NASA/CP-2002-211735

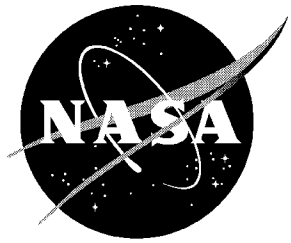

National Educators' Workshop: Update 2001

Standard Experiments in Engineering, Materials Science, and Technology

Compiled by
Edwin J. Prior
Langley Research Center, Hampton, Virginia

James A. Jacobs
Norfolk State University, Norfolk, Virginia

Said Jahanmir
National Institute of Standards and Technology
Gaithersburg, Maryland

June 2002

The NASA STI Program Office . . . in Profile

Since its founding, NASA has been dedicated to the advancement of aeronautics and space science. The NASA Scientific and Technical Information (STI) Program Office plays a key part in helping NASA maintain this important role.

The NASA STI Program Office is operated by Langley Research Center, the lead center for NASA's scientific and technical information. The NASA STI Program Office provides access to the NASA STI Database, the largest collection of aeronautical and space science STI in the world. The Program Office is also NASA's institutional mechanism for disseminating the results of its research and development activities. These results are published by NASA in the NASA STI Report Series, which includes the following report types:

- TECHNICAL PUBLICATION. Reports of completed research or a major significant phase of research that present the results of NASA programs and include extensive data or theoretical analysis. Includes compilations of significant scientific and technical data and information deemed to be of continuing reference value. NASA counterpart of peer-reviewed formal professional papers, but having less stringent limitations on manuscript length and extent of graphic presentations.

- TECHNICAL MEMORANDUM. Scientific and technical findings that are preliminary or of specialized interest, e.g., quick release reports, working papers, and bibliographies that contain minimal annotation. Does not contain extensive analysis.

- CONTRACTOR REPORT. Scientific and technical findings by NASA-sponsored contractors and grantees.

- CONFERENCE PUBLICATION. Collected papers from scientific and technical conferences, symposia, seminars, or other meetings sponsored or co-sponsored by NASA.

- SPECIAL PUBLICATION. Scientific, technical, or historical information from NASA programs, projects, and missions, often concerned with subjects having substantial public interest.

TECHNICAL TRANSLATION. English-language translations of foreign scientific and technical material pertinent to NASA's mission.

Specialized services that complement the STI Program Office's diverse offerings include creating custom thesauri, building customized databases, organizing and publishing research results . . . even providing videos.

For more information about the NASA STI Program Office, see the following:

- Access the NASA STI Program Home Page at ***http://www.sti.nasa.gov***

- Email your question via the Internet to help@sti.nasa.gov

- Fax your question to the NASA STI Help Desk at (301) 621-0134

- Telephone the NASA STI Help Desk at (301) 621-0390

- Write to:
  NASA STI Help Desk
  NASA Center for AeroSpace Information
  7121 Standard Drive
  Hanover, MD 21076-1320

NASA/CP-2002-211735

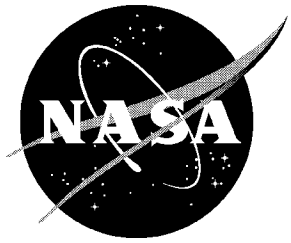

National Educators' Workshop: Update 2001

Standard Experiments in Engineering, Materials Science, and Technology

Compiled by
Edwin J. Prior
Langley Research Center, Hampton, Virginia

James A. Jacobs
Norfolk State University, Norfolk, Virginia

Said Jahanmir
National Institute of Standards and Technology
Gaithersburg, Maryland

Proceedings of a workshop sponsored jointly by the National Aeronautics and Space Administration, Washington, DC; Norfolk State University, Norfolk, VA; the National Composite Center, Kettering, OH; the National Institute of Standards and Technology, Gaithersburg, MD; the Energy Efficiency and Renewable Energy Program, Oak Ridge National Laboratory, Oak Ridge, TN; the United States Automotive Materials Partnership; the Center for Lightweight Materials and Processing, University of Michigan-Dearborn, MI; ASM International Foundation, Materials Park, OH; Gateway Engineering Coalition, Drexel University, Philadelphia, PA; and the University of Maryland, College Park, MD
and held in
College Park, Maryland
October 14–17, 2001

National Aeronautics and
Space Administration

Langley Research Center
Hampton, Virginia 23681-2199

June 2002

Acknowledgments

We greatly appreciate the support provided by these organizations.

National Aeronautics and Space Administration — Langley Research Center

National Institute of Standards and Technology

American Society for Engineering Education

Columbia University

International Council for Materials Education

Johns Hopkins University

Loyola College

Northeast Center for Telecommunication Technologies

United States Naval Academy

University of Maryland — College Park

University of Virginia

Available from:

NASA Center for AeroSpace Information (CASI)
7121 Standard Drive
Hanover, MD 21076-1320
(301) 621-0390

National Technical Information Service (NTIS)
5285 Port Royal Road
Springfield, VA 22161-2171
(703) 605-6000

PREFACE

NEW:Update 2001, scheduled to be hosted by the National Institute of Standards and Technology in Gaithersburg, Maryland, was held October 14–17, 2001 as a part of their Centennial Celebration. However, the September 11th terrorist attack forced the move of the workshop to the University of Maryland, College Park. There we received the excellent coordination of Professor Isabel Lloyd and the Department of Materials and Nuclear Engineering.

The 16th Annual NEW:Update was built on themes, activities and presentations based on extensive evaluations from participants of previous workshops as we continued efforts to strengthen materials education. About 150 participants witnessed demonstrations of experiments, discussed issues of materials science and engineering (MS&E) with people from education, industry, government, and technical societies, heard about new MS&E developments, and chose from ten mini workshops in state-of-the-art laboratories. Faculty in attendance represented high schools, community colleges, smaller colleges, and major universities. Undergraduate and graduate students also attended and presented.

We were fortunate to have excellent support from our hosts. Dr. Said Jahanmir, of the Materials Science and Engineering Laboratory, coordinated NIST researchers, and Dr. Lloyd made most of the arrangements at the University of Maryland and coordinated the workshop schedule for the many scientists, engineers, professors and other staff by providing funding, opening their facilities, and developing presentations and activities.

NEW:Update 2001 participants saw the demonstration of about fifty experiments and aided in evaluating them. We also heard updated information relating to materials science, engineering, and technology presented at mini plenary sessions.

This publication provides experiments and demonstrations that can serve as a valuable guide to faculty who are interested in useful activities for their students. The material was the result of years of research aimed at better methods of teaching materials science, engineering, and technology. The experiments developed by faculty, scientists, and engineers throughout the United States and abroad added to the collection from past workshops. There is a blend of experiments on new materials and traditional materials.

Experiments underwent an extensive peer review process. After submission of abstracts, selected authors were notified of their acceptance and given the format for submission of experiments. Experiments were reviewed by a panel of specialists through the cooperation of the International Council for Materials Education (ICME). Comments from workshop participants provided additional feedback that authors used to make final revisions, which were then submitted to the NASA editorial group for this publication.

Dr. Robert B. Pond, Sr., Professor Emeritus of Johns Hopkins University, was honored by Dr. Lyle Schwartz, President of the Federation of Materials Society, as "Outstanding Materials Educator" for his decades of service to strengthen materials education.

The ICME encourages authors of experiments to submit their work to the Journal of Materials Education (JME). The JME offers valuable teaching and curriculum aids, including instructional modules on emerging materials technology, experiments, book reviews, and editorials, to materials educators.

Critiques were made of the workshop to provide continuing improvement of this activity. The evaluations and recommendations made by participants provide valuable feedback for the planning of subsequent NEW:Updates. NEW:Update 2002 will be held in San Jose, California.

NEW:Update 2001 and the series of workshops that go back to 1986 are, to our knowledge, the only national workshops or gatherings for materials educators that have a focus on the full range of issues on strategies for better teaching about the full complement of materials.

We demonstrated the second edition of Experiments in Materials Science, Engineering, and Technology, (EMSET2) CD-ROM with over 350 experiments from NEW:Updates. This CD-ROM is another example of cooperative efforts to support materials education. The primary contributions came from the many authors of the demonstrations and experiments for NEW:Updates. Funding for the CD came from both private industry and federal agencies. Please see the information on page vi for obtaining the CD.

Special thanks go to our national organizing committee, management team, hosts, sponsors, and especially to those of you who developed and shared your ideas for experiments, demonstrations, and innovative approaches to teaching.

The Organizing Committee hopes that the experiments and technical material updated in this publication will assist you in teaching about materials science, engineering, and technology. We would like to have your comments on their value and your suggestions for improving them. Please send comments to Jim Jacobs, School of Science and Technology, Norfolk State University, Norfolk, Virginia 23504.

MANAGEMENT TEAM

James A. Jacobs
Workshop Co-chairperson
Norfolk State University

Said Jahanmir
Workshop Co-Chairperson
National Institute of Standards and Technology

Isabel K. Lloyd
Workshop Co-Chairperson
University of Maryland

Diana P. LaClaire
Assistant Director
Norfolk State University

Robert Berrettini
International Council on Materials Education

Paul J. Coyne
Loyola College

Jeane Deatherage
ASM International Foundation

Wayne L. Elban
Loyola College

Leonard W. Fine
Columbia University

James Fitz-Gerald
University of Virginia

Gale A. Holmes
National Institute of Standards and Technology

Todd C. Hufnagel
Johns Hopkins University

Kenneth L. Jewett
Materials Science & Engineering Laboratory-NIST

Peter J. Joyce
U. S. Naval Academy

Thomas F. Kilduff
Thomas Nelson Community College

P. K. Mallick
University of Michigan-Dearborn

James V. Masi
Western New England College

Alfred E. McKenney
IBM Corporation, Retired

Angela Moran
U. S. Naval Academy

Edwin Prior
National Aeronautics and Space Administration

Mark Palmer
American Society for Engineering Education

Philip Sklad
Oak Ridge National Laboratory

Fred Wellstood
University of Maryland

The New EMSET2 CD ROM from Jim Jacobs, Al McKenney and Prentice Hall Publishing

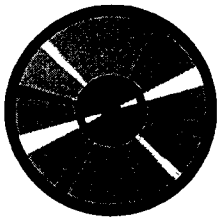

The CD ROM *Experiments in Materials Science, Engineering and Technology 2* (*EMSET2*) will be available soon!

For more than a decade, the National Educators' Workshops have enabled educators to participate in seminars of peer-reviewed experiments and demonstrations in materials science, engineering and technology. Following each workshop, these papers were published in an annual compendium, with the generous support of NASA.

Now, with the assistance from NASA and many other governmental, educational and industrial organizations, we have been able to publish thirteen yearly volumes of these papers in an easily used format, the *EMSET2* CD ROM. This is an expanded and updated version of the original *EMSET* CD ROM. This new version runs on all platforms and uses the universally-accepted Adobe Acrobat format for retrieval, display and printing.

To help the user, the nearly 350 experiments and demonstrations are indexed under the following seven categories: 1)Structure, Testing and Evaluation, 2)Metals, 3)Polymers, 4)Ceramics, 5)Composites, 6)Electronic and Optical Materials, and 7)Materials Curriculum. The user can find the material he or she wants by browsing the tables of contents or by searching for author, title, institution, or key word. Then the documents can be reviewed and used by displaying an exact image of the paper(s), including text, graphs, pictures, formulae, etc. or by printing the paper as written or even by copying the text and/or graphics into a word processor for editing.

To preview an individual demo version please reference ISBN 0130194751 and contact:
Melissa Orsborn
Marketing Assistant
445 Hutchinson Ave. Fourth Floor
Columbus, Ohio 43235
1-614-841-3622
Melissa_Orsborn@prenhall.com
Or
To purchase the complete *EMSET2* CD ROM (available Summer 2000) please reference ISBN 0130305340 and contact:
Prentice Hall Customer Service
1-800-922-0579

CONTENTS

REVIEWERS

Harvey Abramowitz
Department of Engineering
Purdue University – Calumet

Else Breval
Professor of Materials Science
Center for Materials Characterization
University of North Texas

L. Roy Bunnell
Material Science Department
Southridge High School

William Callister
Adjunct Professor of Metallurgy
University of Utah

K. C. Chan
Physics Department of Natural Sciences
Albany State University

Wayne L. Elban
Professor of Engineering
Loyola College, Maryland

Leonard W. Fine
Department of Chemistry
Columbia University in the City
of New York

Richard Griffin
MEEN Department
Texas A&M University

L. J. Martinez-Miranda
Dept. of Materials and Nuclear
Engineering
University of Maryland

James V. Masi
Western New England College
(Emeritus)

Mike Meier
Dept. of Chemical Engineering and
Materials Science
University of California, Davis

Robert Newnham
Solid State Science
The Pennsylvania State University

Edward L. Widener
Department of Mechanical Engineering
Purdue University

Technical Notebooks were provided by
NASA LANGLEY RESEARCH CENTER

Announcements of the workshop were provided by
THE ASM INTERNATIONAL FOUNDATION

Row 1 front (L to R):
R. Garrison, C. Woodall, R. Valenzuela, F. Ekpo, K. C. Chan, L. Martinez-Miranda, S. Jahanmir, W. Elban, S. Keilson, D. LaClaire
Row 2 (L to R):
D. Bushey, K. Song, E. Widener, D. Vigliotti, M. Palmer, J. Fitz-Gerald, J. Dahl, A. McKenney, R. Chung
Row 3 (L to R):
C. Umana, D. Evans, L. Avila, R. Simoes, J. Carpenter, P. Coyne, L. Huang
Row 4 (L to R):
R. Smelser, R. Griffin, R. Berrettini, M. Rudes, Y. Kin, G. Kohne, M. Meier, B. Venkataraman
Row 5 back (L to R):
L. Fine, M. Bagby, R. Crider, J. Gardner, M. Churma, J. Fortman

Participants – National Educators' Workshop 2001

Harvey Abramowitz
Department of Engineering
Purdue University B Calumet
2200 169th Street
Hammond, IN 46323
219-989-2473
harveya@calumet.purdue.edu

Sean Agnew
MSE Faculty Member
University of Virginia

Lori Aldridge
Northwestern High School
2503 W. Main Street
Rockhill, SC 29732
803-417-0863
laldridg@rock-hill.K12.sc.us

Eric J. Amis
Polymers Division (854)
Polymers Building (224), Room A303
National Institute of Standards and Technology
100 Bureau Drive, Stop 8540
Gaithersburg, MD 20899-8540
301-975-6681
eric.amis@nist.gov

Aman Anand
1000 Towers Circle
Apartment South 718
Cape Girardeau, MO 63701
573-339-4376
amanfromcs@hotmail.com

Shahriar Anwar
Arizona State University
1171 N. Tercera Court
Chandler, AZ 85226
480-965-5696
anwar@asu.edu

Luis Avila
Columbia University
Dept. Of Chemistry
116th Broadway
New York, NY 10027
212-854-2587
avila@chem.columbia.edu

Michael Bagby
West Virginia University
School of Dentistry
HSC North
Box 9403
Morgantown, WV 26506-9403
304-293-3370
mbagby@hsc.wvu.edu

Raj Bansal
University of Virginia
2021 Ivy Road, #C-5
Charlottesville, VA 22903
434-923-8794
rajbansal@virginia.edu

Laura M. Bartolo
Associate Professor
Libraries & Media Services
Kent State University
Kent, OH 44141-0001
330-672-1691
lbartolo@kent.edu

Robert Berrettini
209 Kenmar Drive
Monroeville, PA 15146-1717
412-373-7975
e-mail berrettini@stargate.net

John Blendell
National Institute of Standards and Technology
Ceramics Division 223/B324
110 Bureau Drive, STOP 8522
Gaithersburg, MD 20899-8522
301-975-5796
John.Blendell@nist.gov

Duane Bushey
Maury High School
322 Shirley Avenue
Norfolk, VA23517
757-628-3348
dbushey@infi.net

William D. Callister
University of Utah
2419 East 3510 South
Salt Lake City, UT 84109
801-278-8611
bill.callister@m.cc.utah.edu

Joseph C. Carpenter
EE 32
U. S. Department of Energy
100 Independence Avenue SW
Washington, DC 20585
202-586-1022
joseph.carpenter@ee.doe.gov

G. Slade Cargill III
Department MS&E
Lehigh University
5 E. Packer Avenue
Bethlehem, PA 18015
610-758-4207
gsc3@lehigh.edu

John Cassidy
jacassi1@kent.edu

K. C. Chan
Albany State University
Natural Sciences Dept.
504 College Drive
Albany, GA 31705
229-430-1728
kcchan@asurams.edu

Kaushik Chatterjee
University of Virginia
Kc5v@virginia.edu

W. Richard Chung
Department of Chemical and Materials Engineering
San Jose State University
San Jose, CA 95192-0082
408-924-3927
wrchung@sjsu.edu

Michelle Churma
Prentice Hall
445 Hutchinson Avenue
Columbus, OH 43235
614-841-3636
Michelle_Churma@prenhall.com

Toby Cordell
National Composite Center
2000 Composite Drive
Kettering, OH 45420
937-369-1174
tcordell@compositecenter.org

Paul J. Coyne, Jr.
Loyola College
Dept. of Electrical Engineering
and Engineering Science
Baltimore, MD 21210-2699
pcoyne@loyola.com

Roger Crider
2100 Concert Drive
Virginia Beach, VA 23456
757-468-3800
rlcrider@vbcps.k12.va.us

Jeffrey Csernica
Department of Chemical Engineering
Bucknell University
Lewisburg, PA 17837
570-577-1257
csernica@bucknell.edu

Jai N. Dahiya
Professor of Physics & Associate Dean
College of Science & Mathematics
Southeast Missouri State University
One University Plaza, MS 6000
Cape Girardeau, MO 63701
573-651-2163
dahiya@physics.semo.edu

Jeff Dahl
Ford Research Lab
SRL, MD3135
2101 Village Road
Dearborn, MI 48124
313-322-7814
jdahl@ford.com

Sabine Dickens
National Institute of Standards and Technology

Avinash M. Dongare
Materials Science and Engineering
University of Virginia
2021 Ivy Road
University Forum, Apt. #C-5
Charlottesville, VA 22903
434-923-8794
davinash@virginia.edu

Frederick C. Eichmiller
Polymers Division (854)
Polymers Building (224), Room A155
National Institute of Standards and Technology
100 Bureau Drive, Stop 8546
Gaithersburg, MD 20899-8546
301-975-6813
frederick.eichmiller@nist.gov

Efremfon Frank Ekpo
Bethune-Cookman College
640 Dr. M. M. Bethune Blvd.
Daytona Beach, FL 32114
386-255-1401 xd 532
ekpoe@cookman.edu

Wayne L. Elban
Dept. of Electrical Engineering and Engineering Science
Loyola College
Baltimore, MD 21210
410-617-2853
welban@loyola.edu

Don Evans, Director
Center for Research on Education in Science
Arizona State University
Tempe, AZ 85287-5006
480-965-5350
devans@asu.edu

Neda Fabris
Department of Mechanical Engineering
California State University, Los Angeles
5151 State University
Los Angeles, CA 90032-8153
323-343-5218
nfabris@exchange.calstatela.edu

Louis Feng
lfeng@kent.edu

R. J. Fields
National Institute of Standards and Technology
MATLS B252
100 Bureau Drive, Stop 8553
Gaithersburg, MD 20899-8533
301-975-5712
rjf@nist.gov

Leonard W. Fine
Department of Chemistry
Columbia University in the City of New York
Havemeyer Hall
New York, NY 10027
212-854-2017
fine@chem.columbia.edu

James M. Fitz-Gerald
Department of Materials Science & Engineering
Advanced Laser Processing
School of Engineering and Applied Science
University of Virginia
116 Engineer=s Way
Charlottesville, VA 22904-4745
804-243-8830
jmf8h@virginia.edu

John J. Fortman
Department of Chemistry
Wright State University
Dayton, OH 45435
937-775-2188
john.fortman@wright.edu

Douglas Frantz
Community College of Baltimore County
800 S. Rolling Road
Baltimore, MD 21228
410-455-4317
dfrantz@ccbc.cc.md.us

Morton Friedman
Columbia University
500 West 120th Street
Room 510 Mudd
New York, NY 10027
212-854-2986
friedman@columbia.edu

Eli Fromm
Director and P.I. of Gateway Engineering
Education Coalition
fromm@drexel.edu

Edwin Fuller
Ceramics Division (852)
Materials (223), Room A325
National Institute of Standards and Technology
100 Bureau Drive, Stop 8521
Gaithersburg, MD 20899-8521
301-975-5795
edwin.fuller@nist.gov

James Gardner
Technology Commercialization Center
12050 Jefferson Avenue, Suite 350
Newport News, VA 23601
757-269-0025
jgardner@teccenter.org

Kathryn Gargurevich
4920 Strathmore Avenue
Kensington, MD 20895
3/469-6034
garg4@msn.com

Ronald R. Garrison
4653 Priscilla Lane
Virginia Beach, VA 23455
757-460-6052
rrgarris@vbcps.k12.va.us

Charles J. Glinka
National Institute of Standards and Technology
Center for Neutron Research
100 Bureau Drive, STOP 8652
Gaithersburg, MD 20899-8562
301-975-6242
cglinka@nist.gov

Richard B. Griffin
Mahan Hall, C&ME (2001-2002)
United States Military Academy
West Point, NY 10996-1972
845-938-4093
rgriffin@mengr.tamu.edu
Richard.Griffin@usma.edu

Martha Goodway
Archaeometallurgist
Smithsonian Center for Materials
Research and Education
Washington, DC 20560
301-238-3700 x 164
GoodwayM@SCMRE.SI.EDU

Michael Guarraia
Loyola College

Dale Hall, Deputy Director
Materials Science & Engineering Laboratory
National Institute of Standards and Technology
Bldg. 310, Room B309, MS 8500
Gaithersburg, MD 20899-8500
301-975-5658
dale.hall@nist.gov

Justin Hanes
Department of Chemical Engineering
Johns Hopkins University
221 Maryland Hall
3400 North Charles Street
Baltimore, MD 21218
410-516-3484
hanes@jhu.edu

Luke H. Huang
Assistant Professor
Industrial Technology
University of North Dakota
Grand Forks, ND 58202
701-777-2202
luke_huang@und.edu

Yolanda L. Hinton
Department of Engineering
Norfolk State University
700 Park Avenue
Norfolk, VA 23504
757-823-2697
ylhinton@nsu.edu
y.l.hinton@larc.nasa.gov

Todd C. Hufnagel
Dept. Of Materials Science and Engineering
Johns Hopkins University
102 Maryland Hall
3400 North Charles Street
Baltimore, MD 21218
410-516-6277
hufnagel@jhu.edu

Monica Hurley
U. S. Naval Academy
590 Holloway Road
Annapolis, MD 21402
410-293-6534
amoran@usna.edu

James A. Jacobs
School of Science and Technology
Norfolk State Univesity
700 Park Avenue
Norfolk, VA 23504
757-823-8109
jajacobs@nsu.edu

Said Jahanmir
Ceramics Division
Materials, Room B 360
National Institute of Standards and Technology
100 Bureau Drive, MS 8520
Gaithersburg, MD 20899-8520
301-975-3671
said.jahanmir@nist.gov

Greg Jennings
University of Virginia student
258-11 Colonnade Drive
Charlottesville, VA 22903
434-297-3406
gmj3t@cms.mail.virginia.edu

Rodney D. Jiggetts
Metallurgy Division (855)
National Institute of Standards and Technology
100 Bureau Drive, Stop 8555
Gaithersburg, MD 20899-8555
301-975-5122
rodney.jiggetts@nist.gov

Ajit Jillavenkatesa
Ceramics Division (852)
Materials (223), Room A215
National Institute of Standards and Technology
100 Bureau Drive, Stop 8520
Gaithersburg, MD 20899-8520
301-975-5089
ajit.jilla@nist.gov

Peter Joyce
U. S. Naval Academy
590 Holloway Road
Annapolis, MD 21402
410-293-6533
pjoyce@usna.edu

Suzanne Keilson
Loyola College
4501 North Charles Street
Dept. of Electrical Engineering and
Engineering Science
Baltimore, MD 21210
410-617-2722
skeilson@loyola.edu

John N. Kidder, Jr.
Assistant Professor
University of Maryland
Department of Materials Science and Engineering
Bldg. 090, Room 2142
College Park, MD 20742
301-405-0499
kidder@eng.umd.edu

Yulian Kin
Purdue University Calumet
2200 169th Street
Hammond, IN 46323
kin@calumet.purdue.edu

Glenn Kohne
Loyola College
Dept. Of Electrical Engineering
& Engineering Science
Baltimore, MD 21210-2699
410-617-2249
kohne@loyola.edu

Diana P. LaClaire
School of Science and Technology
Norfolk State University
700 Park Avenue
Norfolk, VA 23504
757-823-9072
dplaclaire@nsu.edu

Elodie Leveugle
2728 McElroy Drive
Charlottesville, VA 22903
434-243-7754
el8d@virginia.edu

Isabel Lloyd
Department of Materials and
Nuclear Engineering
Room 2138, Building 090
University of Maryland
College Park, MD 20742-2115
301-405-5221
illoyd@eng.umd.edu

P. K. Mallick
Department of Mechanical Engineering
University of Michigan-Dearborn
Dearborn, MI 48128
313-593-5119
pkm@umich.edu

John Marshall
University of Southern Maine
Mitchell Center
37 College Avenue
Gorham, ME 04038
207-780-5447
jmarshal@usm.maine.edu

L. J. Martinez-Miranda
Dept. of Materials and Nuclear Engineering
University of Maryland
College Park, MD 20742-2115
301-405-0253
martinez@eng.umd.edu

James V. Masi
Western New England College (Emeritus)
242 Spurwink Avenue
Cape Elizabeth, ME 04107-9612
207-767-3196
masij@hotmail.com

Alfred E. McKenney
516 Fairfax Way
Williamsburg, VA 23185
757-221-0476
aem2@prodigy.net

Mike Meier
Department of Chemical Engineering and Materials Science
University of California, Davis
Davis, CA 95616
530-752-5166
mlmeier@ucdavis.edu

Andrew Mercado
313 13th Street NW Apt. 1D
Charlottesville, VA 22903
434-923-8226
alm5w@cms.mail.virginia.edu

Mohsen Mosleh
Howard University
2300 Sixth Street, N. W.
Washington, DC 20059
202-806-6622
mmosleh@fac.howard.edu

Angela Moran
Department of Mechanical Engineering
U. S. Naval Academy
Annapolis, MD 21402
410-293-6534
amoran@gwmail.usna.edu

Frederick W. Oliver
Morgan State University
Baltimore, MD 21251
443-885-3751
fwoliver@morgan.edu

Matthew C. Osborne, Midshipman 1/C
Assistant Professor
U. S. Naval Academy
Mechanical Engineering Dept.
Rickover Hall Room 66
590 Holloway Road M/S 11C
Annapolis, MD 21402
410-293-5528
Osborne@usna.edu

Richard J. Osborne
GMNA Materials & Fastening
MC 480-205-314
Dock #17, Room 306-07
3007 Van Dyke
Warren, MI 48090-9065
810-575-7039
richard.osborne@GM.com

Mark A. Palmer
Kettering University
1700 West Third Avenue
Flint, MI 48504
810-762-7973
mpalmer@kettering.edu

Amy Payne
University of Wisconsin: MRSEC
1101 University Avenue
Department of Chemistry
Madison, WI 53706
608-262-6711
payne@chem.wisc.edu

Thomas Pierce
Norfolk State University
700 Park Avenue
Norfolk, VA 23504
757-823-8109
tapnsu@yahoo.com

Robert B. Pond, Jr.
913 Ellendale Drive
Towson, MD 21286
410-617-5563
rpond@loyola.edu

Merredith Portsmore
Tufts University
Department of Mechanical Engineering
200 College Avenue
Anderson Hall
Medford, MA 02155
617-627-5888
mportsmo@tufts.edu

Adam C. Powell IV
hazelsct@mit.edu

George D. Quinn
Ceramics Division (852)
Materials (223), Room A359
National Institute of Standards and Technology
100 Bureau Drive, Stop 8521
Gaithersburg, MD 20899-8521
301-975-5765
george.quinn@nist.gov

Robert Redfield
Loyola College

Chris Rogers
Associate Professor
Department of Mechanical Engineering
Tufts University
Medford, MA 02155
617-627-2882
crogers@tufts.edu

William Ross
Muskegon Community College
221 S. Quartweline Road
Muskegon, MI 49442
231-777-0367
RossB@muskegon.cc.mi.us

H. Alan Rowe
Professor of Chemistry
Norfolk State University
Chemistry/Center for Materials Research
Norfolk, VA 23504
757-823-2248
harowe@nsu.edu

J. Michael Rowe
NIST Center for Neutron Research (856)
Reactor Building (235), Room A104
National Institute of Standards and Technology
100 Bureau Drive, Stop 8560
Gaithersburg, MD 20899-8560
301-975-6210
j.rowe@nist.gov

Merrill Rudes
Energy Concepts, Inc.
404 Washington Blvd.
Mundelein, IL 50050
847-837-8191
ecisales1@aol.com
mrudes@aol.com

Lourdes Salamanca-Riba
Materials and Nuclear Engineering Department
University of Maryland
College Park, MD 20742-2115
riba@eng.umd.edu

Robert D. Shull
Metallurgy Division (855)
Materials (223), Room B150
National Institute of Standards and Technology
100 Bureau Drive, Stop 8552
Gaithersburg, MD 20899-8552
301-975-6035
robert.shull@nist.gov

Ricardo Simoes
Laboratory of Polymers
Department of Materials Science
University of North Texas
Denton, TX 76203-5310
940-565-3262
rsimoes@unt.edu

Philip Sklad
Grant Tech Monitor
Oak Ridge National Laboratory
skladps@ornl.gov

Ron E. Smelser
University of Idaho
Sixth and Ash
P. O. Box 440902
Moscow, ID 83844-0902
208-885-4049
rsmelser@uidaho.edu

Jonathan D. Stolk
Asst. Professor of Mechanical Engineering
And Materials Science
Franklin W. Olin College of Engineering
1735 Great Plain Avenue
Needham, MA 02492
jonathan.stolk@olin.edu

Kyo D. Song
Norfolk State University
700 Park Avenue
Norfolk, VA 23504
757-823-8105
ksong@nsu.edu

Ichiro Takeuchi
Assistant Professor
Dept. of Materials and Nuclear Engineering
and Center for Superconductivity Research
University of Maryland
College Park, MD 20742
301-405-6809
takeuchi@squid.umd.edu

Vinot Tewary
tewary@boulder.nist.gov

Ming Tung
National Institute of Standards and Technology
100 Bureau Drive,Stop 8546
Gaithersburg, MD 20899-8546
301-975-6823
Ming.tung@nist.gov

Carlos E. Umana
School of Mechanical Engineering
University of Costa Rica
San Pedro, Costa Rica
506-207-4548
caruma@terraba.fing.ucr.ac.cr

Raul Valenzuela
Institute for Materials Research
National University of Mexico
P. O. Box 70-360
Mexico 04510 Mexico
525-622-4653
monjaras@servidor.unam.mx

Bhawani Venkataraman
340 Columbia University
MC 3142 Havemeyer Hall
New York, NY 10027
212-854-4598
bhawani@chem.columbia.edu

Daniel P. Vigliotti
National Institute of Standards and Testing
Division 853
325 Broadway
Boulder, CO 80303-3328
303-497-3351
vigliotti@boulder.nist.gov

Curtiss E. Wall
School of Science and Technology
Norfolk State University
700 Park Avenue
Norfolk, VA 23504
757-823-9571
cewall@nsu.edu

C. David Warren
Bldg. 9204
Oak Ridge National Laboratory
P. O. Box 2099, MS 8050
Oak Ridge, TN 37831-8050
W95@ornl.gov

James Warren
Metallurgy Division (855)
Materials (223), Room A311
National Institute of Standards and Technology
100 Bureau Drive, Stop 8554
Gaithersburg, MD 20899-8554
301-975-5708
jwarren@nist.gov

Edward L. Widener
Purdue University
Knoy Hall 119
West Lafayette, IN 47907-1317
elwidener@tech.purdue.edu

O. C. Wilson, Jr.
Department of Materials and Nuclear Engineering
University of Maryland
College Park, MD 20742-2115

Amy Wilkerson
Applied Research Center
12050 Jefferson Avenue, Suite 713
Newport News, VA 23606
757-269-5760
alwilker@AS.WM.EDU

Charlie Woodall
Norfolk State University
700 Park Avenue
Norfolk, VA 23504
brickcha@hotmail.com

NATIONAL EDUCATORS' WORKSHOP

Update 2001: Standard Experiments in Engineering Materials, Science, and Technology

---

October 14 - October 17, 2001 - Gaithersburg, Maryland

Sponsored by

MSEL

Materials Science & Engineering Laboratories
National Institute of Standards and Technology

Department of Energy
Office of Energy Efficiency and Renewable Energy

National Aeronautics & Space Administration
Langley Research Center

NSU

School of Science and Technology
Norfolk State University

ornl

Energy Efficiency and Renewable Energy Program
Oak Ridge National Laboratory

USAMP

United States Automotive Materials Partnership

Center for Lightweight Materials and Processing
University of Michigan - Dearborn

The ASM International Foundation

The ASM International Foundation

National Composite Center

Gateway Engineering Coalition

With the support of

American Society for Engineering Education
International Council for Materials Education
Loyola College
United States Naval Academy
University of Virginia

Columbia University
Johns Hopkins University
Northeast Center for Telecommunications Technologies
University of Maryland – College Park

MEETING PLACES AND SESSIONS

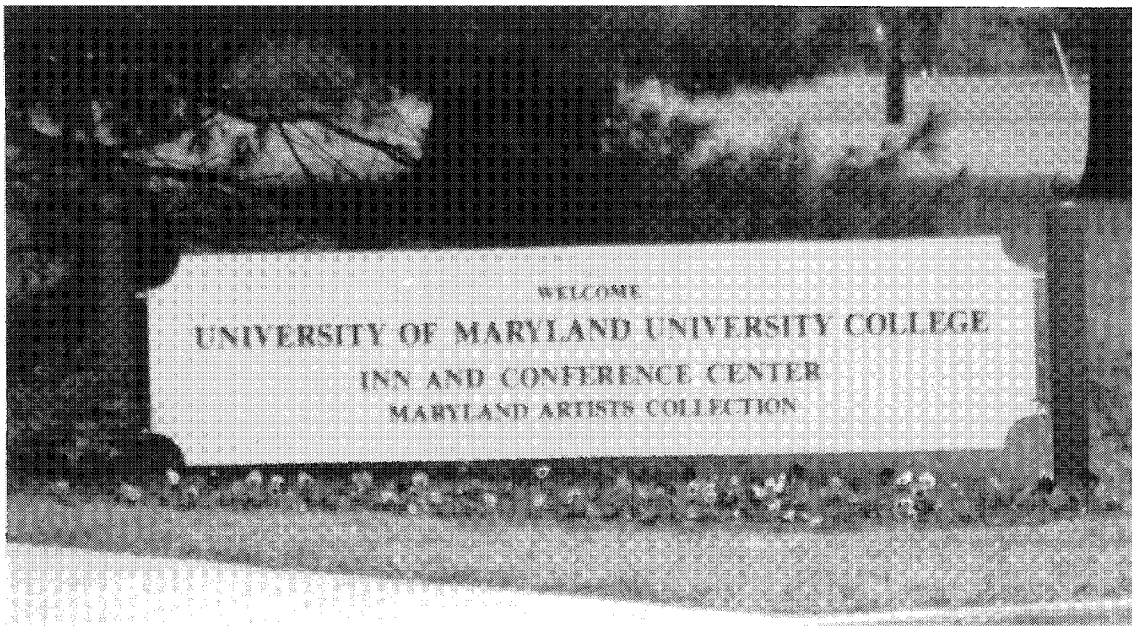

Said Jahanmir
Workshop Co-Chairperson
NIST

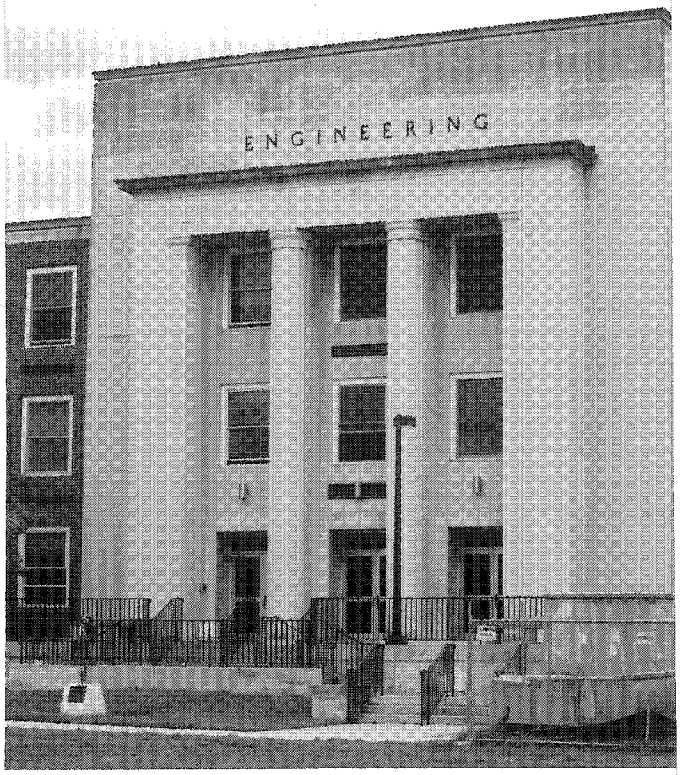
ENGINEERING


ADELF H. STAMP STUDENT UNION
STAMP
STUDENT
UNION
STAMP
STUDENT
UNION
UMCP

SESSIONS

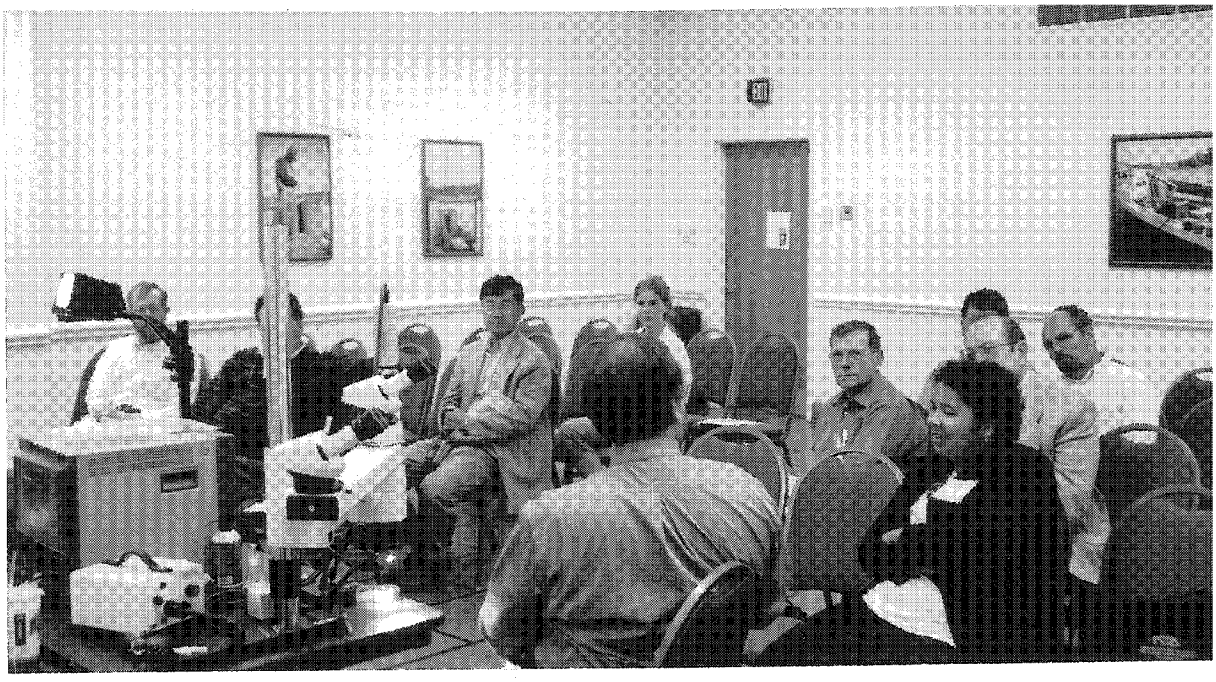

SESSIONS (continued)

SESSIONS (continued)

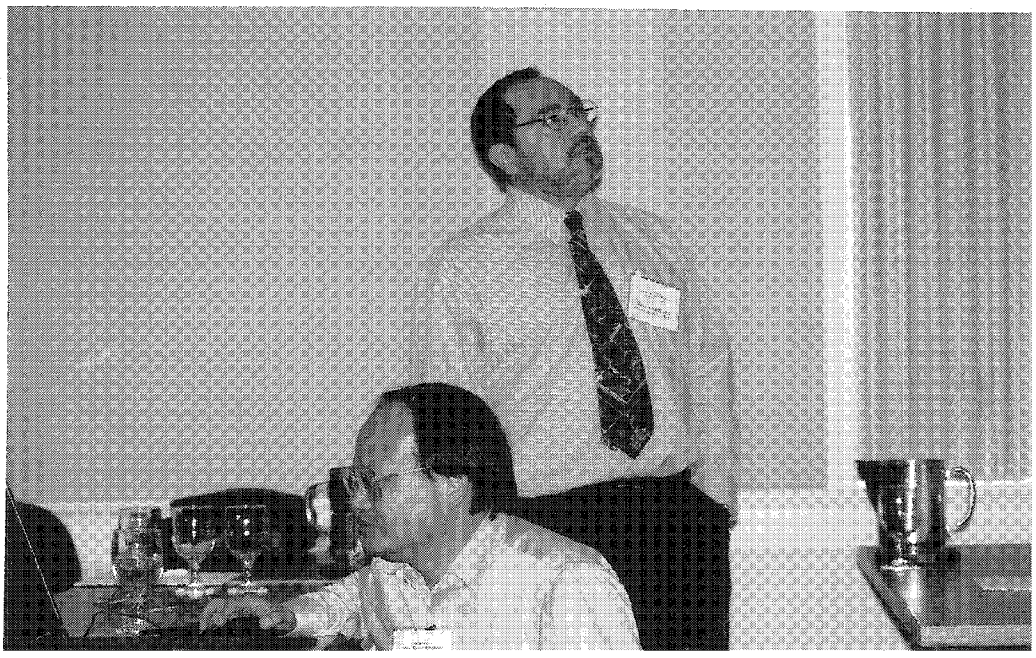

SESSIONS (continued)

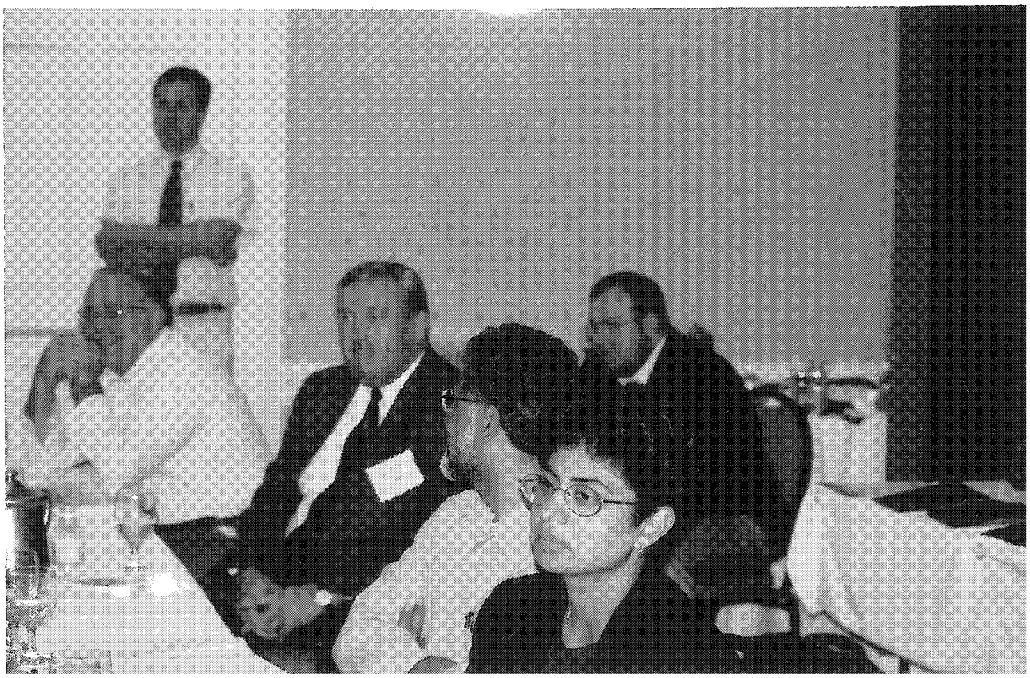

SESSIONS (continued)

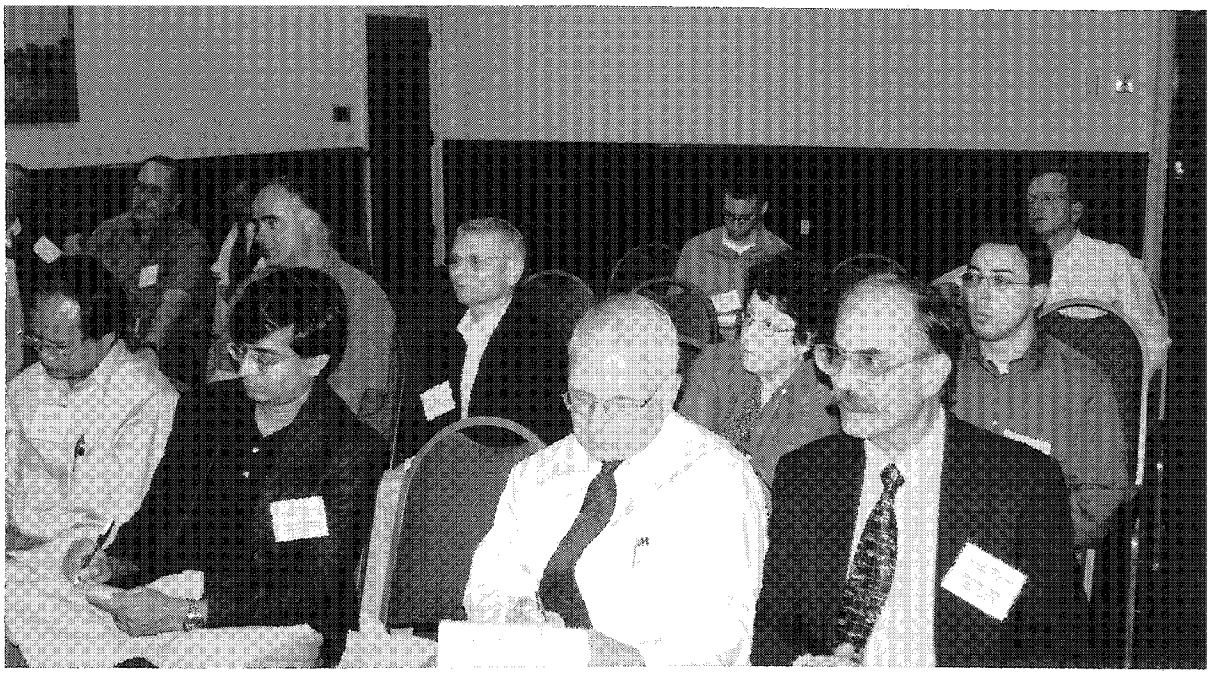

SESSIONS (concluded)

Diana La Claire and Amy Wilkerson

Michelle Churma – Prentice Hall

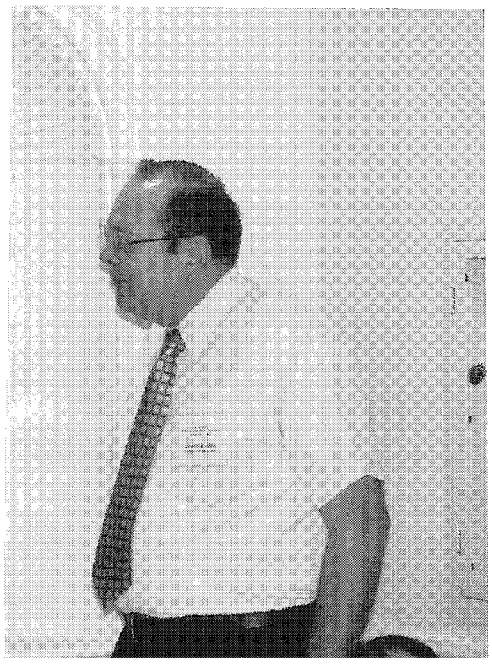

Merrill Rudes – Energy Concepts

BREAKS

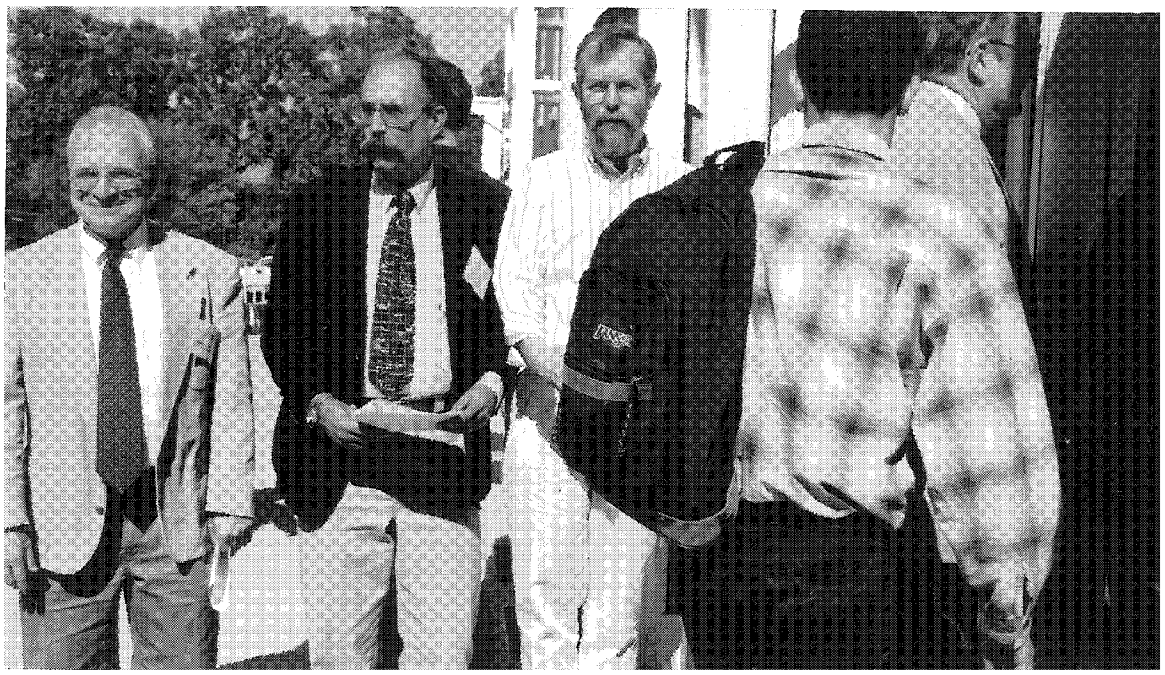

Isobel Lloyd

Al McKenney

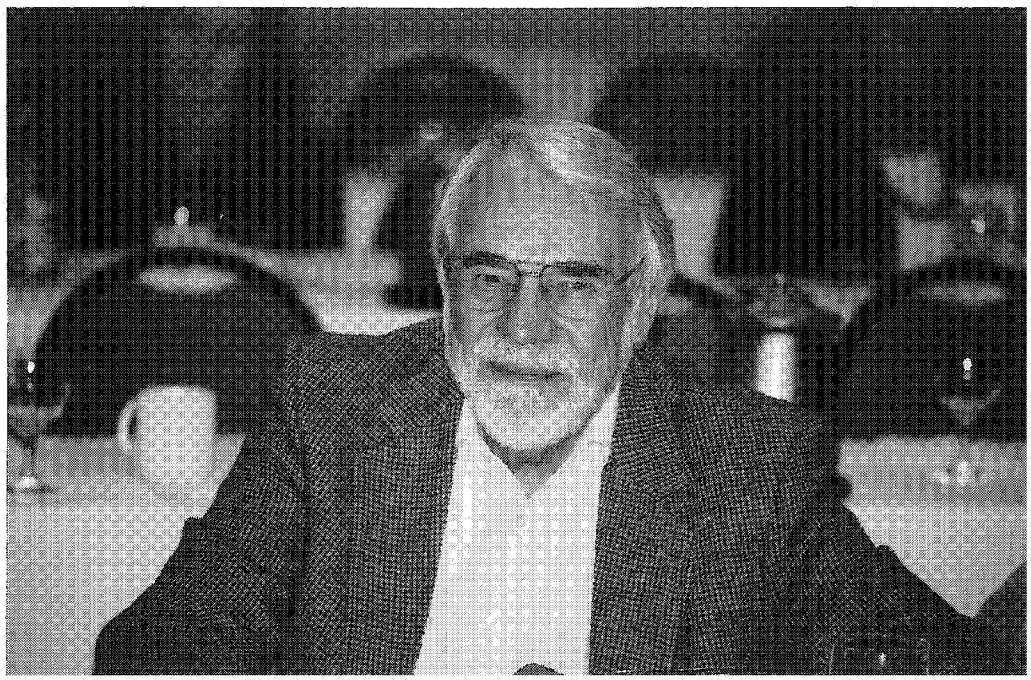

NATIONAL EDUCATORS' WORKSHOP
NEW:UPDATE 2001
SUNDAY PROGRAM

SUNDAY AFTERNOON, October 14, 2001

Welcome and Introduction to the University of Maryland

Materials Science and Engineering at the University of Maryland (Research and UG Program)

Lab tours and Demonstrations

Registration at Conference Center

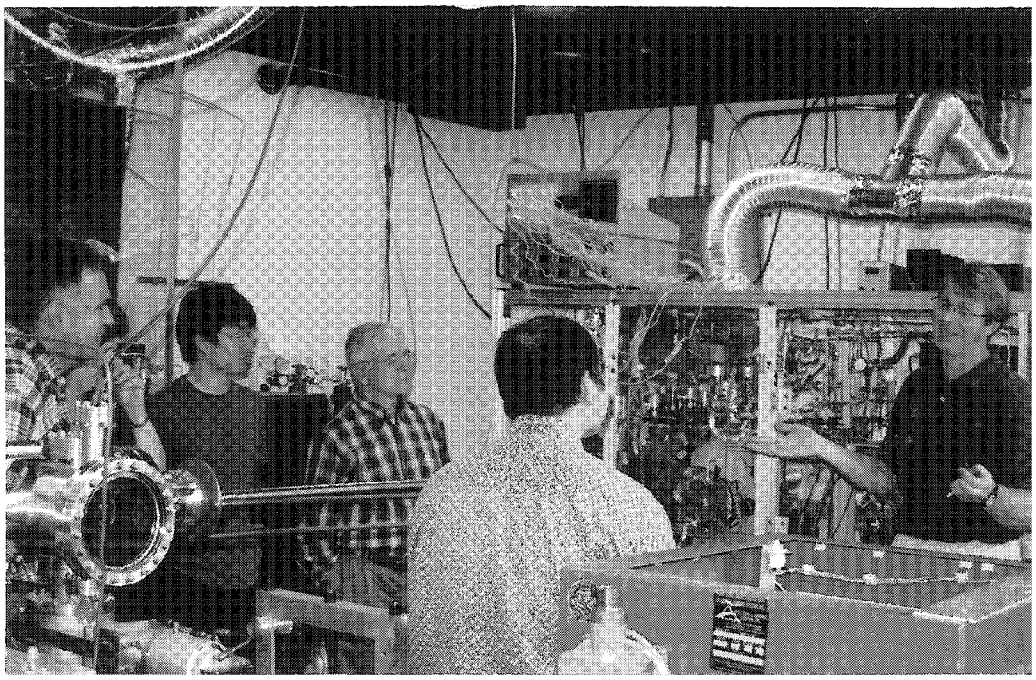

SUNDAY PROGRAM

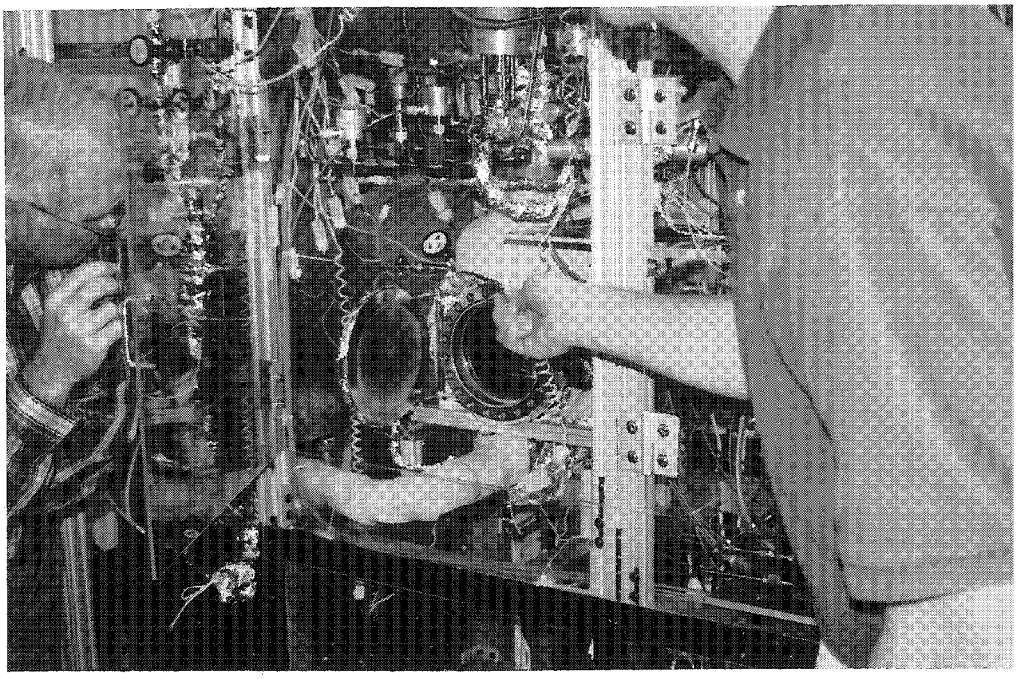

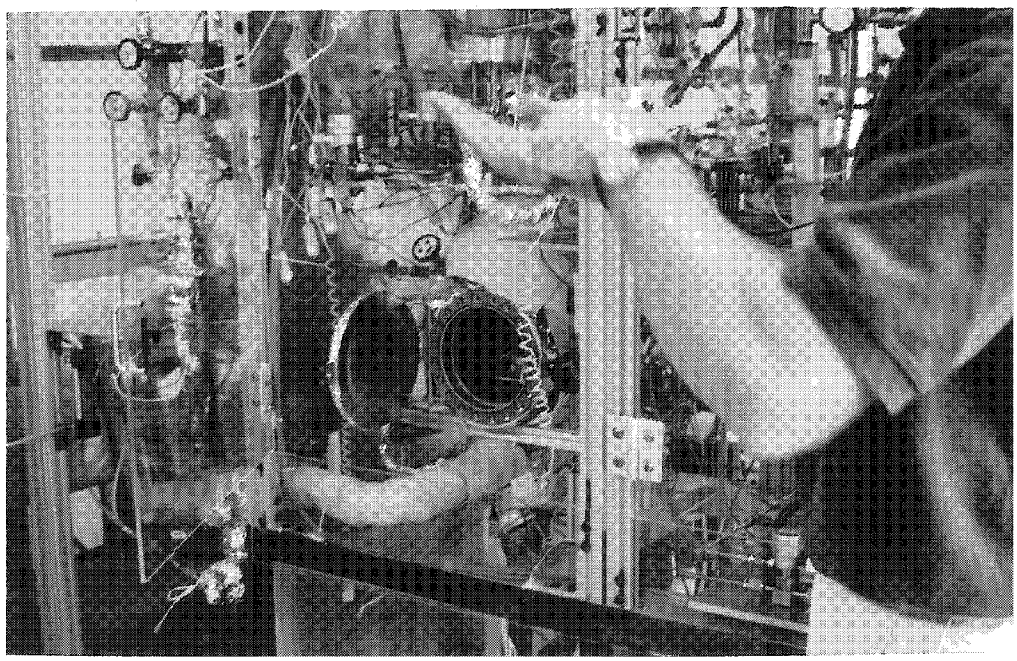

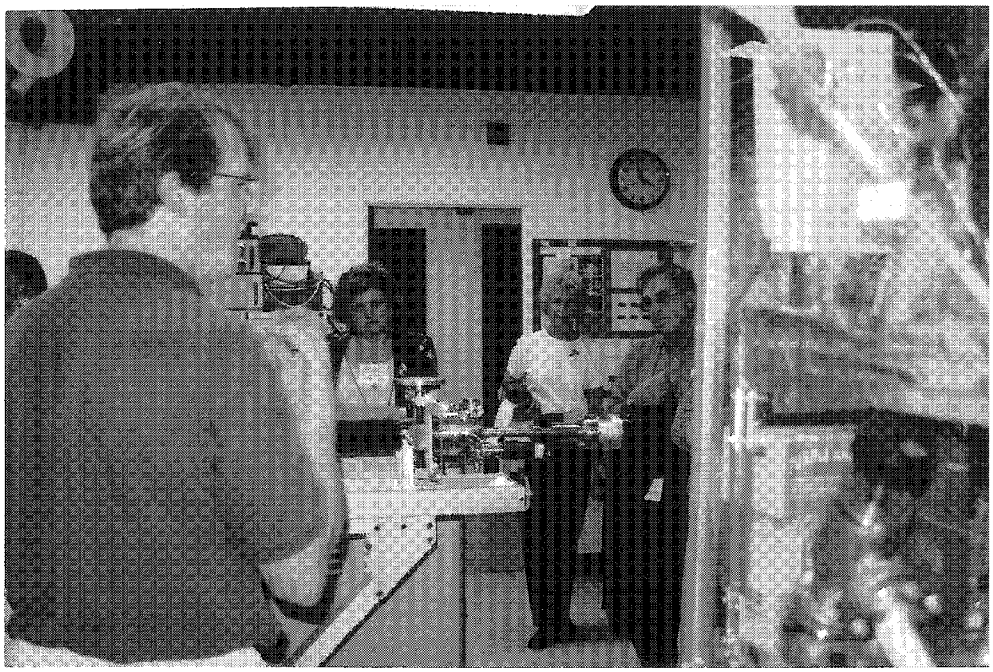

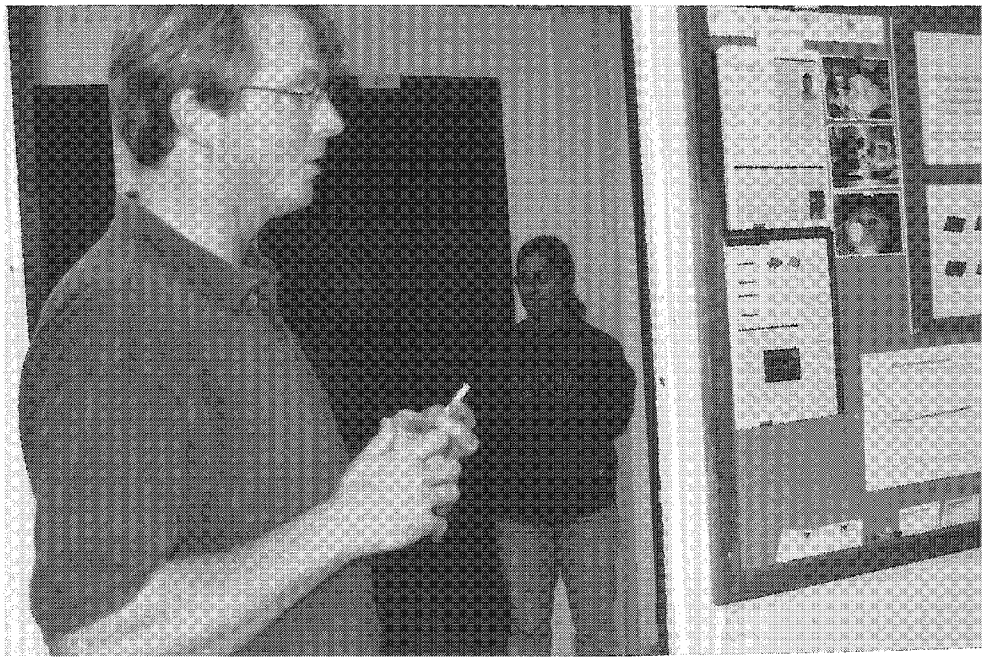

SUNDAY PROGRAM (Continued)

SUNDAY PROGRAM (Continued)

SUNDAY PROGRAM (Continued)

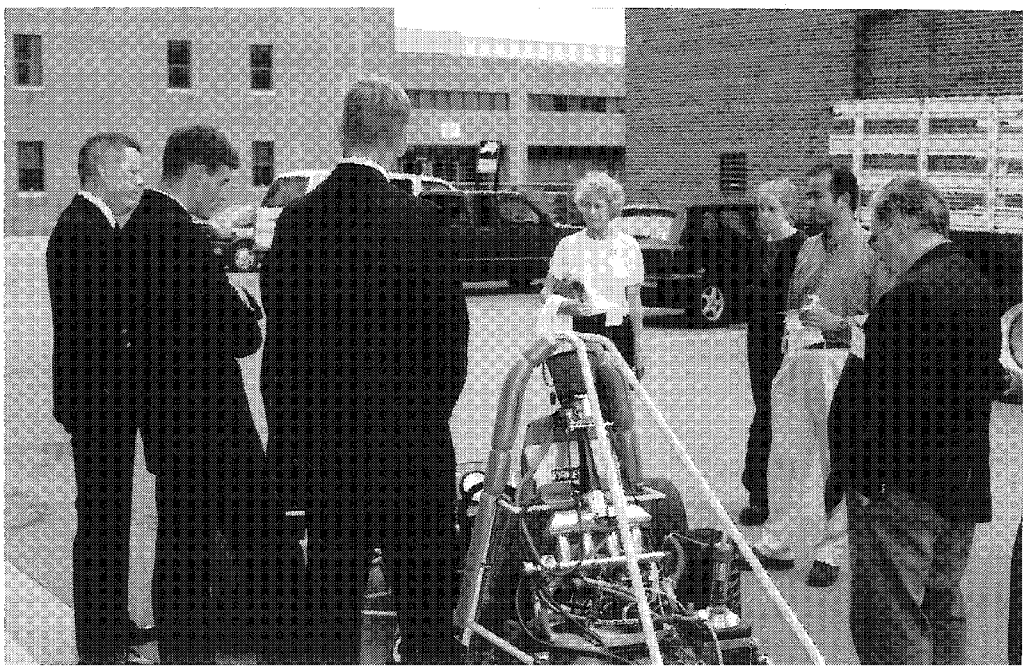

SUNDAY PROGRAM (Concluded)

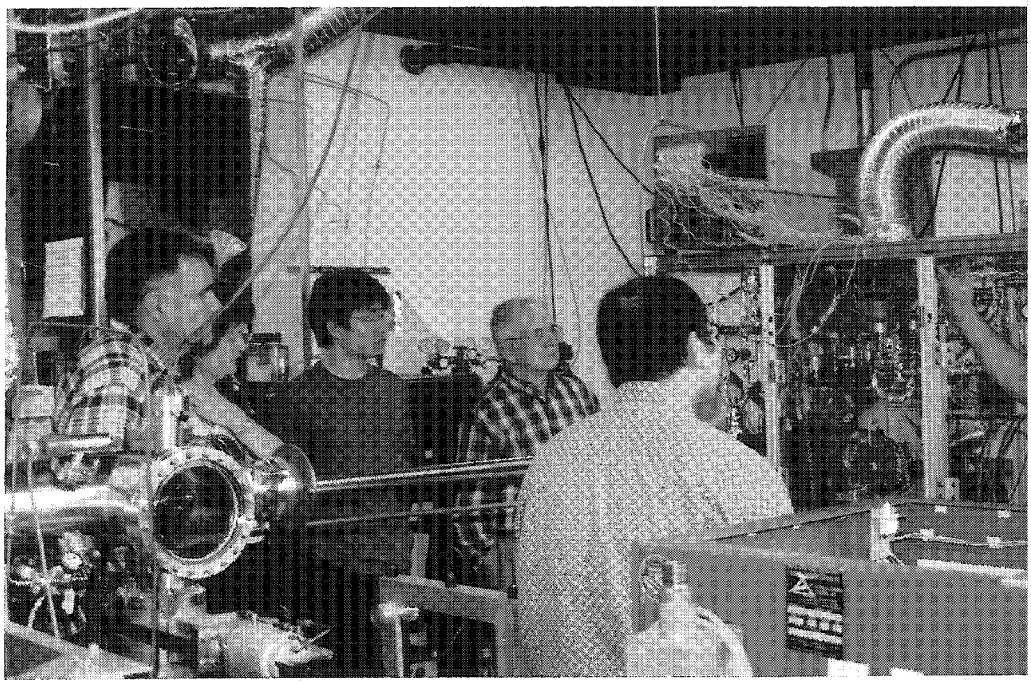

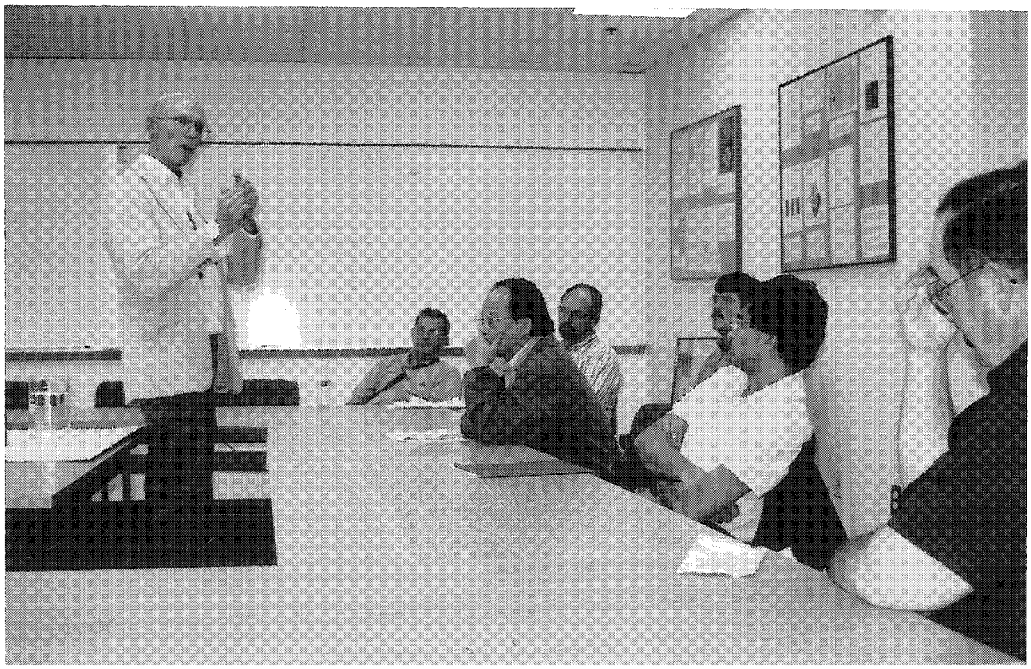

MINI WORKSHOPS

MONDAY AFTERNOON

WONDERFUL WORLD OF POLYMERS
Presented by Eric J. Amix
National Institute of Standards and Technology

CERAMIC FRACTOGRAPHY
Presented by George Quinn
National Institute of Standards and Technology

LIGHTWEIGHT AUTOMOTIVE MATERIALS DATABASE
Presented by P. K. Mallick
University of Michigan-Dearborn

LINEAR ACCELERATOR
Chemical and Nuclear Engineering Building

GREEN'S FUNCTION LIBRARY
Presented by Laura M. Bartolo
Kent State University

TUESDAY AFTERNOON

MICROSTRUCTURAL-BASED FEM MODELING
Presented by Mark R. Locatelli
National Institute of Standards and Technology

NEUTRON RESEARCH FACILITY
Presented by Charles Glinka and Michael Rowe
National Institute of Standards and Technology

CERAMICS AROUND US
Presented by John Blendell and Ajit Jillavenkatesa
National Institute of Standards and Technology

METALS
Presented by Robert Shull
National Institute of Standards and Technology

K-COLLEGE ENGINEERING EDUCATION WITH LEGO BRICKS
Presented by Chris Rogers and Merredith Portsmore
Tufts University

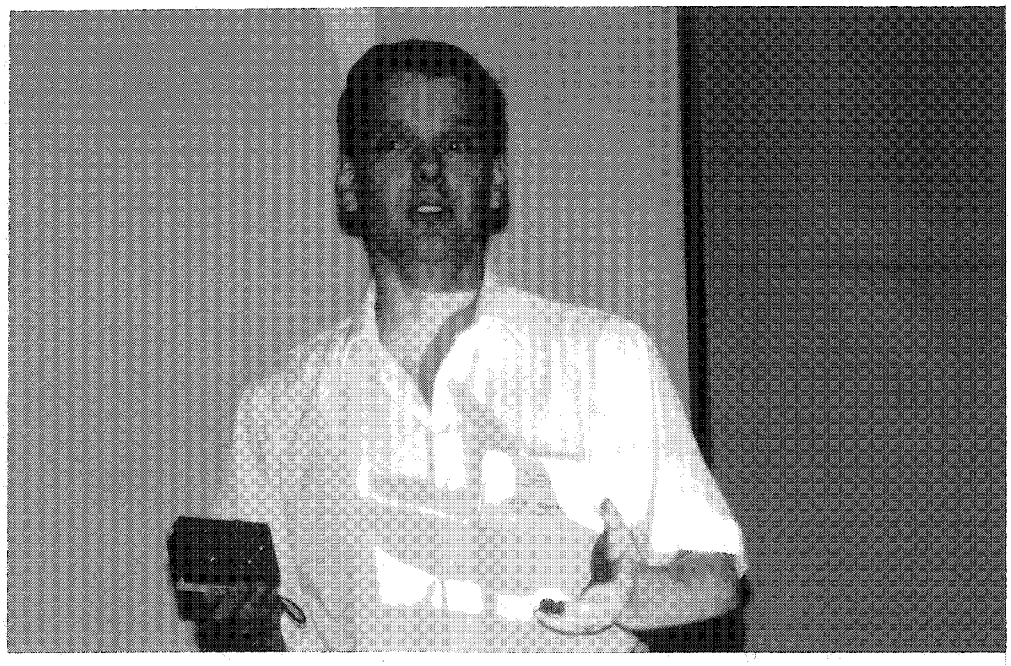

Chris Rogers

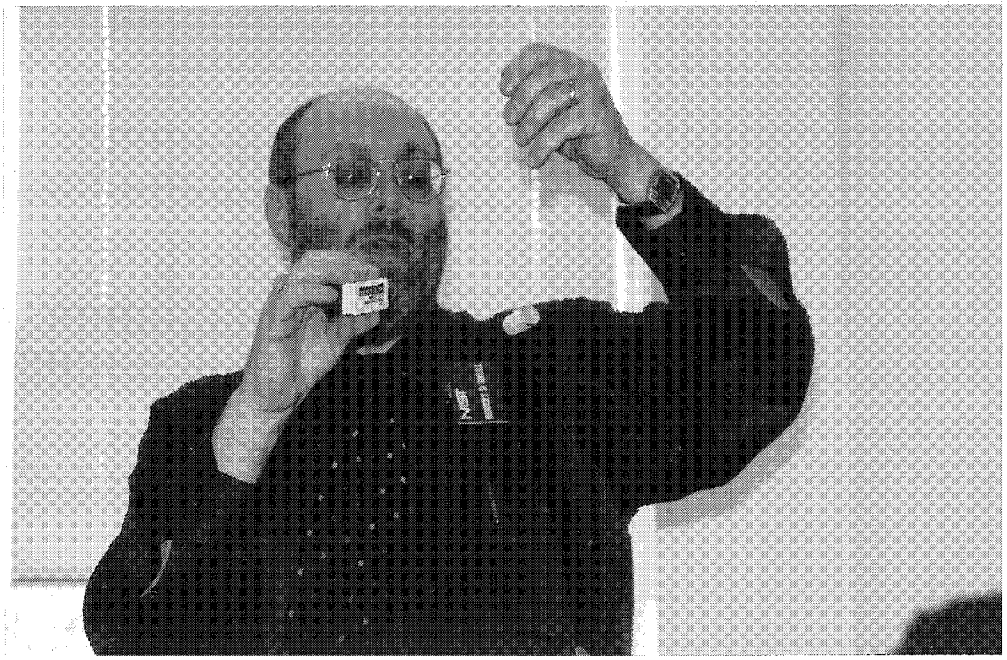

Robert Shull

MINI WORKSHOPS

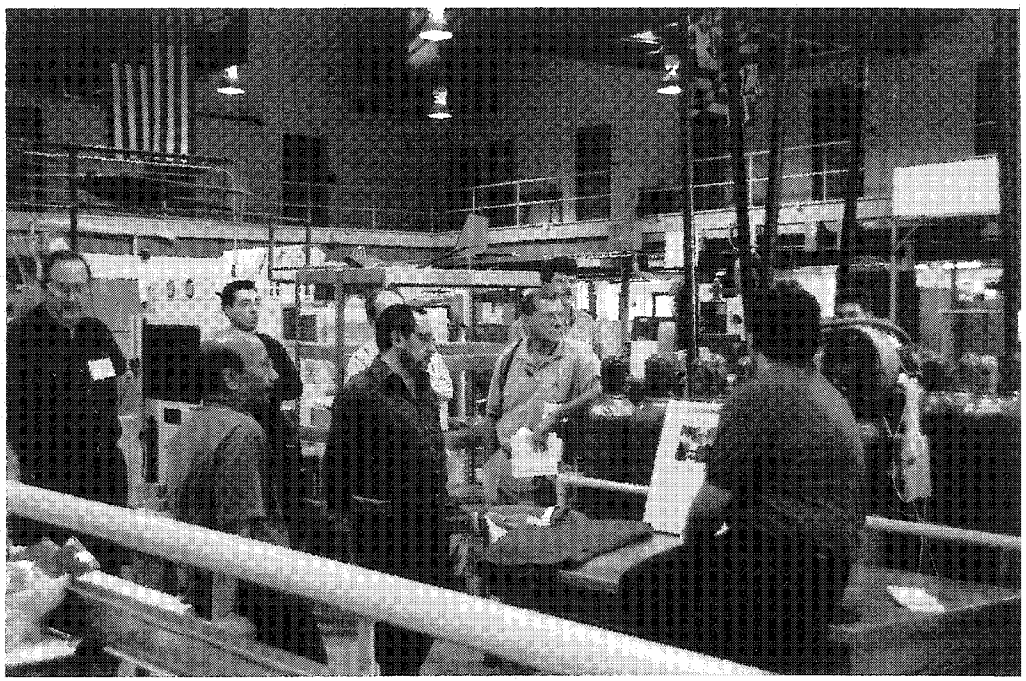

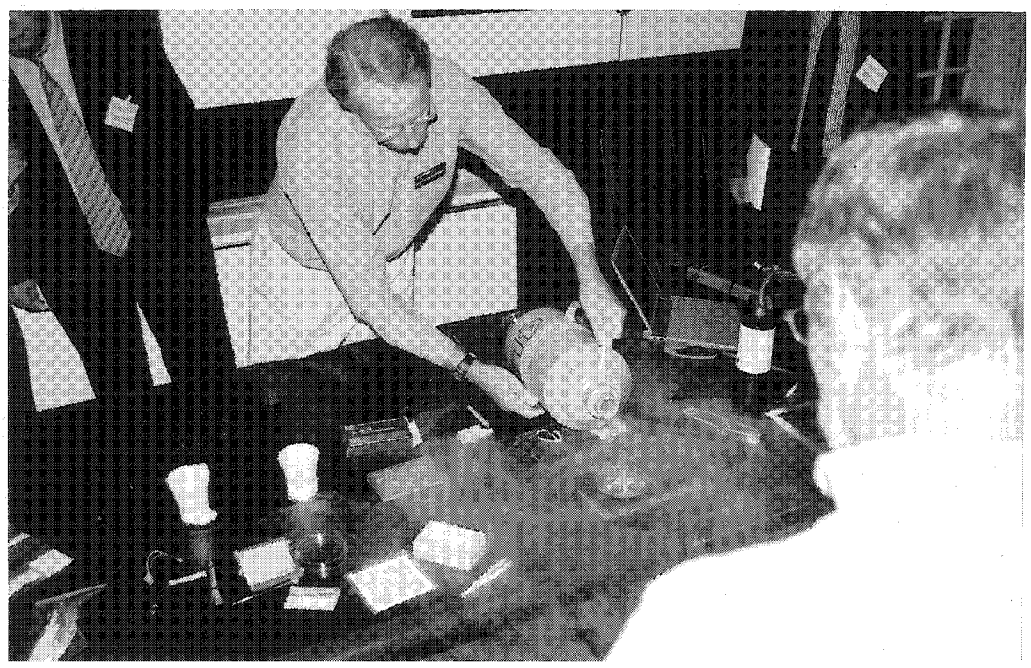

MINI WORKSHOPS (Continued)

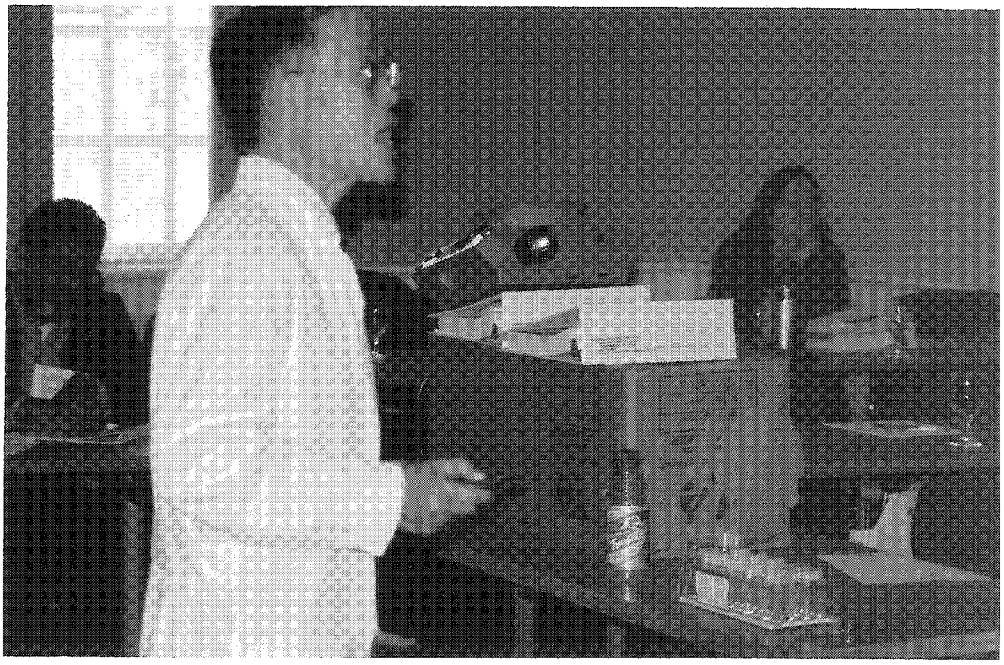

MINI WORKSHOPS (Continued)

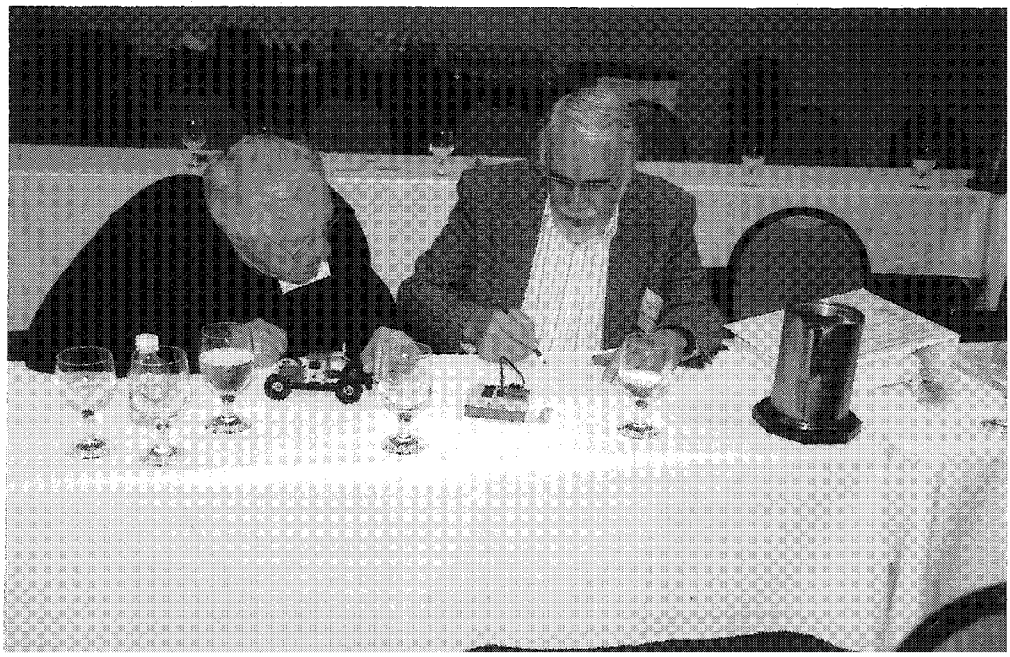

MINI WORKSHOPS (Continued)

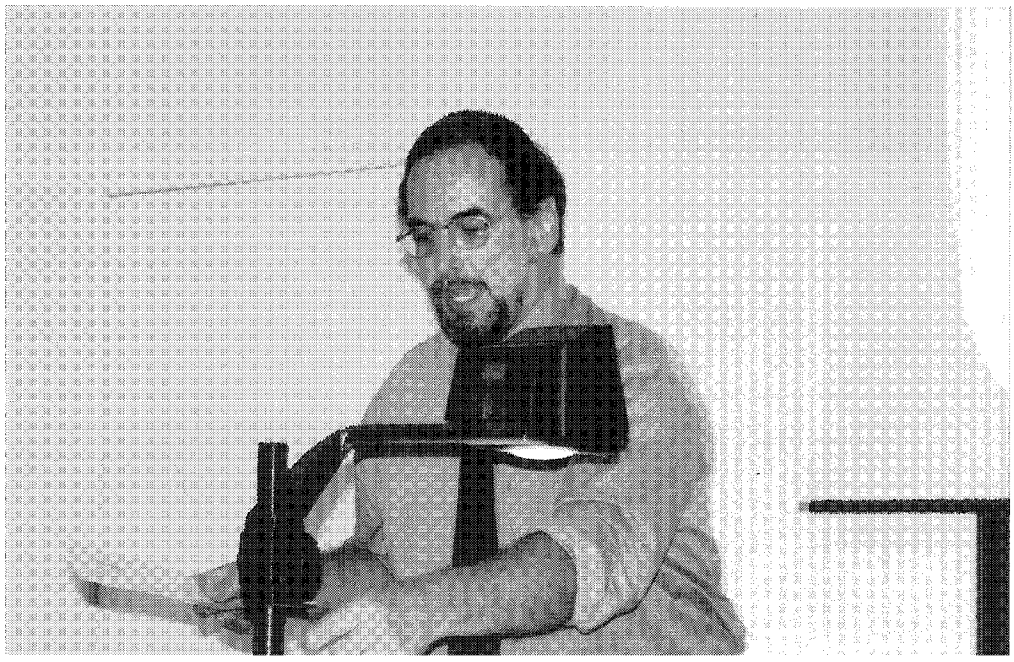

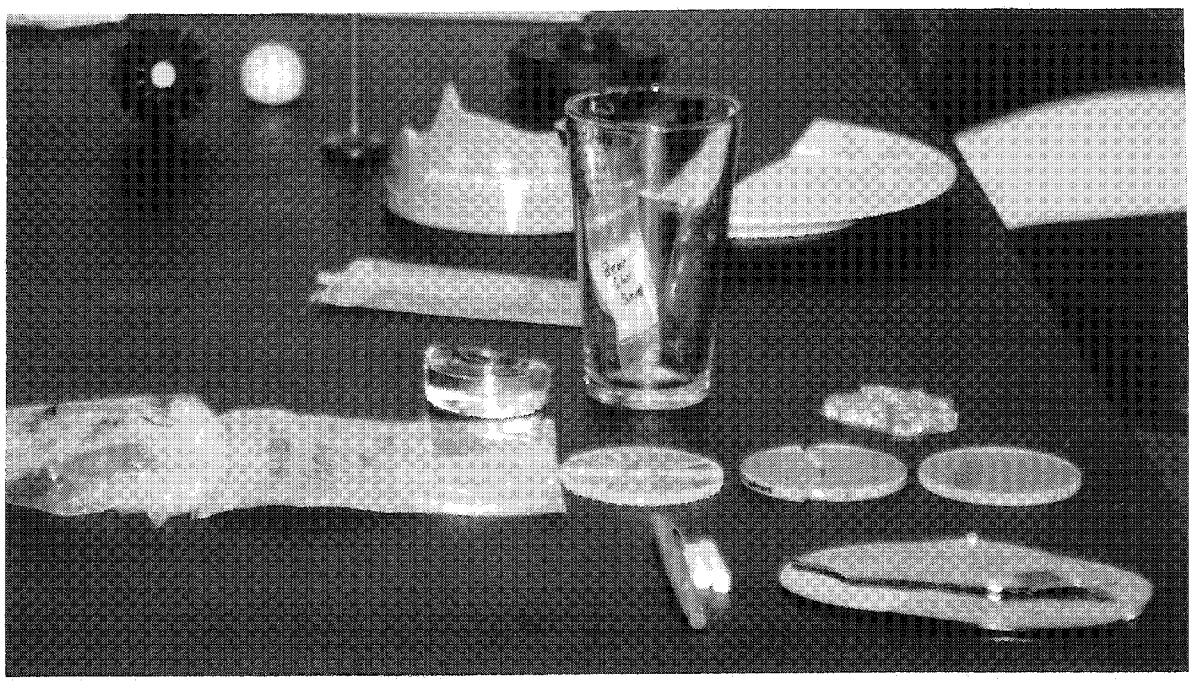

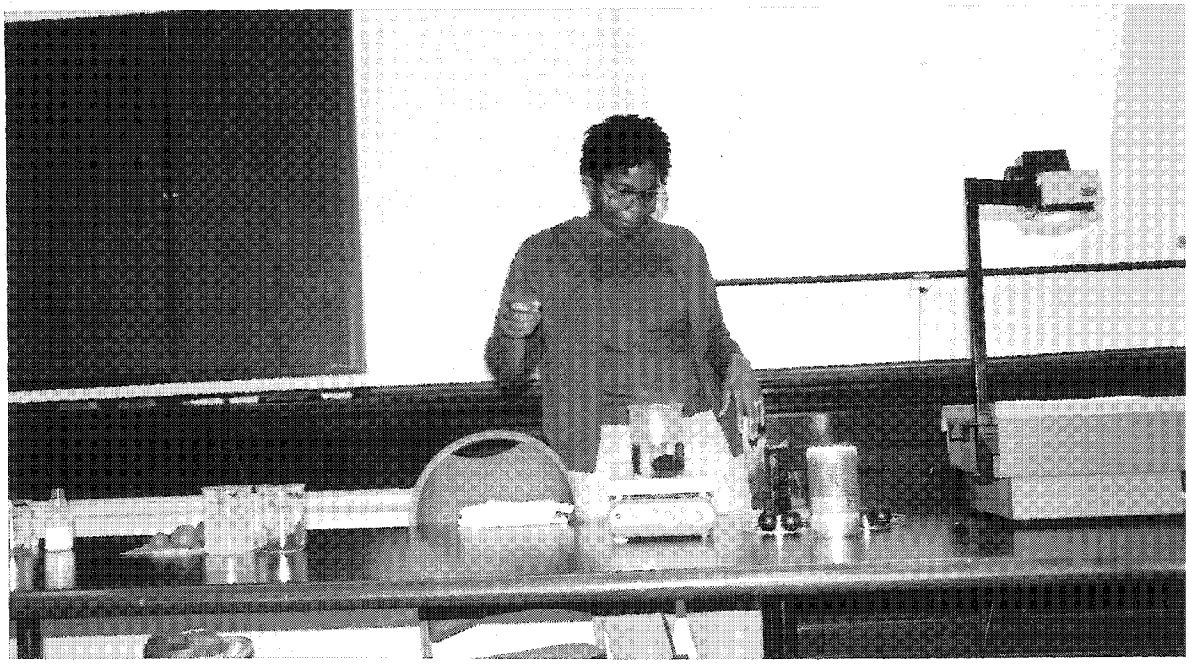

MINI WORKSHOPS (Continued)

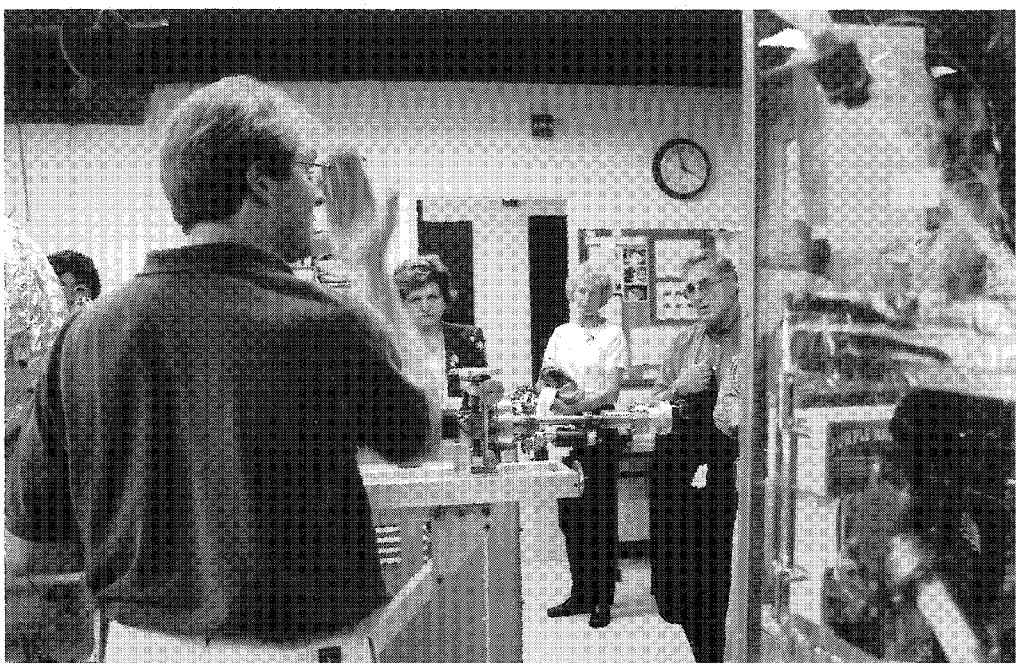

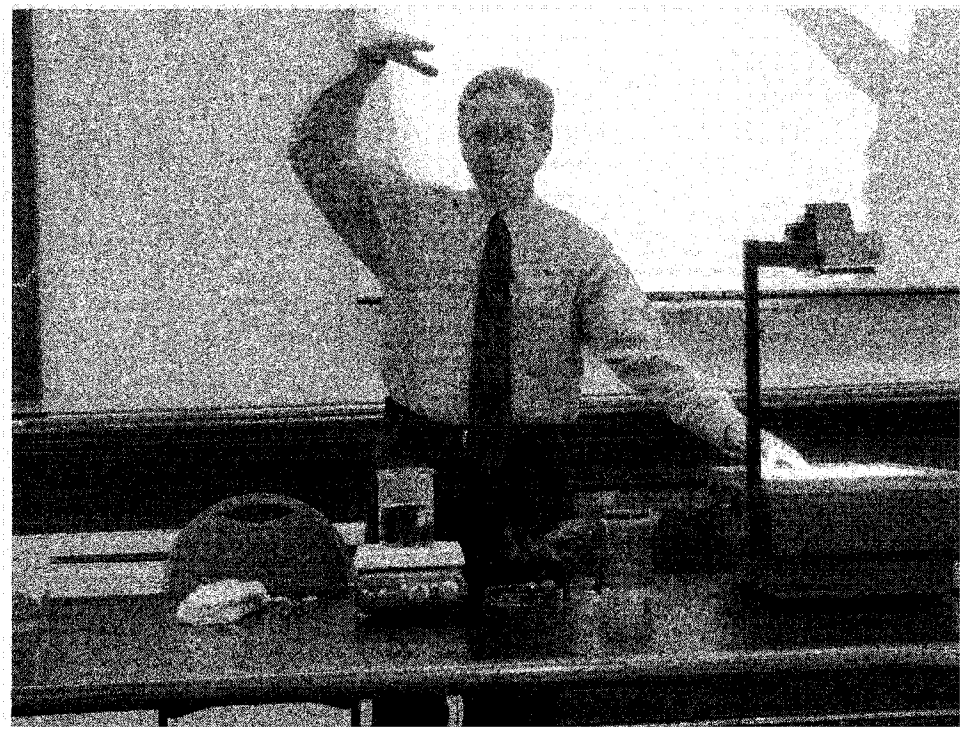

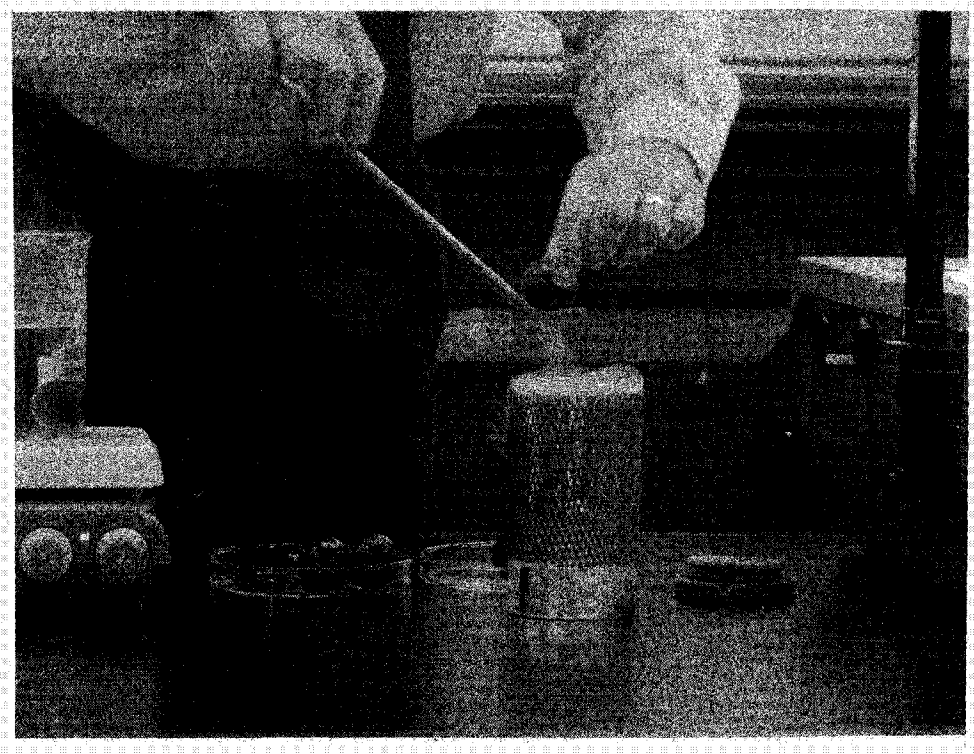

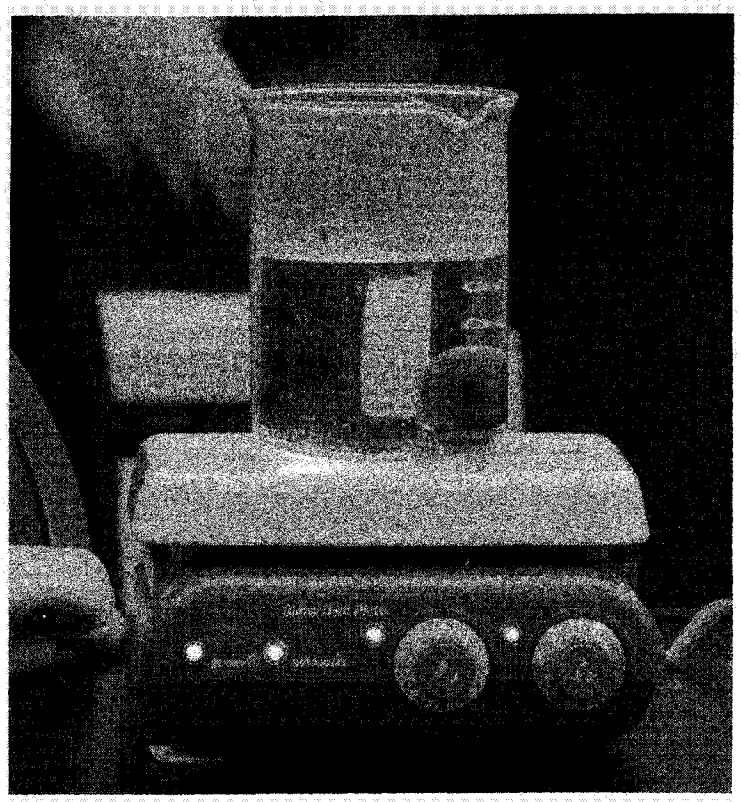

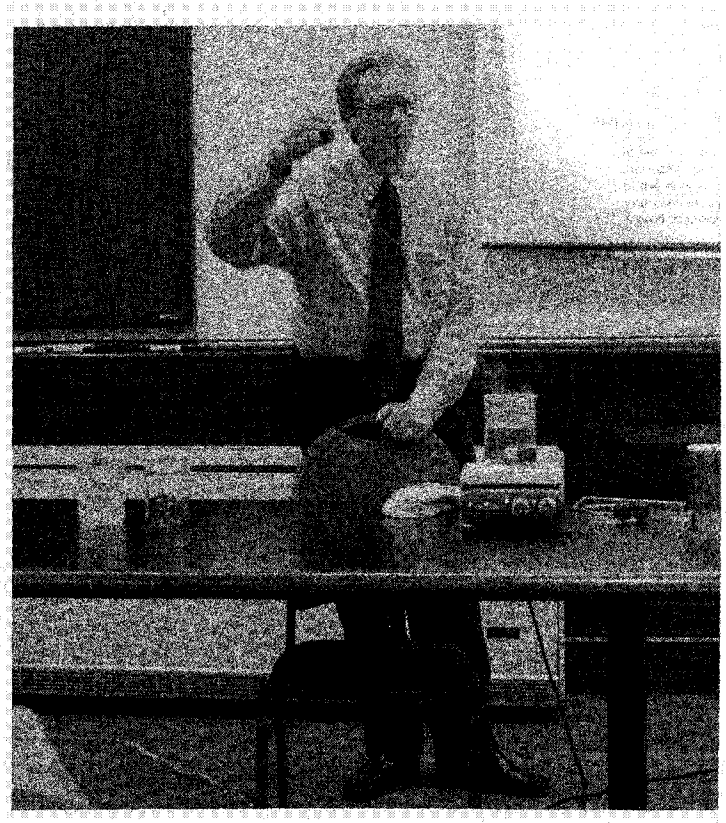

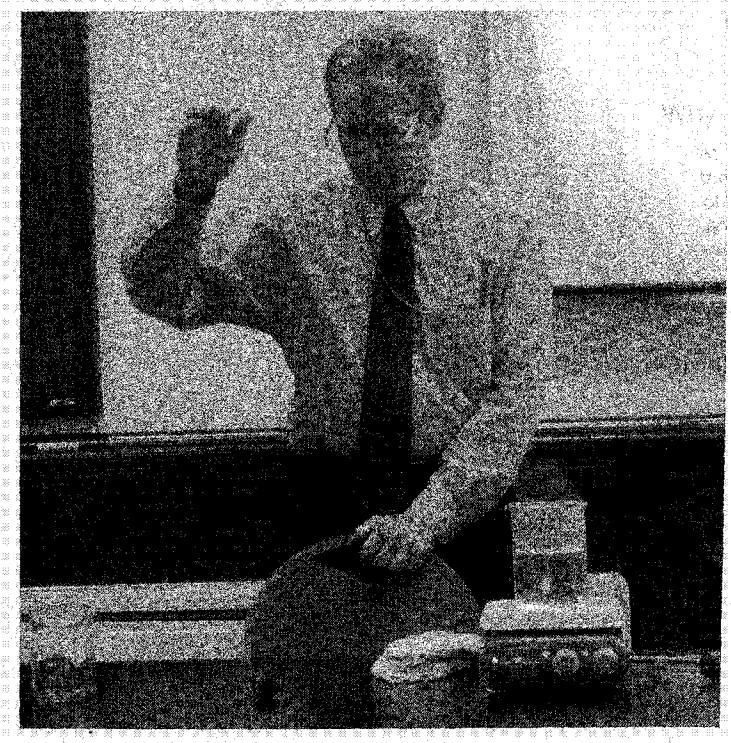

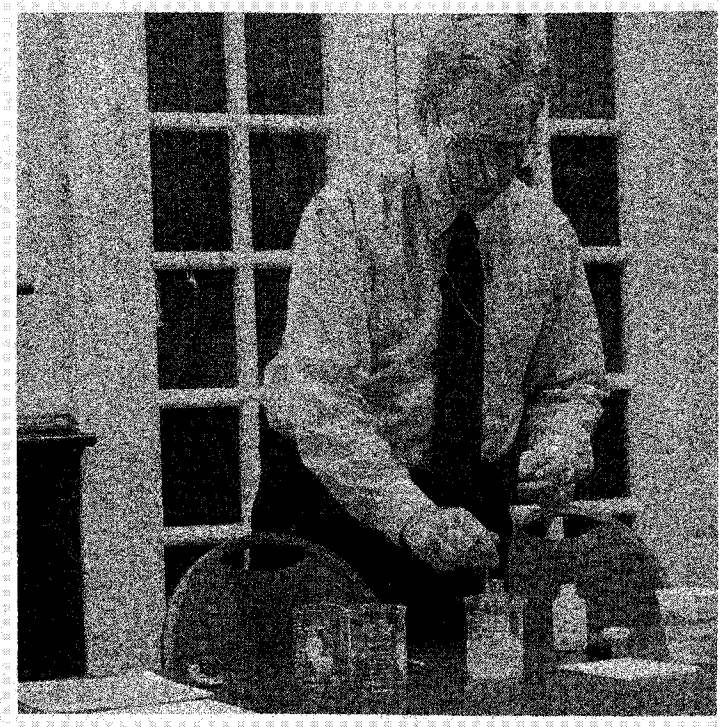

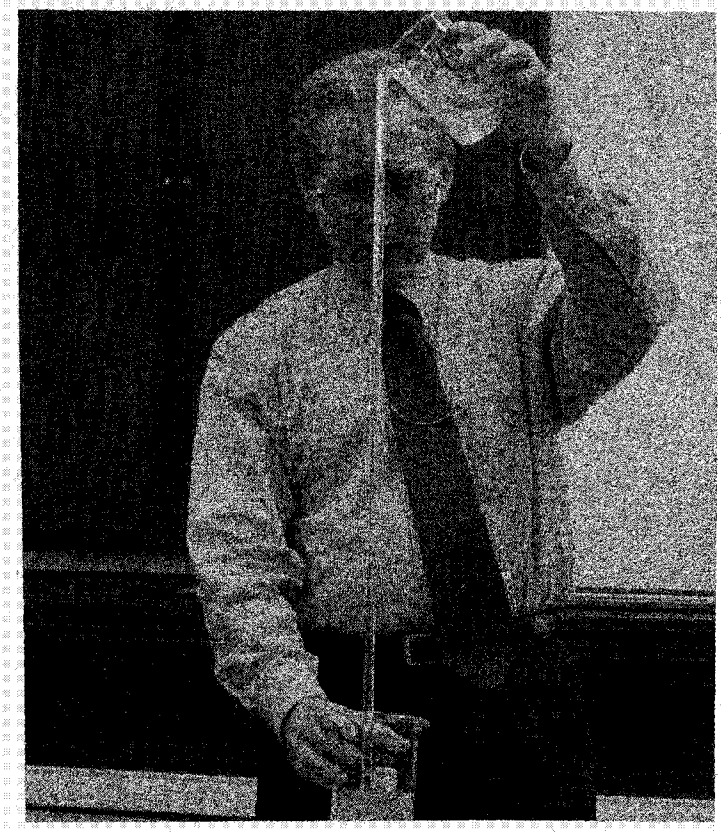

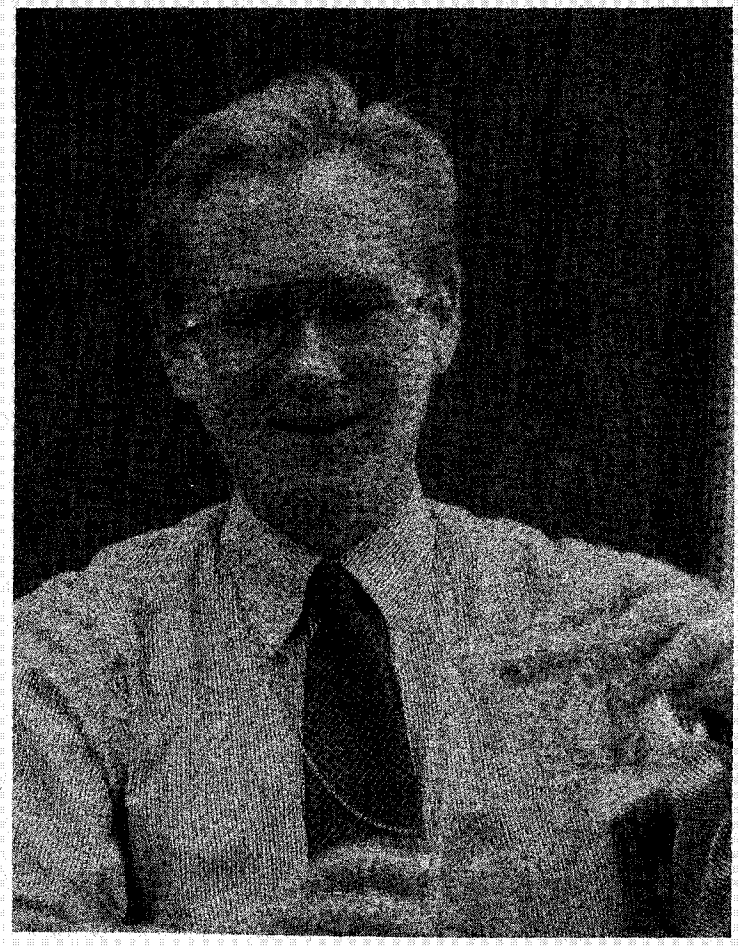

MINI WORKSHOPS (Continued)

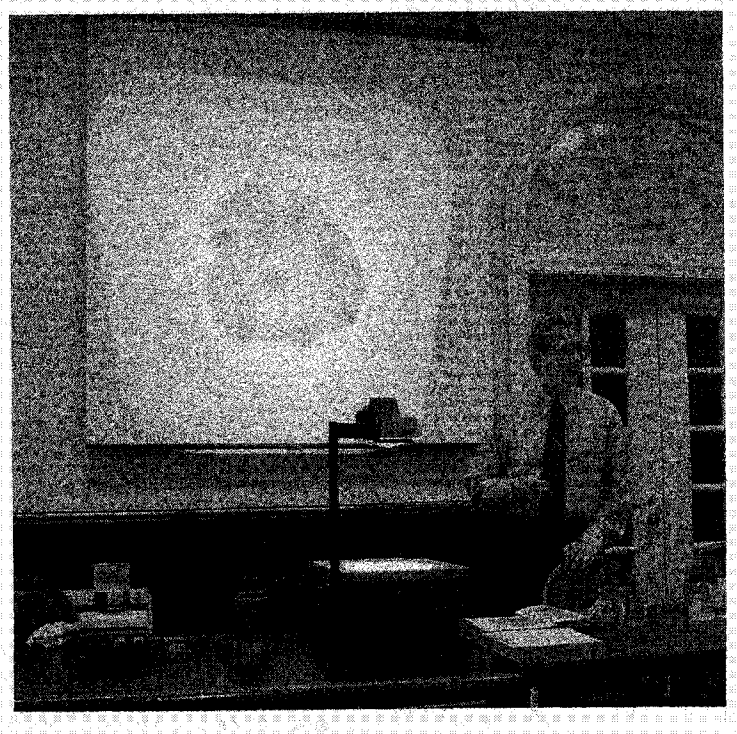

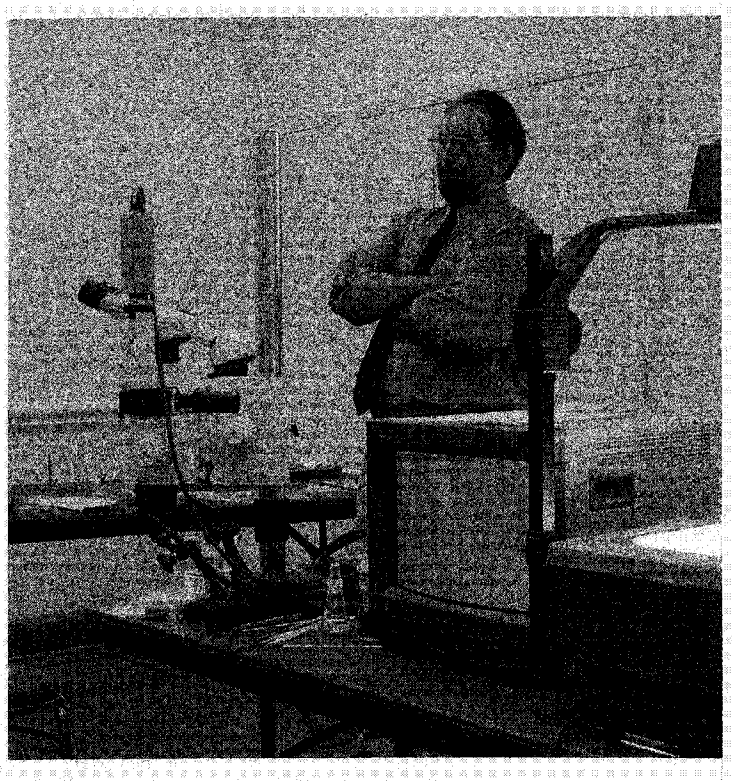

MINI WORKSHOPS (Concluded)

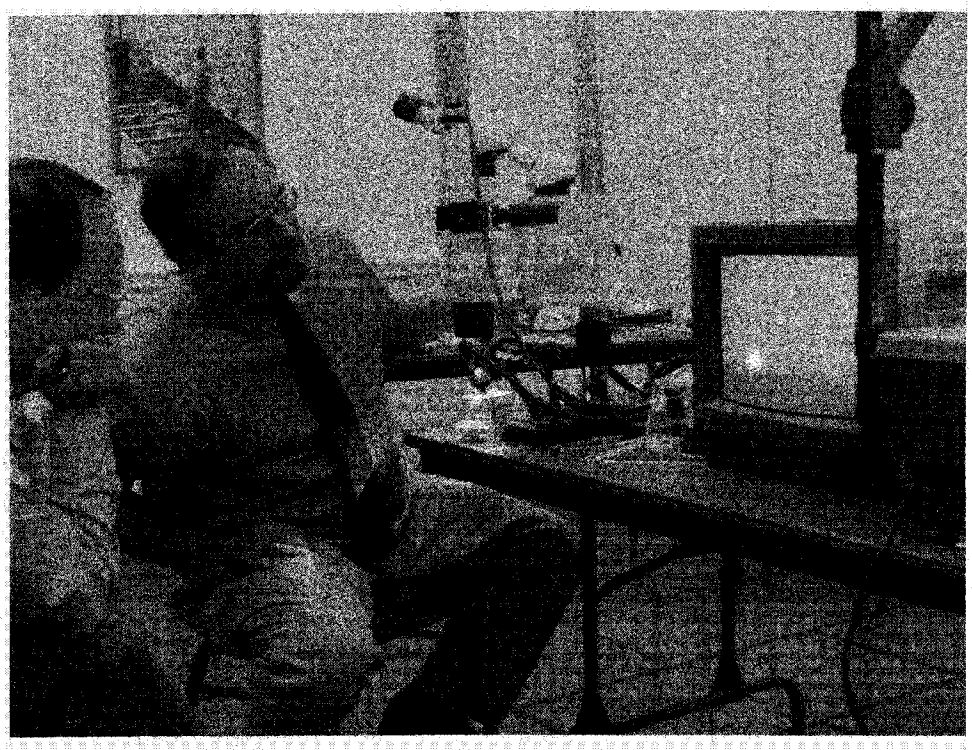

Ceramic Fractography: Broken Pieces Tell the Story

Mr. George Quinn
Ceramics Division, Materials Science and Engineering Laboratory
NIST

A demonstration of the fractographic analysis of fractured ceramic pieces will be presented.

Fractographic analysis is a valuable tool for interpreting laboratory tests wherein ceramics and glasses are broken under controlled conditions. Fractographic analysis also is a powerful tool for forensic investigations of ceramics and glasses that have broken in service. A surprising amount of information may be gleaned from the fractured pieces including the stress in the part at fracture, the mode of loading, and the exact source or cause of fracture. Several case studies will be demonstrated ranging from advanced ceramic laboratory fractures to domestic glass or kitchenware fractures.

The demonstration will feature a "discussion stereo binocular microscope" which enables multiple viewers to simultaneously view the fractured object, either by direct viewing or by projection on television monitors.

Fractographers are detectives!

- Ceramics and Glasses: Examples

- Tools of the Fractographers Trade
  - Mark I eyeball
  - Hand lens
  - Stereo binocular microscope (3X– 200X, extraordinary depth of field)
  - Scanning Electron Microscope (50X – 5,000+X)
  - Other (microscopes, cameras, computers.....)

- Some Fractographic Markings.
  Much of fractography is pattern recognition.
  3 Examples of markings:
  - Twist Hackle ("River lines", "delta patterns")
  - Wallner Lines (curved cracks, direction of crack propagation, "impact ringing")
  - Fracture mirrors (The ***origin*** of fracture, Flaws)

- Quantitative Analysis
  The stress in the part at fracture may be determined.
  Examples:
  - Fragmentation extent
  - Mirror Sizes

- Demos

- Case Studies

For further information:

Book:	*Failure Analysis of Brittle Materials*, V. D. Frechette, American Ceramic Society, Westerville, OH, 1990.
Web Site:	www.ceramics.nist.gov www.ceramics.nist.gov/webbook/fracture/fracture.htm
ASTM standards:	C 1322 Standard Practice for Fractography and Characterization of Fracture Origins in Advanced Ceramics C 1256 Standard Practice for Interpreting Glass Fracture Surface Features

The following fractured parts were available for demonstration:

1. Broken drinking glass.
   Impact origin on inside bottom where knives or forks impacted the surface. Subsequent heating and cooling in the dishwasher propagated the crack.

2. Broken (4 point bending) glass rod
   Classic fracture mirror. One example demonstrated on stereo scope and second one passed around with 10X jeweler's loupe.

3. Automobile side mirrors.
   Examples of Wallner lines and twist hackle. Origin was edge damage on beveled outer rim. Cracks were propagated by thermal heating and contraction, or alternatively, by mechanical bending from mounting stresses.

4. Ceramic rectangular bend bar. 4-point flexure, alumina
   The white ceramic appeared washed out when viewed in the stereo scope, but staining the surface with a green felt tip pen helped the fracture markings come out. Origin was a large pore near the surface.

5. Glass disk specimens tested in biaxial (ring on ring) flexure.
   Demonstrated the extent of fragmentation is proportional to the stress or energy in the part at fracture.

6. Tempered automobile side window.
   Destroyed by tornado impact. Pattern of fracture demonstrated along with actual fracture origin, which was a severe impact site on the outer surface.

Case Studies discussed at end of lecture:

a. Auto windshield (see #6 above)
b. Glass windows ("lights") in a tall office building in Boston. Failure was a multi sequence event.

Stereo Binocular Microscope

Wild (Leica) M-3Z or M-10

with fiberoptic light source.

Stepless magnification changes

Continuous focus

Zoom 6X or 10X

Total Magnifications 5-30X or 10-45X typically, but expensive models can go up to 160 or 200X!

Good working distance (distance between objective lens and object being examined!)

Superb depth of field

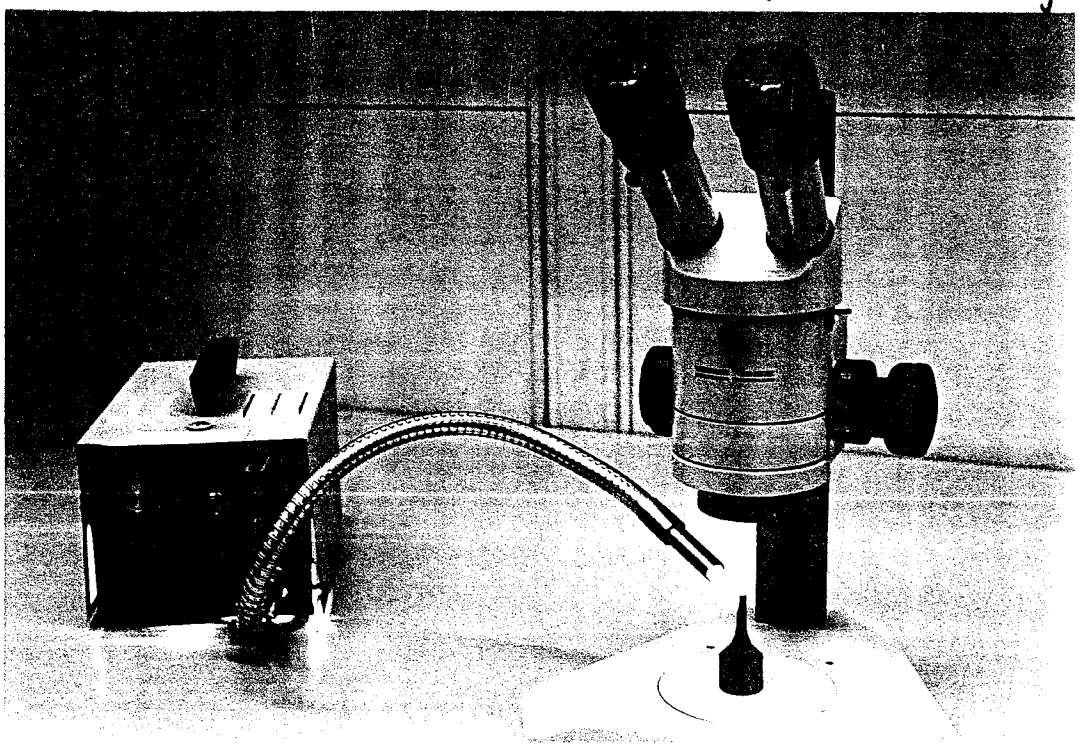

Low angle incident lighting creates shadows that accentuate the fracture features.

Conventional Materials Science Microscope

Reflected light Two eyepieces but not stereo viewing

Very limited depth of field

Very small working distance

No stereo effect

Up to 1000X

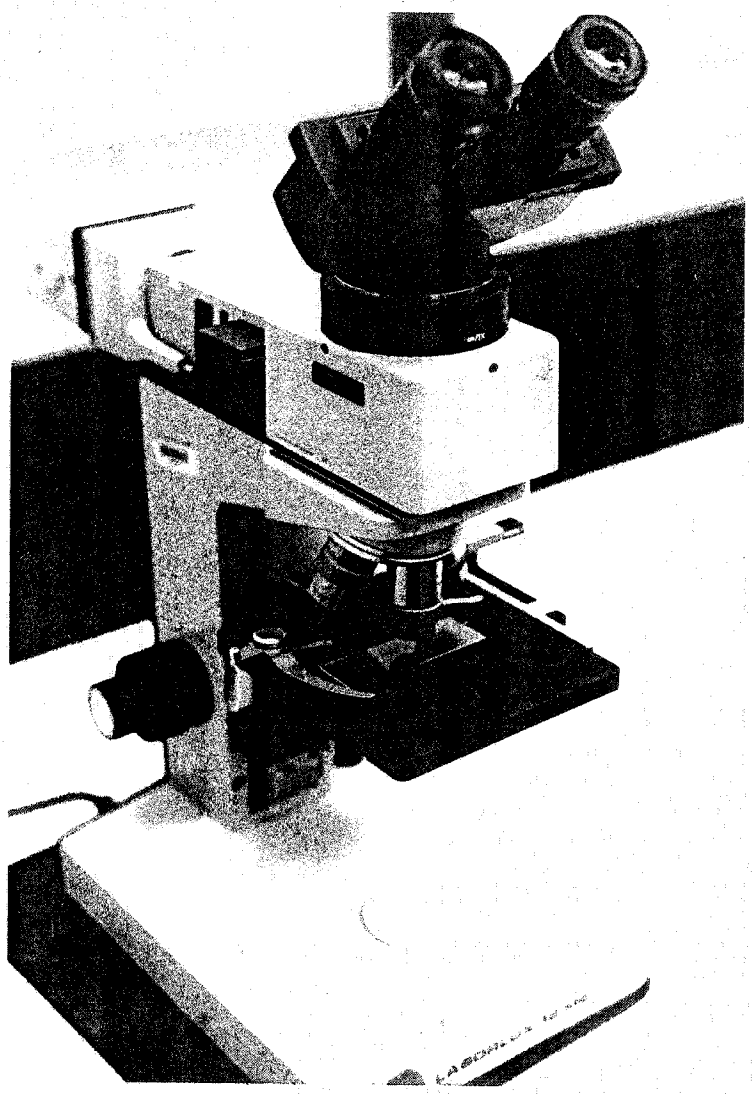

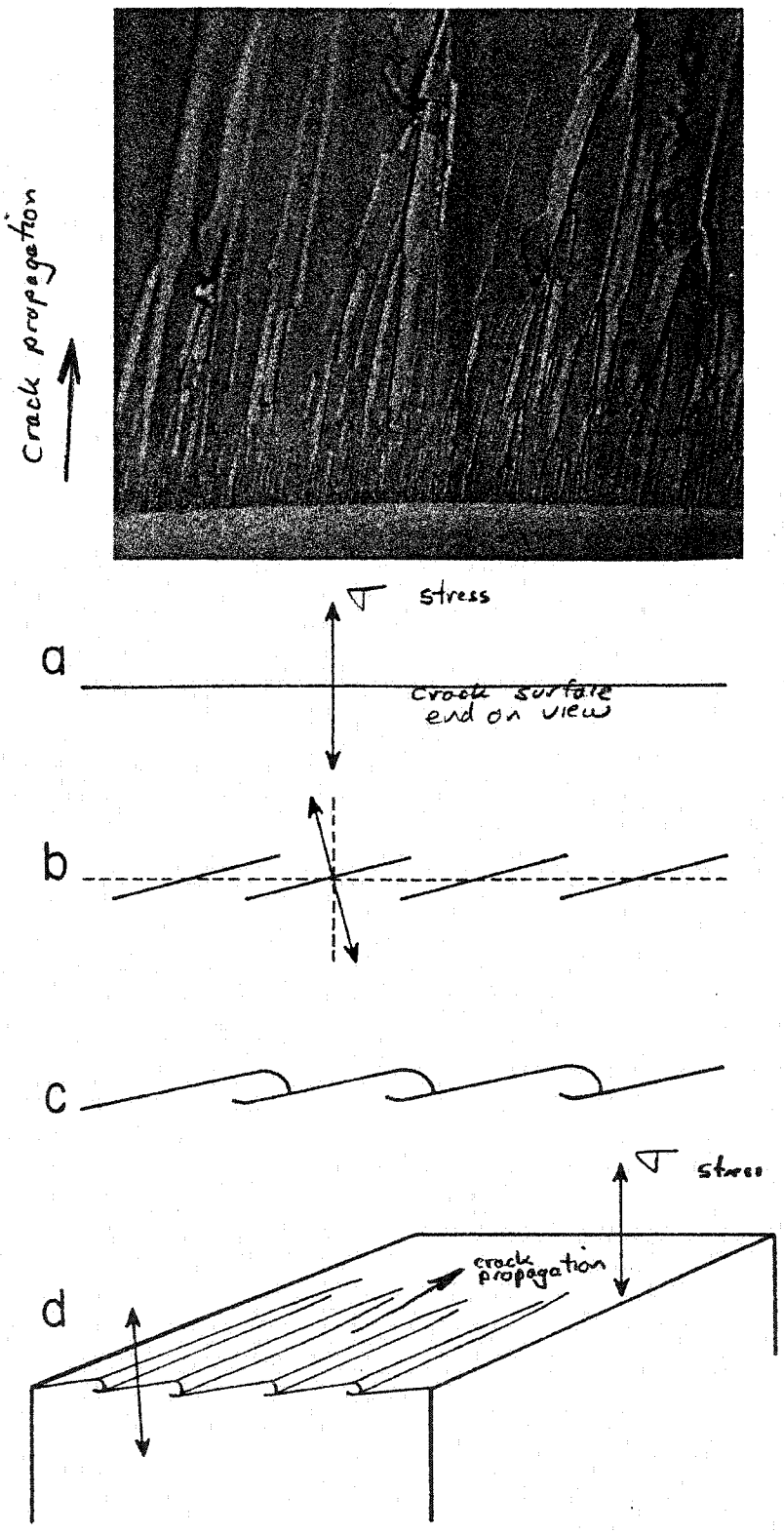

Twist hackle are fine parallel ridges that indicate the direction of crack propagation.

They are caused by a change in the plane of fracture

Fig. 2–14. Stages in the formation of twist hackle: (*a*) Cross-sectional view of the crack surface, forming perpendicular to the axis of principal tension and running away from the observer; (*b*) a lateral twist in the tension axis causes the crack surface to split into unconnected segments, each perpendicular to the new axis of tension, the average crack surface coinciding with the original; (*c*) breakthrough between the segments completes the separation of the specimen into two fragments, forming shallow "risers" in the stairway in which the initial cracks segments are the "treads"; and (*d*) isometric view of the resulting surface.

Wallner lines are slight ripples on the fracture surface. they can indicate the direction of crack propagation and also the stress state!

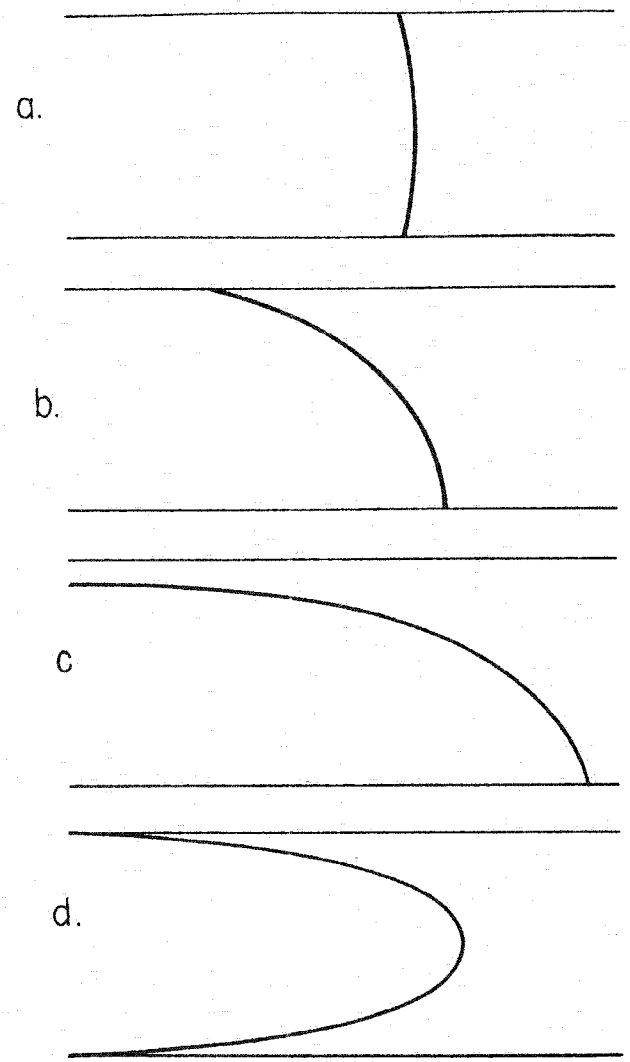

Fig. 2–6. Inference of stress distribution across a thin specimen from Wallner line shape: (*a*) Tensile stress uniform across the thickness; (*b*) tensile stress highest at the lower surface; (*c*) tensile stress highest at the lower surface; upper surface under initial compressive stress; (*d*) tensile stress highest at the midplane.

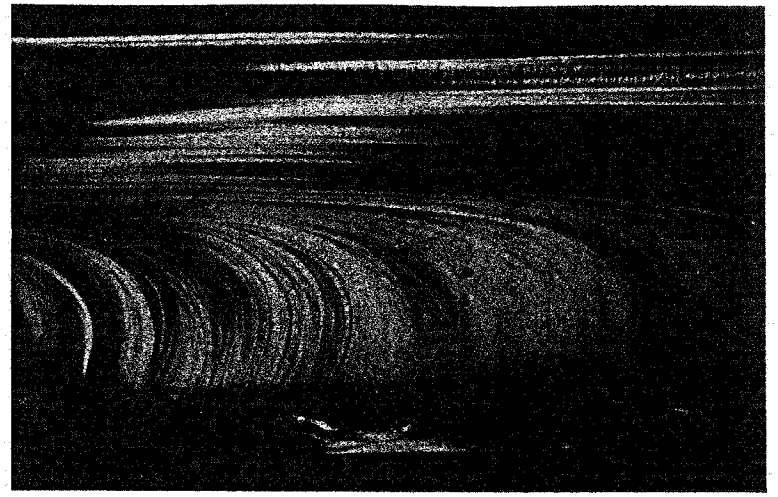

Fig. 2–8. Secondary Wallner lines generated by encounter of the crack front, moving left to right, with mist-hackle roughness (along the bottom, dark in the photo). ×100.

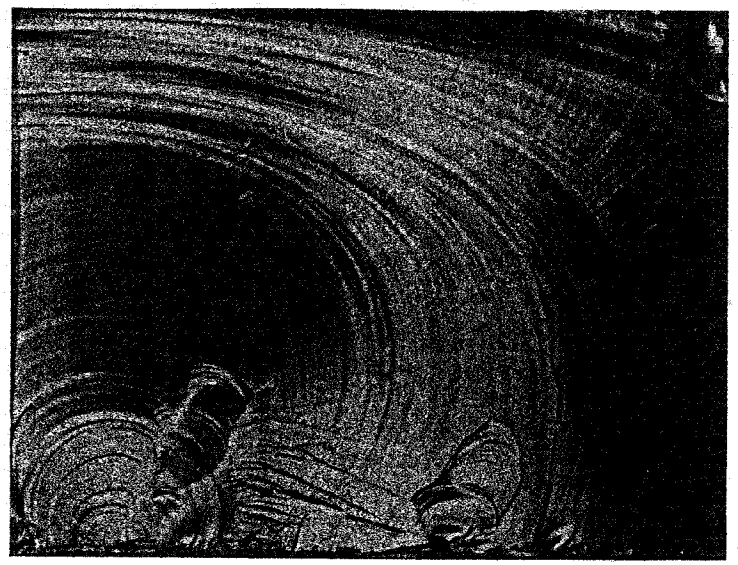

Fig. 2–10. Tertiary Wallner lines, caused by interaction of vibrations, externally generated by impact, with the crack front, expanding from the center of impact at the lower left in the photo. ×100.

3 PHOTOS

1. **Whole Fracture Surface**

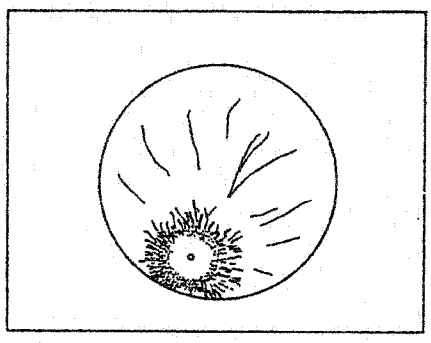

(1-5x)

2. **Fracture Mirror**

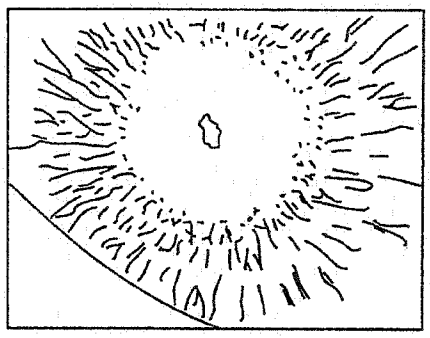

(10-50x)

3. **Fracture Origin**

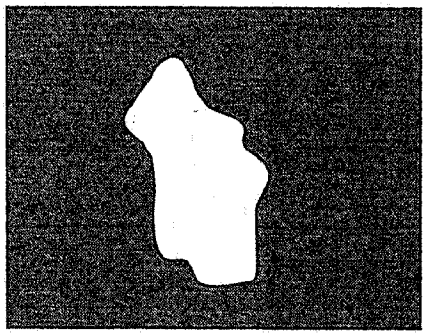

(100-1000x)

QUINN/A1

Fracture Mirrors

Often the fractographer seeks the exact origin of fracture. In many cases, the origin is indicated by a smooth circular zone centered on the flaw.

the mirror corresponds to the region where the crack is accelerating to its terminal velocity. Once the crack reaches terminal velocity ($\sim$1500 m/sec in glass), the crack may split or bifurcate.

Mirrors
(Glass)

The fracture mirror is a relatively smooth, flat area surrounding the origin. The mirror is typically 10–13X larger than the origin flaw.

glasses often fracture from surface flaws. Hence the mirror is semielliptical or semicircular.

64x

note
flaw
mirror
hackle

flaw is a 9 μm deep crack from polishing

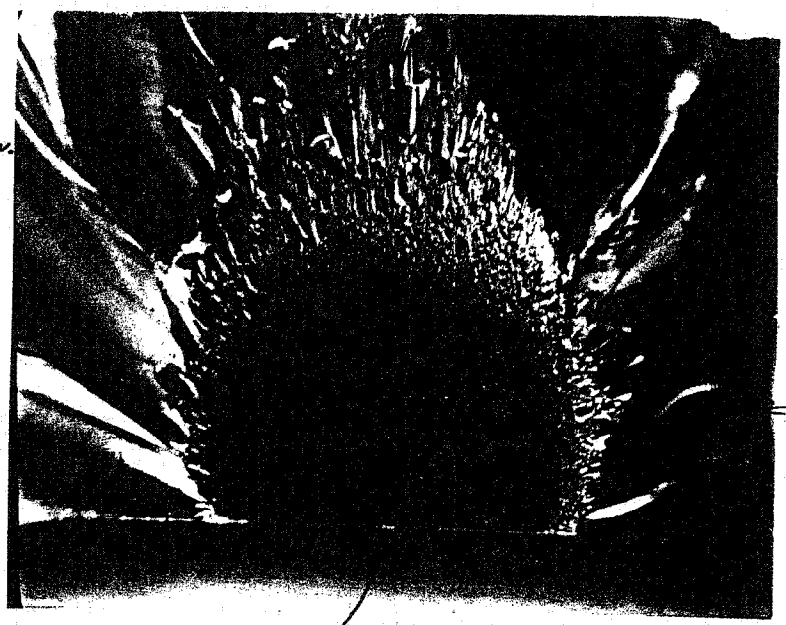

origin is the tiny crack in the center of the mirror.

identical specimen

different lighting

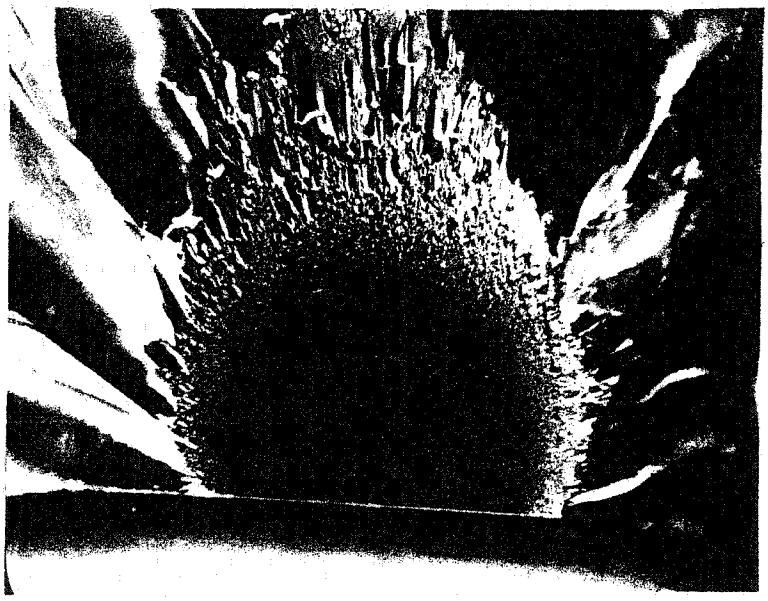

Fracture Mirror in Ceramic Tension Specimen

PAD B SiC

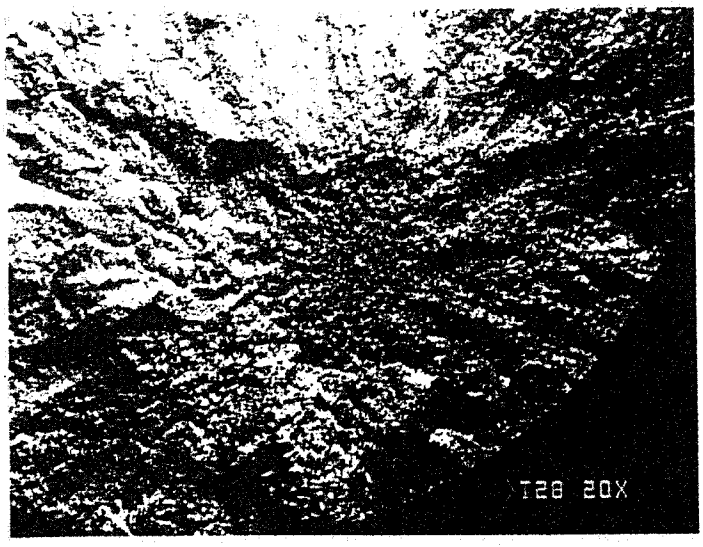

In ceramic, the mirror is rougher – but still is discernable.

317 MPa

origin is a pore buried in the interior of test piece

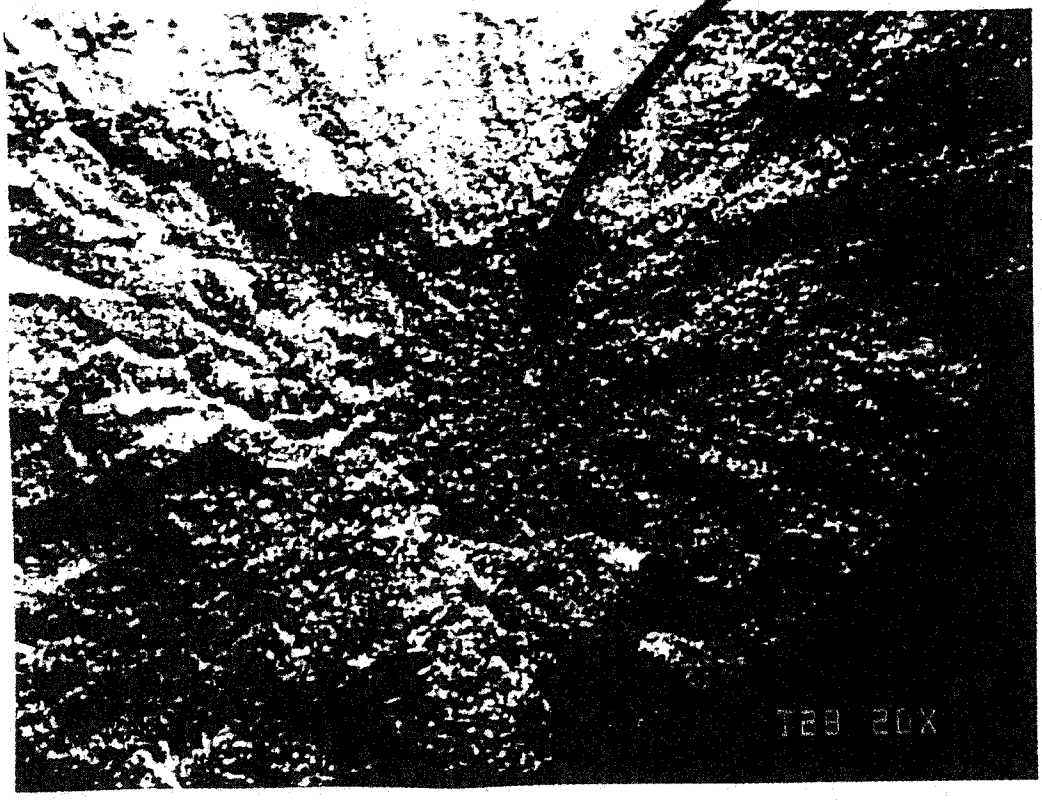

Flexure Testing is a simple method to break ceramics and find flaws!

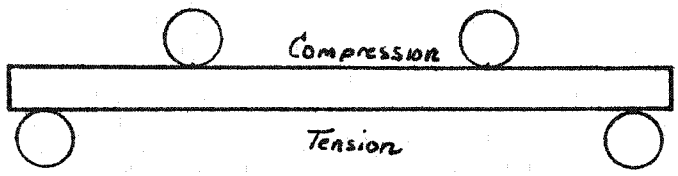

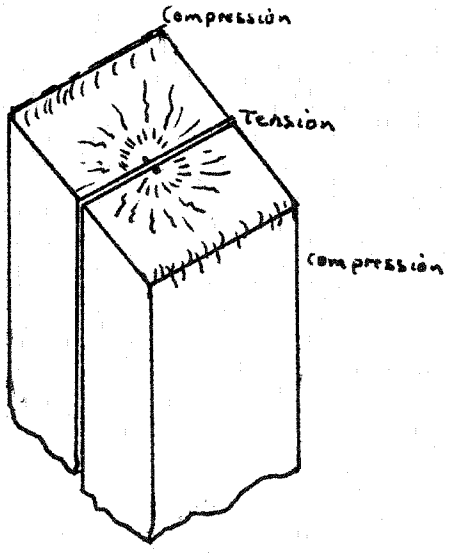

a nice technique is to mount the matching halves back to back so you can view both simultaneously.

Fracture Surfaces

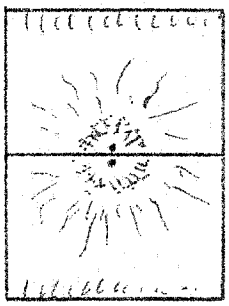

Fracture patterns in bend bars.

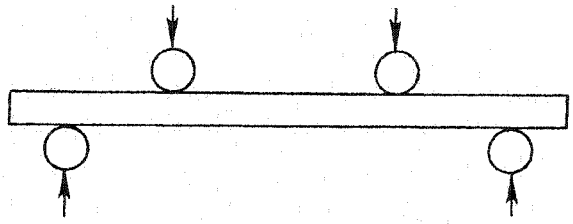

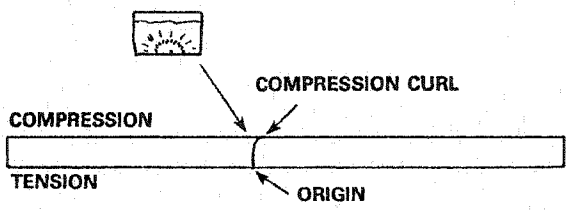

LOW ENERGY FAILURE

FRACTURE SURFACE IS PERPENDICULAR TO TENSILE SURFACE

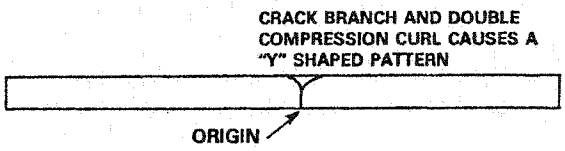

MEDIUM - HIGH ENERGY FAILURE

UPPER FRAGMENT IS NOT IMPORTANT AND CAN BE DISCARDED

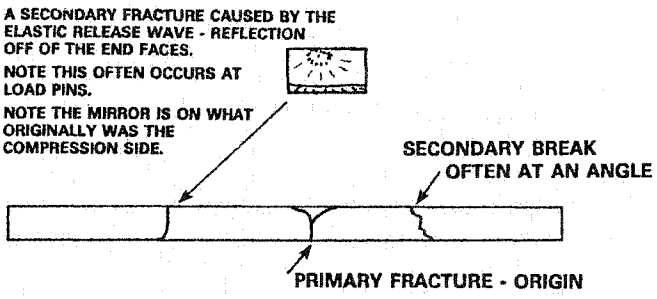

MEDIUM - HIGH ENERGY FAILURE

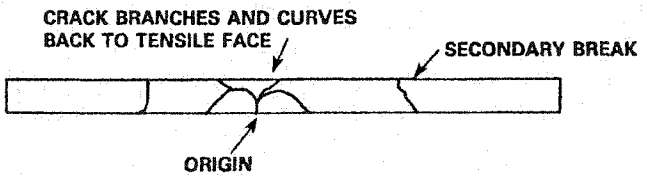

HIGH ENERGY FAILURE

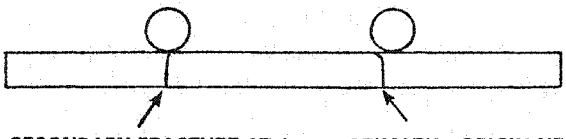

MEDIUM - HIGH ENERGY FAILURE

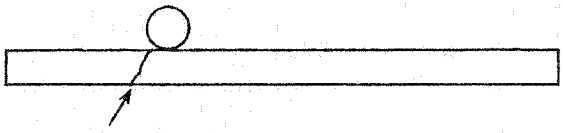

BREAK AT OR NEAR LOAD PIN.
BEWARE OF MISALIGNMENTS OR TWISTING ERRORS
NOTE ANGLE TO TENSILE SURFACE

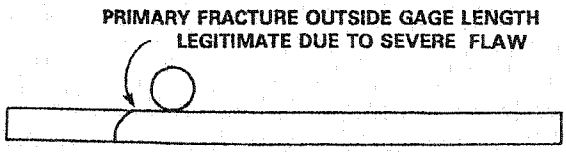

LOW ENERGY FAILURE

Comparison: Optical versus SEM views of the same origin

Reaction Bonded
Silicon Nitride
Norton NC 350 grade
$\sigma = 316$ MPa

view of whole fracture surface

Optical Photo
~25X

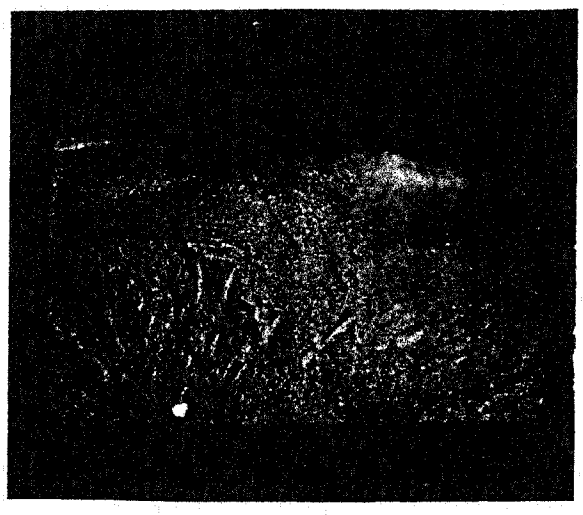

Flaw is a white spot near the bend bar surface →

closeup of flaw at the origin

SEM
Closeup
~500X

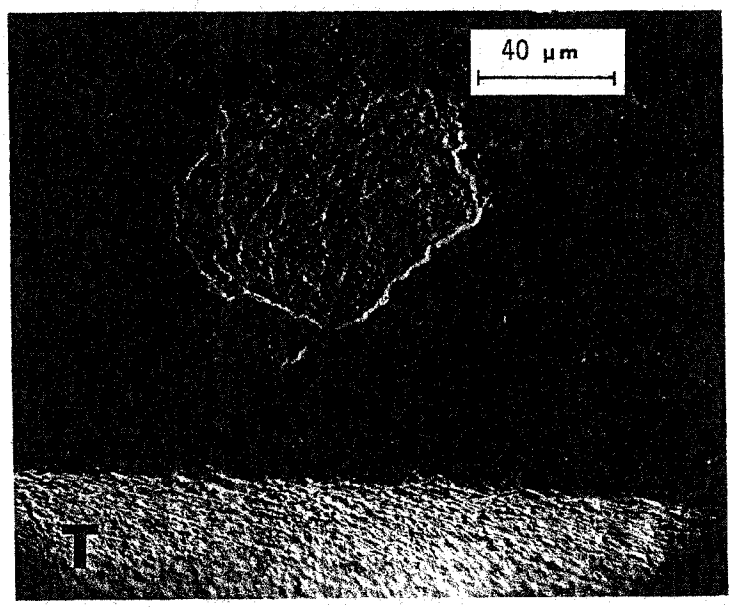

Specimen tilted back to show tensile surface "T" which is in good condition.

Flaw is NOT machining damage.

Sometimes microcracks induced by machining (surface grinding) the part can become the strength limiting flaws!

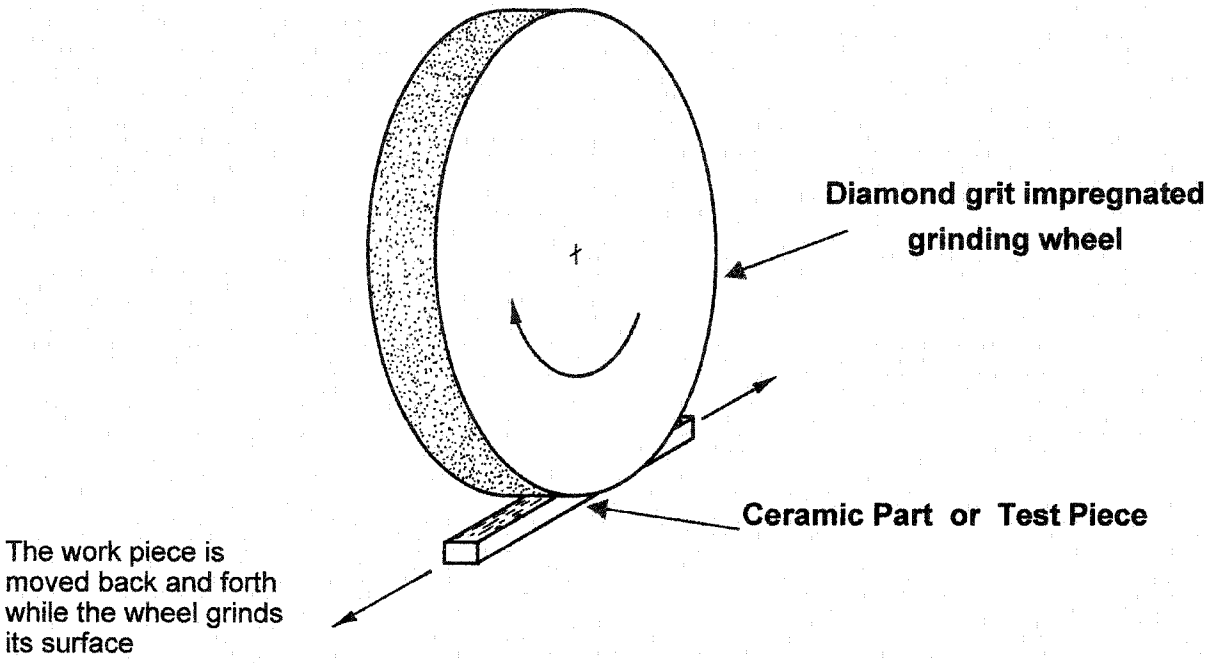

The diamond particles impact the surface and cause microcracks to form.

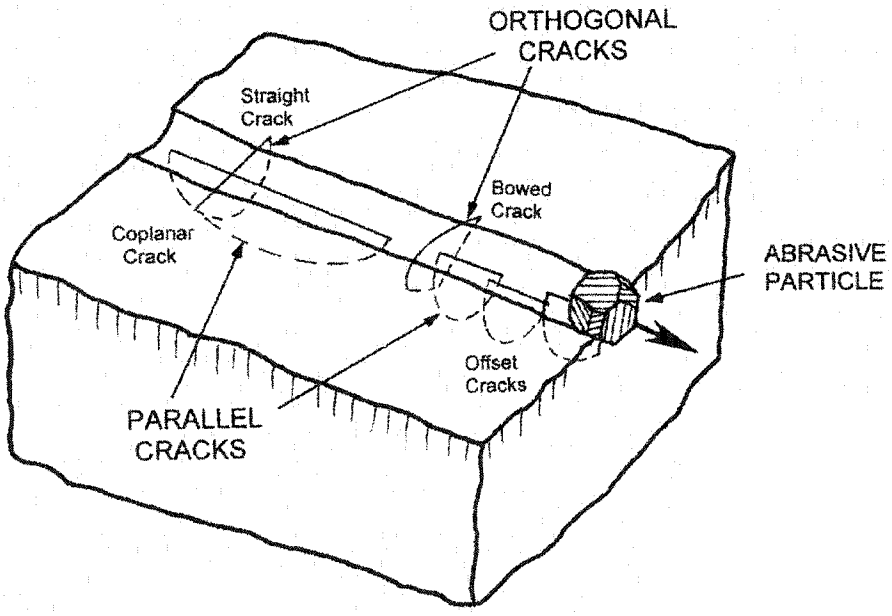

Example:
Silicon Nitride Test bar

machining damage crack in a bend bar (flexure specimen)

broken bend bar

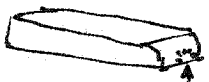

fracture surface

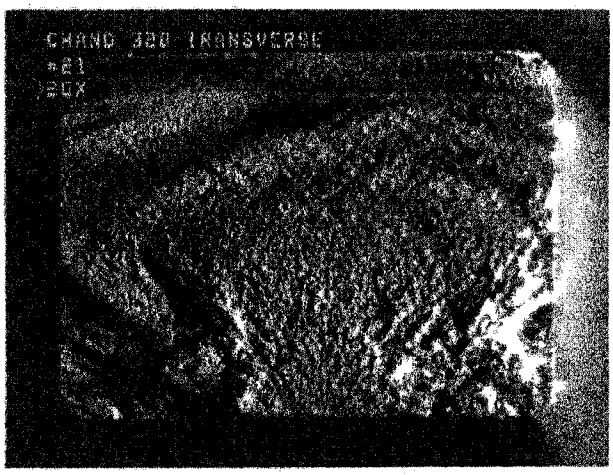

Chand
320
Transverse
#21
487 MPa
weakest

20x

mirror
flaw

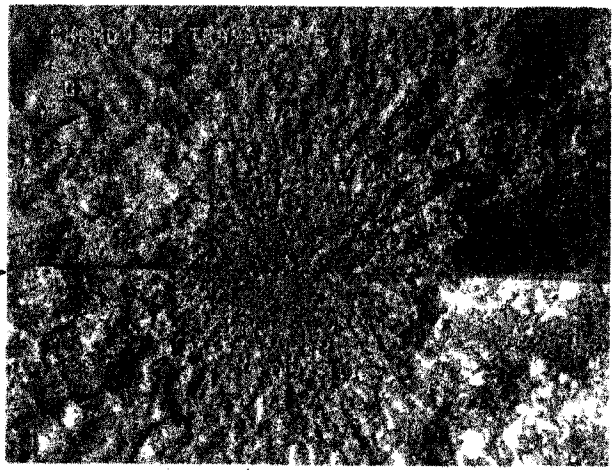

optical photo

mirror

Closeup of the mirror — both fractured halves mounted back to back

40x

Fracture Surface

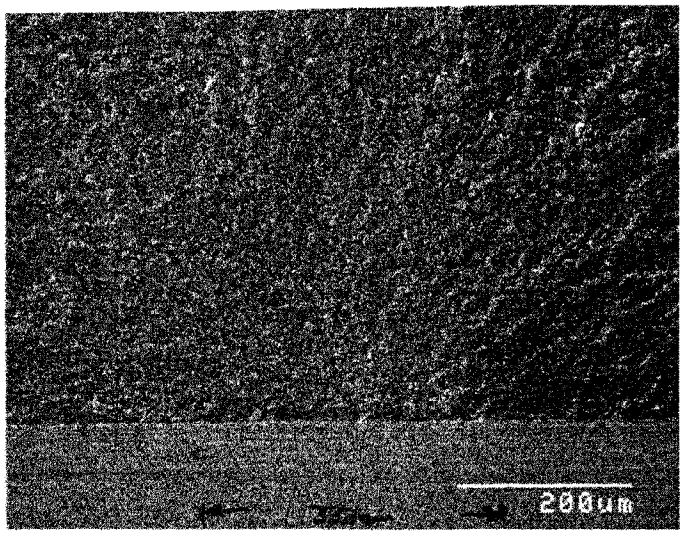

Scanning Electron Microscope photo whole mirror

254μm deep
x 300+ μm long

flaw is 25μm deep machining crack

Specimen is tilted back so that the ground surface is visible

Characterization of Fracture Origins

Examples of Inclusions

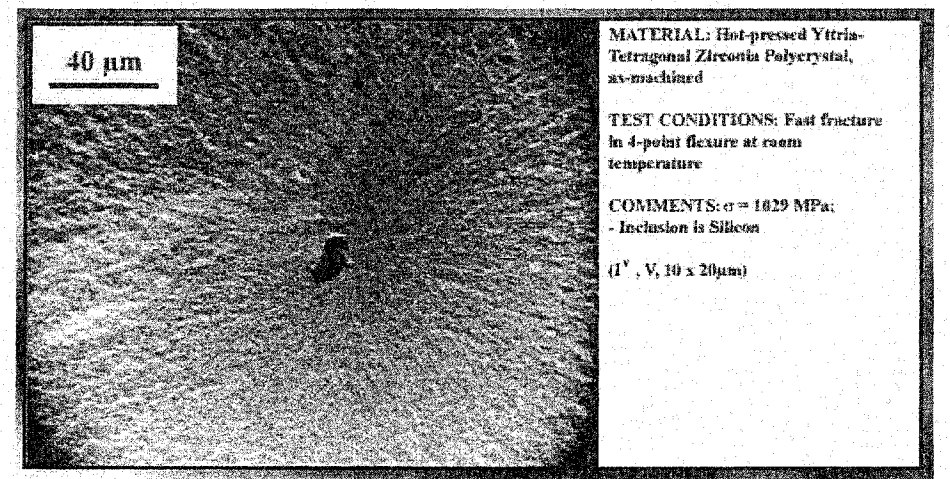

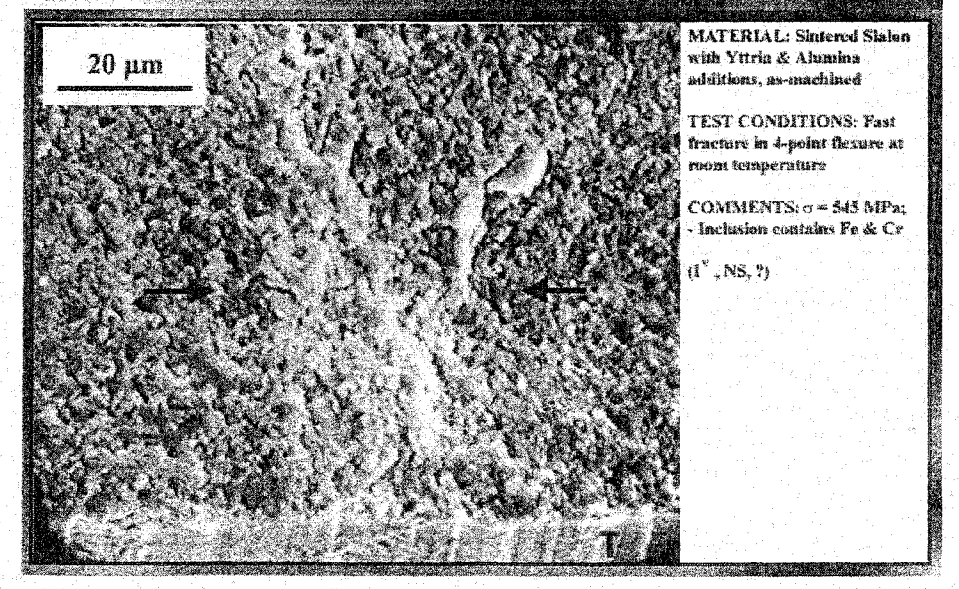

For More Information on Flaws and Fractography, visit the NIST Ceramic Fractography Web Site

Quantitative Fractographic Analysis

Biaxial Disk Strength Testing
Ring on Ring

The extent of fragmentation is a measure of the stress or stored energy in the component at the instant of fracture

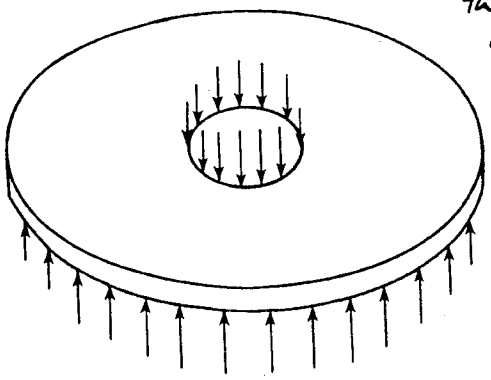

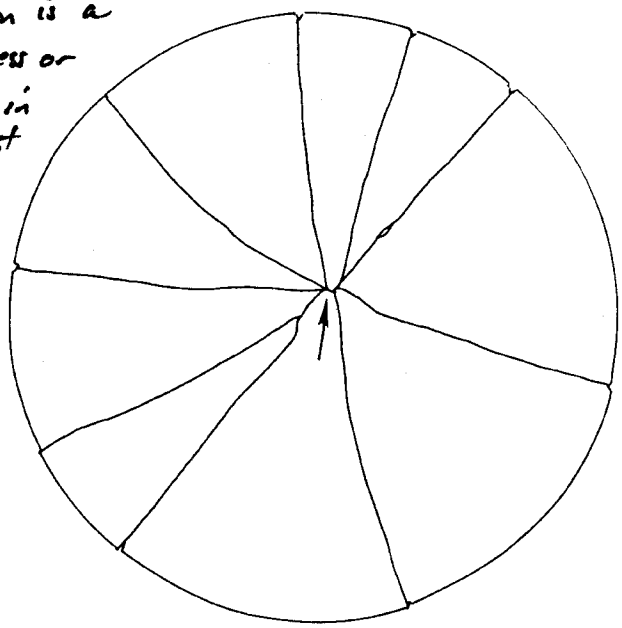

HIGH STRENGTH - HIGH ENERGY

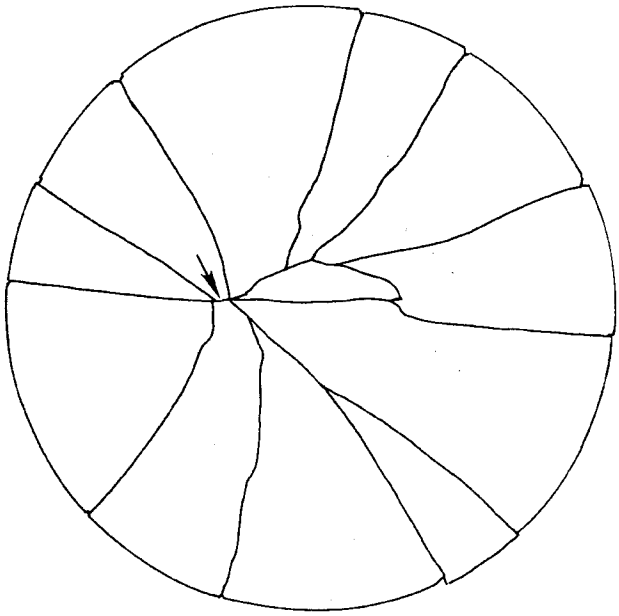

HIGH STRENGTH - HIGH ENERGY

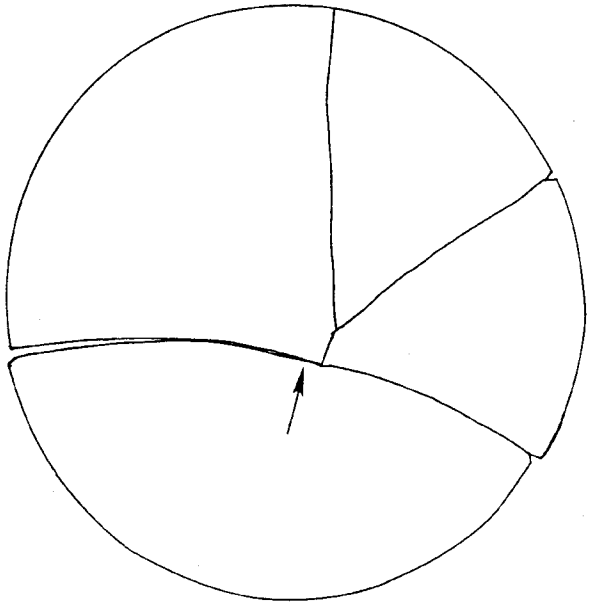

LOW ENERGY

Quantitative Fractography: An Example

Ring on Ring Biaxial Disk Data

BK-7
Borosilicate
Crown
Glass

$N = .96\ \text{Stress}^{1.35}$

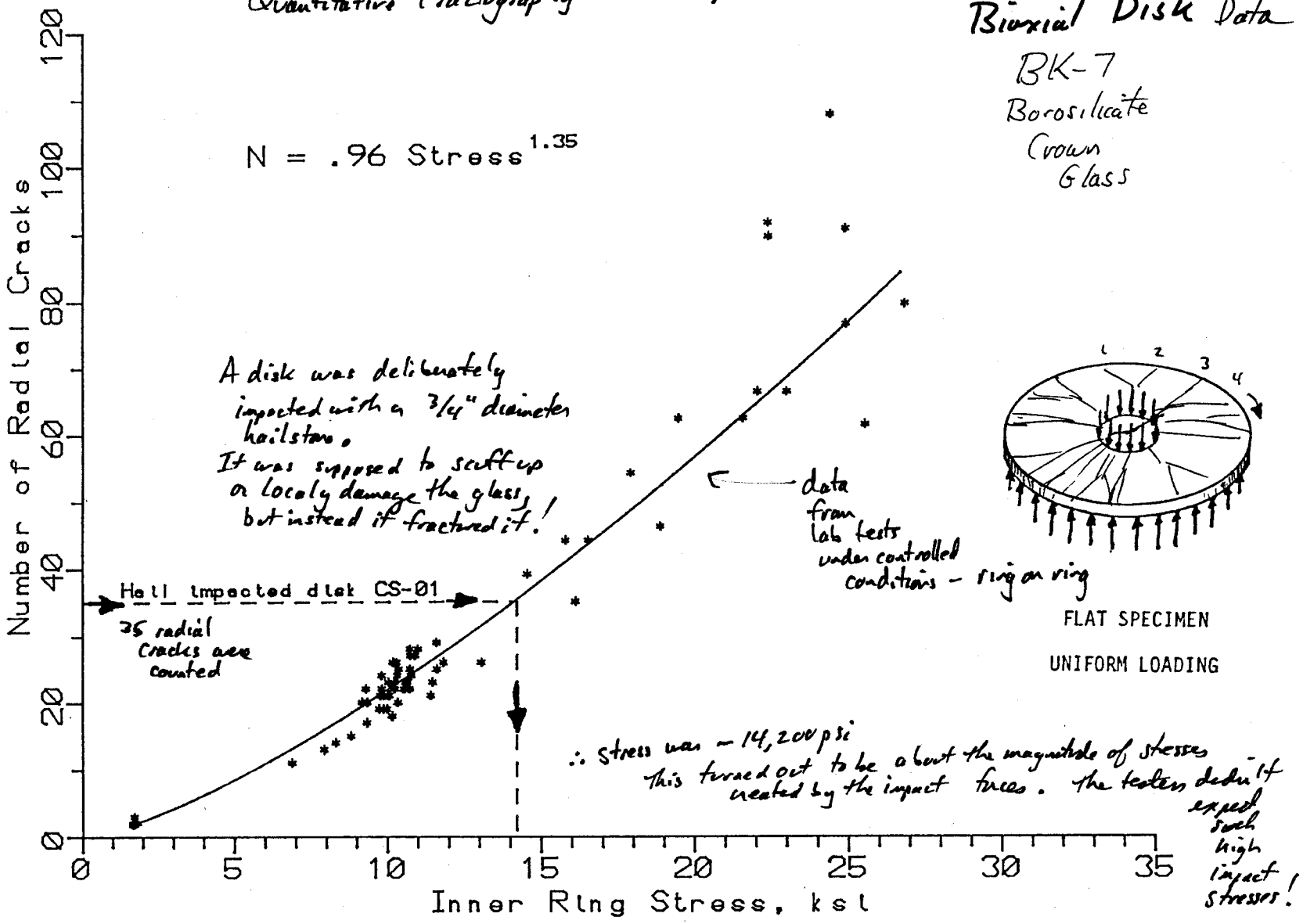

Other geometries and modes of loading will have other curves. For example, Frechette's book has # of cracks versus stress for pressurized Coke bottles!

Fracture Mirrors

$$A = \sigma \sqrt{R}$$

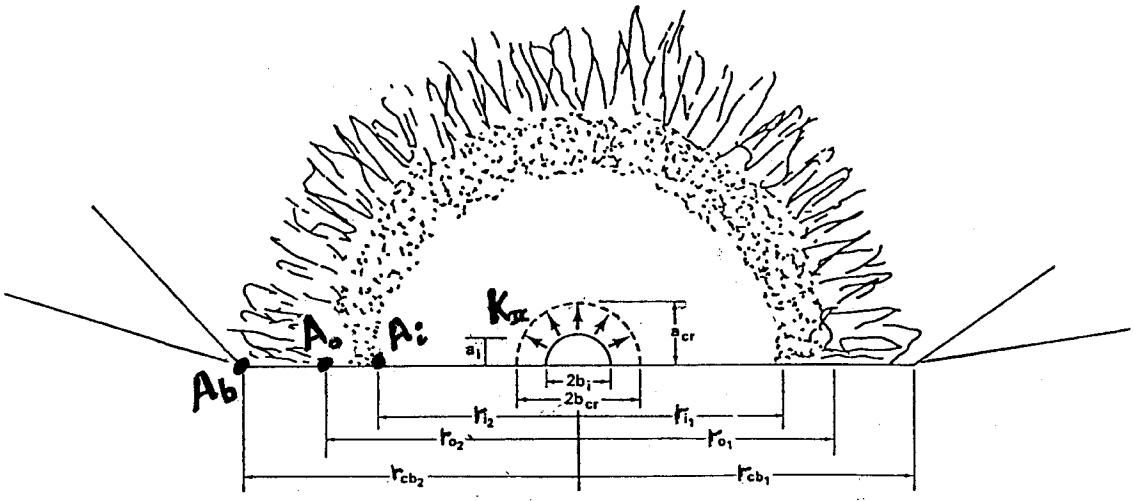

Fig. 1. Schematic of fracture surface of a brittle material subjected to a constant subcritical load, σ. The solid semielliptical line at the center represents the initial flaw size, and the dashed line outlines the critical flaw before catastrophic failure. The inner (r_i), outer (r_o), and crack branching (r_{cb}) mirror radii are shown with subscripts 1 and 2 to indicate that mirrors may be unsymmetric.

Ref. Mecholsky, Gonzalez, Freiman, "Fractographic Analysis of Delayed Failure in Soda-Lime Glass," J. Amer. Ceram. Soc. 1979, Vol. 62, #11-12 p 577 - 580.

Inner Mirror (mirror/mist)	$A_i = A_{inner} = \sigma\sqrt{R_i}$
Outer Mirror (mist/hackle)	$A_o = A_{outer} = \sigma\sqrt{R_o}$
Branch Point	$A_b = A_{branch} = \sigma\sqrt{R_b}$

A's have units of Force / length$^{1.5}$ ie. $MN/m^{1.5}$ or $MPa\sqrt{m}$ or $ksi\sqrt{in}$

Note the Hierarchy:

K_{Ic}	at the flaw
A_{inner}	at the mirror/mist boundary
A_{outer}	at the mist/hackle boundary
A_{branch}	at the branching distance

Theories:

Velocity	Yoffe, 1951	Phil Mag, 42, 1951, p 739.
Energy	Johnson and Holloway, 1966	Phil Mag, 14 (1966) p 731.
Stress	Orr, 1972	"Practical Analysis of Fractures in Glass Windows, Mater. Res. and Stand., Jan. 1972, pp 21-23, 47
Stress Intensity	Clark, Irwin, 1966; Kirchner, 1987	Expl. Mech., 23 1966, p 321.
		H. Kirchner and J. Conway, "Criteria for Crack Branching in Cylindrical Rods: Part I, Tension, and part II, Flexure, J. Amer. Ceram. Soc. 70 #6 1987 pp 413-425.
Strain Intensity	Kirchner, 1986	H. Kirchner, "Brittleness Dependence of Crack Branching in Ceramics," J. Amer. Ceram. Soc., 69 #4 1986, pp 339-342.

cer-mir4.grf
February 10, 2000
uses Cerm-all.xls and cerm.al2.xls files which have all data
then uses FIT function
corrected 2/10/2000
includes NIST 600 grit

Fracture Mirror Size Analysis
stress = $A_o / \sqrt{R}$

* Stress is corrected for location for the rod origins.
* Residual stress assumed to be zero.
* Mirror radius is the average of deepest R, and 2R along surface, or average of two diameters if origin in interior.
* Wild stereo M-10 microscope at 32-63X only!
* Mirror boundary is onset of hackle and major roughness change relative to the "bumpy" mirror characteristic of this material.

New data collected at NIST on a new Commercial Si_3N_4 Ceramic.

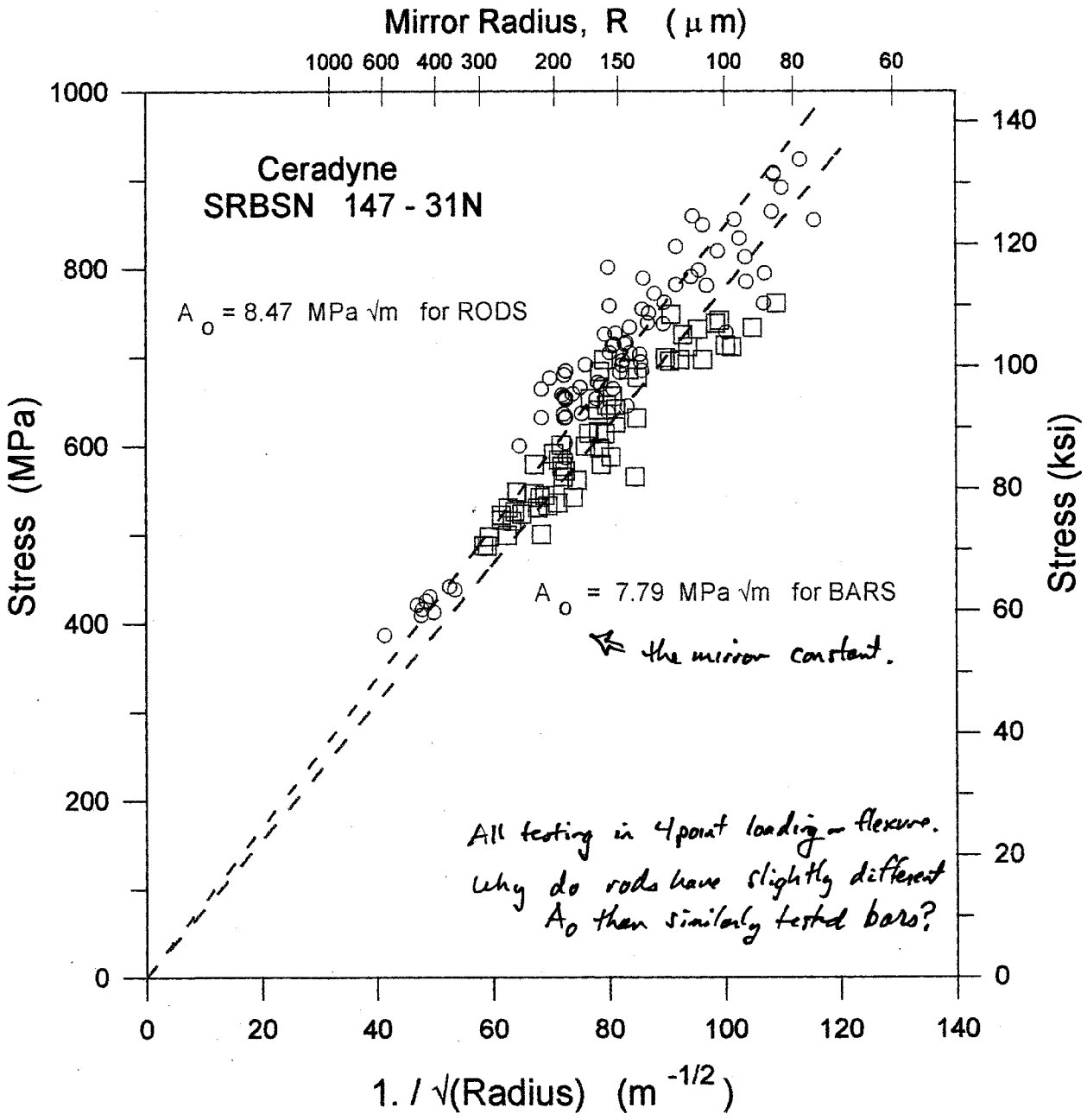

Mirrors - Applied Quantitative Fractography

FRACTOGRAPHY OF CERAMIC FEMORAL HEADS

in Fractography of Glasses + Ceramics IV, 2001

Roger Morrell and Liam Byrne
National Physical Laboratory,
Teddington,
Middlesex, TW11 0LW, UK

Michael Murray
Morgan Matroc Ltd,
Bioceramics Unit,
St Peter's Road,
Rugby, Warwickshire
CV21 3QR, UK

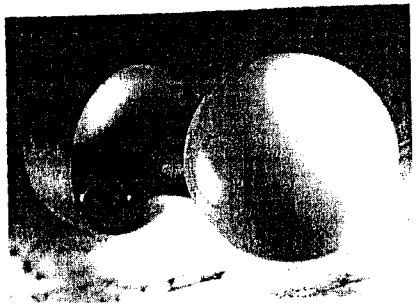

Ceramic Ball Hip Joint

A ball that fractures in service may be analyzed after extraction. The fracture mirror can tell what the stress was at fracture.

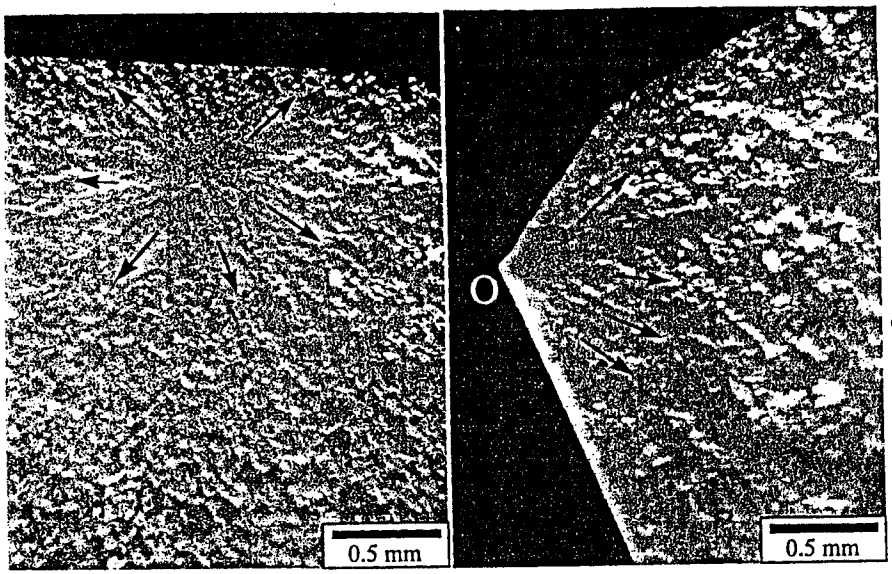

(a) (b)

Figure 4 Examples of fracture origins in mechanically tested Y-TZP femoral heads, (a) internal origin from a pore, (b) surface origin ('O') at the end of the

Mirror data is collected ahead by lab tests with controlled fracture.

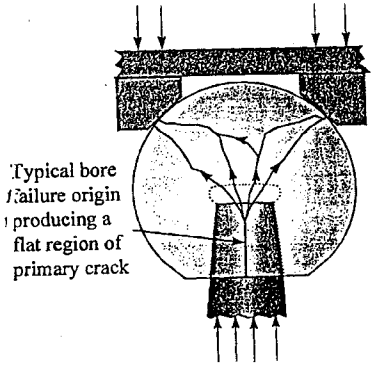

Lab controlled fracture.

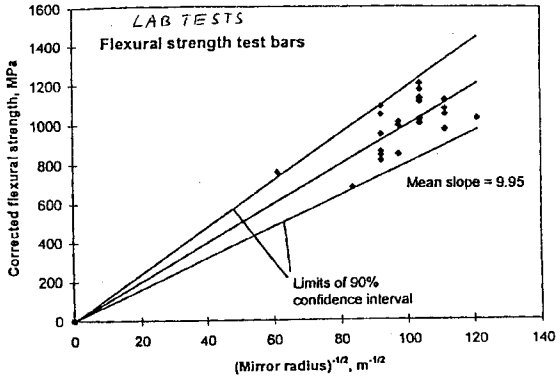

Figure 6 Plot of position-corrected flexural strength of Y-TZP test bars against 1/(mirror radius)$^{1/2}$. The central line gives a slope for the mirror constant of 9.95 MPa m$^{1/2}$; the other lines represent the limits of the 90% confidence interval.

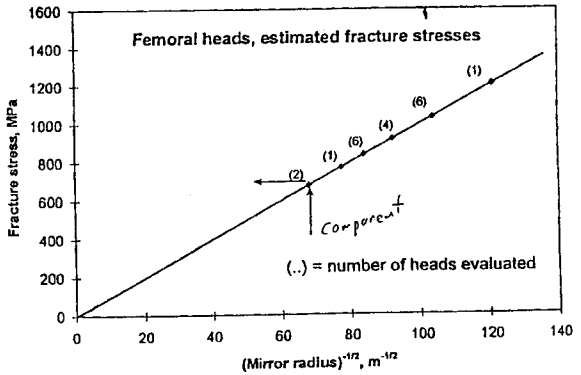

Figure 7 Fracture mirror plot for femoral heads, plotting fracture mirror radii onto the line representing the mean fracture mirror constant determined in Figure

The Quinns' 1982 Ford Mustang
A Fractographic Case Study

The car after a full restoration in 1999.

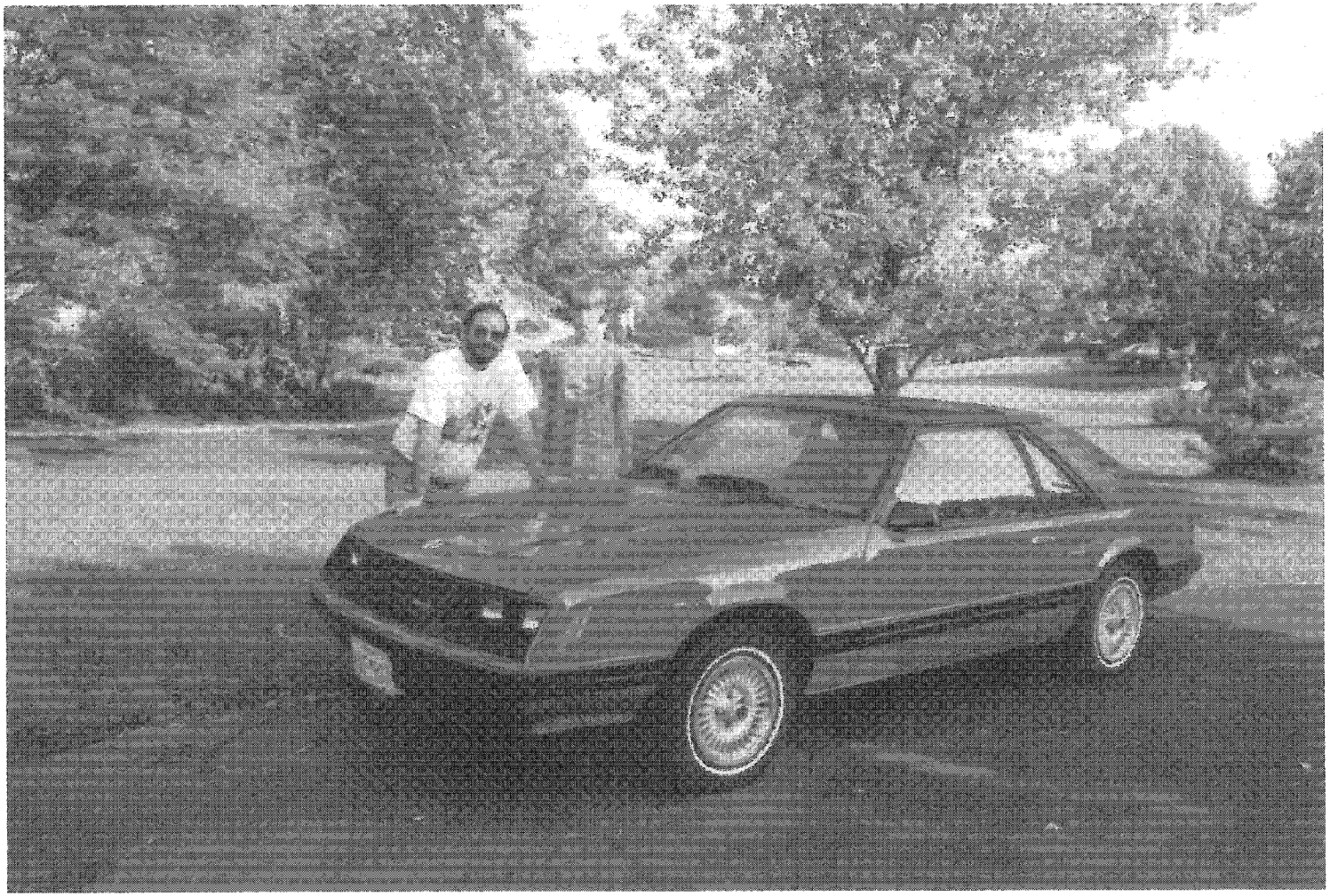

Here it comes.
September 2001 at the
University of Maryland

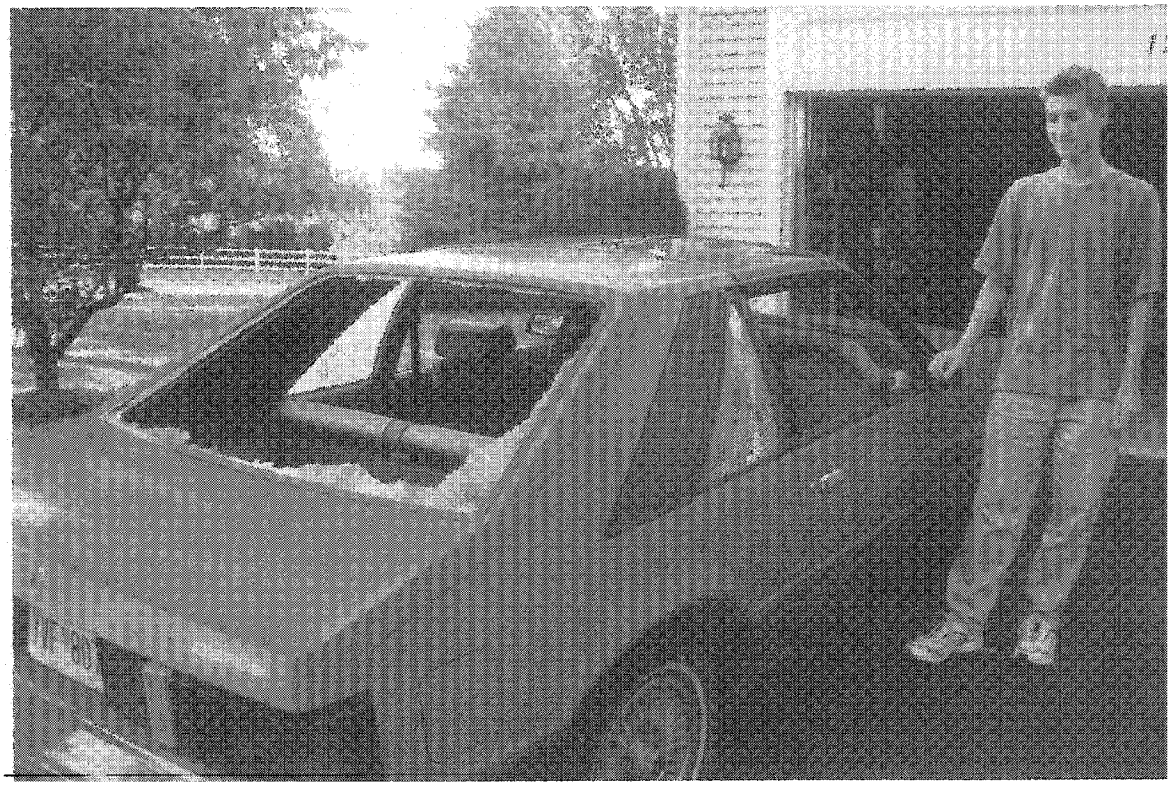

The car was totaled, based on the glass and body paint damage.
The rear hatch, driver's door, two side panels, and one side mirror were destroyed.

Side window fracture. Tempered glass.

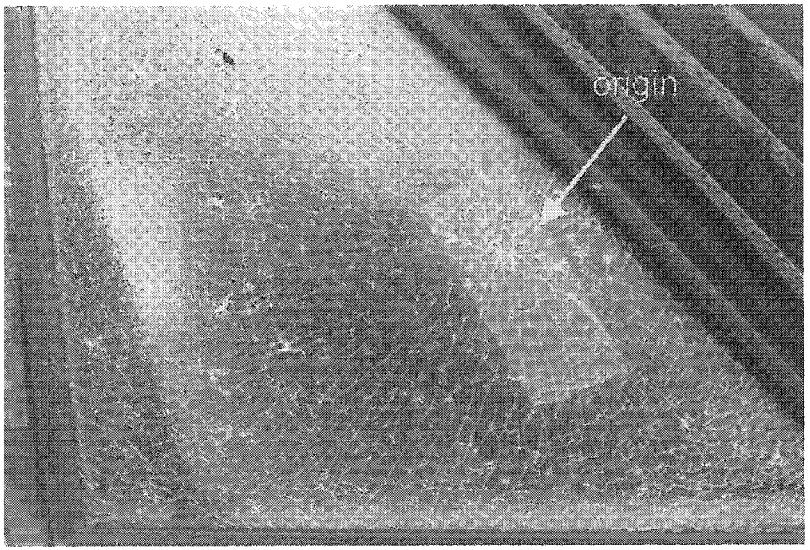

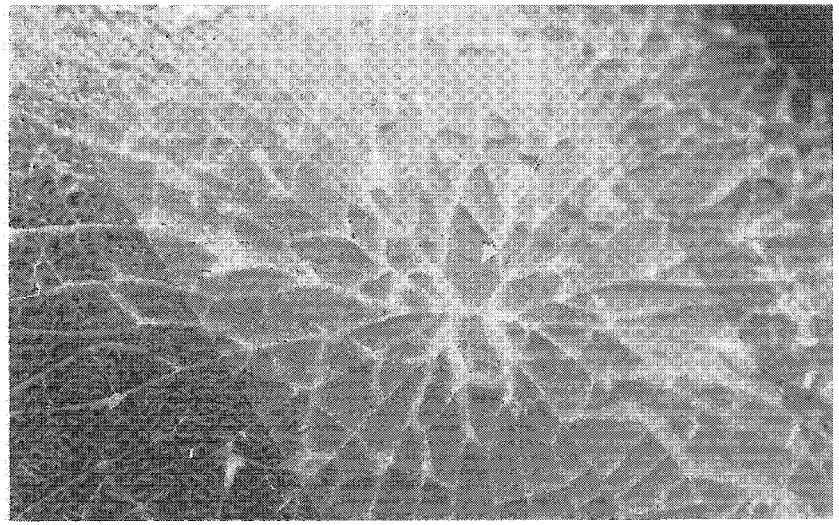

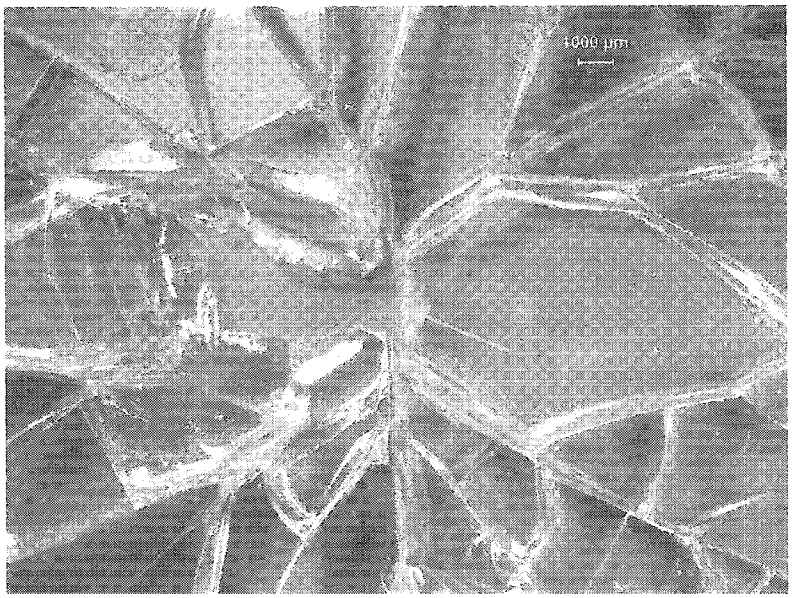

Hackle
Mist
Fracture
Mirror
Wallner
Lines
1000 μm

For More Information

Characterization of Fracture Origins

The strength of many advanced ceramics reflects the flaws present in the material and the material's intrinsic fracture toughness. Monolithic ceramics and some composite ceramics (i.e., particulate- or whisker-reinforced) will fail in a brittle fashion when stressed due to unstable propagation of cracks from preexisting flaws.

The terms "flaw" and "fracture origin" are used interchangeably in this context. Scientists and engineers in the ceramics community traditionally have used these terms to describe the fracture initiation site in ceramics and other brittle materials. These terms are used in the context of fracture mechanics whereby a singularity or microstructural irregularity acts as a stress raiser from which fracture commences. It should be understood that the use of the term "flaw" does not imply that a ceramic product has been prepared improperly or is somehow defective.

Strength-test results must be interpreted in the context of these flaws, whether the strength testing has been done for quality control, materials development, or design purposes. Fractographic observations should be coupled directly to strength results. Fractographic montages and labelled Weibull graphs are an exceptionally versatile means of accomplishing this. See ASTM C1239 for more details on Weibull analysis of strength data.

American Society for Testing of Materials (ASTM) developed C1322 "Standard Practice for Fractography and Characterization of Fracture Origins in Advanced Ceramics". This practice provides an efficient and consistent methodology to locate and characterize fracture origins in advanced ceramics. The table below outlines the fracture origin characterization scheme and the linked figures show examples of the most common types of flaws observed in advanced ceramic materials. (See Fracture Origin Characterization and the Flaw Catalog.)

Any questions or comments about ASTM C1322, the fracture origin examples given here, or fractography of ceramics can be addressed to Jeffrey Swab (jswab@arl.mil) or George Quinn (geoq@nist.gov).

Fracture Origin Characterization and the Flaw Catalog

The fracture origin in each specimen/component shall be characterized by the following three attributes: identity, location, and size as summarized in the table below.

IDENTITY	LOCATION	SIZE
Nomenclature and inherent spatial distribution: •Volume-distributed •Surface-distributed	Spatial location of an individual origin in a specific specimen •Volume-located •Surface-located •Near-Surface-located •Edge-located	•Estimate of the diameter for equiaxed origins •Minor and major axes of volume-distributed origin •Depth and width of surface-distributed origins

Please note that the descriptive terms "volume" and "surface" may have two distinctly different uses.

Lyle Schwartz, President of Federation of Materials Society
Recognizes Robert B. Pond, Sr.
for his contribution to materials education

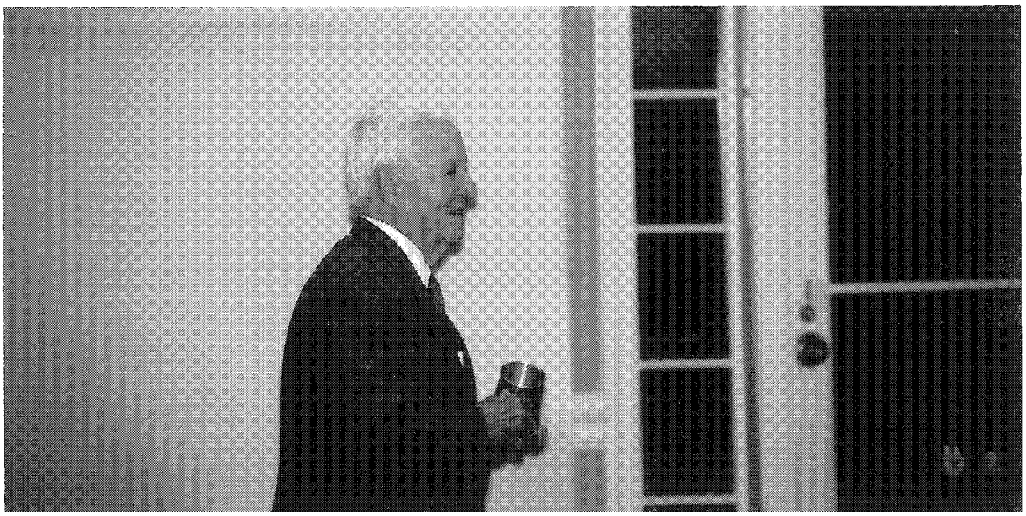

Robert B. Pond, Sr.

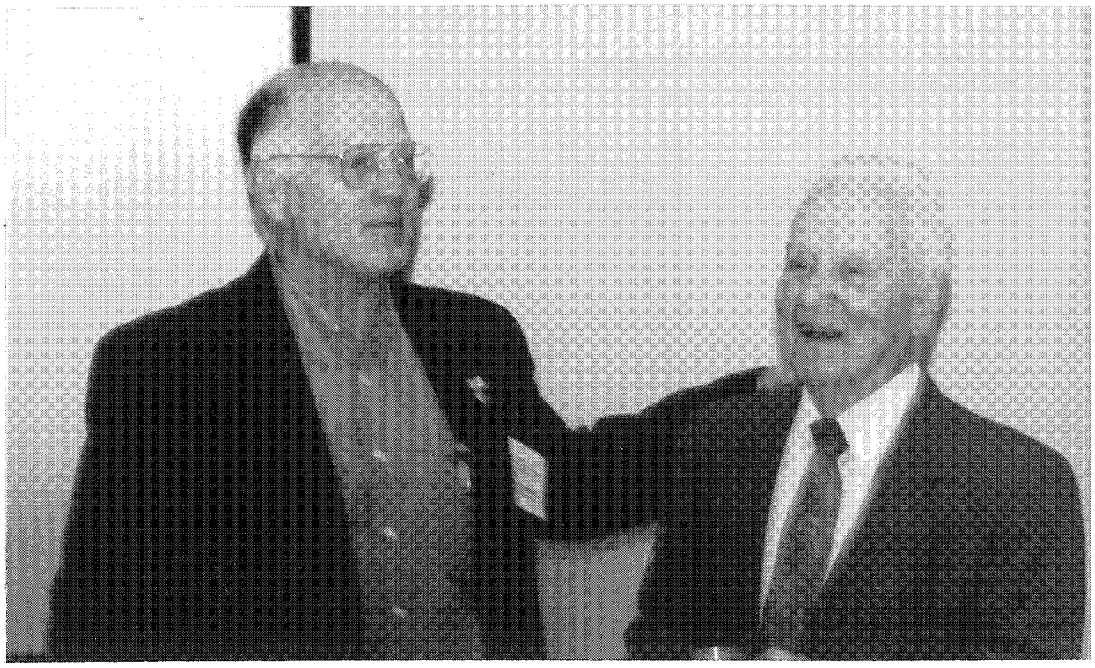

Jim Jacobs and Robert B. Pond, Sr.

Martha Goodway
Archeometallurgist
Smithsonian Center
For
Materials Research and Education

MATERIALS SOLUTIONS TO MEDICAL PROBLEMS

Justin Hanes
Johns Hopkins University

ENERGY CONCEPTS MATERIALS SCIENCE AT MAURY HIGH SCHOOL

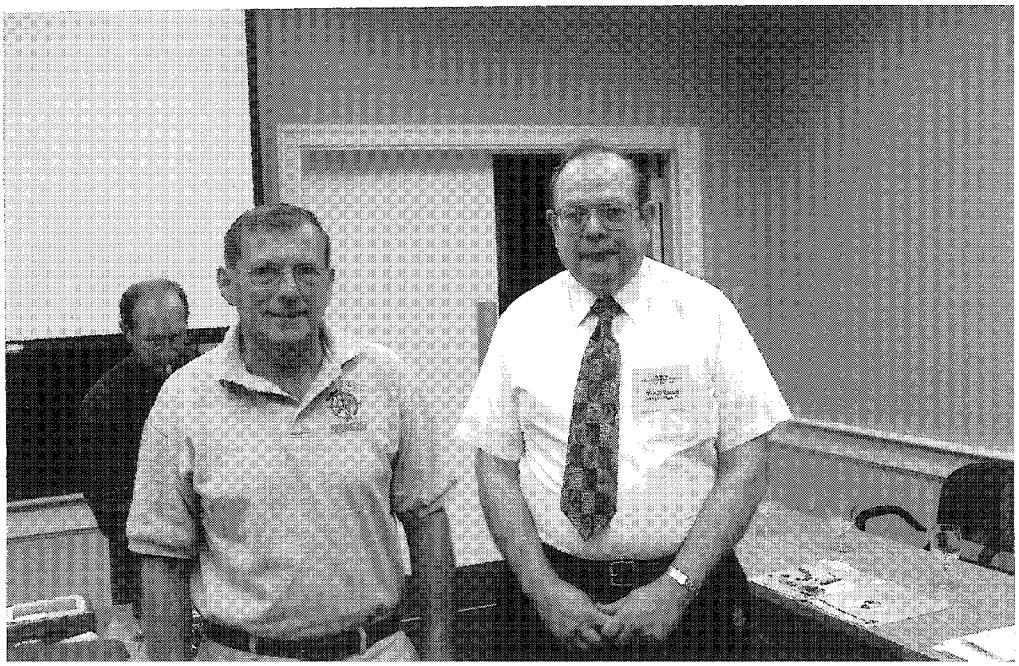

Duane Bushey and Merrill Rudes
Maury High School and Energy Concepts, Inc.

MATERIALS RESEARCH AT NIST - CENTURY OF PROGRESS

Dale Hall

Deputy Director
Materials Science & Engineering Laboratory
National Institute of Standards and Technology
Bldg. 310, Room B309, MS 8500
Gaithersburg, Maryland 20899-8500

Telephone: 301-975-5658
e-mail dale.hall@nist.gov

Dale Hall

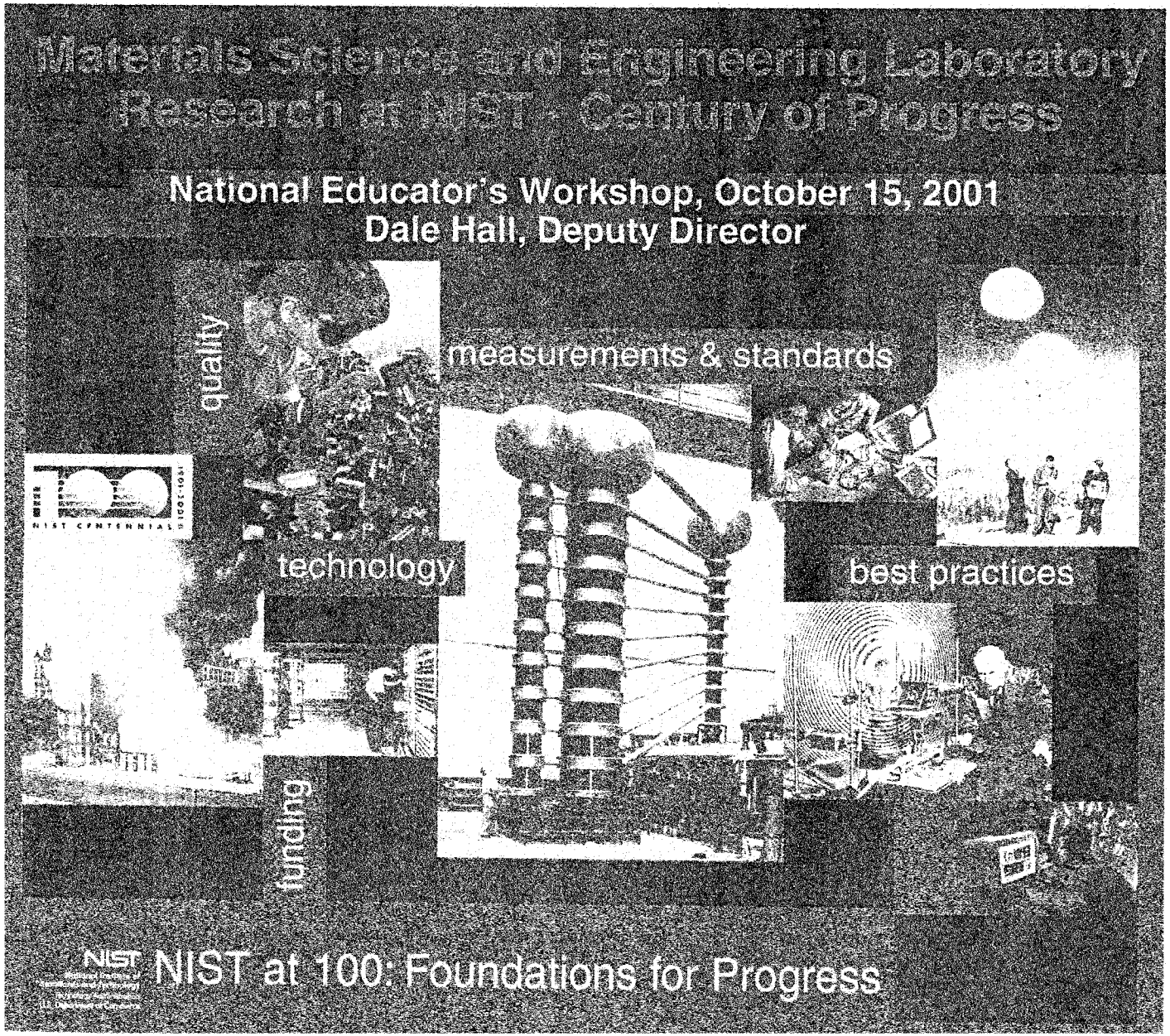
Materials Science and Engineering Laboratory
Research at NIST - Century of Progress
National Educator's Workshop, October 15, 2001
Dale Hall, Deputy Director
quality
measurements & standards
technology
best practices
funding
NIST at 100: Foundations for Progress

National Institute of Standards and Technology

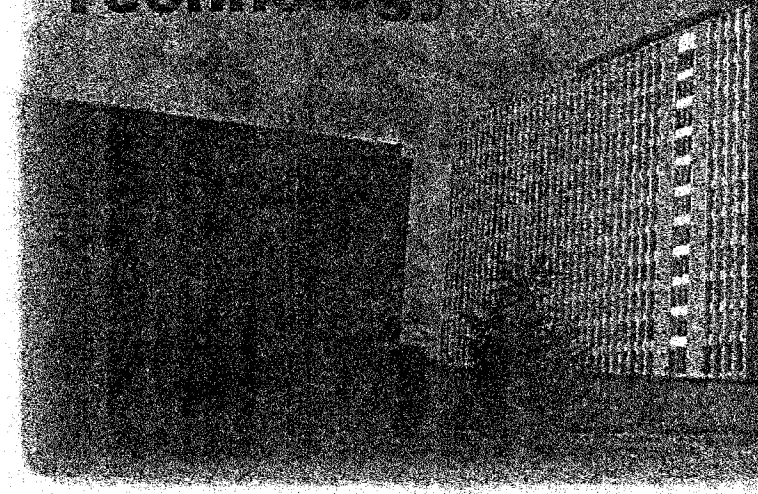

NIST's primary mission is to promote economic growth by working with industry to develop and apply technology, measurements, and standards.

NIST carries out its mission through a portfolio of four programs:

MEASUREMENTS AND STANDARDS PROGRAM

ADVANCED TECHNOLOGY PROGRAM

MANUFACTURING EXTENSION PARTNERSHIP PROGRAM

NATIONAL QUALITY PROGRAM

NIST's Laboratories

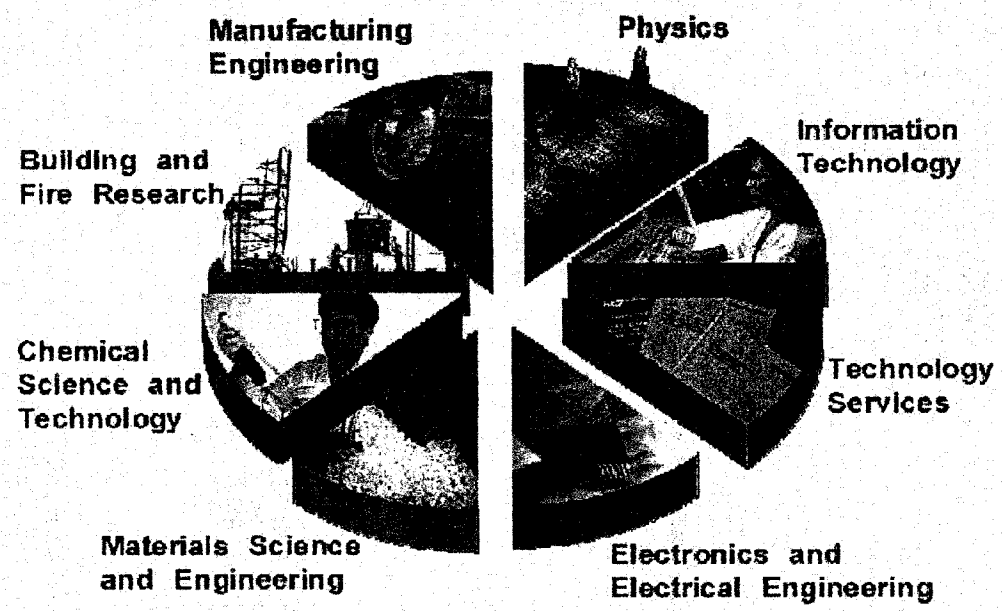

- Enhance US industrial competitiveness and economic growth through critically-needed standards, measurements, and data

- Highly leveraged measurement and research capabilities supporting trillions of dollars in products and services

Establishment of NBS

THE EVENING STAR, MONDAY, MARCH 11, 1901

CORRECT MEASURES

Function of the New Bureau of Standards.

LABORATORY TO BE ERECTED

Prof. Stratton, the Director, Details Need of Establishment.

A HANDICAP REMOVED

A new bureau of the government, authorized by the last Congress, will be established in this city in the near future and will give employment to a number of persons. It is to be known as the national bureau of standards and is to be under the control of the Treasury Department. A separate building for a laboratory, to cost not to exceed $250,000, is to be erected on a site to be purchased at a cost of $25,000.

Mr. Samuel W. Stratton of Chicago has been appointed by the President to be chief of the bureau at an annual salary of $5,000. Prof. Stratton is to have the following assistants, to be appointed by the Secretary of the Treasury: One physicist, at an annual salary of $3,500; one chemist, at $3,500; two assistant physicists or chemists, each at an annual salary of $2,200; one laboratory assistant, at $1,400; one laboratory assistant, at $1,200; one secretary, at $2,000; one clerk, at $1,200; one messenger, at $720; one en-

Director Stratton.

1915 Organization Chart

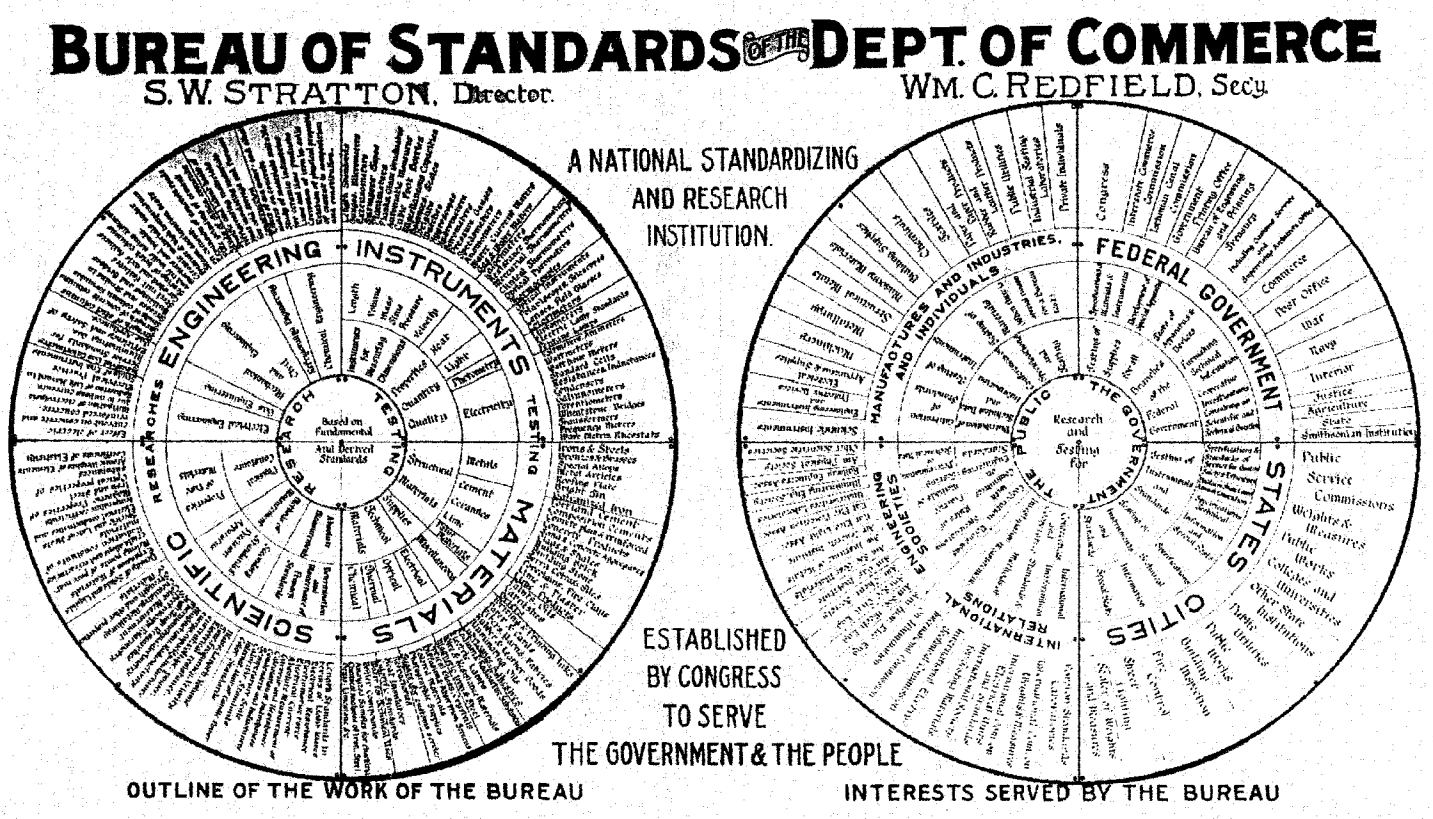

Materials research in 1915 involved Metals, Cement, Ceramics, Paint, Ink, Paper, Fibers, Yarns, Fabrics, Rubber and Leather Goods

NBS Railway Scale Test Car for Standardization of Railroad Track and Master Scales

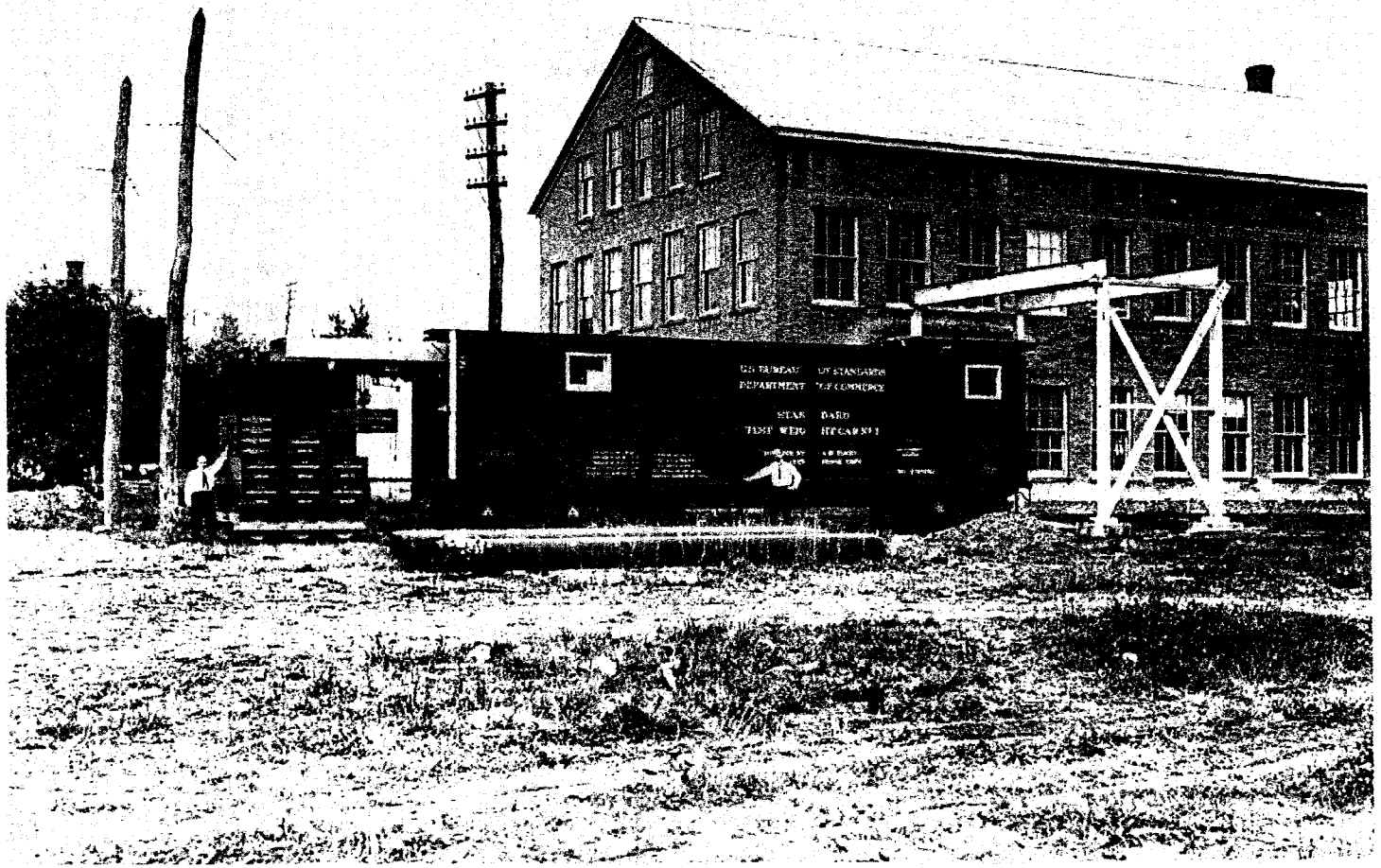

Looms, Spinning Frames, and Warpers to Test Cotton as a Substitute for Wool

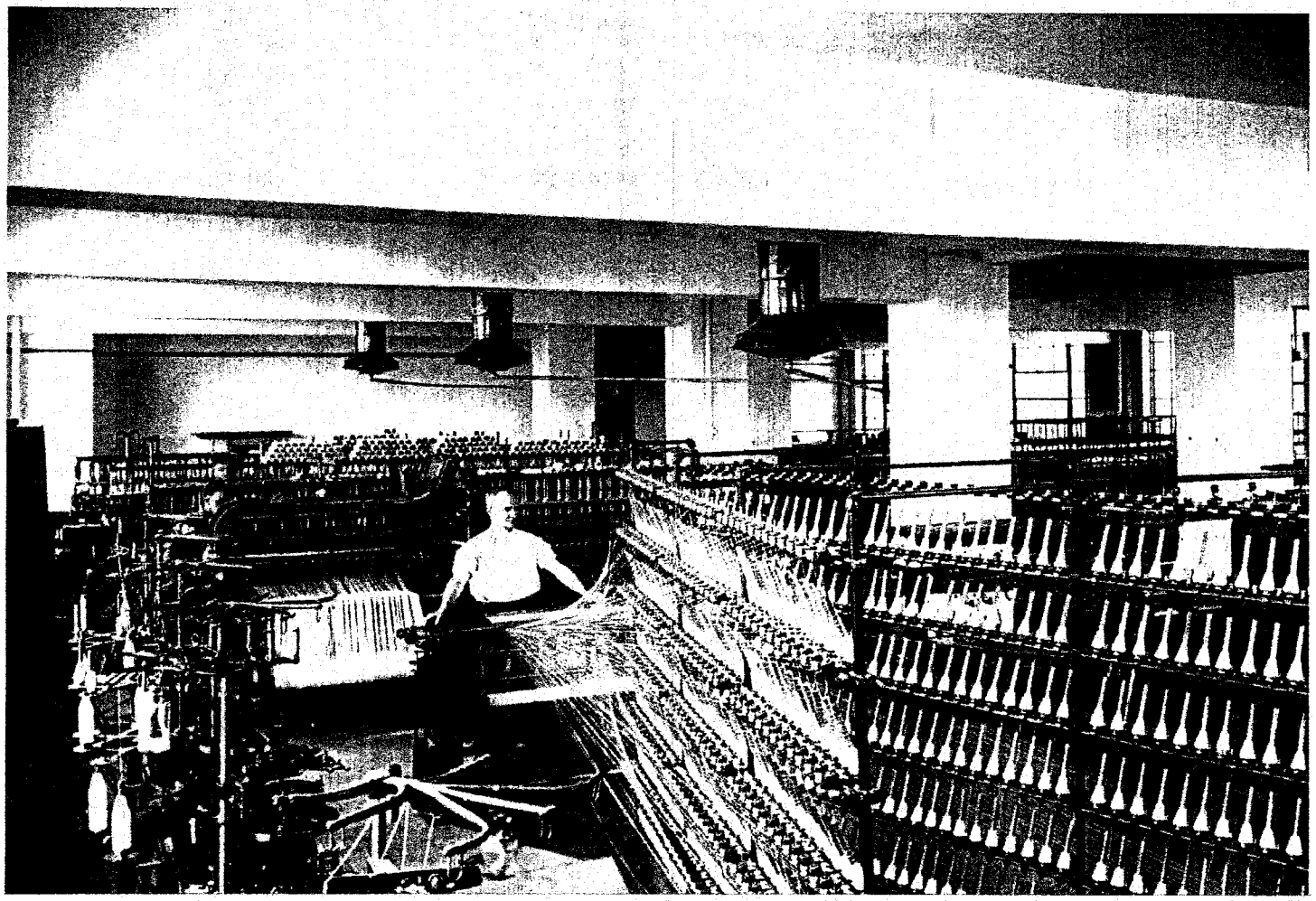

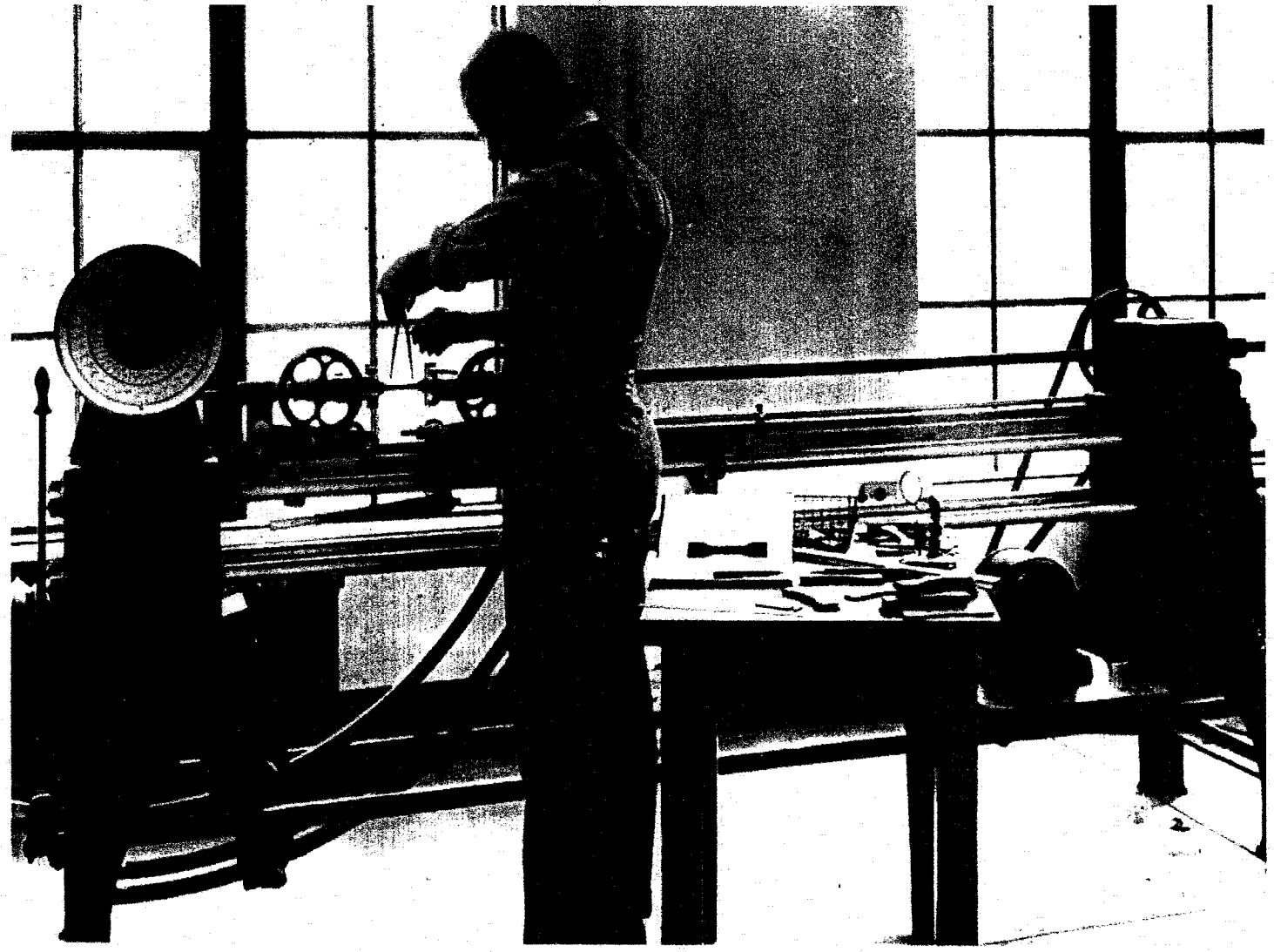

Testing of Leather to Enable the Search for Substitutes

The Dynamometer Laboratory for Testing the Durability of Vehicle Tires

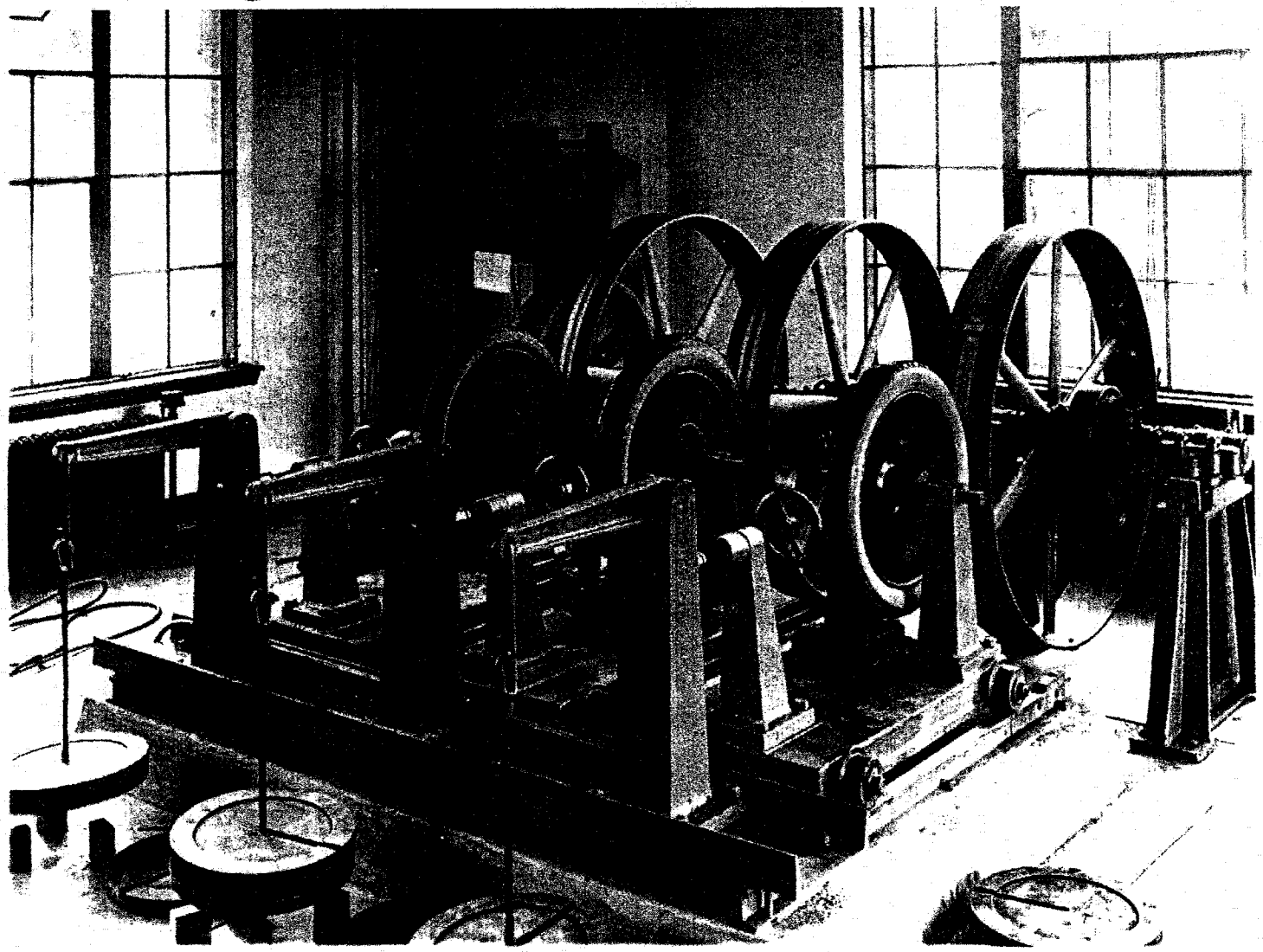

NIST Maintains Scientific Integrity Despite Political Pressures

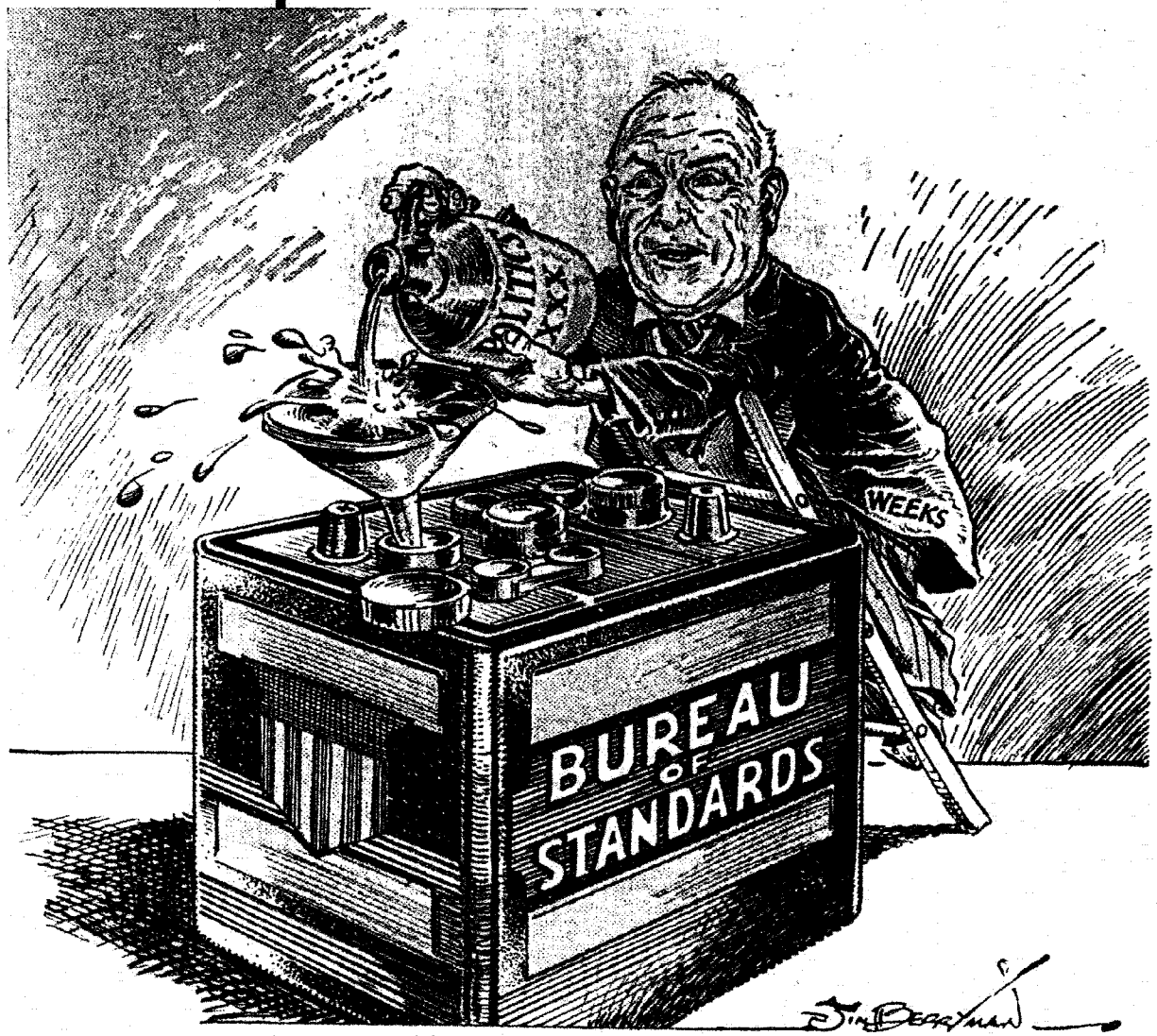

New Battery Additive

Director Austin Exhonorated by Secretary of Commerce Weeks

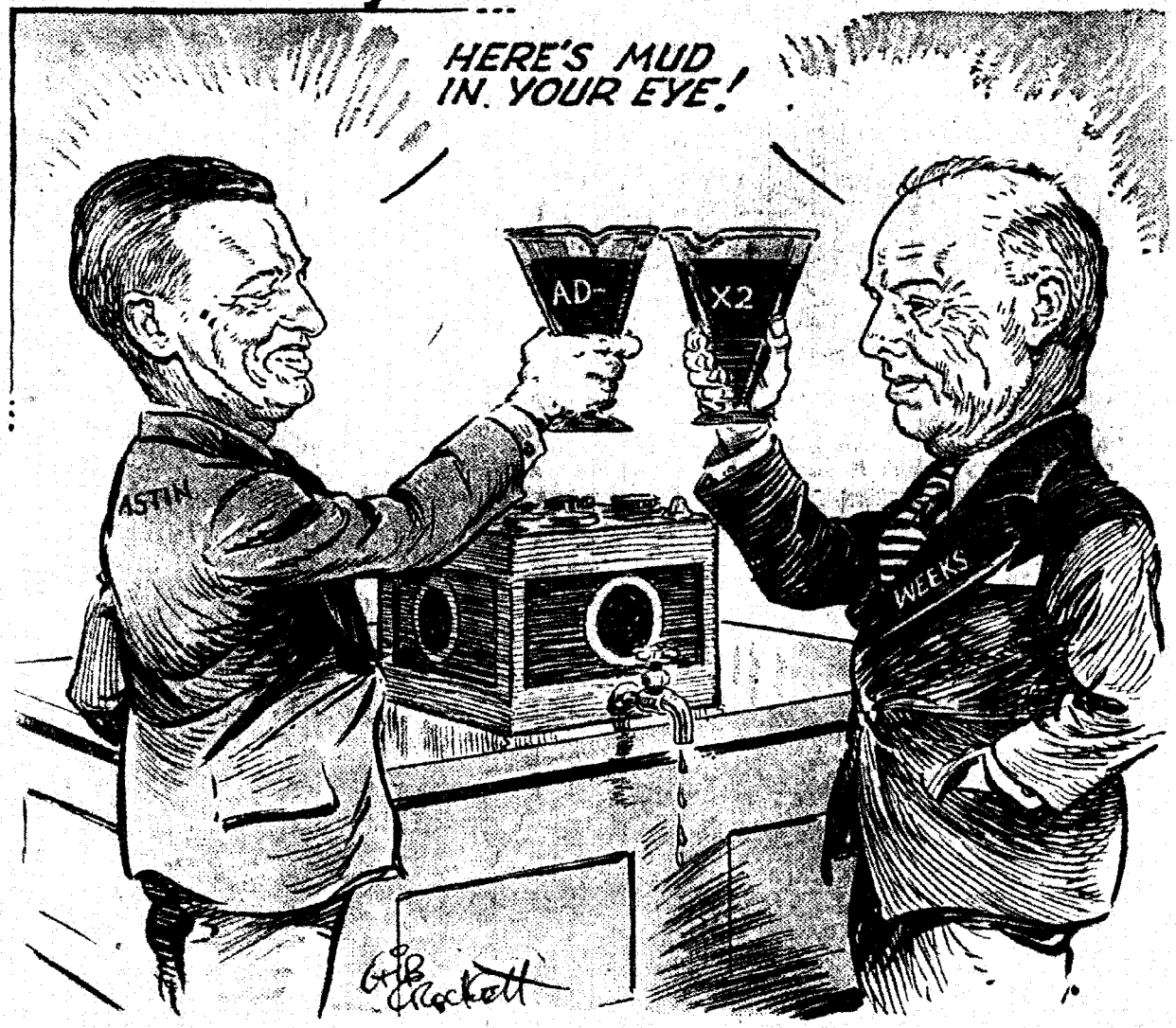

Happy Days!

NBS Completes High-Flux REACTOR

Because neutrons are deflected only by collisions with other particles and not by electric charge, they have wide experimental application in studies of the nature and properties of matter. "Fast" (up to 10 MeV) neutrons are used to study nuclear reactions. Crystallographic arrangements of atoms are explored by "slow" (about 0.025 eV), or "thermal," neutrons.[1] "Cold" neutrons (having energies on the order of 0.001 eV) are uniquely suited to the study of the dynamics of molecular systems.

The intense thermal neutron beams provided by the reactor will constitute a powerful tool in the analysis of the structure of solids and liquids by neutron diffraction. This technique can be applied to investigate various aspects of crystal structure, such as the location of hydrogen atoms, magnetic crystal properties, intermolecular force constants, and chemical bond strength.

of purposes, such as activation analysis and tracer t
tion, as well as for distribution as radioactivity sta

In addition, studies of the effects of radiation
terials will be carried out with the reactor by in-pi
diation of bulk matter. The information obtained
way should be of great value, both for basic knc
in solid state and chemical physics and for applica
radiation processing and altering the properties o
tural materials.

Basically, the reactor consists of an enriched u
core, moderated and cooled by heavy water and co
in a large aluminum vessel. Thermal and bio
shields surround the core vessel and attenuate the
tion (which reaches a level of 10^{14} neutrons/cm
to biological and instrument tolerance level. T
beam tubes, or ports, running outward from th

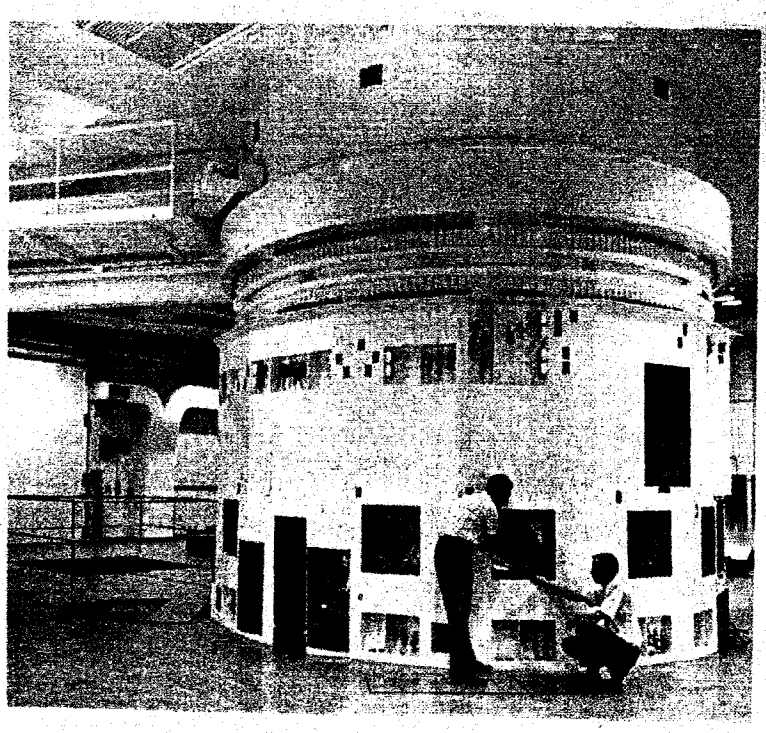

NBS technicians inspect one of the 13 beam ports of the Bureau's new 10-megawatt nuclear reactor, which has just been completed. The radioactivity will be confined by the 2-m-thick concrete wall to a small space at the height of the ports. The ports will be plugged, or open only to shielded experimental areas, so that no radiation hazards will be present. Fuel will be loaded and operation monitored and controlled from the level above.

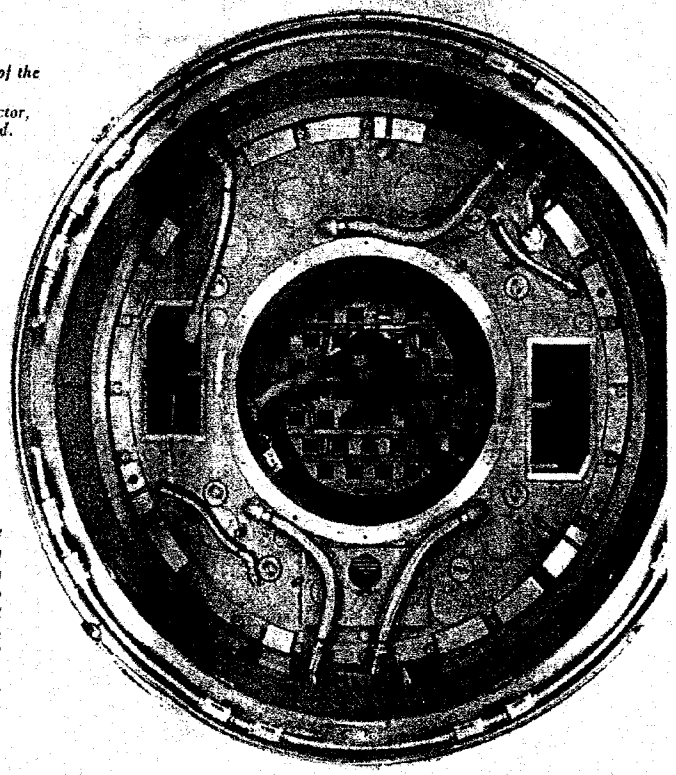

Charles Hook, of the NBS staff, stands on the upper grid plate in the Bureau's reactor to show size of the fuel transfer area. This area will be completely sealed by a top plug, before the reactor is placed in operation, and the cavity around it also closed.

Encasement of the Declaration of Independence and Constitution

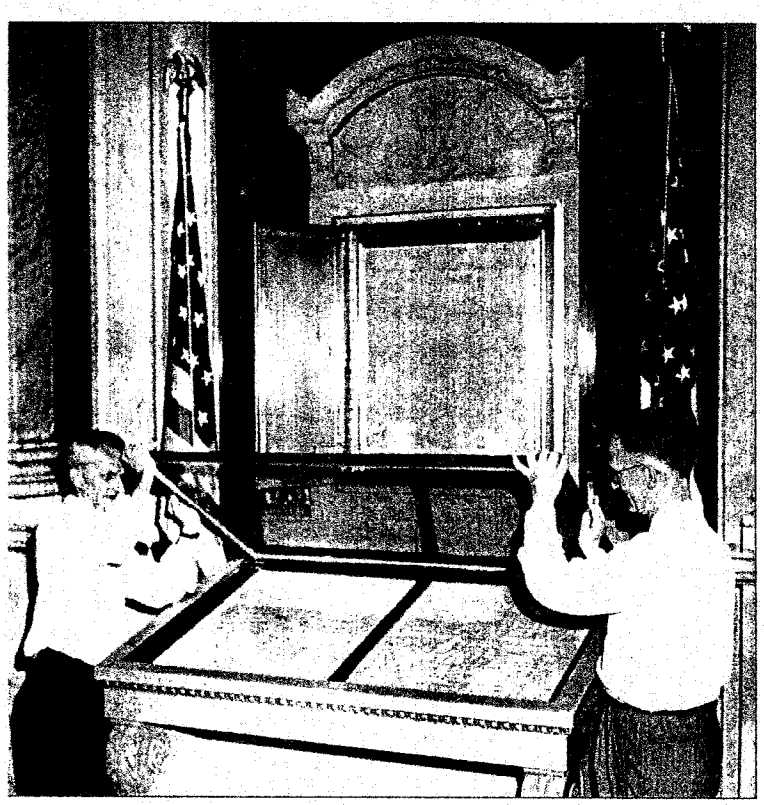

1950

Leslie E. Smith, left, and Richard Rhorer with a model casement for the Declaration of Independence, the Constitution and the Bill of Rights.

1999

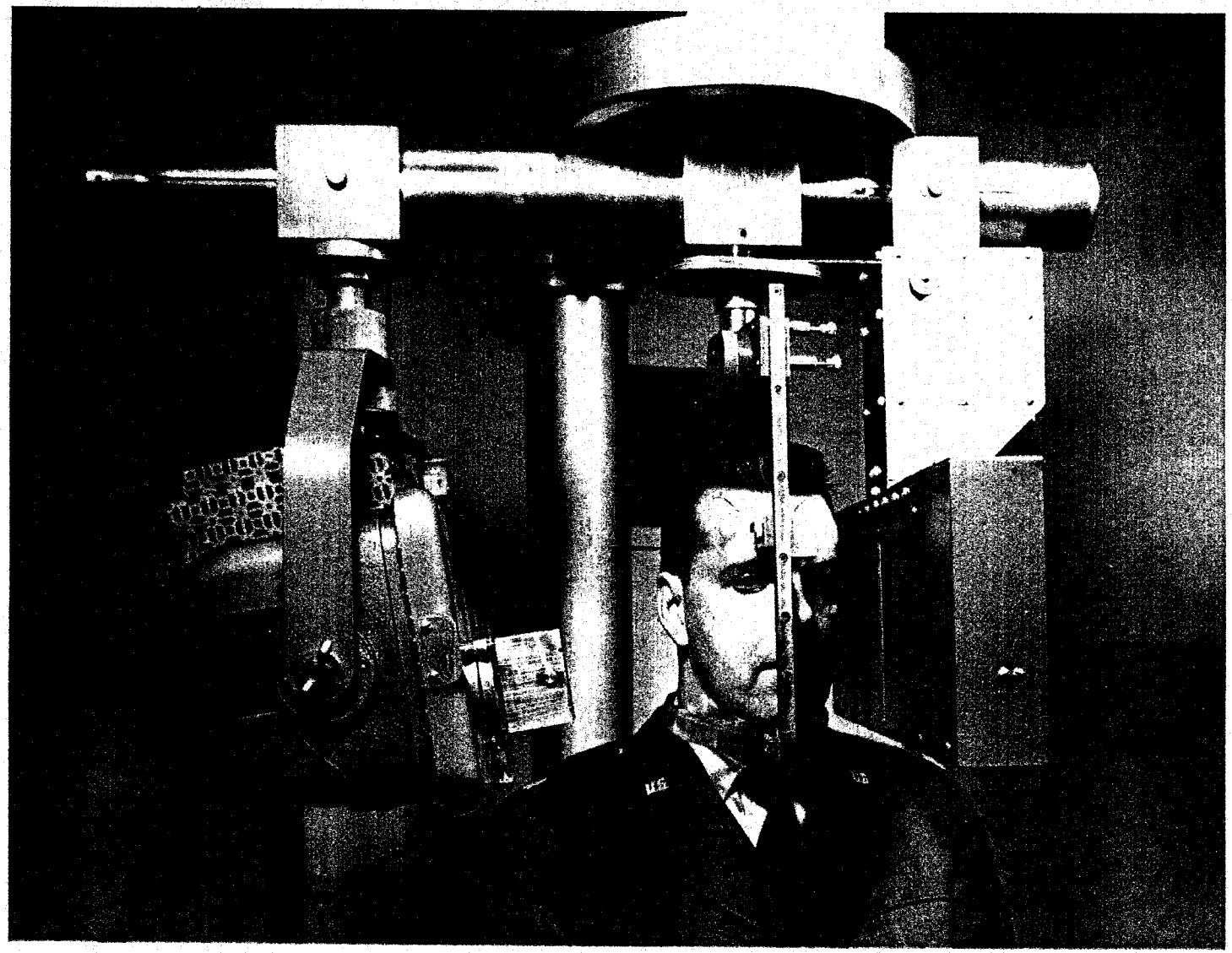

NBS and the American Dental Association Health Foundation Developed the Panoramic X-ray

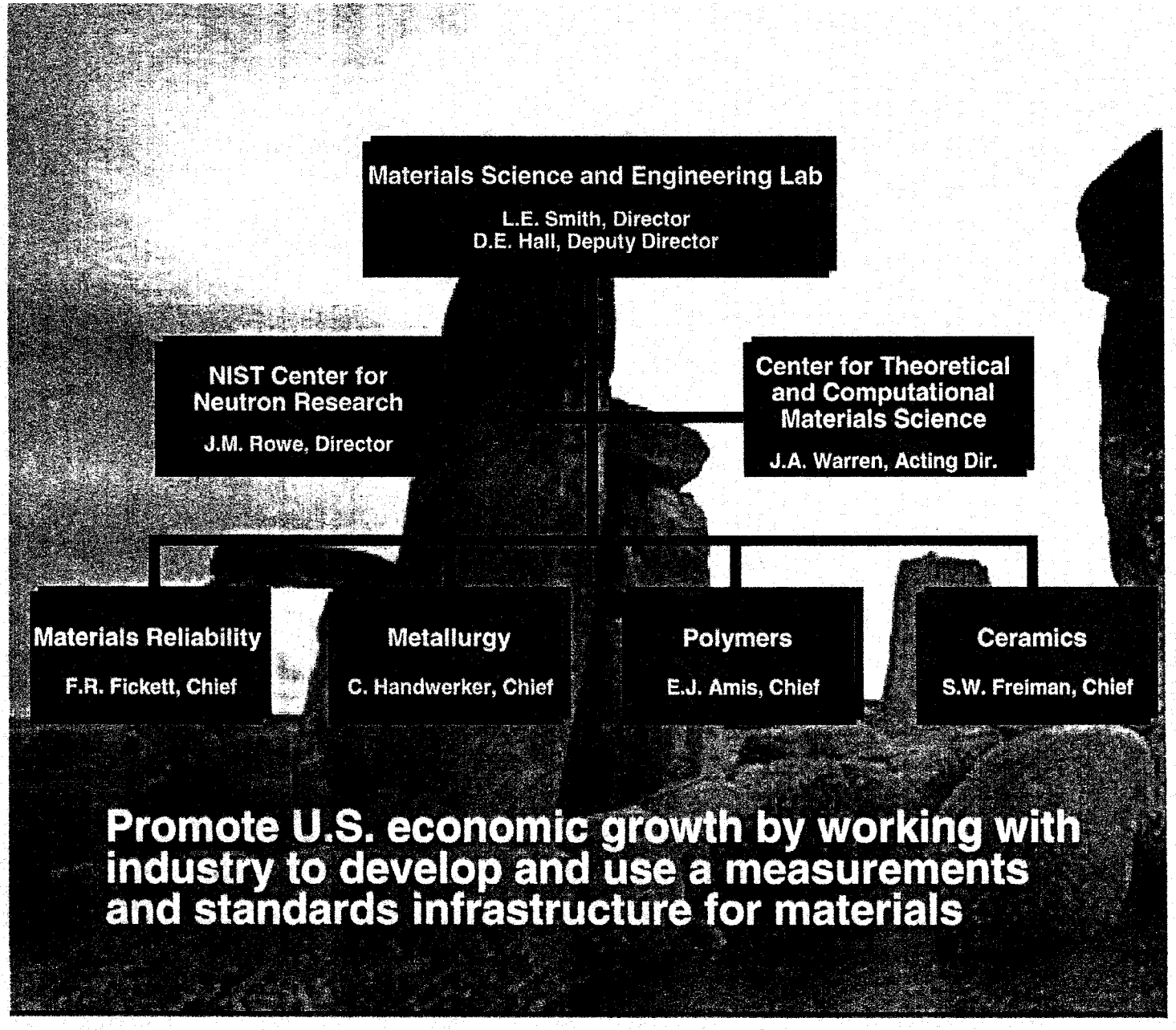
Materials Science and Engineering Lab
L.E. Smith, Director
D.E. Hall, Deputy Director
NIST Center for Neutron Research
J.M. Rowe, Director
Center for Theoretical and Computational Materials Science
J.A. Warren, Acting Dir.
Materials Reliability
F.R. Fickett, Chief
Metallurgy
C. Handwerker, Chief
Polymers
E.J. Amis, Chief
Ceramics
S.W. Freiman, Chief
Promote U.S. economic growth by working with industry to develop and use a measurements and standards infrastructure for materials

Trends in Materials Science and Engineering

- Rapid technical advances in electronic materials, nanotechnology, smart materials
- Scale of materials research and measurement getting smaller
- Growth of biomaterials and "soft" materials
- Greater emphasis and excitement in functional materials
- Fundamental physics to predict materials properties
- Increased use of computation and modeling for all aspects of materials research and engineering
  - Integration of modeling scales
- Characterization is expensive; need to share unique facilities
- Products contain combinations of materials
- Use of information technology as a tool for collaboration and knowledge dissemination

Key Markets

Health Care

Medical Instrumentation
Artificial Replacement
Tissue Engineering

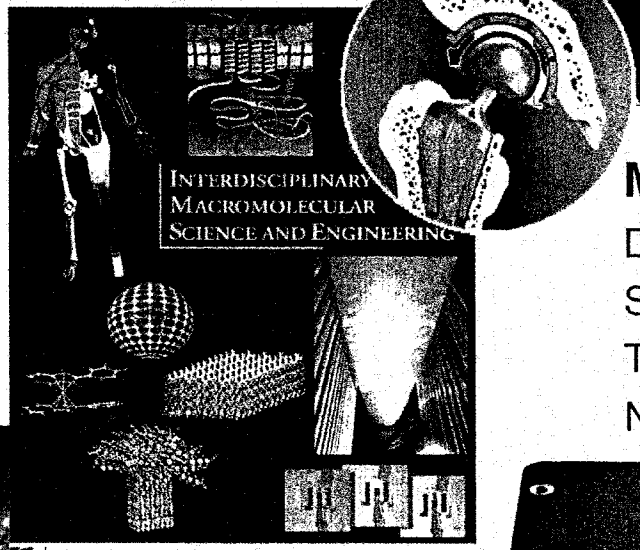

Electronics

Optoelectronics
Wireless Communication
Electronic Commerce
Display Devices

Magnetics

Data Storage
Superconductors
Thin Films
Nanomaterials

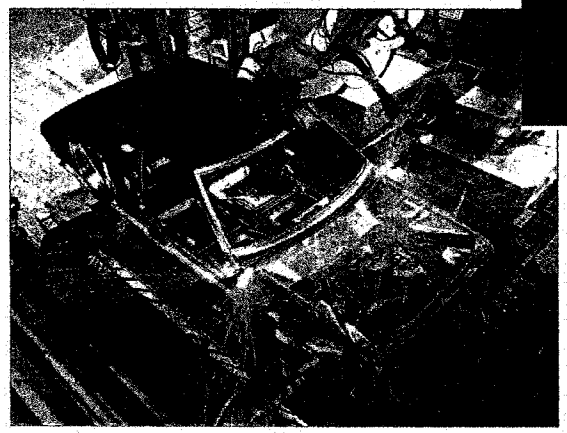

Automotive

Lightweight Materials
Energy Storage
Electronics

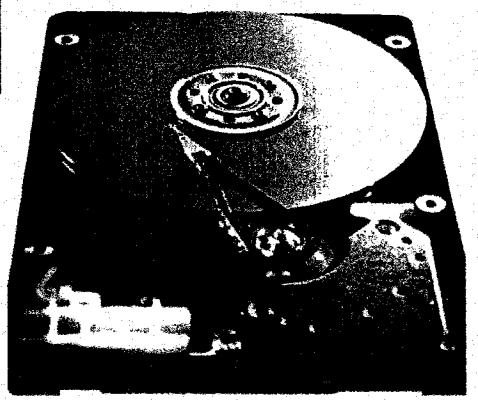

NIST Center for Neutron Research

- A National user facility, serving
  - -2/3 of U.S. users in 2000
  - -50 U.S. industrial laboratories
  - -115 U.S. universities
  - -34 U.S. government laboratories

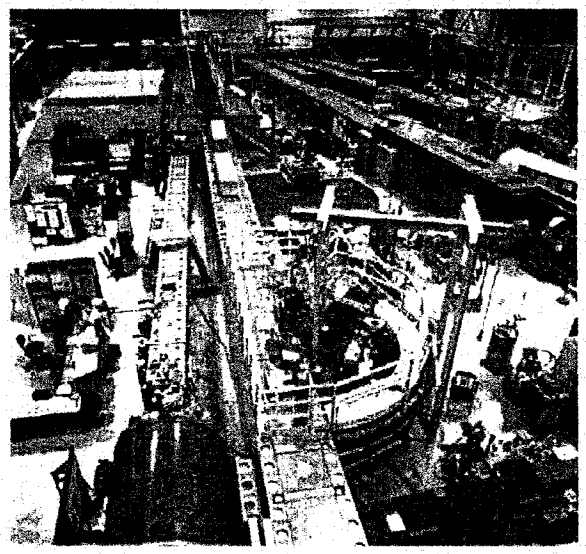

NIST Cold Neutron Instruments in the Guidehall

- Leadership areas
  - -The most cost effective neutron source in world
  - -Measurement of nanoscale structure
  - -Unique U.S. probes of polymers and molecules
  - -Forefront research on protein dynamics, chemical sieves and catalysts

Center for Theoretical and Computational Materials Science

- Materials Theory and Modeling
  - Novel computational approaches
  - Integration of NIST science
  - Collaborations among industry, academia, government

Molecular Dynamics Melt Simulations

- Focus Areas
  - Object Oriented Finite Element Software (OOF)
  - Prediction of phase behavior
  - Simulations of filled polymers
  - Phase field modeling of microstructure

Object Oriented Finite Element (OOF) Modeling Software

- Computes macroscopic properties of materials from their complex microstructures
- Operates on data from real images or simulations of microstructures
- Provides user friendly and web accessible public domain software
- Significantly reduces amount of laboratory experimentation

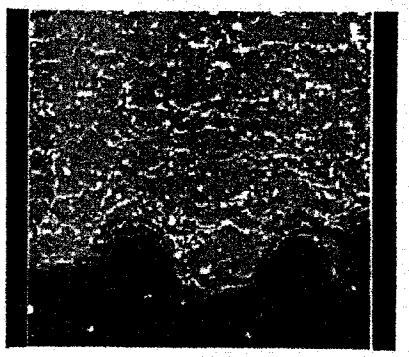

Virtual Test

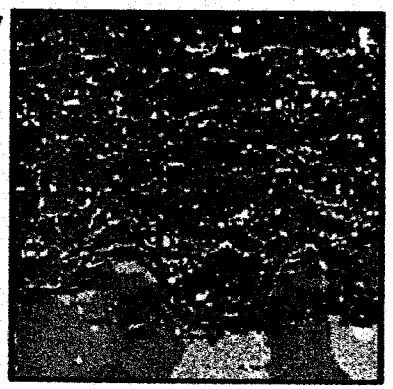

Visualize and Quantify

IW

1999 Technologies of the Year Award

NIST National Institute of Standards and Technology

Solder Interconnect Design Team

Industry Uses Tools to Design Smaller, More Reliable Electronic Packages

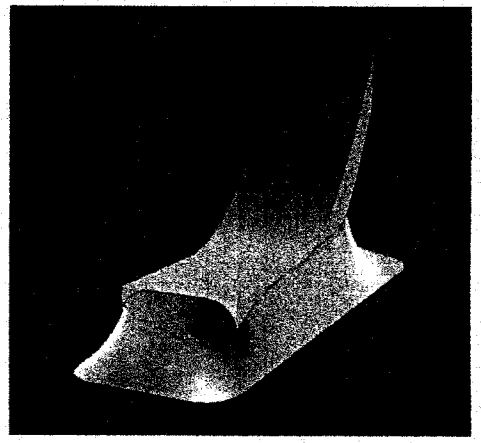

"Gull Wing" Solder Joint on PC Board Simulation

Technical Challenge:

- With many electronic devices having upwards of 100,000 solder interconnects, accurate prediction of solder joint reliability is critical

MSEL Response:

- Convened Solder Interconnect Design Team (SIDT) and held workshops for leaders in the electronics industry
- Created software tools that model the shape, spreading, reaction, and solidification of solder, allowing the prediction of joint reliability
- Disseminated tools through collaborative workshops, and the Theory Center web site

Impact:

- Companies are using SIDT tools in their in-house modeling programs to improve their electronic packages

The Ceramics WebBook
Sharing Information

- Evaluated data
  - -high temperature superconducting materials database
  - -structural ceramics database
  - -property data summaries for advanced materials
- Guide to data centers and sources
  - -NIST-based
  - -external
- Tools and resources
  - -software
  - -other materials resources

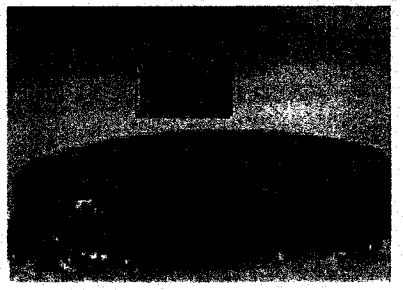

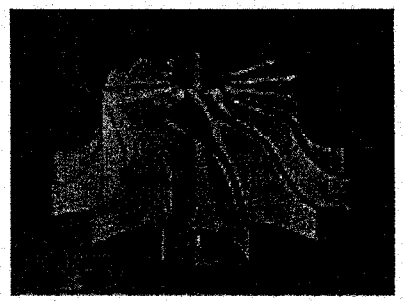

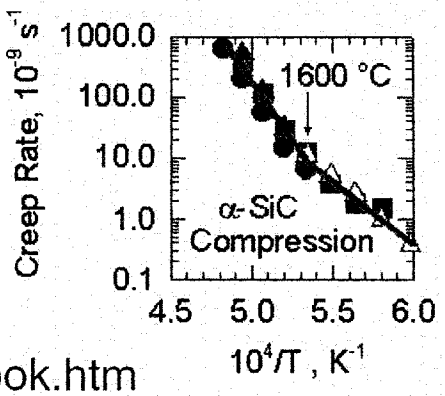

http://www.ceramics.nist.gov/webbook/webbook.htm

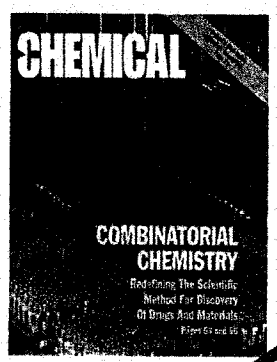

special report

Materials À La Combi

Despite the challenges, a growing number of corporate and other labs see promise in studying materials combinatorially

special report

COMBINATORIAL CHEMISTRY

Redefining The Scientific Method

Recent concepts and advances in this dynamic field involve combinatorial animals, target-guided ligand assembly, fluorous mixtures, microencapsulation, and nanoelectrospray technology

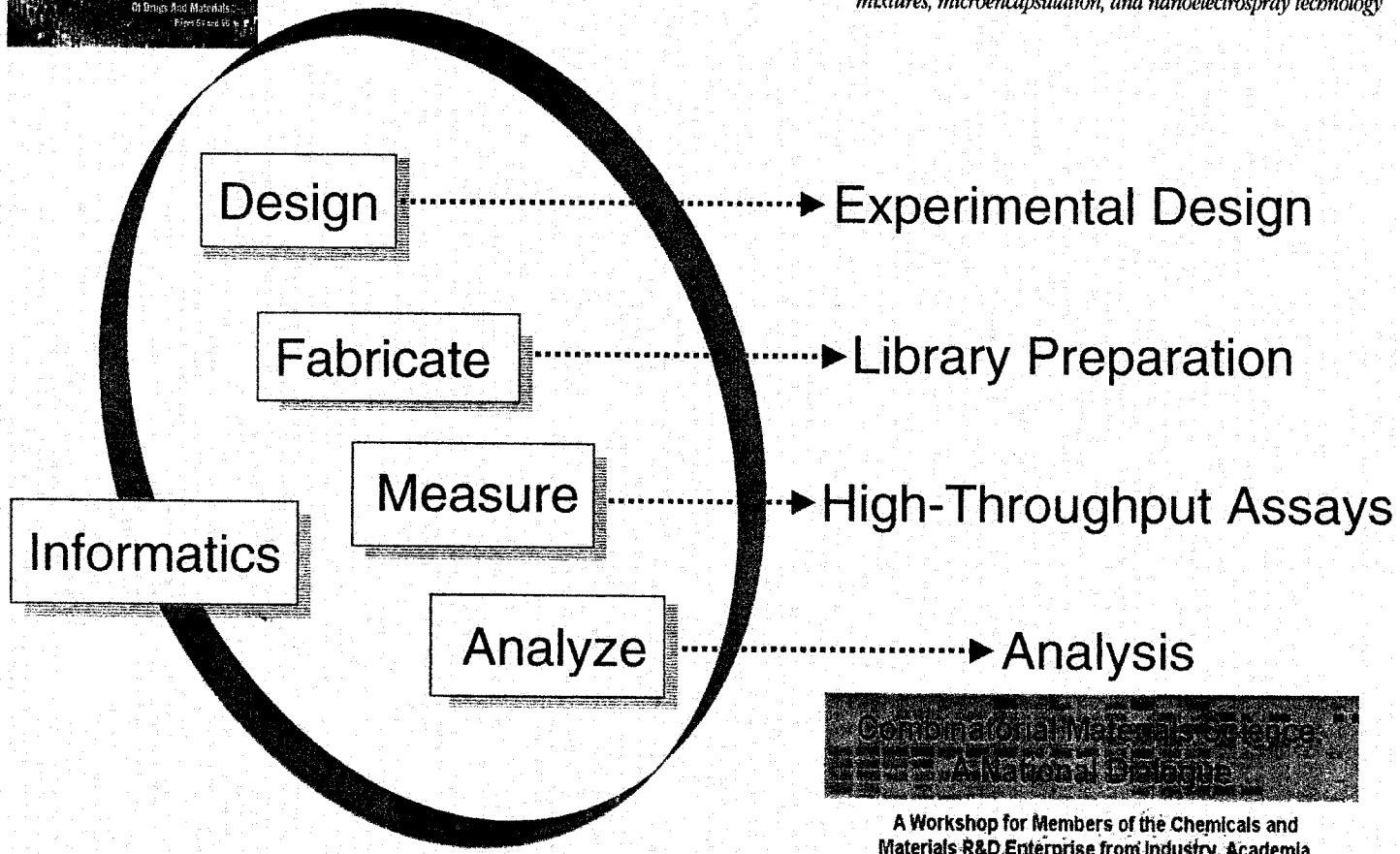

Combinatorial Materials Science: A National Dialogue

A Workshop for Members of the Chemicals and Materials R&D Enterprise from Industry, Academia, and Government

Gaithersburg, Maryland
May 31 - June 1, 2000

NIST National Institute of Standards and Technology

Combinatorial Dewetting Analysis of Polymer Thin Films

- Coatings
- Adhesives
- Electronics
- Biomaterials

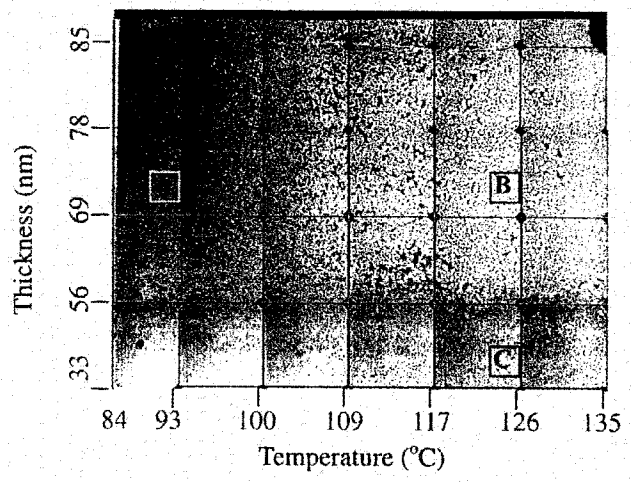

Polystyrene on Silicon Wafer

AFM Images

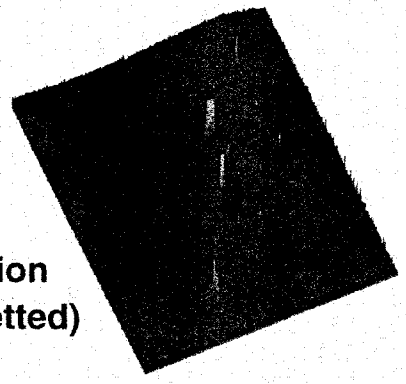

Intact Film Section (not dewetted) Region A

— 20 μm

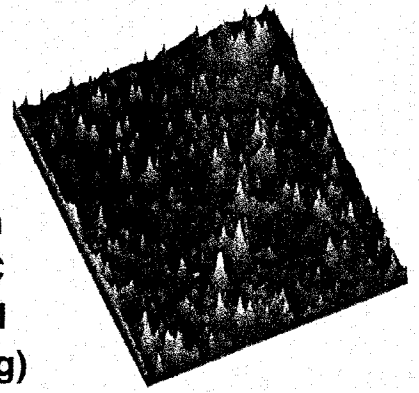

Capillary Waves in Region C (spinodal dewetting)

NIST National Institute of Standards and Technology

ELECTROLYSIS OF WATER IN THE K-12 CLASSROOM

H. Alan Rowe

Chemistry/Center for Materials Research
Norfolk State University
700 Park Avenue
Norfolk, Virginia 23504

Telephone: 757-823-2531
e-mail harowe@nsu.edu

Dr. Rowe is currently a Professor and Chair of the Chemistry Department at Norfolk State University. He is a graduate of UNC-Chapel Hill, North Carolina State University, and was a postdoctoral fellow at Wake Forest University. Dr. Rowe was honored as a Research/Lecturing Fulbright Scholar in South Asia and has been awarded the Teacher of the Year at Norfolk State University. He is the author of numerous research publications as well as several articles on chemical education.

Electrolysis of Water in the K-12 Classroom

Dr. H. Alan Rowe
Professor of Chemistry
Norfolk State University
Norfolk, Virginia 23504

Key Words
Electrolysis, oxygen, hydrogen, electrodes

Pre-requisite knowledge
From none to a general theory of electrolysis depending on the level of the student to which the experiment is presented

Objective
To understand the reactions that occur when water molecules are subjected to an electrical current

Equipment and Materials

3" x 3" piece of cardboard, two pencils sharpened on each end, 100 ml beaker, two wires with alligator clips on each end, salt, 9volt battery, optional materials –other metals and salts

Introduction

When an electrical current is passed through water, hydrogen and oxygen gas is produced. Since distilled water is a non-electrolyte, a source of ions must be added to conduct the current. Optionally, bromothymol blue or other appropriate pH indicators can be added to test for the acid/base changes at each electrode.

$$2\ H_2O \text{ ----------} \rightarrow 2\ H_2 + O_2$$

If models are available have the students make 2 water molecules and then reassemble as per the equation above

Construct the electrolysis apparatus by placing the two sharpened pencils 1" apart through the piece of cardboard. Use the alligator clips to attach the wire to the sharpened pencils and the 9V battery.

Procedure:

1) Put distilled water in the beaker. Predict what will happen when the electrodes are attached. Attach the electrodes to the battery (be sure the wire has a good connection to the graphite of the pencil) and record your observations and conclusions.

DISTILLED WATER IN BEAKER WITH GRAPHITE ELECTRODES

PREDICTION(S):

OBSERVATION(S):

CONCLUSION(S):

2) Put a small amount of sodium chloride [about 0.25g, about ¼ teaspoon in a cup (250 ml) of water and connect the apparatus.]

DILUTE SALT IN BEAKER WITH GRAPHITE ELECTRODES

PREDICTION(S):

OBSERVATION(S)

CONCLUSION(S):

3) Add a large amount of sodium chloride (about 2 g, or 2 teaspoons) and connect the apparatus

CONCENTRATED SALT WITH GRAPHITE ELECTRODES

PREDICTION(S):

OBSERVATIONS(S):

CONCLUSION(S):

4) Several other variables can be studied. Different objects can be used for the electrodes [galvanized and non-galvanized nails (the formation of insoluble Zn salts are observed), copper, steel, different coins, etc)]. Different materials can be used for the electrolyte. In all of the above activities, after observing for a few minutes the connections can be reversed and the results noted.

Comments

At the cathode (negative electrode), sodium and hydrogen ions are available for reduction. Since hydrogen ions are reduced far more easily than sodium ions, they will react to form hydrogen gas

$$2\ H^+\ (aqueous) + 2\ e^- \longrightarrow H_2\ (gas)$$

At the anode (positive electrode), hydroxide and chloride ions are available for oxidation. Hydroxide ions are oxidized more easily than chloride ions in dilute solution so they will react to form oxygen gas.

$$4\ OH^-\ (aq) \longrightarrow O_2\ (g) + 2\ H_20\ (liquid) + 4\ e^-$$

[Hydrogen and oxygen gas should be expected to be produced in what ratio ?]

While there is no net change in pH, there is a localized change. Examining the equations above there should be a loss of hydrogen ions at the cathode and a loss of hydroxide ions at the anode. Added bromothymol blue is blue, green, and yellow at pHs that are basic, neutral, and acid, respectively. [Which electrode will become more acidic? Explain]

TESTS FOR GASES PRODUCED

Hydrogen and oxygen gas have low solubilities in water and will appear as bubbles. Chlorine gas, if it forms, is more soluble and will not form bubbles until the water is saturated. [Give the balanced equation for the production of chlorine gas at the anode]

If the gases are collected, oxygen gas will cause a glowing splint to flare, hydrogen gas will cause a glowing splint to pop, and chlorine will cause a solution of KI to turn brown. Both Hydrogen and oxygen gas are colorless and odorless, chlorine gas is greenish-yellow and has a strong unpleasant odor (Take care to provide adequate ventilation).

References

Brown, LeMay, and Bursten, *Chemistry, The Central Science,* 8th Edition, Prentice-Hall (2000)

TEACHING UNDERGRADUATES RESULTS FROM RECENT RESEARCH AS PART OF A LABORATORY CLASS: X-RAY DIFFRACTION EXPERIMENT

L. J. Martínez-Miranda

Department of Materials and Nuclear Engineering
University of Maryland
College Park, Maryland 20742-2115

Telephone 301-405-0253
e-mail martinez@eng.umd.edu

L. J. Martinez-Miranda

Biography:

L. J. Martínez-Miranda is Associate Prof. of Materials in the Dept. of Materials and Nuclear Eng at the University of Maryland – College Park. She received her bachelor's and master's degree in Physics from the Universidad de Puerto Rico in Río Piedras, a bachelor's in Music degree from the Conservatory of Music of Puerto Rico and her doctoral degree in Physics from Massachusetts Institute of Technology. At Maryland she has been responsible for designing the junior level laboratory undergraduate course with the help of her colleagues, and has taught the introductory design course and the physics of materials course. She is the faculty coordinator for the NSF-MRSEC Research Experiences for Undergradautes and is a co-PI in the University's G K-12 program. Her interest is in X-ray scattering from liquid crystals and related nanomaterials and solid films.

Teaching Undergraduates Results From Recent Research As Part of a Laboratory Class: An X-ray Diffraction Experiment

L. J. Martínez-Miranda
University of Maryland, Dept. of Materials and Nuclear Eng., College Park, MD, 20742-2115

Key Words: X-ray diffraction, powder, texture, nanocrystalline and nanometer size sample, time-dependent structure

Prerequisite Knowledge:

What is X-ray diffraction?
What characteristics of a material can X-ray diffraction measure?
In what size range does it measure these (angstroms, microns)?
What is a powder sample?
What is a textured sample?

Objective:

How can X-rays be used to distinguish between samples prepared using different methods, i.e., different times? How can X-rays be used to distinguish between samples of different thickness?

Equipment:

1. An X-ray diffractometer
2. Two samples prepared at different times
3. A computer with any plotting program

Introduction:

Copper samples prepared using electrodeless deposition on Aluminum Nitrade (AlN) substrates have been studied for interconnections. The method of deposition is less intrusive than other methods, which require the use of catalysts on an electrically insulated surface. The quality of the samples depends both on the direction of coating and the time the solution is refluxed. The samples which were prepared horizontally (parallel to the bottom of the flask) seemed to contain more Cu_2O than the samples prepared vertically (perpendicular to the bottom of the flask)[1,2]. In both samples, the structural evolution was that Cu was more textured for lesser times and more polycrystalline for longer times in the reflux. The students will look at the effect of time on the structure of the films[3].

polycrystalline for longer times in the reflux. The students will look at the effect of time on the structure of the films[3].

Samples of lead-zirconium-titanium (PZT) oxide have been prepared using pulsed laser deposition (PLD to different thickness on lanthanum aluminate (LAO). LAO is chosen because its lattice constant is almost matched to that of the a-lattice constant of tetragonal PZT. Because it is not exactly matched, variation on the c-lattice of PZT can be observed which in turn reflects the variation of the a-lattice parameter as a function of thickness[4]. This has consequences on the properties of the PZT, in particular the ferroelectric properties. Although the students do not look at the ferroelectric properties, there is a discussion on how the structure is related to them and how altering the lattice parameters (a and c) will affect the polarization of the film. The need for this film to be grown in single crystal form (epitaxy) is also discussed.

Procedure:

The students begin by looking at a standard silicon sample to become familiar

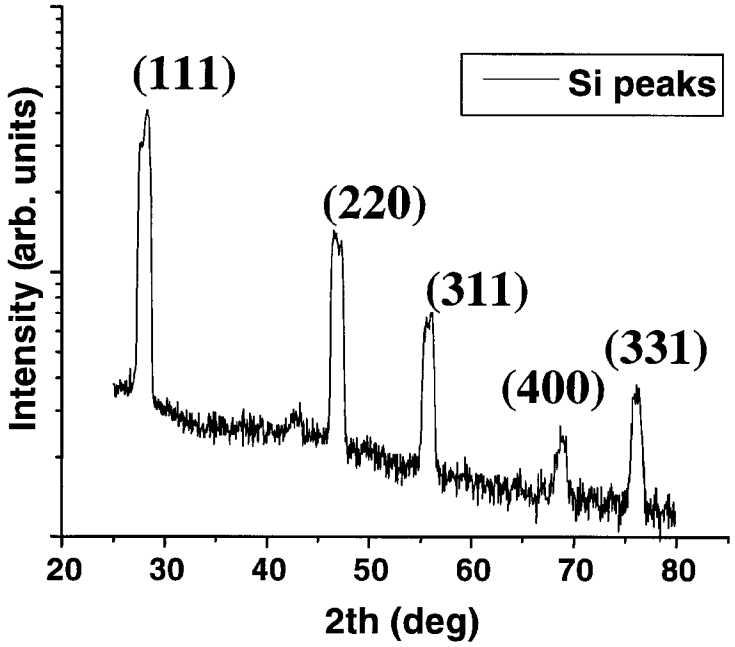

Figure 1. Results of the scan in a standard silicon sample.

with the structural analysis of powders. They do a $\theta - 2\theta$ scan, illustrated in Figure 1. Students are asked to compare the peaks observed with those given in the X-ray cards (which they are asked to bring) and to see how the intensities compare.

Two films of cupper prepared at 20 minutes and 30 minutes are analyzed, using θ–2θ scans. Depending on class size, one group does the analysis for the 20 minute film and the other the 30 minutes. They have gone to the library to find the card for Cu. We

also ask them to get the cards for Cu_2O and for AlN. They have used the cards to compare the scans obtained for the crystalline sample and to see that the relative intensities compare with the ones cited on the cards.

After obtaining the θ–2θ scans, they compare it to the cards and identify each peak observed. They take the relative intensity of the x-ray peaks, especially the stronger ones, and comment on the results. If two groups are doing different samples, they get together and compare and exchange results. They comment on the different times the sample spent on the reflux. Their results are similar to those presented in Figure 2.

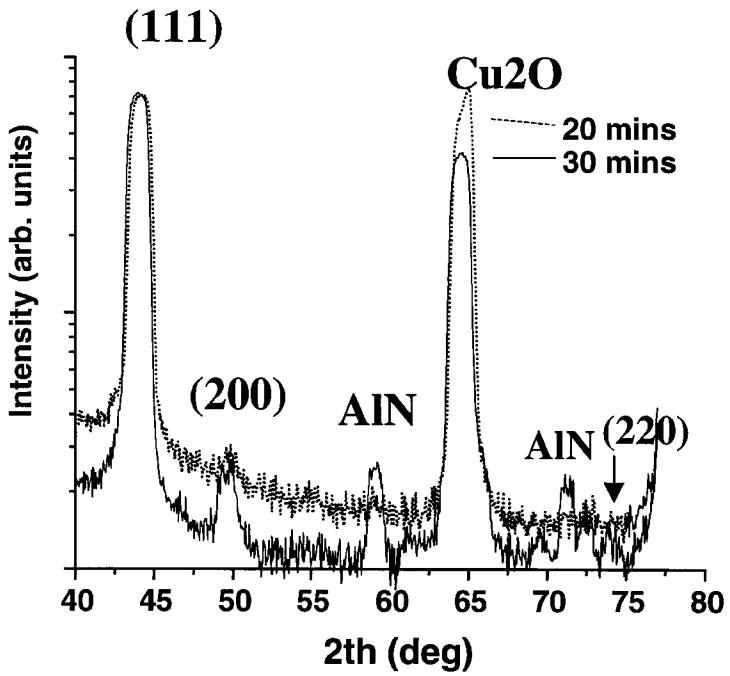

Figure 2. Results of the scan obtained from the Cu samples prepared at 30 minutes and 20 minutes.

The students proceed to look at a single crystalline sample. We chose LAO, because that is the crystal on which the films of PZT are deposited. They are taught how to center the sample such that the peak is maximized. The students go to a known peak, at 23.4°. They proceed to rock the sample about θ, until the maximum θ is obtained. The value of θ maximum is defined as one-half of 23.4°. Then they take a θ–2θ to make sure the centering has been done correctly and to check the maximum. The process is illustrated in Figures 3 and 4.

The students then study the PZT films as a function of thickness. One group receives the 500Å sample and the other receives the 2500Å. The sample is centered according to the previous paragraph, at the same 2θ as before, since the films have been

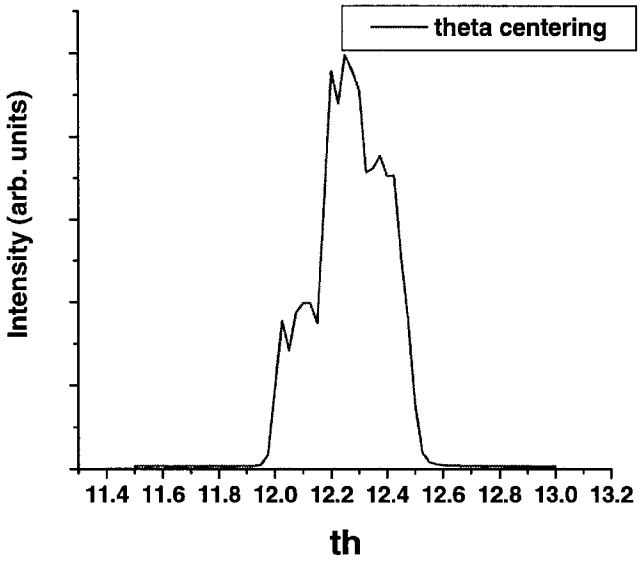

Figure 3. Theta centering at 2theta equal 23.4°. The maximum theta at 12.25° is set to 11.7°, or half of 23.4°.

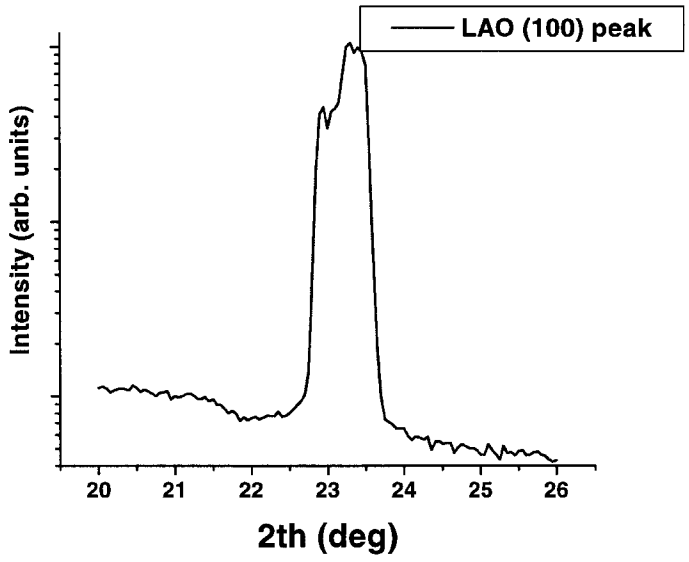

Figure 4. θ–2θ scan of the 23.4° peak of LAO, after θ was reset as explained in Figure 3.

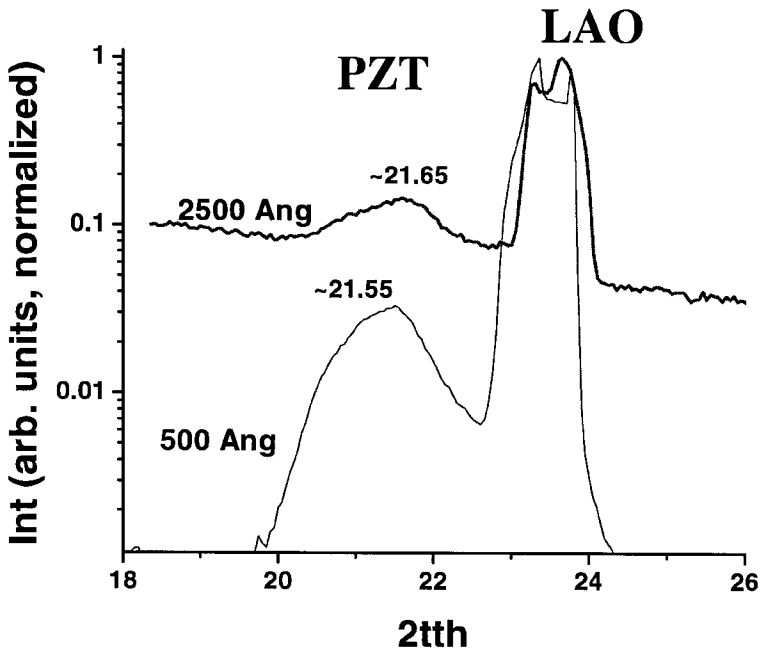

Figure 5. Superposition of the 500Å and 2500Å films, showing that for 500Å film has a larger c-axis parameter (a smaller 2θ). The 500Å was a larger sample: that's why it has a stronger signal.

grown on LAO. A θ–2θ is then taken to look at the peak from the film plus the peak at 23.4° from LAO. This last peak is recentered such that it coincides in both scans, the one on the 500Å and the one on the 2500Å. The students compare the positions of the peak to those presented in reference 4. The students discuss the evolution of the c-peak as the films get thicker. A discussion on the effect of the substrate on the lattice parameters of the epitaxial film follows. Results are shown in Figure 5.

Comments:

This experiment aids in introducing the students to the effects of materials processing on sample structure. The experiment serves as a study of textured samples alone. Any kind of processing that leads to a different structure can be used, as well as any kind of material. The aim is for the students to realize how useful X-ray diffraction can be.

The students are asked what is different about each sample, and how do they think the structure comes about. The purpose is to get them to think about how processing affects the structure and also the properties. The instructor can mention how properties are affected by the orientation of the crystal. This discussion is very basic; the students

have seen this in elementary terms in their introduction to materials class, and will see it later in the physics of solids class.

In the part that concerns the Cu materials in the report, the students are asked to: a. Plot both graphs; b. Write down the relative intensities of the different peaks; c. Identify, if possible the other peaks, based on the cards; d. Comment on how the preparation time affects the structure of the sample. They are not asked to calculate the texture of the samples: the experiment, due to limitations in equipment is done on a machine which cannot take angles higher than 90°. More angles are needed to measure the texture. For the PZT films on LAO, the students are asked to: a. plot both graphs; b. explain how they go about centering a single crystal and epitaxial film in the diffractometer; c. compare the position of the c-axis peak to the one obtained from reference 4 and given by the instructor.

When time allows, the instructor gives the students more details on the research. For example, the instructor tells the student that studies on the samples were done with different X-ray energies, and that these energies and the absorption properties of the sample can limit the depth the X-rays can penetrate, into the sample which allows for a study of the structure as a function of depth.

All of the results presented were taken as part of the class in the Fall of 2001.

References

1. G. M. Chow, L. K. Kurihara, D. Ma, C. R. Feng, P. E. Shoen, and L. J. Martínez-Miranda, Appl. Phys. Lett., 70, 2315 (1997).

2. L. J. Martínez-Miranda, Yiqun Li, G. M. Chow and L. K. Kurihara, NanoStructured Materials, 12, 653 (1999).

3. Samples donated by Lynn K. Kurihara (NRL).

4. V. Nagarajan, I. G. Jenkins, S. P Alpay, H. Li, S. Aggarwal, L. Salamanca-Riba and R. Ramesh, JAP, 86, 595 (1999).

THE DISTRIBUTION OF ELECTROMAGNETIC ENERGY IN A MICROWAVE OVEN

J. N. Dahiya

and

Wendy Decker

Physics Department
Southeast Missouri State University
One University Plaza
MS 6600
Cape Girardeau, Missouri 63701

Telephone: 573-651-2390
e-mail dahiya@physics.semo.edu

and

Aman Anand

Computer Science Department
Southeast Missouri State University
One University Plaza
Cape Girardeau, Missouri 63701

e-mail amanfromcs@hotmail.com

Aman Anand

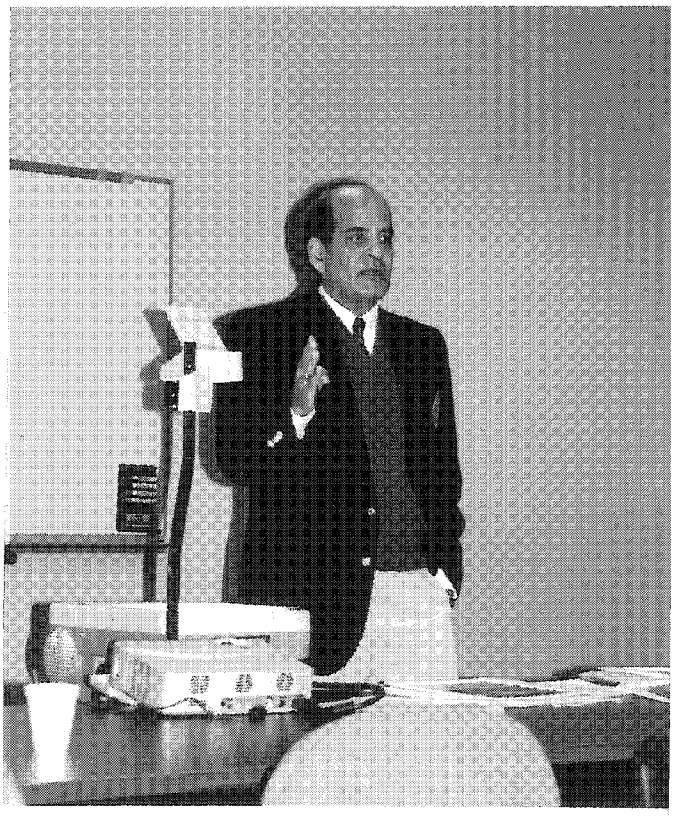

J. N. Dahiya

The Distribution Of Electromagnetic Energy In A Microwave Oven

Jai N. Dahiya & Wendy Decker
Physics Department
dahiya@physics.semo.edu
And
Aman Anand
Computer Science Department
amanfromcs@hotmail.com

Southeast Missouri State University
One University Plaza,Cape Girardeau, Mo-63701

KEY WORDS

Microwaves, Temperature, Heat Distribution, Frequency

OBJECTIVES

The main Objective of this experiment is to study the distribution of temperature in a food sample placed inside the microwave oven.

SUMMARY

Electromagnetic Distribution of the microwave field is studied by placing the food sample inside a microwave oven. This distribution is studied in terms of change of temperature as the microwaves are absorbed by a particular food sample. A series of thermometers are probed in a circular fashion in the food sample. The penetration depth of these thermometers are kept constant. The microwave oven is turned on for a certain time and the thermometers are read as quickly as possible as discussed in the procedure section of this paper. The distribution of temperature is related to the microwave field pattern inside the microwave oven.

Introduction And Theory

This paper is being written for the scientific investigators who wish to understand in detail the concept of microwave spectroscopy and use in their research laboratories the techniques of microwave heating. A mental or a physical picture of complete electromagnetic spectrum as a classified array of energy sources is a valuable aid to the scientists. In this experiment over microwave heating certain tests are performed and conclusions are drawn about the spectrum developed within a microwave oven.

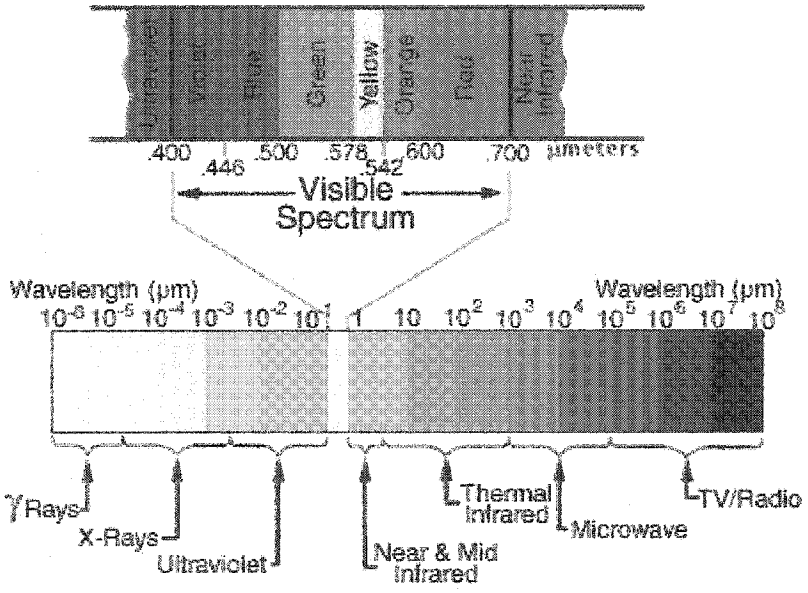

Figure A. Electromagnetic Spectrum from radio waves to gamma rays

The picture in figure A above, is an electromagnetic spectrum and the frequency ranges between 300 MHz to 300 GHz for the microwaves. The microwaves within the microwave oven is 2.4 GHz. We know that in general, the food placed within the microwave oven has water contents. The water is a polar compound and has a permanent

dipole. Within the microwave oven these water molecules develop a dipole moment and experience a force (torque between the two charges separated by a distance) and in turn these dipoles then start oscillating with the same frequency as those of the microwaves. With these oscillations the water molecules follow the frequency of the microwaves and then transfer the heat content to the material. In the process of Free Induction Decay the water particles in food sample placed inside the microwave oven get converted into vapor phase and get induced dipole charges which promotes heating.

Figure B. Free Induction Decay

Depending on how many spectral lines are in the region being scanned these FID's can be simply, a singly oscillating (sinusoidal or cosinusoidal) function with a superimposed exponential decay. However when more than one line is present in the region being

scanned we often see two or more different frequencies in the FID pattern (such as the one above). These frequencies correspond to differences between the natural absorbance frequency of the molecule and the frequency of the light in the cavity. We can accurately determine the natural frequency of the molecule by doing a Fourier Transform of the FID and adding (or subtracting) the difference frequency from the frequency of the light in the cavity. The Fourier Transform of this FID is shown in figure C.

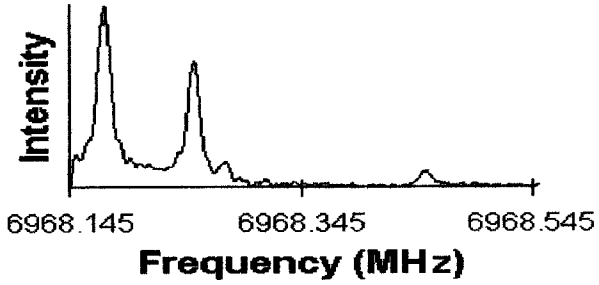

Figure C. Fourier Transform

PROCEDURE

Following procedure was used in conducting this experiment:

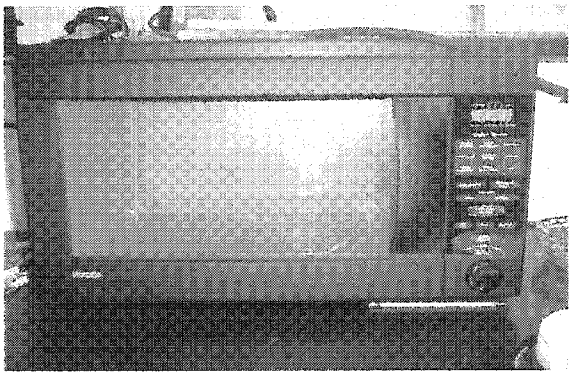

Figure D. The Microwave Oven used in this experiment

1. The sample taken into consideration was frozen New York Style Cheese Pie.
2. Then the dimensions(diameter , depth of the sample were recorded.)
3. Using a protractor and compass 9 different plots were made in an octagonal form for placing the thermometers dipped in water initially at room temperature as shown in the figure below:

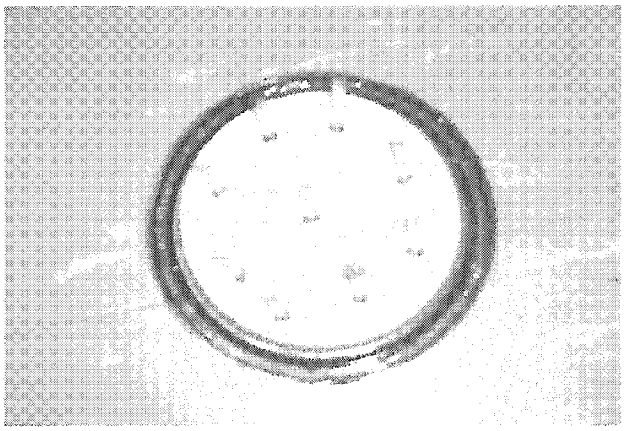

Figure E. Distribution of Thermometer probes inside the food sample

4. The initial temperature of thermometer was recorded.

5. Thermometers were inserted and they were marked 1 – 9 clockwise as shown in figure E.
6. The initial temperature of the cheese pie was recorded for all the 9 plots.
7. The sample was placed with thermometers into a microwave oven as shown in figure D, and experiment was performed in two different parts

PART A:

1. The frequency of the thermometers was kept 50 % and the time was 30 seconds and the turntable of the oven was also off.
2. The microwave oven was switched on and after 30 seconds of heating the final temperature was recorded for all the 9 plots . It was made sure that the temperature recording was done most efficiently.
3. The sample was kept in deep freezer for cooling for 5 hours. This was done just to make sure that next time the experiment was performed the sample reaches the same temperature as for the first reading.
4. The whole procedure (step 1-3) was repeated for 5 different times.

PART B:

1. Now this time the frequency of the microwave oven was increased to 100 % and the time was 30 seconds, but the turntable was left on.
2. Then the microwave oven was switched on and after 30 seconds of heating the final temperature was recorded for all the 9 plots. It was made sure that the temperature recording was done most efficiently.
3. Then the sample was kept in deep freezer for cooling for 5 hours. This was done just to make sure that next time the experiment was

performed the sample reaches the same temperature as for the first reading.

4. The whole procedure (step 1-3) was repeated for 5 different times.

From both the styles of observations we determined the temperature shift and tried to determine the relation between the frequency and temperature change within a microwave oven. Experiment was conducted a number of times by changing the variables such as the diameter of the plots, turntable, frequency and the time interval of heating. The data of the experiment performed has been shown as tables underneath with their supporting graphs.

ANALYSIS:

From the experiment conducted above there are certain inferences that were drawn.

1. The temperature efficiency depended upon the probes distribution(circular,linear)
2. The thermometers labeled 8^{th} and 9^{th} showed the maximum temperature change.
3. The efficiency of heating was more when the turntable was left on.
4. There were certain regions that was close to the magnetron that received maximum heat waves.
5. During the experiment between two readings food sample was placed in deep freezer for 5 hours , so that the initial temperature was always the same.
6. When the frequency of the microwave oven was kept 100% maximum efficiency was obtained.

7. The data taken for various runs is shown in data tables 1 – 8 and the final results are shown in graphs 1 - 8.

References

1. Cutnell & Johnson, Physics, 5th Edition, Wiley Publishing Co, 2000
2. Watson ,"Microwave Semiconductor Devices And Their Circuit Applications", McGraw Hill Company 1969
3. V. L. Granatstein, "Applications Of High Power Microwaves", Archtech House Inc, 1994
4. David A. Copson, "Microwave Heating", The Avi Publication, 1975
5. Przybylinska przyby@ifpan.edu.pl
6. J. Van Bladel, Electromagnetic Fields, McGraw Hill, New York, Ch.10,1964
7. C.H. Townes and A.L. Schawlow, Microwave Spectroscopy, McGraw-Hill, New York, 1961

Trial 1/Table 1

Eight thermometers were placed in a circle of radius 4 cm.
The ninth thermometer was placed in the center.
The depth of each thermometer was set at 2.3 cm.
The microwave was on for 30 seconds at full power.
The turntable was ON.

Location of thermometer probe (x axis)	Location of thermometer probe (y axis)	Change in temperature (°C)
0	-4	5.125
2.828	-2.828	4.5
4	0	4.9
2.828	2.828	5.83333
0	4	6.89286
-2.828	2.828	6.85714
-4	0	6.39286
-2.828	-2.828	6.85714
0	0	5.66667

Trial 2/Table 2

Eight thermometers were placed in a circle of radius 4 cm.
The ninth thermometer was placed in the center.
The depth of each thermometer was set at 2.3 cm.
The microwave was on for 30 seconds at full power.
The turntable was OFF.

Location of thermometer probe (x axis)	Location of thermometer probe (y axis)	Change in temperature (°C)
0	-4	4.16667
2.828	-2.828	5.8
4	0	5.25
2.828	2.828	3.92857
0	4	5.61111
-2.828	2.828	4.5
-4	0	4.625
-2.828	-2.828	3.5
0	0	4.27778

Trial 3/Table 3

Eight thermometers were placed in a circle of radius 4 cm.
The ninth thermometer was placed in the center.
The depth of each thermometer was set at 2.6 cm.
The microwave was on for 30 seconds at full power.
The turntable was ON.

Location of thermometer probe (x axis)	Location of thermometer probe (y axis)	Change in temperature (°C)
0	-4	3.4375
2.828	-2.828	4.125
4	0	5
2.828	2.828	5.25
0	4	6.3125
-2.828	2.828	6.5
-4	0	6
-2.828	-2.828	5.0625
0	0	4.07143

Trial 4/Table 4

Eight thermometers were placed in a circle of radius 4 cm.
The ninth thermometer was placed in the center.
The depth of each thermometer was set at 2.6 cm.
The microwave was on for 30 seconds at full power.
The turntable was OFF.

Location of thermometer probe (x axis)	Location of thermometer probe (y axis)	Change in temperature (°C)
0	-4	3.83333
2.828	-2.828	4.91667
4	0	3.14286
2.828	2.828	4.64286
0	4	4.85714
-2.828	2.828	5.08333
-4	0	3.83333
-2.828	-2.828	4
0	0	4.85714

Trial 5/Table 5

Eight thermometers were placed in a circle of radius 5 cm.
The ninth thermometer was placed in the center.
The depth of each thermometer was set at 2.3 cm.
The microwave was on for 30 seconds at full power.
The turntable was ON.

Location of thermometer probe (x axis)	Location of thermometer probe (y axis)	Change in temperature (^{o}C)
0	-5	4.08333
3.535	-3.535	4.6875
5	0	5.5
3.535	3.535	6.8125
0	5	7.21429
-3.535	3.535	6.88889
-5	0	6.42857
-3.535	-3.535	5.35714
0	0	5.1875

Trial 6/Table 6

Eight thermometers were placed in a circle of radius 5 cm.
The ninth thermometer was placed in the center.
The depth of each thermometer was set at 2.3 cm.
The microwave was on for 30 seconds at full power.
The turntable was OFF.

Location of thermometer probe (x axis)	Location of thermometer probe (y axis)	Change in temperature (^{o}C)
0	-5	5.83333
3.535	-3.535	5.57143
5	0	6
3.535	3.535	3.83333
0	5	4.0625
-3.535	3.535	5.42857
-5	0	4.57143
-3.535	-3.535	5.5
0	0	4

Trial 7/Table 7

Eight thermometers were placed in a circle of radius 5 cm.
The ninth thermometer was placed in the center.
The depth of each thermometer was set at 2.0 cm.
The microwave was on for 30 seconds at full power.
The turntable was ON.

Location of thermometer probe (x axis)	Location of thermometer probe (y axis)	Change in temperature (°C)
0	-5	4.92857
3.535	-3.535	5.14286
5	0	6.5
3.535	3.535	6.375
0	5	5.91667
-3.535	3.535	6.16667
-5	0	5.85714
-3.535	-3.535	6
0	0	4.71429

Trial 8/Table 8

Eight thermometers were placed in a circle of radius 5 cm.
The ninth thermometer was placed in the center.
The depth of each thermometer was set at 2.0 cm.
The microwave was on for 30 seconds at full power.
The turntable was OFF.

Location of thermometer probe (x axis)	Location of thermometer probe (y axis)	Change in temperature (°C)
0	-5	4.58333
3.535	-3.535	7.4375
5	0	7.57143
3.535	3.535	5.64286
0	5	4.21429
-3.535	3.535	6.66667
-5	0	4.2
-3.535	-3.535	6.25
0	0	4.25

Figure 1

Average Change in Temperature (°C)

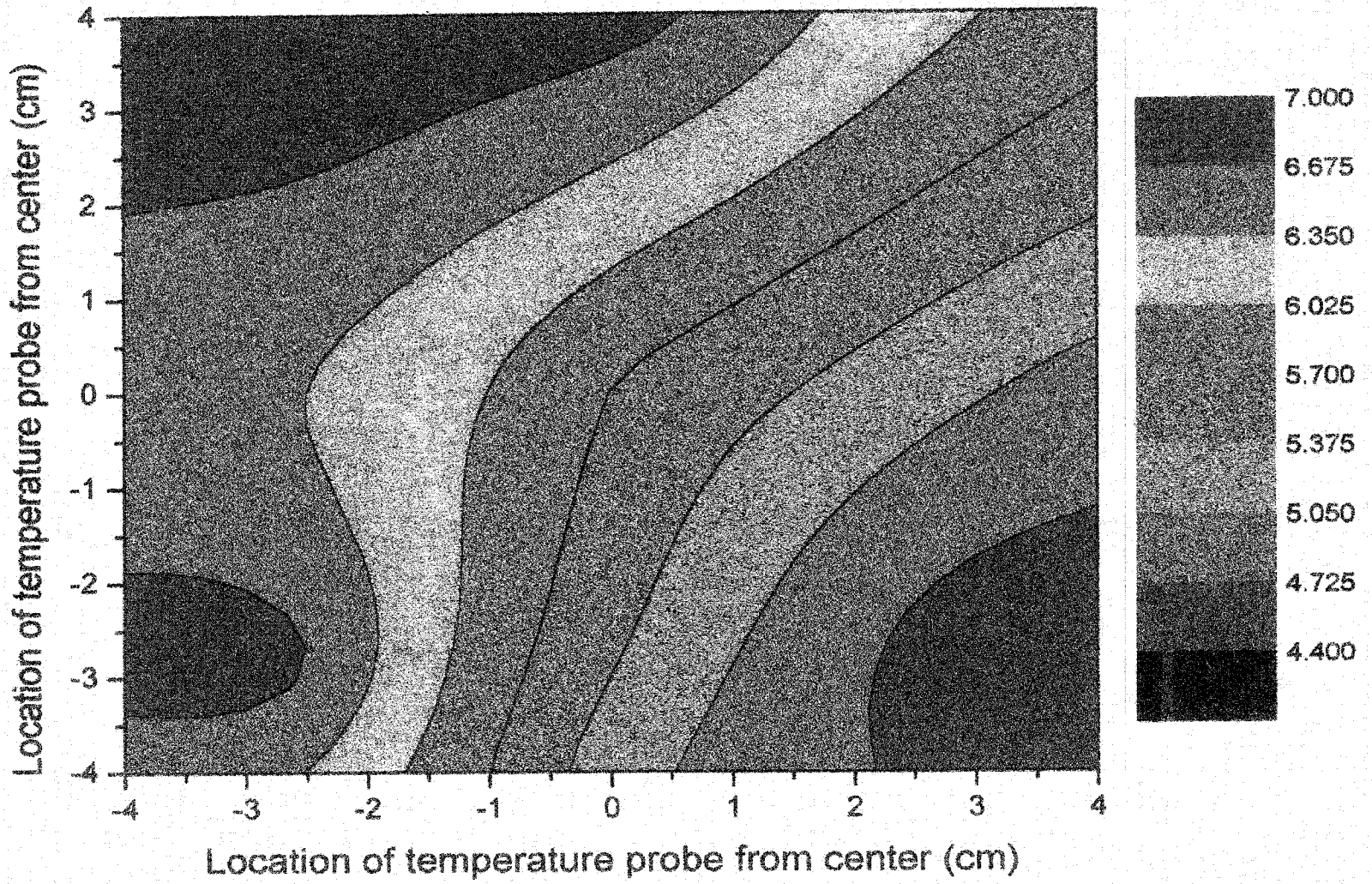

Figure 2

Average Change in Temperature (°C)

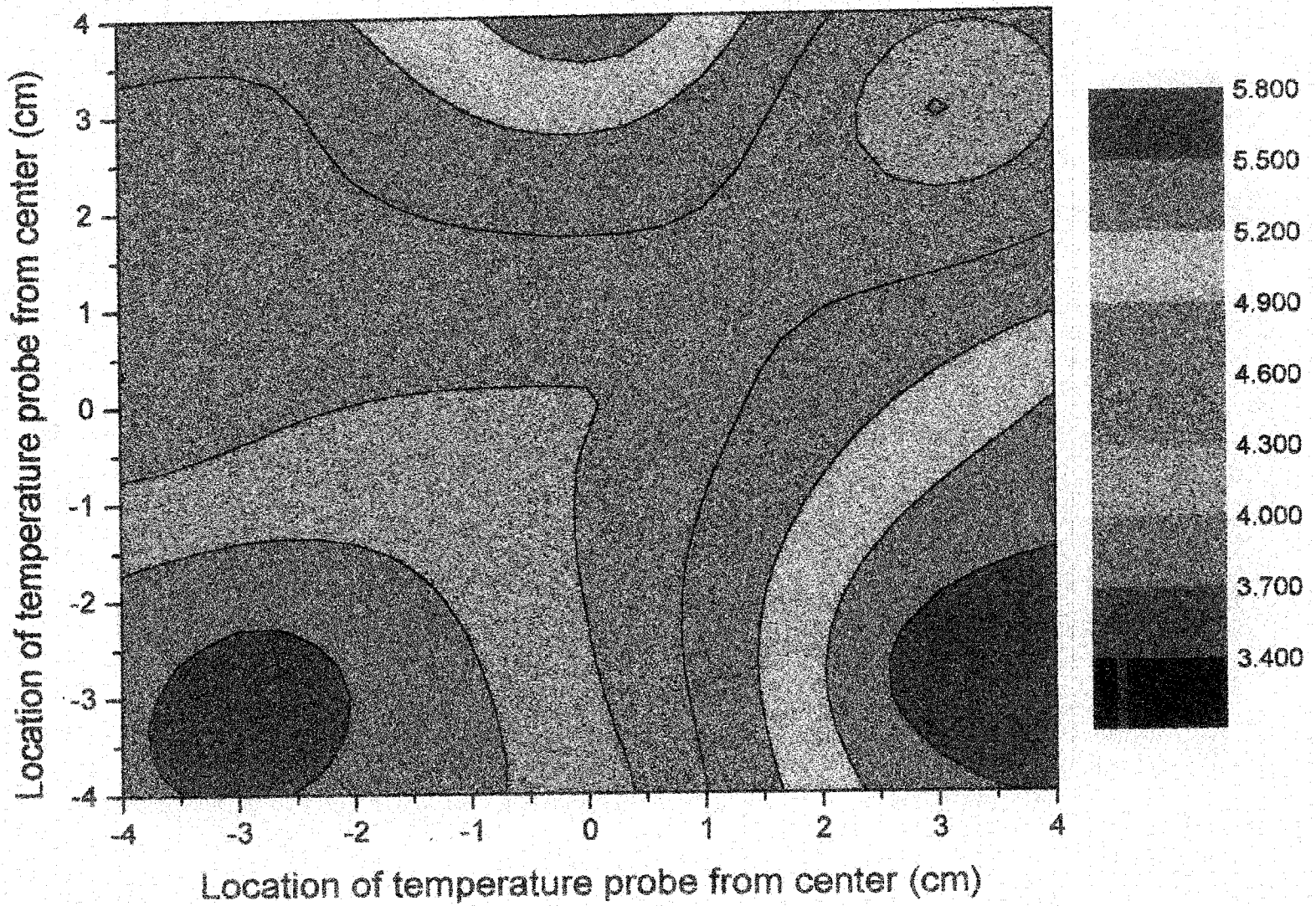

Figure 3

Average Change in Temperature (°C)

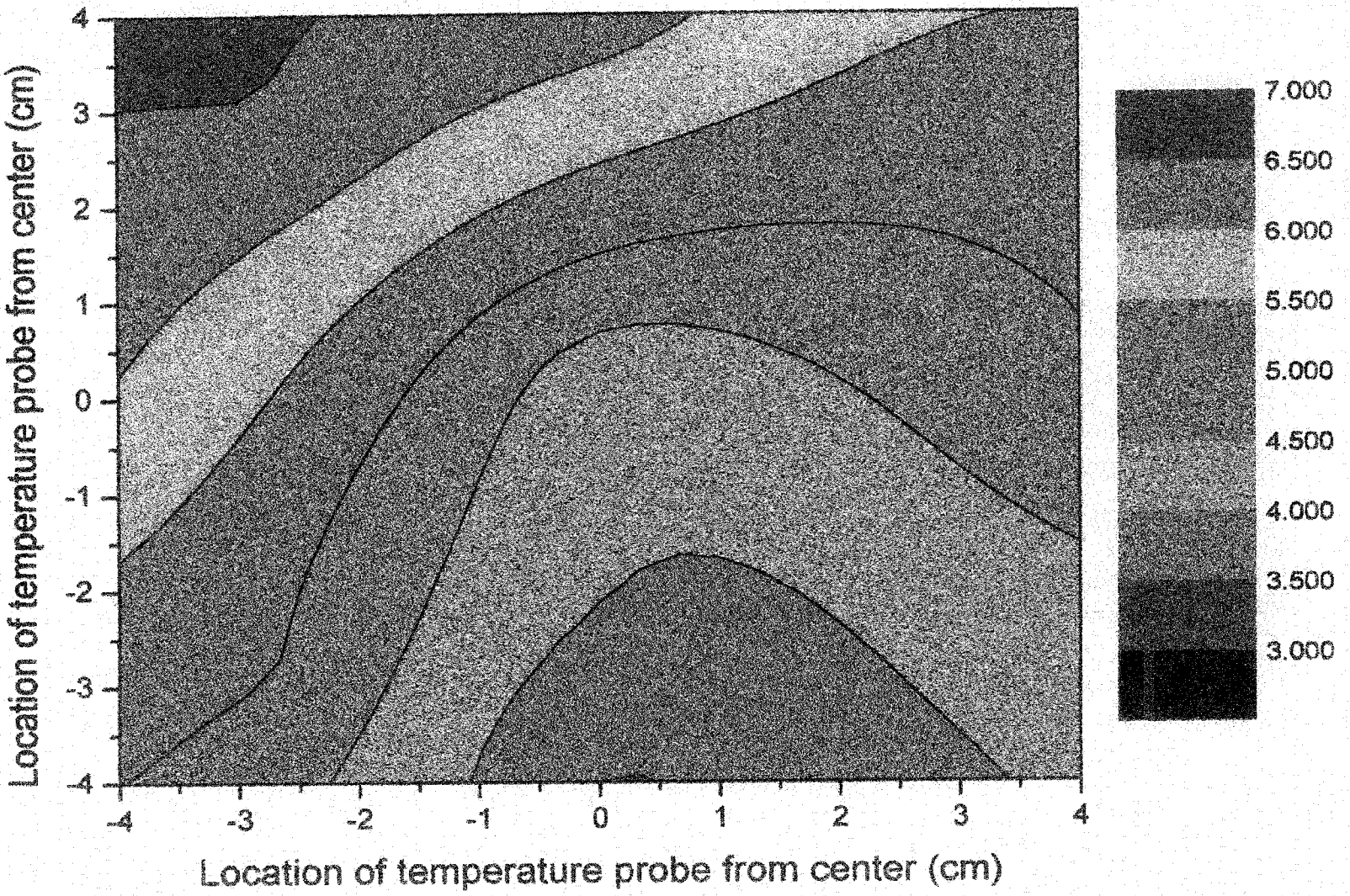

Figure 4

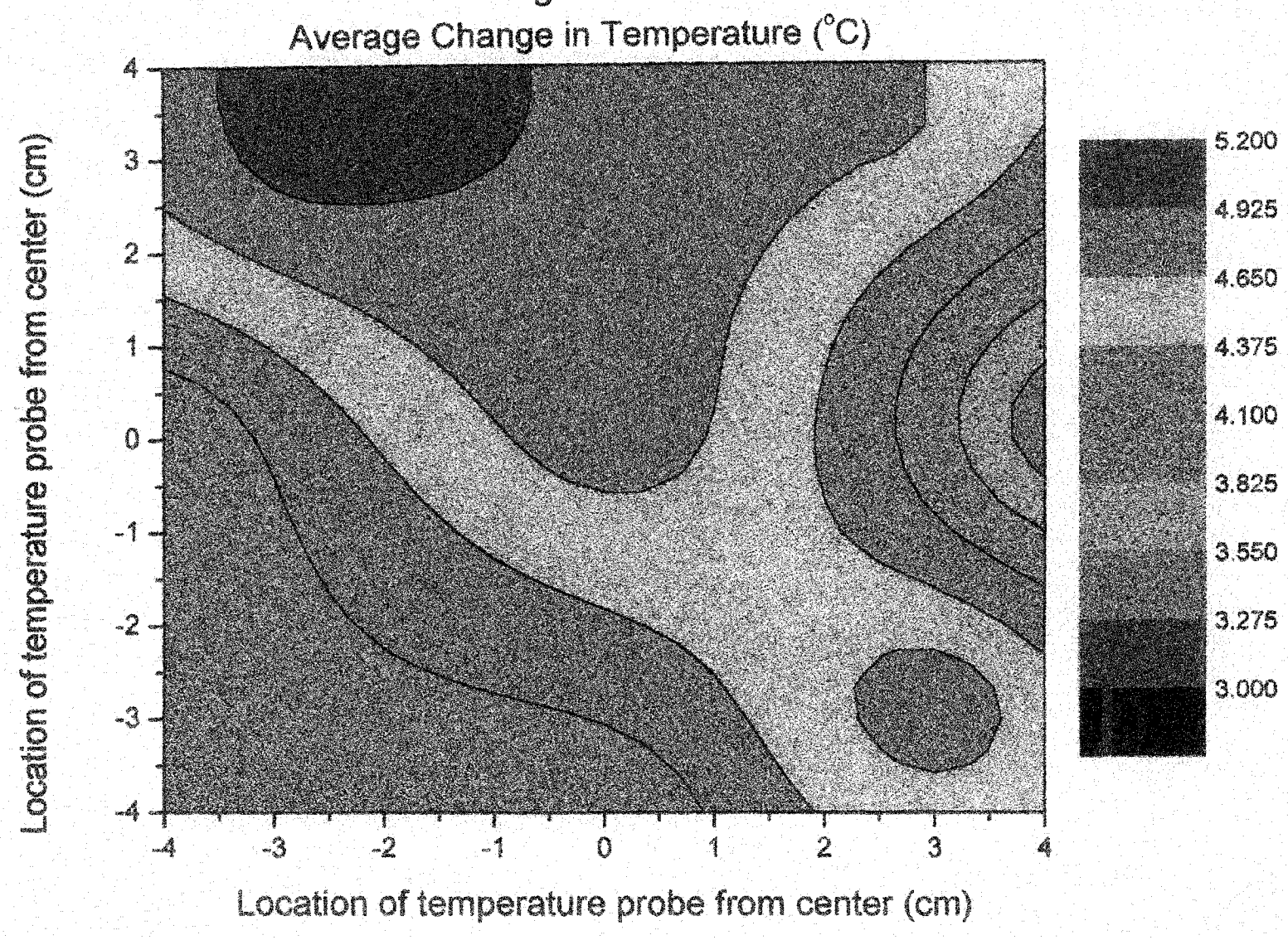
Average Change in Temperature (°C)
Location of temperature probe from center (cm)
Location of temperature probe from center (cm)
4
3
2
1
0
-1
-2
-3
-4
-4
-3
-2
-1
0
1
2
3
4
5.200
4.925
4.650
4.375
4.100
3.825
3.550
3.275
3.000

Figure 5

Average Change in Temperature (°C)

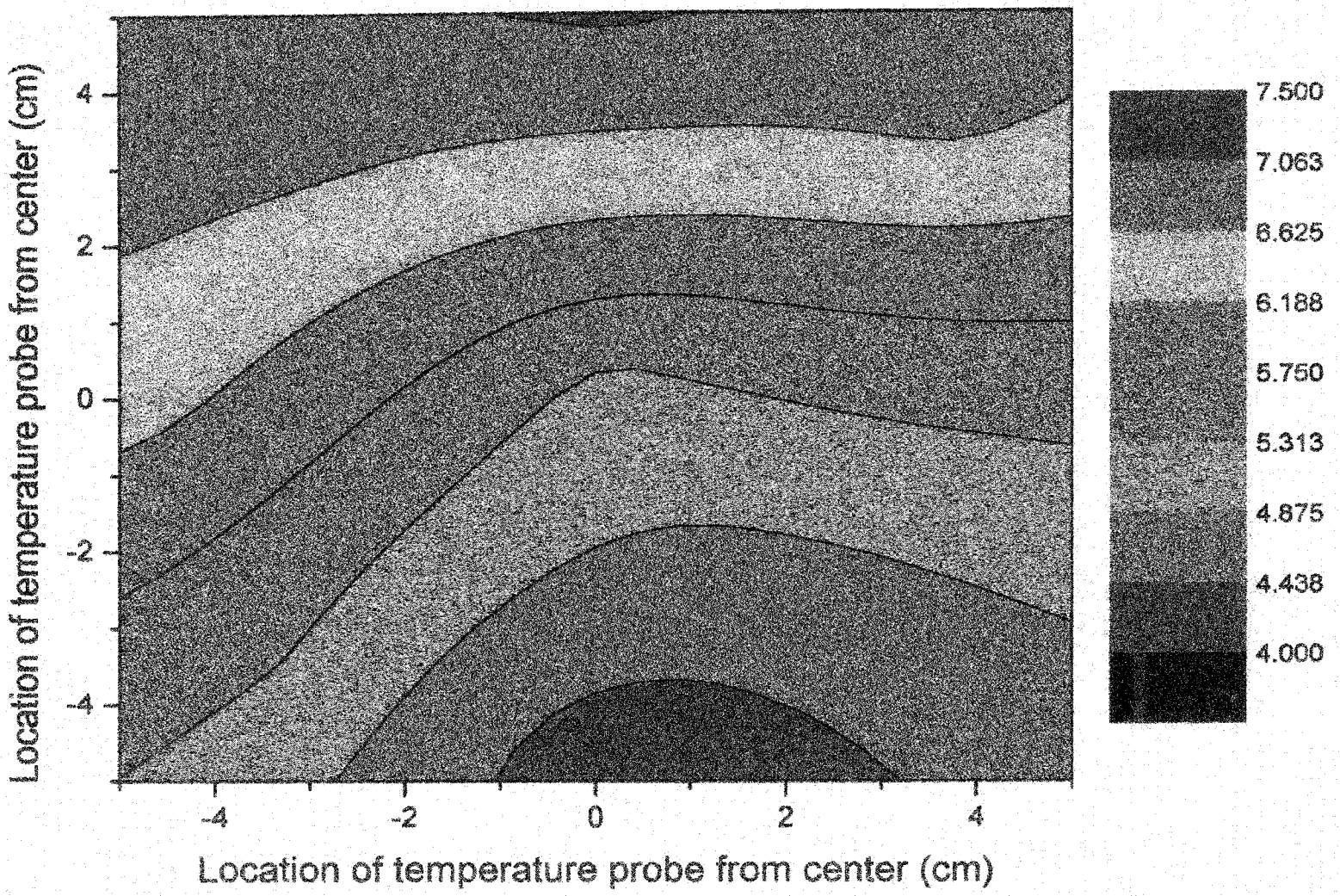

Figure 6

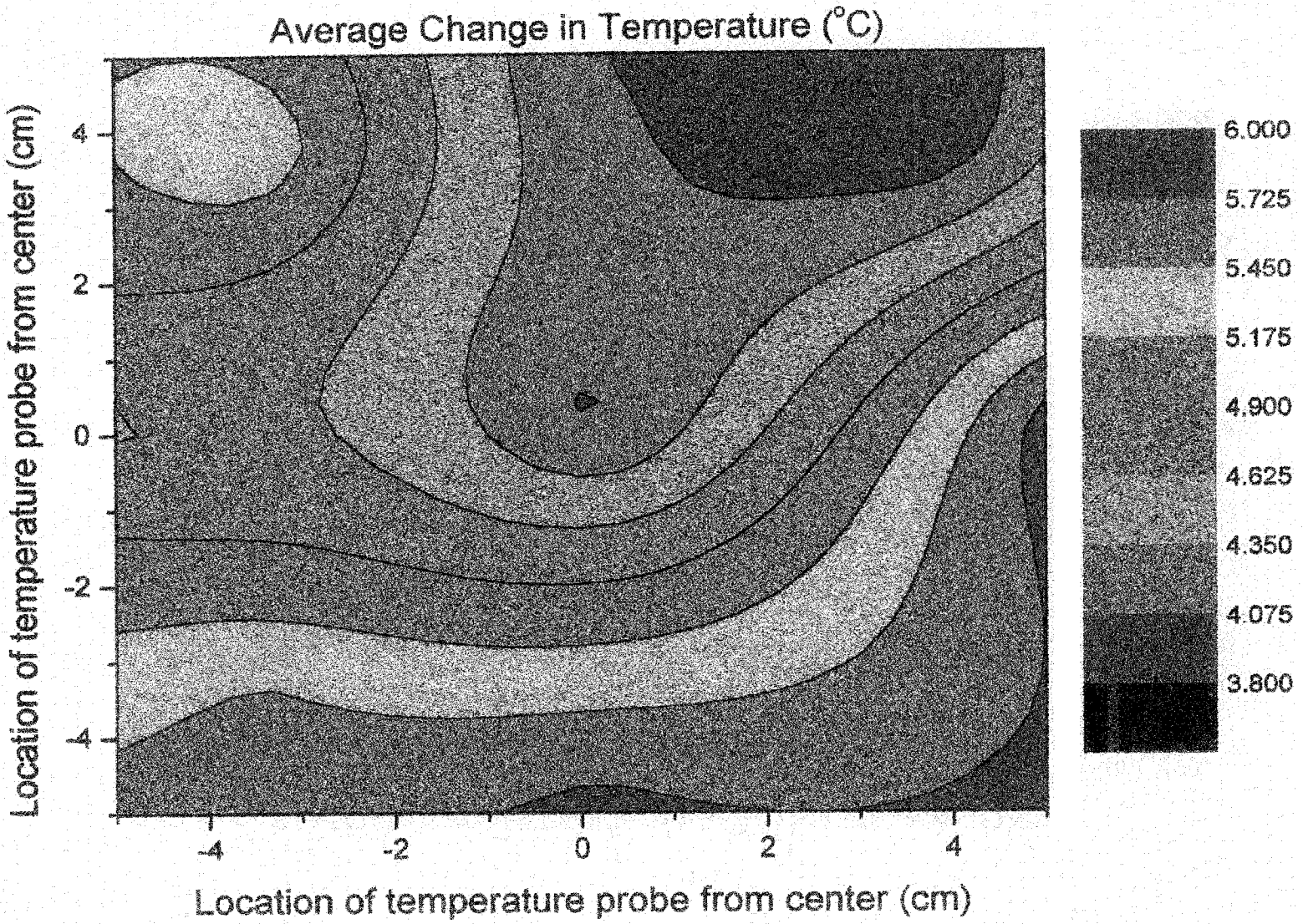
Average Change in Temperature (°C)
Location of temperature probe from center (cm)
4
2
0
-2
-4
-4
-2
0
2
4
Location of temperature probe from center (cm)
6.000
5.725
5.450
5.175
4.900
4.625
4.350
4.075
3.800

Figure 7

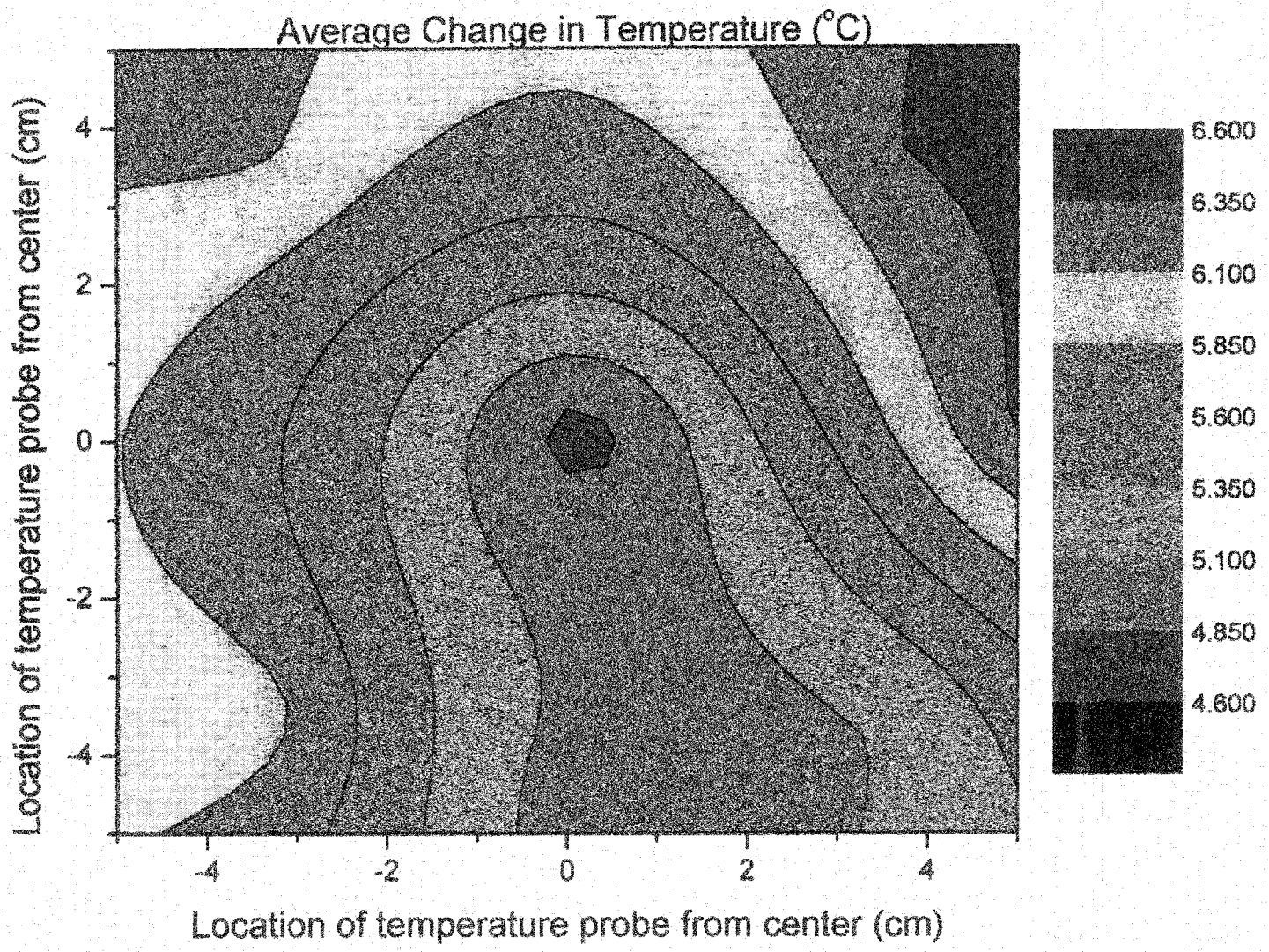
Average Change in Temperature (°C)
Location of temperature probe from center (cm)
4
2
0
-2
-4
-4
-2
0
2
4
Location of temperature probe from center (cm)
6.600
6.350
6.100
5.850
5.600
5.350
5.100
4.850
4.600

Figure 8

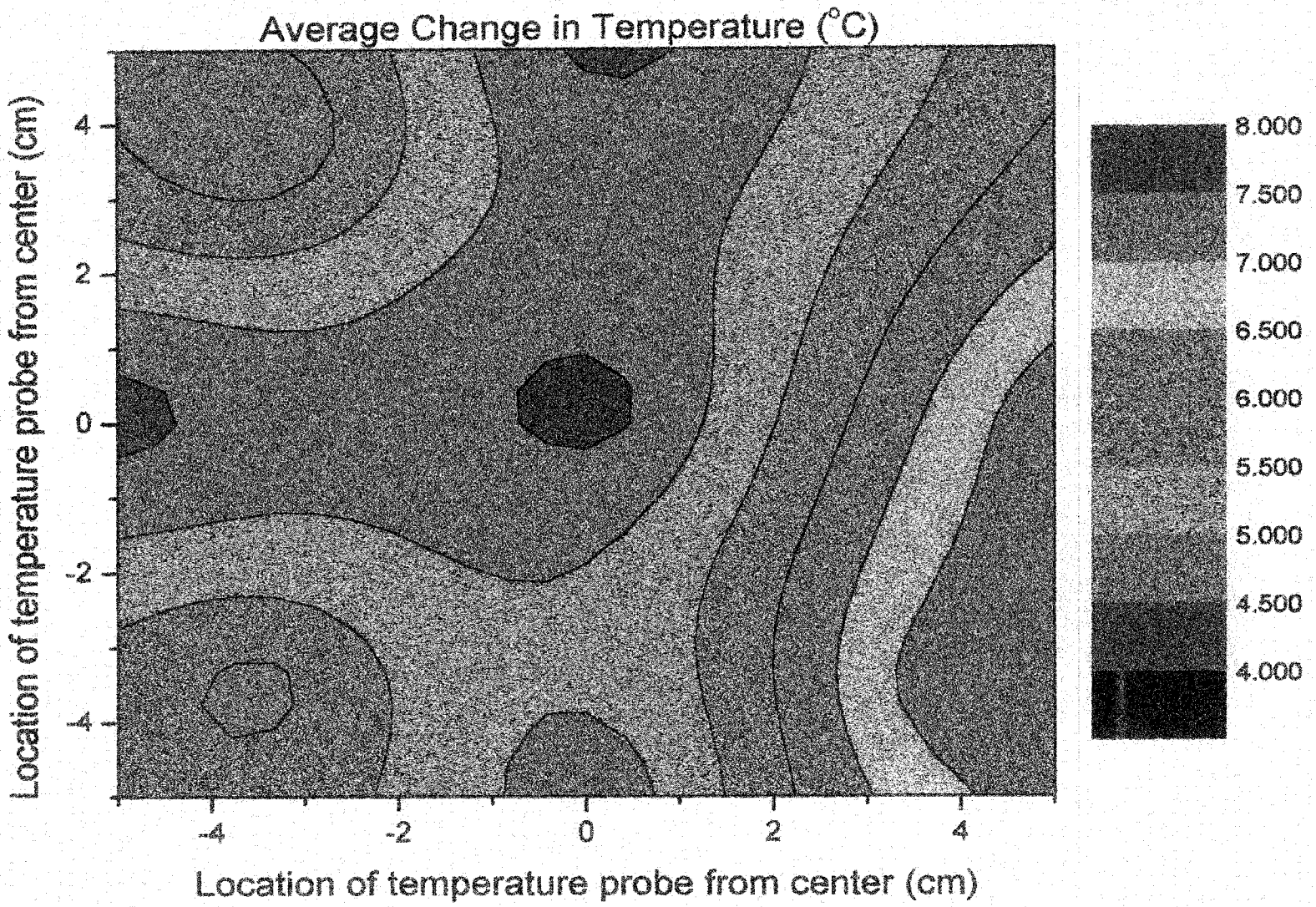
Average Change in Temperature (°C)
Location of temperature probe from center (cm)
4
2
0
-2
-4
-4
-2
0
2
4
Location of temperature probe from center (cm)
8.000
7.500
7.000
6.500
6.000
5.500
5.000
4.500
4.000

ACTIVE AND INTELLIGENT MATERIALS

John A. Marshall

School of Applied Science
University of Southern Maine
Gorham, Maine 04038

Telephone 207-780-5447
e-mail jmarshal@usm.maine.edu

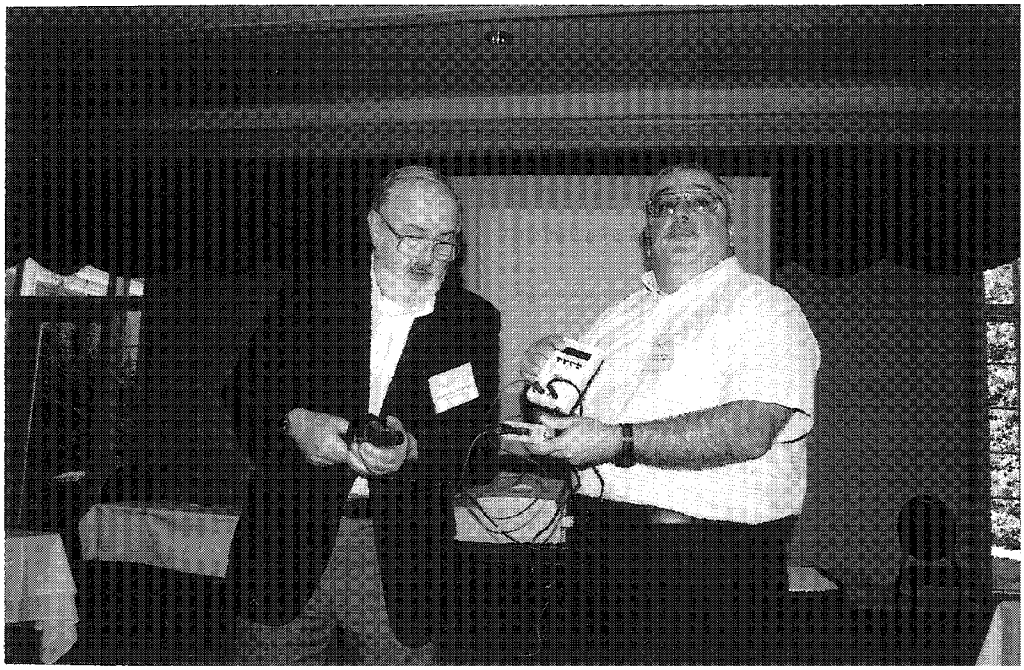

Biographical Information:

Dr. JOHN ALLEN MARSHALL taught senior high school prior to receiving his Ph.D. from Texas A&M University. He has eighteen years of university teaching experience, and is currently the Coordinator of the Industrial Power and Control curriculum and laboratories as well as the Internship Coordinator for the University of Southern Maine's Department of Technology.

Active and Intelligent Materials

John A. Marshall, PHD
University of Southern Maine

Key Words:

Hydraulics, mechanical power transmission, and rheology.

Perquisite Knowledge:

Elementary concepts of power transmission.

Objective:

To observe the tunable characteristics of one of the most active and intelligent materials, magneto-rheological fluids. To understand the potential power transmission advantages of these fluids.

Equipment and Supplies:

Magneto-rheological clutch assembly and power supply.

Introduction:

Magneto-rheological fluid is an active and intelligent material that changes its flow characteristics when subjected to an electrical field. Response, which takes only milliseconds, is in the form of a progressive gelling that is proportional to field strength. With no field present, the fluid flows as freely as hydraulic oil (Korane, 1991).

Magneto-rheological fluids represent a technology that has the potential to widen the performance range of automated electromechanical and electrohydraulic equipment. Research and ongoing developments are refining this active material and experts predict an important future for these fluids.

Importance of Magneto-rheological Fluids:

Current automation capabilities are not advanced enough to build a robot that could play tennis. Even though cameras and computers could direct the robot towards a ball, robot's move in an awkward, lumbering fashion because conventional hydraulic valves cannot keep pace with the commands of the computerized controllers.

With an active material such as magneto-rheological fluid, this type of response time is possible. This technology will allow devices that can operate instantly and without mechanical valves. Increased productivity and better product quality through more dependable and responsive automated equipment is just a small part of what this maturing technology can deliver.

How This Active and Intelligent Material Functions:

Magneto-rheological fluids are composed of two primary components. They are the carrier fluid and the suspended particles. The carrier fluid needs to be a good insulator, compatible with the materials they contact. Typical particle materials include polymers, minerals, and ceramics (Scott, 1984).

When a magnetic field is applied to the active fluid, positive and negative charges on the particles respond by separating, so each particle then has a positive end and a negative end. Particles of the magneto-rheological fluid then link together in the same manner that the north pole of one magnet is attracted to the south pole of another magnet (Duclos, 1988).

Potential Applications:

Magneto-rheological fluids can activate from solids to liquids so fast, they will work well with fast-acting computers. These characteristics suggest a number of unusual engineering applications such as fluid clutches and vibration isolators (Duclos, 1988).

According to Hans Conrad, professor of materials science and engineering at North Carolina State University, magneto-rheological fluids will lead to a whole new generation of brakes, automatic transmissions, actuator devices, hydraulic valves, pump parts, and motors (Conrad, 1992).

Procedure:

Safety Considerations:

1. Protective eye wear is mandatory for all those in the lab area.

2. Read the operating instructions that accompany the active magneto-rheological clutch assembly and power supply.

3. Obtain a "Material Data Safety Sheet" on the fluid from the supplier. Read the sheet completely and ask questions to any information you do not understand.

Observing the tunable clutch assembly:

1. With the power supply off, notice how easily the shafts can be rotated by hand.

2. Increase the power output through the range of 4, 8, 16, 32, 60, and 80 % and record your findings on the data sheet.

3. Vary the cycling frequency through the range of 4, 8, 16, and 32 Hz and notice the pulsating sensation while rotating the shafts. Record your findings on the data sheet.

Sample Data Sheet:

Record below the characteristics of the clutch when varying the power output.

Record below the characteristics of the clutch when varying the cycling frequency.

Instructor Notes:

1. The power being transmitted through the clutch increases proportionally when the power output is increased.

2. The impulses of power transmission increase as the cycling frequency is increased.

References:

Korane, K.: Putting ER Fluids To Work. Machine Design, May 9,1991, pp. 52-57.

Scott, D.: Amazing Hardening Fluids Open a New World of Hydraulic Drives. Popular Science, April 1984, pp. 42-46.

Duclos, T.G.: Electrorheological Fluids and Devices. Automotive Engineering, December 1988, pp.45-48.

Conrad, H.: The Impact of ER Fluids. Compressed Air Magazine, March 1992, pp.14-17.

"Procedure Demonstration Power Supply Controller" directions which accompany the tunable clutch.

Source of Supplies:

Internet resource to supplies and additional information:

http://www.rmit.edu.au/departments/ch/rmpc/

UNIVERSITY OF MARYLAND MRSEC RESEARCH EXPERIENCE FOR UNDERGRADUATES: CULTIVATING TOMORROW'S RESEARCHER

Jennifer Stott [(a)]

Donna Hammer [(a)]

E. D. Williams [(a, b)]

and

L. J. Martinez-Miranda [(a,c)]

a. Materials Research Science and Engineering Center
b. Department of Physics
c. Department of Materials and Nuclear Engineering
University of Maryland
College Park, Maryland 20742-2115

Telephone 301-405-0253
e-mail martinez@eng.umd.edu

University of Maryland MRSEC Research Experience for Undergraduates: Cultivating Tomorrow's Researcher

Jennifer Stott[a], Donna Hammer[a], E. D. Williams[a,b] and L. J. Martínez-Miranda[a,c]
a. Materials Research Science and Engineering Center
b. Dept. of Physics
c. Dept. of Materials and Nuclear Engineering
University of Maryland, College Park, MD 20742

Key Words: Scientific research, engineering research, undergraduate program

Prerequisite knowledge:

None, specifically.
Freshman chemistry, physics, first year materials

Objective:

What is involved in doing a research project?
What other aspects we must consider when doing research: communication, awareness of what other people are doing, how research is done in other environments.

Equipment:

Varies with the project.

Introduction:

The University of Maryland MRSEC Summer Research Experience for Undergraduates provides the students with a well rounded educational experience doing materials research. Supplemental activities enhance the laboratory experience and provide students with opportunities to advance into graduate school and careers in science. Approximately 6 – 8 sophomores and juniors with science and engineering backgrounds participate in the 10-week program. The REU offers a diverse range of research topics and includes a weekly seminar series, industrial tours of several neighboring facilities, and a tutorial on how to conduct oral and poster presentations. Research programs are available in Physics, Chemistry, Materials Science, and Electrical Engineering. The students get to present their research results twice during the course of the program.

Procedure:

The 6 – 8 students are selected by national competition. This competition is not limited to large universities, with graduate programs. People from small colleges which do not necessarily have a research program in place are especially encouraged to apply. They choose three projects in order of preference, from which one is chosen by the faculty in charge. If there are many students who ask for the same project as their first choice, the advisors are consulted. The students come to the University with their projects already assigned. In their orientation, they meet with their advisors, who summarize the project. They begin to work the next day.

The advisors are informed ahead of time that there are certain activities which the students need to attend. These are the seminar series and the tour series. The seminar series is presented by faculty in the MRSEC, some of whom are not advisors and work in projects different than what the students are working. The faculty are advised that the audience will be mostly undergraduates and that they must prepare the talk such that people with only basic knowledge in the field will be able to understand it. Occasionally, the talk may be accompanied by a mini-tour of the faculty's laboratory. The purpose of the tours is to introduce the students to how research is done at different laboratories and how experiments with a small amount of sample are taken to industrial quantities.

The students have the opportunity to present their work twice as part of the seminar series. They are given a seminar on how to present their results considering time limitation. Many of the students have presented work before, but many have not presented it under the strict time limitations required here or in any professional meeting. Others have not presented at all. Generally, they have a poster and an oral presentation, so they get to practice for both. In addition, they must present a final written report. They are provided with a set of instructions on how to prepare the report, and in addition are told to look into the articles they have read as references for additional style and language requirements in their field. This helps not only the students, but also the advisors, who get a write-up on the Summer research that can serve a student coming in the fall to continue the work or to do related research.

Comments

At the end of the 10-week period, the students are given a series of questions aimed at evaluating how successful the program has been. The purpose of this is to find ways to improve on the offerings and if they have served the purpose we intended them to serve. They are also encouraged to write telling us about their progress. Some comments we have received during the years include (not exact citation):

"I don't know if I will go to graduate school or do research, but now I know what it involves and will be able to make an informed decision."

"Before coming to the program, I was in a program that really did not encourage me to continue. After the program, I made my own program (approved by the dean), and feel I can continue now."

"The tour (of NASA) inspired me to apply to NASA when I finished."

"The tour of (Grace) industrial laboratory helped to see how things are scaled up. I thought that was 'really cool'."

"I had never presented anything in class. I am so nervous." This student did a great presentation. She appreciated the opportunity to do it.

Other students have told their friends about the program, and these have in turn applied. In this last application pool, we received applications that referred to our specific activities (the presentation of a report, the tours) as a reason for applying to Maryland.

Acknowledgements:

This work was supported by NSF Grant No. DMR-0080008.

ROOM TEMPERATURE CREEP OF Pb-Sn and Sn-Ag-Cu EUTECTIC SOLDERS

Matthew C. Osborne

Monica Hurley

and

Angela L. Moran

Department of Mechanical Engineering
U. S. Naval Academy
590 Holloway Road
Annapolis, Maryland 21402-5042

Telephone: 410-293-5528
e-mail osborne@usna.edu

Telephone: 410-293-6534
amoran@usna.edu

Angela Moran

Room Temperature Creep of Pb-Sn and Sn-Ag-Cu Eutectic Solders

Assistant Prof. Matthew C. Osborne
MIDN1/C Monica Hurley
Associate Prof. Angela L. Moran
Department of Mechanical Engineering
U.S. Naval Academy
Annapolis, MD 21402-5042

Key Words: Lead (Pb), Tin (Sn), Copper (Cu), Silver (Ag), Creep

Prerequsite Knowledge:

Objective: To provide the students with a fundamental understanding of time-temperature-load behavior of materials and the creep behavior of two similar metal alloys.

Equipment: Wood and nails to build a frame, Solder, Dial Indicator, U-joint

Introduction:

When a metal or an alloy is under a constant load or stress, it may undergo a progressive plastic deformation over a period of time. This time-dependent strain is called creep. Creep occurs at different rates, the rate being dependent on the stress level, material properties, and the application temperature. If a constant stress level is applied to a material, an increase in temperature can increase the creep rate. This characteristic is termed as a thermally activated process. Creep rate is also affected by the microstructure of the material, its prior processing and mechanical history, and its composition. When considering long term applications such as steam plants, nuclear power plants or gas turbine engines, it can be seen that creep rate is an extremely important property of a material to understand, for it can be regulated and controlled by the materials processing, environment, and application.

Creep tests are run to determine the creep rate of a material. These tests are either run at a constant temperature with varying stresses, or at a constant stress with varying temperatures. The change in length of the specimen over a period of time is plotted against time increments, which is termed a creep curve (see Fig. 1). The slope of the creep curve is creep rate of the material ($d\epsilon/dt$). During primary creep, the metal strain-hardens to support the applied load and the creep rate decrease with time as further strain hardening becomes more difficult. During secondary creep, processes involving highly mobile dislocations counteract the strain hardening so that the metal continues to elongate at a steady rate. During this stage the creep resistance of the metal or alloy is the highest. Then for a constant-loaded specimen, the creep rate accelerates in the tertiary stage of creep due to necking of the specimen and also to the

formation of voids, particularly along grain boundaries. The complete time it takes for the specimen to fracture is termed the rupture time. Either a higher stress of a higher temperature reduces the rupture time and increases the creep rate. In essence, the creep test measures the resistance of a material to deformation and failure when subjected to a static load below the yield strength at an elevated temperature, or to a constant temperature at a varying stress. The temperature at which creep becomes significant is generally considered to be approximately 0.4 T_m where T_m is the absolute temperature so for lower melting point materials such as lead –tin solders, creep can become an issue at room temperature.

The experimental tests described in this paper were designed to give quantitative results which allow students to see room temperature changes in a commonly used material. This experiment compares common solder materials with a new solder alternative, a mixture (alloy) of tin, silver and copper. Figure 1 gives a typical creep curve of strain vs time.

Common lead (Pb)- tin (Sn) solder can be found in a range of mass fractions of Pb and Sn. This study used 38% Pb by mass and 62% Sn by mass which results in a single melting point of 183°C. The lead free alloy tin (Sn)-silver (Ag)-copper (Cu) is a combination of 95% Sn by mass, 4% Ag by mass and the remainder is Cu. The Sn-Ag-Cu alloy has a melting point of 219°C.

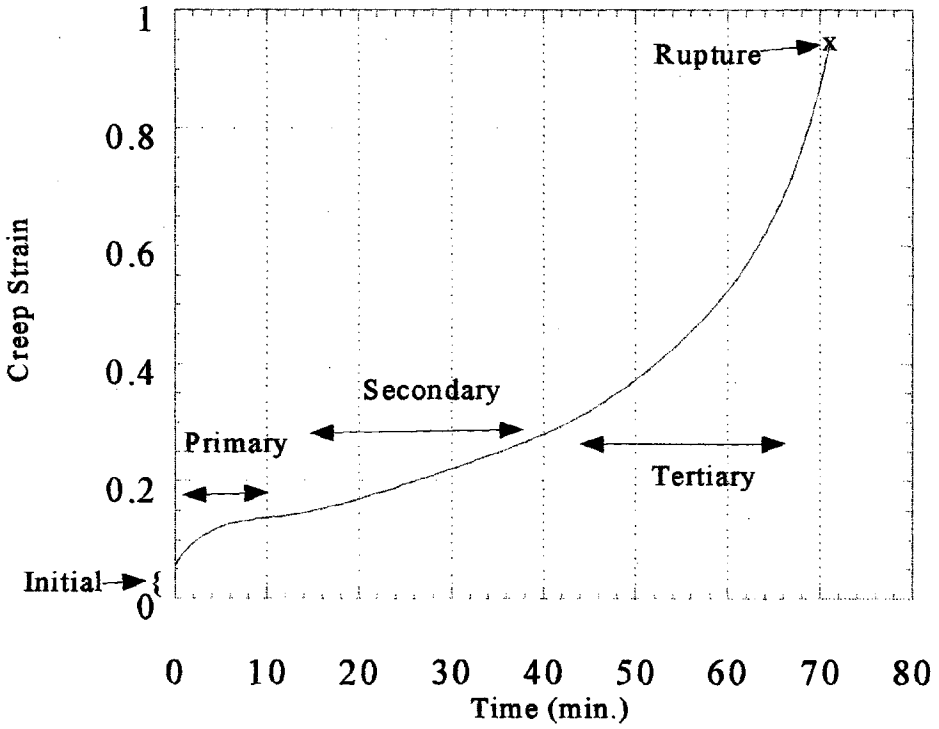

Figure1. Example Creep Curve with Labeled Regions

Experimental Methods:

The Sn-Ag-Cu alloy was provided by OMG. The Pb-Sn was manufactured at USNA by melting Pb and Sn pellets mixed in the appropriate mass fractions. Melting was done in a small crucible in a furnace at 400°C to produce ingots which were subsequently cut into ½" thick blocks measuring 1"x 2" in size. The cut blocks were rolled (or pressed) to a 1/16" thick 3' long strip approximately 1 ½" wide. These were then punch cut according ASTM D 1708 to form the specimens shown in Figure 2.

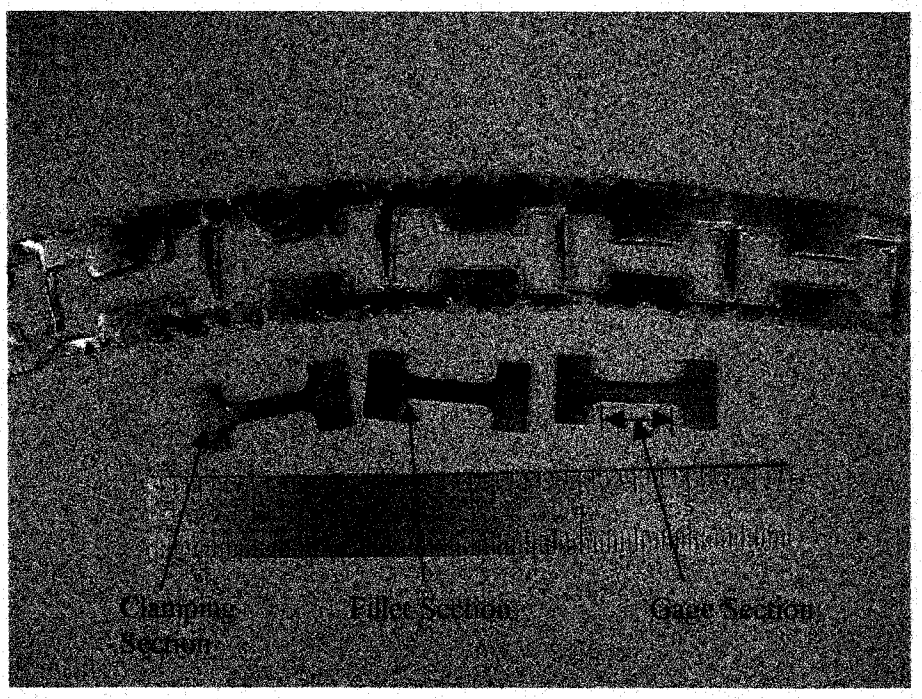

Figure 2. Cut Sn-Ag-Cu Tensile Specimens

The specimen is hung from a frame using special fixtures to allow for application of the load and to prevent the specimen from slipping as shown in Figure 3. The grip is made of aluminum, the pins are made of brass which prevent the specimen from sliding out of the grips. The thumb screws and steel strip inserts apply pressure to the wide flat face of the specimen so that the soft solder is not pulled by the brass pins.

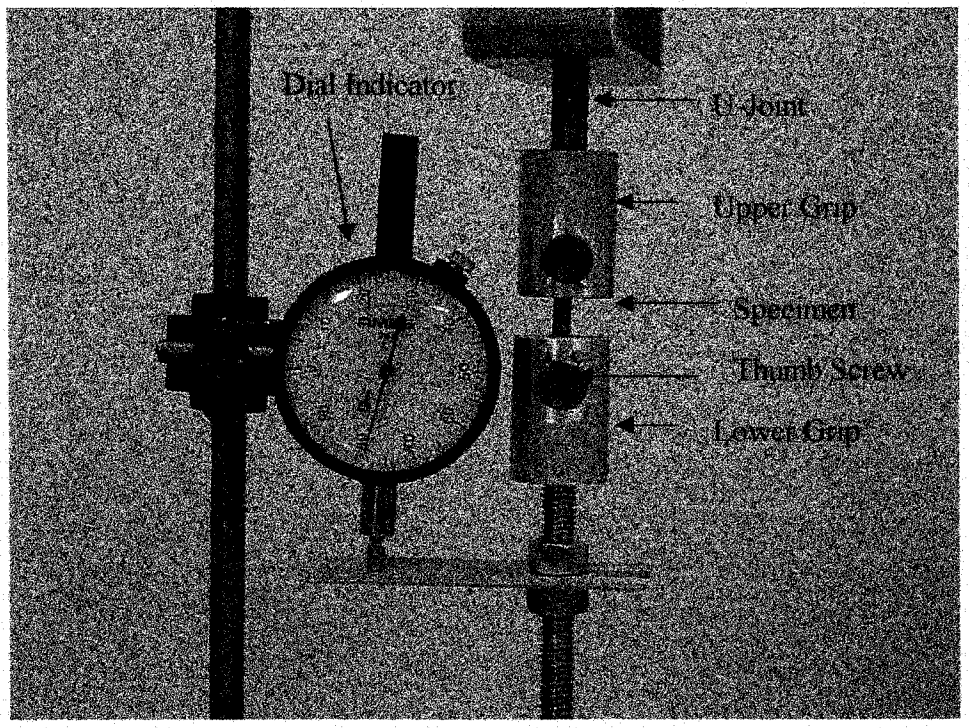

Figure 3. Specimen Mounting in Grip Fixture.

The complete experimental set-up, with grip fixtures at both ends of the specimen, is shown in Figure 4. The upper grip fixture is connected to a small U-joint to prevent specimen bending. The entire load is aligned parallel to the long axis of the specimen. The lower grip fixture is attached to an aluminum hangar for the weights. The hangar is composed of a threaded rod and a disc with a threaded hole in its center. The hangar hangs free in space. The weight of the bottom grip fixture and hangar is 1.8 lbs.

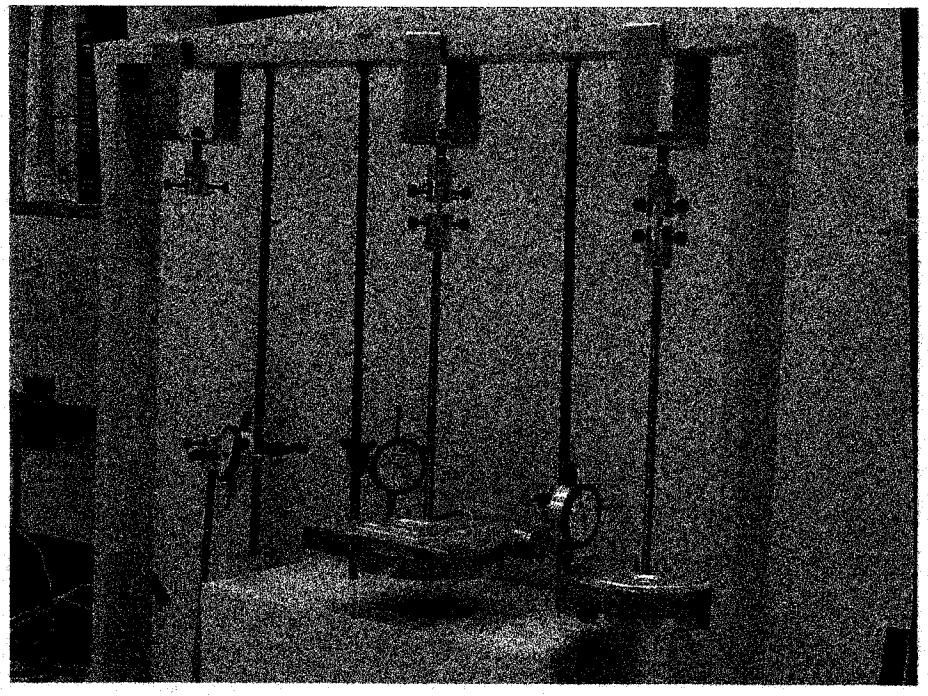

Figure 4. Creep Experiment in Test Frame

To measure deflection, a dial indicator is mounted next to the hanging specimen as seen in Figure 3 or directly above the weight as seen in Figure 4. Rigorous experimentation would not measure deflection in such a manner since errors are inherent when not measuring directly from a gage section. For demonstration purposes, the errors are considered unimportant but can be discussed as follows. These errors are minimized for this type of material since creep is essentially non-existent in the Al parts as they are operating at 0.314 times the melting point while the Sn-Ag-Cu and Pb-Sn solders are at 0.596 times and 0.643 times, respectively, their melting points. Generally in materials, the closer one comes to the melting point the softer and more easily a material will deform. The only true error will be the deflection measured from the fillet section as the gage section transitions to the clamping section. This error is expected to be small since the gage section is much larger than the filleted sections.

Procedure and Results:

The specimens were mounted as described above and data was recorded at different intervals depending upon the time to failure. The specimen loadings were 30 and 20 lbs. for the Sn-Ag-Cu solder and 20, 10 and 5 lbs. for the Pb-Sn solder. All tests were performed at room temperature.[1] Typical results are presented in Figure 5 thru 7. Figure 8 has images of the failed specimens.

[1] A walk in freezer can provide low temperature effects and a Plexiglas enclosure with a small heater can provide a higher temperature effect.

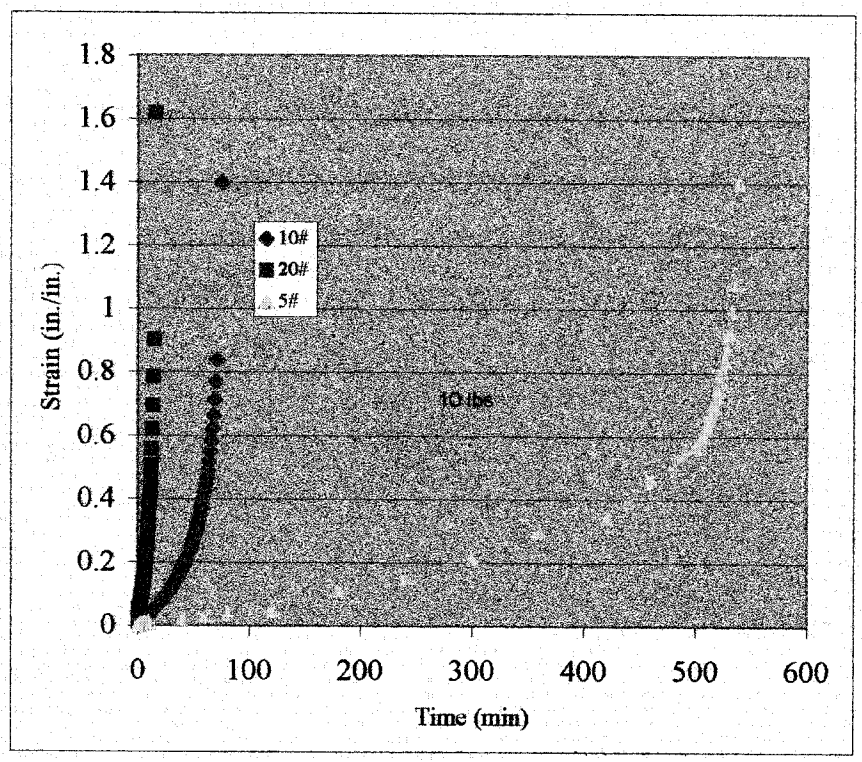

Figure 5. Creep Strain vs. Time for Pb-Sn solder at Room Temperature (20°C)

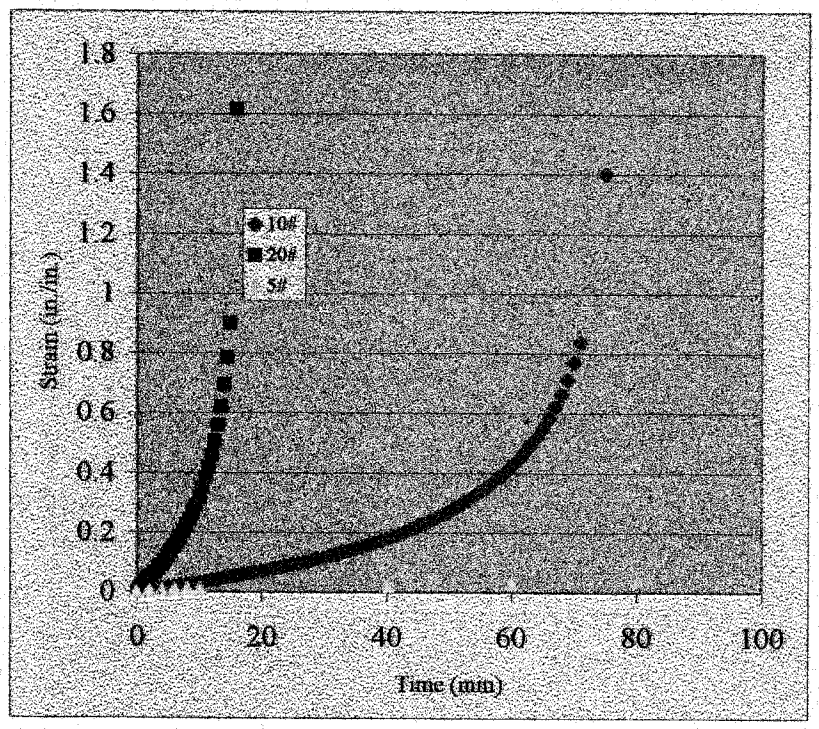

Figure 6. Creep Strain vs. Time for Pb-Sn solder at Room Temperature (20°C) (Expanded view of Figure 5)

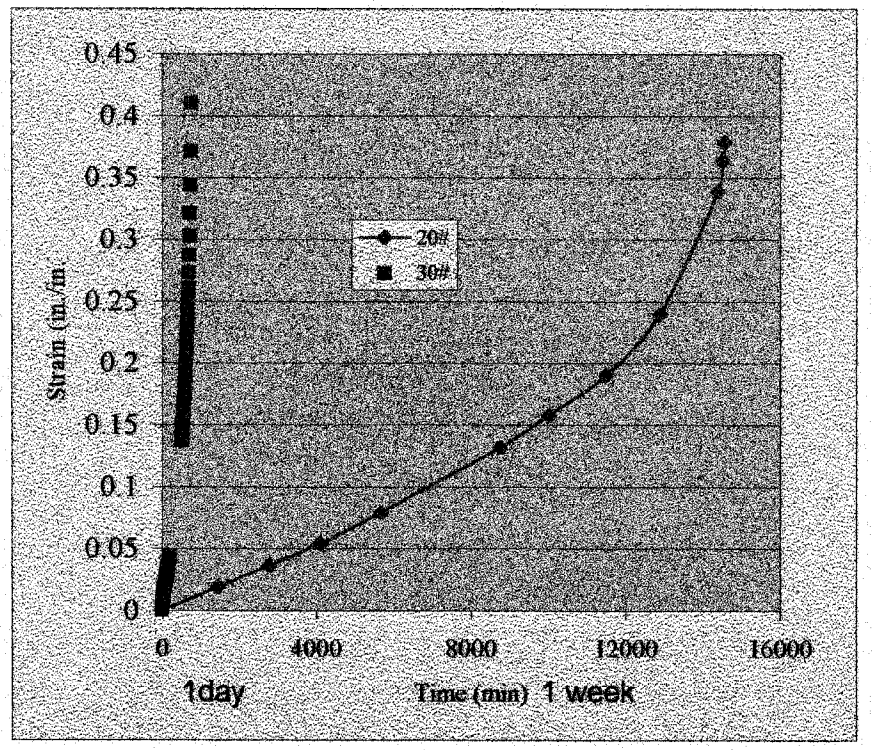

Figure 7. Creep Strain vs. Time for Sn-Ag-Cu solder at Room Temperature (20°C)

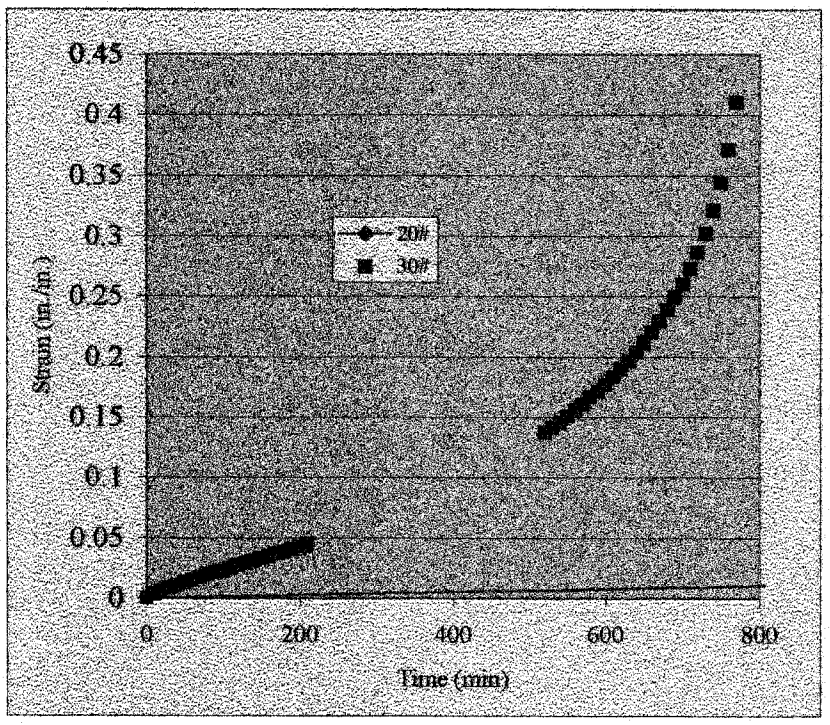

Figure 8. Creep Strain vs. Time for Sn-Ag-Cu solder at Room Temperature (20°C)

As can be seen in these figures, two different solders with close melting points have very different creep behaviors. Also by examining Figures 5-8, one can see that the steady state creep rate increases as loading increases, the slope is higher. The Pb-Sn failed the quicker than the Sn-Ag-Cu solder but it had much greater deformation. This effect can also be seen by examining the failed specimens in Figure 9.

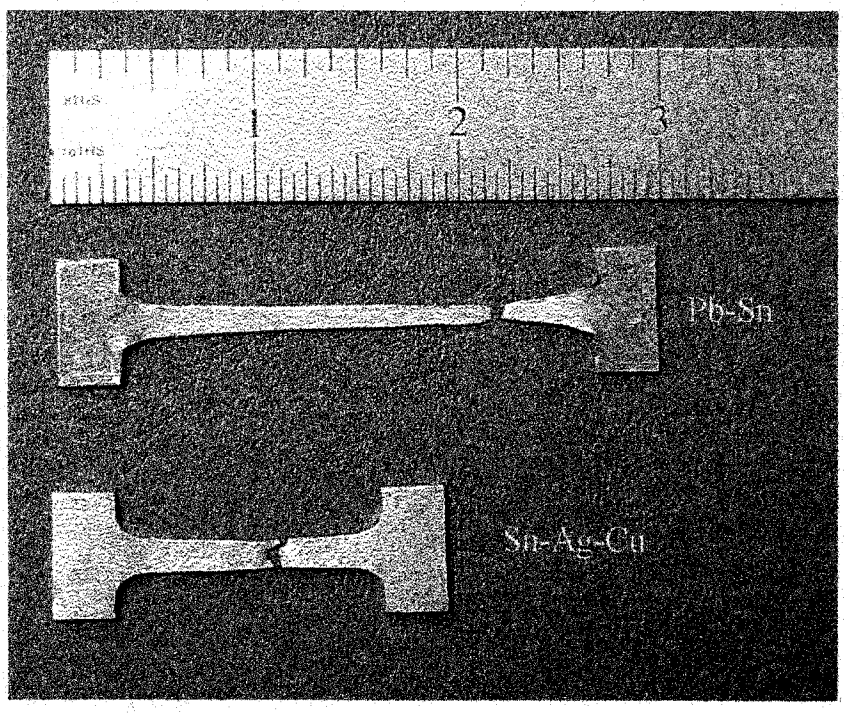

Figure 9. Creep Specimens after failure at 20 lb. loading and at Room Temperature (20°C)

Summary:

This experiment was designed to provide the students with a fundamental understanding of the time-temperature-load behavior of materials and the creep behavior of two similar metal alloys. It is hoped that the students will take note of the following:

- When a metal or an alloy is under a constant load or stress, it may undergo a progressive plastic deformation (creep) over a period of time.
- Creep occurs at different rates, the rate being dependent on the stress level, the material properties, and the application temperature.
- For constant – stress tests, alloys having different melting temperatures will exhibit different strain – time behavior.

References:

1. W. Callister, Materials Science and Engineering: An Introduction, John Wiley & Sons (2000).
2. American Society for Testing and Materials, Annual Book of ASTM Standards, Philadelphia PA .

WINDMILL-POWERED, PROPELLER-DRIVEN BOAT DESIGN-BUILD ENGINEERING PROJECT

Matthew A. Carr

Mechanical Engineering Department
U. S. Naval Academy
590 Holloway Road, MS 11C
Annapolis, Maryland 21402

Telephone: 410-293-6504
e-mail macarr@usna.edu

Matthew A. Carr

Windmill-Powered, Propeller-Driven Boat Design-Build Engineering Project

CDR Matthew A. Carr, USNR
Mechanical Engineering Department, United States Naval Academy, Annapolis, MD 21402

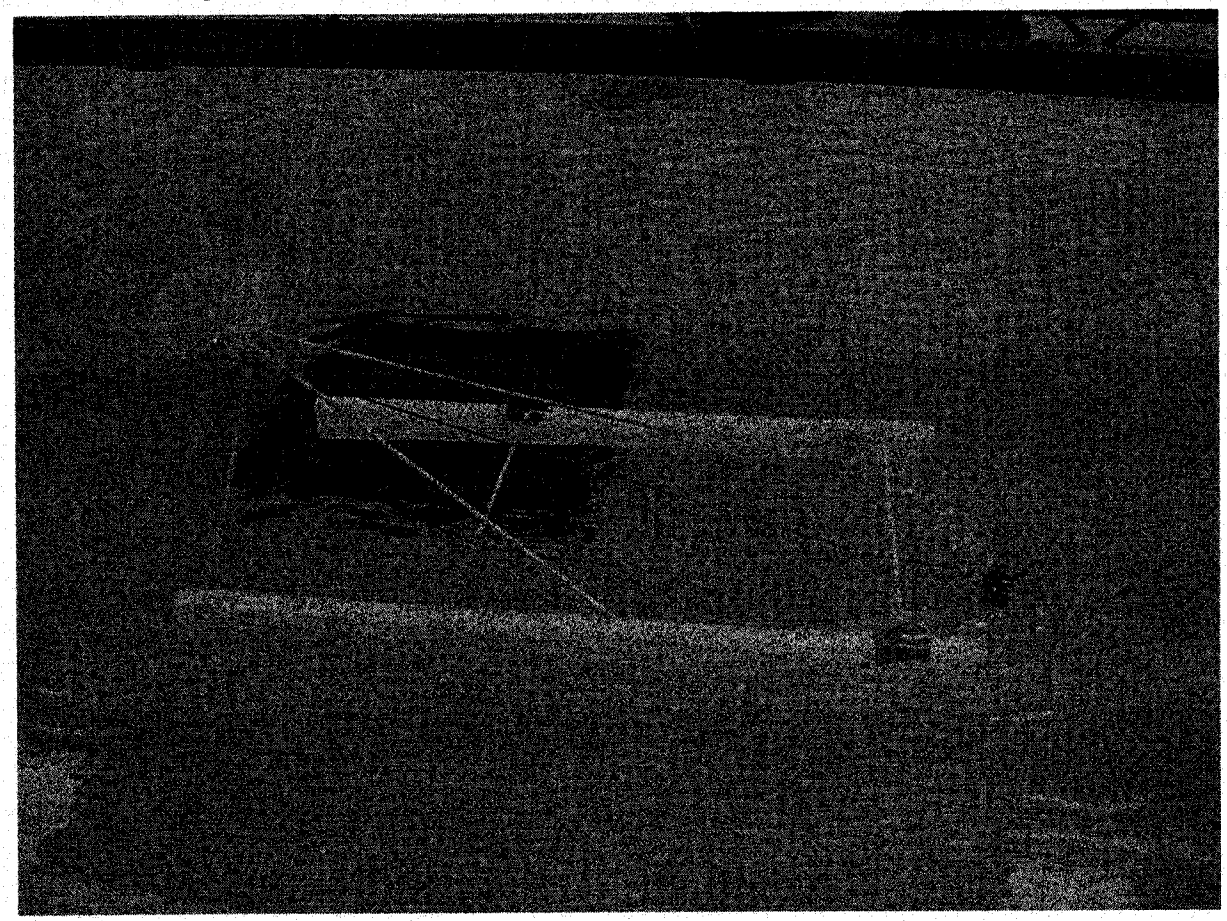

Abstract: This engineering project answers the question: "Can a boat use wind power to propel itself directly into the wind?" The solution is a model boat with a windmill mounted on it that is connected to a propeller that, in turn, propels the boat. This project is designed as a team competition and is suitable for students ranging from high school physics through college-level engineering students. Concepts taught and/or reinforced by this design-build experience include: fluid statics, buoyancy and stability; strength of materials; machinery design, friction, and power transmission; and fluid drag resistance of various shapes. This article is structured to provide a general overview of the supporting theory and key terminology, resources for additional information, project rules for the student teams, and a supplies list for executing this project. Where possible, the references cited are commonly available at public or larger high school libraries.

Introduction: Anyone with sailing experience knows that a sailboat cannot sail directly into the wind. However, can a boat use wind power to propel itself directly into the wind? The answer is "yes," if properly designed and constructed, and can be done on a model scale with the skills of most college-track high school students.

Project Considerations:

Facilities. This project requires access to a body of water of sufficient depth to allow the boat propellers to clear the bottom and of sufficient length to allow a reasonable run. This is easily met by an in-ground swimming pool, but can also be conducted in self-supporting, shallow,

plastic pools with a recommended length of at least six feet and a depth of at least six inches. A multi-speed fan (large desk-top, box, or pedestal fan) provides the "wind." Electric power for the fan is necessary. Students need to be informed of the dimensions of the pool for consideration in their design. The length of the required run must be adjusted for the available facility, but a run of at least three feet is recommended for scoring purposes.

Materials. Materials for the boat hulls may either be provided in a kit form or left to the students' resourcefulness. Suitable materials for the hulls may be wood (balsa or construction lumber), plastic (soft drink bottles or PVC pipe sections from a plumbing supply store), or foam (Styrofoam or other insulation boards from a building supply store). Materials for the rest of the boat structure typically include wood dowels, coat hanger wire, and cardboard. The windmill and propeller are typically made from soft drink cans, balsa wood sheets, Venetian blind slats, and pre-molded plastic fan blades and model airplane or boat propellers. Power transmission is typically via a straight steel rod, with threaded ends, mounted on an angle such that the windmill is on one end and the propeller is on the other. The rod may include small bearings or plastic or Teflon tubing bushings to reduce friction. Other useful materials include graphite powder, duct tape, super glue, and a plumber's epoxy stick. (Plumber's epoxy is clay-like and is hand-molded into the desired shape. The action of kneading the clay sets off a rapid curing process.) The material cost to build each boat should be less than $15 to $20, if materials such as foam are purchased in sheets and cut down to blocks and provided, recycled materials such as wire coat hangers or soft drink containers are used, and excluding tools.

Tools. This project may be constructed with hobby craft hand tools that include a small hammer and various punches (nails are a suitable substitute), tin snips, coping saw, razor knife, wire cutters/pliers, sand paper and a sanding block. A hand-held power drill and various small drill bits are helpful, but not necessary if foam is used for the hulls. If construction lumber were used, then access to a band saw or scroll saw would be helpful.

Safety. The fan must be located adjacent to the pool. The fan must be restrained from falling into the water. Electric power for the fan should be provided via a ground-fault interrupting circuit breaker or extension cord. The extension cord should be kept dry.

Terminology and Definitions:

Boat. Also known as a "vessel."

Hull – The "body" of a boat.

Catamaran – A boat with two parallel hulls aligned in the direction of motion. Note that most of the designs will probably be catamarans.

Trimaran – A boat with three parallel hulls aligned in the direction of motion; the center hull typically being longer than the other two.

Bow – The front of the hull.

Stern – The rear end of the hull.

Aft – Toward the stern of the vessel.

Displacement – The weight of the entire vessel. Archimede's Principle states that a floating object displaces a volume of fluid that will weigh the same as the floating object.

Propeller. Good visual aids for a boat propeller are either a set of fan blades from a desk fan or a small boat propeller from a marine parts store.

Propeller – A propeller is analogous to a screw and "advances" through the fluid in much the same way as a screw advances through wood. The typical propeller used on boats is a multi-blade screw propeller with two, three, or (sometimes) four or more blades (Naval vessels typically have five or more blades on their propellers). The blades attach to the

"hub" of the propeller. The hub is connected to the propeller "shaft."

Blade – Each blade attaches to the hub at its "root." The opposite end is called the "tip." The "face" is the blade surface generating pressure. The "back" is the surface opposite the face. Suction is generated on the back of the blade.

Blade Angle – Also known as the "pitch angle." The angle measured between the blade, at some radius from the hub, and a line perpendicular to the shaft. If the blade angle is zero degrees, then no pressure is generated on the blade face and no thrust is produced as the propeller rotates. If the blade angle is 90 degrees, then all the pressure is directed sideways and not aft.

Pitch – The axial distance that the propeller theoretically advances in one revolution. The pitch of a "fixed pitch" propeller can not be changed during operation. A "controllable pitch" propeller can be changed during operation, such as with a turboprop airplane. A solid propeller (one piece) may also be classified as "constant pitch" or "variable pitch." A constant pitch propeller has the same blade angle at each radius away from the hub. The blade angle is different at each radius for a variable pitch propeller.

Slip – The difference between the theoretical and actual advance per propeller revolution. (This effect will be addressed in the actuator disc theory discussion.)

Design Rules: (Instructor to adapt as necessary) Each team shall design and build its own boat. Total length shall not exceed XX inches (instructor specify; recommend 30). Width and height limitations are XX and XX (instructor specify; USNA chose the dimensions to fit inside an available display cabinet). Power transmission from the windmill to the propeller may incorporate direct-drive, gears or belt drives, with or without speed reduction. There is no limit on the choice of materials, but the total material expenditure, including sales tax paid, shall not exceed $XX (instructor specify) for the team. Note - if larger quantities are procured and only a portion used, the total cost of the item shall be counted. Free or scrap materials may be obtained from XX (instructor suggest sources such as local technical support shop or other sources), but the owner's permission is required to use any free materials not retrieved from scrap or recycling containers. Remember that the top finishing boats will be placed on display, so that the boats and their component parts will not be returned. Expenses shall be shown on a spreadsheet and included as an enclosure to the design report. Receipts shall be maintained and copies turned in as an enclosure to the design report.

Competition Rules: (Instructor to adapt as necessary) A static tank (describe the tank) will be used for the competition and will be available (instructor's judgment) for preliminary testing. A multiple speed fan (instructor describe the fan) will be provided and placed adjacent to the tank. Each team may set the speed of the fan for their run. The speed and direction of the fan many not be changed during the run. The team may add a nozzle to the fan (typically duct-taped cardboard), but once placed the nozzle may not be removed during the run. The boat may be placed at any location, s_i, not touching the walls. The run time will start when the boat is released at s_i. The time will stop when the boat crosses s_f, as measured by a string stretched perpendicularly across the tank (or contact with the tank wall or as viewed by a judge, at the instructor's option). Two runs may be made on the day of the competition. The boat may be modified between runs, but all modifications must be accomplished and subsequent run completed within the class period. The best score of the two runs will be the score for the competition. If $\Delta s < 3$ ft, the grade is a D. If $t < 5$ sec, the grade is a D. If the boat capsizes twice, the grade is a D.

Contest Scoring: The team's score is based primarily upon the performance factor, G. The value of G is determined from the following equation.

$$G = 100 * (s_i - s_f) / t = 100 * \Delta s / t$$

Where, t = time of travel (seconds); must be greater than 5
s_i = initial distance from the reference point (ft)
s_f = final distance from the reference point (ft)
$\Delta s = s_i - s_f$ (ft); must be > 3 ft

Each team shall submit a design report and their lessons learned in memorandum format for the balance of the grade on this project (See Reporting Requirements section, below).

Construction Pointers to Students: Hulls have been made from foam blocks, plastic bottles, PVC pipe, and balsa wood. Propeller shapes have been purchased, or fabricated from scrap aluminum or tin can lids. This project can be built with common hand tools. Students may find tin snips useful in fabricating propeller shapes. Good local sources of materials for this project include hardware stores, arts and crafts/hobby stores, and marine parts stores. Students may find it advantageous to tour these types of stores with a concept in mind in order to get ideas on materials and shapes available to facilitate boat construction. Bearings, should they be desired, are available on-line from model parts companies (Small Parts Inc., Boca Bearings, et. al.).

Key concepts to consider in your plan include drag of both the air and the water on your boat and friction in the machinery components. Also consider what happens to the drag and propeller/windmill forces when the boat starts to turn.

Preliminary testing, well in advance of the competition, is vital to achieving the optimum performance from your vessel. Plan on adjusting or even rebuilding your team's vessel from what you will learn from a properly conducted series of tests.

Reporting Requirements: (Instructor adapt) (1) Four weeks prior to the competition, submit a concept sketch of what your team intends to build. (2) Two weeks prior to the competition, each team provide a written progress report of what you have done and describe your plan to complete and test your entry prior to the day of the competition. (3) On the day of the competition, each team is to submit a design report in memorandum format describing your vessel, how it is constructed, and how it was tested. Include the financial spreadsheet as an enclosure. (4) Within the week following the competition, provide lessons learned from this experience by each person on the team and specifically answer what you would do differently given the opportunity to do it over again.

Prizes and Awards: (Instructor adapt) The total score of this competition is worth XX. (Also suggested) The instructor will treat the top place team to dinner. The top team from each class will have their boat and team photograph placed on display.

Theory and Derivation:

W. J. M. Rankine (1869) and R. E. Froude (1889) applied momentum theory to conceptualize the ideal propeller. The propeller was modeled as an actuator disk or mechanism that imparted an increase in pressure to the fluid passing through its cross-sectional area. The theory ignores how this increase in pressure is achieved. We know that fluid flows in response to a pressure gradient, thus the propeller and windmill terms can also be looked at using upstream and downstream velocities. Applying actuator disc theory for both the propeller and the windmill, the propeller equations are written in terms of the axial "interference factor," a,

$$a = \tfrac{1}{2} [V_2/V_1 - 1) \qquad (1)$$

where, V_1 is the water entry speed relative to the propeller's plane, and
V_2 is the water exit (wake) speed relative to the propeller's plane.

In other words, the change in velocity of the water entering and exiting the propeller's control

volume is directly related to the interference factor.

The thrust, T, is

$$T = 2 A \rho V^2 (1+a) a \quad (2)$$

where, A is the propeller circumscribed area,
D is the water density, and
V is the velocity of the vessel (Note that $V_1 = V$, see Equation 1).

The power absorbed, P, is

$$P = 2 A \rho V^3 (1+a)^2 a \quad (3)$$

The efficiency is the ratio of useful work obtained to the work expended.

$$\eta = T V / P = 1 / (1+a) \quad (4)$$

Similar relations can be set up for the windmill. The power generated is

$$P_w = 2 A_w \rho_w (U+V)^3 (1-a_w)^2 a_w \quad (5)$$

where, U is the wind velocity,
(U+V) is the relative velocity of the wind to the vessel (and to the windmill),
A_w is the windmill area,
D_w is the air density.

and the windmill's drag, D_w is

$$D_w = 2 A_w \rho_w (U+V)^2 (1-a_w) a_w \quad (6)$$

and the windmill interference factor is

$$a_w = \frac{1}{2} [1 - (U_2+V)/(U+V)] \quad (7)$$

where, U_2 +V is the relative leaving velocity.

If the boat is in steady motion, the forces must balance, so that

Propeller Thrust = Windmill Drag + Air Drag on Hull + Water Drag on Hull (8)

Assuming that the hull is low riding so that the air drag is negligible as compared to the windmill drag (this is really important to the success of the boat), we can now consider whether the boat can travel against the wind, i.e., whether V>0 is possible. For the limiting case, V=0, there is also no water drag and the combination of (2) and (6) then yields the force balance.

$$2 A \rho V^2 (1+a) a = 2 A_w \rho_w (U+V)^2 (1-a_w) a_w \quad (9)$$

Furthermore, if the power generated is fed into the propeller *neglecting friction and actual inefficiencies*, then equations (3) and (5) may be equated to yield

$$2 A \rho V^3 (1+a)^2 a = 2 A_w \rho_w (U+V)^3 (1-a_w)^2 a_w \quad (10)$$

Dividing (10) by (9) results in

$$V (1+a) = (U+V) (1-a_w) \quad (11)$$

or

$$V = (U+V) [(1-a_w) / (1+a)] \quad (12)$$

Since the ranges of the interference ratios are

$$0 \leq a_w \leq \frac{1}{2} \quad \text{and} \quad 0 \leq a \leq \infty \quad (13)$$

V>0 is possible.

For the theoretical optimum windmill condition, a = 1/3, so that

$$V = 2U / (3a+1) \tag{14}$$

in the absence of drag or inefficiencies. The necessary propeller/windmill area ratio can be estimated from

$$A/A_w = [\rho_w/\rho]\,[(1+a)/a]\,[a/(1-a_w)] \tag{15}$$

where, for $a_w = 1/3$ and $\rho_w/\rho = 1833$, then the area ratio is

$$A/A_w = [1/1700]\,[p(1+a)/a] \tag{16}$$

Since reasonable values of "a" are on the order of a = ½, a fairly large area ratio is indicated. This reduces to a diameter ratio of about 23.8.

Now, we know that there are a variety of windmill designs and not all of them will posses the same efficiency. For windmills, the efficiency term is called the power coefficient, C_p

$$C_p = P_{actual} / P_{ideal} = 4a_w (1-a_w)^2 \tag{17}$$

The power coefficient of an ideal wind machine rotor varies with the ratio of blade tip speed to free-flow wind-stream speed and approaches the maximum of 0.593 when this ratio reaches a value of 5 or 6 and coincides with $a_w = 1/3$.

Supplementary Reading:

The following references apply to this specific project.

Experiment #37, *Experiments in Fluid Mechanics*, R. A. Granger, 1988.

Engineering Applications of Fluid Mechanics, Hunsaker & Rightmire, McGraw Hill, 1947, pp. 382-383.

The following reference provides useful background information for various aspects of this project. Annotations describe the content used in this project.

Marks Standard Handbook for Mechanical Engineers, 10th Ed, Avallone & Baumeister, 1996.
- Section 3.2 - discusses friction.
- Section 3.3 - discusses vessel stability.
- Section 9.1 - discusses wind power.
- Section 11.3 - provides ship and propeller taxonomy.
- Section 11.5 - discusses actuator disc theory and airplane propellers.

Students may also find useful books on wind-powered machines under the wind energy, alternative energy, or renewable energy key words.

EXPERIMENTS FOR FIRST YEAR ENGINEERING STUDENTS USING Sn-Bi ALLOYS

Mark A. Palmer

Manufacturing Engineering
Kettering University
1700 West Third Avenue
Flint, Michigan 48504-4898

Telephone: 810-762-7973
e-mail mpalmer@kettering.edu

and

Kurt Wainwright

Lung C. Fok

and

Benjamin Jones

Virginia Commonwealth University

Mark A. Palmer

Experiments for First Year Engineering Students Using Sn-Bi Alloys

Mark A. Palmer[1], Kurt Wainwright, Lung C. Fok, Benjamin Jones
Virginia Commonwealth University

Abstract

An introductory course, the completion of which will enable first year students to make design decisions based on experimental data and using their knowledge of structure and processing identify possible alternative materials has been developed at VCU and RPI. The order of topics selected for this course is based on the paradigm that Processing effects Structure which effects Properties which in turn determines Performance and is the basis for design. To make this course successful laboratory experiments and hands-on exercises have been incorporated into the studio-based recitation which is the key learning experience. Alloys based on Sn and Bi have been used to demonstrate eutectic melting and diffusion in the solid and liquid states

- validate the Sn-Bi phase diagram through determination of the amount of proeutectic constituent,
- demonstrate coarsening of second phase particles,
- demonstrate sintering using Sn-Bi solder paste,
- and demonstrate grain growth using Sn.

The success of these experiments/demonstrations and how they were integrated into a course without a separate lab or lab grade will be discussed.

This was funded by the National Science Foundation's CCLI Program

Introduction

A second semester first-year course, Applied Materials Science (or Materials Chemistry II) was taught at Virginia Commonwealth University. This course evolved out of a course originally developed at Rensselaer Polythechnic Institute. The course seeks to respond to several of the criticisms regarding freshman engineering education specifically, that much of the dissatisfaction and disinterest in engineering occurs during the first two years of an engineer's education when they are exposed to the scientific concepts they will apply during their careers[1]. These criticisms include,

1. A vast majority of engineering students who described the quality of teaching as poor overall, and that the focus on weed-out objectives and use of poor teaching practices in the first two years had given them a shaky foundation for higher level work.
2. A lack of student-teacher dialogue, which was perceived to reflect faculty indifference. Large classes which are mainly one-way lectures, compared unfavorably to the high school experiences of many students. Recitations taught by non-faculty did not adequately address this.
3. A disjointed laboratory experience frequently annoyed students as did cook-book laboratory exercises which were perceived as busy work[2].
4. An ineffective use of instructional technology.

The typical experience therefore is inappropriate for beginning engineering students. Bloom, a noted educational specialist identified a hierarchy of educational levels, each one required to the next, and each higher level being more rewarding[3]. The first four of these of these are

---

[1]Now at Kettering University

1. Knowledge (memorization of facts),
2. Comprehension (restating learned facts),
3. Application (simple one-step application of abstract concepts),
4. Analysis (breaking down a problem into parts and solving it),

The large introductory courses characterized by the criticisms mentioned earlier focus on the first three levels. Consider however, that first graders learn at the knowledge level, fourth graders at the comprehension level, junior high school students at the application level and high schoolers at the analysis level in English and social studies courses. One cannot be surprised that college students do not respond well to being treated like children.

The course description for our course is: *The students will learn how to specify materials for a given performance criterion based on experimental data. Mechanical, chemical (corrosion) and electrical property-performance issues will be discussed, as will the fundamental scientific principles needed to understand how structure and processing effects these properties* [4]. In order to do this students need to be exposed to the interplay between processing, structure, properties and performance. There are two approaches to presenting this material, the tetrahedral [5] and the chain[6] approaches as shown below.

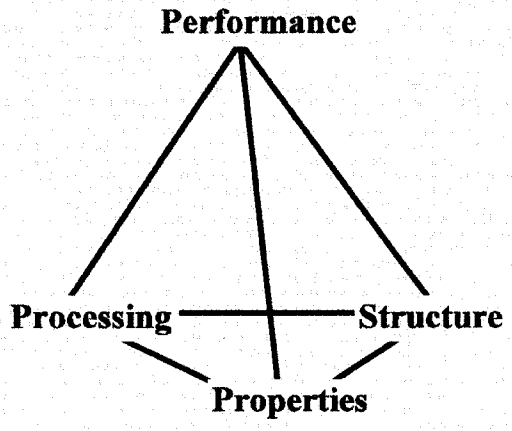

Figure 1: Tetrahedral approach where the constant interplay of performance, properties, structure and processing are emphasized.

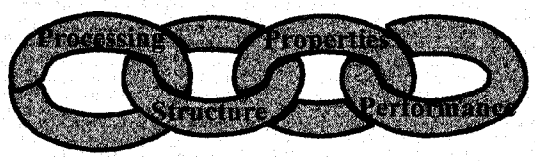

Figure 2: The chain approach where it is presented that processing affects structure, structure affects properties and ultimately performance.

We feel that the chain approach is the most pedagogically sound and therefore present the material in the following order: Structure –> Processing –> Property-Performance Relationships. One cannot tell students how structure is changed without first describing structure and therefore a discussion of structure must precede processing. Once these two issues are covered the students can spend the last one-half of the course applying the theory.

To successfully do this we integrated the laboratory into the course, expanding upon earlier work[7], and identified a set of experiments and demonstrations to enhance the discussion of phase diagrams (structure), coarsening, sintering and grain growth (processing). Because Sn and Bi are low melting temperature metals all of the experiments could be performed on a hot plate[8].

Experiments and Demonstrations

The following experiments and demonstrations were developed and fully integrated into the course.

Structure
Phase Diagrams
Demonstration of Melting Point Depression
Estimation of Relative Amount of ProEutectic Constituent

Processing
Grain Growth of Sn
Coarsening of ProEutectic Constituent
Sintering of Eutectic Sn-Bi Solder Paste

Melting Point Depression

As shown in the phase diagram on the right Sn and Bi both have melting temperatures above 200°C and a eutectic at 58Sn-42Bi and 138°C[8]. Thus when placed on a hot-plate at 200°C chunks of Sn and Bi will not melt. However, when placed in contact diffusion occurs and a liquid forms at the interface. Then melting occurs quickly. Once the alloy is completely mixed, it readily melts at 200°C. Because Sn and Bi have comparable densities equal size chunks can be used.

Following the demonstration the students were asked the following question on the second test. *When two different (oxide-free) metals are placed on a hot-plate at a temperature below the melting point of either material they will not melt. Yet when placed in contact with each other a liquid forms at the point of contact, and then the metals melt more rapidly. Explain both observations.* At least 80% of the students were able to explain that the mixing of atoms caused melting point depression, and about 35% of the students were able to explain that once liquid formed diffusion occurred more rapidly.

Estimation of Relative Amount of ProEutectic Constituent

Determining the amount of proeutectic constituent is a challenge to most students, however during solidification the proeutectic constituent is the most recognizeable. Students were told to prepare a Sn-Bi alloy, measure the amount of proeutectic and compare it to that predicted by the phase diagram as part of the homework assignment. An internet tip was written to guide them through the process should they have trouble. In addition in class they were assigned a team problem to estimate the proeutectic.

Representative Micrographs Showing Proeutectic Constituent in Sn-Bi Alloys

Note the proeutectic is fairly easy to spot.

Grain Growth of Sn

Since Sn melts at 232°C grain growth will occur quite rapidly at 200°C which is 94% of the melting point. Sn can be melted readily on the hot-plate, cooled quickly and the grain boundaries can be exposed using very dilute nitric acid. The Sn was placed in a furnace, although a conventional toaster oven could have been used, for periods between 1 and 4 hours. Results of one experiment are shown below.

Grain Growth of Sn at 200°C for 4 Hours

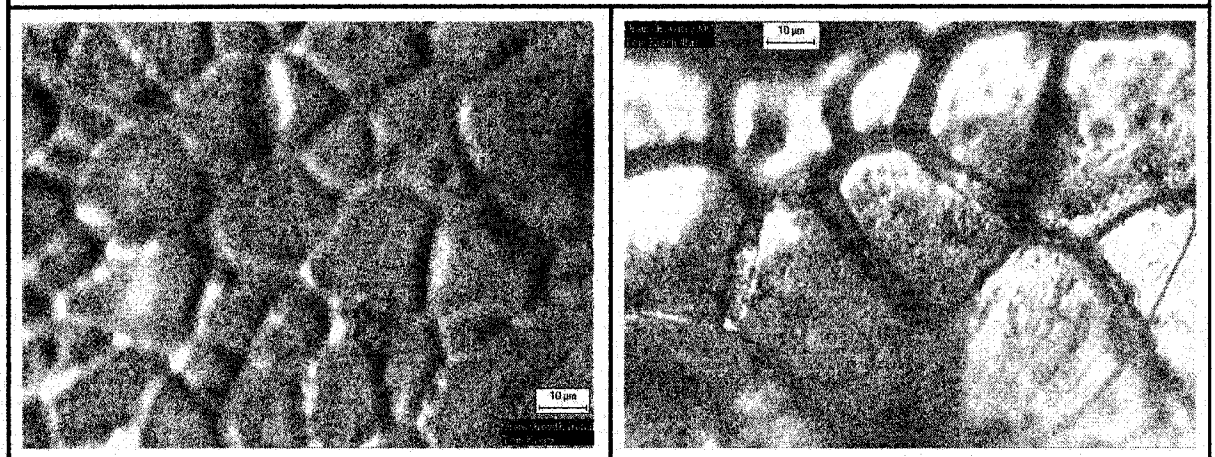

Appreciable grain growth is evident after a short time period.

Coarsening of ProEutectic Constituent

The proeutectic constituent will coarsen at 100°C, students took an initial micrograph and processed the material for up to two hours. Results of one experiment are shown below.

Coarsening of Proeutectic After 90 Minutes at 100°C

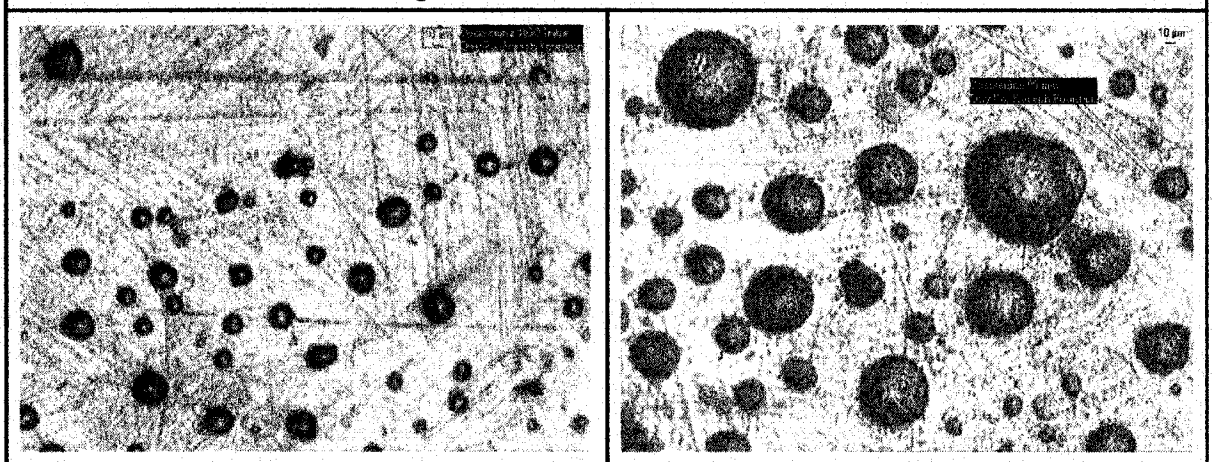

It is evident that the size of the particles has increased.

Sintering of Solder Paste

Eutectic Sn-Bi solder paste is readily available from a number of commercial sources. Prior work has demonstrated that it is possible to sinter solder pastes at low temperatures [9,10]. It is important that to use paste and not powder as the flux will prevent the material from oxidizing. Students took an initial micrograph and then placed the solder paste on the hot plate for up to 3 hours. Results of one experiment are shown below.

Sintering of Sn-Bi Solder Paste at 100°C for 90 Minutes

Note that after 90 minutes it is evident that extensive necking has occurred and pores have begun to form.

Discussion

Students were required to answer questions about the laboratory experiments on homework, quizzes, tests and the final examination. To assist them on homework a series of internet tips was provided so that they could work outside of class[11].

Structure Experiments

Graded performance records demonstrate that the students mastered the reading of phase diagrams with roughly one-half of the students being able to calculate the amount of proeutectic. 50% of the students were able to explain why a 1040 steel would be more fatigue resistant than a 1077 because of the presence of proeutectoid ferrite when asked on the final examination. When asked to rate how well the following learning objective was satisfied, *To understand how multiphase systems are formed, and predict the material properties of such systems* the students rating was: (3.8±0.8)/5.0.

Processing Experiments

Students chose to complete one of the three processing experiments described and were required to analyze their data as part of the following homework assignment. However, nothing can quantify the excitement expressed by the students when they realized that solid state motion had occurred. This confirmed to them that surface energy does exist and that once sufficient energy is provided for atomic motion the microstructure will evolve to minimize surface area.

Graded performance records demonstrate that on the following test over 50% of the students could explain coarsening, grain growth, and annealing and the effect on mechanical properties. On the final examination students were able to explain sintering, but did not make the connection to small grain size. When asked to rate how well the following learning objective was satisfied, *To understand, the principles of material processing and how processing effects structure* the students rating was: (4.2±0.8)/5.0.

Conclusion

This set of simple and inexpensive experiments can be used to teach students two of the most difficult topics in introductory materials science courses. Following a suggestion by reviewers of the assessment package, student teams will present their results to the class at the end of the term. This will allow them to demonstrate their communication skills and help them prepare for the final examination.

Acknowledgment

This was funded by the National Science Foundation's CCLI Program DUE 9980982. The support and encouragement of NSF is appreciated.

References

1. Shaping the Future: New Expectations for Undergraduate Education in Science, Mathematics, Engineering, and Technology; National Science Foundation Document NSF 96-139, © 1996.

2. Kenny S. S.: The Boyer Commission on Educating Undergraduates in the Research University Reinventing Undergraduate Education: A Blueprint for America's Research Universities; Carnegie Foundation for the Advancement of Teaching,

3. Bloom B. S. and Krathwohl D. R.: Taxonomy of Educational Objectives: the Classification of Educational Goals, by a Committee of College and University Examiners. Handbook I: Cognitive Domain; Longmans, Green New York, © 1956.

4. Palmer M. A., Wnek G. E., Hudson J. B.: New Approaches for an Introductory Materials Science Course; ASEE Materials Division 1998 Conference

5. Flemings M. C., Sadoway D. R.: Frontiers of Materials Education; MRS Proceedings v66, ©1985.

6. Linden B., Vanasuppa L., Heidersbach R.: The Structure of Materials Engineering: A New Model for Materials Engineering Curricula; TMS Annual Meeting, Education Symposium (1996).

7. Hudson J. B and Palmer M. A.: Interactive Learning in a Multidisciplinary First-Year Course; ASEE Educational Research and Methods Division 1996 Conference Proceedings.

8. Baker H. (ed): ASM handbook - Volume 3 Alloy Phase Diagrams; ASM International, Materials Park, ©1992

9. Palmer M. A., Alexander C. N., and Nguyen B.: Forming Solder Joints by Sintering Eutectic Tin-Lead Solder Paste; Journal of Electronic Materials, 7/99 pp. 922-925.

10. Palmer M. A., Erdman N., McCall D.: Sintering of High Temperature Solder Materials; Journal of Electronic Materials, 11/99 pp. 1189-93.

11. Palmer M. A., Hudson J. B., Moynihan C. T., Wnek G. E.: Using the Internet in a Freshman Engineering Course; Journal of Materials Education v18, pg. 35, (1996).

FORMATION AND CONVERSION OF CALCIUM PHOSPHATES - A NOVEL APPROACH TO PREVENT CAVITIES AND DENTIN SENSITIVITY

Ming S. Tung

American Dental Association Health Foundation
Paffenbarger Research Center
National Institute of Standards and Technology
100 Bureau Drive, Stop 8546
Gaithersburg, Maryland 20899-8546

Telephone: 301-975-6823
e-mail Ming.tung@nist.gov

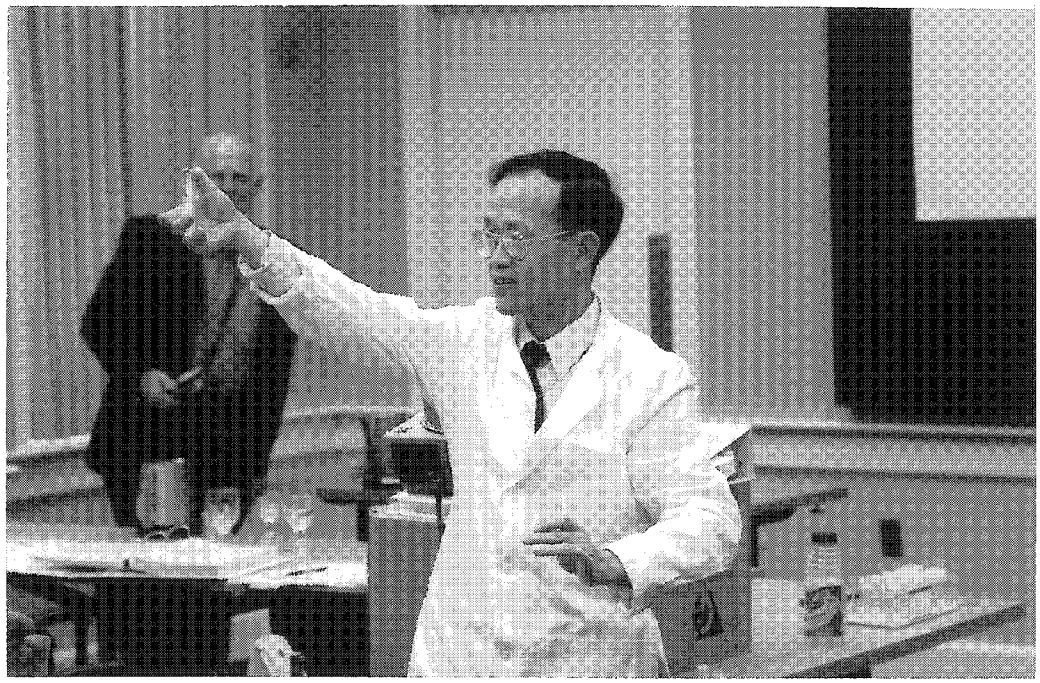

Biography:

Ming S. Tung is a Senior Project Leader at American Dental Association Health Foundation, Paffenbarger Research Center, National Institute of Standards and Technology. He has a B. S. degree in Chemical Engineering from Cheng-Kung University in Taiwan and a Ph.D. in Chemistry from Brown University. His research includes calcium phosphate chemistry and remineralization of the tooth.

Formation and Conversion of Calcium Phosphates- A Novel Approach to Prevent Cavities and Dentin Sensitivity

Ming S. Tung
American Dental Association Health Foundation
Paffenbarger Research Center
National Institute of Standards and Technology
Gaithersburg, MD 20899

Key Words: Amorphous calcium phosphate, Apatite, Cavities, Dentin sensitivity, Gel, Carbonate.

Prerequisite Knowledge: General Chemistry.

Objective: To demonstrate the chemical principle of a novel approach to prevent cavities and dentin sensitivity.

Materials:

1. One mL of calcium chloride solution (1.5 mol/L) and one mL of dipotassium hydrogen phosphate solution (1 mol/L).
2. One mL of 33 mmol/L of calcium chloride and 50.6 mmol/L of acetic acid at pH of 2.5 and one mL of 50.6 mmol/L of potassium carbonate, 7.4 mmol/L of potassium dihydrogen phosphate and 12.6 mmol/L of phosphoric acid at pH of 9.7.

Introduction:

About 95 percent of the tooth enamel is inorganic calcium phosphate crystal, known as apatite. Dental cavities and dentin sensitivity are due to the dissolution or loss of the apatite crystal, demineralization. To prevent and heal these problems, the tooth mineral is deposited back to where it is lost by a novel process of **rapid remineralization**, the recrystallization of apatite. This is accomplished with a new, clinically feasible method: rapid formation on and in the tooth of amorphous calcium phosphates, which then crystallize to apatite slowly after application.[1] The highly concentrated calcium phosphate solutions are applied in two ways: two-step gel and one-step carbonated mouth rinse. Two-step application forms the calcium phosphate gel on the tooth by applying a calcium solution on the tooth followed by applying a phosphate solution. The one-step application rinses a carbonated calcium phosphate which is mixed before application.

Chemical Reactions:[2]

1. Two-step gel application.
When a highly concentrated calcium chloride solution (1.5 mol/L) is mixed with a highly concentrated potassium phosphate solution (1 mol/L) at high pH (pH = 9.5), the initial phase formed is a gel of calcium phosphate, which then converts to the apatite through an intermediary of amorphous calcium phosphate.

$3\ CaCl_2 + 2\ K_3PO_4 + y\ H_2O \rightarrow (Ca_3(PO_4)_2)_x \bullet yH_2O$ (gel) + 6 KCl
$(Ca_3(PO_4)_2)_x \bullet yH_2O$ (gel) $\rightarrow Ca_3(PO_4)_2 \bullet 3H_2O$ (ACP)$\downarrow$ + (y-3) H_2O
$5\ Ca_3(PO_4)_2 \bullet 3H_2O$(ACP) $\rightarrow 3\ Ca_5(PO_4)_3$(OH)(apatite) + H_3PO_4+$12H_2O$

2. One-step carbonated calcium phosphate solution application.
Two solutions are mixed and then used as mouth rinse. One contains 33 mmol/L of calcium chloride and 50.6 mmol/L of acetic acid at pH of 2.5, and the other contains 50.6 mmol/L of potassium carbonate, 7.4 mmol/L of potassium dihydrogen phosphate and 12.6 mmol/L of phosphoric acid at pH of 9.7. Both solutions are stable under atmospheric pressure. Upon mixing, a carbonated calcium phosphate solution is formed; this solution is highly supersaturated with respect to the carbon dioxide and the calcium phosphate. As carbon dioxide evaporates, which is the same as removal of carbonic acid, the pH of the applied solution increases and the amorphous calcium phosphates precipitate rapidly, and then converts to tooth mineral. The reaction can be observed visually in one minute.

$3CaCl_2+2KH_2PO_4+2K_2CO_3+ H_2O \rightarrow Ca_3(PO_4)_2 \bullet 3H_2O(ACP)\downarrow + CO_2\uparrow$
$5Ca_3(PO_4)_2 \bullet 3H_2O(ACP) \rightarrow 3Ca_5(PO_4)_3(OH)$ (apatite) $+H_3PO_4+ 12H_2O$

Demonstration:

1. Two-step gel application.
Two solutions will be mixed: one contains calcium, and the other contains phosphate. The mixing of the two solutions initially induces the formation of calcium phosphate gel within seconds. The gel will precipitate as amorphous calcium phosphate, which then converts to apatite, the tooth mineral. The reaction can be observed visually in one minute.
2. One-step carbonated calcium phosphate solution application.
Two solutions will be mixed: one contains calcium and the other contains phosphate and carbonate. Upon mixing, a highly saturated carbonated mouth rinse is formed. As carbon dioxide evaporates (as in carbonated beverages and beers), the pH of the applied solution increases and the amorphous calcium phosphate precipitates rapidly and then converts to apatite. The reaction can be observed visually in one minute. The evaporation and the pressure of carbon dioxide can be observed and felt.

Comments:

The dissolution of tooth mineral by acids produced by bacteria fermentation in the mouth causes destruction of the dental enamel and dentin. The calcium and phosphate ions in saliva continuously remineralize the tooth, thus repairing this demineralization. When demineralization is faster than remineralization, cavities occur. In vitro studies[3] show that increases in remineralization can reverse the cavities. Unfortunately, this repair takes months since the direct crystal growth of tooth mineral is a very slow process. The clinically feasible remineralization is accomplished by rapid deposition of amorphous calcium phosphate on and in the tooth which then converts to the tooth mineral after application.

References:

1. Tung, M.S. and Eichmiller, F.C. (1999): Dental Applications of Amorphous Calcium Phosphates, *J of Clinical dentistry* 10:1-6.
2. Dorozhkin, S.V. (2001): Systems of Chemical Equations as Reasonable Reaction Mechanisms, *J Chemical Education* 78:917-920.
3. ten Cate, J.M. (2001): Remineralization of Caries Lesion Extending into Dentin, *J Dental Research* 80:1407-1411.

LIGHTWEIGHT AUTOMOTIVE MATERIALS RESEARCH AT THE CENTER FOR LIGHTWEIGHTING AUTOMOTIVE MATERIALS AND PROCESSING (CLAMP)

P. K. Mallick

Department of Mechanical Engineering
University of Michigan-Dearborn
Dearborn, Michigan 48128

Telephone 313-593-5119
e-mail pkm@umich.edu

P. K. Mallick

Lightweight Automotive Materials Research

at the Center for Lightweighting Automotive Materials and Processing (CLAMP)

P. K. Mallick
Professor
University of Michigan-Dearborn

Current Research Topics/Faculty

- Plastics and Composite Materials
- Lightweight Alloys
- Processing

- Dr. P. K. Mallick
- Dr. G. T. Kridli
- Dr. P. Mohanty

Plastics and Composite Materials

- Fatigue Behavior of Thermoplastics and Related Composites
- Long-Term Behavior of Fuel Tank Plastics
- Low-Velocity Impact Damage
- Fatigue Resistant Joints in Automotive Composites
- Crush-Resistant Composite and Metal/Composite Structures

Lightweight Alloys

- Deformation Characteristics of AA 5754
- Thermo-Mechanical Treatment of AA 6061
- Fatigue of Self-Piercing Riveted Joints in Aluminum Alloys
- Forming Characteristics of Metal/Plastic Sandwich Panels
- Corrosion Behavior of Aluminum and Magnesium Alloys

Processing

- Hydroforming: Simulation and Experiments
- Forming of Tailor-Welded Blanks: Simulation and Fatigue Characteristics
- Rapid Prototyping by Spray Forming and Solidification
- Dimensional Control in Injection Molding
- Press Forming of Thermoplastic Matrix Composites
- Filament Winding of Thermoplastic Matrix Composites

Press forming (Stamping) of Thermoplastic Matrix Composites

- Thermoplastic Composite Beams and Tubes for Automotive Applications

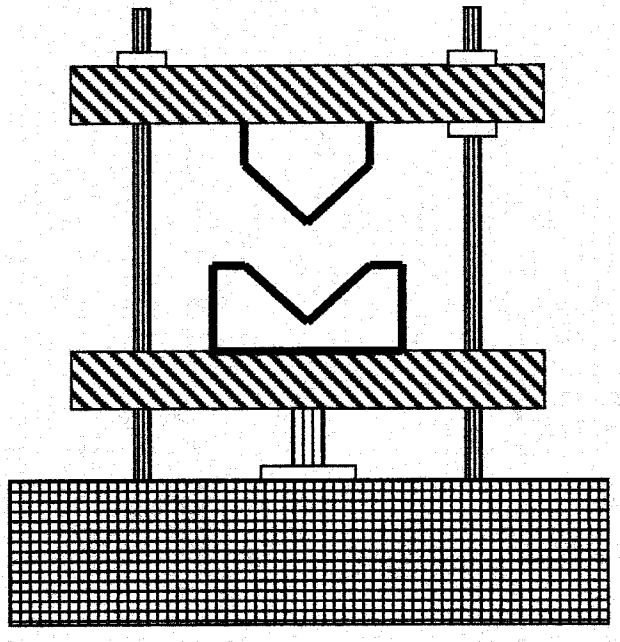

Stamping Press

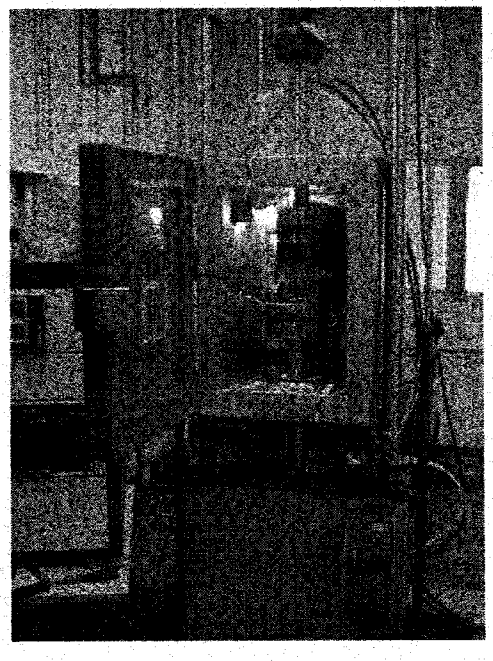

Materials Testing Machine

Press Formed Beams and Tubes

Press Formed Sections

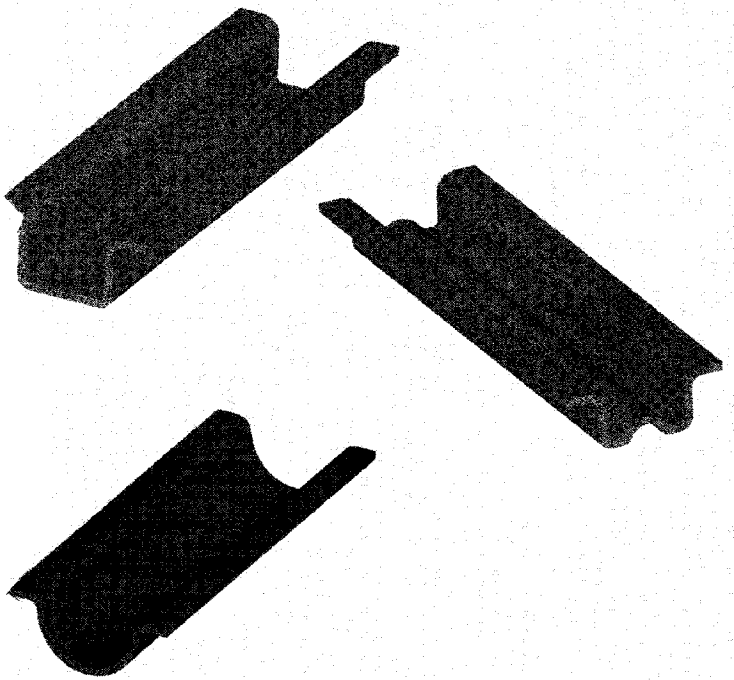

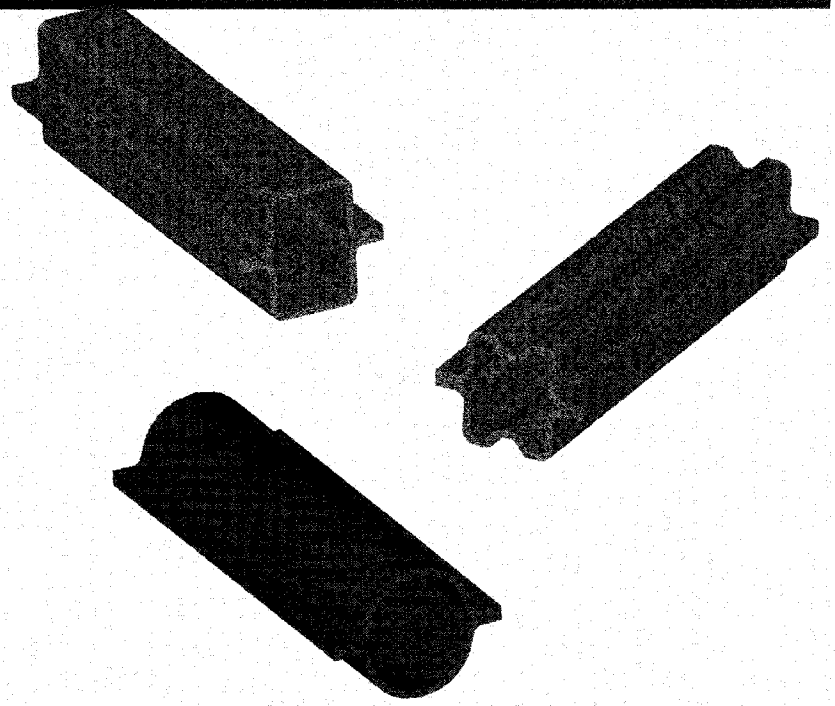

Vibration Welded Sections

Filament Winding

- Filament Winding and Joining of Composite Tubes for Automotive Space Frame Structures
- Filament Winding of Composite and Metal/Composite Tubes for Crush Resistant Automotive Frame Rails

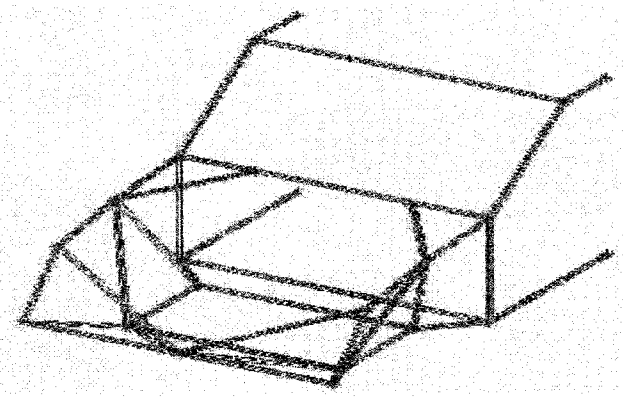

Tube Hydroforming

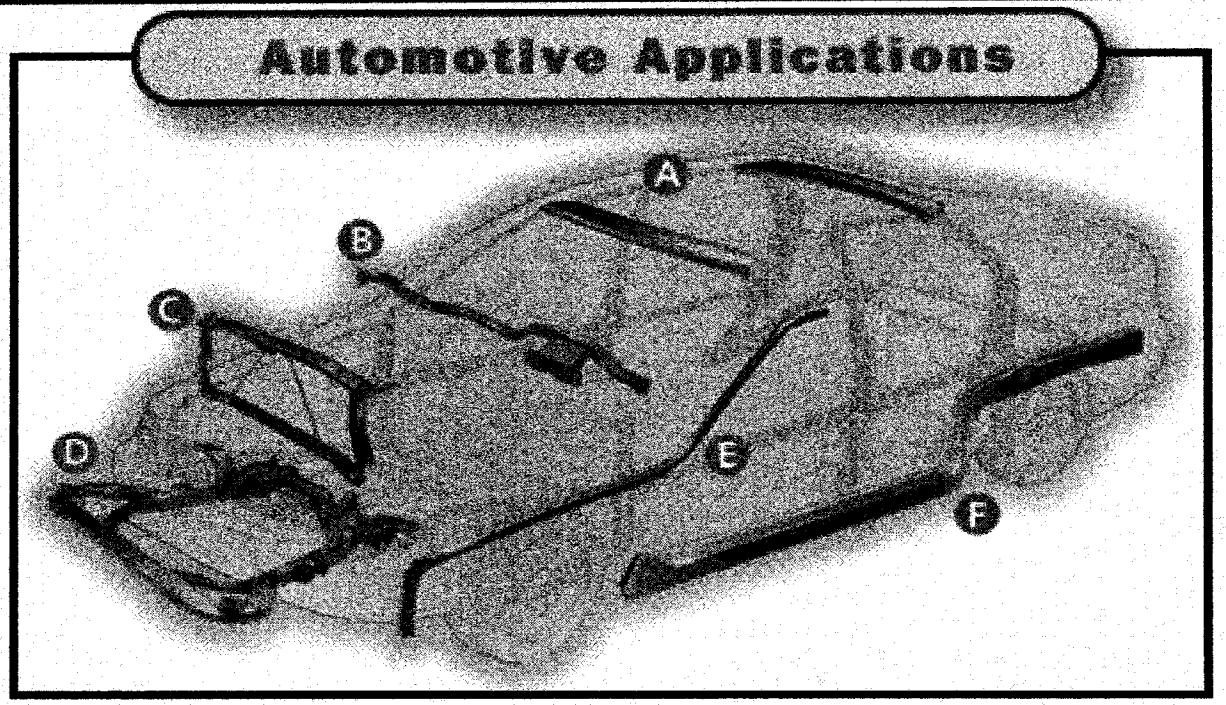

A. Roof Headers B. Instrument Panel Supports C. Radiator Supports D. Engine Cradles E. Roof Rails F. Frame Rails. In addition: Cross Car Beams · Headers · A,B,C Pillars · Seat Frames · Roll Bars · Control Arms (courtesy of Vari-form)

Tube Hydroforming

Objectives:

- Study (both analytically as well as experimentally) the effects of die geometry, material properties, and frictional characteristics on the quality of hydroformed components, such as corner filling, thickness distribution and cracking.

- Develop formability characteristics of tube materials for hydroforming processes.

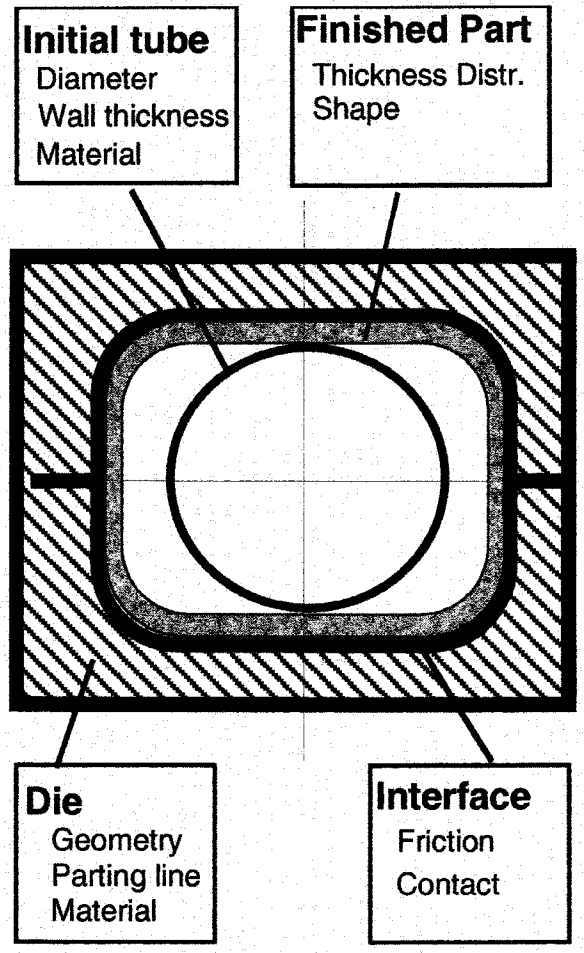

Self-Piercing Riveted Joints

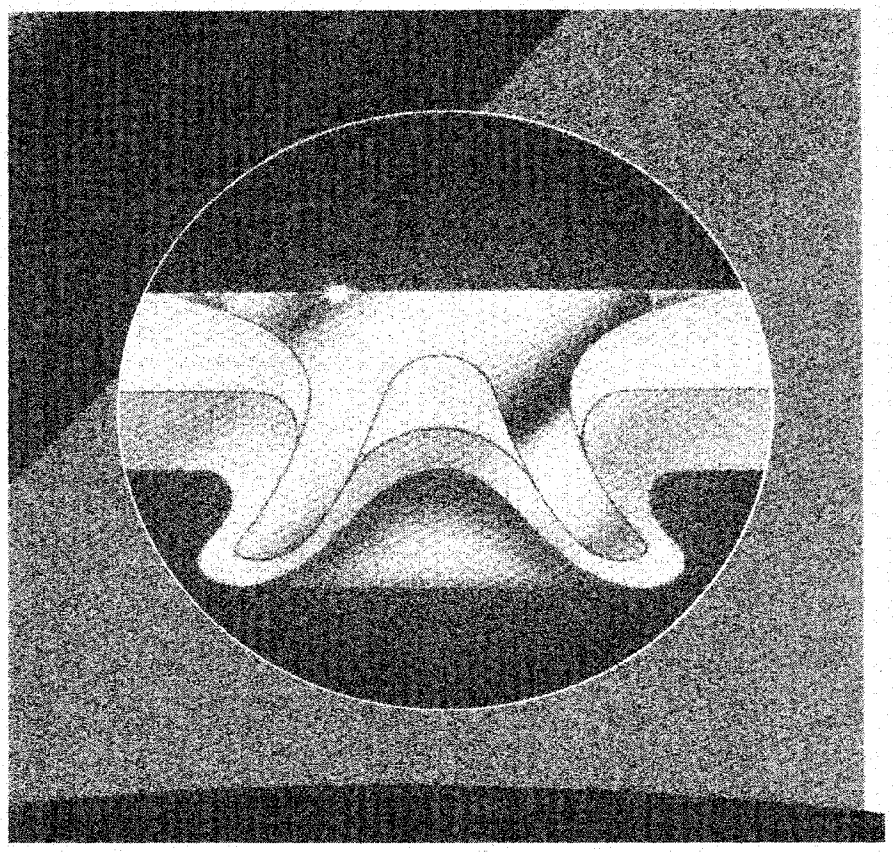

Fatigue of SPR Joints in 611 1 Alloy

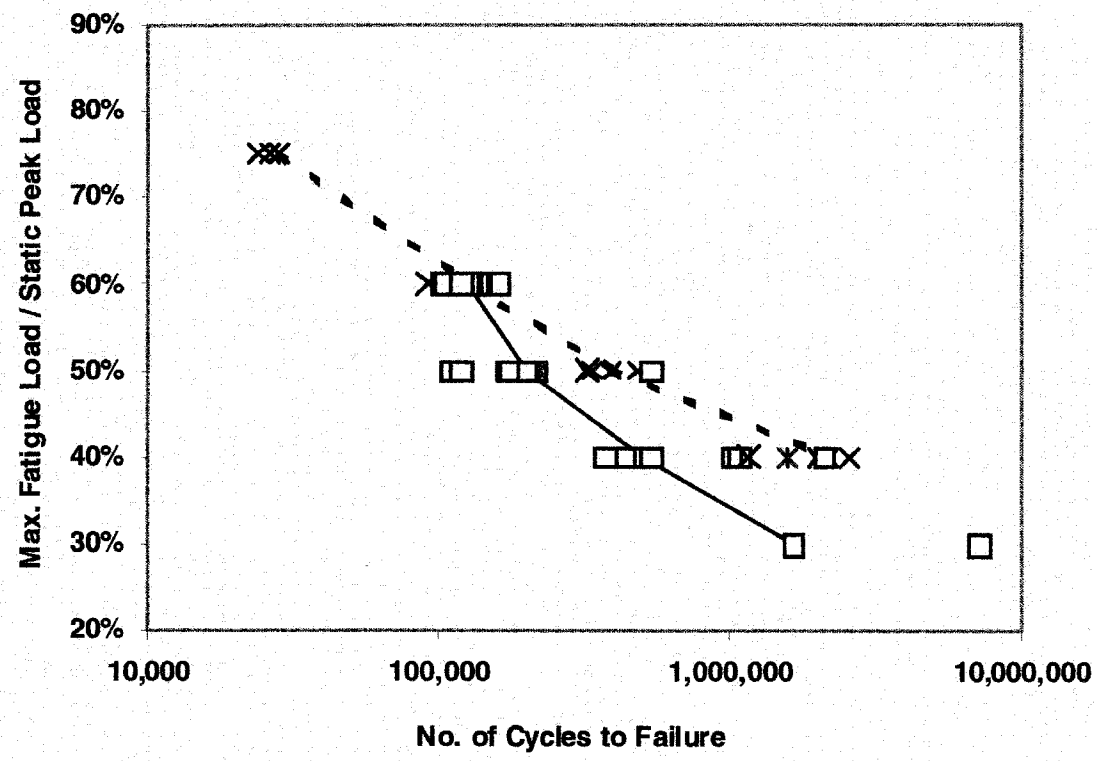

2-mm thick sheet, 5-mm dia. rivet

× 1-mm thick sheet, 3-mm dia. rivet

MEMS AND NANOTECHNOLOGY IN THE 21ST CENTURY

Luc G. Fréchette

Department of Mechanical Engineering
Columbia University in the City of New York
220 S. W. Mudd Building
Mail Code 4703
500 West 120th Street
New York, New York 10027

Telephone: 212-854-2962
e-mail lf307@columbia.edu

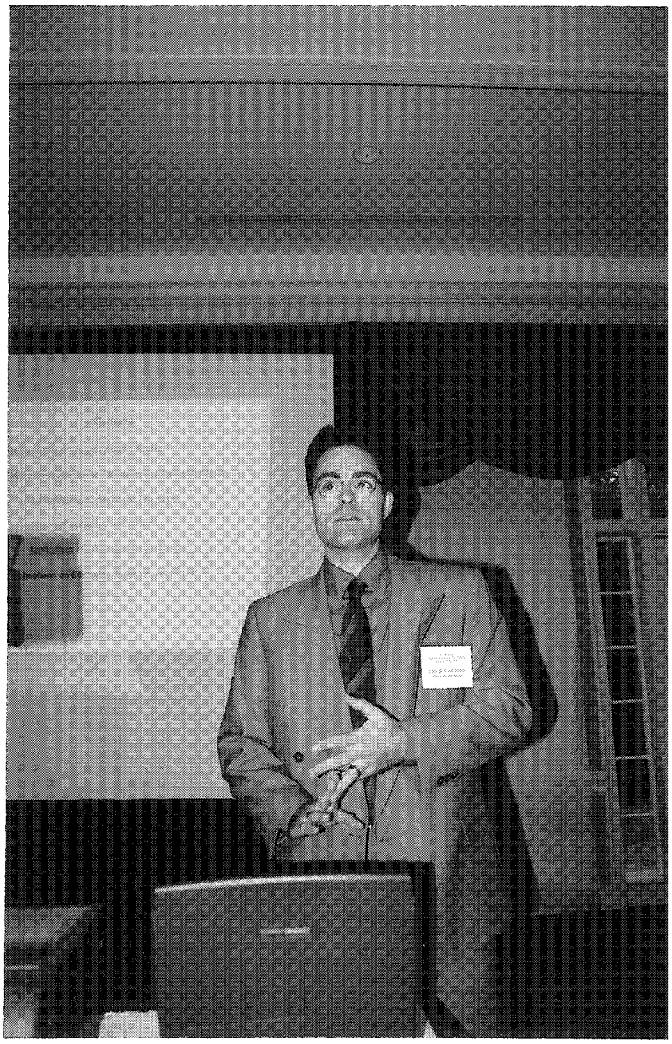

Luc G. Fréchette

Outline

Natural Trend Towards Smaller Scales

MicroElectroMechanical Systems and Nanotechnology

- Building blocks: Science and Technology
- Assembly: Forming Useful Devices
- Applications of MEMS and Nanotechnology

Implications on Education, Industry, and Research

Scale of a device is set by its task

- **Transportation: human scale**
- **Biology: cellular scale**
- **Chemistry: molecular scale**
- **Physics: atomic scale**
- **Information**
  - Processing
    - Microelectronics: Double number of transistors / chip every 18 months (Moore's Law)
  - Gathering
    - Temperature, Force, Acceleration, Chemical composition sensors
  - Storage
    - Magnetic storage: minimum area to store 1 bit of information
  - Transmission
    - Optical (fiber), RF (antenna), Electrical (wire)

Impact of smaller scales

- **Fabrication technology and characterization tools**
  - Manipulate nanoscale elements
  - Measure their characteristics
  - Reproducibility and tolerances
  - Assemble and connect with the macro-world

- **Increased surface area / volume ratio**
  - Dominant forces change
  - Requiring new design principles
  - Signal-to-noise ratio

- **Quantum effects at nanoscale**

⇒ **Leveraged to accomplish unprecedented functionality**

Building Blocks

- **Nature's Elements**
  - Atoms
  - Molecules
  - Cells
- **Nanoscale components**
  - Nanoparticles
  - Nanotubes
- **Microfabrication**
  - Lithography
  - Thin films
- **Fabrication from Bulk**

Brief Description of Carbon Nanotubes

- **1991: multi-wall nanotubes were discovered in the deposits of carbon arc discharge.**
  Iijima, Nature 354, 56 (1991)
- **1993: single-wall nanotubes.**
  Iijima et al. Nature 363, 603 (1993)
- **1995: large scale synthesis of single-wall nanotubes by laser ablation of graphite.**
  Smalley et al, Chem. Phys. Lett. 243, 49 (1995); Science 273, 483 (1996)

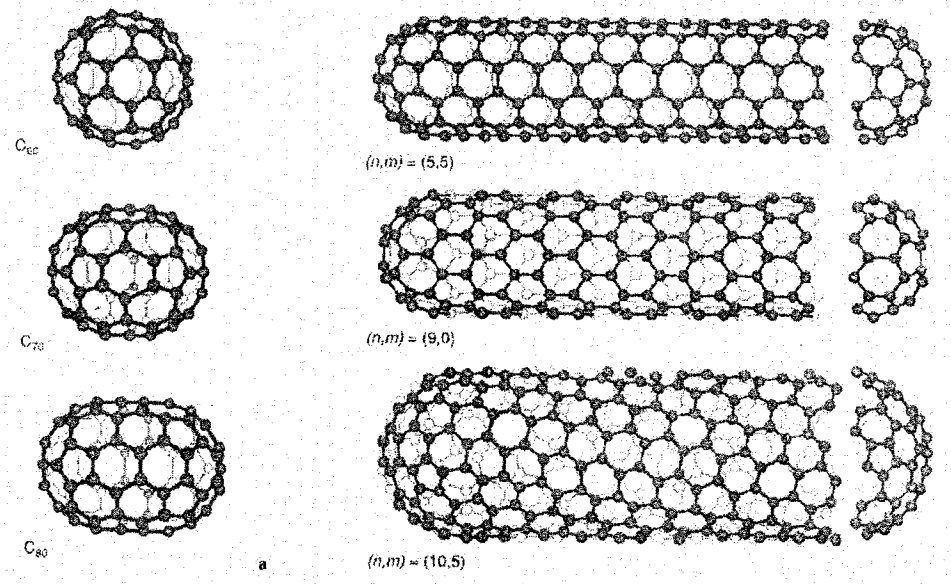

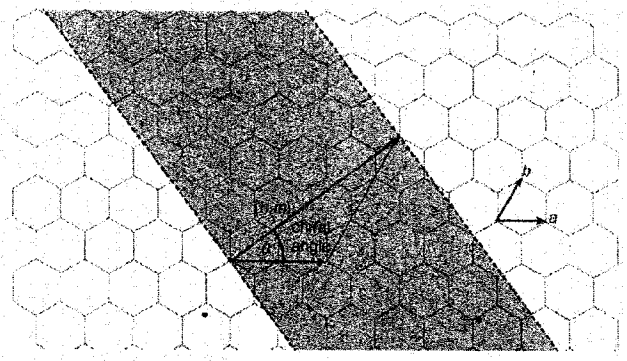

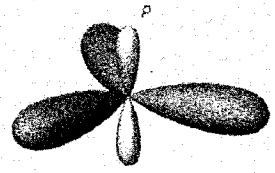

From Smalley website, Rice U.

Single-Wall Nanotube Synthesis

SWNTs made by laser ablation

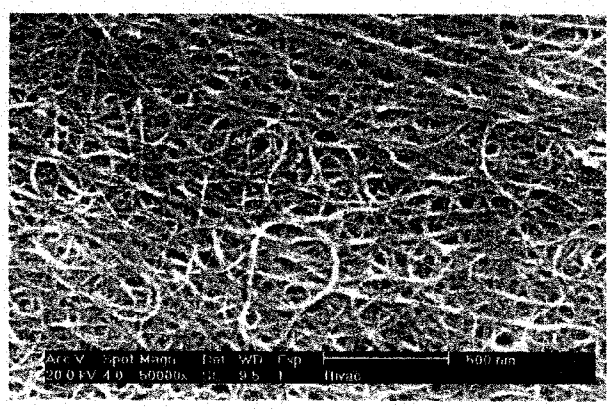

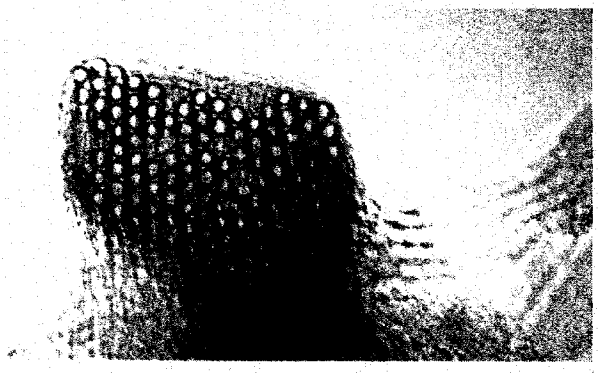

(from Tubes@Rice)

Scanning Tunneling Microscope (STM) image of a SWNT on the surface of a rope.

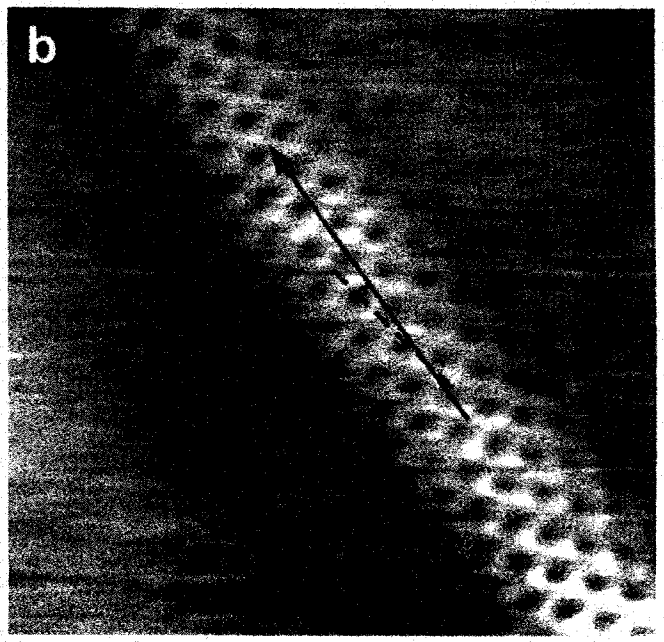

(Lieber group)

Unique Properties of SWNTs

- **Size: Nanostructures with dimensions of ~1 nm diameter (~10 atoms around the cylinder)**

- **Electronic Properties: Can be either metallic or semiconducting depending on diameter and orientation of the hexagons.**

- **Mechanical: very high strength and modulus Good properties on Compression**

- **Physics**
  - 1 D density of electronic states
  - Single molecule `transport' properties Ballistic transport
  - Junctions
  - Heat pipe and electromagnetic pipe

Characterization of SWNTs

Rayleigh scattering spectra of a single thick bundle

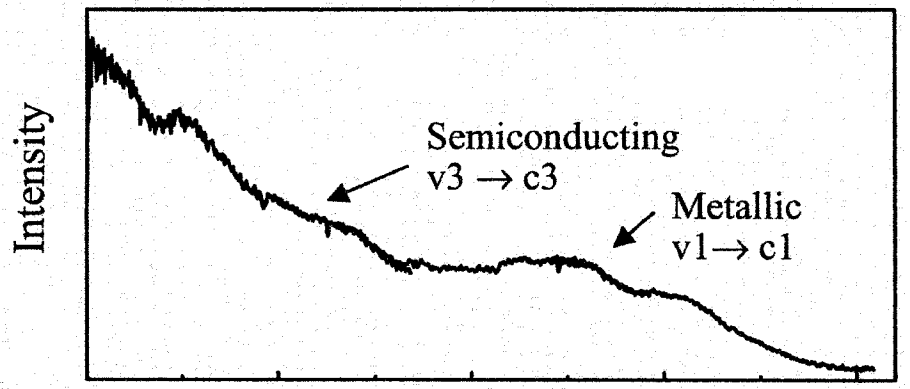

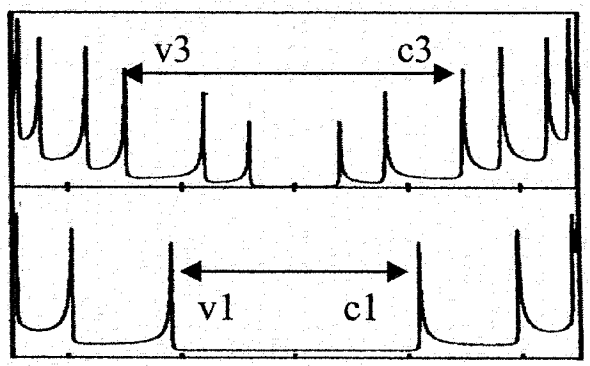

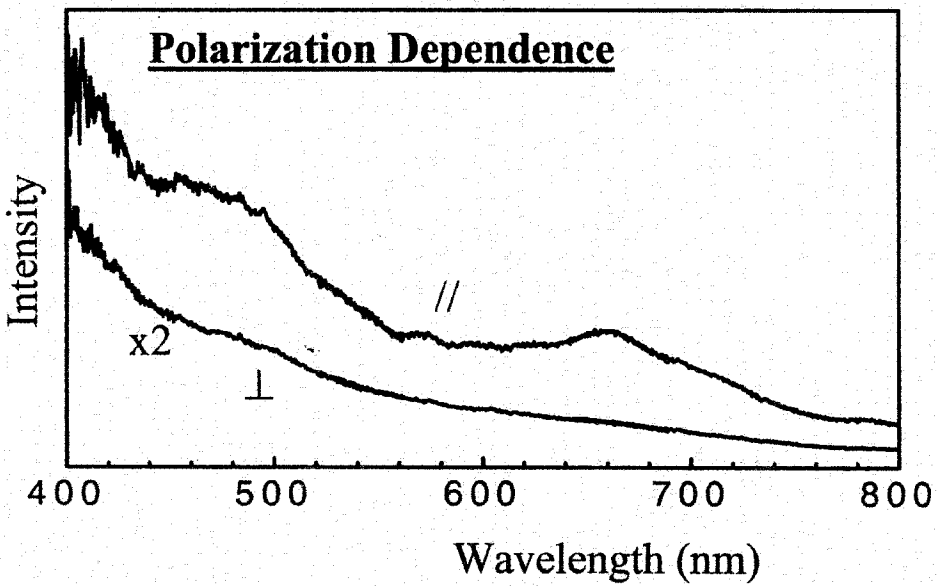

Rayleigh scattering spectrum exhibits resonance peaks due to interband transitions, whose dipoles are shown to be parallel to nanotube axis.

Louis Brus, Chem. Columbia U.

Z. Yu and L. Brus, J. Phys. Chem. *B105*, 1123 (2001).

Assembly: Forming Useful Systems

- **Microfabrication: deposition and patterning at the micron scale**
  - Semiconductor processing for integrated circuits (IC), based on Optical lithography and thin film deposition
- **Guided assembly of nanoscale elements**
  - Individually placing atoms using AFM
- **Self-assembly**
  - Self-assembled atomic monolayer

MEMS technology: down to the micron scale

Micro	**Small scale: micron size features**
Electro	**Electricity and / or electronics**
Mechanical	**Moving parts**
Systems	**Integrated, useful devices**

- Grown to encompass thermal, magnetic, fluidic, optical, chemical, biological components / functions

- Based on microfabrication of semiconductor materials, extending to a broader set of materials.
- Combined material synthesis and assembly

Microfabrication

- Lithography: create sub-micron precision features on dimensional scales from microns to millimeters

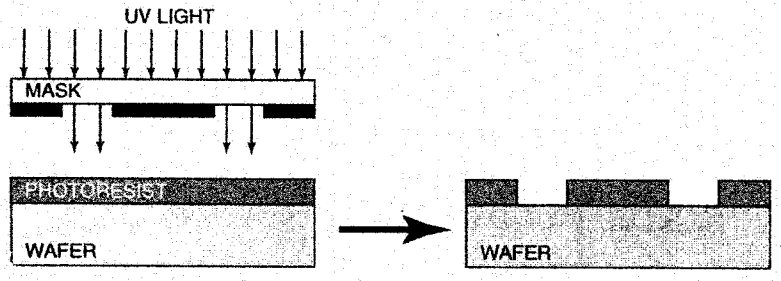

- Etching: removing material in the areas exposed during lithography

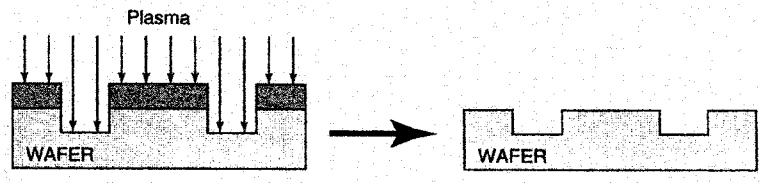

- Deposition of thin films and doping: create multilayered structures with conducting, semiconducting, and insulating components

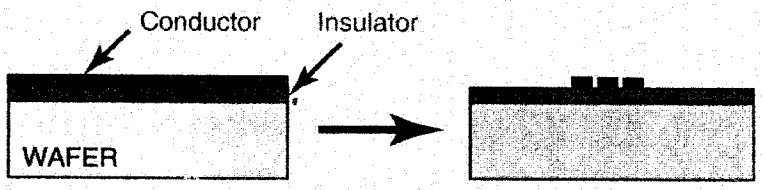

- Wafer bonding and packaging: assemble parts and connect with the macroworld

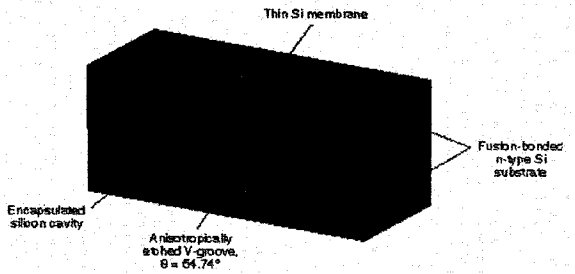

Applications of MEMS Technology

- **MEMS: low cost, small, multifunctional integrated systems:**
  - Ex: Sensors and actuators
- **MEMS as bridge between nanoscale elements and the macroworld**
  - Ex: Lab-on-a-chip
- **MEMS as tools for nanoscale research**
  - Ex: Probing in cellular biology
- **Nanotechnology can enable:**
  - Nanostructured materials by design
  - Nanoelectronics, optoelectronics, megnetics
  - Bio-nanosensors and drug delivery

MEMS Growing Applications and Markets

	1996	2003
	(in million $US)	
• **Pressure measurement**	550	1600
– Automotive, biomedical, industrial		
• **Inertial measurement**	450	1000
– Accelerometers, rate gyros		
• **Optical MEMS**	30	700
– Optical switches, displays		
• **Microfluidic**	450	3800
– Ink-jet, biolab chips, mass-flow sensors		
• **RF MEMS**	-	80
– Cell phone components, devices for radar		
• **Other**	750	1700
– Microrelays, sensors, disk heads		

Source: System Planning Corporation Market Survey (1999)

SURFACE MICROMACHINED COMPONENTS

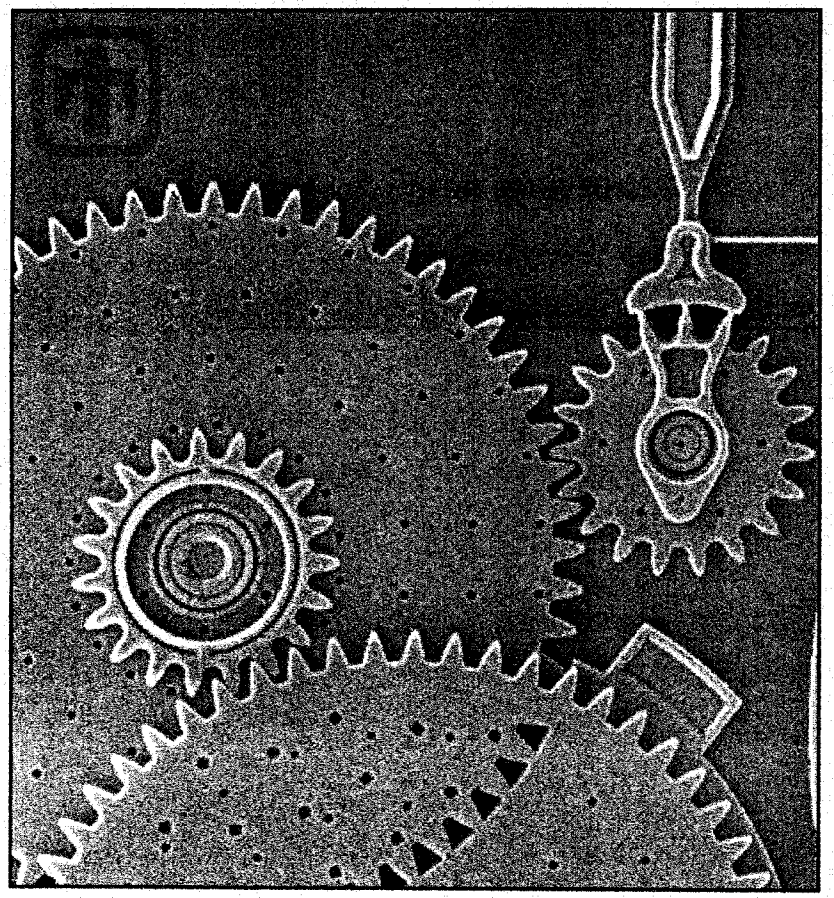

Polysilicon surface-micromachined gear transmission

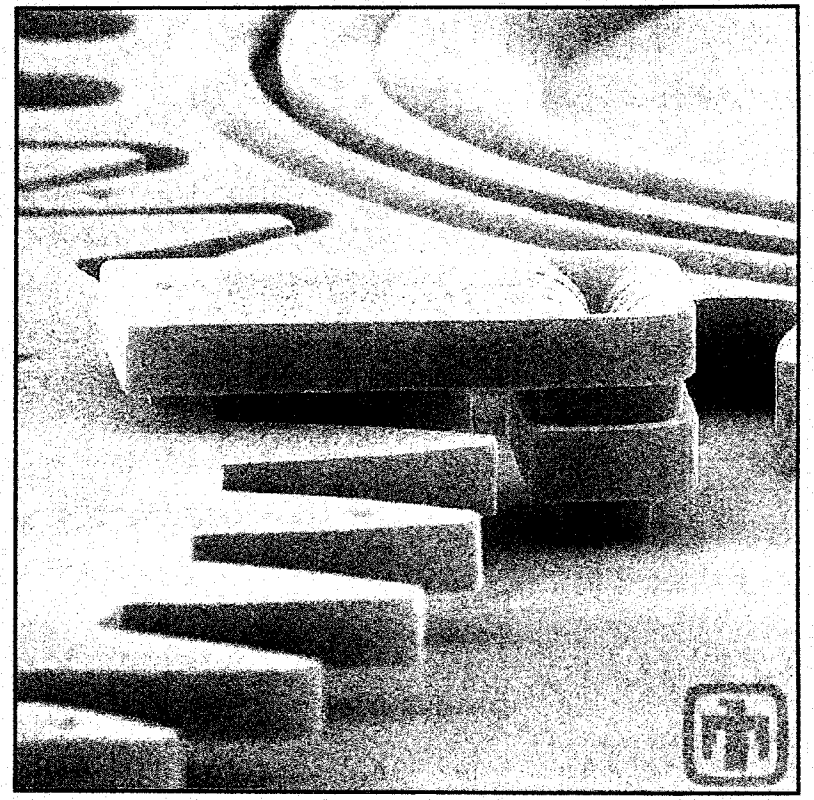

(Sandia National Laboratories)

Micromachines: Fluid-to-Electrical Energy Conversion

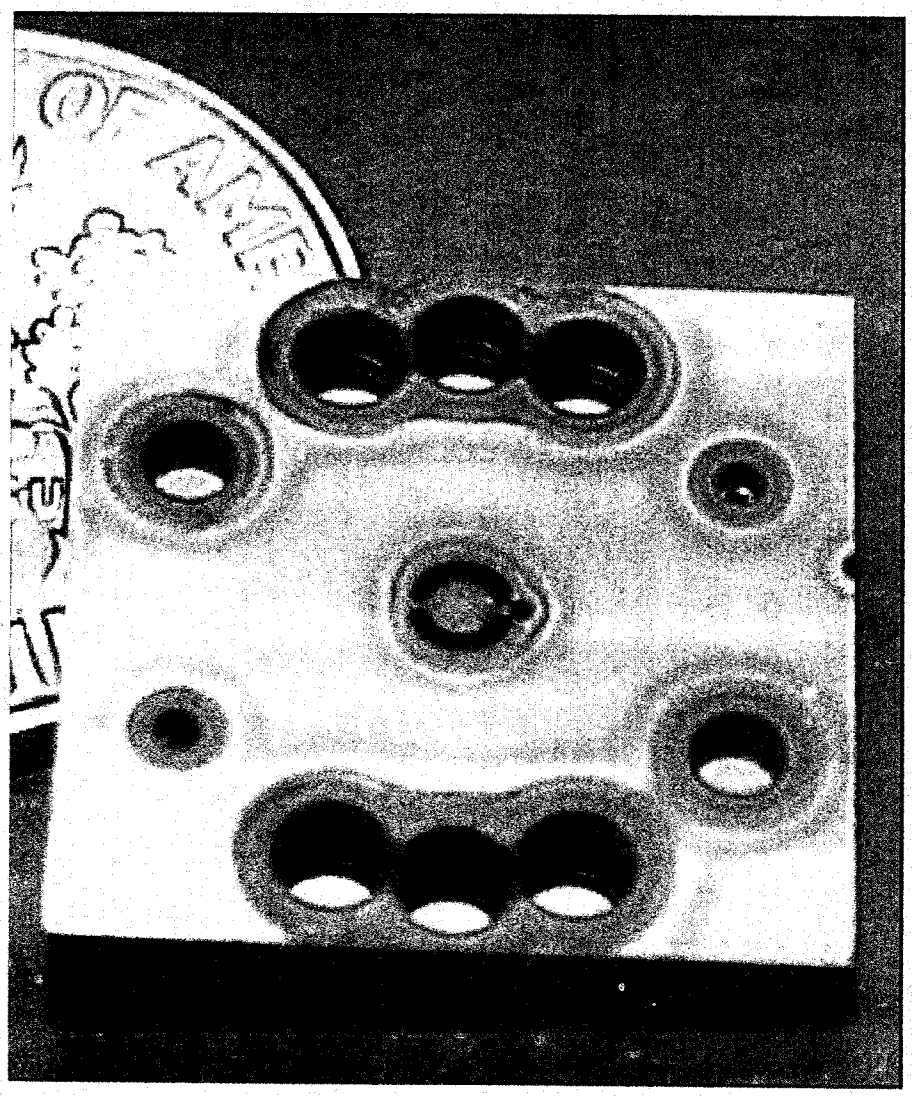

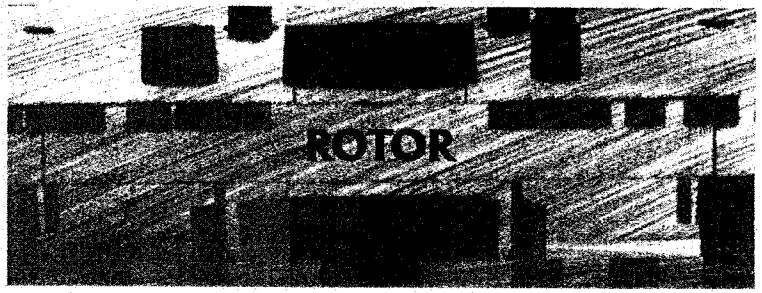

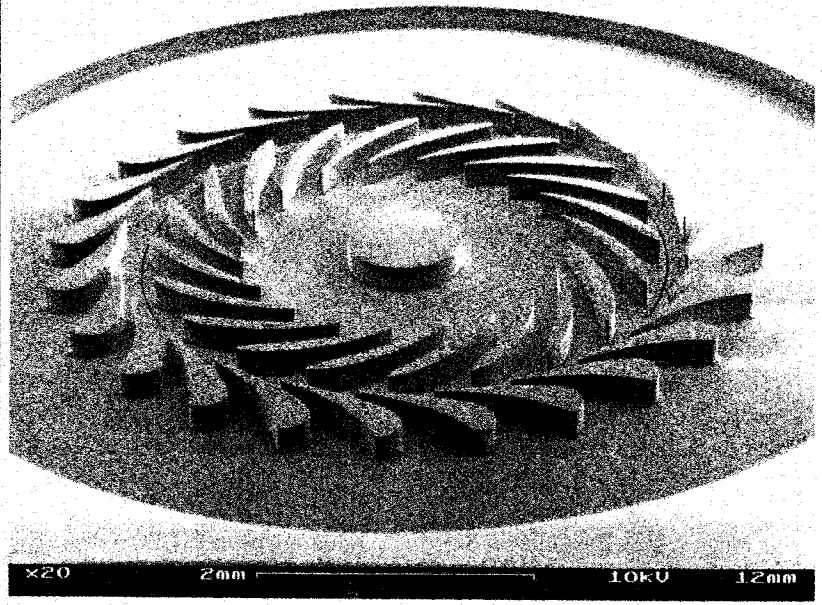

Micro-turbine (MIT)

INTEGRATED MEMS +IC

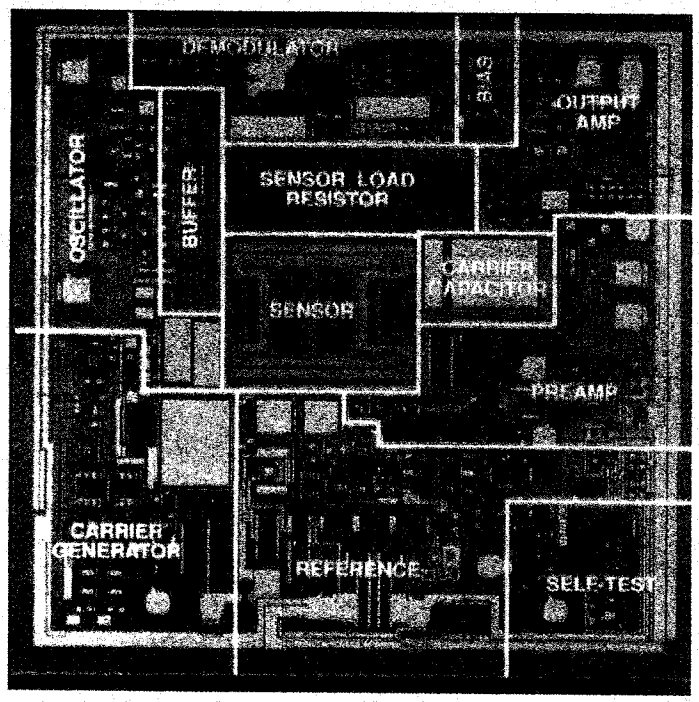

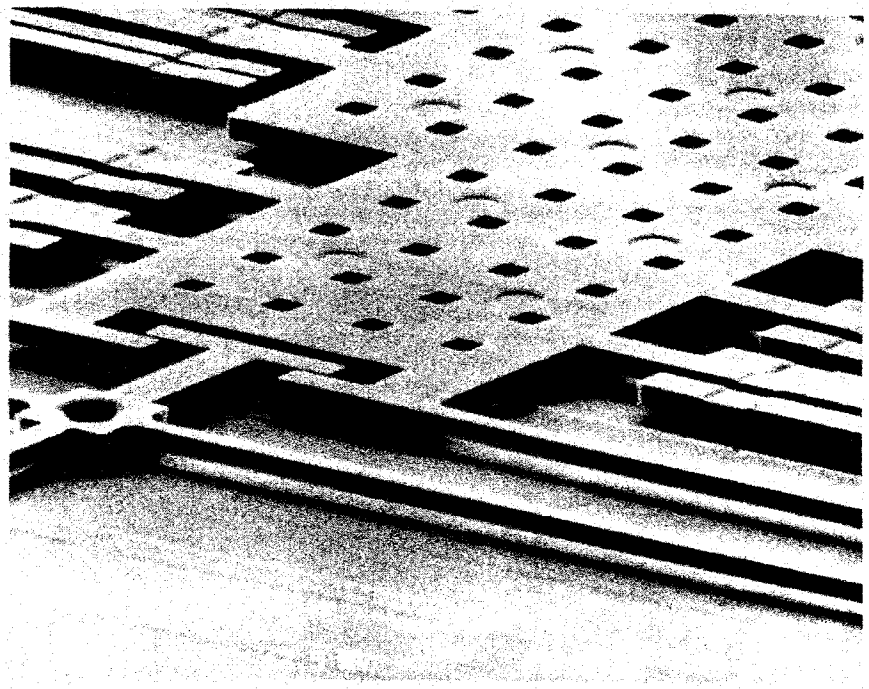

An integrated micromachined accelerometer with:

- **signal processing electronics**
- **micromachined proof-mass**
- **motion sensing capacitance elements**

(Analog Devices)

Micromachined device for measuring traction forces of cells

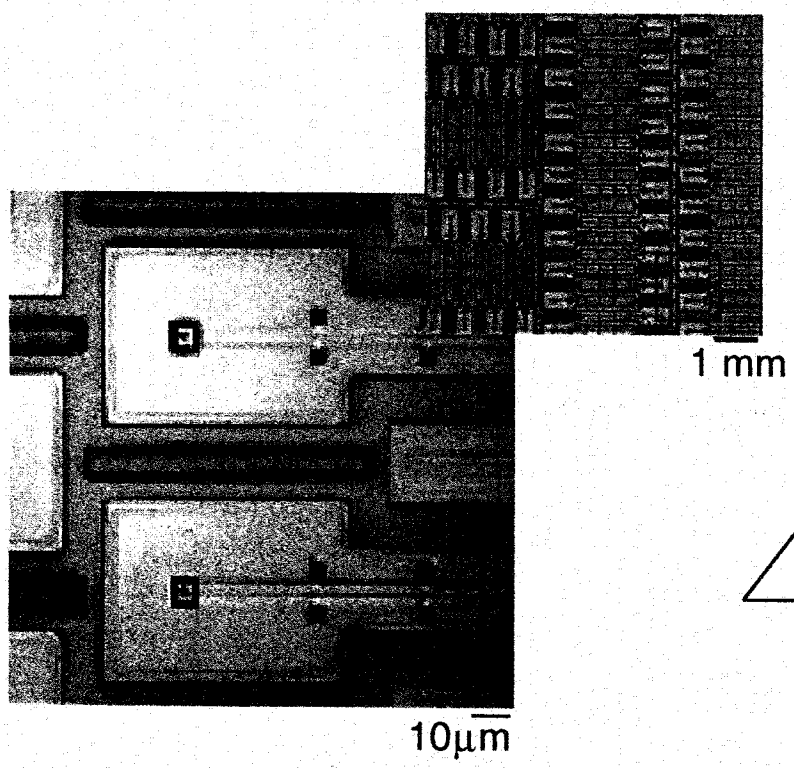

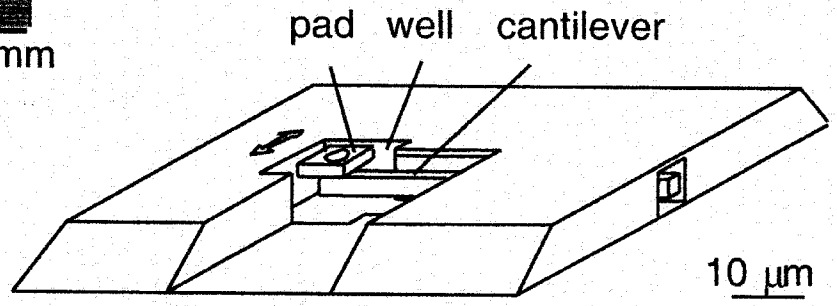

Michael P. Sheetz, Biol. Sci., Columbia U. / MCNC, Research Triangle Park, NC

Galbraith, Catherine G., and Michael P. Sheetz. 1997. A Micromachined Device Provides a New Bend on Fibroblast Traction Forces. Proc. Natl. Acad. Sci. 94:9114-9118.

Galbraith, C. G. and M.P. Sheetz (1999). Keratocytes pull with similar forces on their dorsal and ventral surfaces. J. Cell Biol. 147:1313-1323.

Micromachined device measures:
- Smaller forces than possible other methods
- Sub-cellular spatial resolution

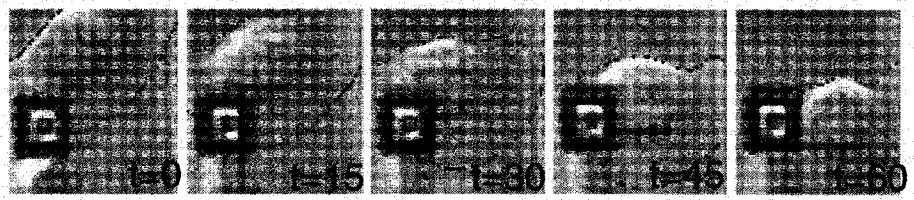

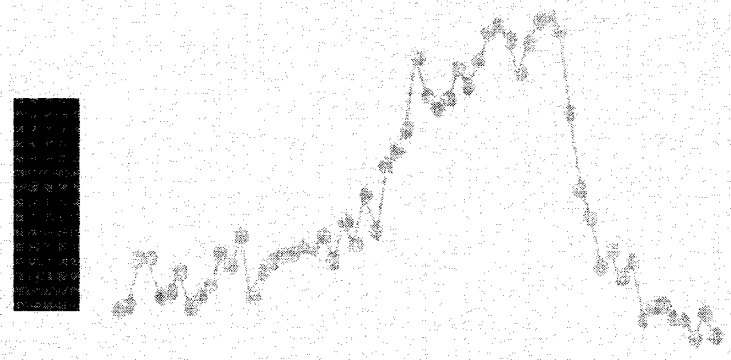

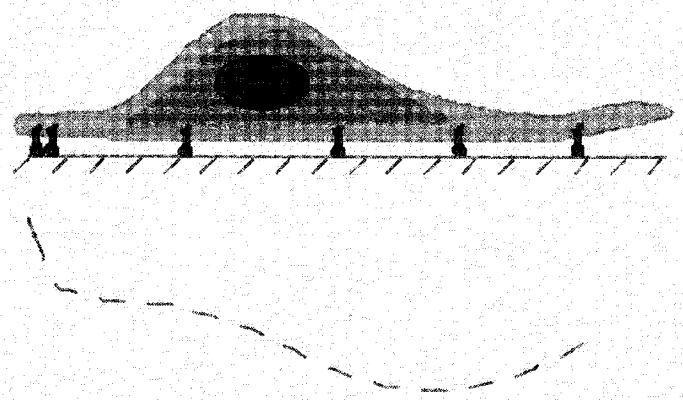

Applications of Nanotechnology

- **MEMS: low cost, small, multifunctional integrated systems:**
  - Ex: Sensors and actuators
- **MEMS as bridge between nanoscale elements and the macroworld**
  - Ex: Lab-on-a-chip
- **MEMS as tools for nanoscale research**
  - Ex: Probing in cellular biology
- **Nanotechnology can enable:**
  - Nanostructured materials by design
  - Nanoelectronics, optoelectronics, megnetics
  - Bio-nanosensors and drug delivery

Columbia Center for Electronic Transport in Molecular Nanostructures

IBM

Lucent Technologies
Bell Labs Innovations

City College
150 YEARS

ROWAN UNIVERSITY

BARNARD

Motivation: Miniaturization of conventional electronic devices will stagnate in early 21 century.
What will be the next technology?

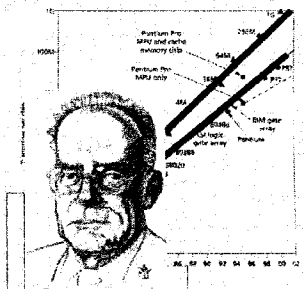
G.E. Moore

Hypothesis: Molecules provide an attractive alternative as switches. Molecular recognition is a starting point for self-assembly.
How can we exploit molecules for electronics?

Proposal: Fundamental research on tailored molecules as primitive electronic components with self-assembly into larger units.
What new principles and concepts will arise?

Heart of the Columbia University Nanocenter:

- ***Fundamental physical understanding of charge transport in molecular materials.***
- ***Synthesis of new materials.***
- ***Collaboration with leading industrial capability.***

Scientific directors:
Horst Stormer
Ronald Breslow
Managing director:
James Yardley

Understanding of electron transport in confined systems…

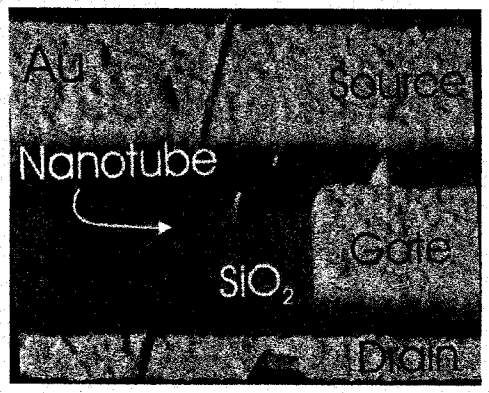

Nanotube transistor

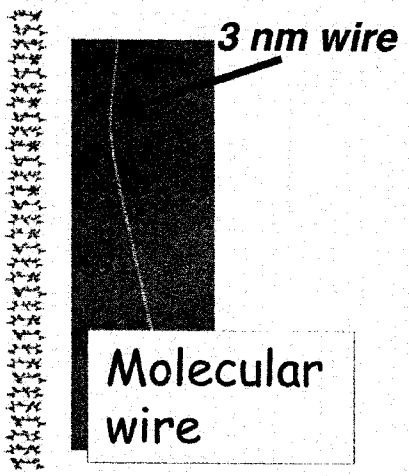

Molecular wire

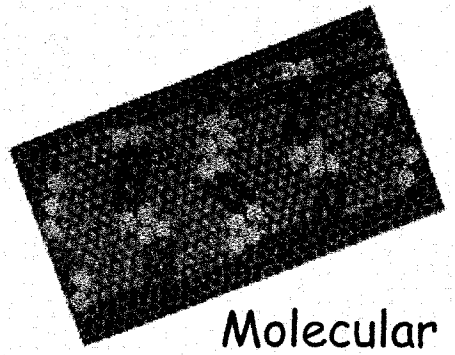

Molecular assembly

…toward development of the molecular transistor.

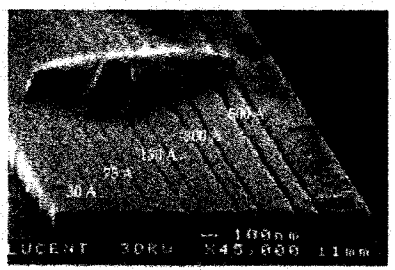

Fig. 5. Lithographic channels as small as 3 nm (Willett, Lucent Tech.)

Scaffold

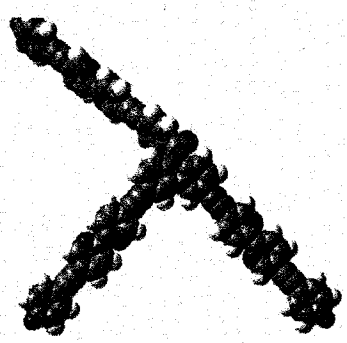

Molecular tripod

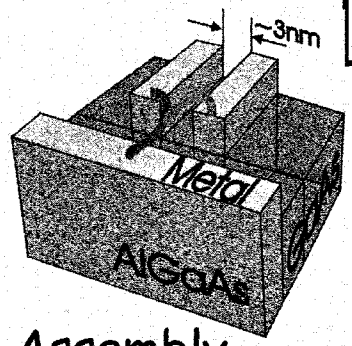

Assembly

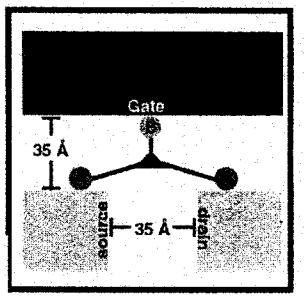

Implications

- **Education**
  - New fabrication technology and materials
  - Quantum effects and surface forces of increasing importance
  - Multidisciplinary training necessary

- **Commercial**
  - Provide paradigm shifts in a growing number of areas, by allowing unprecedented functionality at reduced costs

- **Research**
  - New building blocks
  - Tools to synthesize, characterize, assemble nanoscale elements
  - Modeling of nanoscale phenomena
  - Integration for applications in the macroworld

FISHING LINE KNOT TYING CONTEST: A FRESHMEN EXPERIENCE

Wayne L. Elban

Department of Electrical Engineering and
Engineering Science
Loyola College
4501 North Charles Street
Baltimore, Maryland 21210

Telephone: 410-617-2853
e-mail welban@loyola.edu

and

Douglas L. Frantz

Department of Physics
Earth Science, and Geography
Community College of Baltimore County
Baltimore, Maryland 21228

Telephone: 410-455-4317
e-mail dfrantz@ccbc.cc.md.us

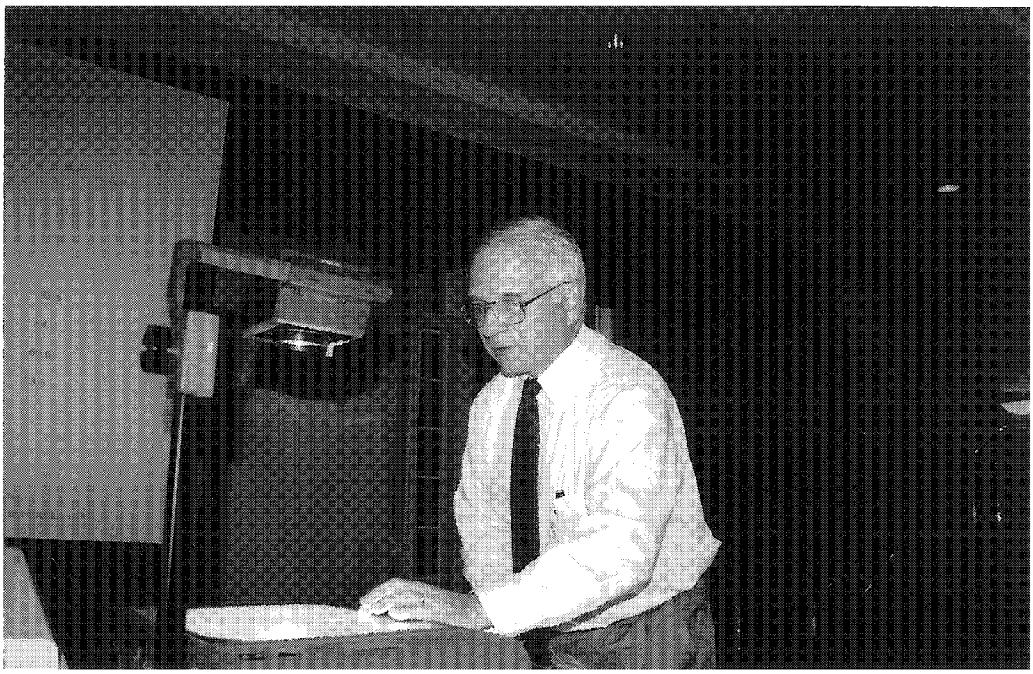

Wayne L. Elban

Wayne L. Elban

Since 1985, Professor Elban has taught engineering science courses at Loyola College, including introductory materials science, materials science lab, mechanical properties of materials, and transformations in solids. He received a BChE with distinction ('69) and a PhD in Applied Sciences: Metallurgy ('77) from the University of Delaware and a MS in Engineering Materials ('72) from the University of Maryland, College Park. From 1969-1985, he was a research engineer at the Naval Surface Warfare Center, White Oak Laboratory, Silver Spring, Maryland. He is a member of ASM International.

Douglas L. Frantz

Doug Frantz has been an adjunct faculty member for the Physics Laboratory at the Community College of Baltimore County (CCBC), Catonsville Campus since 1980. He received his BS in Chemistry ('70) from Towson State College (now Towson University). He serves primarily as Network Administrator for the Mathematics, Science, and Engineering Division at CCBC. His focus as adjunct faculty member is first-year physics laboratory experiences.

FISHING LINE KNOT TYING CONTEST: A FRESHMEN EXPERIENCE

Wayne L. Elban
Dept. of Electrical Engineering and Engineering Science
Loyola College
Baltimore, Maryland 21210

and

Douglas L. Frantz
Dept. of Physics, Earth Science, and Geography
Community College of Baltimore County, Catonsville Campus
Baltimore, Maryland 21228

ABSTRACT: A procedure is described for conducting a knot tying contest for freshmen engineering/physics students using commercial 6 (and 4) lb-test nylon monofilament fishing lines. A bench-top universal testing machine is used to obtain room temperature determinations of tensile breaking load for knots tied to a swivel or hook. Emphasis is given to exposing students to materials testing methodology, modifying a standard test fixture configuration to accommodate the knotted samples, and **(optional activity)** using elementary statistical analysis to assess knot quality. Results from testing samples with a variety of knots, including double overhand, modified double overhand, Palomar, Improved Clinch, Perfection, and Harvey are presented. Experimental determinations of knot efficiencies are compared to values appearing in the literature.

KEY WORDS: Uniaxial tensile testing, fracture, stress concentration, thermoplastic polymers, nylon, monofilament fishing line.

PREREQUISITE KNOWLEDGE: High school mathematics and physics.

OBJECTIVES:

(a) Experimental Goals:

1. to design and tie fishing line knots in order to enter contest for freshmen engineering/physics students;

2. to measure the breaking load (i.e., fracture force) of various fishing line knots tested in uniaxial tension; and

3. to improve on the design of fishing line knots.

(b) Learning Goals:

1. to become familiar with uniaxial tensile testing, a prominent technique for characterizing the mechanical response of materials;

2. to become familiar with measuring dimensions using a dial caliper;

3. to become familiar with the strength properties of common engineering materials;

4. to become exposed to stress concentration and its effect on material deformation/fracture behaviors; and

5. **(optional activity)** to become exposed to rudimentary statistical analysis of experimental data (Instructor Note 1).

EQUIPMENT AND MATERIALS: (1) Chatillon model LRX universal testing machine (bench top model with 500-lb capacity); (2) Wedge-action grip (Chatillon model TG15N); (3) Bollard wire, yarn, and thread grips (Chatillon model TG12N); (4) Metric universal dial caliper (Brown and Sharpe 559-579-13); (5) Ruler; (6) Extruded nylon monofilament fishing line [Berkley Trilene XL 6- (and 4-) lb test (or equivalent)] (Instructor Note 2); (7) 1" x 1-3/4" x 1/4" oak lath with eyehook screwed into the center of the thin dimension (Instructor Note 3); (8) Interlock swivels [Berkley size 7 (or equivalent)]; (9) Fishing hooks [Mustad 9672 3X-8 (or equivalent)] (Instructor Note 4).

SAFETY PRECAUTIONS: Care must be taken to avoid being stuck if fishing hooks are used instead of interlock swivels when tying knots. (Instructor Note 4)

INTRODUCTION:

A. CONTEST RULES (Instructor Note 5)

The objective of this competition is to obtain the knot with the highest fracture force using commercial nylon monofilament fishing line tied to an interlock swivel or fishing hook. It is expected that participation will result in an improved understanding of the important engineering concept of stress concentration and its effect on the strength of polymers and its use in designing with these materials. Listed below are the various constraints and rules that must be adhered to with your entries.

Materials:

1. All knots must be tied using only the fishing line and swivels/hooks supplied in your kit.

2. Each kit consists of:

(a) Five (5) two-foot long pieces of fishing line;
(b) Three (3) No. 7 interlock swivels or 3X-8 fishing hooks; and
(c) Booklet entitled "A Guide to Knots and Lines: Angler's Reference" [1] describing several popular knots used for the type of line provided.

Physical Constraints:

1. An entry (one per individual) shall consist of no more than three (3) knots. These may be of any type -- all the same or a variety. Two (2) additional lengths of line have been provided so practice knots can be prepared.

2. Each knot must be tied to a single swivel/hook with at least 18 in. of line available, so that the knot can be tested as described below.

3. No foreign substance, such as adhesive or glue, may be added to the knot or line.

4. It is expected that each contestant will tie his/her own knots.

Loading:

1. Each knot will be tested in tension using the department's universal testing machine (Chatillon model LRX) operating at a crosshead speed of 1 in./min. Equipped with a couple of different types of grips, the tester is computer controlled and has computer data acquisition capability.

2. The line is elongated at constant rate until one of three events occurs:

   (1) knot fails;
   (2) line fails, leaving knot intact; or
   (3) line fails at the gripping fixture, again leaving knot intact.

   Generally, a grip failure occurs at a load significantly below the test rating of the line as specified by the manufacturer and is considered to be a test artifact.

3. Regardless of failure location, the maximum tensile force is recorded for each of three knots maximum per entry. Only the highest force per entry is used to rank order the entries and for the awarding of prizes. This allows for a maximum number of contest winners.

Qualifications:

1. All knots are subject to the above constraints, and any knot failing to meet any of the constraints will be disqualified by the judges.

2. All decisions of the judges are final.

B. BACKGROUND TOPICS

Nylon is a prominent example of a large class of industrially important materials known as thermoplastic polymers, which usually have a linear structure. Typical uses for nylon include outdoor fabrics, carpet fibers, and monofilament fishing lines (introduced by Berkley in 1957 [2]). The continuous extrusion/drawing process used to manufacture fishing line has been briefly described [3] previously. The most significant feature of the drawing operation is the resultant alignment of molecules along the filament longitudinal axis. Consequently, the highest tensile strength is realized in this direction as desired, for example, in nylon monofilament fishing line.

Stress concentration [4] arises in a material sample experiencing a point applied force or in one of varying cross-sectional area subjected to a uniform applied force. For example in the latter case, a tensile specimen consisting of a bar with reduced cross section in the center has the highest normal stress where the area is smallest. This effect is assessed using a stress-concentration factor, k_t, which is given as

$$k_t = \sigma_{max}/\sigma_{avg}, \tag{1}$$

where σ_{max} = maximum normal stress, and
σ_{avg} = average normal stress at the smallest cross-sectional area.

This ratio provides a quantitative measure of the effect of sample geometry on the local stress at the smallest cross-sectional region. As a result of the stress concentration that occurs at a pre-existing surface flaw (e.g., nick) or a knot, nylon monofilament fishing line exhibits a notch weakening effect. [3]

It is useful to gage the performance of a knot in fishing line, say, by comparing its fracture force with that of the same line without a knot. These two forces allow the calculation of a knot efficiency, η_{knot}, which is defined as

$$\eta_{knot} = F_{knot}/F_o, \tag{2}$$

where F_{knot} = fracture force of knot, and
F_o = fracture force of line without knot.

For 6-lb test Berkley Trilene XL fishing line tested [3] previously, a single in-line overhand knot had an average efficiency of 54.9%. From analogous sets of measurements obtained by other researchers [5] for a variety of 30- and 50-lb test nylon monofilament lines, knot efficiencies were somewhat higher, typically in the 60-70% range. In kernmantle climbing rope, a different class of structural material, efficiencies ranged [6] from 60 to 80% depending on the knot, all of which were more complicated than a single overhand knot.

For repeated experimental measurements of a given quantity, such as knot fracture force, the arithmetic mean or average [7] is generally considered to be the best estimate of the so-called "true" value for a particular set of experimental conditions. However, calculating just the average

conveys no knowledge about the distribution or spread in the data set. To assess this characteristic, statisticians rely on a calculation of root mean square deviation or standard deviation [7]. This parameter provides a measure of the uncertainty due to fluctuations in the measurements.

The purpose of this activity is to provide a "hands-on" experiment designing, preparing, and evaluating various knots tied using nylon monofilament fishing line. To this end, a quantitative evaluation of knot fracture force will be made from uniaxial tensile testing. The current experiment follows on from last year's National Educators' Workshop (NEW) paper [3] describing a procedure for characterizing the fracture behavior of commercial nylon monofilament fishing line. Further, it relates to a previous year's NEW paper [8] that provides a very nice description for evaluating the load reducing (stress concentrating) effect of knots in various lines and threads.

PROCEDURE:

A. INTRODUCTORY TENSILE TESTING OF AS-MANUFACTURED LINE (Instructor Note 6)

1. Measure the diameter of each specimen using a dial caliper prior to tensile testing.

2. Perform tensile testing (specimen gage length = 4¾ in.; crosshead speed (CHS) = 1 in./min -- Instructor Note 7) on five (5) specimens minimum of line (without knot) using bollard grips.

3. For each specimen, note whether failure occurred in the line as desired or where it was clamped corresponding to a testing artifact. In this case, the data should be discarded.

B. KNOT DESIGN

1. Recognizing that knots inherently degrade the strength of nylon monofilament fishing line [3,5] and other materials [8], attempt to identify desirable features of a knot that can serve as a basis for designing a strong, high performance knot.

2. Review various widely used knots appearing in the literature [1,9,10] and on Web sites [11-13] to determine whether and how these design features have been used.

3. To commence designing knots and to become familiar with handling/tying fishing line, prepare several double overhand knots for initial testing.

4. Once the double overhand knot is tested, consider ways to improve it's performance and prepare several modified double overhand knots for testing. (Instructor Note 8)

5. Tie knots of your own design or select knots to tie from the literature to enter the contest.

C. TENSILE TESTING OF KNOTS

1. Perform tensile testing (same specimen gage length and CHS employed previously) using a top bollard grip and a bottom wedge-action grip with eyehook/lath assembly to provide the necessary sample fixtures (Figure 1) for the knots provided.

2. For each specimen, note whether failure occurred at the knot as desired to evaluate its fracture force or elsewhere (where it was clamped or in the line away from the knot). In the latter cases, the data should be discarded in the analysis that follows.

D. ANALYSIS

Perform the following analyses.

1. Tensile testing measurements:

   a. Tabulate the measured values of fracture force.

   b. Calculate [7] the average and **(optional activity)** standard deviation, σ, for this value if a minimum of five (5) specimens of the same type were tested.

2. Fracture strength of as-manufactured line:

   a. Calculate fracture strength, σ_f, for each line specimen without knot using the engineering stress relationship (e.g., Eqn. (2-1), Ref. [14]):

$$\sigma_f = F_f/(\pi d_o^2/4), \qquad (3)$$

   where F_f = fracture force in force-displacement curve, lb_f, and
   d_o = initial diameter of specimen, in.

   b. Calculate [7] the average and **(optional activity)** standard deviation, σ, of this determination.

3. Knot efficiencies:

   a. Calculate the efficiency of a given knot using Eqn. (2), where both forces have units of lb_f.

   b. Calculate [7] the average of this determination.

COMMENTS with Data Sheets and Plots:

All of the experimental steps were repeated to verify that the results are reproducible. The greatest uncertainty is associated with the quality of knots that were tested and not in the

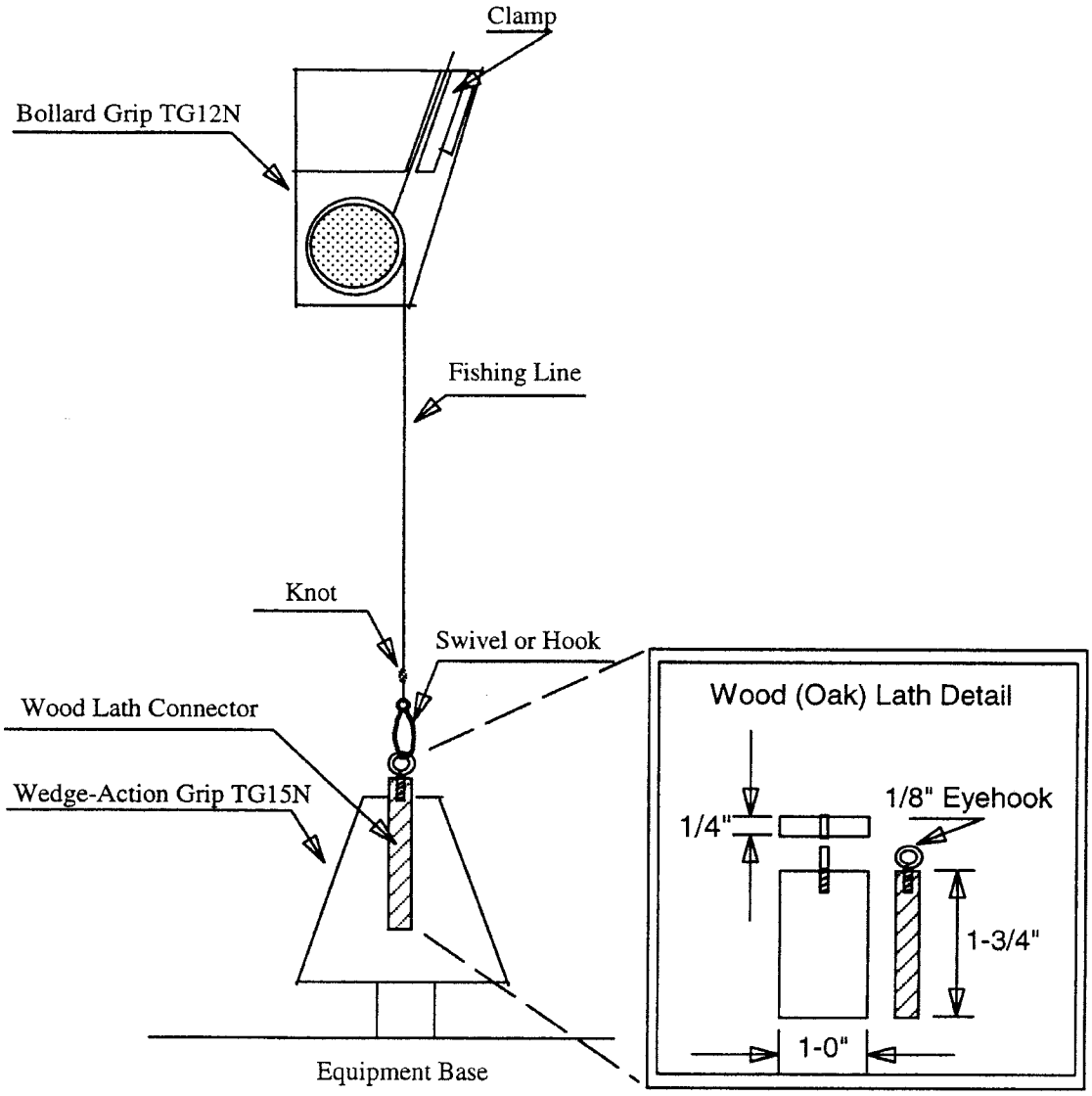

Figure 1. Sample fixture arrangement used in uniaxial tensile testing of fishing line knots.

measurements themselves. The data sets appearing in this section are considered to be representative for Berkley 6-lb test line and the various knots that were evaluated. A complete set of measurements obtained for Berkley 4-lb test line appears in the Appendix. (Instructor Note 2)

Tensile Testing of As-Manufactured Line: Force measurements taken from experimental curves (e.g., Figure 2) are given in the first data set of Table I for Berkley 6-lb test line without knots. The average fracture force was 7.96 lb_f (35.4 N), corresponding to 133% of the line's rating. Four of the six specimens broke in the middle, while fracture in the remaining two occurred at a bollard but away from the clamp. As such, the bollard that takes up the filament before it is clamped in each grip successfully isolates the specimen from the deleterious effect of clamping. Thus, all of these measurements are valid.

Fracture Strength of As-Manufactured Line: The average fracture strength was computed to be 141,000 psi (972 MPa). For comparison purposes, this value appears in Table II along with (ultimate) tensile strengths for several other materials [15-19] that have familiar applications. The relatively (and surprisingly) high fracture strength of the fishing line is attributed to the polymer molecules becoming aligned during the drawing operation along what is to become the tensile axis. As such, a relatively high percentage of strong intramolecular bonds oppose the applied force.

Tensile Testing of Knots and Their Efficiencies: Force measurements taken from experimental curves (e.g., Figure 3) are given in the remaining data sets of Table I for various knots in the 6-lb test line. The double overhand knot yielded an average maximum force of 3.10 lb_f (13.8 N), corresponding to an efficiency of 39.0%. For this knot, failure occurred by filament pull through rather than by breaking. Modifying this knot by providing an additional loop in the swivel to decrease line slippage increased the average maximum/fracture force to 4.77 lb_f (21.2 N), corresponding to an improved knot efficiency of 59.9%.

All of the standard knots except the Perfection failed at loads that exceeded the line's rating. The average fracture force for the Palomar, Improved Clinch, and Harvey knots were 6.58 lb_f (29.3 N), 6.76 lb_f (30.1 N), and 6.66 lb_f (29.6 N), respectively, corresponding to very similar knot efficiencies (82.6, 84.9, and 83.6%). The Perfection knot exhibited poorer performance on the order of the modified double overhand knot; the average fracture force was 4.82 lb_f (21.4 N), resulting in an efficiency of 60.6%.

With the exception of the double overhand knot which did not actually break, all of the knots had higher average efficiencies than the in-line single overhand knot evaluated [3] previously. Thus, these current knots have improved designs that lessen the deleterious effect of stress concentration.

(Optional activity) Insights from Standard Deviation: Referring to the standard deviation values appearing in Table I, the only knot whose standard deviation approached that of line without a knot was the double overhand. The greatest fluctuation from the average value occurred for the modified double overhand knot and is attributed to the two distinct failure modes that occurred as denoted under Comments in the Table. Of the standard knots, the Improved Clinch had the

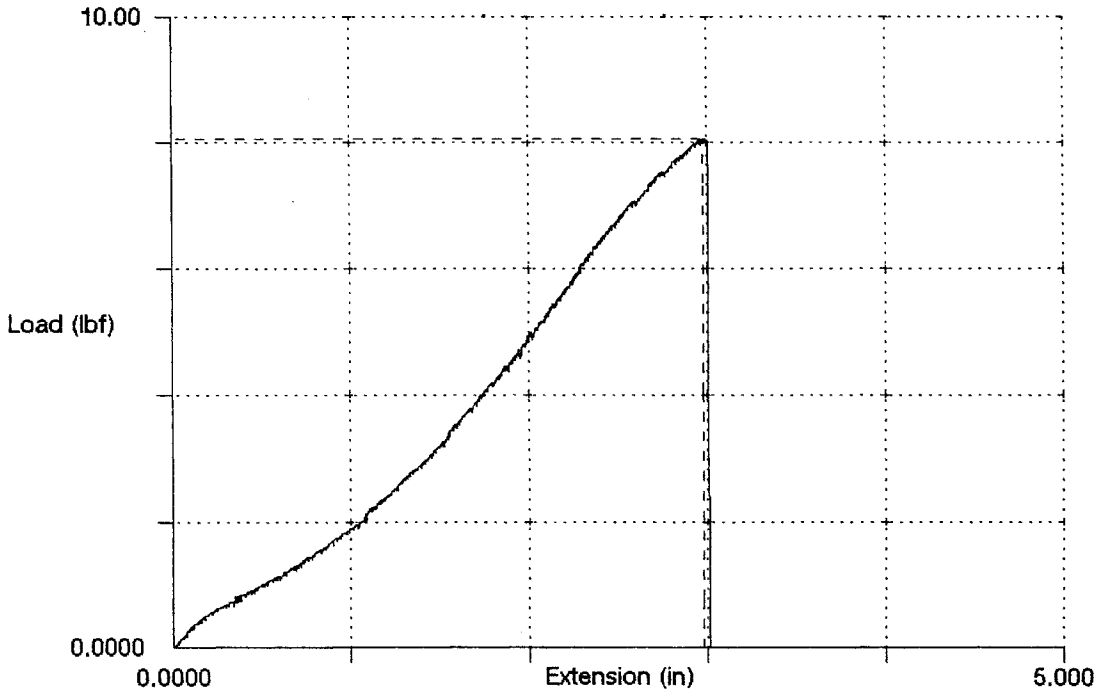

Figure 2. Force-displacement curve for Berkley Trilene XL six-pound test nylon monofilament fishing line (specimen T6XL0401).

Table I. Force Measurements for Berkley Trilene XL Six-Pound Test Nylon Monofilament Fishing Line Having Various Knots

Knot Type	Specimen Designation	Fracture Force* (lb_f)	Comments
Without Knot	T6XL0301	7.588	Fractured at center
	T6XL0401	8.077	Fractured at top of bottom bollard (away from grip)
	T6XL0501	8.077	Fractured at side of bottom bollard (away from grip)
	T6XL0601	7.731	Fractured at center
	T6XL0701	8.097	Fractured at center
	T6XL0801	8.199	Fractured at center
	Avg.:	**7.96 [35.4 N]**	
	σ:	**0.24 [1.1 N]**	
Double Overhand	T6XL0901	2.909**	Knot pulled through without fracture
	T6XL1001	3.092**	Knot pulled through without fracture
	T6XL1101	3.153**	Knot pulled through without fracture
	T6XL1201	3.581**	Knot pulled through without fracture
	T6XL1301	2.991**	Knot pulled through without fracture
	T6XL1401	2.889**	Knot pulled through without fracture
	Avg.:	**3.10 [13.8 N]**	
	σ:	**0.26 [1.1 N]**	
Modified Double Overhand	T6XL1501	4.842**	Knot pulled through without fracture
	T6XL1601	3.764**	Knot pulled through without fracture
	T6XL1701	3.479**	Knot pulled through without fracture
	T6XL1801	6.246	Knot pulled through partially and fractured at knot
	T6XL1901	5.290	Knot pulled through partially and fractured at knot
	T6XL2001	5.005	Knot pulled through partially and fractured at knot
	Avg.:	**4.77 [21.2 N]**	
	σ:	**1.0 [4.5 N]**	

Table I. Force Measurements for Berkley Trilene XL Six-Pound Test Nylon Monofilament Fishing Line Having Various Knots, Cont'd.

Knot Type	Specimen Designation	Fracture Force* (lb_f)	Comments
Palomar	T6XL2101	7.100	Fractured at knot
	T6XL2201	6.734	Fractured at knot
	T6XL2301	5.717	Fractured at knot
	T6XL2401	6.917	Fractured at knot
	T6XL2501	7.243***	Fractured in line (~9/16" away from knot)
	T6XL2601	6.429	Fractured at knot
	Avg.:	**6.58 [29.3 N]**	
	σ:	**0.54 [2.4 N]**	
Improved Clinch	T6XL2701	6.836	Fractured at knot
	T6XL2801	6.653	Fractured at knot
	T6XL2901	7.772	Fractured at knot
	T6XL3001	7.161***	Fractured in line (~3" away from knot)
	T6XL3101	5.554	Fractured at knot
	T6XL3201	6.978	Fractured at knot
	Avg.:	**6.76 [30.1 N]**	
	σ:	**0.80 [3.5 N]**	
Perfection	T6XL3301	4.842	Fractured at knot
	T6XL3401	5.574	Fractured at knot
	T6XL3501	4.171	Fractured at knot
	T6XL3601	6.429***	Fractured at knot; eyelet fixture rotated
	T6XL3701	4.781	Fractured at knot
	T6XL3801	4.740	Fractured at knot
	Avg.:	**4.82 [21.4 N]**	
	σ:	**0.50 [2.2 N]**	

Table I. Force Measurements for Berkley Trilene XL Six-Pound Test Nylon Monofilament Fishing Line Having Various Knots, Cont'd.

Knot Type	Specimen Designation	Fracture Force* (lb_f)	Comments
Harvey	T6XL4501	5.391	Fractured at knot
	T6XL4601	6.368	Fractured at knot
	T6XL4701	6.937	Fractured at knot
	T6XL4801	6.795	Fractured at knot
	T6XL4901	7.283	Fractured in knot
	T6XL5001	7.161	Fractured at knot
	Avg.:	**6.66 [29.6 N]**	
	σ:	**0.70 [3.1 N]**	

* Obtained from computer analysis of force-displacement curve.
** Maximum force reported rather than fracture force since filament pull through occurred rather than fracture.
*** Value not included in statistical analysis for reason cited under Comments column.

Table II. Tensile Strengths of Various Common Engineering Materials

Material	Designation/Condition	Application	Tensile Strength, psi (MPa)	Reference
Aluminum	2014/Heat treated (T6)	Airplane structures	70,000 (483)	15
Copper	C11000/Cold-worked	Electrical wiring	50,000 (345)	16
Plain-carbon steel	1010/Cold-worked	Car fenders	53,000 (365)	17
Stainless steel	430/Cold-worked	Kitchen equipment	90,000 (621)	18
Polyethylene	High density	Milk bottles	4,000 (27.6)	19
Nylon	--	Gears	11,800 (81.4)	19
Nylon	**Monofilament**	**Fishing line**	**141,000 (972)***	**Current work**

* Fracture strength reported, corresponding to the maximum strength.

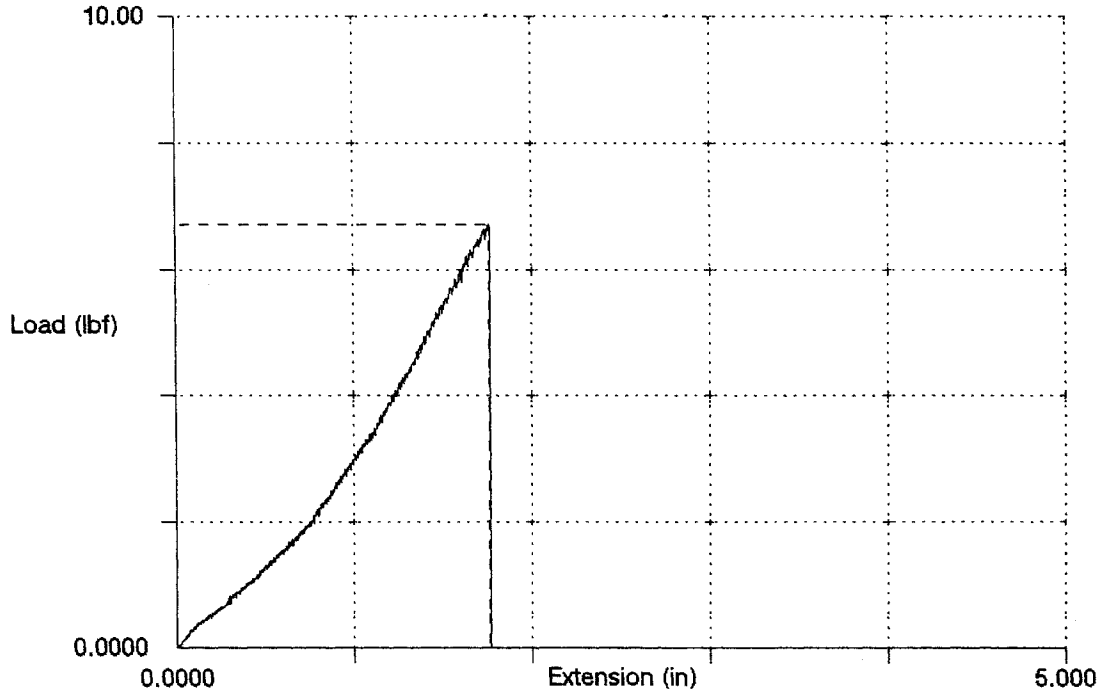

Figure 3. Force-displacement curve for Palomar knot in Berkley Trilene XL six-pound test nylon monofilament fishing line (specimen T6XL2201).

highest standard deviation, indicating that its level of complexity makes it more difficult to achieve highly reproducible performance.

INSTRUCTOR NOTES:

1. To conduct meaningful statistical analysis requires a greater number of specimens than what is called for in the Contest Rules. An ASTM standard for tensile testing of plastics indicates [20] that a minimum of five (5) specimens are to be evaluated.

2. The particular nylon monofilament fishing line selected for this activity was purchased only weeks before it was tested. To relate to last year's experiment [3], 6-lb test Berkley Trilene XL line was chosen as well as analogous 4-lb line. A complete set of data was obtained for both lines. It is recommended that beginners use a larger diameter line since this facilitates knot tying.

3. In order for fishing line tied to a swivel/hook to be tested using a universal testing machine, it is necessary to alter the standard sample fixture by providing some means to attach the swivel/hook. This was accomplished (See Figure 1.) using a eyehook screwed into the center of the longitudinal surface of an oak lath that was cut to the proper length to fit in a wedge-action grip. Here, it is suggested that students be exposed to this sample fixture modification issue. Student designs to solve this problem can be sought, and a group discussion to evaluate them can ensue. It is possible that one or more of the better student designs can even be implemented.

4. While the majority of knots can be tied to swivels, which are much safer for students to handle, some commonly used knots are tied to hooks, particularly involving their shanks. To avoid getting stuck while a knot is being tied, the head of the hook can be embedded into a small cork or piece of rubber.

5. The contest rules were originally specified to be followed by engineering students as part of the 1996 National Engineers Week activities at Loyola College. The procedure has now been expanded with the aim of providing freshmen engineering and physics students with a hands-on laboratory experience. It is envisioned that this would involve preparing student-designed samples for characterization and subsequent data analysis and review that allows development of analytical and critical thinking skills.

6. Students should be shown how to operate the universal testing machine and to position specimens in the machine prior to actual testing.

7. It came [3] to one of the author's (WLE) attention last year that nylon monofilament fishing line is typically tested wet (after soaking in tap water for two hours) using a gage length = 12 in. and a CHS = 10 in./min. Nylon is water conditioned because its mechanical properties decrease when exposed to water, and hence the attempt to simulate service life conditions. While water degrades mechanical properties, the slower CHS used in the current experiment should result in a lower strength because of nylon's strain rate sensitivity. Further, retaining the current experimental conditions allows results to be related to those in last year's workshop paper [3].

8. By performing this step, students are introduced to the iterative process (conception, prototype preparation, testing/evaluation, and improved newer generation prototype) that design methodology often follows.

REFERENCES:

[1] "A Guide to Knots and Lines: Angler's Reference," Form No. L00587, Stren Fishing Lines, Remington Arms Company, Inc., 870 Remington Drive, Madison, North Carolina, 27025.

[2] Evans, S. (Ed.): "Trout Fishing History and Lore," in Sports Afield Trout Fisher's Almanac: Expert Advice from America's Greatest Anglers, The Atlantic Monthly Press, 1997, pp. 1-29.

[3] Elban, W.L.: Fracture Behavior of Nylon Monofilament Fishing Line, in National Educators' Workshop: Update 2000, NASA/CP-2001-211029, 2001, pp. 81-112.

[4] Hibbeler, R.C.: Mechanics of Materials, 4th Edn., Prentice Hall, 2000, pp. 156-161.

[5] Dugger, A.: "Break Point: We Test 50- and 30-Pound Lines," Sport Fishing, Volume 12, April 1997, pp. 48-54.

[6] Gregory, J.F.: Rock Sport: Tools, Training, and Techniques for Climbers, Stackpole Books, 1989, p. 54.

[7] Holman, J.P.: Experimental Methods for Engineers, 7th Edn., McGraw-Hill Book Co., 2001, pp. 62-63.

[8] Karplus, A.K.: Knotty Knots, in National Educators' Workshop: Update 93, NASA Conference Publication 3259, 1994, pp. 369-372.

[9] McClane, A.J.: McClane's Secrets of Successful Fishing: A Complete Guide to the Techniques, Tackle, and Know-How of Sport Fishing, Holt, Rinehart, and Winston, Inc., 1979, pp. 191-210.

[10] Sosin, M; and Kreh, L.: Practical Fishing Knots II, The Lyons Press, 1991.

[11] URL Address (*www.fieldandstream.com/fishing/fsgoodties.html*).

[12] URL Address (*www.fishinglife.com*).

[13] URL Address (*www.jacksonholeflyfishing.com*).

[14] Hertzberg, R.W.: Deformation and Fracture Mechanics of Engineering Materials, 4th Edn., John Wiley and Sons, Inc., 1996, p. 3.

[15] Flinn, R.A.; and Trojan, P.K.: Engineering Materials and Their Applications, 4th Edn., Houghton Mifflin Co. (now John Wiley and Sons, Inc.), 1990, pp. 334-335.

[16] Flinn, R.A.; and Trojan, P.K.: op. cit., p. 346.

[17] Flinn, R.A.; and Trojan, P.K.: op. cit., p. 376.

[18] Flinn, R.A.; and Trojan, P.K.: op. cit., p. 424.

[19] Flinn, R.A.; and Trojan, P.K.: op. cit., pp. 560-561.

[20] "Standard Test Method for Tensile Properties of Plastics," ASTM Designation D638-89 in 1989 Annual Book of ASTM Standards, Section 8: Plastics, Volume 08.01, American Society for Testing and Materials, pp. 156-167.

SOURCES OF SUPPLIES: Commercial-grade nylon monofilament fishing line, swivels and hooks are inexpensive and readily available at numerous retail stores from a variety of vendors. It is also possible that some fishing line manufacturers will supply complimentary small spools of test material and accompanying information. One such example is Pure Fishing Angler Service, 1900 18th Street, Spirit Lake, Iowa 51360. [3]

ACKNOWLEDGEMENTS: Special thanks to Mark A. Elban for analyzing all of the experimental data leading to preparation of Tables I and A-I. Calling on his vast experience tying and using a variety of fishing knots, Jonathan Thompson, Department of Electrical Engineering and Engineering Science, Loyola College, provided helpful discussion regarding the contest rules. Dr. David S. Richards, formerly in the Department of Electrical Engineering and Engineering Science, helped draft the rules and administer the original National Engineers Week contest. The identification of any manufacturer and/or product in this report does not imply endorsement or criticism by the authors or Loyola College and the Community College of Baltimore County.

APPENDIX: A complete set of test data/results for Berkley Trilene XL 4-lb test line appears in Table A-I that follows. (Instructor Note 2)

Table A-I. Force Measurements for Berkley Trilene XL Four-Pound Test Nylon Monofilament Fishing Line Having Various Knots

Knot Type	Specimen Designation	Fracture Force* (lb_f)	Comments
Without Knot	T4XL0301	6.612	Fractured at center
	T4XL0401	6.164	Fractured at top of top bollard (away from grip)
	T4XL0501	6.592	Fractured at side of bottom bollard (away from grip)
	T4XL0601	6.347	Fractured at side of top bollard (away from grip)
	T4XL0701	6.653	Fractured at top of top bollard (away from grip)
	T4XL0801	6.144	Fractured at center
	Avg.:	**6.42 [28.6 N]**	
	σ:	**0.23 [1.0 N]**	
Double Overhand	T4XL0901	2.462**	Knot pulled through without fracture
	T4XL1001	1.973**	Knot pulled through without fracture
	T4XL1101	2.360**	Knot pulled through without fracture
	T4XL1201	2.034**	Knot pulled through without fracture
	T4XL1301	2.218**	Knot pulled through without fracture
	T4XL1401	2.401**	Knot pulled through without fracture
	Avg.:	**2.24 [9.97 N]**	
	σ:	**0.20 [0.90 N]**	
Modified Double Overhand	T4XL1501	2.991**	Knot pulled through without fracture
	T4XL1601	3.906**	Knot pulled through without fracture
	T4XL1701	4.252	Knot pulled through partially and fractured at knot
	T4XL1801	2.991**	Knot pulled through without fracture
	T4XL1901	3.153**	Knot pulled through without fracture
	T4XL2001	4.293	Knot pulled through partially and fractured at knot
	Avg.:	**3.65 [16.0 N]**	
	σ:	**0.62 [2.8 N]**	

Table A-I. Force Measurements for Berkley Trilene XL Four-Pound Test Nylon Monofilament Fishing Line Having Various Knots, Cont'd.

Knot Type	Specimen Designation	Fracture Force* (lb_f)	Comments
Palomar	T4XL2101	5.961	Fractured at knot with knot partially intact
	T4XL2201	6.205***	Fractured in line (~4-3/8" away from knot)
	T4XL2301	4.903	Fractured at knot
	T4XL2401	5.961	Fractured at knot
	T4XL2501	4.679	Fractured at knot
	T4XL2601	5.778	Fractured at knot
	Avg.:	**5.46 [24.3 N]**	
	σ:	**0.62 [2.7 N]**	
Improved Clinch	T4XL2701	6.225	Fractured at knot
	T4XL2801	5.025	Fractured at knot
	T4XL2901	6.653	Fractured at knot
	T4XL3001	3.947	Fractured at knot
	T4XL3101	5.432	Fractured at knot
	T4XL3201	6.388***	Fractured in line (~1/8" away from knot)
	Avg.:	**5.46 [24.3 N]**	
	σ:	**1.1 [4.7 N]**	
Perfection	T4XL3301	3.438	Fractured at knot
	T4XL3401	3.865	Fractured at knot
	T4XL3501	3.926	Fractured at knot
	T4XL3601	4.049	Fractured at knot
	T4XL3701	3.621	Fractured at knot
	T4XL3801	3.723	Fractured at knot
	Avg.:	**3.77 [16.8 N]**	
	σ:	**0.22 [1.0 N]**	

Table A-I. Force Measurements for Berkley Trilene XL Four-Pound Test Nylon Monofilament Fishing Line Having Various Knots, Cont'd.

Knot Type	Specimen Designation	Fracture Force* (lb_f)	Comments
Harvey	T4XL4501	5.839	Fractured at knot
	T4XL4601	5.635	Fractured at knot
	T4XL4701	4.801	Fractured at knot
	T4XL4801	5.127	Fractured at knot
	T4XL4901	4.415	Fractured in knot
	T4XL5001	4.191	Fractured at knot
	Avg.:	**5.00 [22.3 N]**	
	σ:	**0.66 [2.9 N]**	

* Obtained from computer analysis of force-displacement curve.
** Maximum force reported rather than fracture force since filament pull through occurred rather than fracture.
*** Value not included in statistical analysis for reason cited under Comments column.

DETERMINATION OF REDUNDANT WORK IN EXTRUSION USING VISIO-PLASTICITY

Neda S. Fabris

Mechanical Engineering Department
California State University, Los Angeles
5151 State University
Los Angeles, California 90032

Telephone 323-343-5218
e-mail nfabris@exchange.calstatela.edu

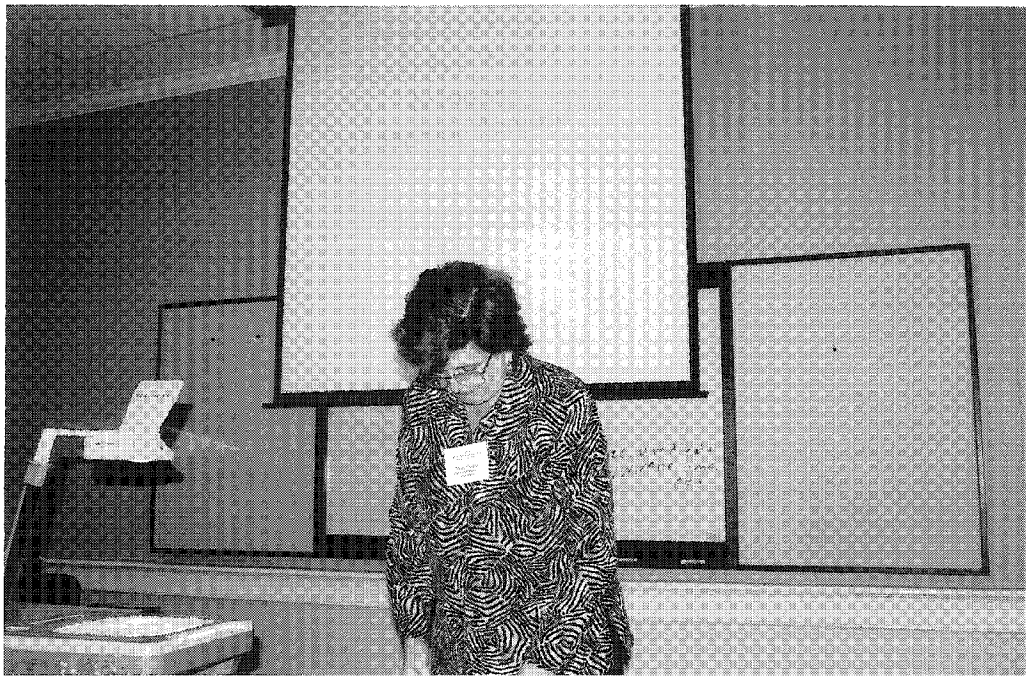

Biography:

Neda Saravanja-Fabris is a Professor of Mechanical Engineering Department at California State University (CSLA) in Los Angeles. She holds Diploma Engineer degree in Manufacturing from University of Sarajevo Bosnia and Herzegovina, M.S. and Ph.D. in mechanical engineering at Illinois Institute of Technology, Chicago Illinois. Her work experience includes teaching at University of Sarajevo and University of Illinois, research position at Technical University in Aachen Germany and at Bell Telephone Laboratory in Napperville Ill. At Cal State University she has taught 27 different courses mostly in the area of materials, design, manufacturing and engineering mechanics. She is a member of SME, ASEE, and SWE. In 2001 she has received Society of Women Engineers highest honor, "Distinguished Educator Award", given to one engineering faculty a year.

Determination of Redundant Work in Extrusion Using Visio-Plasticity

Neda S. Fabris,
Professor, Mechanical Engineering
California State University,
Los Angeles, California

Key Words: Extrusion, ideal work, redundant work, frictional work, optimum die angle, Visio plasticity

Prerequisite Knowledge: Basic knowledge of material flow in extrusion process, understanding the difference between ideal, friction and redundant work.

Objective: Visualization of the material flow in extrusion process and influence of the die angle on the homogeneity of deformation. Basic demonstration of the experimental method known as visio-plasticity. Experimental demonstration of the difference between ideal and actual work performed.

Equipment:
Self-manufactured extrusion set up with die inserts with different extrusion angles and glass upper plate allowing students to observe the material flow in extrusion process (machining time one hour, piece of the steel and glass). Extrusion set machined out of steel plate, glass upper, pressure gage (appr. $10), Ply-Doh, different color, for the extrusion media, cost app. $9.

Introduction
In the extrusion process the billet is forced through a die with a substantial reduction, the friction between the billet and the die causes the retardation of the material close to the die and surface of the cylinder, causing non-uniform material flow pattern. That pattern is highly influenced by the die angle, friction coefficient between die and material extruded and temperature of the material.

Ideal Deformation
The total work U_t required to extrude the part in direct extrusion from original area A_0 to final area A_f (or from the original length L_0 to final length L_f), is considered to be the sum of ideal work U_i, frictional work U_f and redundant work U_r, i.e.,

$$U_t = U_i + U_f + U_r \quad (1)$$

U_i is computed from the properties of material and extrusion ratio R, where $R = A_0/A_f$ Also, R can be related to the absolute value of the true strain ε as

$$\varepsilon = \ln (A_0/A_f) = \ln (L_f/L_0) = \ln R \quad (2)$$

For the perfectly plastic material with a yield strength Y, the energy dissipated in plastic deformation per unit volume, u, is:

$$u = Y \varepsilon \tag{3}$$

The ideal work U_i done to deform the billet is:

$$U_i = u A_0 L_0 \tag{4}$$

This work is supplied by the ram force F that travels a distance L_0 as seen in the Fig. 1

$$\text{Work} = F L_0 = p A_0 L_0 \tag{5}$$

where p is the extrusion pressure at the ram.

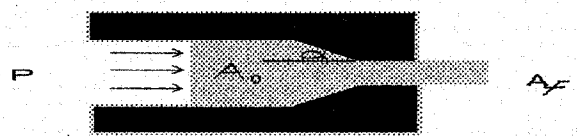

Fig.1. Variables in Direct Extrusion Process

Equating the work of plastic deformation to the external work done, we find that

$$u = p = Y \ln (A_0 / A_f) \tag{6}$$

Ideal Deformation and Friction

Equation (6) pertains to ideal deformation without any friction. It could be shown [1] * that based on the slab method of analysis, the extrusion pressure p for the small die angle α and coefficient of friction μ can be expressed as:

$$p = Y [1 + (\tan \alpha) / \mu] [(R)^{\mu \cot \alpha} - 1] \tag{7}$$

An estimate of pressure can be obtained from the total power P provided by the piston, moving with the velocity V_o and exerting pressure p on the material billet as:

$$P = p V_0 (\pi D_0^2 / 4) \tag{8}$$

The power due to the plastic work of deformation is the product of volume rate of flow and the energy per unit volume. If we assume that, because of the dead zone, material flow in the die region takes place along a 45^0 "die angle" and that the frictional stress is

* Numbers in [ ] represent references at the end of the article.

equal to the shear stress k = Y/2 of the material by equation of the power input to the sum of the plastic deformation and frictional powers, we obtain that [1] :

$$p = 1.7\ Y \ln R \qquad (9)$$

where R is the extrusion ratio $R = A_0/A_f$
If we include in this analysis the force required to overcome the friction at the billet container interface, Eq.(9) becomes

$$p = Y\ (1{,}7 \ln R + 2L/D_0\ ) \qquad (10)$$

Actual Forces
Equation (10) represents a simple estimate of the pressure in extrusion without considering redudandant work i.e. the effect of the inhomogeneous deformation on the required pressure to extrude material. It is also assumed, as mentioned before, that regardless of the actual die angle, material always flows under 45^0 angles, leaving the rest of the material in the dead end zone. Experimental evidence has shown that the die angle influenced the extrusion pressure and the relationship is shown schematically in Fig. 2.

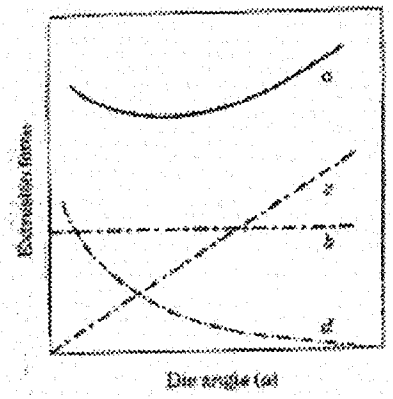

Fig.2 Extrusion force as a function of die angle; (a) total force; (b) ideal force; (c) force required for redundant deformation (d) force required to overcome friction

As can be seen from Fig. 2, the friction component of the force and work done decreases with the increase in die angle due to the decrease in contact between the billet and die, while redundant work (and force) increases with a decrease in the angle of die. There is an optimum die angle for which the extrusion force is the minimum. That angle can be found only experimentally.

Redundant Work in Extrusion
Redundant work is due to the internal distortion in excess of that needed to produce the desired shape [2]. It is the work that goes into inhomogeneous deformation of the

workpiece, which can cause internal defects and non-homogeneous properties of the final product. Because the billet is forced through a die, with a substantial reduction in its cross-section, the metal flow pattern in extrusion is an important factor in the overall process. It is also the amount of work "wasted" in the process, so it is naturally desirable to decrease that work, provided that other components of the work remain constant. It has to be emphasized that it is not the case with friction work in extrusion; therefore, it is desirable to find an optimum angle for a minimum power consumption.

The best way to understand the concept of redundant work is to visualize the flow pattern of the material in the process. The common practice to visualize the flow pattern is to halve the round billet lengthwise and mark one face with the grid pattern. The two halves are then placed together in the container and then extruded. They are taken apart and inspected.

Our Experimental Procedure

We have modified above described approach by designing the extrusion set-up with Plexy glass cover as seen in Fig. 1. The angle of extrusion can be changed using exchangeable dies. The material extruded is common Play-Doh. In order to visualize the material flow, the squares of different colors of Play-Doh are used as shown in Fig. 3. The deformation of each square during the process is easy to follow. The process is scanned to follow subsequent deformation of the squares located in different positions of the specimen. As seen from the figures, the flow of the material is non-uniform, and the material undergoes a much higher deformation than the ideal deformation predicts. The force required to push the material through the die is measured using a fluid USG, (0-300psi) pressure gage. The set-up was scanned in frequent intervals and transformed into image files on Dell Lap-top computer as shown on the picture in the Figure3.

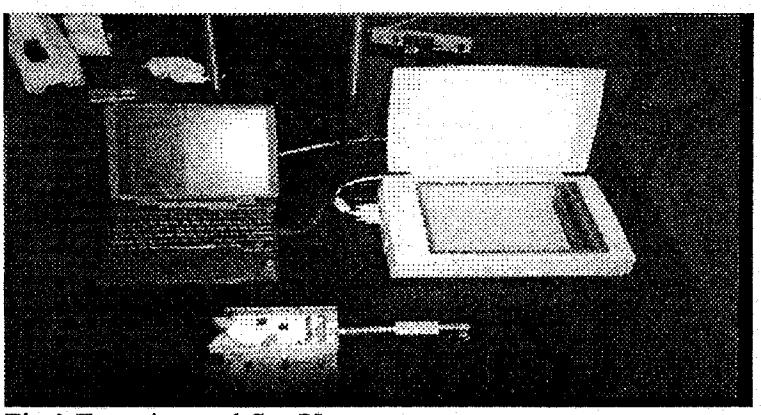

Fig.3 Experimental Set-Up

Experiments have shown that the formation of dead zone in the corners of the dies is highly dependent upon the die angle. They have also shown that the force necessary to push the material through the dies roughly increases 30% when the die angle increases from 30-90 degrees. Actual reading on the pressure gage for the two angles: 60^0 and 45^0 are shown on the Fig.5 and Fig.6. They are 175 psi and 150 psi respectively.

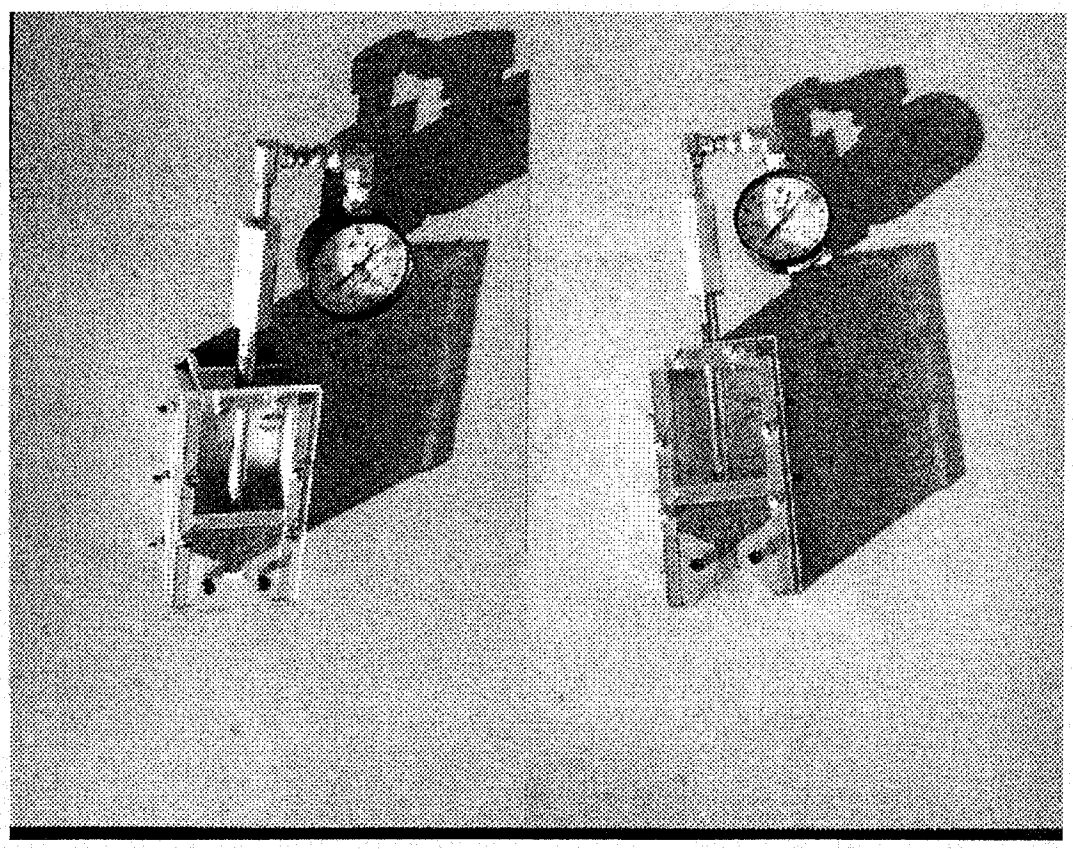

Fig.5 Extrusion angle 60^0 Fig. 6 Extrusion angle 45^0

Several steps of flow of the material during extrusion are shown in pictures below.

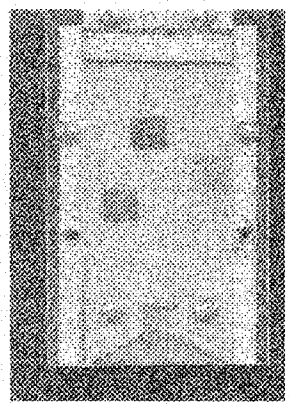

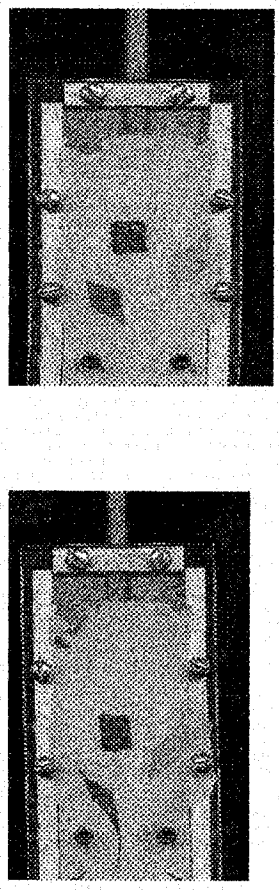

Fig. 7. Material Flow in Extrusion

Conclusions

These experiments are in the development stage. Up to now we did not have a chance to analyze the strains for each particular die angle. It will be interesting to relate the deformation of each square of the model with the amount of force necessary to conduct deformation.

This experimental approach will be also used to verify the validity of Equation 10. All what is needed is the yield strength of the Play-Doh. Also, using this relatively simple experimental set-up we can verify other more sophisticated models of material flow in an extrusion-like upper-bound approach and the slip line theory presented in [2], taught by the author of the paper in a graduate metal forming class.

Visio plasticity is a very successful method in explaining the concept of redundant work in extrusion and the concept of redundant work in general. This powerful method is often neglected in material and manufacturing education. The experiment is similar to flow visualization methods used in fluid mechanics, with possibilities for even more practical applications.

The author of this paper got the idea for the experimental set-up during a visit to the University of Michigan at the NEW 1999 conference. She wants to acknowledge the faculty at that school for developing a similar experimental set-up.

REFERENCES:

1. Kalpakjian S. Manufacturing Processes for Engineering Materials, Third Edition, Addison Wesley, 1997
2. Hosford R.M.C., Caddell R.M., Metal Forming Mechanics and Metallurgy, Second Edition, Prentice Hall, 1993

MAGNETIC FIELD SENSING EXPERIMENTS BASED ON A COMMERCIALLY AVAILABLE GIANT MAGNETORESISTIVE (GMR) SENSOR

Amy Payne[a]

Kara A. Schnell[a]

Franz J. Himpsel[b]

and

Arthur B. Ellis[a]

[a]Department of Chemistry
University of Wisconsin: MRSEC
1101 University Avenue
Madison, Wisconsin 53706

Telephone: 608-262-6711
e-mail payne@chem.wisc.edu

[b]Department of Physics

Amy Payne

Biographies

Amy C. Payne is a Research Intern at the University of Wisconsin-Madison. She has a bachelor's degree from Randolph-Macon Woman's College and performed her doctoral research at the University of California-Davis.

Kara A. Schnell is a Program Assistant at the University of Wisconsin-Madison with a bachelor's degree from the University of Wisconsin-Madison.

Franz J. Himpsel is the Ednor M. Rowe Professor of Physics at the University of Wisconsin-Madison. He received a Diplom and a Ph.D. from the University of Munich. He joined the IBM Research Division at Yorktown Heights in 1997 and moved to the UW-Madison in 1995. Currently, he is investigating how surfaces can be structured on the nanometer scale by self-assembly, with the goal of producing new types of electronic materials.

Arthur B. Ellis is Meloche-Bascom Professor of Chemistry at the University of Wisconsin-Madison. He received a Bachelor's degree from California Institute of Technology and a Ph.D. from M.I.T. He teaches introductory and advanced chemistry courses as well as a graduate course on nanostructured materials at UW-Madison, and coordinates the education efforts of the NSF-funded MRSEC on Nanostructured Materials and Interfaces.

Magnetic Field Sensing Experiments Based on a Commercially Available Giant Magnetoresistance (GMR) Sensor

Amy C. Payne,[a] Kara A. Schnell,[a] Franz J. Himpsel,[b] Arthur B. Ellis[a]
Department of Chemistry[a] and Department of Physics[b]
University of Wisconsin – Madison
Madison, Wisconsin 53706

Key Words: Giant magnetoresistance, magnetic field sensing

Prerequisite Knowledge: magnetic north and south poles, magnetic attraction and repulsion of poles, basic algebra skills, ferromagnetism and antiferromagnetism, electrical resistance.

Objective: The purpose of this lab is to familiarize students with the concept of giant magnetoresistance (GMR)and its applications.

Equipment:
Individual GMR sensor, Figure 1a (Part Number: AA002-02)[a]
GMR Cylinder Position Sensor Assemblies, Figure 1c (Part Number: AG007-07)[a]
Power supply (9 Volt Battery)
Set of 5 refrigerator magnets cut to create different patterns[b]
Multimeter with alligator clips
2 pieces of wire (26 gauge, 3" in length)
bar magnet
liquid nitrogen and styrofoam cup

[a]These items can be obtained from NVE Corporation, (800) 467-7141, http://www.nve.com
[b]Bulk refrigerator magnets can be obtained from office supply (e.g., Office Max) or sign stores.

Introduction:

The experiments being presented are based on a relatively inexpensive, commercially available giant magnetoresistive (GMR) sensor. Magnetoresistance is a phenomenon in which the resistance of a material changes in response to an applied magnetic field.[1] All metals display a small magnetoresistance; however, magnetic multilayers with nanoscale dimensions can display a large magnetoresistance called GMR, which is based on the magnetic reversal of individual layers in the stack. GMR has found its way into many important applications. GMR devices are currently being used as magnetic sensors in the read heads of computer disk drives,[2] as motion sensors in automobiles,[3] and in biosensing assays.[4]

Students will be introduced to GMR concepts and applications by:

1. using a GMR sensor to determine patterns of magnetic fields from a series of refrigerator magnets;
2. observing the GMR effect, calculating the percentage change in resistance of a material in response to a magnetic field, and determining how temperature affects the GMR effect;
3. designing an application for the GMR sensor.

Procedure:

I. Using a GMR Sensor to Detect Patterns of Magnetic Fields.

The GMR sensor, Figure 1a, can be incorporated into a circuit designed to control the power to an LED, shown in Figures 1b and 1c; this device can then be used to sense magnetic patterns. A common refrigerator magnet (RM) can be used to demonstrate this point. A flat RM is different in design from many magnets: Instead of a single north and south pole, a dipole, RMs are arranged in patterns that can be thought of as a set of small horseshoe magnets lined up next to one another.[5] The black and white areas in Figures 2a and 3 refer to the north and south poles of magnetic fields, oriented perpendicular to the page. When the poles are aligned in stripes, magnetic field lines are formed, as shown in Figure 2b.

The Experiment.

A RM with a known magnetic pattern can be used to investigate the way the sensor responds when passed over the surface of the RM.

1. Try dragging the sensor across the RM in a variety of directions.
2. Once you have established how the sensor responds to a known magnetic pattern, characterize the other four RMs in Figure 3 in the same way.
3. How does the GMR sensor respond to magnet A of Figure 3? Does the GMR sensor respond in more than one direction, and, if so, does it respond in the same way in multiple directions?
4. Match the unknown RMs to patterns A-E. What problems, if any, did you have trying to distinguish among the magnetic patterns?

II. What is Giant Magnetoresistance?

Students can work on the following activities in groups of two or three.

GMR can be observed by measuring the resistance of a material with and without an applied magnetic field. These values can then be used to calculate a percentage GMR using the formula

$$\% \text{ GMR} = [(\rho_H - \rho_o) / \rho_o] \times 100\%$$

where ρ_o is the resistance without an applied magnetic field and ρ_H is the resistance with an applied magnetic field. The percentage magnetoresistance is characteristic of the material at a given temperature and can be calculated by two methods: dividing by ρ_o, which provides a more conservative value for the MR, or by ρ_H, which is often used for values that appear to saturate at 100% when calculated with ρ_o in the denominator. The response of the GMR sensor is dependent not only on the strength of the magnetic field, but also on the temperature. This dependence can be examined by measuring and comparing the GMR effect at room temperature and liquid nitrogen temperature.

The Experiment.

1. Strip the protective coating off both ends of two pieces of wire.

2. Connect the end of one stripped wire to pin 1 of the individual sensor by wrapping the wire around the pin several times (see Figure 1a). Repeat for pin 4 with the second wire.
3. Set the multimeter to measure ohms. Connect the leads attached to the individual sensor to the multimeter. Does it matter which multimeter lead is attached to which pin?
4. Measure the resistance of the sensor without a magnetic field present. Record the resistance.
5. Now bring a magnet up to the sensor. Move the magnet around the sensor to find the orientation that causes the largest change in resistance. Record the resistance.
6. Submerge the sensor in liquid nitrogen (contained in a styrofoam cup) and wait for the multimeter readout to stabilize. **CAUTION: Liquid nitrogen is extremely cold. Do not allow it to come into contact with skin or clothing, as severe frostbite may result.**
7. Bring the magnet next to the outside of the cup that holds the liquid nitrogen and record the resistance of the sensor with and without the magnet present. Play with the position of the magnet and the sensor, still submerged in liquid nitrogen, to find the direction that gives the greatest change in resistance.
8. Using the resistance values, calculate the percentage of the magnetoresistance effect at room temperature and at liquid nitrogen temperature, 77K. Compare both sets of data. What effect does the temperature have on the resistance of the material? On the percentage of the magnetoresistance effect?

III. Design a New Application for a GMR Sensor

The GMR effect has made a significant impact in the computer industry; these materials are used in the read heads of computer hard drives. The use of GMR materials has enhanced read head sensitivity, allowing the areal density of hard drives to increase significantly. Read heads take advantage of the larger magnetoresistive response of GMR materials, which allows smaller magnetic fields on the hard disk to be read. GMR sensors have also been used in anti-lock braking systems to determine wheel speed. A magnetic gear wheel provides a defined number of magnetic "teeth" for the sensor to detect per rotation that can be converted to speed.

The Experiment.

With these applications in mind, what other ways could the sensor be used?

1. Design a new application for the GMR sensor.
2. What kind of detection schemes are possible? Can you keep the GMR sensor constantly lit? How would you make the GMR sensor blink periodically?
3. How is the GMR sensor oriented with respect to the magnet? Does the orientation of the magnet matter?
4. What are the advantages and disadvantages of using this design?
5. Describe the application.

Comments:

The concepts an instructor chooses to highlight are entirely dependent on the audience. For example, the GMR sensor can be used to introduce the concepts of a wheatstone bridge, ferromagnetism and antiferromagnetism, the composition of materials that exhibit magnetoresistance, and the mechanism of magnetoresistance in multilayers.[6]

The GMR sensor is composed of four resistors made of a GMR material and arranged in a Wheatstone bridge configuration (Figure 4). An opposing pair of the four resistors is shielded from the magnetic field and serve as a reference, while the other opposing pair of resistors responds to the applied magnetic field. The sensor detects the change in resistance when a magnetic field is present and converts this change into an output, which can be connected to an amplifier or a transducer such as a buzzer or a light-emitting diode (LED). Figure 1b shows a GMR sensor that has been incorporated into a circuit designed to power a yellow LED.

The GMR structure comprises layers of magnetic (e.g., Fe, Co, Ni) and nonmagnetic (e.g., Cu, Cr) metals that are nanometers in thickness. The magnetic layers are either a single ferromagnetic (FM) metal or an alloy of several FM metals, while the nonmagnetic layer is usually composed of a single element. The FM layers are naturally oriented antiparallel, and the electrical resistance of the material is relatively high. However, in the presence of an external magnetic field, the FM layers undergo a reorientation so that the layers are FM coupled, and the electrical resistance of the material decreases. Figure 5 shows the response of the magnetic multilayer to the external magnetic field.[7]

Use the magnetic field pattern exercise to introduce the concept of magnetic sensing and to familiarize students with the interaction between the GMR sensor and the magnetic field. Students should discover that the GMR sensor has an axis of sensitivity that responds to the magnetic field of the RM when the magnetic field lines are aligned with the axis of sensitivity. When the axis of sensitivity is oriented perpendicular (rotated 90° in the plane of the refrigerator magnet) to the magnetic field lines, there is no response regardless of the movement of the sensor on the refrigerator magnet. Magnetic flux concentrators used to enhance the magnetic field at the unshielded GMR resistors create this directional sensitivity of the sensor. The axis of sensitivity is labeled for each sensor in Figure 1 (note that the axis is different for the two sensors). Some magnetic field patterns (i.e., the diagonal patterns D and E in Figure 3) may be more difficult to distinguish than others, so students should be encouraged to predict the response of the GMR sensor to each of the five magnetic patterns shown in Figure 3 and find a systematic way to examine the magnets.

Measuring the resistance of the individual sensor gives the students a direct demonstration of the magnetoresistive properties of the sensor. At room temperature, the resistance of the GMR sensor decreases in the presence of a magnetic field and a percentage GMR of ~10 % is calculated. The result is similar for liquid nitrogen (LN2), where the percentage GMR is ~14 %. The resistance with and without a magnetic field is much lower when measured in LN2. This demonstrates metallic behavior; the resistance decreases as the temperature decreases because of a reduction in the thermal motion of the atoms in the metal.[8]

Visit http://mrsec.wisc.edu/EDETC/cineplex/GMR/ to see videos of experiments I and II as well as other demonstrations that can be performed with the GMR sensor.

References:

1. White, R.L. "Giant Magnetoresistance: A Primer." IEEE Transactions on Magnetics. *28*, 2482 (1992).
2. Belleson, J.; Grochowski,E. "The era of giant magnetoresistive heads." http://www.storage.ibm.com/hardsoft/diskdrdl/technolo/gmr/gmr.htm (1998).
3. Treutler, C.P.O. "Magnetic sensors for automotive applications." Sensors and Actuators. *A91*, 2 (2001).

4. Edelstein, R.L.; Tamanaha, C.R.; Sheehan, P.E.; Miller, M.M.; Baselt, D.R.; Whitman, L.J.; Colton, R.J. "The BARC biosensor applied to the detection of biological warfare agents." Biosensors and Bioelectronics. *14*, 805 (2000).
5. Campbell, D.J.; Olson, J.A.; Calderon, C.E.; Doolan, P.W.; Mengelt, E.A.; Ellis, A.B.; Lisensky, G.C. "Chemistry with Refrigerator Magnets: From Modeling of Nanoscale Characterization to Composite Fabrication." J. Chem. Educ. *76*, 1205 (1999).
6. Levy, P.M.; Zhang, S. "Our current understanding of giant magnetoresistance in transition-metal multilayers." J. Magn. Magn. Mater. *151*, 315 (1995).
7. Campbell, D.J.; Lorenz, J.K.; Ellis, A.B.; Kuech, T.F.; Lisensky, G.C.; Whittingham, M.S. "The Computer as a Materials Science Benchmark." J. Chem.Educ. *75*, 297 (1998).
8. Ellis, A.B.; Geselbracht, M.J.; Johnson, B.J., Lisensky, G.C.; Robinson, W.R. Teaching General Chemistry: A Materials Science Companion. American Chemical Society: Washington, D.C., 1993; 198.

Acknowledgment:

We thank Kevin Jones and Tim Hazelton at NVE for technical assistance. We are grateful to the National Science Foundation through the Materials Research Science and Engineering Center (MRSEC) on Nanostructured Materials and Interfaces (DMR 0079983) for generous support of this project.

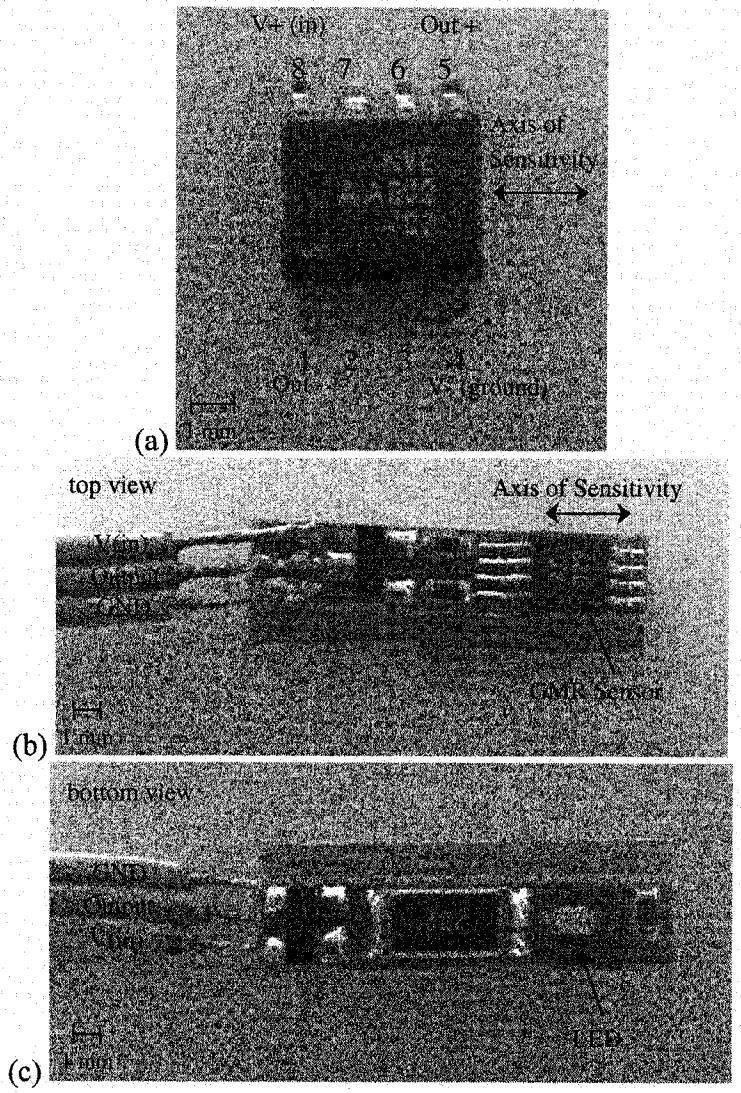

Figure 1. (a) Individual GMR sensor (AA002-02) with pin #'s; (b) and (c) GMR sensor (AG007-07) incorporated into a circuit designed to power a yellow LED .

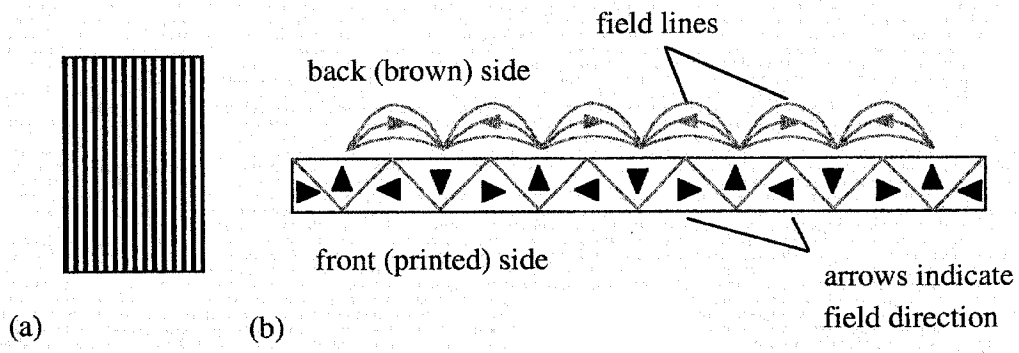

Figure. 2. (a) Top view of the magnetic pattern of a common refrigerator magnet; and (b) a cross-sectional perspective of the same magnet, showing the direction of magnetic field lines.

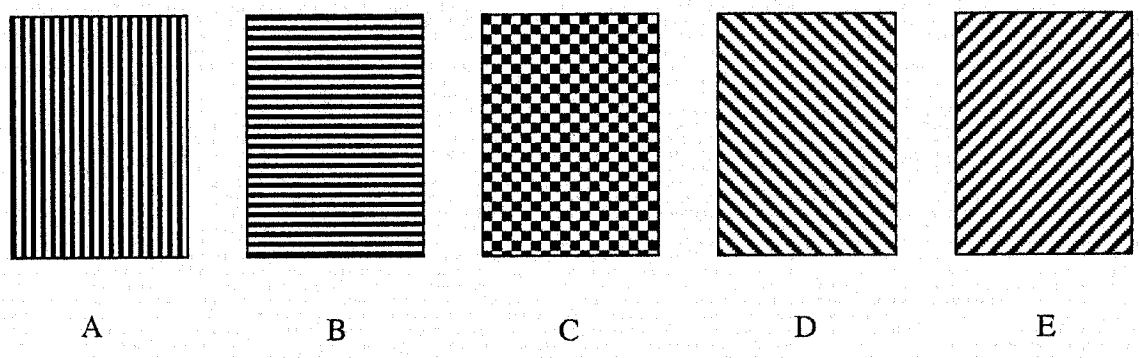

Figure 3. Possible refrigerator magnet patterns. Note that pattern A is the one shown in Figure 2.

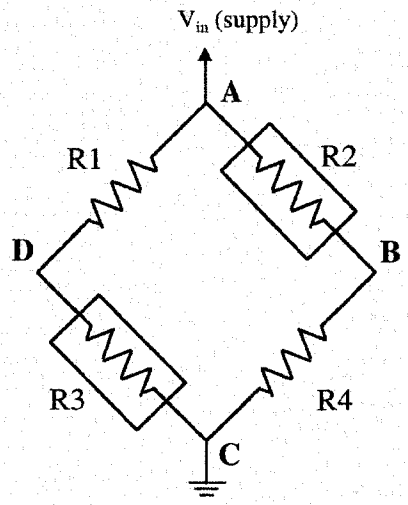

Figure 4. The Wheatstone bridge configuration of a GMR sensor, where all of the resistors are made of GMR multilayer materials. R2 and R3 are magnetically shielded.

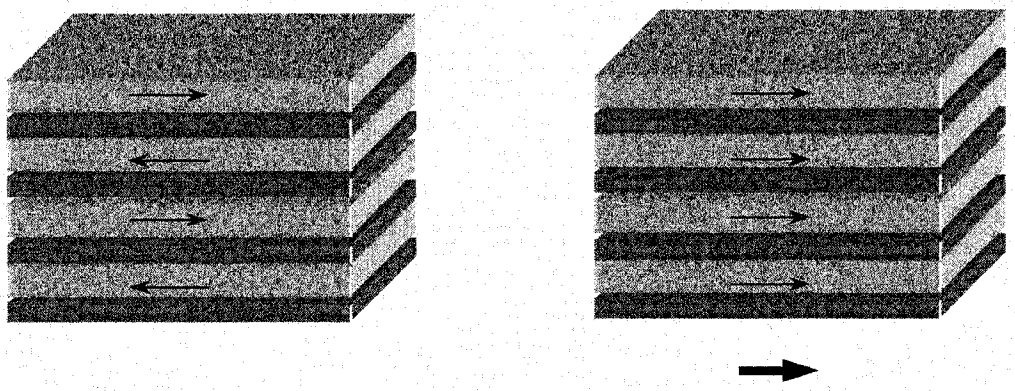

(a) No magnetic field (b) H_a

Figure 5. (a) The ferromagnetic layers of the magnetic multilayer, shown as light grey layers, are coupled antiparallel through the nonmagnetic spacer metal, shown as dark grey layers, in the absence of a magnetic field. (b) When an external magnetic field (H_a) is applied, the ferromagnetic layers reorient to form ferromagnetically coupled layers.

Materials Science Kits from ICE/MRSEC

Qty	Ord No	Item (Standard shipping included.)	US	non US†	Total
_____	90-002	Optical Transform Kit (Second Edition)	$20 00	$45 00	$_____
_____	90-002S	10 copies of 35-mm Unit Cell Slide for Optical Transform Kit	$21 00	$46 00	$_____
_____	93-003S	10 copies of 35-mm Discovery Slide for Optical Transform Kit	$21 00	$46 00	$_____
_____	93-004S	10 copies of 35-mm VSEPR Slide for Optical Transform Kit	$21 00	$46 00	$_____
_____	93-005S	10 copies of 35-mm Plane Groups Slide for Optical Transform Kit	$21 00	$46 00	$_____
_____	92-004	Solid-State Model Kit —deluxe version (includes instruction manual)	$130 00*	$195 00*	$_____
_____	94-006	Solid-State Model Kit —student version (includes instruction manual)	$95 00*	$145 00*	$_____
_____	94-007	Instruction Manual, Solid-State Model Kit (additional copy)	$20 00	$45 00	$_____
_____	99-001	DNA Optical Transform Kit	$22 00	$47 00	$_____
_____	99 001S	10 copies of 35-mm DNA Optical Transform Slide	$22 00	$47 00	$_____
_____	20-001	Exploring the Nanoworld Kit **NEW!**	$26 00	$48 00	$_____
_____	20-002	Amorphous Metal Demonstration Kit **NEW!**	$50 00	$100 00	$_____

Product Subtotal (Standard shipping is included in the price) _____

Discount (If applicable, see Discount Policy below) _____

RUSH Shipping __add $15/item (US) or __$30/item (non US) _____

Indicate items for RUSH Shipping by placing a "#" along with the quantity to be sent RUSH in the left margin on the reverse page

Purchase Order (Attach a copy of the purchase order and add a $10 fee to cover handling costs) _____

Grand Total (Product Subtotal - Discount + RUSH Shipping + Purchase Order) $ _____

†*Customs and import fees are the responsibility of the purchaser*

Discount Policy: 10% for 10–49 copies, 15% for 50 or more Applies only to Product Subtotal *No discounts on Solid-State Model Kits

Payment Policy: Orders from individuals must be prepaid Business and institutional purchase orders will be accepted with the addition of a $10 fee to cover the cost of paperwork involved Payment must be in US funds drawn on a US bank by magnetically encoded check, credit card, or international money order payable to ICE There will be a $30 charge on all returned checks Books and kits are not available for preview No refunds, returns, or exchanges

Method of Payment.

☐ Payment* enclosed $ _____

☐ Mastercard® ☐ Visa®

CREDIT CARD # _____ _____ _____ _____ (Fill in phone number below)

Expiration date: Month ____ Year ____ Signature _____

Daytime phone number ___ ___ / ___ ___ - ___ ___ ___ ___

Ship to: (Please print)

Name _____

Institution _____

Street Address _____

City _____

State/Country _____

Zip (Postal code) _____

Credit Card Billing Address: (If different)

Name _____

Institution _____

Street Address _____

City _____

State/Country _____

Zip (Postal code) _____

Return Orders, with Payment, to:

INSTITUTE FOR CHEMICAL EDUCATION
University of Wisconsin-Madison
Department of Chemistry
1101 University Avenue
Madison, WI 53706-1396

Phone 608/262-3033
Toll-Free 800/991-5534
Fax 608/265 8094
email ICE@chem wisc edu
www http //ice chem wisc edu

Prices effective through June 30, 2001

GATEWAY ENGINEERING COALITION

Morton Friedman

Columbia University
500 West 120th Street
Room 510 Mudd
New York, New York 10027

Telephone: 212-854-2986
e-mail friedman@columbia.edu

and

Eli Fromm

Director and P. I. Of Gateway Engineering
Education Coalition

fromm@drexel.edu

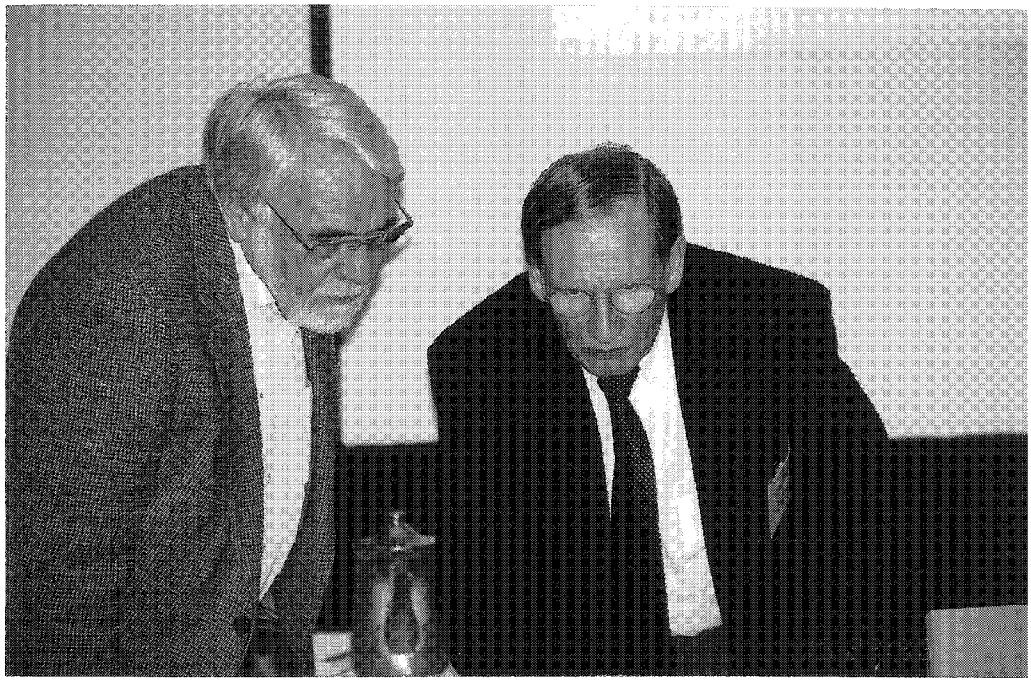

Eli Fromm

Gateway Engineering Education Coalition
www.gatewaycoalition.org
- Drexel - Cooper - USC - Ohio State - Academic Associates - Polytechnic - NJIT - Columbia

Initial Program – The Start
- Single Institution -
- Lower Division Curriculum -

- **Integrated and Interwoven Components:**
  - **Engineering Up-Front and the Intellectual Centerpiece**
  - **Math, Science, and Engineering in parallel and concurrently**
  - **Extensive Experiential Learning**
  - **Interdisciplinary Themes**
  - **Concurrent integration of communication, organizational management, group dynamics, teamwork skills, and social responsibility**

Gateway Coalition - Broadly Defined Goals

- Extend the Drexel freshman/sophomore program to other Coalition members and to the upper division of undergraduate engineering education.
- Create and maintain a curriculum that moves from a focus on course content to the development of human resources and the broader experience in which individual projects are connected, integrated, and multidisciplinary at lower and upper divisions.
- Create, build on, and extend, the program of faculty development to draw engineering faculty to a dedicated investment in the teaching of undergraduates and enhance the pedagogical abilities of faculty to enable the skilled practice of undergraduate engineering education.
- Recruit and retain to the bachelor's degree an increasing percentage of women and minorities to undergraduate engineering education.
- Implement & institutionalize curriculum and related developments moving from pilot model to implementation and incorporation into the mainstream of each institution's programs (Institutionalization).
- Use modern assessment methods to measure, assess and guide the Coalition.
- Change the Culture of the Undergraduate Engineering Educational Enterprise.
- Establish strong relationships and an active program of dissemination among schools within the Coalition, other Coalitions, and with the wider engineering community.

GATEWAY STRATEGIES

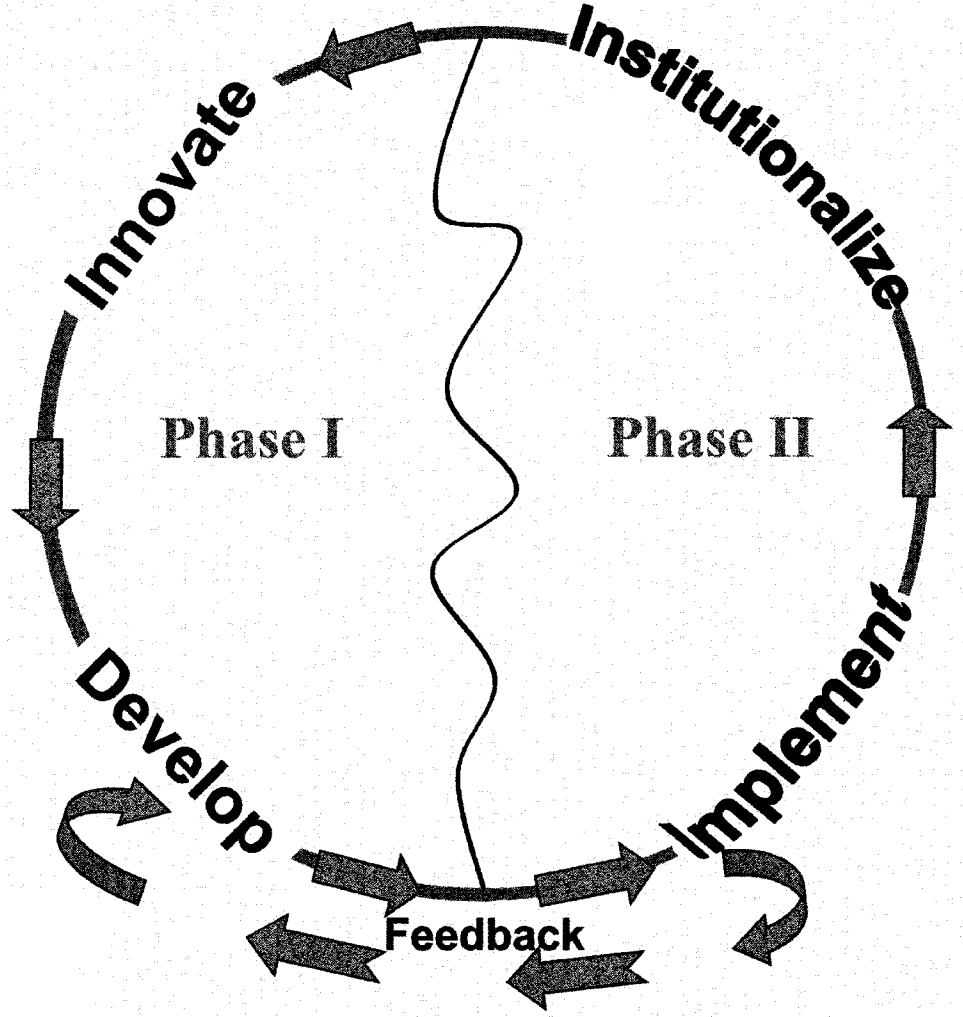

- Curriculum
- Prof.Dev.
- Underrep. Pop.
- Technologies
- Assessment
- Linking/Sharing (Partnerships)

GATEWAY STRATEGIES

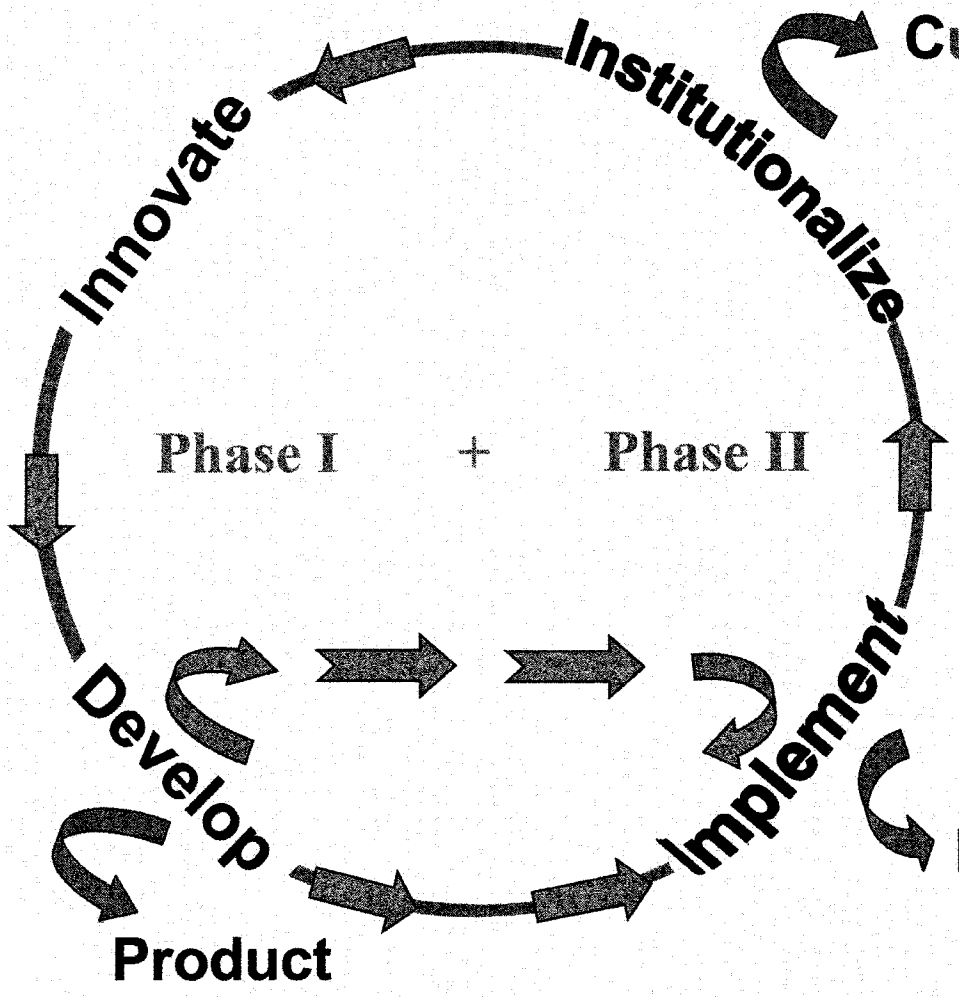

- Curriculum
- Prof.Dev.
- Underrep. Pop.
- Technologies
- Assessment
- Linking/Sharing (Partnerships)

Curricular Objectives

- **Extending the Initial Set of Integrated and Interwoven Components**
  - **Engineering Up-Front and the Intellectual Centerpiece**
  - **Math, Science, and Engineering in parallel and concurrently**
  - **Extensive Experiential Learning**
  - **Interdisciplinary Themes**
  - **Concurrent integration of communication, organizational management, group dynamics, teamwork skills, and social responsibility**

- **Design as a motivator and driver throughout the curriculum and the use of advanced technology as a vehicle for its development and delivery**

- **Shift educational focus from primarily course content to student learning outcomes.**

- **Major push on multi-disciplinary, upper division courses**
  - **Biotechnology, MEMs, & Genomic Engineering**
  - **Engineering Horizons/Emerging Technologies**
  - **Environmental & Earth Systems**
  - **Manufacturing & Concurrent Engineering/Concurrent Design**

A Closer Look at Curriculum

- Lower Division
  - Engineering Up-Front
    Remote experimentation
  - Learning Fundamentals
    Tools & Tactics of Design, Introduction to the Design Process,
    Fundamentals of Problem Solving, Physical Foundations of Engineering
    Structure and Properties of Matter, Systems, etc.
  - Bringing Multimedia into the classrooms (course modules example)
- Multi-disciplinary, upper division courses
  - Biotechnology, MEMs, & Genomic Engineering
  - Engineering Horizons/Emerging Technologies
  - Environmental & Earth Systems Engineering
  - Manufacturing/Concurrent Engineering
- Overall
  - Integrating Technology into the Educational Process
  - On-Line Assessment and Evaluation Processes
  - Web-Based Course Delivery

Professional Development and the Educational Process

- Student Development
  - Ethics
  - Communication
  - Teamwork
- Faculty Development
  - Linkages across coalition institutions for faculty teaming in instructional design, networked facility sharing, and student teaming for design and fabrication.
  - Outcome-based assessment
  - Institutional support for new media technologies
  - Collaborative teaching and learning

Upper Division Cross-Institutional Programs using Technology as a Bridge

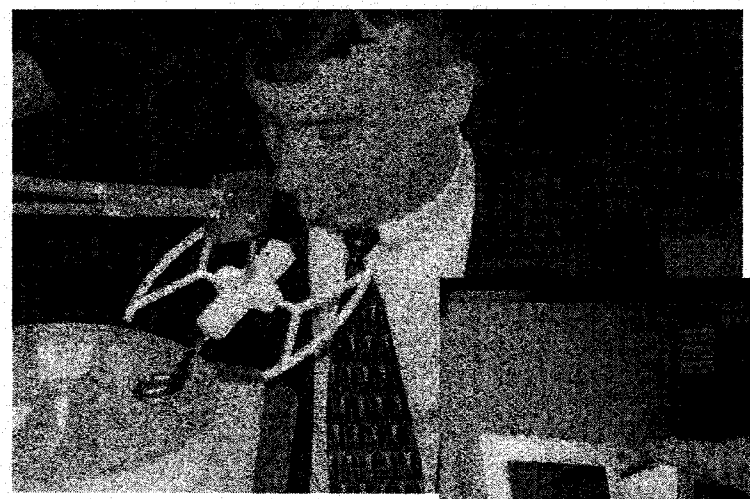

Concurrent Engineering

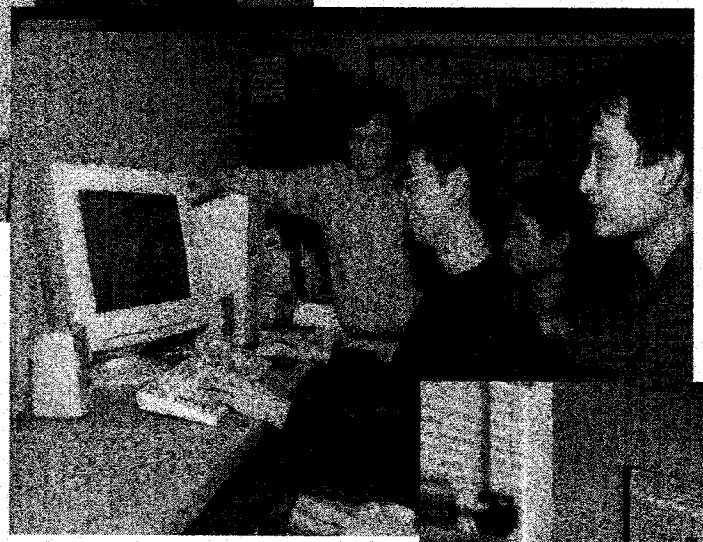

Rapid Prototype Design

Outreach/Mentoring Programs

- Linking with 2 yr. higher education institutions
- Engineering to the high school
- Engineering students in the k-12 classroom
  - Education minor for engineers
- Mentoring and bridge programs
- Building on existing institutional initiatives, implement specific programs to increase enrollment and retention of underrepresented populations.
- Established several programs designed to support the diverse needs of students.

Assessment Process & Initiatives

- Providing Coalition and non-Coalition institutions with a structured process to *imbed* assessment and evaluation, as well as continuous improvement as a fundamental ingredient of the educational process.
  - Developed and implemented a battery of outcome-based assessment processes including:
    - Department and Faculty Workbooks
    - Technology mediated assessment processes including course evaluations, student surveys, alumni surveys, and the Team Developer, a computer based assessment and feedback program (John Wiley & Co.)
  - Over 75 engineering and non-engineering programs are following the structured assessment program.
  - Coalition workshops have been attended by over 1000 participants from 50 engineering schools.
  - Provided a turnkey complete web-based assessment program available to any institution through the Gateway Web Repository.
  - Ongoing collection and monitoring using Gateway metrics

Lower Division

Freshman Participating in Engineering Design Experience

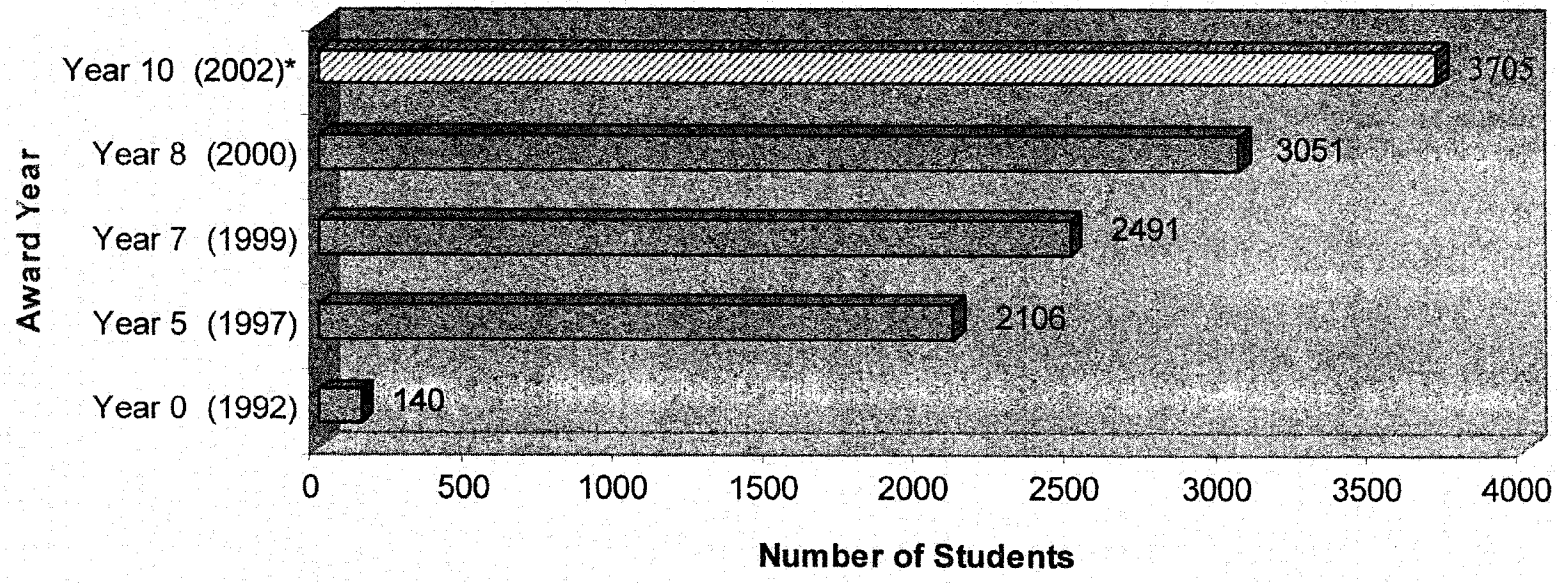

* Projection

Upper Division Courses Taught by Interdisciplinary Teams of Faculty

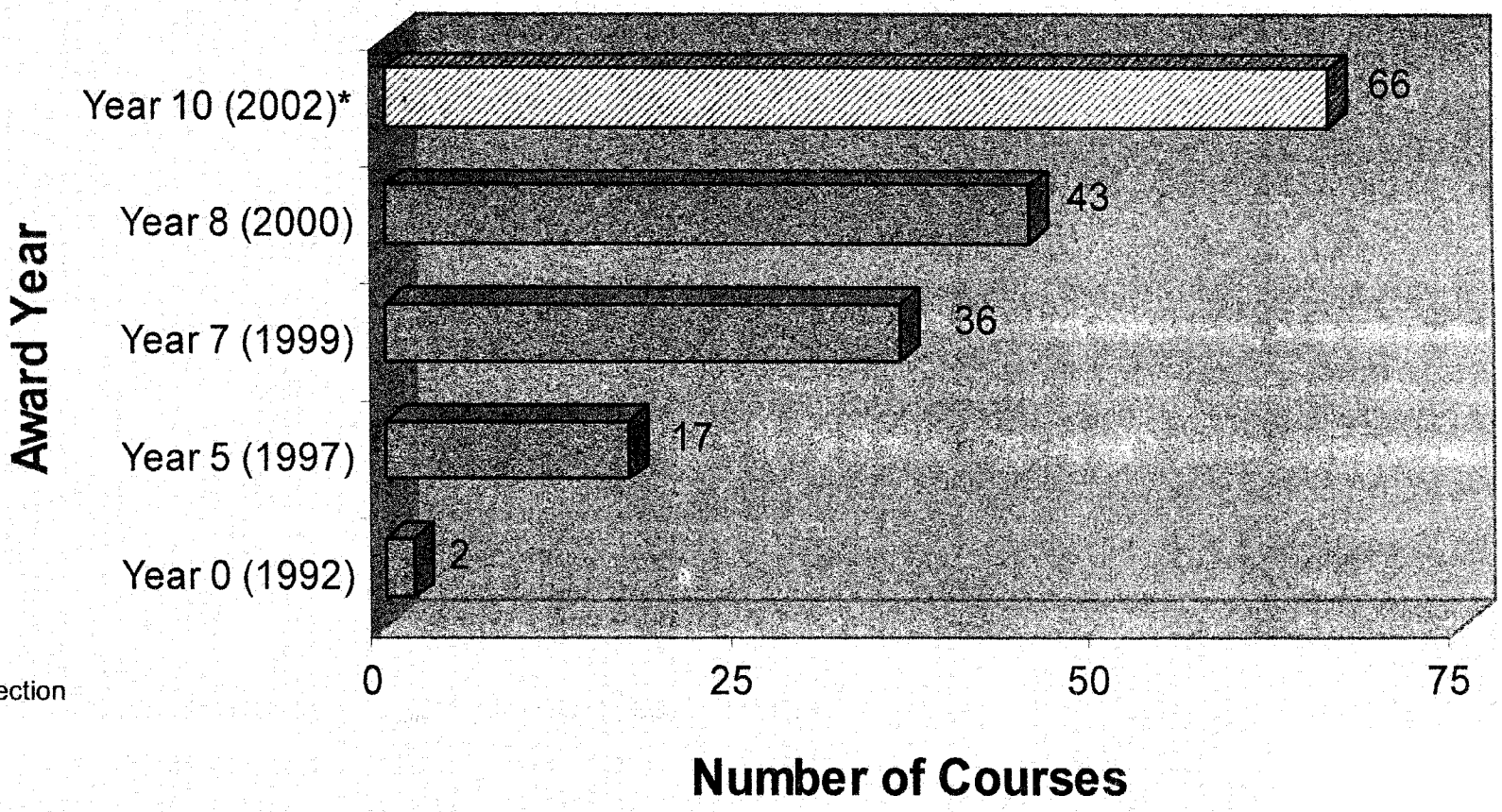

* Projection

Retention Rates

Gateway Coalition Retention Rates from 1st to 2nd Year

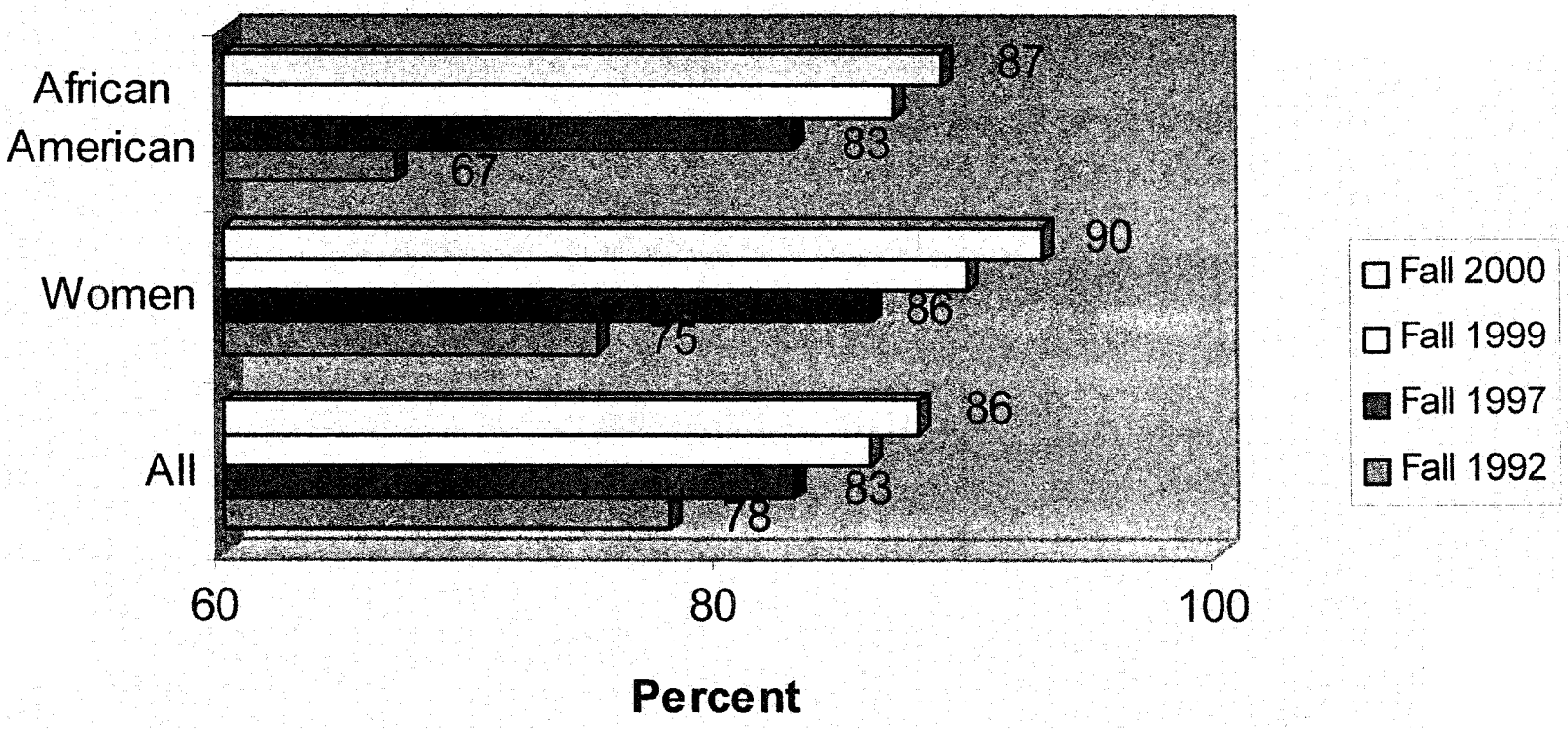

Retention Rates

Gateway Coalition Retention Rates from 2nd to 3rd Year

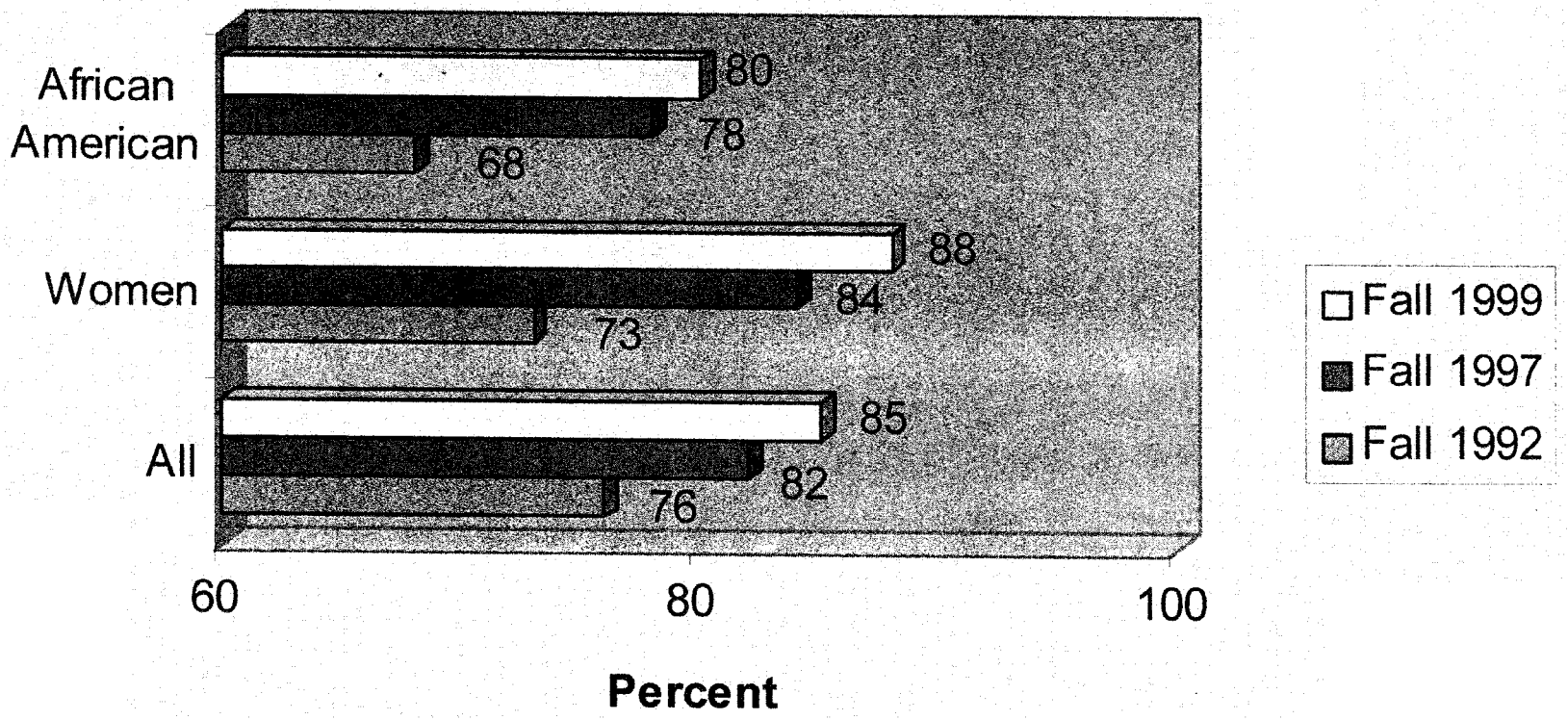

Minority Student Graduation Rates

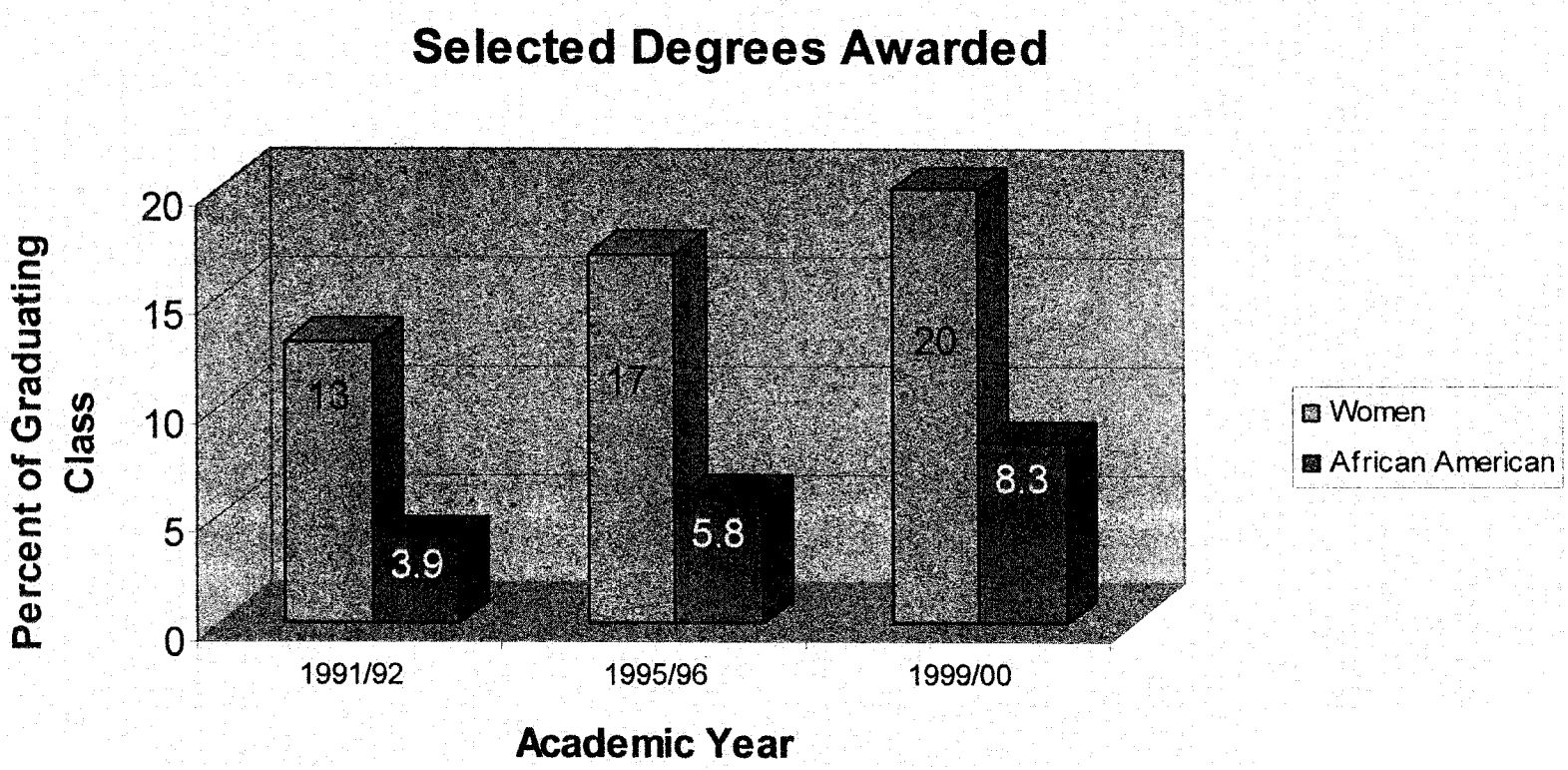

Students Participating in Courses that Formally Integrate Communication Skills and Ethics

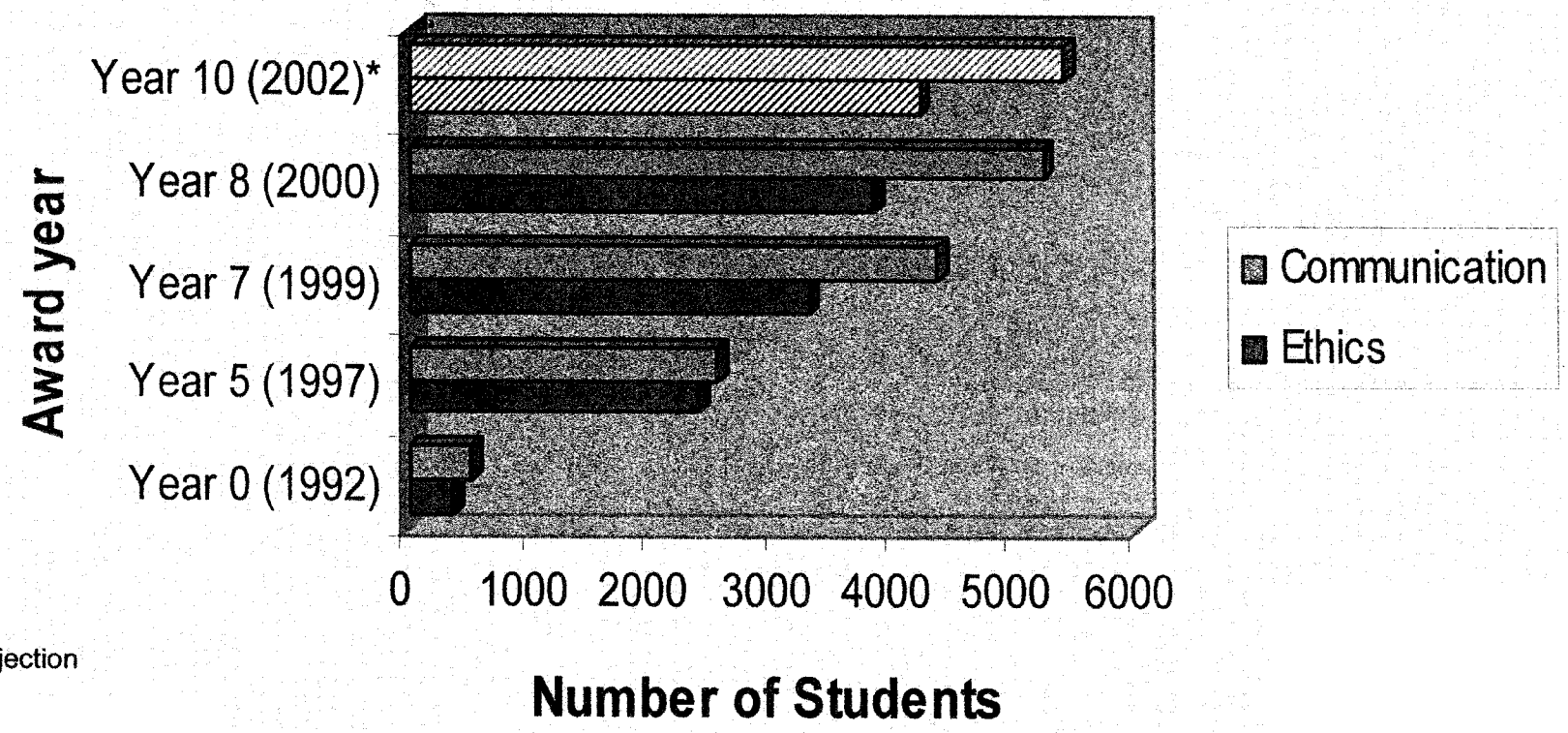

* Projection

Students Participating in Outcome Assessment Processes

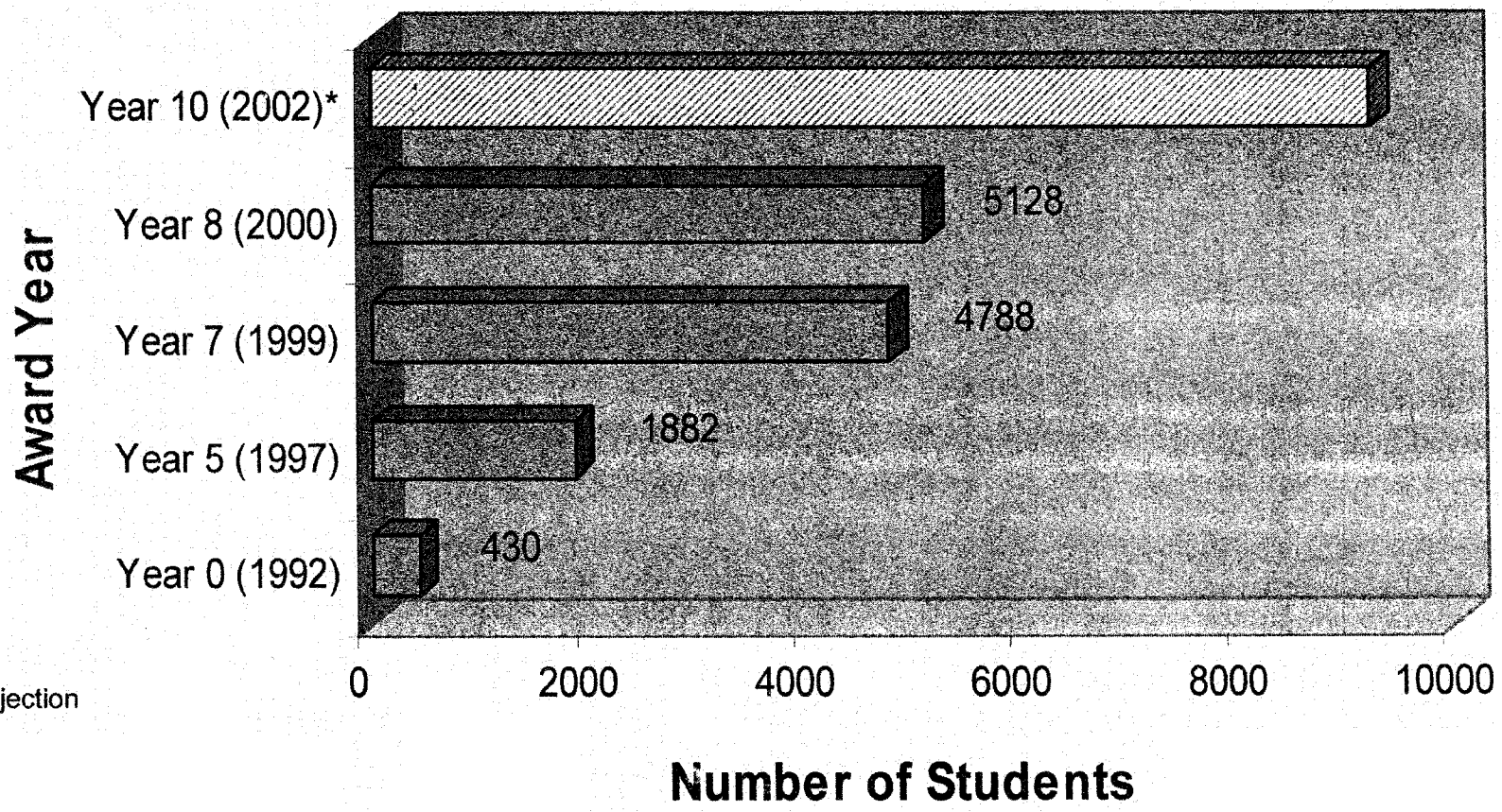

* Projection

Non-Coalition Institutions Impacted by Coalition Initiatives

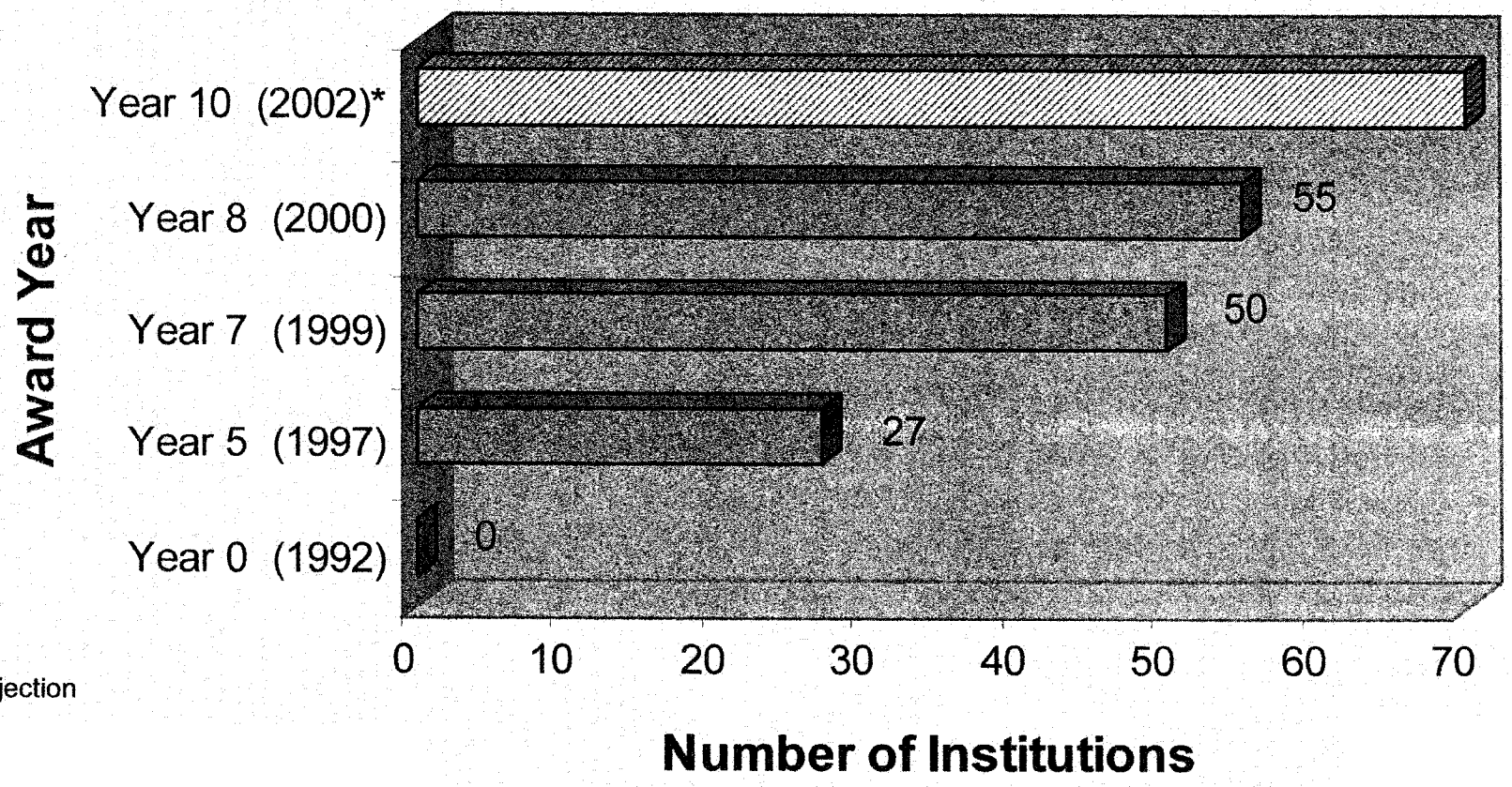

* Projection

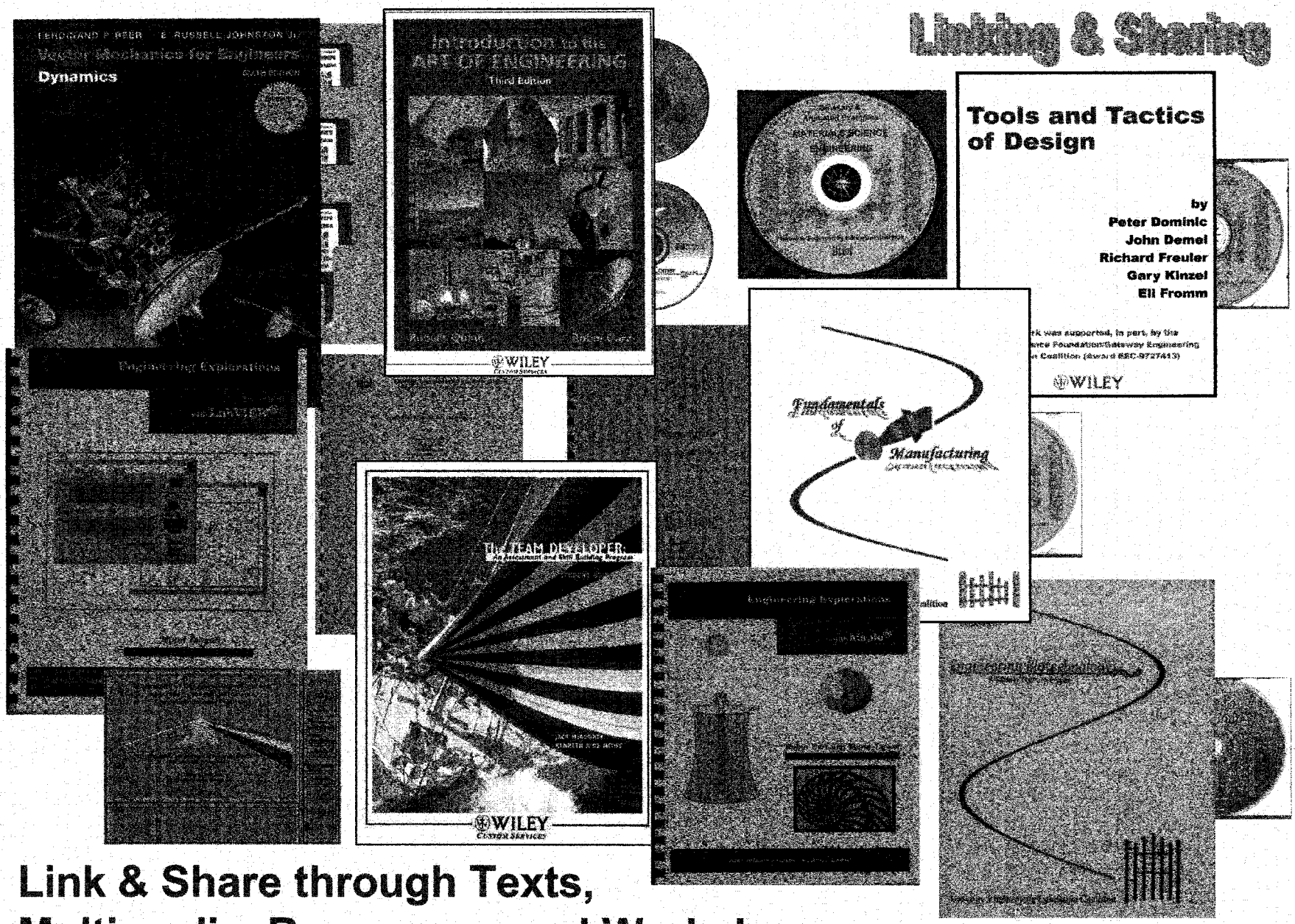

Link & Share through Texts, Multimedia Resources, and Workshops

GATEWAY ENGINEERING EDUCATION COALITION
~ Changing the Culture of Engineering Education ~

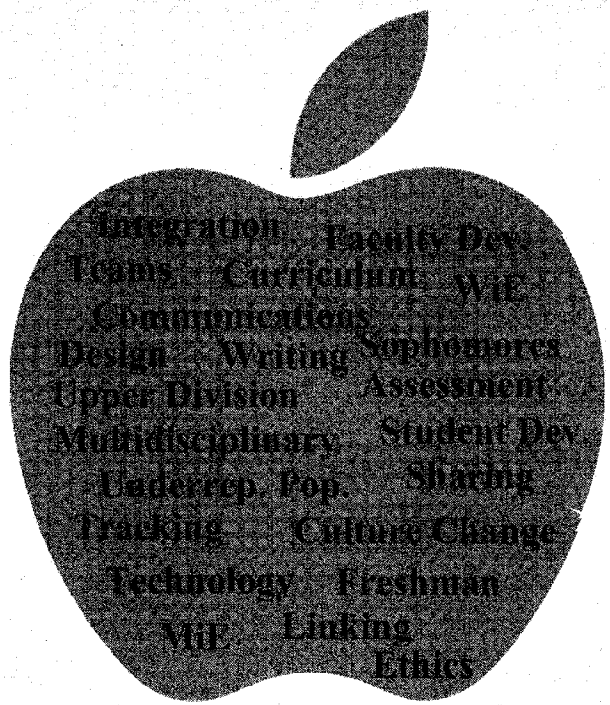

Sustainable Systemic Change of the Undergraduate Educational Enterprise

Developing the Emerging Engineering Professional
~ A Complex Integrated System ~

Gateway Web Repository - The Legacy

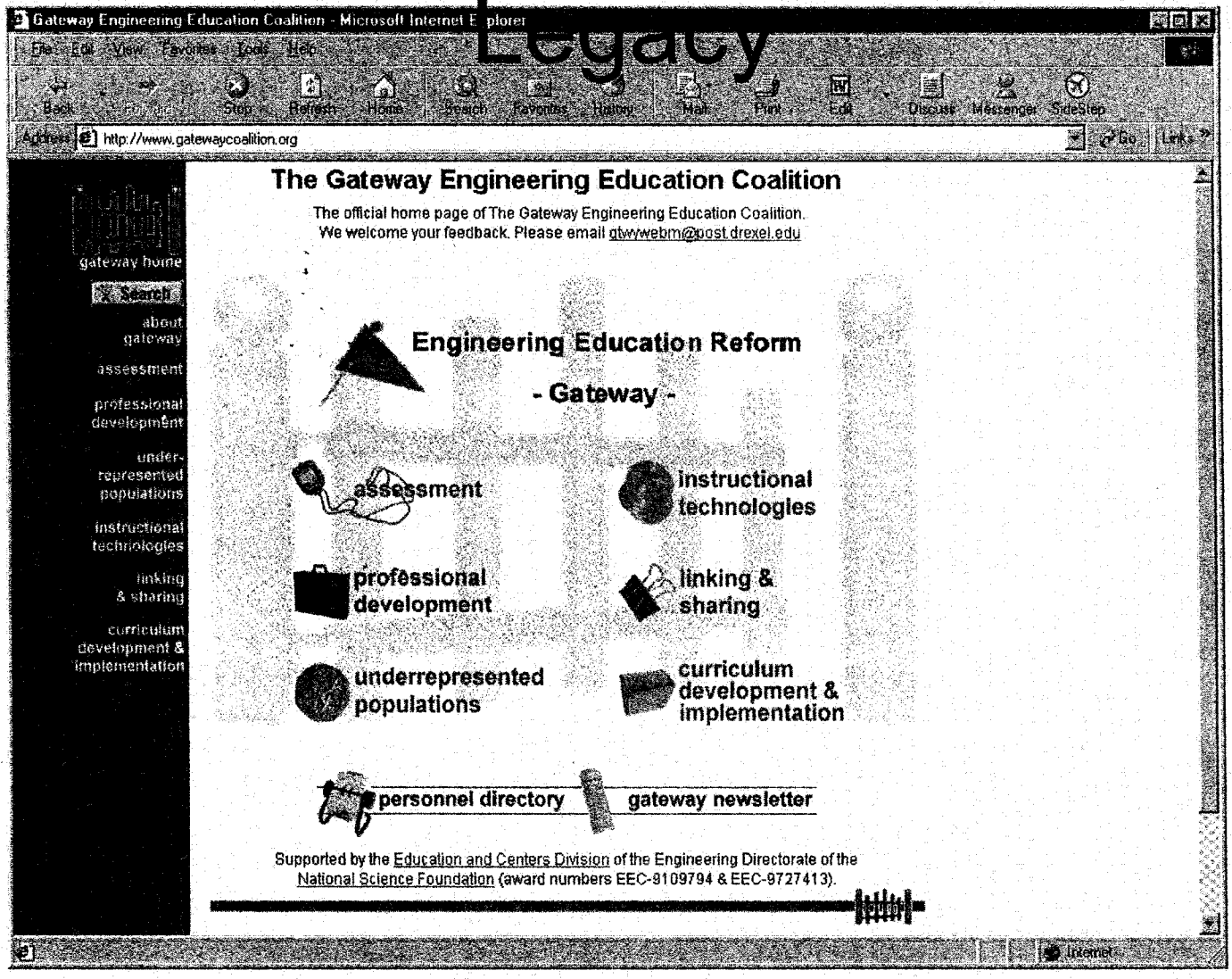

COMBINATORIAL APPROACH TO MATERIALS DISCOVERY

Ichiro Takeuchi

Department of Materials and Nuclear Engineering and
Center for Superconductivity Research
University of Maryland
College Park, Maryland 20742

Telephone 301-405-6809
e-mail takeuchi@squid.umd.edu

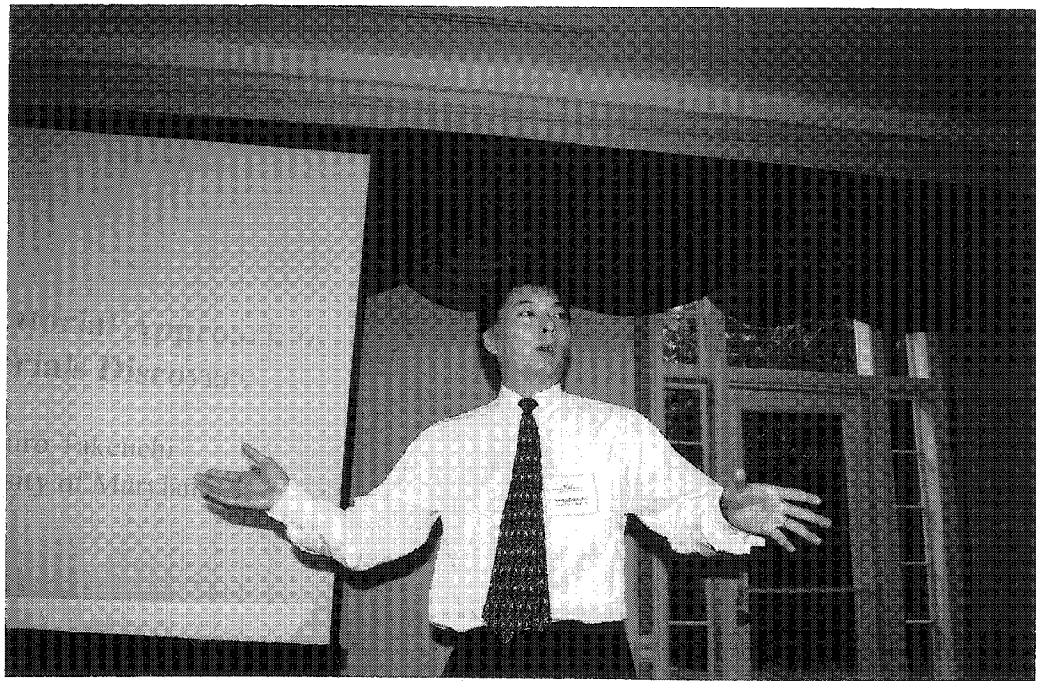

Ichiro Takeuchi

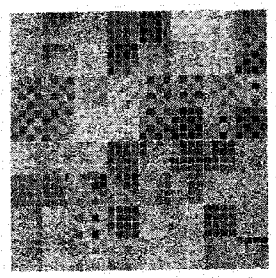

Combinatorial Approach to Materials Discovery

Ichiro Takeuchi
University of Maryland

Opportunities in Materials Science

Electrical	Magnetic	Optical	Chemical
Ferroelectric/ dielectrics	Permanent magnets	Nonlinear optics	Catalysts
Thermo-electrics	Magneto-resistive materials	Photo-refractives	Chemical sensors
Super-conductors	Magneto-strictive materials	Transparent conductors	
Piezoelectrics		Phosphors	

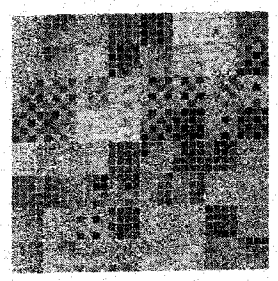

Combinatorial Approach to Materials

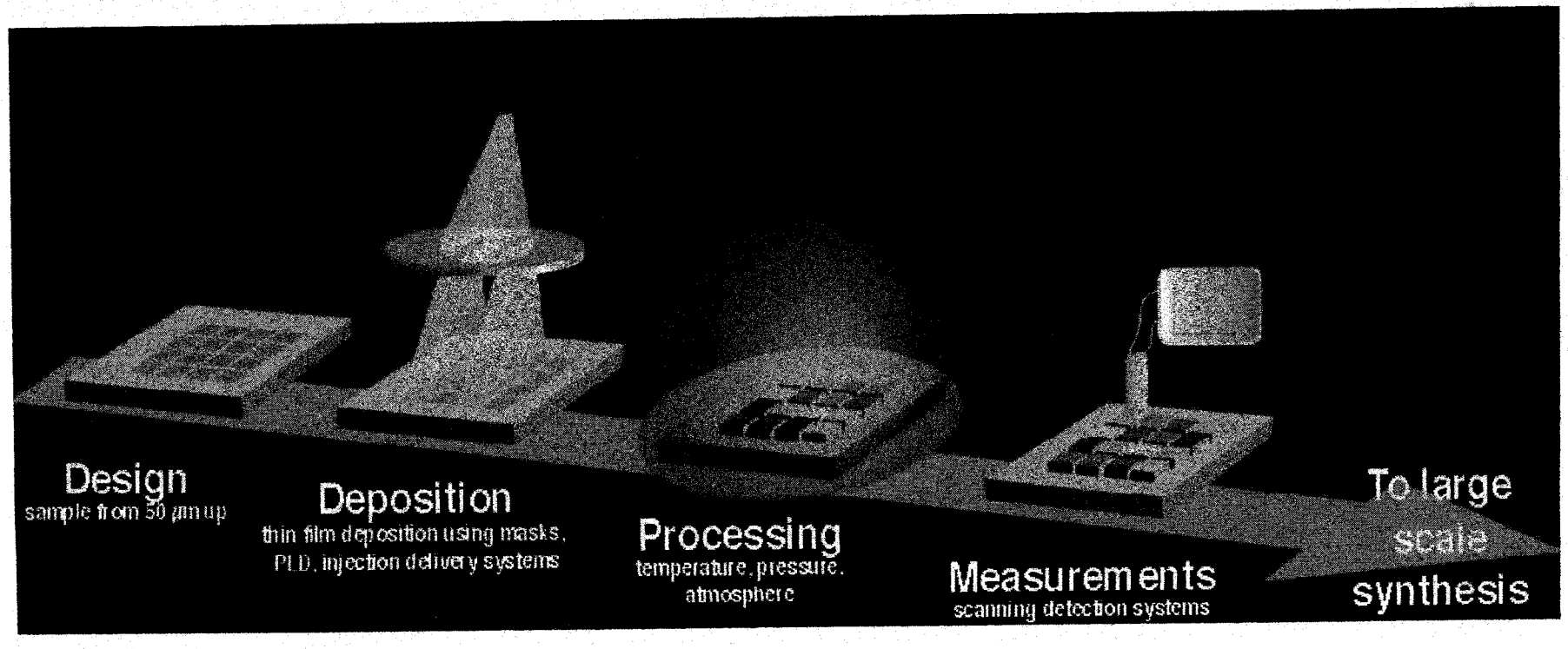

Making New Materials

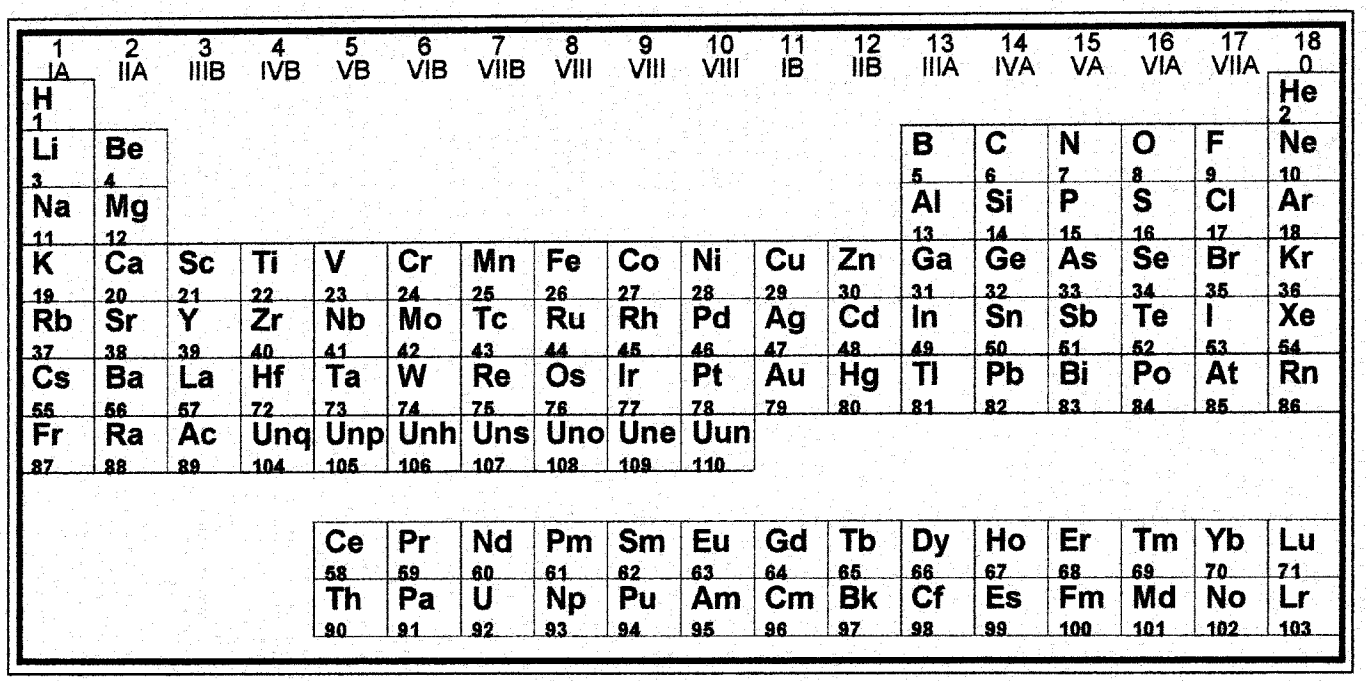

1 IA	2 IIA	3 IIIB	4 IVB	5 VB	6 VIB	7 VIIB	8 VIII	9 VIII	10 VIII	11 IB	12 IIB	13 IIIA	14 IVA	15 VA	16 VIA	17 VIIA	18 0
H 1																	He 2
Li 3	Be 4											B 5	C 6	N 7	O 8	F 9	Ne 10
Na 11	Mg 12											Al 13	Si 14	P 15	S 16	Cl 17	Ar 18
K 19	Ca 20	Sc 21	Ti 22	V 23	Cr 24	Mn 25	Fe 26	Co 27	Ni 28	Cu 29	Zn 30	Ga 31	Ge 32	As 33	Se 34	Br 35	Kr 36
Rb 37	Sr 38	Y 39	Zr 40	Nb 41	Mo 42	Tc 43	Ru 44	Rh 45	Pd 46	Ag 47	Cd 48	In 49	Sn 50	Sb 51	Te 52	I 53	Xe 54
Cs 55	Ba 56	La 57	Hf 72	Ta 73	W 74	Re 75	Os 76	Ir 77	Pt 78	Au 79	Hg 80	Tl 81	Pb 82	Bi 83	Po 84	At 85	Rn 86
Fr 87	Ra 88	Ac 89	Unq 104	Unp 105	Unh 106	Uns 107	Uno 108	Une 109	Uun 110								
				Ce 58	Pr 59	Nd 60	Pm 61	Sm 62	Eu 63	Gd 64	Tb 65	Dy 66	Ho 67	Er 68	Tm 69	Yb 70	Lu 71
				Th 90	Pa 91	U 92	Np 93	Pu 94	Am 95	Cm 96	Bk 97	Cf 98	Es 99	Fm 100	Md 101	No 102	Lr 103

Searching for the Right Combination in Complex Materials

For Example, Superconductors $HgBa_2CaCu_2O_7$?

Parameters that Affect Properties of Materials

1. **Compositions**
   - •identity of components
   - •stoichiometry
2. **Dopants**
   - •identity
   - •concentration
3. **Processing Conditions**
   - •temperatures
   - •pressures
4. **Presence of Defects**
5. **Microstructures**

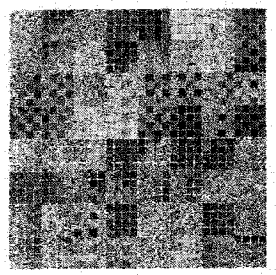

Synthesis of combinatorial libraries and composition spreads

Rapid characterization and screening of physical properties

Materials diagnostics

Designing the libraries and precursor deposition

- **maximize diversity (maximize the density)**
- **quick turn-around**
- **accuracy of deposited thicknesses**

4xn depositions

4^n combinations

n=5
20
1024

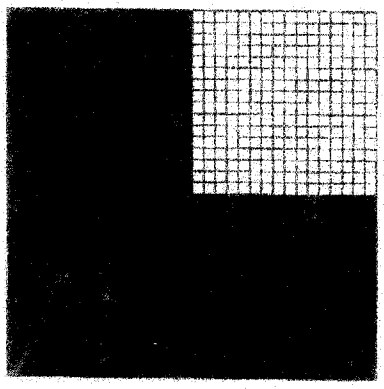

A

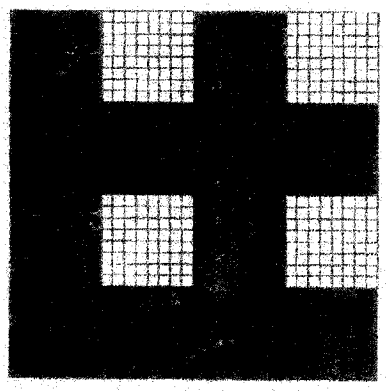

B

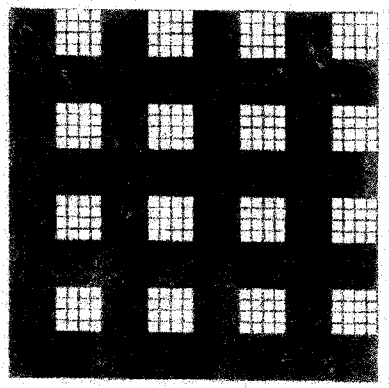

C

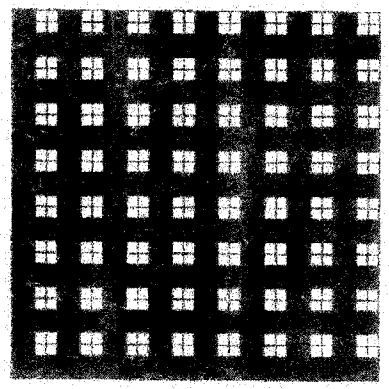

D

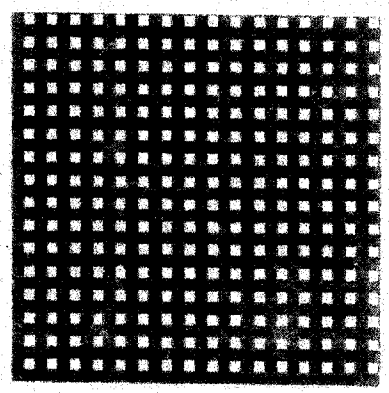

E

Quaternary mask patterns for fabricating libraries. Masks are applied successively from A to E. Each mask is used in 4 depositions, each time rotated by 90 degrees. A total of 1024 different combinations of precursors can be obtained as a result.

Compound

ABCDE

Library fabrication using precursors

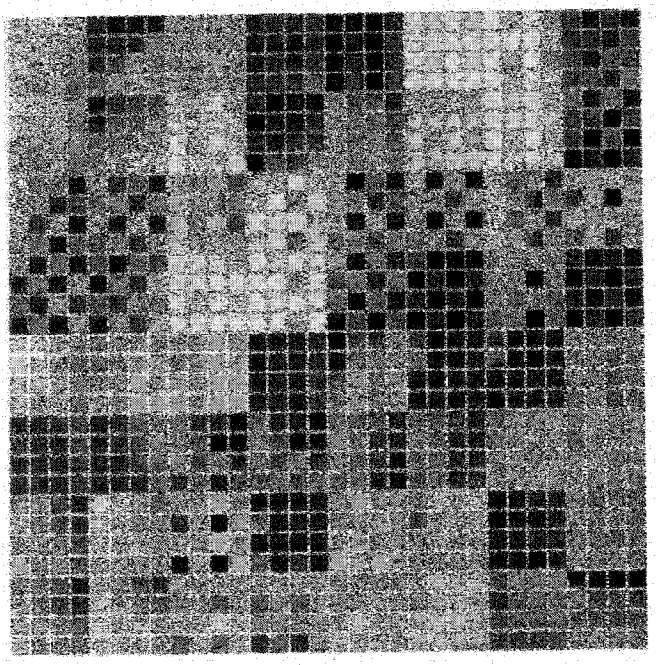

1024-member
luminescent material
library
Science 279, 1712 (98)

Amorphous precursor multilayer

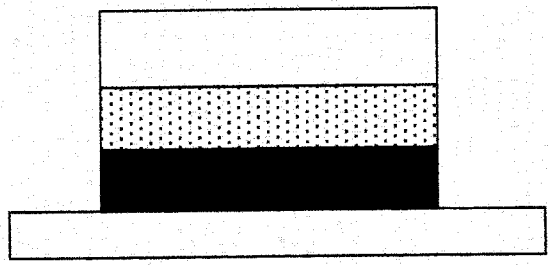

Substrate

Crystalline (epitaxial) film

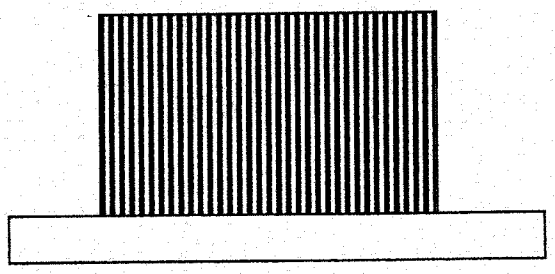

Substrate

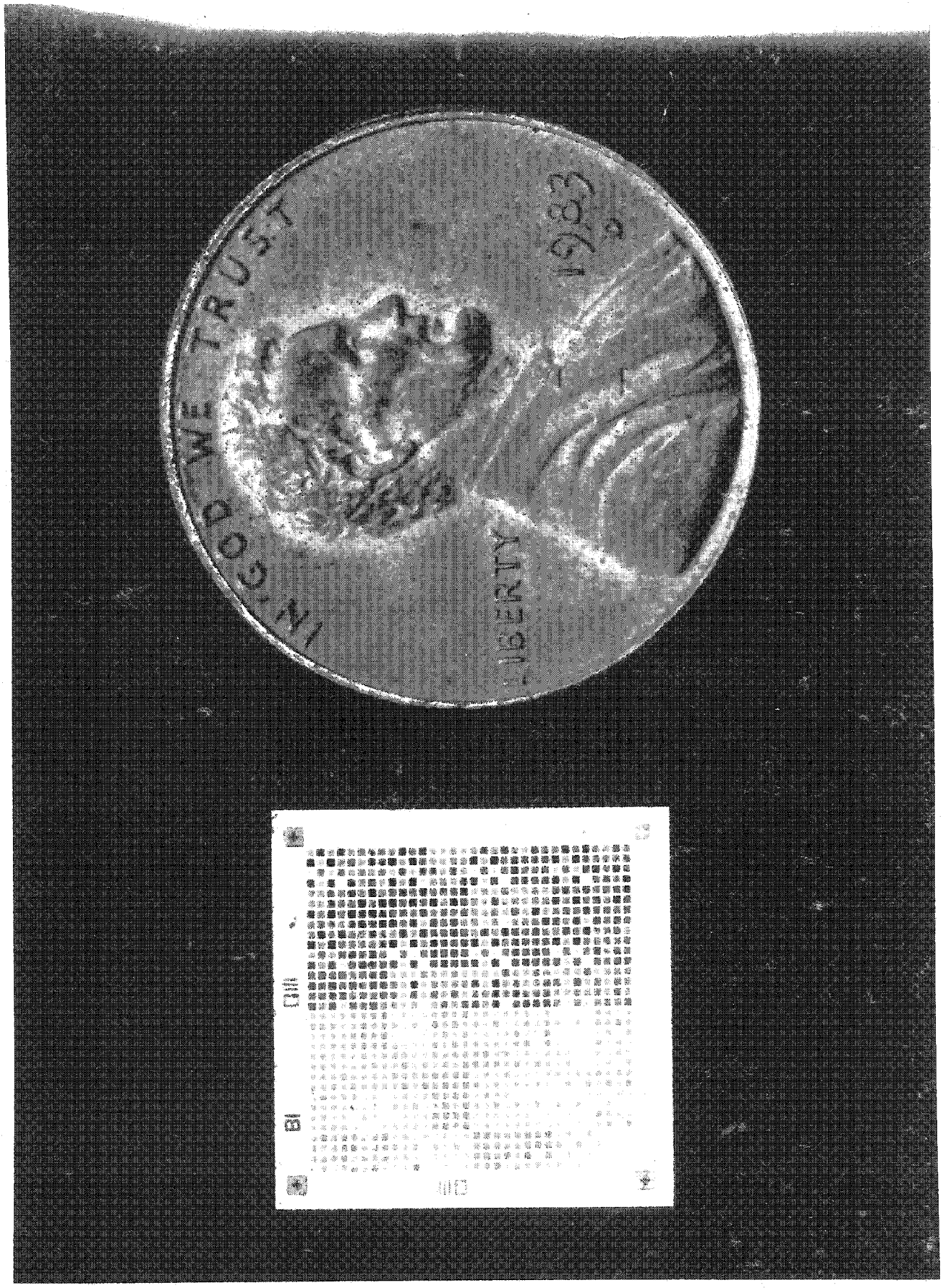
IN GOD WE TRUST
LIBERTY

Combinatorial Capacitor Library

$BaTiO_3$ $Ba_{0.7}Sr_{0.3}TiO_3$ $Ba_{0.5}Sr_{0.5}TiO_3$

Ce 0% → 3%

Y

La

W

Composition Spread of $Ba_{1-x-y}Sr_xCa_yTiO_3$

(imaging obtained with microwave microscope)

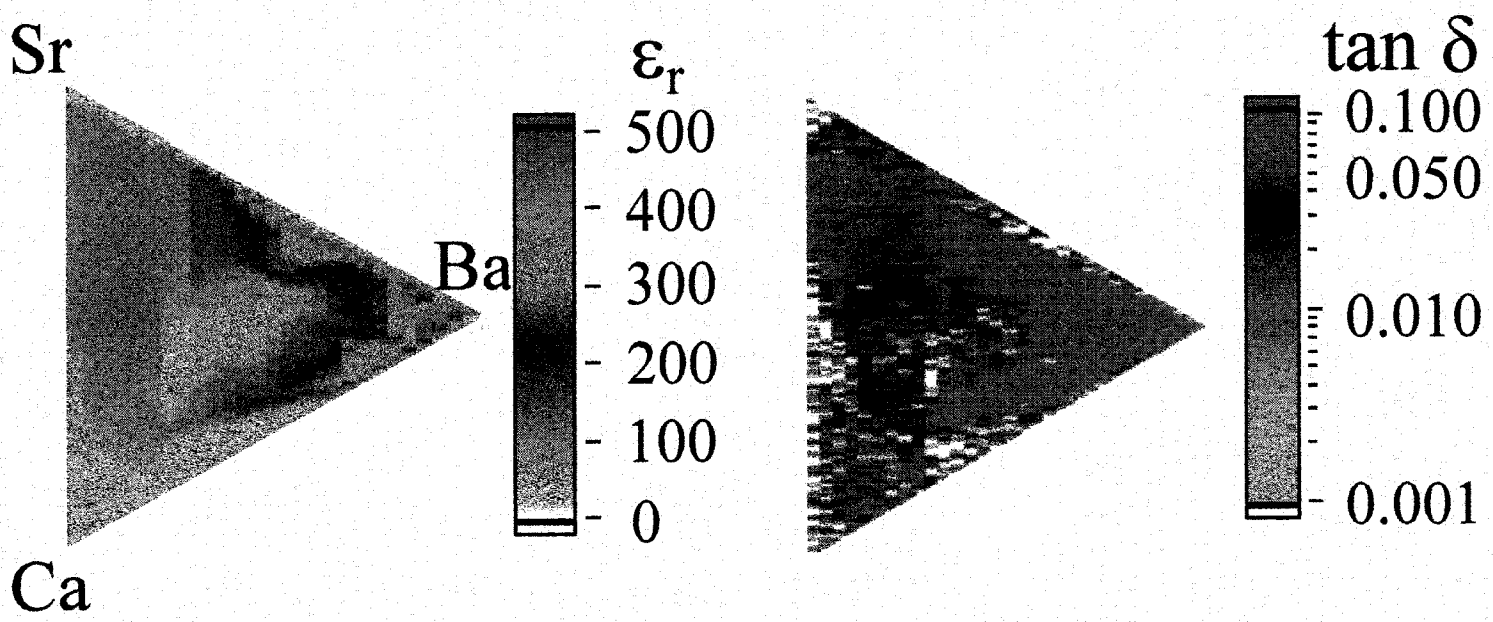

Low loss region: $Ba_{0.12-0.25}Sr_{0.35-0.47}Ca_{0.32-0.53}TiO_3$

Appl. Phys. Lett. 74, 1165 (1999)

Precursor phase diagram

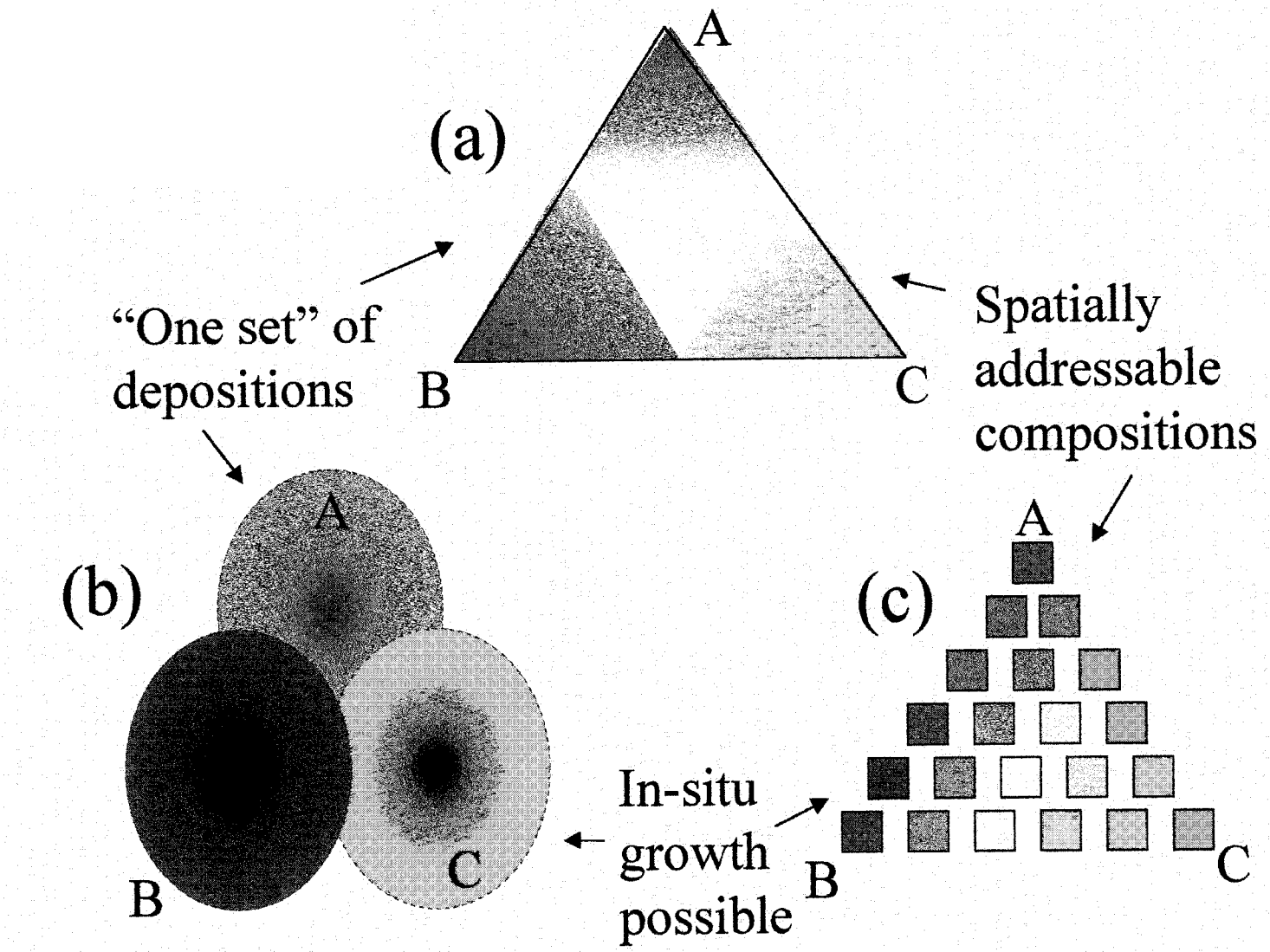

Natural composition spread **Discrete phase spread**

I. Takeuchi, Applied Surface Science, in press

Combinatorial Pulsed Laser Deposition Flange

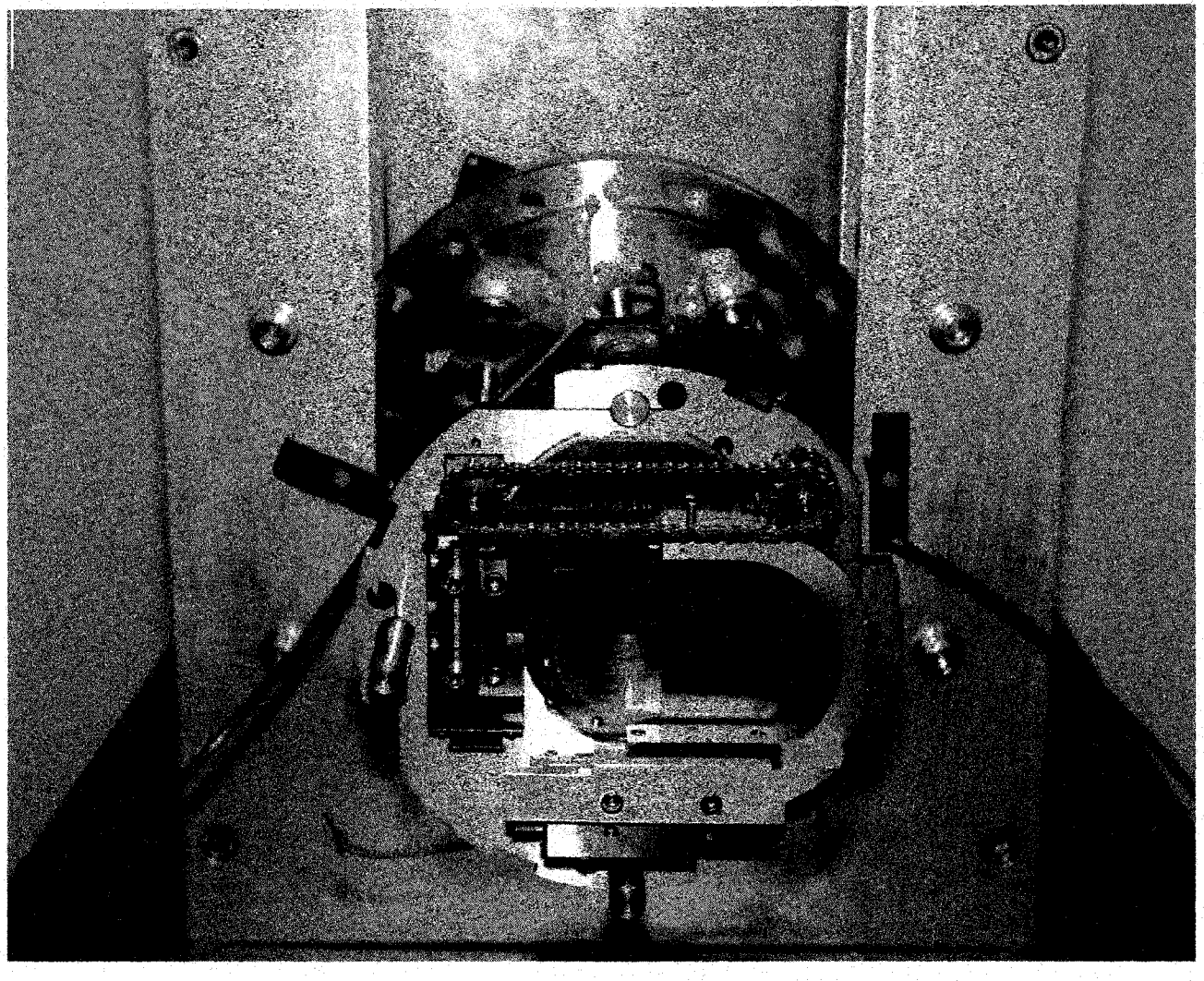

Modular and compact 8" flange

Rotatable heater

2D shutter system

Combinatorial UHV Sputtering System

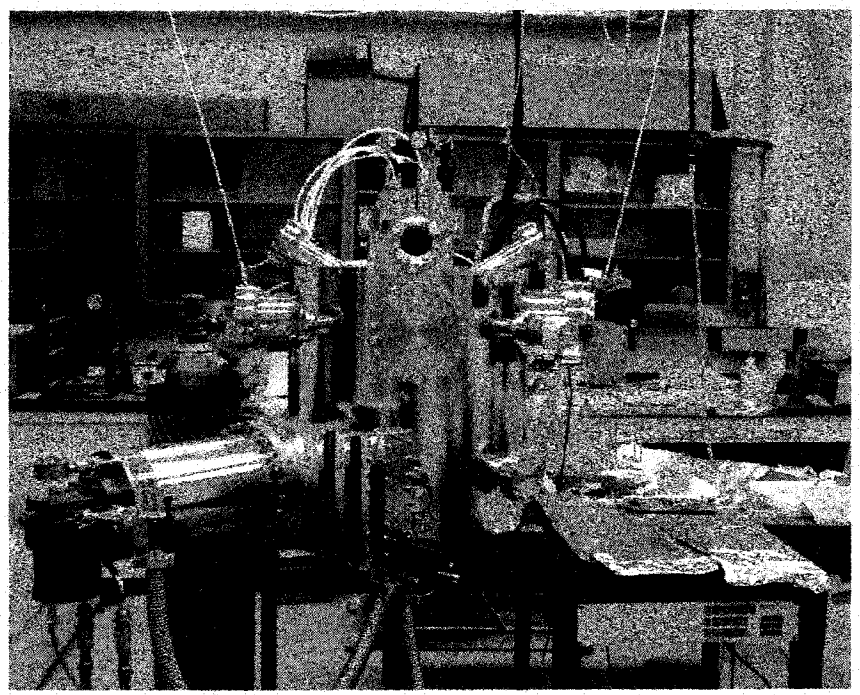

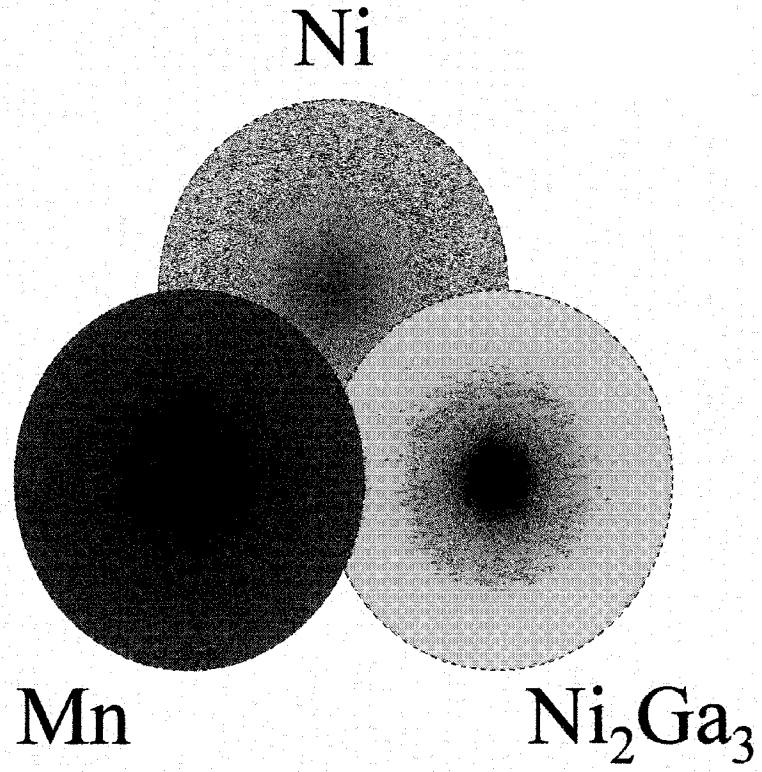

I. Takeuchi, UMD

Characterization of the libraries

•rapid measurements

(scanning and/or parallel detections)

•non-destructive measurements

(non-contact)

•accurate quantitative measurements

Multi-mode Variable Temperature Scanning Microwave Microscope

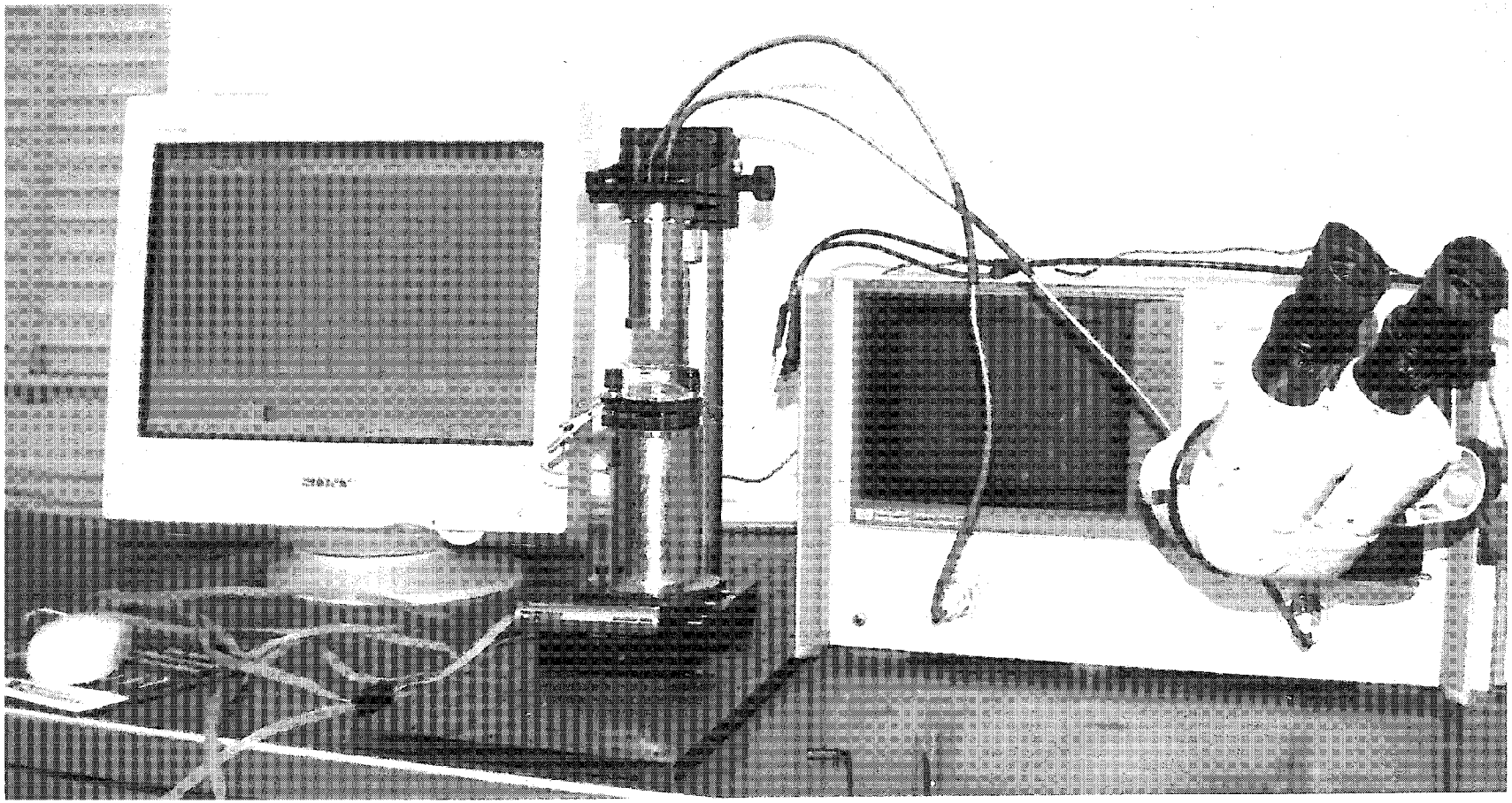

I. Takeuchi, University of Maryland

Screening for Possible New Superconductor Materials

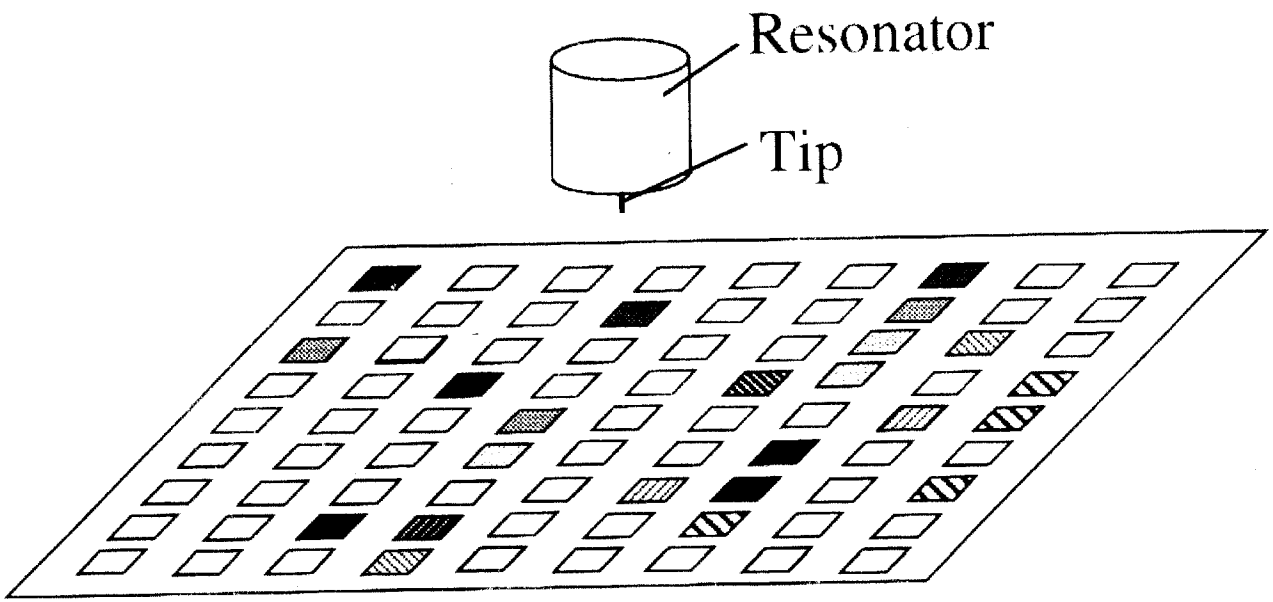

Thin Film Library of Superconductor Materials

Scanning SQUID Microscope

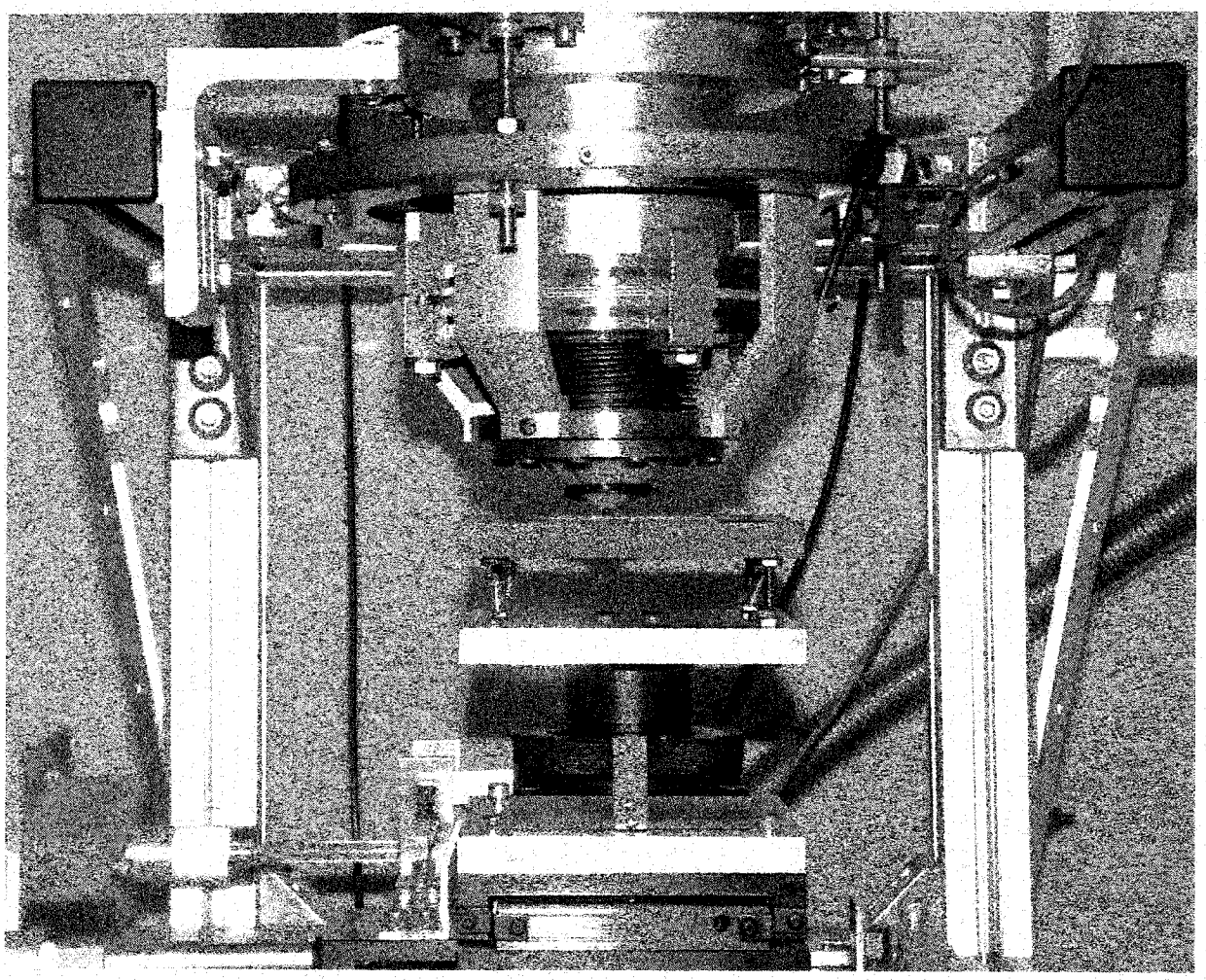

F. Wellstood

Scanning X-ray Diffractometry
$BaTiO_3$-$SrTiO_3$ Composition Spread

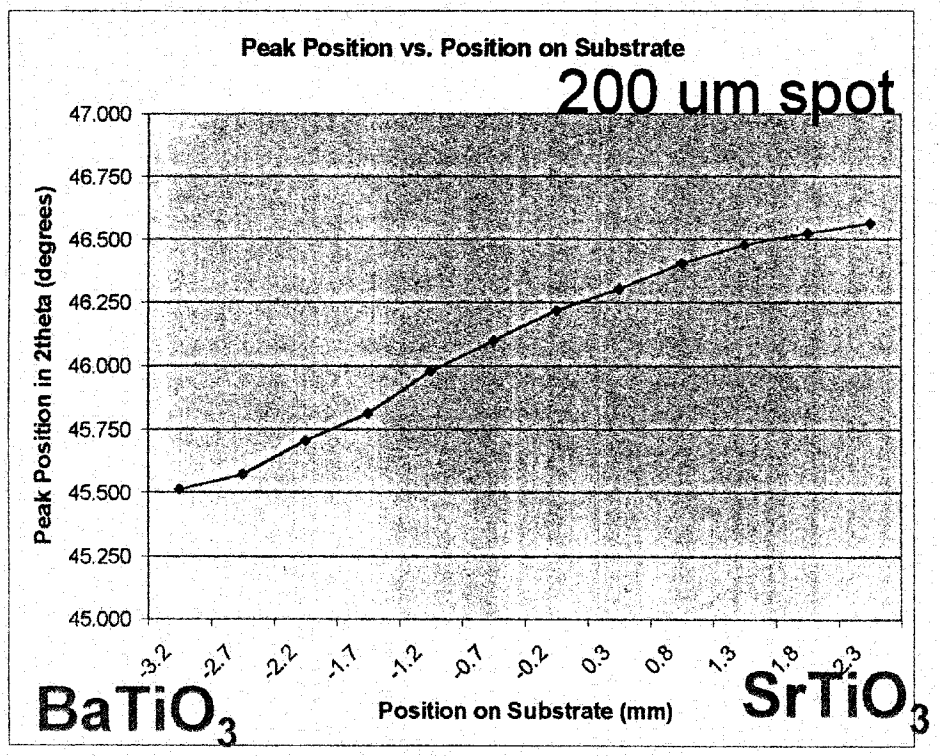

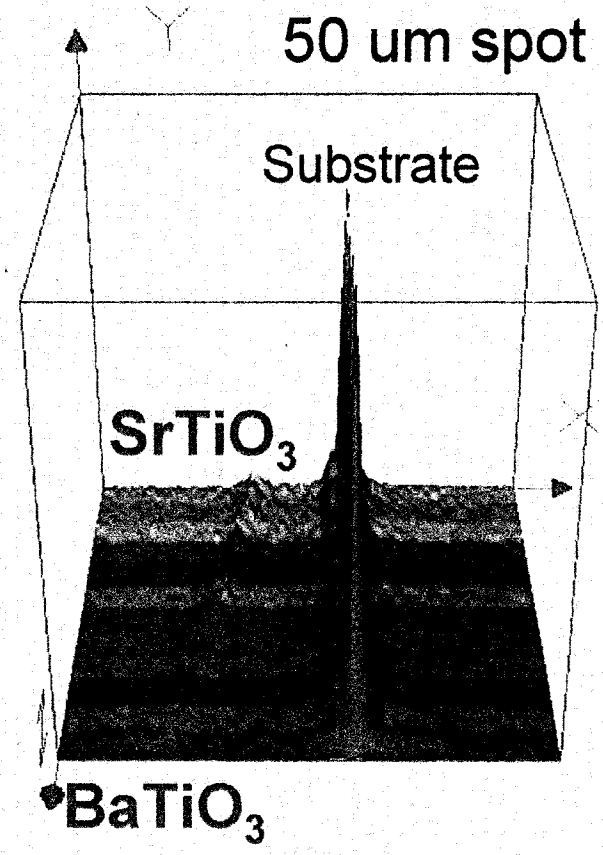

I. Takeuchi, University of Maryland

Combinatorial Materials Research:

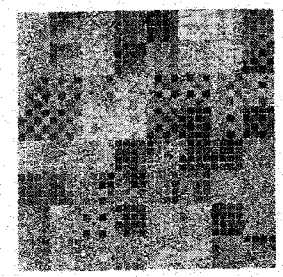

- **Environmentally sound approach**
  Leads naturally to reduction in resources used in research.

- **Great educational tool**
  Covers a wide range of compositions in one breadth.
  Provides highly interdisciplinary research and training environment.

EXPERIMENTS IN ELECTRICALLY AND MAGNETICALLY ACTIVE POLYMERS: NOT JUST INSULATING PLASTICS

James V. Masi

Western New England College (emeritus)
242 Spurwink Avenue
Cape Elizabeth, Maine 04107

Telephone 207-767-3196
e-mail masij@hotmail.com

James V. Masi

Experiments in Electrically and Magnetically Active Polymers: Not Just Insulating Plastics

James V. Masi
Western New England College (emeritus)
Springfield, MA 01119
(207)767-3196, masij@hotmail.com

Abstract: The advent of organic materials for electroluminescent devices has allowed a wide variety of applications in displays, communications, sensors, and the like. The demonstration of organic magnetic materials has offered the challenge of finding polymer (organic) materials in which there is sufficient electronic exchange as well as stability in both thermally and chemically. The intrinsically conductive and semiconductive polymers have allowed designers the liberties of flexibility and conductivity to meet needs from batteries to solar cells. This paper gives an overview of this search past, present, and future and the synthesis of promising new complex polymer building blocks which can yield conductive, semiconductive, luminescent, ferro-, ferri-, and super-paramagnetic materials for devices of the future in power, storage, displays, and communications devices. The use of these materials to produce electrically active polymeric materials has changed our way of thinking about how to fabricate devices with properties heretofore unrealizable.

Key Words: Electrical Polymers, Magnetic Polymers, Luminescent Polymers, Molecular Electronic Materials.

Prerequisite Knowledge: The student should be familiar with the basics of materials science, metallography, and chemistry. Levels at which these experiments are performed are second semester junior year and either semester senior year. The students are first given lectures the properties of materials including polymers and magnetic, luminescent and conductive polymeric materials (as shown in the appendix). They should have already had a laboratory experiment on metallography and sample preparation.

Objectives: The objectives of these experiments are to show how the unique properties of polymers lend themselves to applications involving electrical, magnetic, and optical properties and how they are incorporated in a variety of devices. These experiments contain all of the elements of good design, with the caveat that a novelty in structure is sometimes a part of design. The students learn the process of designing materials for the world of device applications, analyze those already used, and suggest possible solutions to the problems involved with present technology.

Equipment and Supplies:

(1) Metallurgical preparation and polishing apparatus (e.g. Buehler Co., Port Washington, NY).
(2) Varieties of monomers (Roche Chemical Div., Hoffmann-LaRoche Inc., Nutley, NJ; Baker Chemical, U. of Utah Materials, Salt Lack City. National Starch (Beta Cyclodextrin).

(3) Low voltage d.c. and 60Hz power supply (Edmund Scientific)
(4) Miscellaneous graduates, glassware, ovens (Fisher Scientific),
(5) Indium-tin oxide coated glass and plastic (Tecknit Corp., Cranford, NJ)
(6) Miscellaneous meters and power supplies.
(7) Metallurgical microscope (Olympus, Zeiss, etc.).
(8) Small photoresist spinner (Fisher Scientific).

Introduction

Molecular Magnetic Materials

When the early civilizations made the discovery that iron was indeed attracted to lodestone, the era of magnetism and its devices and effects was launched. After that time, the earliest device recorded was the compass, an invention of the Chinese. Since then, ferromagnetic (Fe, Ni, Co, etc.), ferrimagnetic (e.g. F_3O_4), and paramagnetic materials have been used in technology applications such as magnets, magnetic tapes and disks, magnetic resonance imaging contrast enhancers, and magneto-optic memories, to name a few. Organic/molecular based materials, with *p* or *d* orbitals aiding the magnetic properties, have been a source of scientific curiosity for a number of years[1,2], but only recently have such materials become a reality[3,4,5].

This new class of magnetic materials is, for the most part, non-metallic, being made from simple to complex organic molecules. Their structure can be uni- or bi-dimensional and need not have the three-dimensional format necessary for conventional ferromagnetic, ferrimagnetic, paramagnetic, and antiferromagnetic materials. These materials can be simply fabricated from a variety of solvents at or near room temperature. These should not be confused with bimetallic complexes such as those formed by pyrolisis or partial oxidation.[6] Other work postulated the use of a new class of pi-biradicals called the non-Kekule polynuclear aromatics, shown in Figure 1 below.[3] The high spin nature of these systems should drive

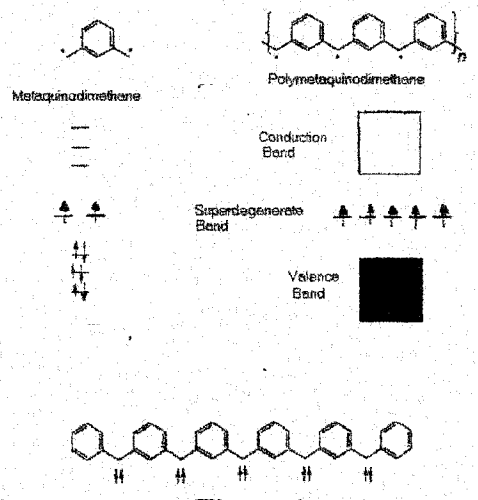

Figure 1
Representation of pi-molecular structure of metaquinodimethane, the associated spins, and an oligomer

ferromagnetic coupling in charge transfer complexes. This is best served by having the centers covalently bonded together, namely, a polymer system made up of repeating molecular segments sharing the framework of the high-spin systems, quinodimethanes based on the benzene, naphthalene, and biphenyl nuclei.

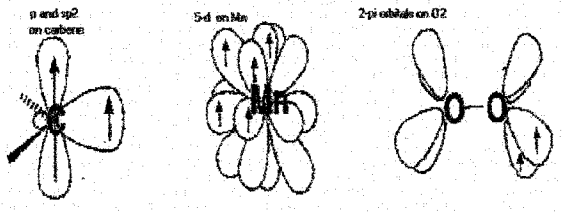

Figure 2
Possible model for magnetic spin coupling

Figure 2 shows a possible model for magnetic spin coupling where spins align in orthogonal orbitals in a small spatial region.[1] Figure 3 shows six possible configurations of parallel and anti-parallel spins, along with canted ones for reference, to describe paramagnetic, ferromagnetic, antiferromagnetic, Ferromagnetic canted ferromagnetic, and correlated spin glass (disordered structure). A description of the materials is given in Appendix A.

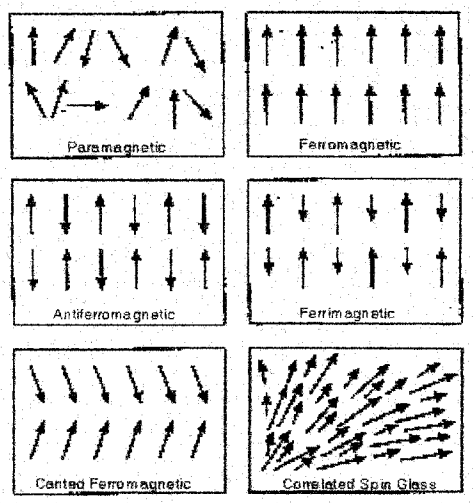

Figure 3
Spin configuration directions for magnetic types

Experiment 1. Making and testing magnetic polymers

The work described here involves a formulation of a solution, the mechanism definition, and results for this formulation. These materials are deposited on a variety of surfaces from alumina to modified vinyl. This method enables the user to deposit a magnetic polymer on a wide variety of surfaces and topographies. These polymers retain the electrically insulating properties, while exhibiting ferromagnetic behavior.

Cyclodextrins, Cyclic oligosaccharides, were discovered approximately 100 years ago. In the pharmaceutical industry , Cyclodextrins have mainly been used as complexing agents to increase the aqueous solubility of poorly water-soluble drugs , and to increase their bio-

availablity and stability . Cyclodextrins are produced by a highly selective enzymatic synthesis consisting of Six, Seven, or Eight glucose monomers averaged in a donut shaped ring, which are denoted alpha, beta or gamma Cyclodextrin respectively. The specific coupling of the glucose monomers gives the Cyclodextrin a rigid conical molecular structure with a hollow interior of a specific volume. This internal cavity, which is hydrophobic in its nature, is a key structural feature of the Cyclodextrins, providing the ability to complex and contain a variety of "guest" molecules (e.g. aromatic, alcohol, halides and hydrogen halides, fatty acids and other esters, ferromagnetic ions, etc.). The guests must satisfy the size criterion of fitting at least partially into the Cyclodextrin internal cavity, resulting in an **inclusion complex**. The Empirical Formula is $(C_6H_{10}O_5)_7$ and is basically a carbohydrate. A graphic simulation of β-cyclodextrin is shown in Figure 4.

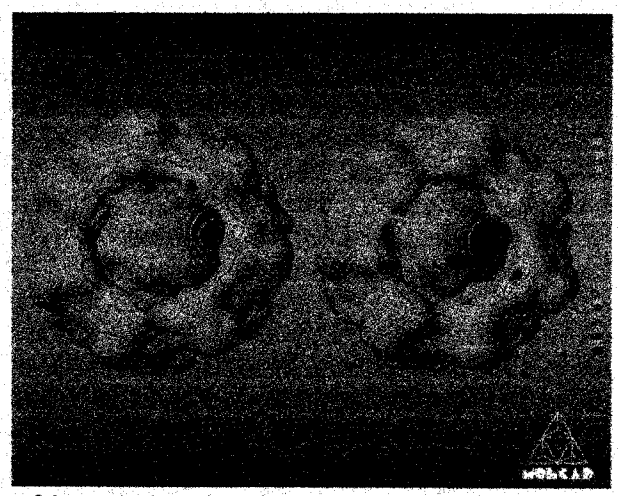

Figure 4. Simulation of β-cyclodextrin with central hole filled with ferromagnetic material. [courtesy MOLCAD]

Table I shows the important parameters associated with the β-cyclodextrin used in this work. As can be seen, the size parameters fit very well with the size of the iron ion (1.17Å).

Table I: Important molecular parameters of β-Cyclodextrins (CD)

	β-CD
glucose residues	7
molecular weight	1135
cavity diameter (Å)	6-6.6
cavity height (Å)	7.9
cavity volume (ml/mol)	262

II. DISCUSSION

Procedure

A. General

The purpose of the process is to treat and polymerize a ferromagnetically modified cyclodextrin polymer and cast it into solid shapes for use in high-speed magnetic devices (inductors, transformers). This is done in aqueous solutions, with alcohol added as a dispersant.

B. Materials Needed

Substrates (alumina, printed circuit G-10, modified, ceramic-filled vinyl, and glass), $FeCl_3$, Beta Cyclodextrin, isopropyl alcohol.

C. The solution

The solution is prepared by mixing 1 mole of $FeCl_3$ With 1 mole of β-cyclodextrin in an aqueous solution. By weight, the amounts are: 26.9 g $FeCl_3$, 16.2 g β-cyclodextrin, added to 50 g water. Alcohol is added, drop by drop, until the solution becomes homogeneous in appearance.

D. Polymerization

The material is condensation polymerized by pouring onto the glass substrates and heating to 85 C until a thick film of the material is formed. This material has a d.p. of about 5000 and is capable of being thermally compression molded into shapes at 150 C.

A electron photomicrograph of sample of the solution dried at 85 C onto a glass substrate is shown in Figure 5. The voids are due to shrinkage and lack of wetting. This morphology differs, dependent on time at temperature.

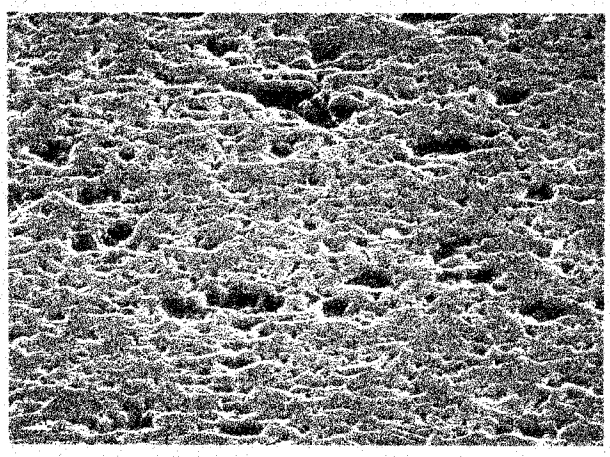

Figure 5. β-cyclodextrin:Fe condensation polymerized and baked at 85 C on glass. 1000x.

The properties of the films as measured at 250MHz at room temperature were:
Resistivity : $>10^9$ ohm-m
Permeability (μ_r): 70-120
Loss tangent: $<10^{-3}$

Coils can be wound on the shapes fabricated and relative permeability can be deduced from the inductance measured on a non magnetic core of the same dimensions.

Conclusions (magnetic)

This process offers many advantages over conventional polymerization methods. The process is simple, low-cost, and effective. The materials used are not toxic, no special procedures need be used, and multiple applications can be made with great accuracy. The surface need not be a plane. Marking, drilling, and deposition can be done on a variety of substrate topologies. The polymer used must be non-hydrated, in order to avoid loss in the material at high frequencies due to water. Further studies are being performed on other metal/substrate systems with other polymer systems as well.

Luminescent Polymers

Introduction

Electroluminescent devices are showing promise for applications in future flat panel displays. Current flat panel display technology depends on inorganic light emitting diodes, backlit liquid crystal displays, and vacuum fluorescent displays with field electron emission onto phosphors. The problem for manufacturers lies in how to reduce the cost of illuminated displays, while increasing their capacity and efficiency. Organic/molecular films may hold the solution to this problem.

Observation of light emission has been observed in various polymers and copolymers of arylene vinylene, Polyphenylene vinylene (PPV) being the most efficient to date. However, a number of conjugated homopolymers, copolymers, and polymer blends have been investigated. These materials have light emission over the entire visible range. [10-13] Though imbalances in the injection and carrier charge transport properties are partially responsible for low efficiencies in polymer light emitting devices, there is hope of overcoming these drawbacks with the use of separate transport layers, electron withdrawing groups, and electron accepting additives and modifications. In addition to PPV, there are other materials which show promise. These are: poly (2,6-quinoline vinylene) (PQV), poly (phenylene vinylene-co-quinoline vinylene) (PPVQV), poly(p-pyridine) (PPP), poly(phenylene vinylene) (PPV), cyano-poly(phenylene vinylene) (CNPPV), and poly(2,3-diphenyl-5-hexyl-p-phenylene vinylene) (DP6-PPV). Two of these compounds are shown in Figure 6. [14] A detailed description of electroluminescent polymeric materials and structures is given in Appendix B.

PPV PPP

Figure 6. PPV and PPP

Experiment 2. Making and testing luminescent polymers

The experimental setup is shown in Figure 7. The transparent electrodes are the same as those shown in the experiment on Liquid Crystals (NEW Update 2000). The layers are spun onto the conductive glass using the solvents shown below. Electrodes may either be evaporated or "painted" on with conductive silver epoxy. Construction can also be of the SCALE variety as shown in Figure B2 in Appendix B.

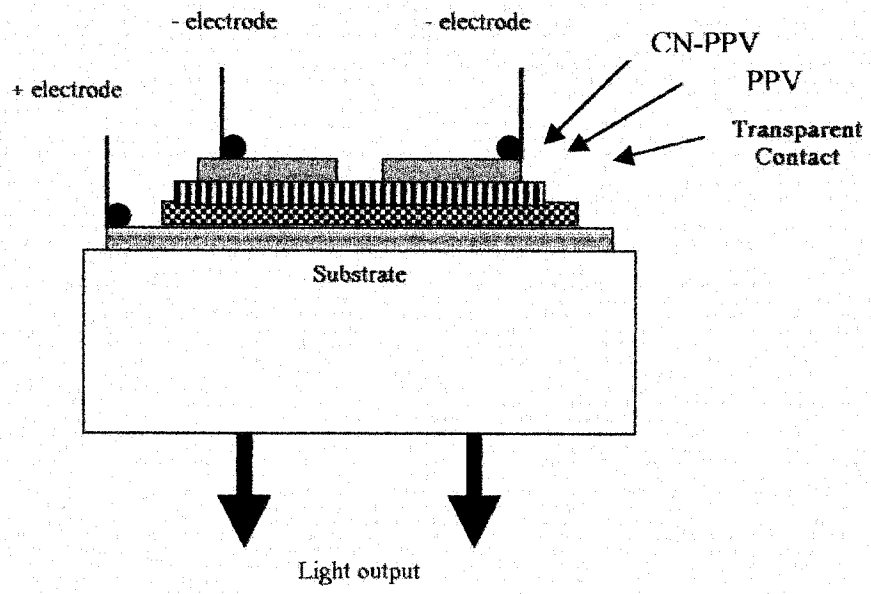

Figure 7. Light emitting polymer diode construction

Violet: Oxydodecyl poly(paraphenylene) (DDO-PPP)
-π -π * absorption band maximum at 340 nm
-PL band in the violet; 0-0 transition at 400 nm
-Soluble in toluene or THF for processing

Green: unsubstituted Poly(paraphenylenevinylene) (PPV)
-π -π * absorption band maximum at 400 nm
-PL band in the green; 0-0 transition at 520 nm
-Available as the precursor in aqueous solution for ease of processing

Red: Oxydodecylmethoxy-poly(paraphenylenevinylene) (DOO-PPV)
-π -π * absorption band maximum at 510 nm
-PL band in the red; 0-0 transition at 570 nm
-Soluble in toluene

The cyano-layer can be fashioned on any of these materials by adding potassium cyanide (1% solution) to the monomer. The cure cycle is 110 C for 20 minutes.

Measurements of current vs. voltage can be made and log I vs V can yield the activation energies and effective bandgap of the materials.

Conductive Polymers

The conductive and semiconductive polymers have properties which allow device, cost, and interconnection attributes not available with conventional inorganic materials [16]. It should be noted that there are no polymers based on carbon backbones that are intrinsically conductive to the extent of metallic or carbon/graphite loaded polymers. These polymers are usually made electrically conductive by adding either electron donors or acceptors to the host polymer, either by charge transfer complexes or dopant atoms (as in semiconductors) [17,18]. A comparison of organic and inorganic materials is given in Figure 8.

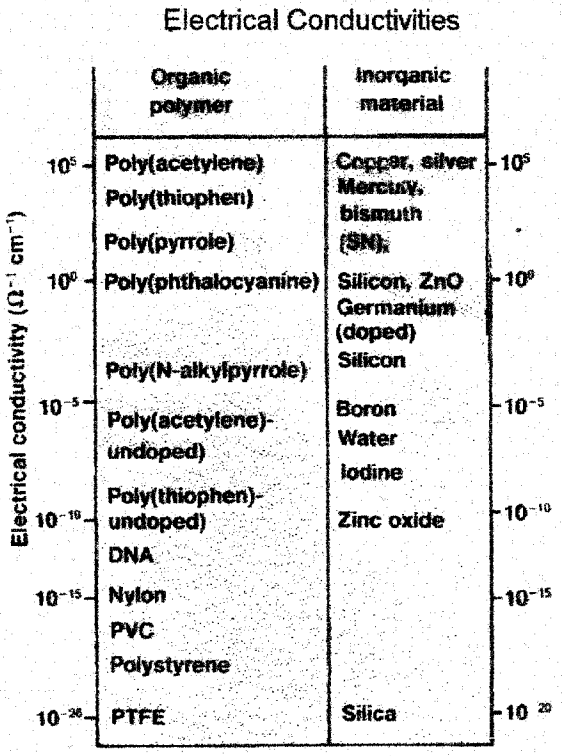

Figure 8. Electrical conductivities compared

Though silver and copper are, in reality, an order of magnitude higher than polyacetylene, the organic materials have certain electrical, electrochemical, and optical properties which make their use preferred. Some of the methods for making polymers conductive are shown in Figure 9. The proposed model for charge transfer is called percolation and in shown schematically as chain-like pathways for conduction.

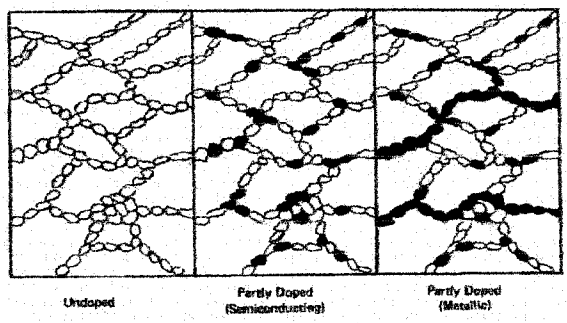

Figure 9. Percolation through polymers causing conduction

A scanning electron micrograph of trans-polyacetylene is shown in Figure 10 [16]. The chain-like structure is quite visible in this photo and supports, at least visually, the model of conductive pathways.

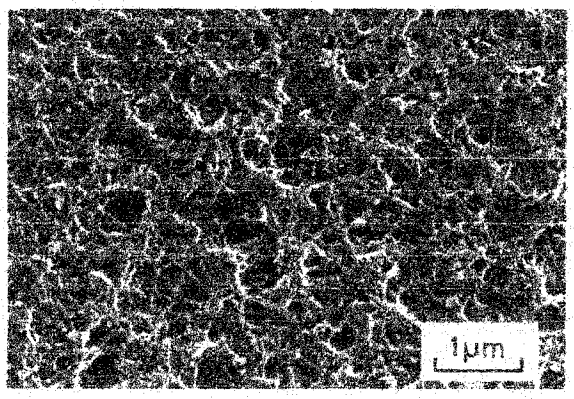

Figure 10. Scanning electron micrograph of trans-polyacetylene [16].

Some of the uses for these semiconductive and conductive polymers are: battery electrodes, polymer electrolytes for batteries, solar cells, compatible contacts for light emitting polymers, and high frequency window filters for microwaves, to name a few. Some of the conductive polymers presently in use are shown in Figure 11.
As newer materials are synthesized and new properties develop, applications will, as for most new materials, finally find uses for these emerging polymers.

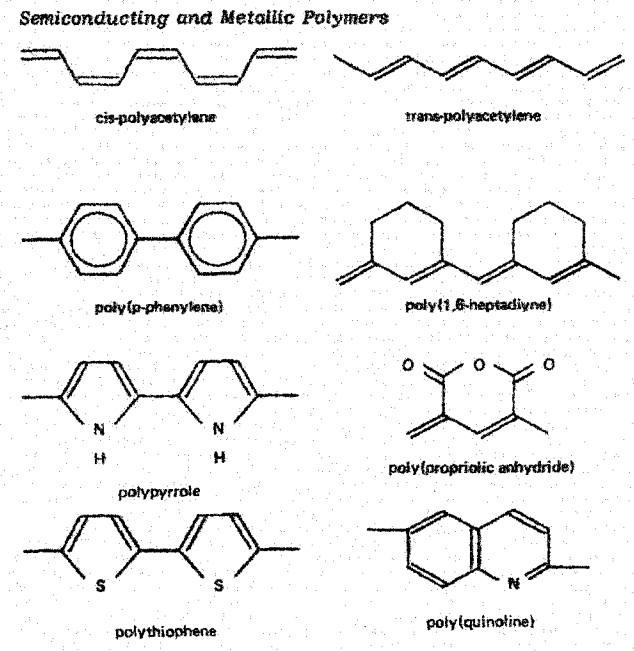

Figure 11. Some conductive/semiconductive conjugated polymers

Polyaniline (PANi)
-Available as emeraldine hydrochloride or as emeraldine base.
This material is easily spun onto a conductive glass substrate or an insulative substrate. The graph of resistivity vs. 1/T should be made using either a 4-point probe or silver epoxy contacts. By using an ITO substrate and silver epoxy on the rear of the sandwich, a photovoltaic cell can be shown to give approximately 0.35 volts at 1 mA/10 sq. cm.

Conclusions (General)

The future of magnetic materials using molecular/organic substances as their basis will be dictated by the ability of scientists to find new materials or modifiers which force high, coupled electron spin densities into 1-, 2-, or 3-D network bonding using cooperative phenomena. The potential for modifying the physical properties through conventional organic synthesis techniques makes this class of materials very attractive to the magnetics community. The polymer light emitting devices are well on their way to impacting the industry as easily produced, low cost devices. They have the present drawback of having lifetimes shorter than those demanded by the telecommunications industries and the industry as a whole. The conductive and semiconductive polymers have properties that allow device, cost, electrochemical, electro-optic, electronic, and interconnection attributes not available with conventional inorganic materials. This may lead to their use in photonic, electronic, and magnetic devices to make lower cost, high performance telecommunications, electrical, and electronic systems.

ACKNOWLEDGMENTS

It is important to recognize the efforts of pioneering researchers and the efforts that they expended in bringing this science to the level mentioned in this overview. Drs. J. Miller and A. Epstein of Ohio State University have taken polymeric formulations and turned them into working devices, both magnetic and luminescent. Dr. A. Heeger of the University of Santa Barbara and Dr. A. McDiarmid of the University of Pennsylvania pioneered many of the early conductive polymer efforts, especially the advances in polyacetylene and other electrically active polymers. Dr. T. Skotheim has advanced the understanding of conjugated polymer structures and allowed many other efforts to be published through his comprehensive treatise on conducting polymers. For all of these and many more whose efforts have made a substantial difference, but are not mentioned here, we are forever grateful.

REFERENCES:

1. J. S. Miller and A. J. Epstein, *J. Am. Chem. Soc.*, **109**, 3850 (1987).
2. J. M. Williams *et al.*, *Acc. Chem. Res.*, **18**, 261 (1985).
3. G. Allinson *et al.*, *J. Mat. Sci.: Mat'ls in Electr.*, 5, 67 (1994).
4. D. Gatteschi, *Adv. Mat.*, **6**, 635 (1994).
5. J. S. Miller and A. J. Epstein, ed. "**Proceedings of the Conference on Molecule-Based Magnets**", *Molec.Cryst., Liq. Cryst.*, 271-274 (1995).
6. A. Lukasiewicz, *et al.*, *Mat. Lett.*, **14**, 127 (1992).
8. J. V. Masi and W. Thibault, **New, High Frequency Transformer Topologies,** in Proc. of the EMCWA, IEEE Press, N.J., 1995, pp 157-162.
9. J. S. Miller and A. J. Epstein, *C & E N*, 30, Oct. 2, (1995).
10. J.H. Burroughs, et al., Nature 347,539 (1990)
11. I. Sokolik, et. al., J. Appl. Phys. 74,3584 (1993)
12. C. Zhang, et al., Synth. Met. 62,35 (1994).
13.R.K. Kasim, et al., Mat. Res. Soc. Symp. Proc, 488, 51-56 (1998).
14. A.J. Epstein, et al., Synth. Met. 78 (3), 253 (1996)
15. J.V. Masi, **Novel Magnetic Materials for High Frequency Devices,** in Proc. of the EMCWA, IEEE Press, N.J., 2001 to be published.
16. Terje A. Skotheim, *Handbook of Conducting Polymers*, Marcel Dekker Publishers, 1986, 1992.
17. J.R. Ellis and R.S. Schotland, *Market Opportunities for Electrically Conductive Polymeric Systems*, Princeton Polymer Laboratories Inc. and Schotland Business Research, Inc., Princeton, NJ, 1981
18. A.G. MacDiarmid and A.J. Heeger, in *Molecular Metals* (W.E. Harfield, ed), Plenum Press, NY, 1979.

Appendix A. New Magnetic Materials Design

Since standard stand-alone materials gave way to polymeric techniques, the possibilities of cooperative phenomena became more feasible. Since magnetic materials are only useful below

their Curie temperature, this temperature should be above room temperature. To obtain these higher Curie temperatures, one must induce some order (local disorder leads to random and inconsistent interactions). In 1985, the first molecule based magnetic materials were reported.[1,2] These materials were ionic salts (containing alternating donors and acceptors, of tetracyanoethylene and tetracyanoquinodimethane, TCNE and TCNQ in a "...DADA..." configuration, producing high multiplicity spin radicals. A ferromagnetic $[FeCp^*_2]^{\bullet+}$ $[TCNE]^{\bullet-}$ forming chains of alternating donors (cations) and acceptors (anions)can be modified from ferromagnetic to metamagnetic by replacing TCNE with TCNQ or when $[C_3(CN)_5]^-$ is added magnetic coupling is no longer effective. (Cp^* is pentamethylcyclopentadienide). A symbolic representation is shown in Figure A1.[9]

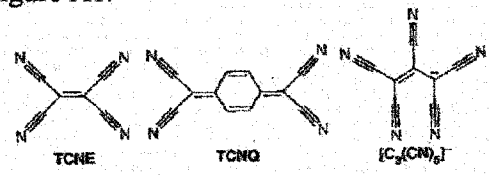

Figure A1. TCNE and TCNQ salts with ...DADA...

Up to 1991, the Curie temperatures were low, only in the tens of degrees Kelvin. Though the performance in magnetization in all forms of magnetic behavior degrade with increasing temperature, a few materials show promise for the future.[9] Some of these are shown in Figures A2 and A3.

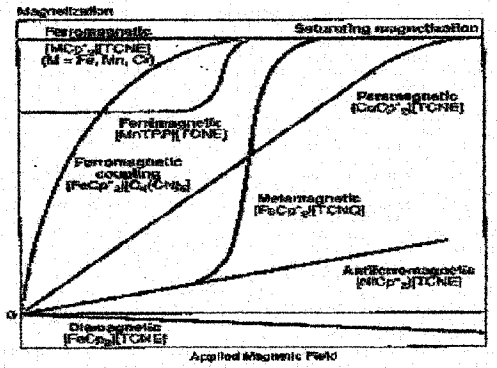

Figure A2. Magnetization vs applied magnetic field for some materials

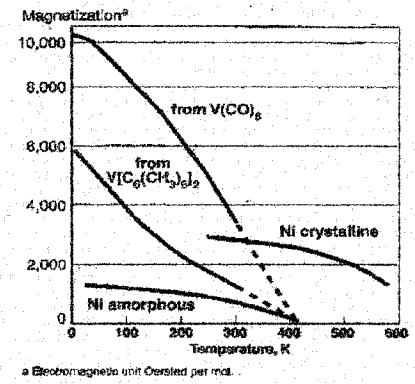

Figure A3. Vanadium salt $V(TCNE)_x \cdot y(CH_2Cl_2)$ prepared from $V(CO)_6$

As can be seen from the figures above, the magnetic behavior, magnetization, and temperature profile vary greatly with host (TCNE, TCNQ, etc.), salt (vanadium, iron, cobalt, nickel, etc.) and precursor. It may suggest that there is a greater order than previously suspected, implying that 3-D order might be more prevalent.
Some new saccharides, in the class of cyclodextrins (called inclusion compounds) are showing promise because of their ease of ion incorporation in the "nooks and crannies" of the molecule [15].

Magnetic Testing
Impedance measurements, giving the relative permeability and dielectric constant as well, and multi-port tests on the materials can be made on an 8700 series HP Network analyzer as shown in Figure 8. "Donuts" were 3 mm thick, made to fit in the coaxial air line.

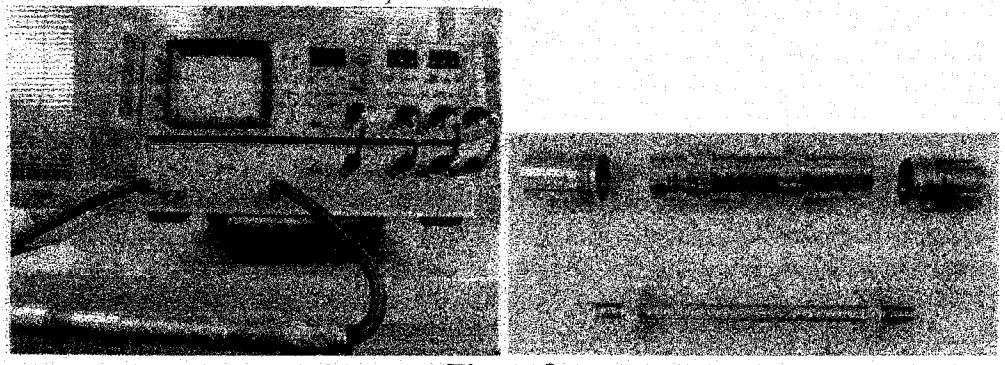

Figure 8
Network Analyzer/Coaxial Setup

High frequency measurements vary on these materials with the vanadium salts showing permeabilities of 60 at room temperature at 100 MHz. More work needs to be performed on these materials at high frequencies to determine what models are justified by these measurements.

Appendix B. Electroluminescent Polymers

The polymers mentioned in the body of this paper have been used to fabricate conventional light emitting diodes as shown in Figure B1.

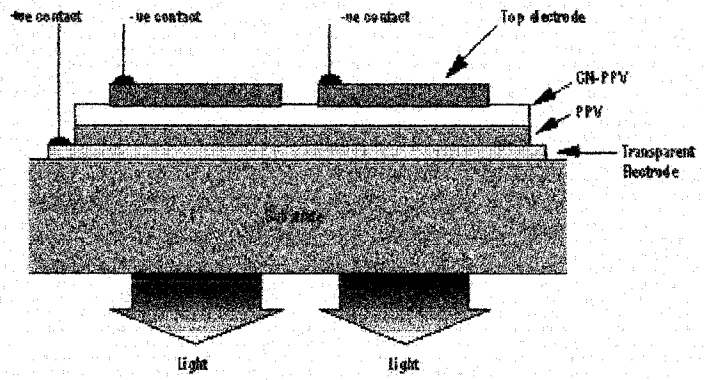

Figure B1. Conventional Diode Structure

New devices called system configured a.c. light emitting (SCALE) devices are shown in Figure B2.

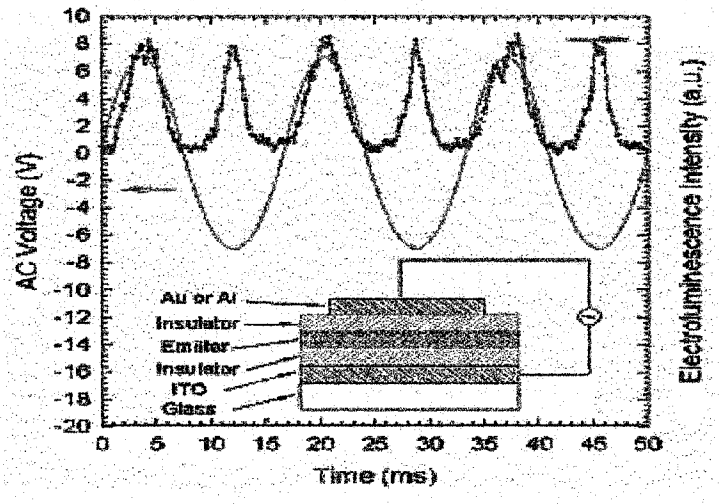

Figure B2. SCALE Device

These devices show a wide range of emission wavelengths, dependent upon the composition, as shown in Figure B3.

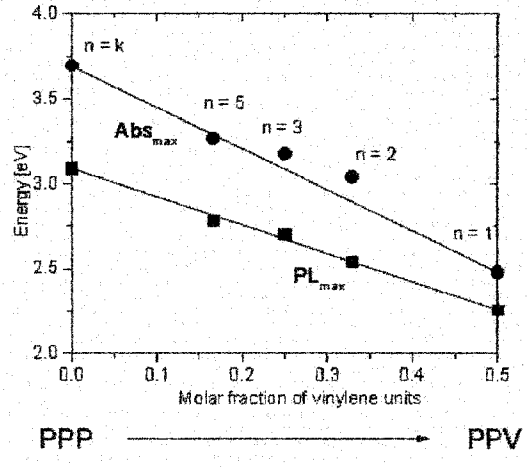

Figure B3. Variation in output energy (color, wavelength) with composition

Some of the advantages of polymer devices include flexibility, semi-transparency, full color range, diffuse light, large area devices, robustness, low driving voltage, and low power consumption.

LOW-BUDGET EPITAXY: COPPER ON SILICON

John N. Kidder, Jr.

and

Luz Martinez-Miranda

Department of Materials Science and Engineering Science
University of Maryland
Building 090, Room 2142
College Park, Maryland 20742

Telephone: 301-405-0499
e-mail kidder@eng.umd.edu

Telephone: 301-405-0253
e-mail martinez@eng.umd.edu

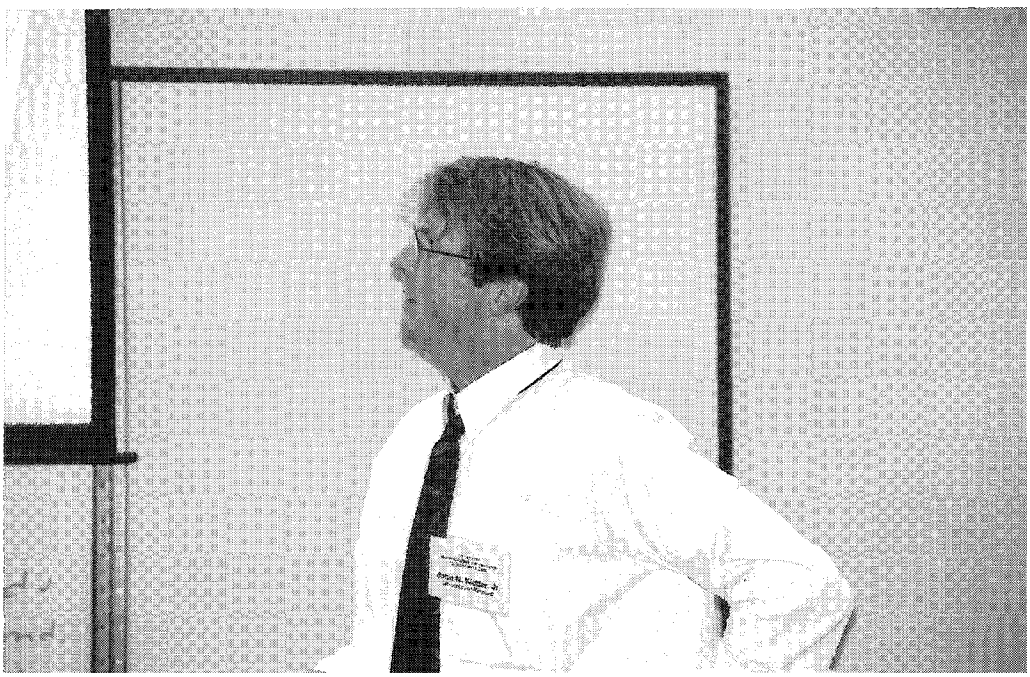

John N. Kidder

Biography:

John N. Kidder is an Assistant Professor of Materials Science and Engineering at the University of Maryland, College Park MD. He has A.B. degree from Occidental College and a M.S. degree from the University of Vermont in Physics and a Ph.D. degree from the University of Washington in Materials Science and Engineering. At Maryland he teaches freshmen engineering and undergraduate courses in Microprocessing of Materials and Electronic and Optical Properties of Materials. His research is in the area of thin film growth and in-situ process diagnostics.

Luz Martinez-Miranda is an Associate Professor of Materials Science and Engineering at the University of Maryland, College Park MD. She received B. S. and M. S. degrees in Physics from the University of Puerto Rico at Río Piedras and a Ph.D. degree in Physics from the Massachusetts Institute of Technology. At Maryland Prof. Martinez-Miranda teaches courses in freshmen engineering, undergraduate Materials Science and Engineering laboratory, and the Solid State Physics for Materials undergraduates. Her research is in the area of X-ray diffraction and nano-structured materials.

LOW-BUDGET EPITAXY: COPPER ON SILICON

John N. Kidder, Jr. and Luz Martinez-Miranda
University of Maryland
Materials Science and Engineering

Key Words:
Thin films, epitaxy, deposition, surfaces, crystal structure, copper, silicon

Prerequisite Knowledge:
Crystal structure, X-ray diffraction, principles of vapor pressure, kinetic theory of gases, evaporation.

Objective:

To become familiar with thin film deposition by thermal evaporation and the role of interface energy in thin film formation. The objective is to introduce students to the principles of thin film growth, generation of an atomic flux, deposition rate, surface cleaning in silicon processing, surface structure and chemistry, interface energy and epitaxy, and metallization in semiconductor technology.

Equipment and Materials:
Bell jar thermal evaporator; high purity copper wire; glass and plastic beakers; dilute HF acid, acetone, methanol, deionized water; silicon wafer (001) orientation; scribe; steel and plastic tweezers; scale; duster or clean dry compressed air; safety garments, X-ray diffractometer.

Introduction:

This exercise combines a thin film deposition experiment with X-ray diffraction measurements. This exercise is a good supplement to undergraduate laboratory course that includes X-ray diffraction by providing a way for students to create their own samples for analysis. In this experiment copper thin films are deposited on (001) oriented silicon substrates with two different surface treatments. All of the samples are cleaned using solvents and high purity water. Some of the substrates are also etched in dilute HF acid solution *immediately prior* to the deposition, which removes the native oxide from the surface and leaves a stable hydrogen-terminated silicon surface. Copper films are then deposited on the etched and unetched silicon substrates to compare copper films deposited on the amorphous native oxide and the crystalline surface. To prepare for the exercise several questions are discussed: Why would a FCC metal film form in one preferred orientation or texture? What orientation might be expected on an amorphous surface? What orientation of copper might be expected on a crystalline silicon surface? How are the Cu(001) planes and Si(001) geometrically similar? These questions can be discussed in terms of low-energy planes in a crystal and the crystal structure of copper (*face-centered cubic, a=3.61 Å*) and silicon (*diamond, a=5.43 Å*). The experiment postulates that the HF etch creates a stable surface that promotes oriented growth with the Cu(001) planes parallel to the Si(001) surface. (see figure 1)

Procedure:

Divide the silicon wafer into small pieces by using a diamond scribe to score the unpolished side and apply pressure over the edge of a microscope slide. Clean the Si substrates by soaking in acetone, methanol, and deionized water for approximately 60 sec at each step and then blow-dry with clean dry gas. Prepare the HF etched samples by dipping in 10-vol% HF aqueous for approximately 60 seconds. Use acid resistant (i.e., plastic) tweezers for this step and hold the sample by the edges. When removing the silicon piece slowly pull it from the solution. The hydrogen terminated surface is hydrophobic so the polished surface should be dry when pulled from the solution. Any droplets on the surface indicate contamination or defects and these samples should not be used. Remove residual liquid solution on the backside of the wafer and at the edges by blowing dry. A lab tissue can be used to wick away liquid from the edges. The surface will reoxidize after several minutes so deposition should be done immediately after the HF etching step. The need for an exquisitely clean surface should be emphasized – a lesson that reflects processing practices in the semiconductor industry.

To prepare for each deposition, wrap the copper wire on to the evaporation source (e.g., tungsten filament). Place the samples at a fixed distance from the source (see figure 2). We recommend placing a shutter between the source and the substrates during the first few seconds of evaporation to block the flux of impurities emitted from the surface of the metal source during initial heating. After loading the substrates pump the system down to below 10^{-5} Torr. The procedure for pumping down the vacuum evaporator will depend on what type of system is used. With a modest vacuum pump a single deposition run can be accomplished within approximately 15 minutes, allowing several depositions per lab session. Once the system reaches 10^{-5} Torr or less, turn on filament power and turn up current, and then immediately move the shutter to begin deposition on to the substrate. After a fixed time, rotate the shutter back to the position between substrate and filament. Turn off filament power, close pump valve, and back-fill chamber to atmospheric pressure. Remove samples.

The lab can be run as a process line with different students responsible for each step. The students doing the solvent clean need to use safety glasses, lab coats and gloves, and the student doing the HF etching should also use a acid lab apron and a face shield. The copper wire should be wiped clean with a solvent and handled with gloves to minimize surface contaminants. If possible deposit on etched and unetched substrates simultaneously to allow direct comparison.

X-ray diffraction measurements are required to observe the orientation of the copper films. This is indicated by a variation in the relative intensity of the Cu(111) and Cu(002) diffraction peaks. Figure 2 shows an example of θ-2θ scans for etched and unetched samples where a significant increase in the relative intensity of the Cu(002) peak was observed.

Comments:

Microelectronic technology is largely based on electronic devices fabricated from layered and patterned thin films. The process for fabrication a micro-device from thin films involves three primary steps: Deposition of a film, lithography for pattern

formation, and etching to remove material and form the selected pattern. This experiment aims to use simple deposition equipment - a bell jar thermal evaporator - to demonstrate and study vapor-phase thin film epitaxy using technologically relevant materials. This exercise is a good introduction to thin film processing and can serve as a prerequisite for a more extensive thin film processing lab. The experiment was adapted from an article by Longiaru *et al.*[1] which is an excellent reference for the exercise. In that article they used a sputtering system but we have found this experiment can also be done using a thermal evaporator. Bell jar evaporators are generally less expensive and more available on college campuses, and can easily be operated by undergraduate students. We adapted a thermal evaporator system used for coating electron microscopy samples for the deposition exercises.

It may be beneficial to process films of different thickness. This can be done in two different ways. If it is assumed that the evaporation rate is relatively constant over that period of time, then for fixed filament power the shutter can be opened for different periods of time (5, 10, 20 seconds). Another method is to use different weights of wire and leave the filament on and the shutter open for an extended time (~60 s) to completely evaporate the piece of wire. In this case the thickness can be roughly estimated using the mass of the wire, the distance between the source and the substrate, and the density of the deposited material using the expression:

$$Film\,Thickness = \frac{M_{Cu\ wire}}{\rho_{Cu}\,(4\pi r^2)}[cm]$$

In this expression, $M_{Cu\ wire}$ is the mass of the wire [grams], r is the distance between the source and the substrate [cm], and ρ_{Cu} is the density of copper (8.94 g/cm^3). This expression assumes certain assumptions such as that the substrate surface is facing normal the source (see figure 2) and that and the dimensions of the filament are much smaller than the distance between the source and the substrate (i.e., it acts as a point source). The actual thickness may be offset due to the shuttering at the start of the evaporation, but this expression can be used to generally predict the maximum thickness and to estimate what mass of wire is needed. A typical range of thickness for this experiment is 10 – 250 nm.

In summary, the experiment combines a thin film deposition experiment with X-ray diffraction measurements. This exercise provides excellent hands-on activity to teach several important topics including, kinetic theory of gases, atomic flux, film deposition, vacuum science, surface structure and chemistry, and semiconductor processing practices. It is an excellent module for an undergraduate materials processing laboratory, and provides a way for students to create their own thin film samples for characterization experiments (X-ray diffractometry). The experiment can also serve as a platform for lab-based lessons in vacuum science, lift-off lithography for circuit fabrication, and experiments that study process property effects (electrical characterization, roughness).

In future work we hope to develop complementary exercises that involve other deposition techniques. For example copper can be deposited by simple thermal CVD using

Cu(II)2,4-pentanedionate (Cu acac) as a precursor, which is easy-to handle (not air sensitive) and non-toxic.[2] Sol-gel spin coating is another straightforward and relatively low cost approach for depositing thin films which would be appropriate for undergraduate materials science and engineering laboratory curriculum.

References

[1] "Epitaxy above 10^{-5} Torr: A Students Introduction to Thin Film Growth and Characterization" Minsu Longiaru, E.T. Krastev, R.G. Tobin, J. of Vac. Sci. and Technol. A 14(5) 2875 (1996)

[2] "Materials Synthesis, Processing and Characterization Laboratory Course", Carmela Amato-Wierda, Univerity of New Hampshire, poster presented at Gordon Conference on Innovations in College Teaching of Materials Science, Plymouth N.H., July 1998

General references on thermal evaporation
Milton Ohring, "The Materials Science of Thin Films" (Academic Press, San Diego, CA, 1992)
Donald L. Smith, "Thin-Film Deposition: Principles and Practice" (Mcgraw-Hill, New York, 1995)

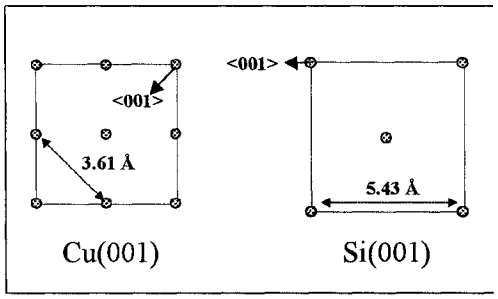

Figure 1 Atomic arrangements in the (001) planes of silicon and copper.

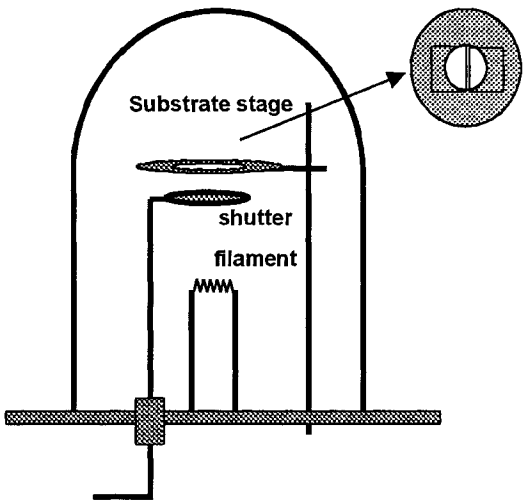

Figure 2 Schematic of the filament source, shutter, and substrate stage in the thermal evaporator for copper film deposition.

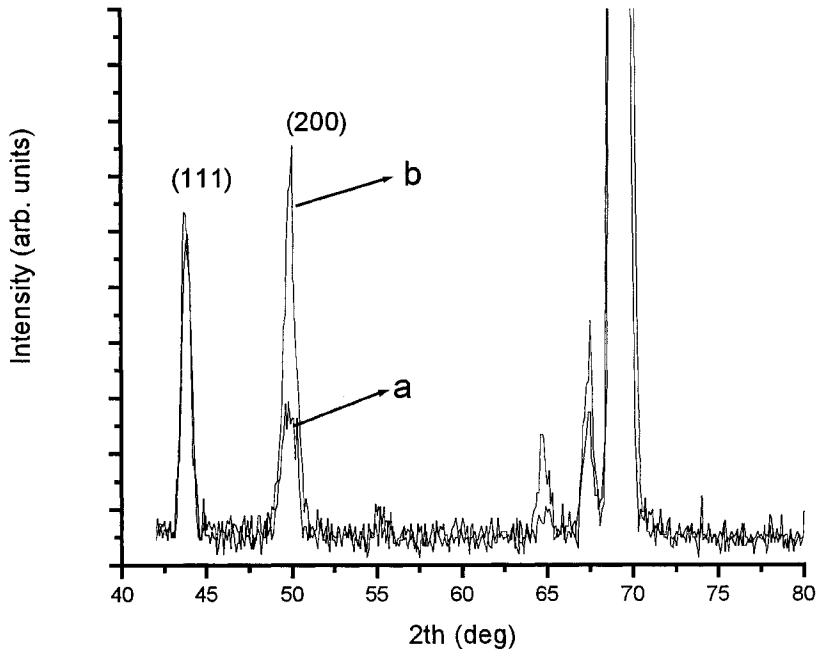

Figure 3 X-ray diffraction data for copper films on (001)Si substrates. Sample (a) was the unetched substrate and sample (b) was the etched substrate. The copper film deposited on the etched silicon shows a stronger (001) orientation.

MAGNETOIMPEDANCE: A USEFUL PHENOMENON FOR MAGNETIC, ELECTRIC AND STRESS SENSORS

Raul Valenzuela

Institute for Materials Research
National University of Mexico
P. O. Box 70-360
Mexico 04510

Telephone: 525-622-4653
e-mail monjaras@servidor.unam.mx

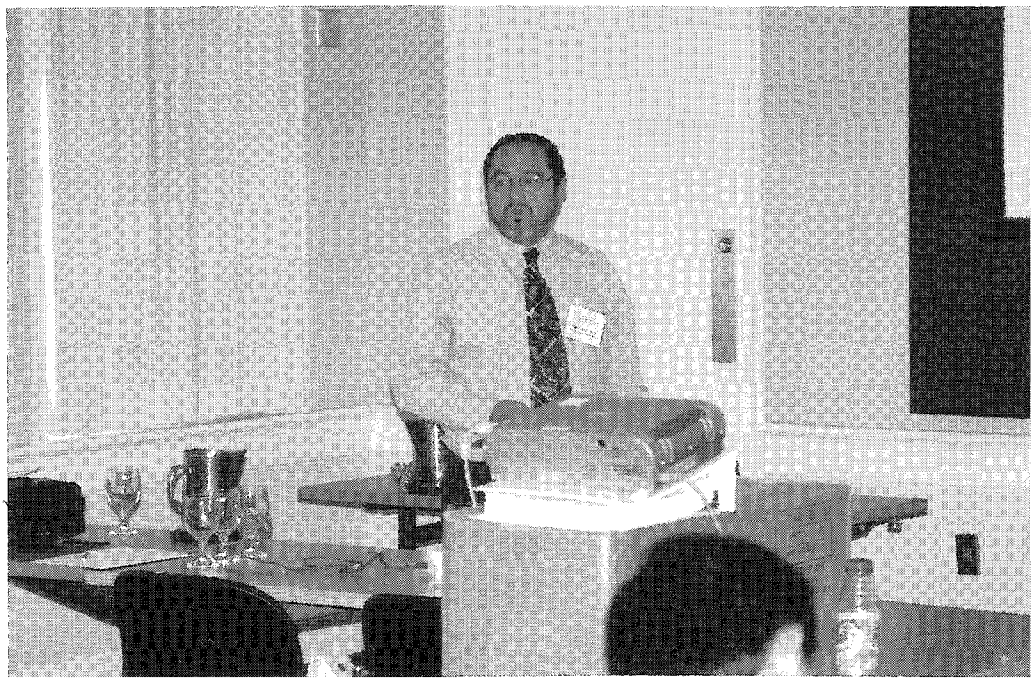

Raul Valenzuela

Magnetoimpedance: a Useful Phenomenon for Magnetic, Electric and Stress Sensors

R. Valenzuela

Institute for Materials Research, National University of Mexico, Mexico, p.o. Box 70-360, Mexico D.F. E-mail: monjaras@servidor.unam.mx

Key Words: electromagnetism, magnetic domains and magnetic domain walls, magnetic permeability, skin depth effect.

Prerequisite Knowledge: basic knowledge on atomic structure including spin moment, basic magnetic properties of ferromagnetism.

Objective: to understand a basic electromagnetic phenomenon involving the magnetic structure of ferromagnetic materials.

Equipment:

1. A magnetically soft ferromagnetic wire or ribbon
2. A permanent magnet (barium ferrite or metallic, NdFeB type), or a solenoid (250 turns) powered by a DC source
3. A signal generator (100 kHz-10 MHz frequency range, 1 mA *RMS* current amplitude)
4. A measuring instrument such as a voltmeter, an oscilloscope, or an impedance analyzer
5. A standard resistor (10-50 Ω)

Introduction:

When a conducting ferromagnetic material (best results have been obtained with amorphous wires and ribbons in the CoFeBSi system) is subjected to an AC current of small amplitude (less than 10 mA *RMS* to avoid any heating of the sample), it shows an impedance larger than the value corresponding solely to its DC resistance. If a DC magnetic field is applied, the impedance decreases to a value very close to the DC conditions. The impedance change increases as the current frequency increases, and is quite sensitive to the DC magnetic field. This phenomenon is known as Giant Magneto-impedance (GMI) and has attracted much interest due both to its technological applications in magnetic field sensors, and to its basic electromagnetic nature.

Procedure:

a) Connect in series both the resistor and the ferromagnetic material to the signal generator (Fig. 1). The purpose of the resistor is to limit the current flowing through the sample, which is in short circuit since it is a good conductor
b) Connect the measuring device (voltmeter) to the sample ends
c) {If a solenoid is available, put the sample inside the solenoid}
d) Establish a small current on the system (for most ferromagnetic materials, a 10 V drop at 1 MHz is obtained when the current amplitude is in the mA range)
e) Observe the voltage drop when the permanent magnet is far away from the sample (say, more than 1 m)
f) Place the permanent magnet very close to the sample (it is more efficient if the magnetic field produced by the permanent magnet is parallel to the axis of the sample) and observe the voltage drop
g) Move the permanent magnet with respect to the sample, increasing the distance between them (thus decreasing the magnetic field on the sample); make a plot of voltage as a function of distance
h) If the system includes the solenoid, carry out measurements at different levels of DC magnetic field, and plot the voltage as a function of the field

Comments:

The results should show a decrease in the voltage drop in the sample as the DC magnetic field increases, as shown in Fig. 2 (i.e., the permanent magnet is approached to the sample), which means that the impedance of the sample *decreases* under the effects of the DC magnetic field. This effect, known as magnetoimpedance (or giant magneto-impedance, GMI) is quite sensitive as compared with giant magnetoresistance (GMR), since in the former, a few oersteds lead to changes as large as 50% in the impedance value, while GMR needs at least a few tens or hundreds of oersteds to show such resistance changes. In fact, as can be seen in Fig. 2, GMI plot shows that the maximum in impedance appears for a non-zero DC magnetic field, which compensates for the earth's magnetic field.

Impedance:

While resistances are used to measure the effects of an element in a DC electric circuit, impedances are used to measure the changes produced by an element in an electric circuit subjected to an AC current. Impedance, **Z**, is formed by a real part, Z' and an imaginary part, Z'' and is a vector:

$$\mathbf{Z} = Z' + jZ'' \qquad (1)$$

where j is the basis of imaginary numbers, $j = \sqrt{-1}$. For calculations, the total impedance is used, and is calculated as :

$$Z_{tot} = [(Z')^2 + (Z'')^2]^{1/2} \qquad (2)$$

In an AC circuit, the presence of a resistor leads to changes in the current amplitude as shown in Fig. 3, while elements such as capacitors and inductors produce changes not only on current amplitude, but also on the current phase, Fig. 3. The relationship between voltage, V, and current phasors, I, is similar to the DC expressions, except that total impedance is used instead resistance:

$$I = V / Z_{tot} \tag{3}$$

The variations in Z_{tot} therefore produce proportional variations in voltage (assuming that the current amplitude is constant):

$$V = Z_{tot} I \tag{4}$$

Magnetic Structure:

Ferromagnetic materials are solids formed by atoms that possess a magnetic moment mainly from non-paired electronic spins. Most of them have transition metals as iron, nickel and cobalt, which have an incomplete 3d orbital where the electronic spins are oriented in the same direction. In addition to these magnetic moments, there is an interaction (known as the "exchange" interaction) that favors a parallel arrangement of spins of neighboring atoms, see Fig. 4. For antiferromagnetic materials, the arrangement with the lowest energy is the antiparallel order.

The existence of such a parallel ordering (leading to a high magnetization state) in a given sample should lead to high magnetic flux around all ferromagnetic materials. We know that it is not the case, as far as many metallic objects with a high content of iron do not show any attraction or repulsion forces between them. The explanation for this is that the generation of a strong magnetic field outside the material needs high energy. The total energy is decreased by changing the magnetization direction toward the opposite direction in half the sample. Magnetic "domains" are thus formed; by combining several directions, "closure" domains are also created to maintain all the magnetic flux inside the sample, as shown in Fig. 5. Since the magnetization direction in domains oppose each other, the total magnetization is zero. Magnetic domains are separated by domain "walls", where the spins of neighboring atoms rotate from the direction of a domain toward the direction of the next domain, Fig. 6. In the case of materials such as pure iron, the 180° angle between opposing domains is distributed among some 100-300 atoms [1].

In the case of permanent magnets, a non-equilibrium condition is produced to maintain more domains with a magnetization in a particular direction than in others, and therefore to have a stable magnetix flux outside the sample.

When a magnetic field is applied to a ferromagnetic material, it is magnetized by means of different magnetization processes. For example, the external field can produce a rotation of all the spins in the sample toward the magnetic field direction. In another process, the applied field can lead to domain wall movements favoring the increase in volume of domains with the same direction than the field, at the expense of domains with a direction opposing the field. If the applied field is strong enough, both the domain wall movements and the spin rotation processes can lead to the elimination of walls and the total ordering of spins in the field direction. The sample is then "saturated", as in Fig. 4.

In soft ferromagnetic materials, the response to magnetic fields is very sensitive; domain walls are easily displaced leading to large changes in magnetized volumes, and hence to large variations in global magnetization. These changes can be measured by the permeability, μ, which is defined as the ratio between the induction, B, and the applied field, H. Permeability units are different in the two main unit systems, c.g.s. and SI; however, the value of absolute permeability normalized by the value of vacuum permeability, μ_0, is the same in both systems, and this "relative permeability", μ_r, is the most used parameter:

$$\mu_r = B / (H \mu_0) \qquad (5)$$

Domain wall movements are quite fast and therefore they are able to follow applied fields of varying frequencies. However, for field frequencies above ~500 kHz, domain walls are too slow to be able to follow the field, and they show a **relaxation**. To understand this relaxation processes, it can be recalled that in all dynamic processes several terms contribute, as is generally expressed by a motion equation:

$$m\mathrm{d}^2x/\mathrm{d}t + \beta \mathrm{d}x/\mathrm{d}t + \alpha x = \mathrm{F}(t) \qquad (6)$$

with an inertia term (related to the mass of the system), $m\mathrm{d}^2x/\mathrm{d}t$, a damping term (associated with the dissipation processes), $\beta \mathrm{d}x/\mathrm{d}t$, a restoring term (tending to taking the system back to the initial condition), αx, all driven by a force with a given dependence on time. A **resonance** is observed when the inertia term (the mass) is comparable to the damping and the system possess a natural vibration frequency, f_s. As the excitation frequency approaches f_s, the vibration amplitude (x) increases, reaches a peak, and drops down to negative values, before going back to zero as frequency increases further. In contrast, when the damping term is significantly larger than the inertia term, the system simply decreases the vibration amplitude as the excitation frequency increases over the **relaxation** frequency, f_x. In most soft ferromagnetic materials, domain walls have exhibited a relaxation character.

For field frequencies above any of these two values, only spin rotation is fast enough to follow the excitation field.

Skin Effect:

When a ferromagnetic conductor is submitted to an AC magnetic field, the strong variations in magnetic flux inside the material give rise to electric currents due to the Faraday's law of electromagnetic induction:

$$emf \propto \mathrm{d}\phi / \mathrm{d}t \qquad (7)$$

Where *emf* is the electromagnetic force generated by the rate of change in magnetic flux, $\mathrm{d}\phi / \mathrm{d}t$. In turn, the electric currents generated produce magnetic fields that are oriented against the applied field. The global result is that there exists an opposition to the penetration of the AC field into the material, which can then be limited to a small surface

fraction or "skin depth" δ. The skin depth depends on the frequency of the applied field, f, the magnetic permeability, μ_r, and the resistivity of the conductor, ρ:

$$\delta = 1/[2\pi (\mu_r f / \rho)^{1/2}] \qquad (8)$$

The skin effect provides an explanation for the gant magnetoimpedance phenomenon, as follows. When a ferromagnetic conductor is submitted to an AC current of high frequency (say above 1 MHz) there are at least two sources of impedance in addition to the DC resistance: the coupling of the AC magnetic field (generated by the AC current) to the ferromagnetic domain structure, and the opposition of the material to the penetration of the AC magnetic field (due to the skin effect). If a saturating DC magnetic field is applied, the domain walls are eliminated and the spins are oriented into the DC field direction, leading to a strong decrease in permeability. In agreement with Eq. (7), this results in an increase in skin depth, and therefore, a decrease in the impedance response.

Applications:

There are many technological applications of GMI, as far as this phenomenon provides a sensitive relationship between DC magnetic fields an impedance response. The most obvious is the fabrication of magnetic field sensors, which can be made as quite small (miniature) devices [2]. An interesting application is a device to detect and control moving vehicles [3]. Since DC magnetic fields can be obtained in a controlled way from coils powered by DC currents, it is also possible to provide miniature DC current sensors [4]. Also, since the magnetization processes are affected by mechanical stresses through magnetostriction, the deformation of the ferromagnetic material leads to differences in the impedance response, and a correlation between impedance and deformation has been found. GMI can also be applied in tensile, compression and torsion sensors.

References:

[1] C. Kittel. *Introduction to Solid State Physics*. Wiley, N.Y., 1995.
[2] M. Vázquez, M. Knobel, M.L. Sánchez, R. Valenzuela and A.P. Zhukov. *Sensors & Actuators* **A59** (1997) 20
[3] R. Valenzuela, M. Knobel, M. Vázquez and A. Hernando. *J. Appl. Phys.* **79** (1996) 6549.
[4] R. Valenzuela, J.J. Freijo, A. Salcedo, M. Vázquez and A. Hernando. *J. Appl. Phys.* **81** (1996) 4301.

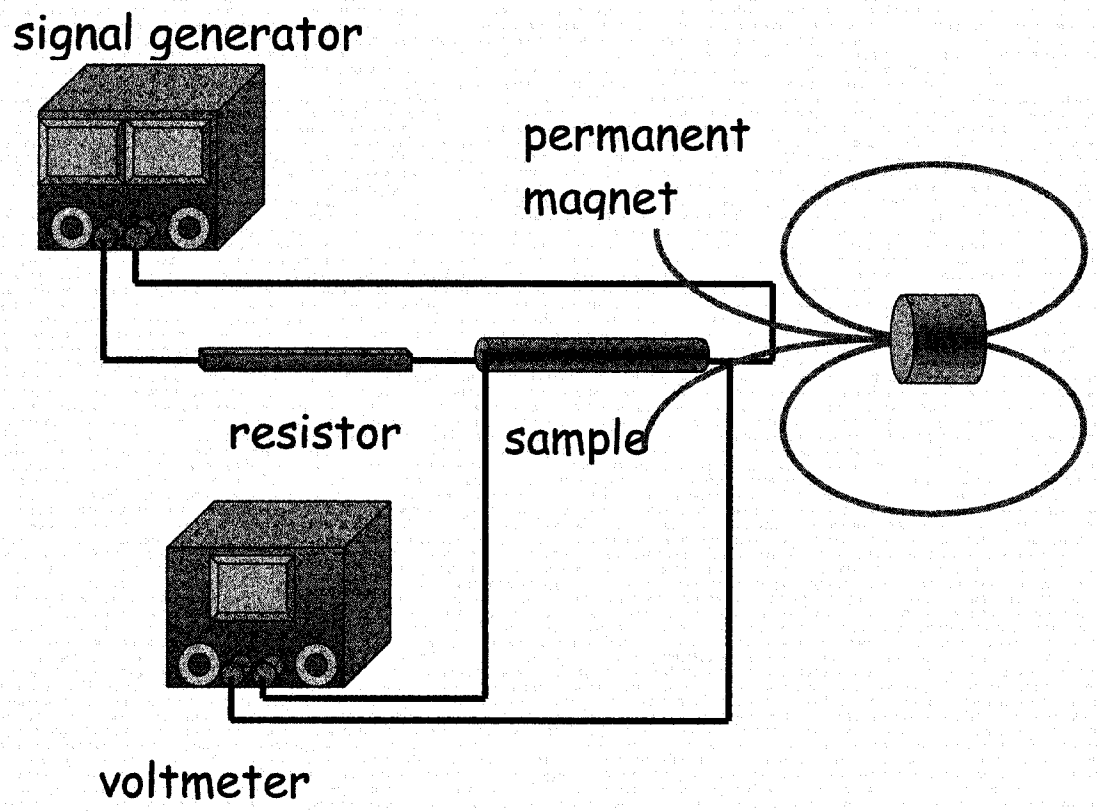

Fig. 1. Layout of the equipment required for the experiment.

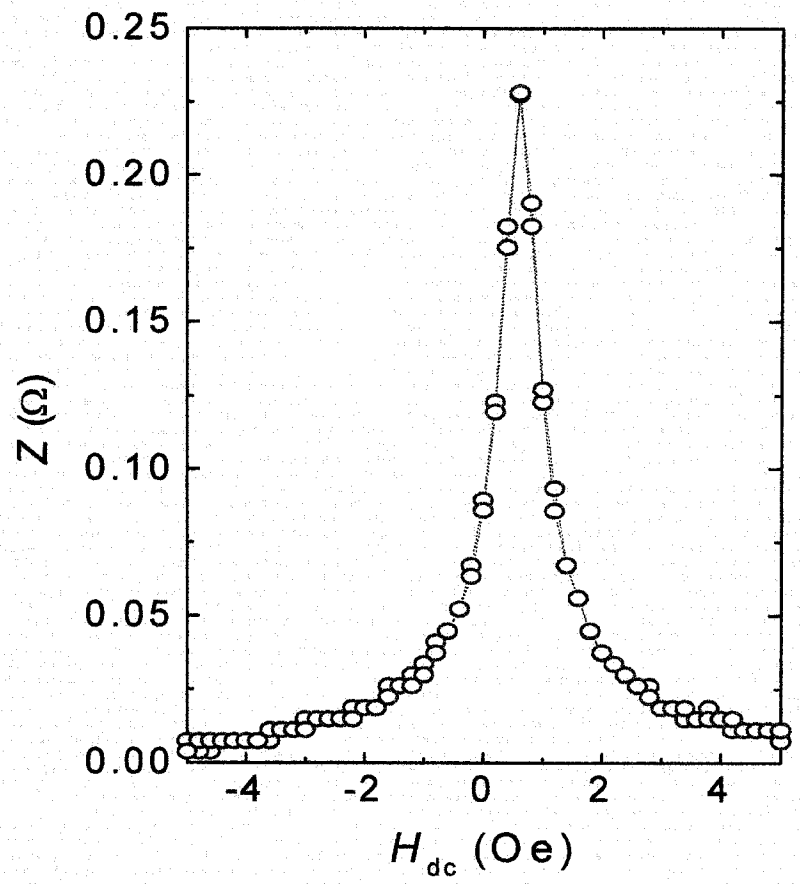

Fig. 2. Typical results obtained with as-cast, amorphous CoFeBSi wires, at a frequency of 10 kHz and a current amplitude of 1 mA (RMS). The maximum is not found at $H_{dc} = 0$ because of the earth's field, which has to be compensated.

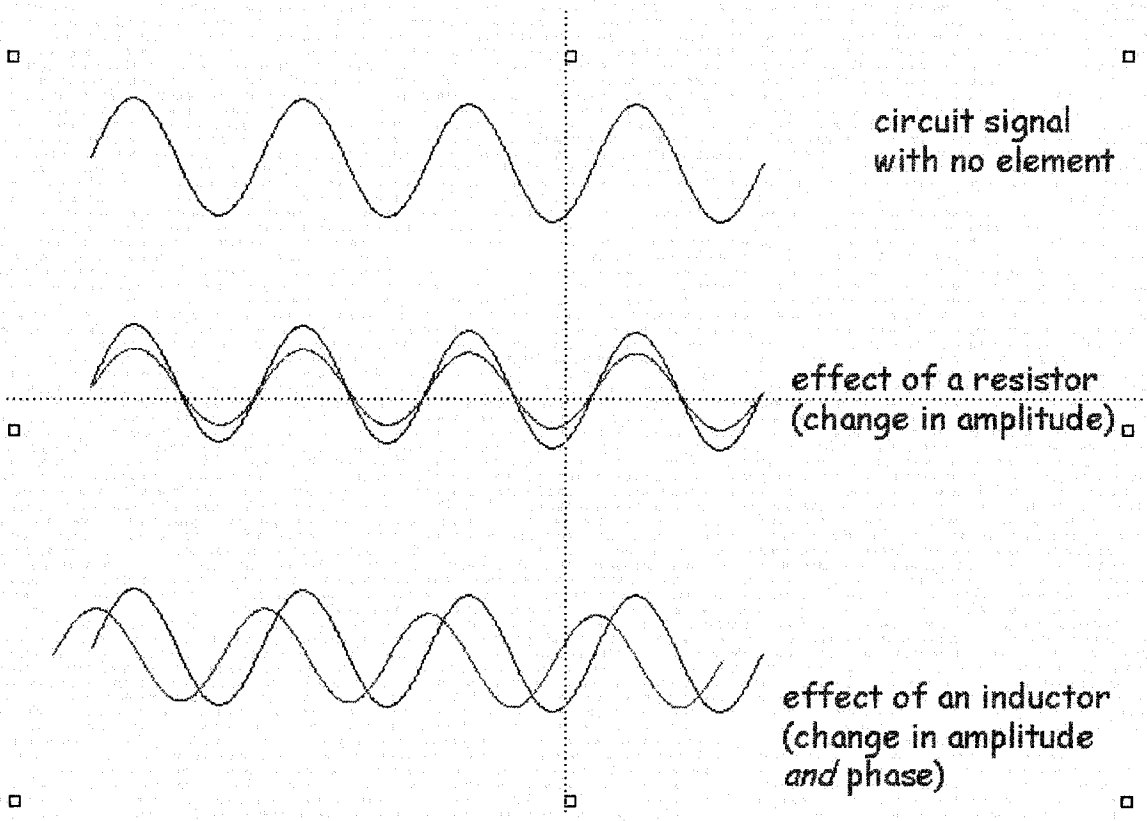

Fig. 3. Schematic comparison of effects on amplitude and phase of resistors and inductors, to help explain the notion of "impedance".

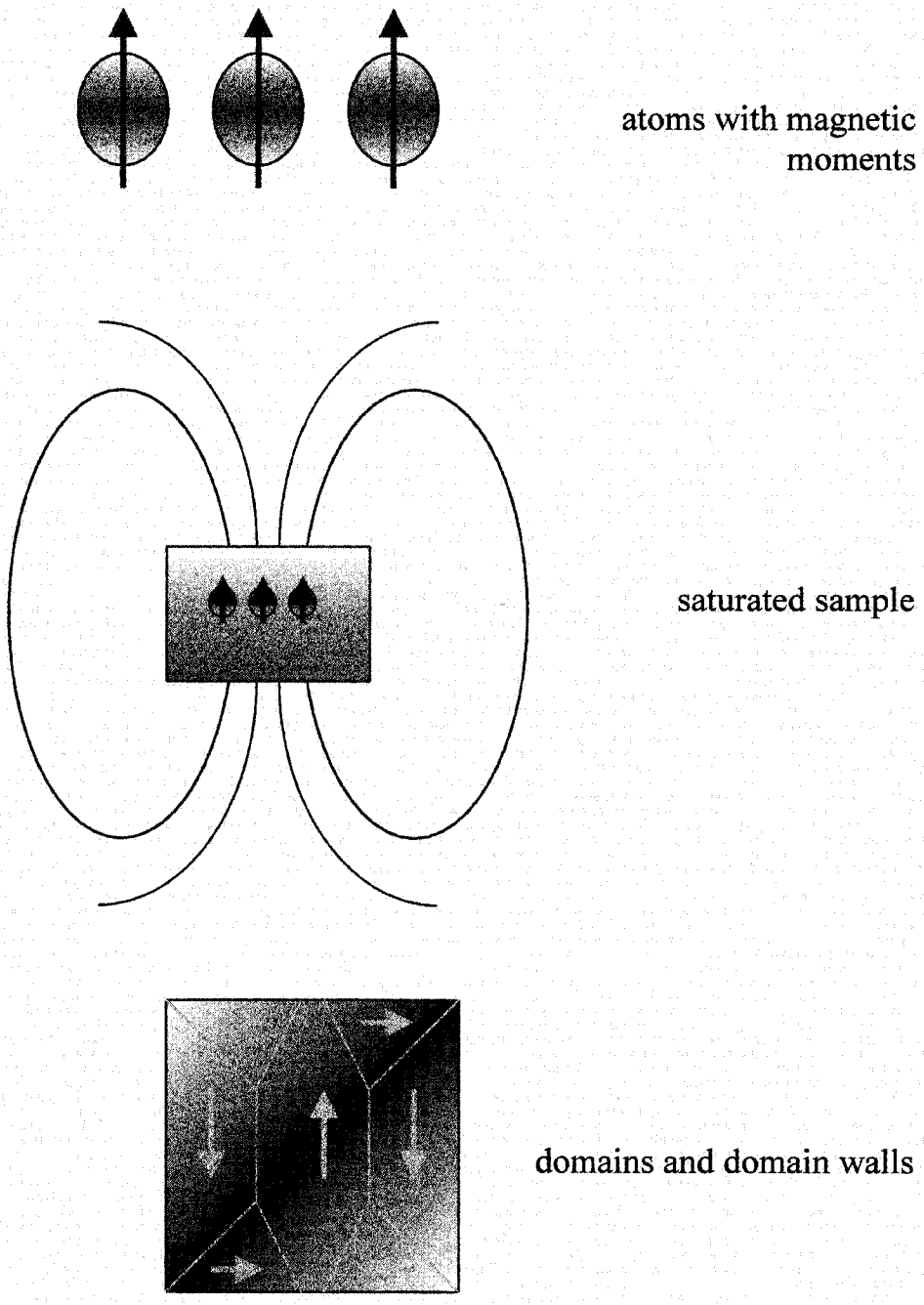

Fig. 4. Simplified explanation for the appearance of magnetic domains and domain walls in ferromagnetic materials.

CHARACTERIZING ALLOY MICROSTRUCTURES FOR SEMI-SOLID FORMING

Robert B. Pond, Jr.

Department of Electrical Engineering and Engineering Science
Loyola College in Maryland
4501 Charles Street
Baltimore, Maryland 21210-2699

Telephone: 410-617-5563
e-mail Rpond@Loyola.edu

and

Scott N. Hornung

Lucent Technologies
Baltimore, Maryland

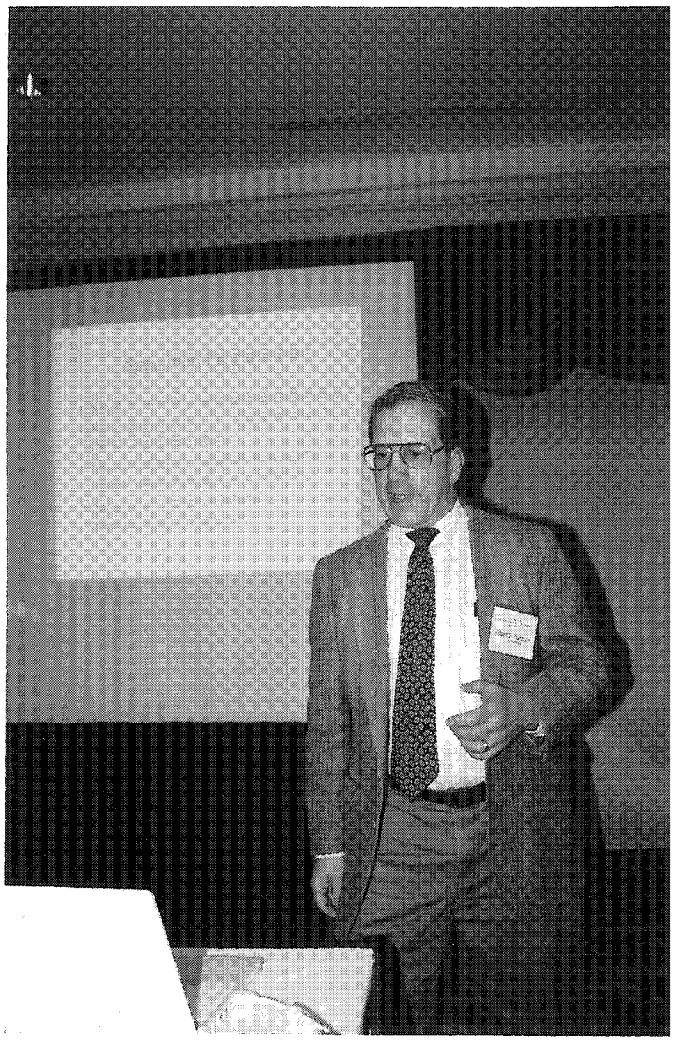

Robert B. Pond, Jr.

Biography:

Robert B. Pond, Jr. is Chair of the Electrical Engineering and Engineering Science Department at Loyola College in Maryland. He has a bachelor's degree in Engineering Mechanics from Johns Hopkins University in Baltimore, Maryland and a Master's and Doctorate of Engineering in Metallurgical Engineering and Materials Science from the University of Pennsylvania in Philadelphia, Pennsylvania.

Scott N. Hornung developed this data as a part of his senior design project at Loyola College in MD. He received a Bachelor's Degree in Engineering Science and he is employed by Lucent Technologies in Maryland.

Characterizing Alloy Microstructures for Semi-Solid Forming

Robert B. Pond, Jr
Electrical Engineering and Engineering Science Department
Loyola College in Maryland
Baltimore, MD

Scott N. Hornung
Lucent Technologies
Baltimore, MD

Key Words: Microstructures, Image Processing, Quantitative Metallography, Casting, Semi-solid Forming.

Prerequisite Knowledge: Basic knowledge of materials science, phase diagrams, the relationships between microstructures and phase diagrams, fundamentals of heat treatment, and competence in metallographic specimen preparation and metallography.

Objective: To understand the three-dimensional aspects of microstructure, the relationships between phase diagrams and microstructures and the metallurgy of semi-solid forming for commercial applications.

Equipment:
1. Alloy A357.0 prepared for semi-solid forming (1)
2. Small muffle furnace
3. Microhardness machine
4. Metallographic equipment and film or digital camera
5. Computer, scanner (for film records) and NIH Image software

Introduction:

Properties of alloys are dependent on microstructure. The three dimensional characterization of microstructure, although important is not often developed in a laboratory course, because the acquisition and processing of data is usually time consuming and expensive. However, three-dimensional microstructure characterizations can be easily made within the scope of a senior engineering project.

In this case a commercial semi-solid forming aluminum- 7.0 silicon- 0.5 magnesium alloy was used (A357.0) (Figure One (2)). This alloy was of interest because the thixotropic properties of the alloy when heat-treated in the liquid plus solid phase field are dependent on the size, shape, fraction solids, and interconnections between the primary phase particles.

This laboratory exercise provides an easy method to examine three-dimensional microstructures and specifically to measure and characterize the microstructures of an aluminum-silicon-magnesium hypoeutectic alloy used for commercial semi-solid forming.

1. A specimen is heat treated and prepared for metallography.
2. The specimen surface is indexed with three microhardness indentations and successively polished and etched.
3. The microstructural data is digitized and analyzed using NIH Image (3) software to present and measure the nature of the microstructure.

Procedure:

The laboratory exercise is augmented by the use of the free software, NIH Image, which originally was established and is used extensively for characterizing microbiological systems. This software works as well for evaluating alloy microstructures.

1. The student cut a specimen from aluminum alloy stock (A357.0) for thermal treatment.
2. The specimen was heated to 590° C for 20 minutes to simulate the commercial heat treatment prior to forming and then quenched in water to capture the high temperature primary phase distribution.
3. A mount of the specimen was metallographically prepared after the thermal treatment.
4. The mount was indexed with three neighboring microhardness indentations. These indentations provided a means to locate, orient and take sequential micrographs of the same region.
5. Micrographs were made of the indented area after each micropolishing step.
6. The micrographs were identified, digitized and stored.
7. The computer images were processed, analyzed and displayed using the NIH Image software. Microstructural features were used to register the successive slices through the microstructure.
8. The fraction solids of the primary phase, their sizes, shapes and the interconnected nature of the structure are apparent and accessible for microstructural measurements.

Comments:

The shaping of aluminum alloys heated to a two-phase, liquid plus solid condition is facilitated when the primary alpha phase is rounded and interconnected (4). This microstructural condition allows for the handling of heated blanks of material as a solid. Under shear loads the interconnections between the solid alpha particles break and the material becomes a slurry, allowing low temperature forming in casting dies.

The rendering of a three dimensional microstructure for visualization and quantification is easily and inexpensively done in a metallographic laboratory using the free imaging software. The successive polishing steps included one-minute of polishing on a wheel using 5 μm alumina powder followed by a minute each with 1 μm and 0.05 μm gamma-alumina powders. The etchant, a 1% aqueous solution of hydrofluoric acid was applied for 30 seconds with a swab.

The micrographs were taken at 100X magnification and were recorded on Polaroid film. The prints were digitized at a resolution of 150 dpi using a flat bed scanner.

A single micrograph from a series is seen in Figure Two along with analytical results for the fraction solids made using the NIH Image software. A montage of part of the microstructure is seen in Figure Three. A dynamic presentation was made of the sequence of data files in the form of a movie.

The sequential microstructures are located and oriented using three microhardness indentations. The load used was 500 gf using a Vickers indenter. The change in size of the indentations after polishing provides a means to measure the depth of material removal for each polishing step. Two applications of polishing eradicated the indentations and new indentations were placed directly on top of old ones.

The student was able to measure the fraction of primary solid of the alloy in the high temperature condition and demonstrate the interconnected structure of the primary phase, which explains the thixotropic behavior of the alloy. The student also experienced the use of the laboratory and software tools while gaining an appreciation for the three dimensional aspects of an alloy microstructure.

NIH Image software originally was available only for the Macintosh Operating system. A Macintosh computer needs to have an operating system of 7.0 or higher and available at least 16 MB of RAM to run the software. The software accepts images in the form of TIFF, PICT, PICS, and Quick Time files. NIH Image provides analytical capability for measuring areas, averages, centroids, and perimeter lengths of user defined regions of interest. The software also performs automated particle analysis and provides tools for measuring path lengths and angles. The program is easy to use and the documentation is very useful. All the analysis was performed on a Macintosh G3 computer using the NIH Image program, developed at the U.S. National Institutes of Health and available on the Internet.

There is a new program for Windows operating systems that is currently available from Scion Corporation (5). This company made NIH Image and now has developed a Windows equivalent, which is also free.

We anticipate the use of other alloy systems for laboratory demonstrations of the influence of many variables on the microstructures of alloy systems. The effect of heat treatment of steels on microstructure, the examination of different eutectic morphologies, the characterization of intermetallics and of porosity and other discontinuities, including pitting profiles may be made with this technique. Measurements of composite material microstructure and grain shapes are additional areas of interest for this laboratory exercise.

References:

(1) *Aluminum and Aluminum Alloys*, 1993, ASM International, Materials Park, Ohio, pg. 720.
(2) *Binary Alloy Phase Diagrams*, 1996, Second Edition, CD-ROM Version 1.0, ASM International, Materials Park, Ohio.
(3) *NIH Image* software from U. S. National Institute of Health at http://rsb.info.nih.gov/nih-image.
(4) Merton C. Flemings, "Behavior of Metal Alloys in the Semisolid State", 1990 Edward Campbell Memorial Lecture, 1991, *Metallurgical Transactions B*, Vol. 22B, June, pp. 269-293.
(5) *Scion Image* for Windows from Scion Corporation at www.Scioncorp.com.

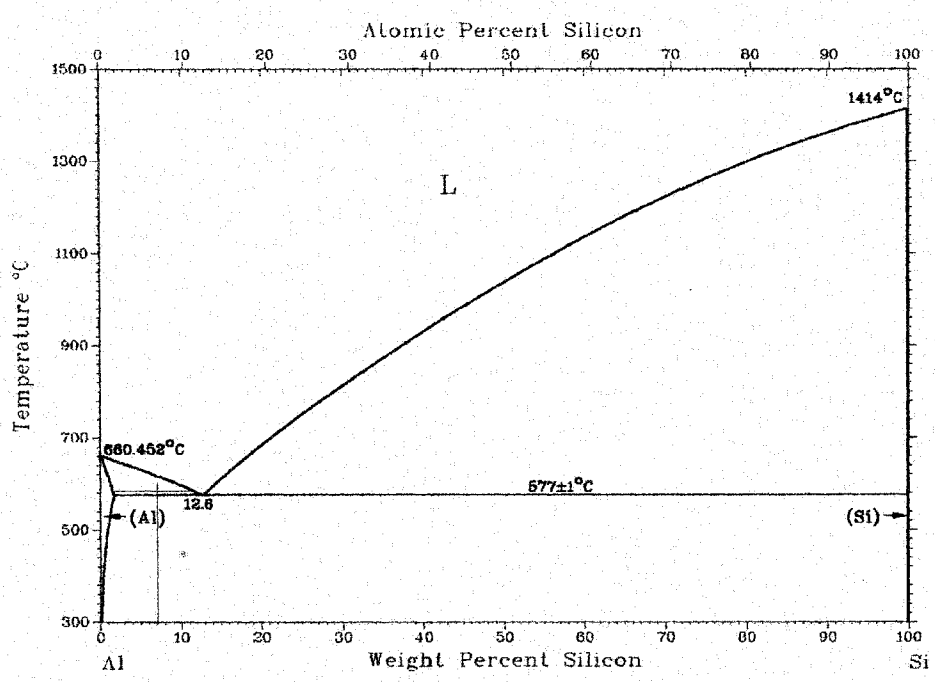

Figure One. The binary Al-Si diagram (2) showing silicon composition (7%) and the semi-solid heat treatment temperature of 590°C.

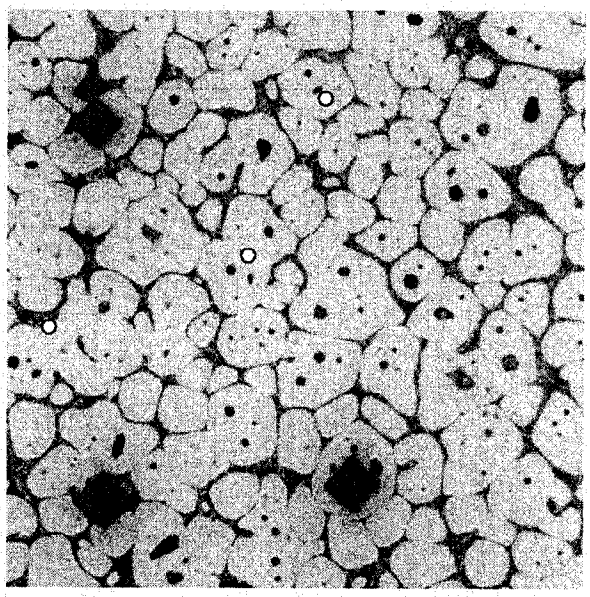

Figure Two. A single microstructural slice.
The fraction liquid (eutectic area) is 22.1%.

The three Vickers indentations were used to locate and orient the specimen for metallography. The three circular registry marks were added later to spatially coordinate the successive data sets.

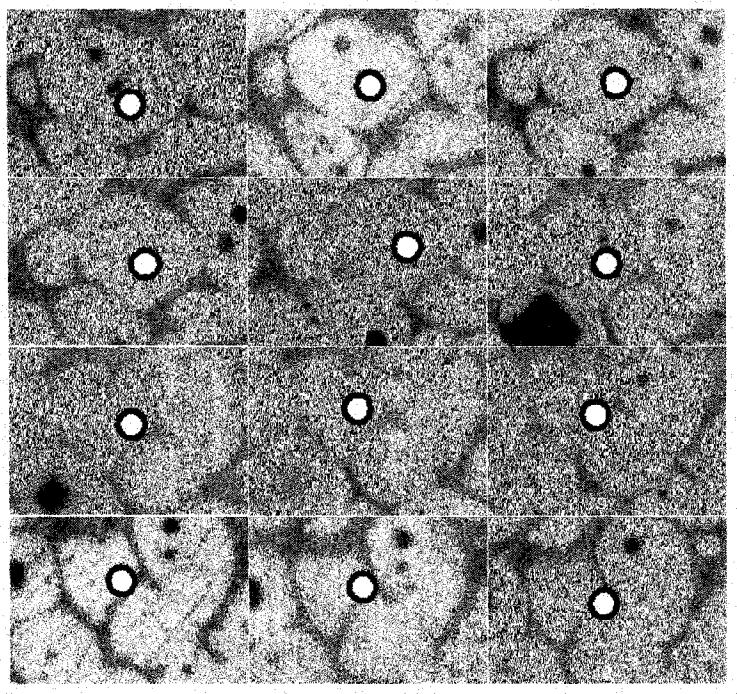

Figure Three. A montage of a local area of microstructure. Interconnecting points between primary aluminum particles and re-entrants of eutectic as a source of occluded liquid in alpha are seen.

P4 PREFORMING TECHNOLOGY: PROCESS DEVELOPMENT UTILIZING CARBON FIBER ROVINGS

Norman G. Chavka

and

Jeffrey S. Dahl

Senior Technical Specialist
Ford Research Lab
SRL MD3135
2101 Village Road
Dearborn, Michigan 48124

Telephone: 313-322-7814
e-mail nchavka@ford.com

Telephone: 313-322-7814
e-mail jdahl@ford.com

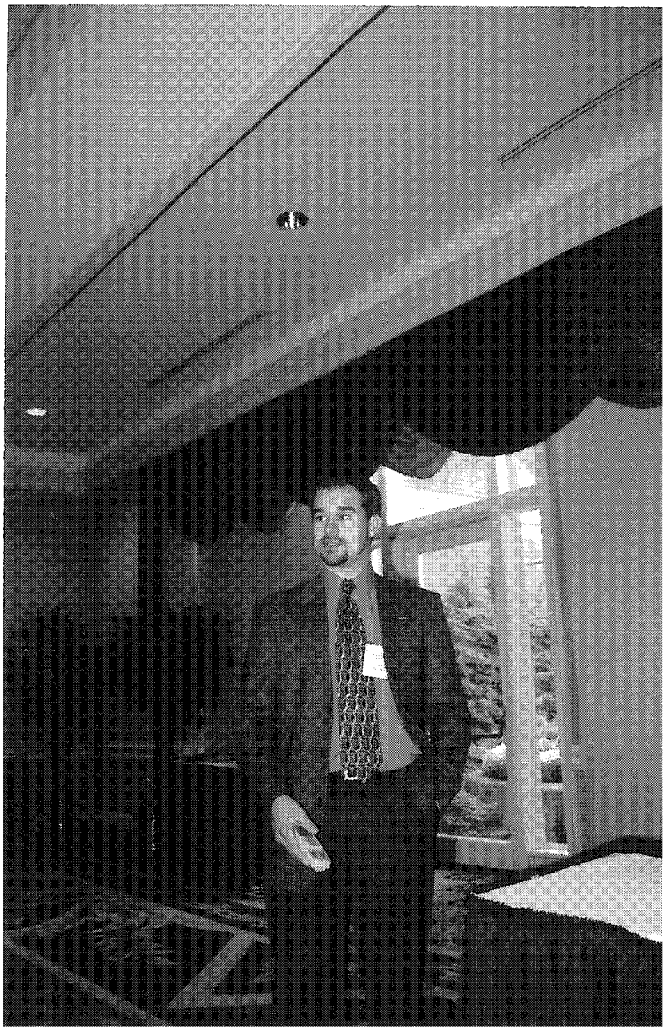

Jeffrey S. Dahl

Automotive Composites Consortium

P4 Preforming

P4 Preforming Technology: Process Development Utilizing Carbon Fiber Rovings

Norman G. Chavka and Jeffrey S. Dahl

Automotive Composites Consortium/Ford Motor Company

National Educator's Workshop

P4 Carbon Fiber Preforming

- **Background Information**
- **Carbon Fiber Roving Specification**
- **Experimental Equipment and Tooling**
- **Experimental Testing and Results**
- **Future Research Activities**

Automotive Composites Consortium

P4 Preforming

Working Groups

- **Energy Management**
- **Joining**
- **Processing**
- **Materials**

Automotive Composites Consortium

P4 Preforming

Focal Projects

- **Focal Project I: Front End Structure**
- **Focal Project II: Pickup Box**
- **Focal Project III: CF Body-in-White**

P4 Programmable Powder Preforming Process

P4 Preforming

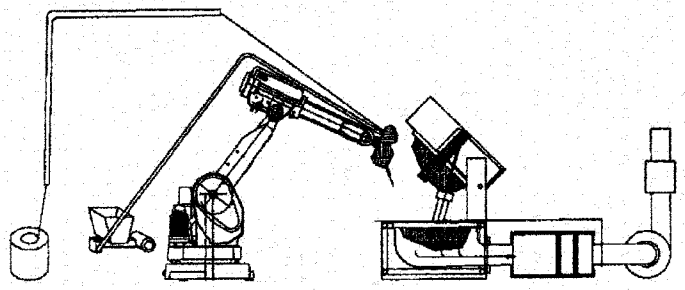

Glass Deposition:
Glass and Binder
Applied to Screen
via Robotic Glass
Deposition Routines

Consolidation:
Preform Compacted
Hot Air Melts and
Cures Binder

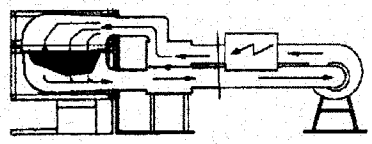

Stabilization:
Cold Air Cools Binder
and Rigidizes Preform

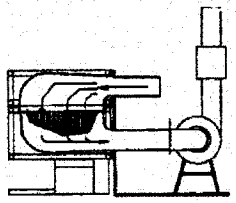

De-Molding:
Tool Opens and Preform
Removed from Tool

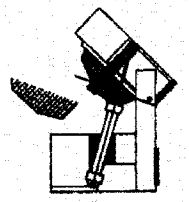

P4 Preforming Process Technical Advantages (1)

- **Low Cost**
  - **Lowest cost raw materials: rovings**
  - **Low scrap (< 3%)**
  - **Net shape/size (i.e. no trimming)**
- **High Speed**
  - **High output chopper guns (4 kg/min)**
  - **Fast setting binders**
  - **4 minute part throughput**

P4 Preforming Process Technical Advantages (2)

- **Reliability/Quality**
  - **Fully automated, robotic preforming**
  - **Within preform areal density consistency**
  - **Preform to preform areal density consistency**
  - **Consolidated net-shape, net-size preform**
- **Flexibility**
  - **Variable fiber output and fiber length**
  - **Complex shape capability**

ACC P4 Machine: Truck Box Preforming

P4 Preforming

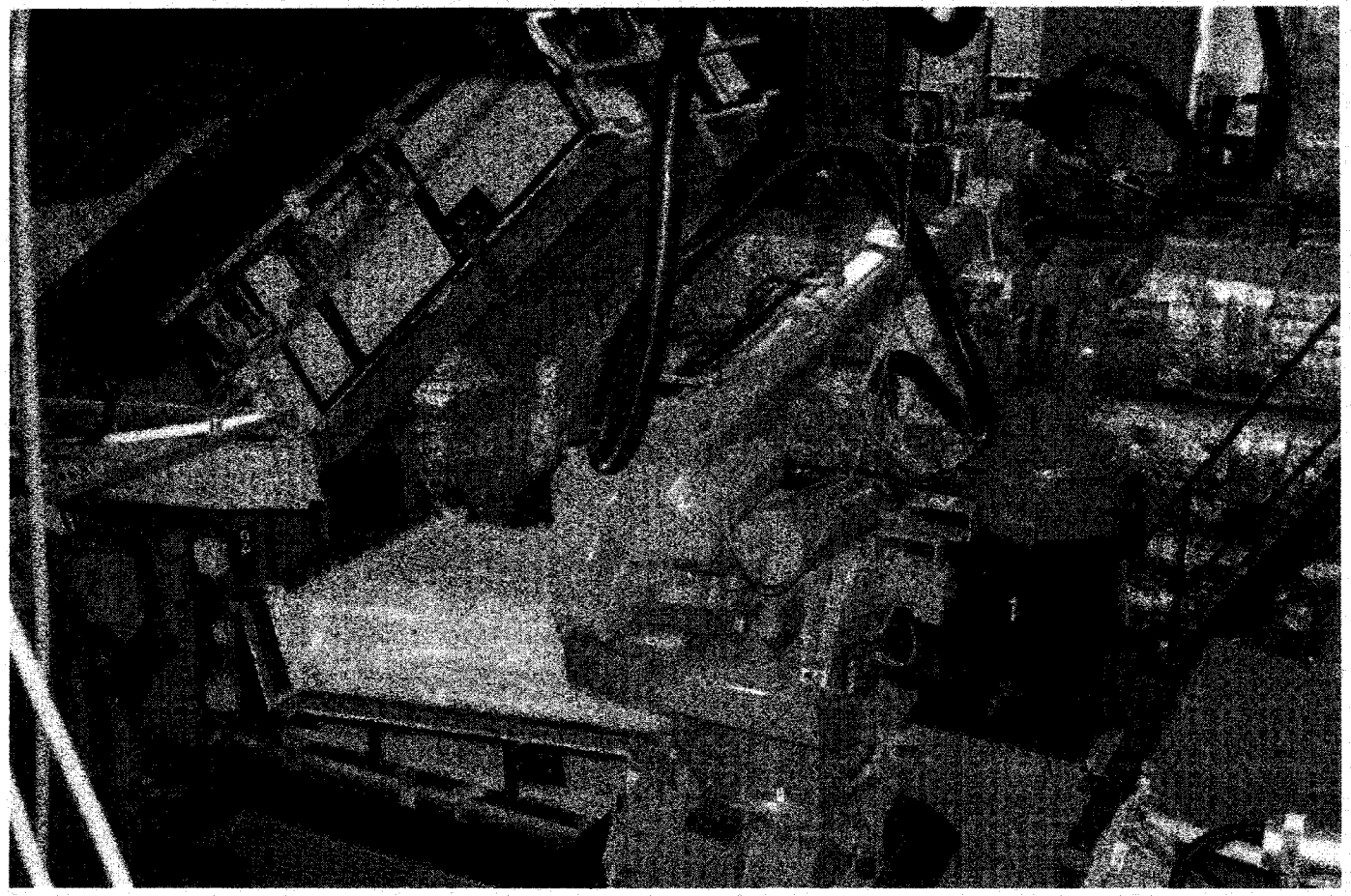

Carbon Fiber Roving Specification

P4 Preforming

- Currently available 'off the shelf' carbon designed for other processes
- Carbon tows not suitable for chopped fiber preforming applications
- Carbon fiber specification developed using glass fiber rovings as a guideline
- Specification not yet achieved by carbon suppliers

P4 Carbon Fiber Roving Specification

P4 Preforming

		P4 Glass Roving	Sample Carbon	P4 Carbon Roving
		OCF 357 D-AA 3120	Roving To Date	Not available
Density	(g/cm^3)	2.56	1.81	1.81
Fiber Diameter	(microns)	12	7.2	7.2
Single Filament Cross Sectional Area	(m^2)	1.1E-10	4.1E-11	4.1E-11
Bundle Cross Sectional Area	(m^2)	1.8E-08	1.7E-07	1.8E-08
Total Roving Cross Sectional Area	(m^2)	1.3E-06	1.9E-06	1.3E-06
Number of Bundles		70	11	70
Number of Filaments Per Bundle		160	4182	444
Total Number of Filaments		11200	46000	31111
Bundle TEX	(g/1000 m)	44	308	33
Roving TEX	(g/1000 m)	3120	3390	2293

Carbon Fiber Rovings and Suppliers

P4 Preforming

- Rovings from five carbon manufacturers have been tested
- Supplied by Fortafil, Hexcel, TOHO, Toray, and Zoltek
- 19 different rovings in total

P4 Carbon Fiber Ranking Criteria

P4 Preforming

- **Gun/FDS Fuzz**
- **Chopping Quality**
- **Strand Integrity**
- **Areal Density Distribution**
- **Shape Conformability**
- **Loft Control**
- **Cost**

Experimental Preforming Equipment

P4 Preforming

- **ACC's P4 Preforming Machine**
  - **2 robots, 2 station**
- **Aplicator SMART Chopper**
  - **Electric servo control**
  - **Continuously variable fiber output and fiber length**
  - **Maximum fiber speed 10 m/s**

P4 Preforming Machine

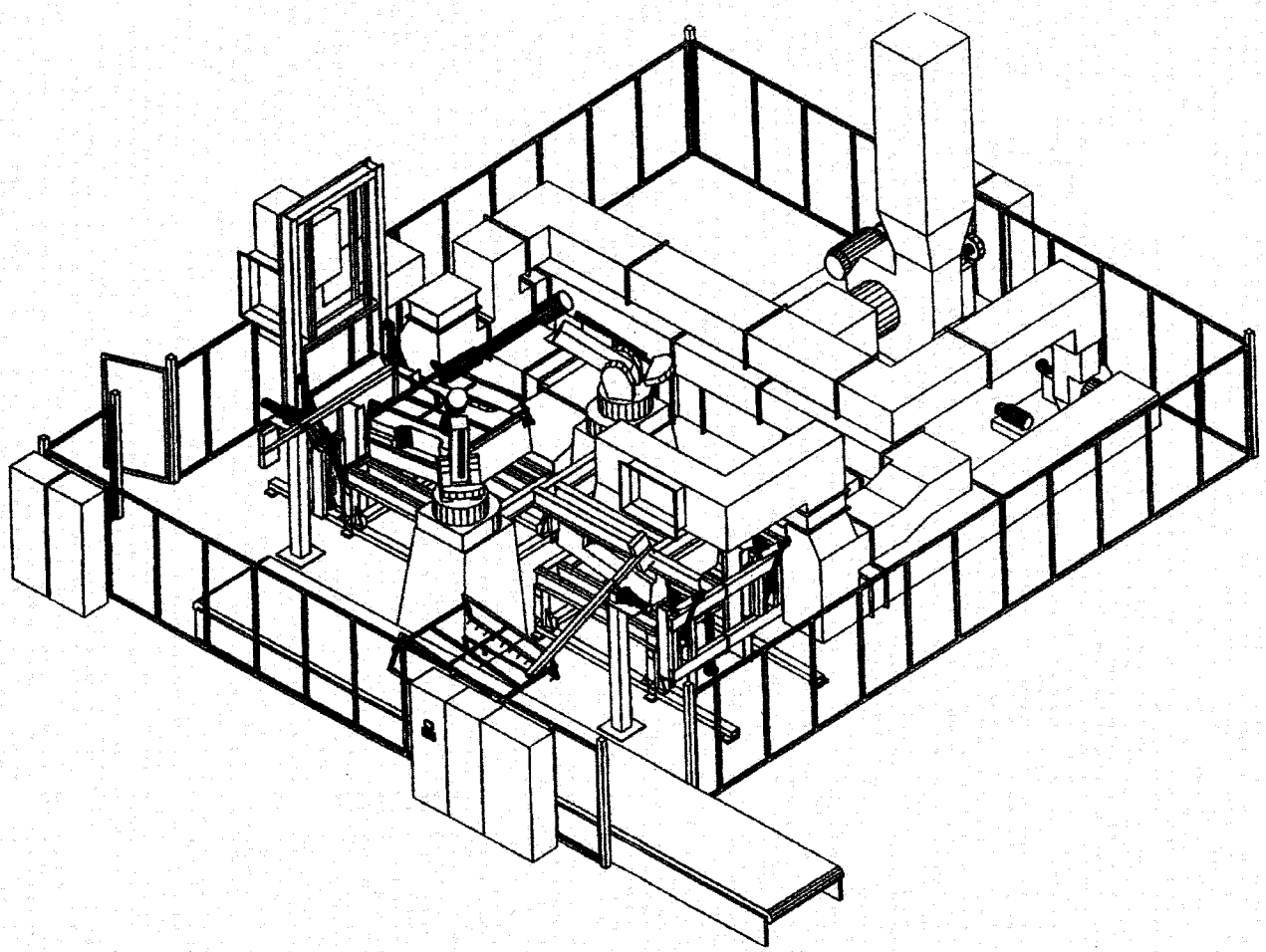

Experimental Tooling:

Flat Plaque and Shape Preform Tools

P4 Preforming

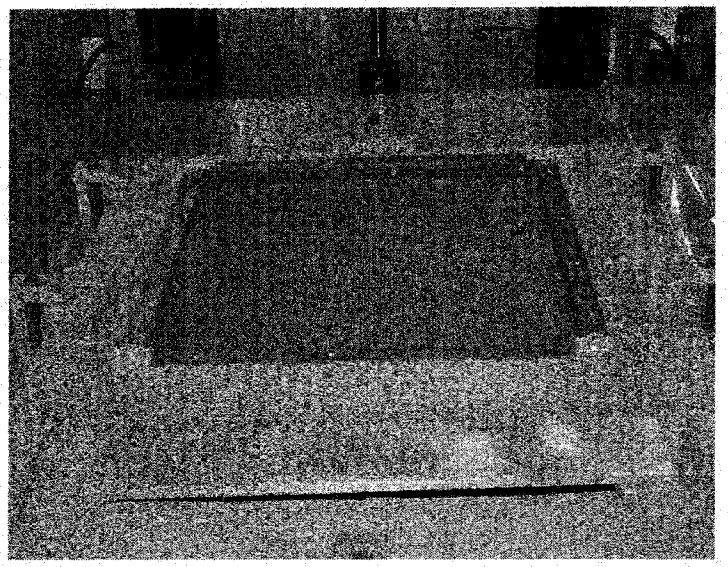

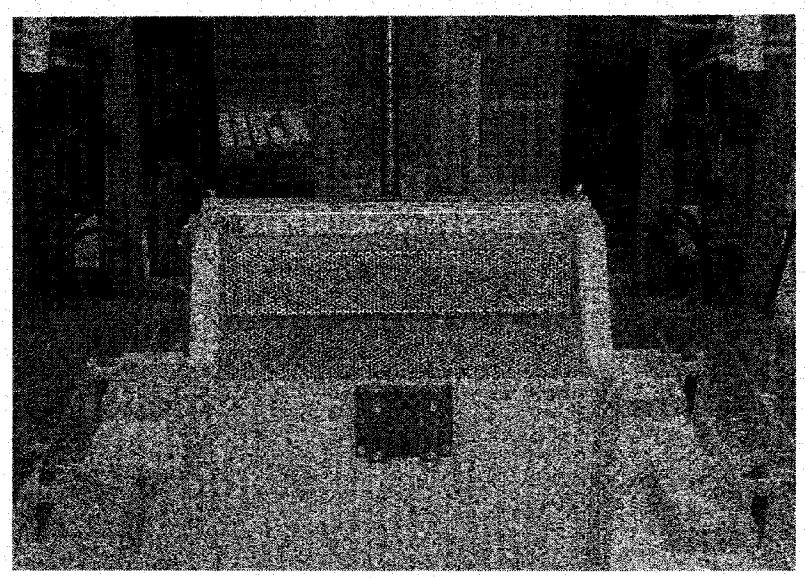

Flat Plaque Preforming Tool

- **700 x 700 mm**
- **Flat panels for molding and mechanical testing**

Shape Preforming Tool

- **0°, 90°, 45° oriented surfaces**
- **Inner and outer radii**

Experimental Preforming Method

P4 Preforming

- Stationary chopping: fiber output and fiber length ramping program
- Flat plaque and shape tool preforming
- Flat plaque and shape tool areal density sampling
- Observation of processing characteristics during all chopping and preforming trials
- Ranking of processing characteristics according to preset critieria

Experimental Preforming Results

P4 Preforming

Manufacturer	Ranking Criteria (1 = Best, 5 = Worst)							Total	Ranking
	Gun/FDS Fuzz (x4)	Chop (x3)	Integrity (x2)	Distributio n (x3)	Conforma bility (x2)	Loft (x3)	Cost (x2)		
A1	2	3	2	1	1	1	2	33	1
A2	1	3	2	2	2	1	2	34	2
B1	1	3	1	1	1	5	1	37	3
C1	2	1	2	2	3	1	5	40	4
A3	3	1	3	3	1	2	2	42	5
C2	1	1	3	3	4	1	5	43	6
B2	2	2	4	4	2	2	1	46	7
D1	2	2	4	3	2	2	3	47	8
D2	2	2	4	3	3	3	3	52	9
A4	4	3	2	3	1	3	2	53	10

P4 Carbon Fiber Preforming: Roving Trial Conclusions

P4 Preforming

- Trials performed to date on available materials from five carbon manufacturers
- Most materials are not 'new' or 'advanced' from previously available product forms
- Individual bundle size is too large, sizing is too stiff
- Roving form is not acceptable for high volume chopped fiber preforming applications
- Additional development is necessary at the carbon supplier to improve raw material form

P4 Carbon Preforming: Ongoing Research

P4 Carbon Roving Development

- Develop unique rovings for P4 with suppliers
- Currently encouraging carbon suppliers to fabricate multi-ended rovings
- Testing of 1k, 3k, 6k, 12k, 24k carbon materials to examine effect of bundle size on preforming and mechanical properties
- Continue with roving development and down-selection

P4 Carbon Preforming: Future Work

- **Support plaque molding and mechanical property evaluation program**
- **Focal Project 3 'B' pillar bodyside section**
  - **Tooling manufacture**
  - **Experimental preforming with variable thicknesses**
- **String binder development with carbon fiber**
- **Class 'A' surface capability**
  - **SRIM and/or Epoxy RTM**
  - **Glass veil vs. Carbon veil**

THE MAGSET K-12 CURRICULUM PROJECT

Don L. Evans

Director, Center for Research on Education
in Science, Math, Engineering, and Technology
Arizona State University
Tempe, Arizona 85287-5006

Telephone: 480-965-5350
e-mail devans@asu.edu

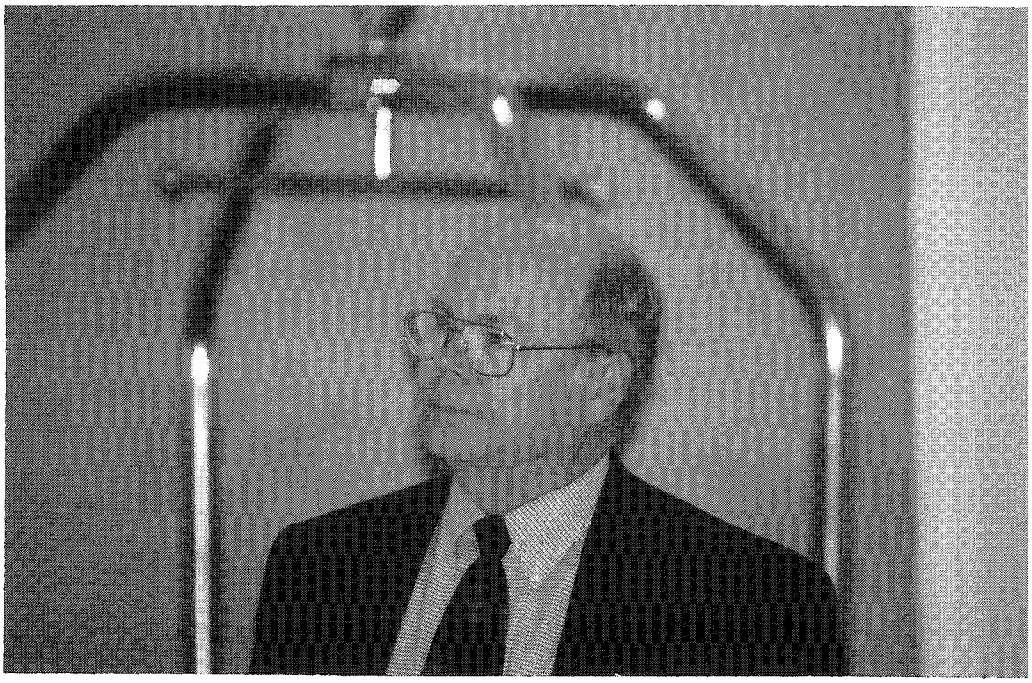

Don L. Evans

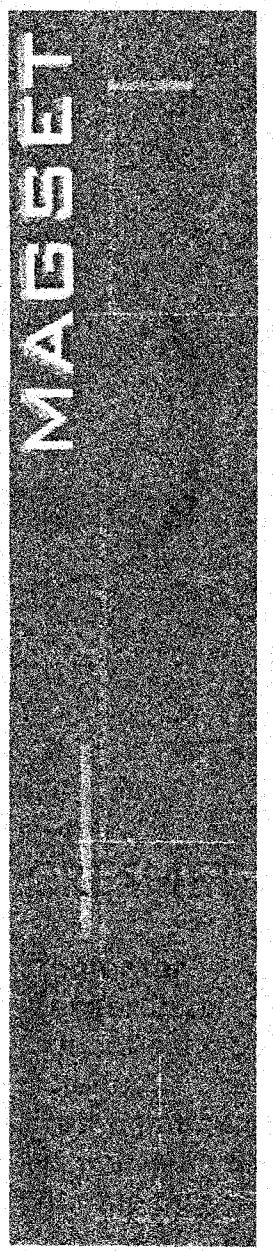

MAGSET

Materials As the Gateway (and Glue) for Science, Engineering and Technology (MAGSET)

A Consortium of Eleven Institutions
Addressing K-12 Education

Slide 1

MAGSET

U. S. Needs

- A more broadly prepared, diverse work force for the future;
- A creative, problem-solving emphasis in education programs;
- A scientifically and technologically savvy citizenry for the global economy.

Slide 2

MAGSET

K-14 Science Literacy Needs Reform

- The typical science curriculum is "over-stuffed"
- Few curricula address "relevance to the learner;"
- Most curricula do not address equity - the needs of under-represented and under-served students;
- There is a lack of interdisciplinary, structured, ***coherent***, and articulated curricula;
- Addressing all science standards with existing curricula is problematic.

Slide 3

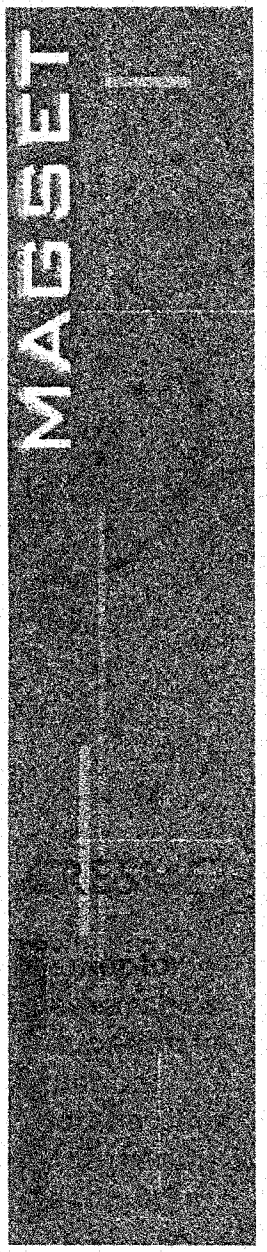

MAGSET

Materials As the Gateway (and Glue) for Science, Engineering and Technology

Presentation

Why Materials?

Goals of MAGSET

Who is MAGSET?

MAGSET Experience

Reform Plan

How to Join Us

Why Materials

- All citizens deal with materials every day (see, touch, and use)
- Chemistry, physics, biology are all linked to materials
- Materials cover the range from highest tech semiconductors and superconductors, to bone repair, to concrete and fly ash
- Can focus on a theme, not a discipline.

MAGSET

MAGSET Goal

Utilize materials as diverse as metals, plastics, semiconductors, ceramics "geomaterials" and biomaterials, as the gateway and the glue in which science, mathematics, engineering and technology (SMET) learning can be effective for the general population.

MAGSET Target Groups

- All K-14 students, especially,
  - Non-SMET-majors;
  - At-risk populations - equity.
- All pre-service and in-service K-12 teachers.
- All SMET faculty and instructors in Community College, 4-year College, and University general education programs.
- Supporting infrastructure people.

MAGSET

MAGSET: Local Points of Presence connected within a National Partnership

Steering Committee Members

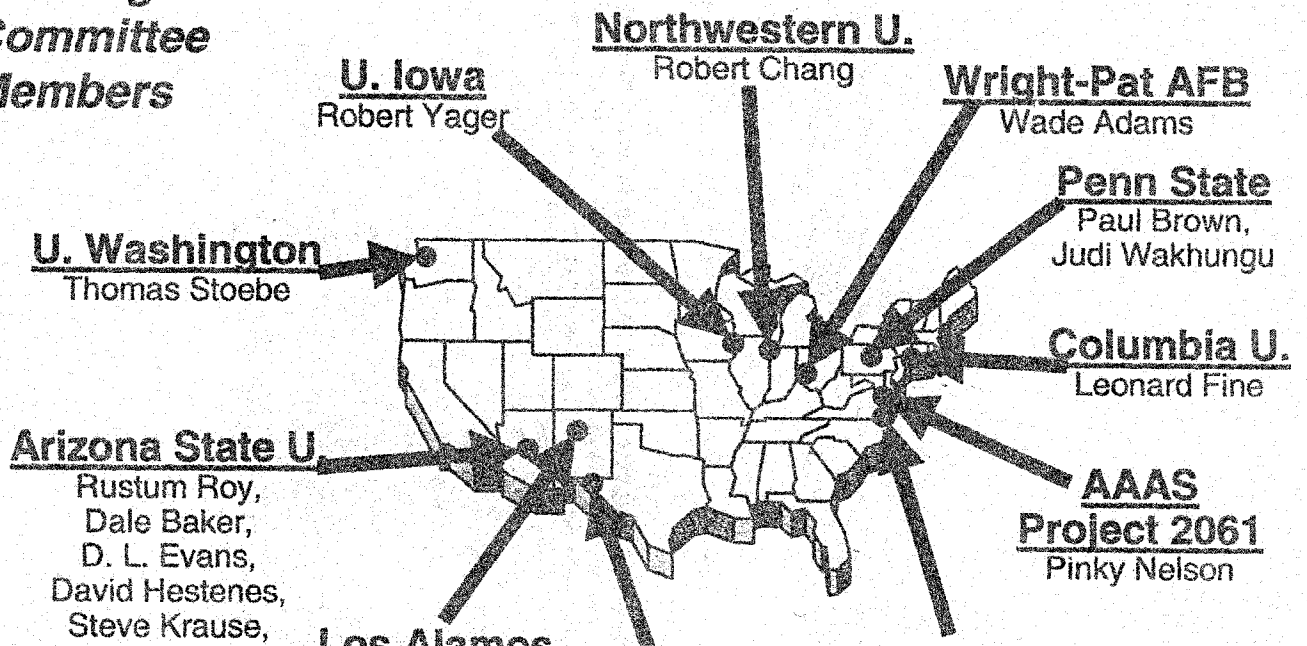

MAGSET

MAGSET Uniqueness

- Established national network of school/university partnerships serve as points of presence for local reform;
- Participants are close to the problems:
  - Effective partnerships;
  - Insures adaptability.
- Uses National Design and Coordination Teams:
  - Teams are diverse collections of stakeholders;
  - Meet quarterly w/one day of overlap;
  - Yearly national meeting (co-sponsored by various professional societies).
- Conducts multiple, geographically distributed pilots that are aggregated nationally;
- Focus on a theme, not a discipline, is unique.

MAGSET

MAGSET Approach to Curriculum Reform

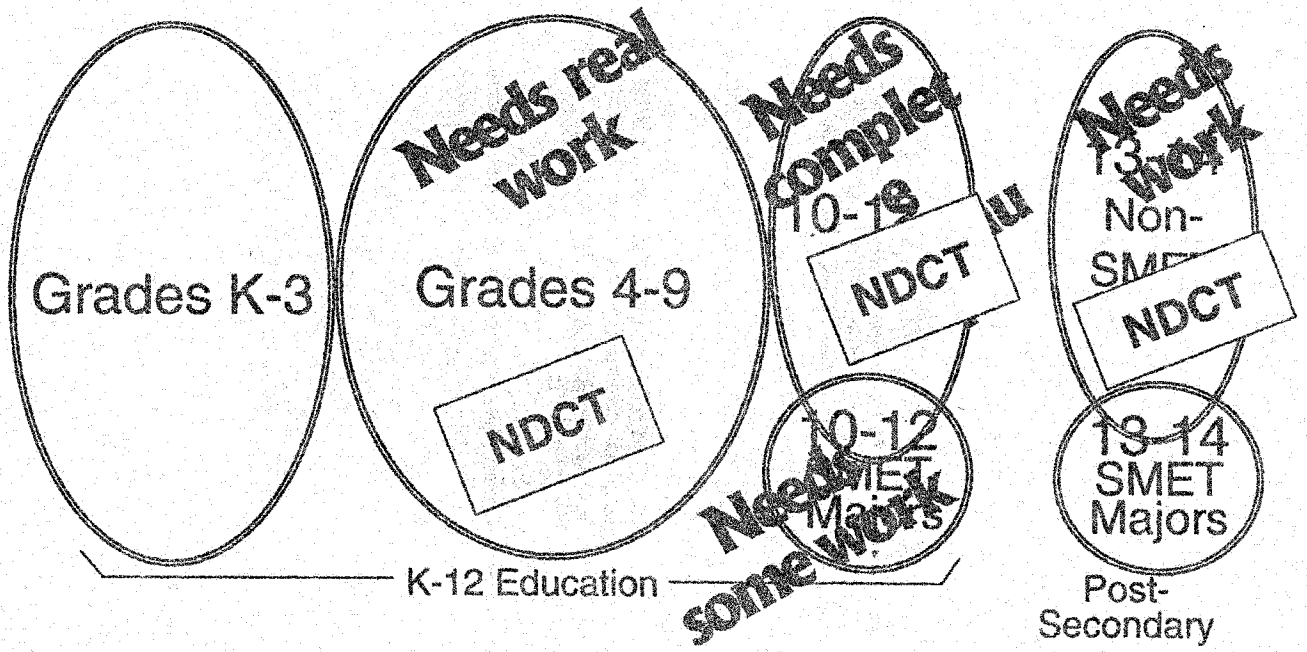

NDCT National Design & Coordination Team

MAGSET

MAGSET: A Start-Up Effort to Improve Science Literacy in K-14 Education

MAGSET Project Overview

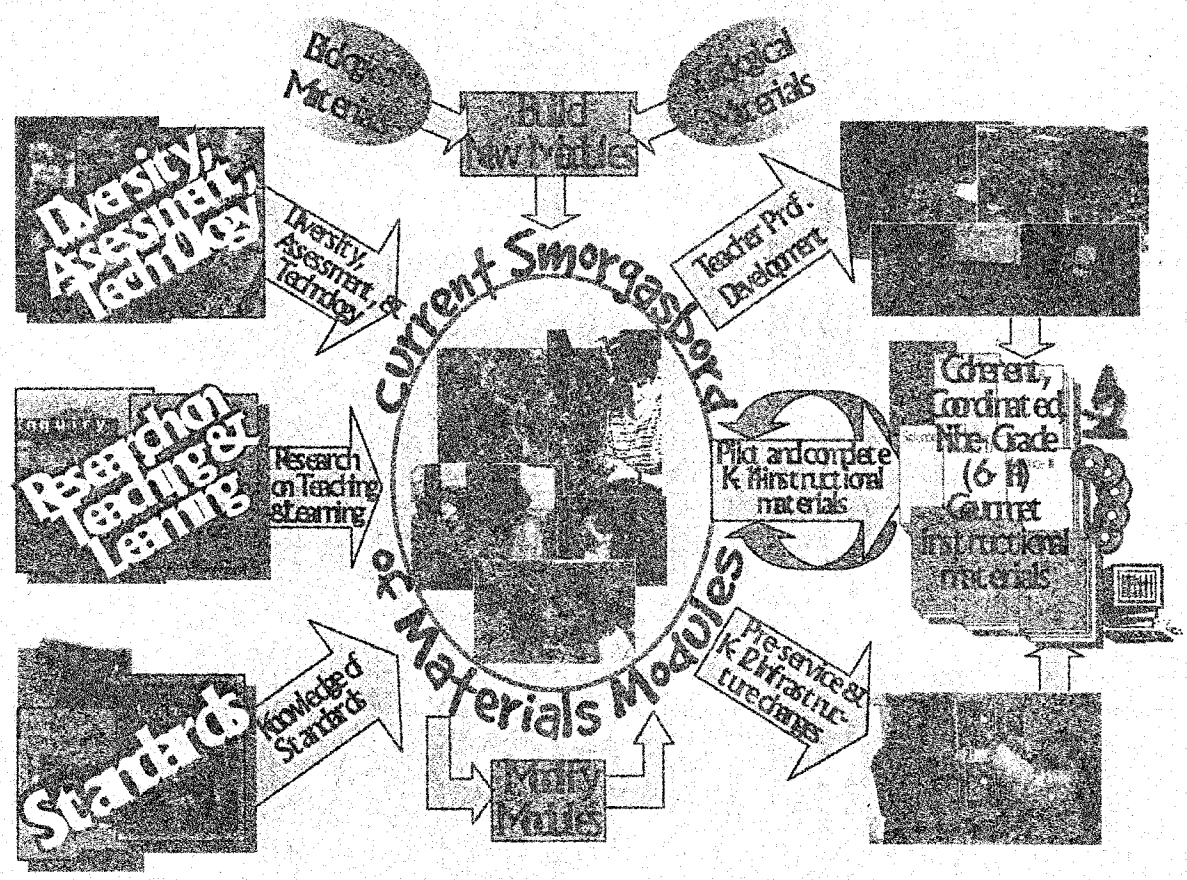

Slide 11

NORTHWESTERN UNIVERSITY
ASU ARIZONA STATE UNIVERSITY
NORFOLK STATE UNIVERSITY
The University of Texas at El Paso
THE UNIVERSITY OF TOLEDO

MAGSET

MAGSET

National Kickoff

A National Forum on Thematic, Cross-Disciplinary Approaches to Scientific and Technological Literacy in K-12 Education

A national, open meeting on this approach to science education was held in Washington D.C. on May 3rd, 2001, to announce MAGSET and to solicit input from a wider audience.

A Proceedings is Forthcoming

Slide 12

ASU ARIZONA STATE UNIVERSITY NORFOLK STATE UNIVERSITY The University of Texas at El Paso

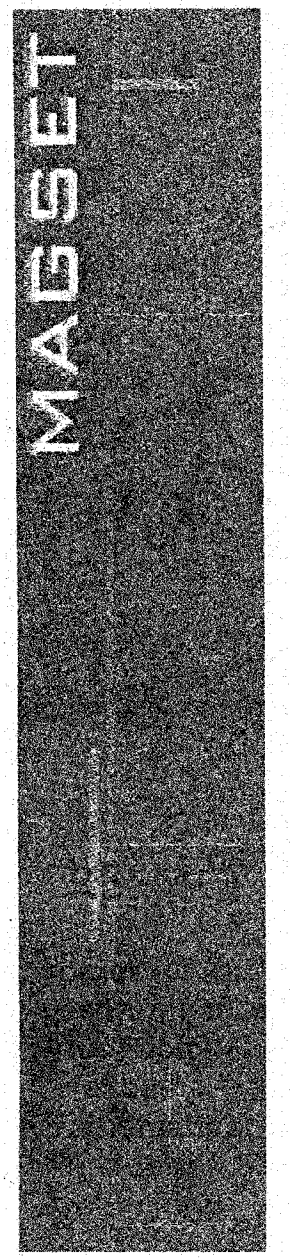

Forum Speakers

Welcome and Introductions: **Rustum Roy,** Visiting Prof. of Materials, *Arizona State University*

The Nation and Technological Literacy: **William Wulf,** President, *National Academy of Engineering*

Technology Literacy(Forum Keynote): **George Bugliarello,** Chancellor, *Polytechnic University of New York*

Why a Different Approach to Science Education for the Masses is So Important: **Rustum Roy,** Visiting Prof. of Materials, *Arizona State University*

The 2061 Platform: **George "Pinky" Nelson:** Director, *Project 2061, AAAS*

What We Know About How Children Learn: **Dale Baker,** Professor, *Arizona State University*

The Diversity of Solutions to Science Education: **Robert Yager,** Science Education Center, *University of Iowa*

MAGSET: One Approach to Thematic Cross-Disciplinary K-14 Education: **D. L. Evans,** Director, *CRESMET, Arizona State University*

Case-Study: "Materials" Courses in K-12: **Thomas Stoebe,** *University of Washington*

Slide 13

MAGSET

Want to Contribute/Participate?

- To place your project/activity in the MAGSET database, fill out the interactive form found linked to:

  www.eas.asu.edu/~magset

- National Design and Coordination Teams are being formed. To tell us of your interests and to get on our distribution list, send an email to

  magset@asu.edu

LECTURE ACTIVITY WORK KITS FOR INTRODUCTORY MATERIALS ENGINEERING CLASSES

Stephen Krause

and

Shahriar Anwar

Arizona State University
1171 N. Tercera Court
Chandler, Arizona 85226

e-mail skrause@asu.edu

Telephone: 480-965-5696
e-mail anwar@asu.edu

Shahriar Anwar

Lecture Activity Work Kits for Introductory Materials Engineering Classes

Stephen Krause* and Shahriar Anwar
Department of Chemical and Materials Engineering
Arizona State University
Tempe, AZ 85287

Abstract: This paper describes a series of hands-on activities that use student-centered learning for a diverse group of engineering students enrolled in larger sections of an engineering core class, "Structure and Properties of Materials". The "Lecture Activity Work Kits" supplement knowledge development from the more traditional teacher-centered blackboard lectures. The "Lecture Activity Work Kits" involve short, 10 to 20 minute, team-based classroom activities, which relate directly to the topical material in the course at that time. Typical activities include manipulations of crystal structure models, polymer deformation, and examination or metal, polymer, and ceramic samples. Results of the activities are being tied to assessment of course objectives and outcomes through student surveys, quizzes, and tests. An initial assessment of activities by students has been quite positive. Results and techniques are being disseminated to other course faculty. There is good progress toward improvements in student interest, participation, and comprehension in the learning process.

Key Words: Lecture activity work kits, student-centered learning, hands-on activities.

Prerequisite Knowledge: Freshman physics.

Objectives: To involve the students in team based activities to supplement lecture material topics such as crystal structures, crystal defects, polymers and their deformation, and classification of materials. In particular, learn to classify materials according to their electrical, mechanical, thermal & optical properties; learn crystal directions and Miller indices; identify crystalline defects of vacancies, dislocations, and grain boundaries in 2-D models; understand principle of condensation polymerization.

Equipment and Materials: 1. Materials "grab bag' consisting of some everyday material for less than $1 each. 2. Crystal geometry kit consisting of Styrofoam balls held together with glue or toothpicks, for about $0.50 per model. 3. Crystal structure kit from Klinger Educational Products (1-800 522-6252 www.klinger-educational.com/), for about $20 each. 4. Crystal Defects Kit assembled with CD ROM jewel case and BBs for about $1 each. 5. Silly putty polymerization kit consisting of Elmer's glue and Borax solution for about $0.25 each. 6. Metals cold working kit consisting of as-received and annealed

* Contacting author: skrause@asu.edu (480) 965-2050

copper wires available from local hardware stores for a negligible amount per kit. 7. Condensation polymerization kit assembled from ball-and-stick models for about $60 per kit. Models are available from Indigo Instruments (1-877-746-4764 www.indigo.com)

Introduction

A wide variety of approaches are used today to communicate subject matter in materials engineering and other technical courses. Although the majority of classes taught in the Materials Engineering Program at Arizona State University rely upon the traditional blackboard lecture method, this approach can be supplemented by methods that increase the involvement of students during the lecture. These methods, which are not unique and are being used to varying extents at other institutions, include classroom demonstrations and individual or team-based exercises and experiments. A variation of these methods that can be used is "Lecture Activity Work Kits". These economical kits have been created for classes of 60 to 70 students with 20 to 25 teams of 3 to 4 students each. Student involvement and satisfaction has been measured with surveys and student comprehension will be measured with test and quiz scores.

The Lecture Activity Work Kit Method

"Lecture Activity Work Kits" are being developed and used for inquiry-based learning in order to promote a deeper understanding of the course material by shifting knowledge development from teacher-centered to student-centered learning. This is being achieved by developing team-based activities that provide direct, hands-on activities that are directly linked to the course content in structure, processing, and properties of materials (metals, polymers, ceramics).

A set of a more than a dozen different "Lecture Activity Work Kits" were developed for an engineering core class, "Structure and Properties of Materials". In the five sections of this yearly course there are over 200 students enrolled from Bio, Mechanical, Aerospace, Industrial, and Materials Engineering. The course teaches critical prerequisite content for disciplinary courses in manufacturing, design, and advanced material classes. Thus, an enhancement of the understanding of the material presented in this class will have a positive impact on a variety of subsequent classes in each student's discipline. The kits were created by two undergraduate students with a small grant from the university's Center for Research on Education Science, Math, Engineering, and Technology (CRESMET). Some examples of the activities will now be described.

The Kits

The first kit was a "Materials Grab Bag" (Figure 1), which consisted of real-world examples of metals, ceramics, and polymers. The objects in a plastic "baggie" were sets of: ceramic tile, marble, and chalk; metal coin, large-gage wire, and rock-climbing hook; and polymer inner tube sample, clear fork, polyethylene dropper, and rubber band. The student teams were asked to organize the samples into families and then specify what physical properties were used to develop the classification system. After some time

students began to realize differences in behavior of different families of materials based on thermal, mechanical, electrical and optical properties. The knowledge acquired provided a lead into upcoming material on atomic bonding (metallic, ionic, covalent, and secondary bonding) and associated properties. The cost of each kit was a few dollars and some of the samples were revisited with later activities.

Another two kits used early in the course were the "Crystal Structure Kit" and the "Crystal Geometry Kit" (Figure 2). In an earlier course assessment, it was shown that students did not develop an adequate knowledge of crystal geometry and structures. One kit used to address this problem was the "Crystal Structure Kit". This kit used styrofoam balls stuck together with toothpicks and glued in place with a small glue heat gun. Small, half-inch balls were assembled into face-centered-cubic (FCC), body-centered-cubic (BCC), and hexagonal-close-packed (HCP) structures. Larger one-inch balls were sliced and assembled into FCC and BCC unit cells. The student teams then used these models to determine structural features such as atoms per unit cell and stacking sequence of layers in FCC and HCP structures. The students found the kits helpful in visualizing three-dimensional structures and also later, when the kits were reused to study deformation slip systems and mechanical properties of metals. These were inexpensive kits that cost a couple dollars each.

The "Crystal Geometry Kit" (Figure 2) used a commercial stick-and-ball simple cubic structure purchased from Klinger Educational Products for about $20 each. Crystal geometries were illustrated for directions and Miller index planes. The directions were created with sticks and the planes with styrofoam cutouts for (100), (110), and (111) planes. Visualization of the planes (and families of planes) was supplemented by a small cardboard cube with bevels along edges and corners with all faces labeled with specific (100), (110), and (111) planes. The students again appreciated the 3-D visualization, although the effectiveness will be determined in test performance.

Another kit on crystals is the "Crystal Defects Kit" (Figure 3) which is also inexpensive, about a dollar, and enjoyable to use. It is based on Bragg's bubble raft model of atoms in a 2-D lattice. For the model here a CD ROM case was filled three-quarters with BBs and sealed with clear tape on the one open edge. There is room for just a single layer of BBs and when the case is jiggled and tilted it is possible to generate an infinite variety of configurations of the BBs, which usually include grains, grain boundaries, edge dislocations, and vacancies. The instructor can also point out these features to the class by placing the case on an overhead projector and pointing out the defects. The model is a bit noisy, but that seemed to enhance the enjoyment of the activity by the students.

There are useful kits for each of the material families. For polymers four activity kits were developed. The first two were an "Addition Polymerization Kit" and a "Condensation Polymerization Kit" (Figure 4). In the first kit, ball-and-stick models of monomers and an initiator were given to teams and they were asked to construct models that showed the mechanisms of initiation, propagation, and termination for addition (or free-radical)

polymerization of polyethylene. In the second kit (figure 4) the monomers for nylon 6/6, hexamethyline diamine and adipic acid were given to student teams. They had to break and form appropriate bonds in order to give reactions, which gave the condensate molecule, water, and the characteristic amide linkage group between the two molecules. As before, students felt this activity helped them understand the 3-D nature of the molecules as well as the chemistry of the reactions that form polymers. These kits, which were more expensive, were the Student Organic Chemistry Model Kits obtained from Indigo Instruments. It took two kits, at $30 each, to make the two sets of polymerization models. The cost could probably be cut in half if just the components needed for the specific models had been purchased in quantity separately, since many balls and sticks were left over.

A third polymer kit was the "Silly Putty Polymerization Kit". With this kit a polymer was synthesized in a plastic "baggie" from Elmer's glue and borax solution. Solutions were premixed and placed in plastic vials so that the activity could be done efficiently for teams in a large class. In one vial there is 20 ml of glue plus 20 ml of water. In the other vial there is 20 ml of a *5%* Borax solution. The two vials are then poured into a baggie and kneaded for more than five minutes. A viscous moist gel is created that students enjoy handling. The vials can be returned and recycled for the next demonstration. Although the knowledge content of this activity is limited the students seemed to enjoy it the most. The cost of each kit is limited with the vials at 40c each and the consumables about *25c* per activity.

One last description of another kit is the "Metal Cold Working Kit". With this kit samples are given to all students in class since they just consist of 6" lengths of large gage, 1/8" diameter copper wire. Large gage copper wire can be purchased from a local electrical supplier or Home Depot. It is heavily cold-worked in the as-received condition and can be softened by annealing at 600°C for 15 minutes. Samples of as-received and of annealed wire are given to the students for comparison of yield strength and for cold working of annealed material. Although this is a simple and inexpensive exercise, the students develop an appreciation of the degree of strengthening possible by cold work.

A number of other Activity Kits have been created, but will only be given here by title. There have been "Grab Bag Kits" also created for polymers, metals, and ceramics. A "Polymer Deformation Processing Kit" has been used with a Ziploc "baggie" and a polyethylene. Other kits are being worked on for hardening of steels and precipitation hardening of aluminum alloys. Other kits being considered are related to solar cells, transistor behavior, electrical conductivity, piezoelectric crystals, and fracture toughness. If anyone has activities, or suggestions on activities, in these or other areas please contact me (skrause@ asu.edu).

Short assessments of the use of "Lecture Activity Work Kits" in comparison with previous classes without the kits were conducted. The results are quite positive as shown below by survey results of students in a larger class of 51 students. The responses vary from 1 to 5

corresponding to "strongly disagree" to "strongly agree".
1) Interest in subject matter is increased — 4.34
2) Subject matter more easily understood — 4.26
3) Homework more easily understood — 3.64
4) Opportunities for classroom participation are increased — 4.30
5) Overall, my performance has been enhanced — 3.89
6) In the future, I would prefer greater usage of the kits — 4.13

The survey generally shows a strong endorsement of "Lecture Activity Work Kits" by students in most areas. However, the survey also indicates that the kit activities should be more closely tied in with homework and also course outcomes. It should be possible to modify the activities so they are more closely linked with student work and course outcomes.

Summary and Conclusions

A brief summary of the advantages and disadvantages of the "Lecture Activity Work Kits" method of teaching materials engineering courses is summarized below. The advantages of the technique include":

* increased participation of students in class
* increased attention of students during filling in notes
* increases student involvement and opportunities for interaction in large classes
* increased highlighting of important content and concepts
* increased student thinking, questioning, and dialogue

Some disadvantages of the "Lecture Activity Work Kits" technique include:

* increased time required for activities reduces amount of course content
* logistic issues in preparing, distributing and collecting kits in larger classes
* development of "Lecture Activity Work Kits" consumes some time

The main goal of this article on "Lecture Activity Work Kits" has been to illustrate the concept and give some examples, which could be expanded upon. These kits do not replace the other insightful, full-length, laboratory-based materials science and engineering experiments, many of which have bee described at this conference. Rather, a series of short activities have been created to complement lecture content, especially in larger classes. If anyone would like the write up on any of these activities please contact me for these (skrause@ asu.edu).

Overall, the "Lecture Activity Work Kits" technique has proven to be a useful method to enhance communication of subject matter in materials engineering by shifting toward student-centered learning that improves student participation in lectures and enhances student learning. It has the flexibility to be adapted by instructors by varying the particular kits that are used and provides a basis for instructors developing their own kits. The modular format allows easy sharing and modification of content by other instructors teaching courses with similar content.

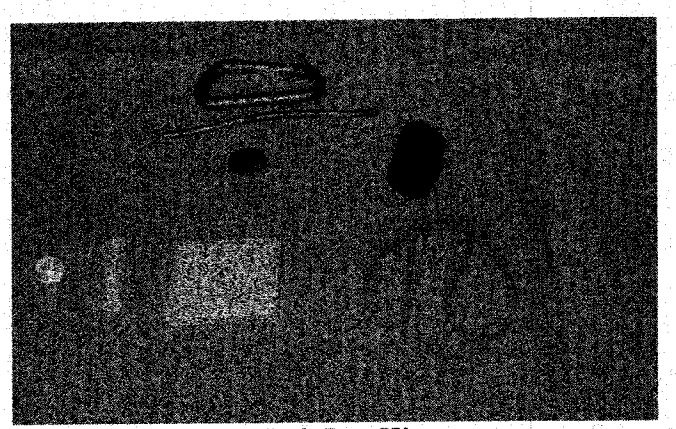

Figure 1. Materials Grab Bag Kit

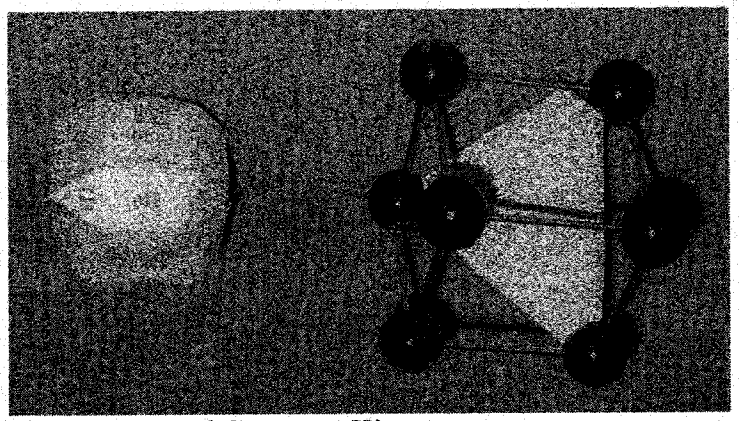

Figure 2. Crystal Geometry Kit

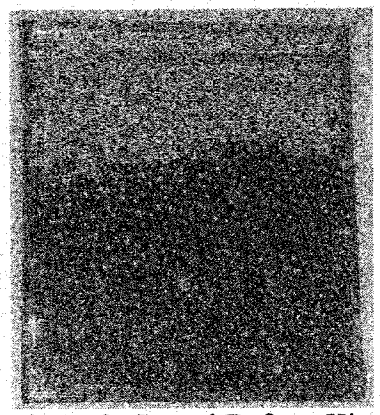

Figure 3. Crystal Defects Kit

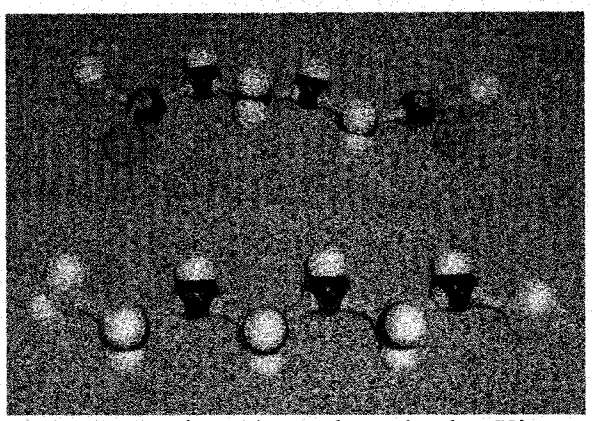

Figure 4. Condensation Polymerization Kit

LÜDER'S BAND FORMATION IN STEEL

Mike L. Meier

and

Aaron Broumas

Department of Chemical Engineering and Materials Science
University of California, Davis
Davis, California 95616

Telephone: 530-752-5166
e-mail mlmeier@ucdavis.edu

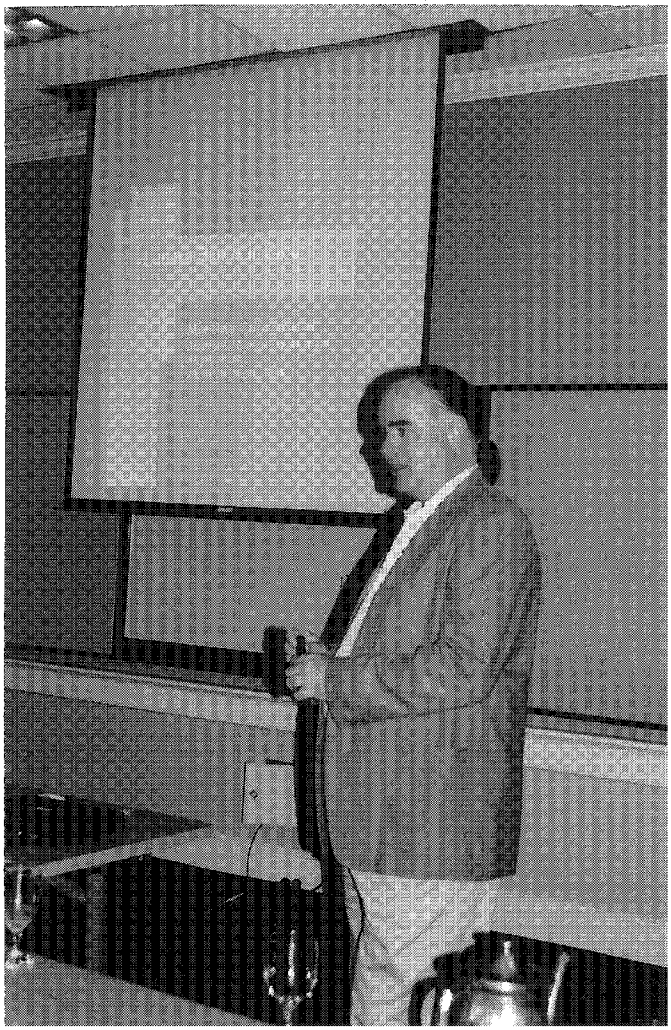

Mike Meier

Biographical Information

Michael L. Meier received his B.S. in Materials Engineering from North Carolina State University in 1979 and his M.S. (1986) and Ph.D. (1991) in Materials Science and Engineering from the University of California, Davis. After a two-year post-doctorate position at the Universität Erlangen-Nürnberg in Erlangen, Germany he returned to UC Davis where he is now the director of Materials Science Central Facilities.

Aaron Broumas is in his junior year at the University of California, Davis and is majoring in materials science. He is proficient in metallography, specimen preparation techniques, scanning electron microscopy and EDS which he learned outside of normal courses. He has yet to take his core materials science courses. Aaron is currently working full time in Materials Science Central Facilities supporting users of and operating our two scanning electron microscopes. He is also engaged in the analysis of dust samples collected over Puerto Rica and in the northern deserts of China.

LÜDERS BAND FORMATION IN STEEL - VIDEO

Mike L. Meier, Aaron Broumas
Department of Chemical Engineering and Materials Science
University of California, Davis
Davis, CA 95616

Keywords: Microstructure, microstructural evolution, tensile testing, digital video, Lüders bands, upper yield stress, lower yield stress.

Prerequisite Knowledge: Basic knowledge of the following is required: mechanical properties of low-carbon steels, formation and propagation of Lüders bands, tensile testing, digital video using the PC and basic video editing techniques.

Objectives: The objectives of this paper are:
1. To describe how we made a video showing the formation and propagation of Lüders bands during tensile deformation of a low-carbon steel
2. Provide instructions on how to make a video for classroom instruction
3. Encouraged others to create and share their own videos of in-situ observations or other materials processes.

Also, projects such as this are excellent student laboratory projects and produce course materials that an instructor can use in the classroom, and which the student can show to friends who might be interested in majoring in materials science and engineering.

Equipment: The equipment used to make the videos consisted of the following:

- Oven – An oven capable of reaching 300°C.
- Tensile testing system – in this case an Instron model 4204 (computer controlled, 50 kN capacity)
- Digital camera – A CCD video camera with composite video output.
- Video Capture – The computer used in this project was a 733 MHz Pentium III-based PC running Windows 98. It had 256 MB of SDRAM and a 30 GB ATA-100 hard drive. The video capture board, a miroVIDEO DC30 Pro, was capable of digitizing full motion video at 640x480x24 bits and 30 frames per second (fps).
- Video editing software – Adobe Premiere 5.1
- Optical Microscope – the microscope used in this experiment was a Zeiss-Herrberg stereo-zoom microscope capable of providing magnifications from 5 to 75X and at a working distance of several inches.
- Illumination – Fostec light source utilizing a quartz lamp and ring or dual-light pipe fiber optic illuminators.
- Other Microscopes – an FEI XL30-SFEG scanning electron microscope was used to obtain high-resolution images of the Lüders bands while a metallograph was used to obtain color images of the Lüders bands at ordinary magnifications.

Introduction: Lüders bands formation and propagation are fascinating aspects of the deformation of a number of materials. This can be seen in figure 1 as the curious feature of the stress-strain curve, the upper and lower yield strengths and yield point extension. This behavior is characterized by an initially high yield stress followed immediately by a sudden drop in stress. With continued straining the stress stays nearly constant for several percent strain before normal strain hardening behavior begins. This behavior always elicits questions from students. An explanation involves a discussion that deals with how dislocations break free of the solute atoms, a localized process which produces the Lüders bands which in turn propagate until they cover the whole specimen. Lüders bands may appear as elongated surface markings or depressions, often visible with the unaided eye. Many textbooks contain pictures of Lüders bands we can show to the students, or, we can polish up a specimen and let the students watch the Lüders bands from during a tensile test. If this is not convenient then one can use our video that shows Lüders bands forming and propagating on the surface of a polished steel tensile specimen.

In this video project, specimens of steel were annealed, polished and tensile tested. Changes in the surface of a specimen observed using an optical microscope were recorded using a VCR and a PC-based digital video capture system. In this paper we describe how this was done.

Procedure:

Materials

The steel used in this experiment was a 1-inch (25.4 mm) wide, ⅛-inch (3.175 mm) thick strip of 1018 steel. These were machined into tensile specimens having a gage length of 1.50 inches (38.1 mm) and a gage width of 0.50 inches (12.7 mm).

Heat Treating

The tensile specimens were annealed in air at 300°C for one hour then air cooled. The objective of this heat treatment was to maximize solute locking of dislocations without causing much grain growth.

Specimen Polishing

After heat treating the specimens were mounted in a specially designed holder (figure 2), ground and polished using an automated polisher/grinder (8-inch wheels, 240-600 grit SiC, 6 μm diamond) and finally with 0.05 micron alumina on a flocked cloth (Buehler's Micropolish B on Microcloth). The result was a set of flat and highly polished steel tensile specimens (figure 3).

Tensile Testing

Tensile testing was conducted using crosshead speeds ranging from 0.6 mm per minute to over 6 mm per minute. In all tests the lower crosshead was stationary while the upper crosshead moved at the specified rate. During each test the load-elongation data was recorded and saved to disk.

Video Capture

Several tests were done to allow us to monitor Lüders bands activity at different magnifications. A stereo-zoom microscope was mounted horizontally and focused on the surface of the specimen. The magnification of each video segment was noted by recording images of a ruler. A color video camera was attached to the microscope's C-mount adapter and its output was connected to the PC, a VCR (in case the PC video capture failed) and to a color monitor (figure 4). After making a few short test recordings to ensure everything was working properly the video capture system and the VCR were started and a few seconds later the tensile test was started. The video was recorded at the highest available resolution and

frame rate (640x480x24-bits, 30 fps).

A total of seven tests were conducted and recorded, many giving poor results due to poor lighting. Proper illumination of the specimen was difficult due to the highly reflective nature of the specimen and the low contrast of the Lüders bands. The original setup consisted of a color camera with a macro lens and a light source consisting of a dual light-pipe illuminator and a polarizer (figure 5). These problems were solved by doing all recordings using the stereo-zoom microscope and a ring illuminator (figure 6). The resulting videos were similar to microstructures seen using dark-field illumination. The specimen itself appears dark with bright edges and the Lüders bands showed up as bright streaks on the otherwise dark specimen.

Video Processing

All video processing was done on the same PC that was used for the video capture. Adobe Premiere was used to create the title screens, transitions and micron bars, to cut and splice the video and to assemble the final video. The final video shows segments of three different tests. It starts by showing the whole specimen as it is deformed. About half way through the video two segments showing the close-up views of individual Lüders bands. The final video was produced in three formats: 640x480x24-bits, 320x240x24-bits and 160x120x24 bits, all at a frame rate of 15 fps. These videos were also accelerated so that their runtimes would be less than the recommended three minutes.

CD-ROM

The videos, the data from the tensile tests, several frames from the videos and SEM and optical microscope images were written to a CD-ROM.

Comments: Videos such as this one are challenging projects and fun to do with students. They have the added benefit of producing something which can be used to help teach other students. This project requires a thorough understanding of the phenomenon, the testing procedures, advanced computer skills and a knack for presenting the results in a straightforward manner. It also requires a degree of creativity and promotes a sense of ownership which motivates students to do their very best work.

This video, like the videos showing the orange peal surface develop in annealed brass that we made a few years ago [1], was meant to be used as a short video clip in which the instructor provides the background information and narration. The appendix at the end of this paper summarizes some of the details of the sharp yielding phenomenon and Lüders band formation.

This video, the tensile test data, and still images may be downloaded from our web site at www.matsci.ucdavis.edu/ meier/NEW-Update2001. Note that the 640x480 video is a 108 MB file and the 320x240 video is in the neighborhood of 40 MB. Download times may be impractical and you will also need enough hard drive space to store these large files. If you would like to get a copy of these videos you can write or email the authors to request copies of the CD-ROM.

References:

1. M.L.Meier, K.H.Ewald, The Underlying Structure of Engineering Materials, Proceedings of the National Educator's Workshop-Update 98, Brookhaven National Laboratory (1998).

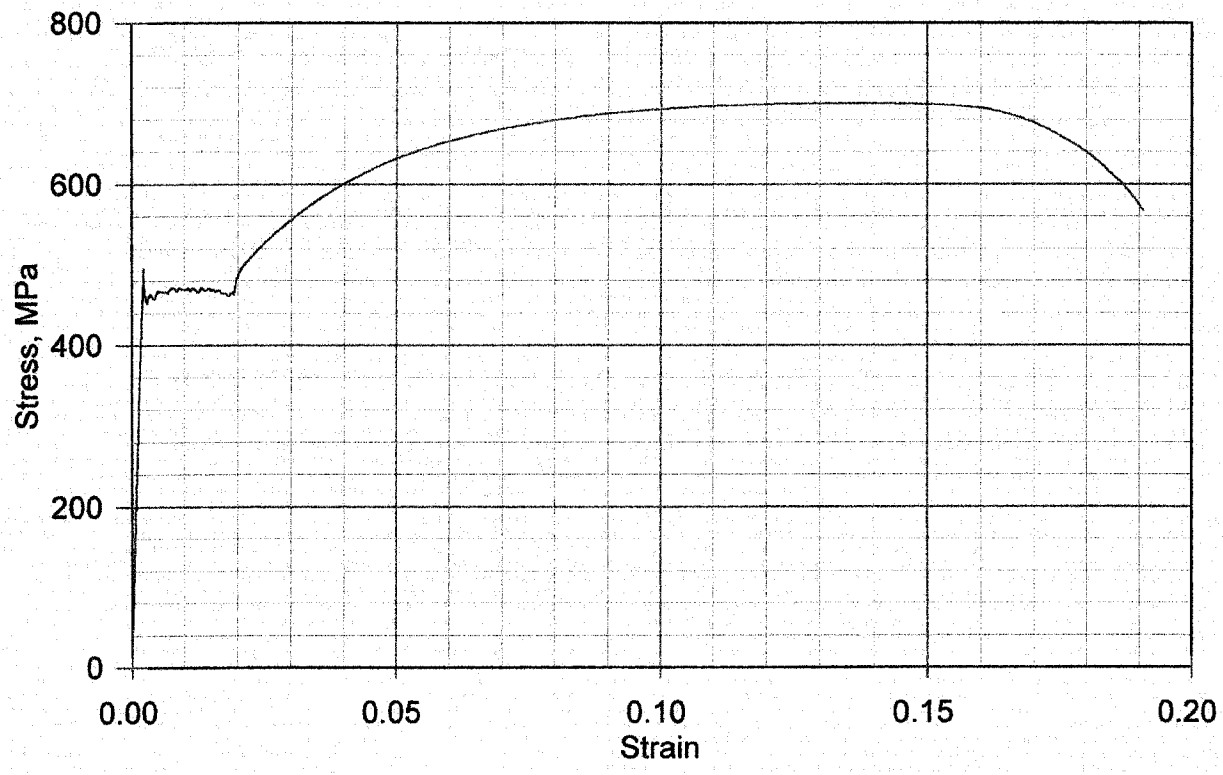

Figure 1 Stress-strain curve for a low-carbon steel. Not the upper and lower yield stresses.

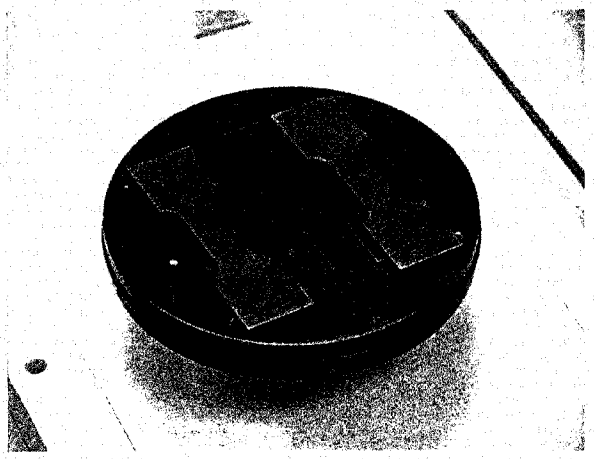

Figure 2 The fixture used to hold the specimens during grinding and polishing.

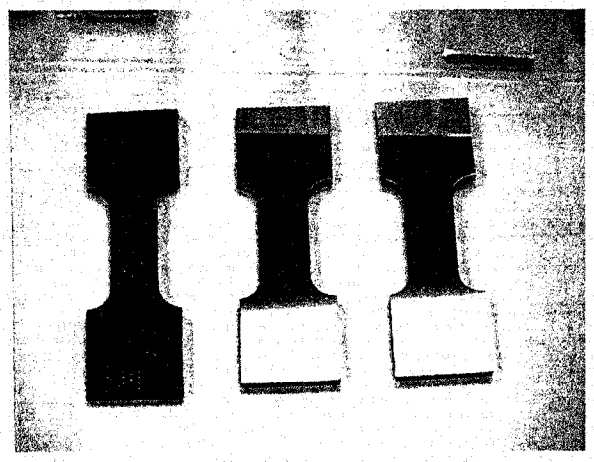

Figure 3 Tensile specimens before and after polishing.

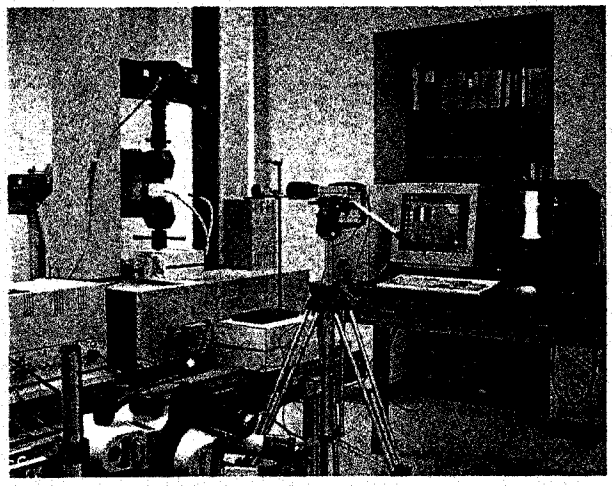

Figure 4 The original setup showing the tensile tester, the camera and illumination setup, the computer, VCR and monitor.

Figure 5 The original camera and lighting setup. The camera and macro lens are mounted on a tripod. The illumination system consists of a dual-light pipe quartz illuminator and a polarizer.

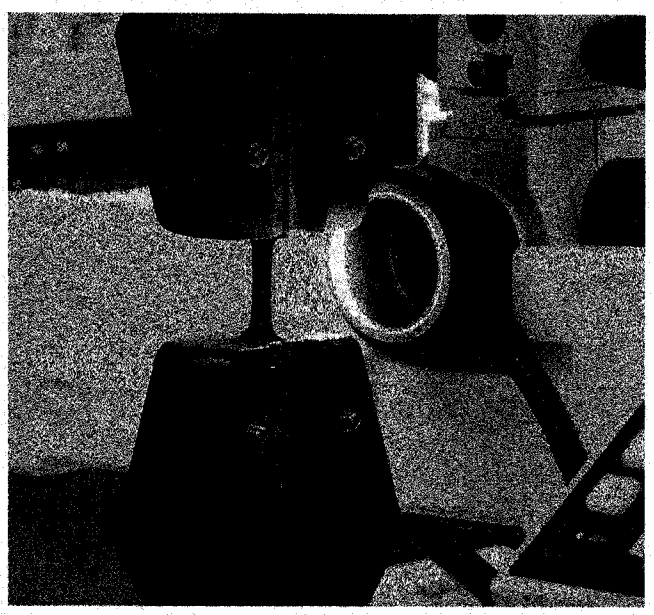

Figure 6 The final setup used for the close-up shots. The ring illuminator provided the best results when videoing the polished steel specimens.

Appendix

This appendix provides a more detailed description of the phenomenon of upper/lower yield point phenomenon and of Lüders band formation and propagation. [1]

General Aspects

Consider a tensile test conducted at a constant rate of strain. Strain rate due to dislocation processes can be expressed as

$$\dot{\epsilon} = \rho b v \qquad (1)$$

where ρ is the density of mobile dislocations, b is the magnitude of the Burgers vector and v is the average velocity of the mobile dislocations. At the upper yield stress the strain rate is

$$\dot{\epsilon}_U = \rho_U b v_U \tag{2}$$

and at the lower yield stress the strain rate is

$$\dot{\epsilon}_L = \rho_L b v_L. \tag{3}$$

Since the strain rate is constant

$$\dot{\epsilon} = \dot{\epsilon}_L = \dot{\epsilon}_U \tag{4}$$

we can write

$$\frac{\rho_U}{\rho_L} = \frac{v_L}{v_U}. \tag{5}$$

The relationship between stress and velocity is generally written as

$$v = k\tau^m \tag{6}$$

where τ is the shear stress acting on the dislocations and m is the strain rate sensitivity. Combining equations 5 and 6 we can express the ratio of the upper and lower shear stress in terms of the ratios of the densities and velocities of dislocations

$$\frac{\tau_U}{\tau_L} = \left(\frac{\rho_L}{\rho_U}\right)^{\frac{1}{m}} = \left(\frac{v_U}{v_L}\right)^{\frac{1}{m}}. \tag{7}$$

This last equation summarizes the general aspects of the upper/lower yield stress phenomenon. At the upper yield stress the mobile dislocation density is low but the average dislocation velocity is high. At lower yield stress there are many more mobile dislocations but they are not moving as fast. Lüders bands are nucleated at the upper yield stress and propagate at the lower yield stress with ρ_L and v_L representing the deformation that is occurring in a narrow zone ahead of the advancing Lüders band.

Advanced Aspects

Please note the dependence of the ratio of upper and lower yield stress on the strain rate sensitivity m. The strain rate sensitivity of a material is measure of the stability of the neck that forms at the UTS which is in turn related to strain hardening index $n=\epsilon_{UTS}$, a measure of the material's resistance to necking. The strain rate sensitivity can readily be measured from the Lüders strain and the initial slope of the stress-strain curve [2].

$$\frac{1}{m} = \frac{\Delta\sigma}{\sigma} - \epsilon_L \tag{8}$$

The early theories of Cottrell-Bilby [3] and others were given in terms of solute atom locking of dislocations. Initially, dislocations are pinned but at the upper yield strength they break away, the mobile dislocation density increases, the dislocation velocity decreases and the stress decreases to the lower yield stress. A later theory proposed by Petch [4] addressed the effect of grain size on the upper yield stress. At the upper yield stress only a few grains contain mobile dislocations and these dislocations move quickly relative to the average velocity for the whole specimen. As more grains acquire mobile dislocations the velocity drops, the macroscopic stress drops and so does the stress required to penetrate grain boundaries. A Lüders band forms and from that point on the number of active grains remains constant as it propagates through the specimen.

The Hall-Petch equation

$$\sigma = \sigma_f + kd^{-\frac{1}{2}} \tag{9}$$

where d is the grain size and σ_f is a the inherent strength of the material without grain boundaries, defines the lower yield stress. In Petch's model σ_f is expressed as

$$\sigma_f = \sigma_0 + \Delta\sigma_0 \log\left(\frac{1}{Nd^3}\right) \tag{10}$$

where σ_0 is the inherent strength when all grains are deforming uniformly and N is the number of active grains per unit volume. The difference between the upper and lower yield stresses is given by the second term in the equation above.

As for the lower yield stress, an important factor is the extension of deformation past or through grain boundaries. The lower yield stress was seen as the stress forcing grain boundaries ahead of the Lüders band and the propagation of the Lüders band involves a process of generating dislocations in the next grain, adjacent to the boundary.

Practical Aspects

It is difficult to measure the true upper yield stress due to practical difficulties in testing, such as the specimen design, grip design, alignment, etc. Consequently the lower yield stress is usually considered the material's yield strength. When these difficulties have been eliminated experiments have shown that the upper yield stress can be twice as high as the lower yield stress.

Lüders bands, also called stretcher strains, are unsightly and may spoil the finish during sheet forming operations. Prior rolling can minimize this, but strain aging can restore it. Strain aging sufficient to cause stretcher strains can occur after a few days at room temperature or only an hour at 60-100°C.

References

1. Honeycombe, *The Plastic Deformation of Metals*, Edward Arnold, London, pp.149-157 (1984).
2. U.F.Kochs, A.S.Argon and M.F.Ashby, *Thermodymanics of Slip*, Pergamon Press, Oxford, pp. 261-264 (1975).
3. A.H.Cottrell and B.A.Bilby, *Proc. Phys. Soc*, **A62**, 490 (1949).
4. N.J.Petch, *The Upper Yield Strength of Polycrystalline Iron, Acta Met.* **12**, 59 (1964).

TRANSMISSION ELECTRON MICROSCOPY OF SELF-ORGANIZED MAGNETIC STRUCTURES IN $La_{0.67}Sr_{0.33}Mn$ FILMS

Lourdes Salamanca-Riba

and

L. J. Martinez-Miranda

Materials and Nuclear Engineering Department
University of Maryland
College Park, Maryland 20742-2115

Telephone: 301-405-0253
e-mail martinez@eng.umd.edu

e-mail riba@eng.umd.edu

Lourdes Salamanca-Riba

Biography:

L. Salamanca-Riba is a Professor of Materials Engineering in the Department of Materials and Nuclear Engineering at the University of Maryland-College Park. She received her BS degree in Physics from the Universidad Autonoma Metropolitana, Mexico City and her PhD degree in Physics from the Massachusetts Institute of Technology. At the University of Maryland she has been involved in teaching courses in electron microscopy, electronic properties of materials and defects in materials. Her research interests are in the areas of effect of defects on the physical properties of materials for devices, semiconductor quantum structures and self assembly in semiconductors.

L. J. Martínez-Miranda is Associate Professor of Materials in the Department of Materials and Nuclear Engineering at the University of Maryland – College Park. She received her bachelor's and master's degrees in Physics from the Universidad de Puerto Rico in Río Piedras, a bachelor's in Music degree from the Conservatory of Music of Puerto Rico and her doctoral degree in Physics from Massachusetts Institute of Technology. At Maryland she has been responsible for designing the junior level laboratory undergraduate courses with the help of her colleagues, and has taught the introductory design course and the physics of materials course. Her research interest is in X-ray scattering from liquid crystals and solid films.

Transmission Electron Microscopy of Self-Organized Magnetic Structures in $La_{0.67}Sr_{0.33}Mn$ Films

L. Salamanca-Riba and L.J. Martinez-Miranda
Materials and Nuclear Engineering Department
University of Maryland
College Park, MD

Key Words: Transmission electron microscopy (TEM), electron diffraction, structure identification, self-organized structures, magnetic structures, thin films

Prerequisite Knowledge: Basic knowledge of diffraction, Bragg's Law, concept of reciprocal lattice and its relation to the real space lattice, Fourier transform.

Objectives:

- To understand the dependence of diffraction on structure factor from crystals with different structures,
- To understand the relationship between real space imaging and diffraction as Fourier transforms of one another.
- To become familiar with the capabilities of TEM in the analysis of the structure of thin films.
- To learn the concept of dislocation formation in thin films.

Equipment:

1. A high resolution transmission electron microscope
2. High resolution scanner
3. One plan-view and one cross-sectional TEM samples of a $La_{0.67}Sr_{0.33}MnO_3$ (LSMO) thin film containing MnO inclusions and deposited on $LaAlO_3$ by pulsed laser deposition (PLD).
4. A computer with image processing software and photo shop.

Introduction:

$La_{1-x}Sr_xMnO_3$ (LSMO) is a magnetic oxide that shows a very large change in its electrical resistance in the presence of a magnetic field. The elements in the LSMO are ionic, namely, La^{3+}, Sr^{2+}, a mixture of Mn^{3+} and Mn^{4+}, and O^{2-}. The properties of the LSMO depend on the Mn^{3+}/Mn^{4+} ratio, which can in turn be controlled by the La^{3+}/Sr^{2+} ratio and the oxygen content. To obtain films with desirable properties it is necessary to control the composition of the LSMO. In this project the structure of LSMO films grown by pulsed laser deposition on $LaAlO_3$ substrates is studied for the characterization of a two-phase material. During the deposition of the films the LSMO transforms into two phases. The transformation takes place by phase separation in the form of self-assembled structures. One phase consists of columns of MnO with square base that extend from the film/substrate interface to the film surface embedded in a matrix of LSMO (second phase). The MnO remains epitaxial with the matrix and with the $LaAlO_3$ substrate. The columns have a different structure (cubic, a =0.445 nm)) from the LSMO matrix (tetragonal, a =0.38 nm, c=1.32 nm) in which the out-of plane interplanar distance of the LSMO

and that of the MnO are approximately the same. In contrast, the in-plane interplanar spacings are different giving rise to in-plane misfit dislocations between the MnO and the LSMO.

This exercise is carried out after the students in the class have performed a standard x-ray diffraction experiment so that they are already familiar with Bragg's Law, Miller indices, and the concept of diffraction in general. In this project, electron diffraction patterns are obtained from the LSMO film and substrate. The pattern from the substrate is used for calibration. Images are obtained using objective apertures of different sizes to include the transmitted or direct (BF) beam only, a diffracted (DF) beam only, the transmitted and several diffracted beams at the same time. The table below shows the different types of pictures that are obtained in this experiment with an explanation of how to carry them out.

Name	Abbreviation	Explanation	How to carry out
Selected area diffraction pattern	SADP	Pattern of the (hkl) reflections allowed by the structure factor of the sample	1. Insert a selected area aperture to isolate the area that we want the SADP pattern from 2. Switch to diffraction mode and the diffracted beams are observed on the screen 3. Take a picture
Bright field image	BF	Image of the sample using only the transmitted (not diffracted) beam	1. Obtain a SADP 2. Insert a small objective aperture to select only the transmitted beam 3. Go to imaging mode 4. Increase the magnification to ~50,000X 5. Focus on the image and take a picture
Dark field image	DF	Image of the sample using only one diffracted (hkl) beam	1. Obtain a SADP 2. Insert a small objective aperture to select only one diffracted beam 3. Switch to imaging mode 4. Increase the magnification to ~50,000X 5. Focus on the image and take a picture
High resolution electron microscopy	HREM	Image of the sample formed by the interference of several beams (transmitted and diffracted beams)	1. Obtain a SADP 2. Insert a larger objective aperture that includes the transmitted beam (at the center of the aperture) and several diffracted beams 3. Switch to imaging mode and increase the magnification to

			~400,000X 4. Focus on the image and take a picture

Procedure:

The class is divided in groups of five to six students so that they all can see the microscope screen. Each group works with a graduate student or postdoctoral fellow who operates the TEM. The students are required to obtain the following images from the LSMO thin film sample.

a) A SADP from an area including both the MnO inclusions and the LSMO matrix.
b) A bright field (BF) image of the thin film at a magnification of approximately 50,000X.
c) Two dark field (DF) images, one using a diffracted spot from the MnO inclusions and one with a diffracted spot from the LSMO matrix, also at a magnification of ~50,000X.
d) A high-resolution lattice image from the film (approximate magnification of 400,000X).

Note: the pictures can be taken from either the plan view or the cross-sectional sample, or both (if time allows).

After the demonstrations the students are asked to

a) Scan the TEM negatives obtained during the laboratory session and print the pictures. Note the scale on each negative. Label the phases in the bright and dark field images. Examples of the pictures obtained in a), c) and d) are shown in Figures 1-4.
b) Obtain the interplanar distances, d_i from the diffracted spots from the MnO and LSMO using the formula $d_i = L\lambda/r_i$, where L is the camera length printed on the negative of the SADP, λ the wavelength of the electrons used (0.00197 nm for 300,000 KeV) and r_i is the distance from the transmitted beam to a diffracted beam.
c) Perform necessary image processing by adjusting the contrast to the images and
d) obtain the fast Fourier transform of the different regions in the high resolution images and the diffraction pattern.
e) Compare the interplanar distances obtained from the diffraction patterns to the ones obtained from the FFTs from the high resolution lattice image of each region (MnO inclusions and LSMO matrix). To get interplanar distances using the FFTs the students use the HREM image of the substrate for calibration.

Comments:

Prior to the laboratory demonstration the students are introduced to the operating principles of the TEM and how the various image types are obtained. The students are also asked to read a reference paper on the structure of LSMO films,[1] which contains images like the ones they have to analyze in this experiment. They are also introduced to the differences and similarities between a transmission optical (light) microscope and a TEM. The instructor also explains briefly how a TEM sample is prepared so that the electrons can actually go through it without being completely absorbed.

To help visualize the relationship between real space lattice and reciprocal lattice the students are asked to compare

- The FFT obtained from the diffraction pattern to the lattice image and
- The FFTs from the MnO and LSMO regions in the lattice image to the corresponding spots in the diffraction pattern.

The instructor also demonstrates how by the different DF images one can identify which regions of the sample give rise to the different spots in the diffraction pattern. Namely, the dark field images obtained with MnO spots contain bright regions where the inclusions are and a dark background for the matrix. The contrast is reversed when the spot selected for the dark field image is from the matrix. (See Fig. 2)

During the demonstration, and later when the students print the pictures, the instructor emphasizes the fact that dislocations can be clearly seen at the interfaces between the inclusions and the matrix in the plan view images while they are not visible in the cross section images. This is because the out of plane interplanar distances are continuous across the interfaces (i.e., the (002) MnO spot overlaps with the (006) LSMO spot). In contrast, in the plan view images none of the MnO spots overlap with any of the LSMO spots.

The instructor describes how the LSMO film has formed a fairly regular structure of columns of MnO in a LSMO matrix even though nothing special was done during the deposition of the film. This is an example of self-assembled structures in a magnetic material.

Acknowledgments

This work was supported by the National Science Foundation (MRSEC) under grant No. DMR 00-80008

References:

1. Y.H. Li, L. Salamanca-Riba, Y. Zhao, S.B. Ogale, R. Ramesh and T. Venkatesan, J. Mater. Res. 15, 1524-7 (2000).

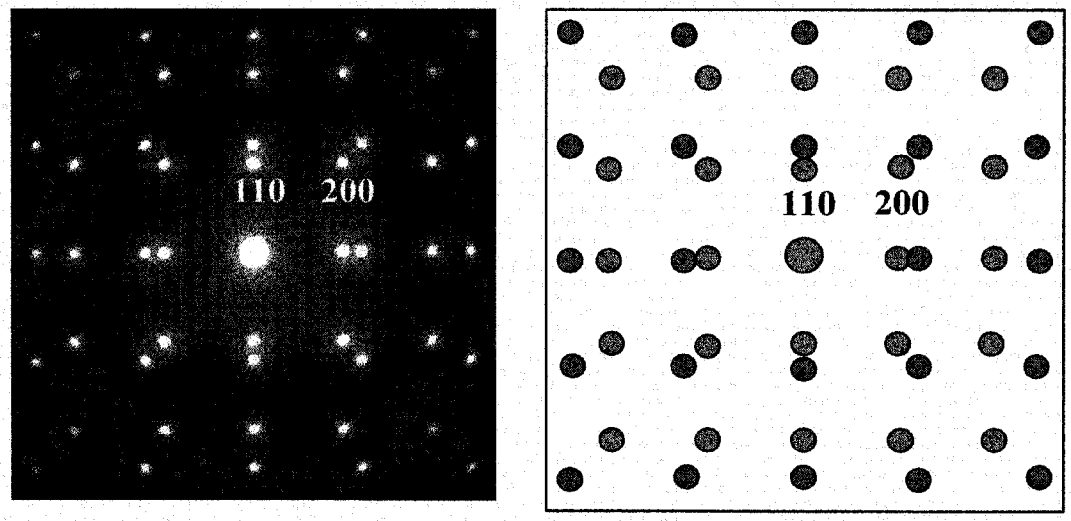

Fig. 1 SADP of LSMO film. Superposition of two patterns as shown in schematic on right is indicative of two structures present in the film.

THE ATOMIC MASS UNIT AND THE AVOGADRO CONSTANT: AN APPROACH TO INTRODUCE THESE CONCEPTS

Carlos E. Umaña

Department of Materials
School of Mechanical Engineering
University of Costa Rica
San Jose, Costa Rica

Telephone: 506-207-4548
e-mail caruma@terraba.fing.ucr.ac.cr

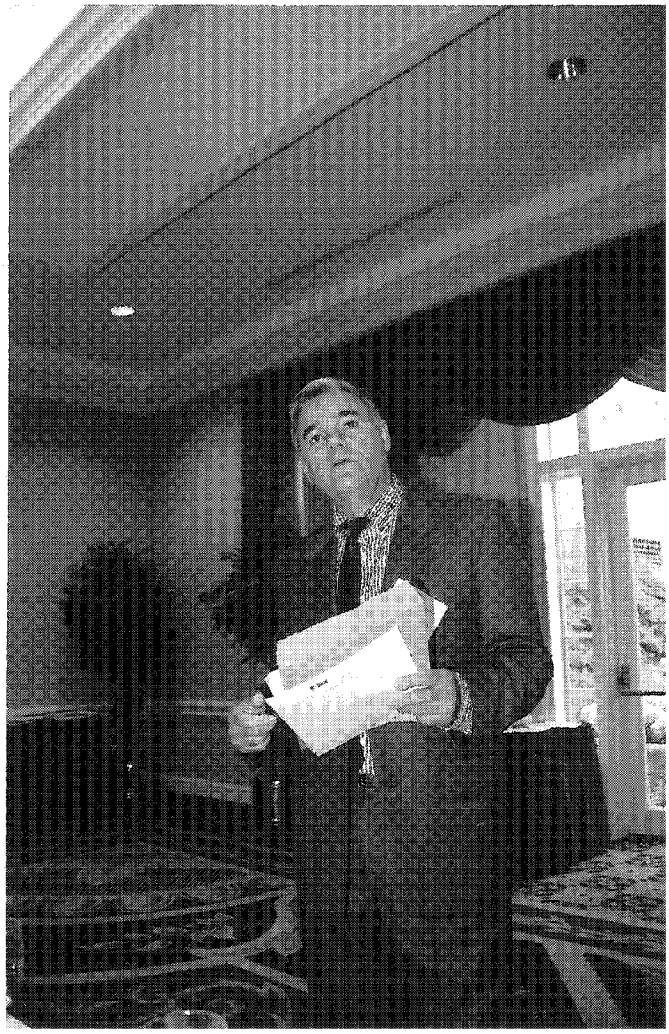

Carlos E. Umaña

THE ATOMIC MASS UNIT AND THE AVOGADRO CONSTANT: AN APPROACH TO INTRODUCE THESE CONCEPTS

Carlos E. Umaña
Department of Materials
School of Mechanical Engineering
University of Costa Rica
San José, Costa Rica

KEY WORDS: Absolute and relative scalar quantities, International System of Units (SI), isotope, mass spectrometer.

PREREQUISITE KNOWLEDGE:
Have an introduction to the atomic mass parameters and a basic understanding of the Dempster spectrometer.

OBJECTIVES:
1. To analyze scalar quantities and propose an atomic mass nomenclature.
2. To explain in a logical sequence how the atomic mass unit and the Avogadro constant are defined and related to each other.
3. To show how the values of these constants have been changing during the last thirty years.

INTRODUCTION:
Most textbooks in the fields of chemistry, physics and materials science present an incomplete or a weak treatment of the origins and fundamentals of the atomic mass unit and the Avogadro constant. Sometimes explanations do not follow a logical sequence or the key concepts are omitted. As a result confusion or misunderstanding about these basic constants is usually generated amongst students and even amongst instructors.
Two main problems are identified: In the first place it is not usually clearly stated that mass spectrometers play a very important role concerning the necessity of having a relative atomic mass unit definition, due to the fact that absolute atomic masses cannot be experimentally obtained with mass spectrometers. Secondly the direct relationship existing between the Avogadro constant and the atomic mass unit is not usually well established.
It is the intention of the author that the content of this paper should be helpful as an introduction to these topics in any basic course in chemistry, physics or materials science.

SCALAR QUANTITIES:
In order to make the demonstrations on which this work is based, it is necessary to go beyond the traditional definitions and take into account that scalar quantities actually consist of two components: a coefficient or numerical value and some sort of unit that defines the nature of the scalar quantity, e.g., mass, energy, length, etc. These units are either absolute or relative. The absolute units are the ones defined by the International System of Units (SI) and are classified into basic and derived units. The relative units consist of absolute units modified by numerical coefficients other than one (See Appendix A). Some examples of relative units are:

The angtrom [Å], defined as: $[Å] = 10^{-10}[m]$

Where: 10^{-10} is the numerical value of the relative unit [Å].
The meter [m] is a basic SI unit.

The electron volt is also a relative unit and is defined as: $[eV] = 1.602 \times 10^{-19}[j]$

Where: 1.602×10^{-19} is the numerical value of the relative unit [eV]
The joule [j] is a derived SI unit.

The atomic mass unit is also a relative unit but it will be analyzed in the following sections.

NOMENCLATURE:

Regarding the atomic mass parameters representation, it is important in the first place to promote the use of international symbols. For quantities not defined, it is convenient that symbols proposed, at least be in agreement with most occidental languages. Two basic parameters are the atomic mass unit and the atomic mass. In English the first quantity is usually identified as a.m.u. (Atomic mass unit) and in Spanish as u.m.a. (Unidad de masa atómica). Nevertheless, and regardless of the language, the international symbol that must be used is "u". This symbol was adapted in 1960 by the IUPAP and the IUPAC [1]. On the other hand the letters A.M. stands for atomic mass while in Spanish the letters M.A. (masa atómica) represent atomic mass. In this work the letter M is proposed and used as the symbol for mass. It has the advantage of avoiding language influence.
Since the atomic mass is a scalar quantity that can be either expressed with absolute or relative units, it is necessary to introduce symbolic expressions to take into account both cases. The absolute atomic mass of an isotope ${}^{A}_{Z}X$ will be represented as $M'_N\left({}^{A}_{Z}X\right)[kg]$, where $M'_N\left({}^{A}_{Z}X\right)$ is the scalar numerical value and $[kg]$ the absolute unit in kilograms. A and Z are the atomic mass number and the atomic number respectively. The relative atomic mass will be represented as $M_N\left({}^{A}_{Z}X\right)[u]$, where $M_N\left({}^{A}_{Z}X\right)$ is the scalar numerical value and $[u]$ the relative atomic mass unit.

THE MASS SPECTROMETER, THE ATOMIC MASS UNIT AND THE ISOTOPIC RELATIVE ATOMIC MASS CALCULATION:

Mass spectrometers are instruments used to find out the relative atomic mass of isotopes. Its operation requires the use of a standard isotope to calibrate the spectrometer. The standard used by international agreement is the ${}^{12}C$ isotope and it is arbitrarily assumed that the absolute atomic mass of this isotope is equal to $12[u]$. In other words:

$$[u] = \frac{M'_N\left({}^{12}C\right)}{12}[kg] \tag{1}$$

Which can also be expressed as:

$$[u] = u_N[kg] \tag{2}$$

Where: u_N is the numerical value of the relative atomic mass unit [u].

The exact value of $M'_N\left({}^{12}C\right)$ is unknown and for that reason the results obtained with the mass spectrometer are given in terms of [u] as is shown below.
The mass spectrometer measurements are based on adjustments of magnetic or electric fields [2]. The adjustment values "V" of the parameters that represent those fields are directly proportional to the isotopic atomic masses. For that reason it is possible to establish the following proportional relationship:

$$V\left({}^{12}C\right) \rightarrow 12 \cdot [u]$$
$$V\left({}^{A}_{Z}X\right) \rightarrow M_N\left({}^{A}_{Z}X\right) \cdot [u]$$

Which can be expressed as an equation, from where the numerical value of the relative atomic mass of an isotope is obtained as it follows:

$$M_N\left({}^{A}_{Z}X\right) = 12\frac{V\left({}^{A}_{Z}X\right)}{V\left({}^{12}C\right)} \tag{3}$$

Where:
$V\left({}^{12}C\right)$ = Adjustment value for the ^{12}C isotope
$V\left({}^{A}_{Z}X\right)$ = Adjustment value for the $\left({}^{A}_{Z}X\right)$ isotope

At this point it is important to emphasize how relative atomic masses are experimentally obtained without either knowing the ^{12}C absolute atomic mass or requiring the Avogadro constant.

With the mass spectrometer it is also possible to obtain the natural isotopic abundance percentage of the elements with a natural abundance different to 100%. The combination of these percentages with the $M_N\left({}^{A}_{Z}X\right)$ values gives rise to the weighted average of the isotopic relative atomic masses, $\overline{M}_N\left({}_{Z}X\right)$. Since more than one isotope are now involved, the symbol A is omitted. In Appendix B it is shown how $\overline{M}_N\left({}_{Z}X\right)$ is obtained.

THE RELATIONSHIP BETWEEN THE AVOGADRO CONSTANT AND THE ATOMIC MASS UNIT:

By definition, one mol of an isotope $\left({}^{A}_{Z}X\right)$ is an absolute scalar quantity with a numerical coefficient equal to the numerical value of the relative atomic mass $M_N\left({}^{A}_{Z}X\right)$ times 10^{-3}. Expressed as an equation,

$$1Mol = M_N\left({}^{A}_{Z}X\right) \cdot 10^{-3}[kg] \tag{4}$$

Taking into account that one mol is a mass amount composed of N atoms, each one with an absolute mass given by $M'_N\left({}^{A}_{Z}X\right)[kg]$; it then follows that,

$$M_N\left({}^{A}_{Z}X\right) \cdot 10^{-3}[kg] = M'_N\left({}^{A}_{Z}X\right) \cdot [kg] \cdot N \tag{5}$$

Hence,
$$N = \frac{M_N\left({}^{A}_{Z}X\right)\cdot 10^{-3}}{M'_N\left({}^{A}_{Z}X\right)} \tag{6}$$

By substituting for [u] from equation (2) into the relative atomic mass expression $M_N\left({}^{A}_{Z}X\right)[u]$, the following equation is obtained

$$M_N\left({}^{A}_{Z}X\right)[u] = M_N\left({}^{A}_{Z}X\right) u_N[kg] \tag{7}$$

From where it follows that the absolute atomic mass is given by

$$M'_N\left({}^{A}_{Z}X\right)[kg] = M_N\left({}^{A}_{Z}X\right) u_N[kg] \tag{8}$$

By combining equations (6) and (8), it is deduced that:

$$N = \frac{10^{-3}}{u_N} \tag{9}$$

In this way it is demonstrated that for a given u_N value there is a constant amount N of atoms in a mol. When u_N is defined according to equation (1), the number N is known as the Avogadro constant N_A.

THE EXPERIMENTAL ORIGIN OF N_A:

The numerical value of the atomic mass unit u_N depends on the numerical value of the absolute atomic mass of the ^{12}C isotope. However, as was mentioned before, this value is unknown and therefore N_A cannot be calculated from equation (9). The value of N_A is experimentally obtained and has been changing through the years as a result of worldwide research that is being done trying to achieve a more accurate value by developing more sophisticated experiments. Table 1 lists four N_A values and the years when they were reported.

There are also experimental efforts being carried out in order to obtain directly the value of u_N [3]. However the values reported until now are calculated by applying the experimental N_A results in equation (9), as can be confirmed in Table 1.

Table 1. Some values of the Avogadro constant and the corresponding atomic mass unit reported at different years.

N_A*	u [kg]*	Year	Reference
6.022169(40) X 10^{23}	1.660531 (11) X 10^{-27}	1969	[4]
6.022045(31) X 10^{23}	1.660565 (9) X 10^{-27}	1973	[5]
6.0221367(36) X 10^{23}	1.6605402 (10) X 10^{-27}	1986	[6]
6.02214199(47) X 10^{23}	1.66053873 (13) X 10^{-27}	1999	[7]

* The numbers within brackets are the standard uncertainty.

ADDITIONAL COMMENTS:

Finally it is important to mention that the atomic mass unit [u] should not be assumed to be numerically equivalent to the proton or neutron mass. All these quantities are independent from each other as it is deduced from the following facts:

1. The proton and neutron isolated masses are not equal, and when these particles joint to form a nucleus their masses become smaller and probably remain different.

2. The isotopic relative atomic masses obtained from mass spectrometers include the electron masses that remain in the atom after ionization. In other words if the atomic mass unit is defined as $\left(M_N^{/}\left({}_Z^A X\right)/A\right)\,[kg]$ in such a way that any isotope of any element can be used as a reference, then the numerical value $M_N^{/}\left({}_Z^A X\right)/A$ will be different in every case while proton and neutron masses remain constant. Observe that the established $M_N^{/}\left({}^{12}C\right)/12$ value is only a specific case out of many possibilities.

REFERENCES:

1. B.W. Petley, "The atomic mass unit", IEEE Trans. Instrum. Meas. Vol. 38. N°2. April 1989.
2. K.W. Whitten, K.D. Gailey and R.E. Davis,"General Chemestry", Saunders College Publishing, 3th edition, 1980.
3. M. Glasër,"Proposal for a novel method of precisely determining the atomic mass unit by the accumulation of ions", (PTB) Physikalisch-Technische Bundesanstlt, Braunschweig, Germany, Rev. Sci. Instrum. 62(10), 2493-2494 (1991)
4. B. N. Taylor, W. H. Parker, and D. N. Langenberg, Rev. Mod. Phys., vol.41, pp.375-496, July 1969.
5. E.R. Cohen and B.N. Taylor, "The 1973 least-squares adjustment of the fundamental physical constants", J. Phys. Chem. Ref. Data, vol. 2, pp. 663-734, 1973.
6. E.R. Cohen and B.N. Taylor, "The 1986 adjustment of the fundamental physical constants", CODATA Bulletin 63, Oxford, U.K.: Pergamon, and Elmsford, N.Y, : Maxwell, Dec. 1986.
7. P.J. Mohr and B.N. Taylor, CODATA Recommended Values of the Fundamental Physical Constants: 1998, available at NIST site: http://physics.nist.gov/cuu/Constants/index,html

ACKNOWLEDGMENT:

The author wishes to thank the Universidad de Costa Rica (Vicerrectoría de Investigación), la Fundación de la Universidad de Costa Rica para la Investigación
(FUNDEVI) and the Ministerio de Ciencia y Tecnología - Conicit for giving financial support to attend the NEW : UP DATE 2001.
I also want to thank Prof, Allan Bloomfield for reviewing the grammar and vocabulary of this paper.

Appendix A. SCALAR QUANTITIES

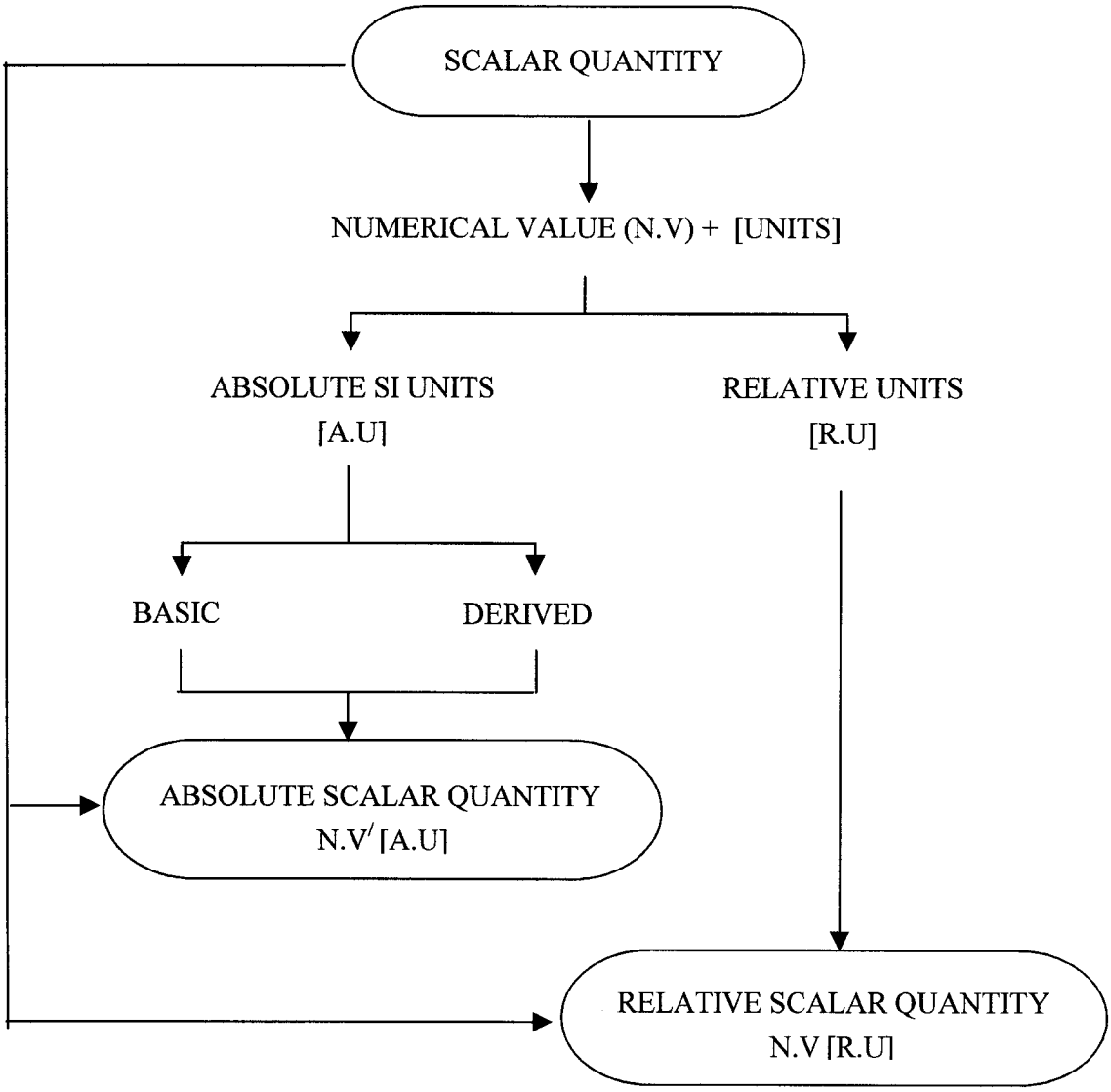

But, $R.U = RU_N\ [A.U]$

Where RU_N = Absolute numerical value of relative units

Substituting R.U and comparing absolute and relative scalar quantities it is obtained:

$$N.V' = N.V\ .\ R.U_N$$

Appendix B. THE WEIGHTED AVERAGE OF THE ISOTOPIC RELATIVE ATOMIC MASSES

Suppose there is an arbitrary amount of an element $({}_{Z}X)$ with a total relative mass given by $M^{T}({}_{Z}X)[u]$. Let us assume that the element has only two natural isotopes with the following characteristics[1]:

Isotope	Relative Atomic Mass [u]	Natural Abundance %
$({}^{A1}_{Z}X)$	$M_N({}^{A1}_{Z}X)$	$\%({}^{A1}_{Z}X)$
$({}^{A2}_{Z}X)$	$M_N({}^{A2}_{Z}X)$	$\%({}^{A2}_{Z}X)$

If the total number of atoms in the sample is taken as N, it is deduced that:

$$M^{T}({}_{Z}X)[u] = M_N({}^{A1}_{Z}X)[u]\ \frac{\%({}^{A1}_{Z}X)}{100}N\ + M_N({}^{A2}_{Z}X)[u]\ \frac{\%({}^{A2}_{Z}X)}{100}N \qquad \text{(A1)}$$

Dividing both members by $[u]$ and N and substituting $\frac{M^{T}({}_{Z}X)}{N}$ for $\overline{M}_N({}_{Z}X)$ it follows that:

$$\overline{M}_N({}_{Z}X) = M_N({}^{A1}_{Z}X)\ \frac{\%({}^{A1}_{Z}X)}{100} + M_N({}^{A2}_{Z}X)\ \frac{\%({}^{A2}_{Z}X)}{100} \qquad \text{(A2)}$$

Where: $\overline{M}_N({}_{Z}X)$ is the weighted average of the isotopic relative atomic masses.

Finally it is important to establish that the symbolic representation of any element in the periodic table, according to the nomenclature already proposed, is the following,

$$\begin{array}{|c|}\hline Z \\ ({}_{Z}X) \\ \overline{M}_N({}_{Z}X) \\ \hline\end{array}$$

For the silicon, as an example, the meaning of the symbols is:

$Z = 14$
$({}_{Z}X) = Si$
$\overline{M}_N({}_{Z}X) = 28.086$

[1] The demonstration applies to elements with any number of natural isotopes.

THE ONSET OF TENSILE INSTABILITY

Mike L. Meier

and

Amiya K. Mukherjee

Department of Chemical Engineering and Materials Science
University of California, Davis
Davis, California 95616

Telephone: 530-752-5166
e-mail mlmeier@ucdavis.edu

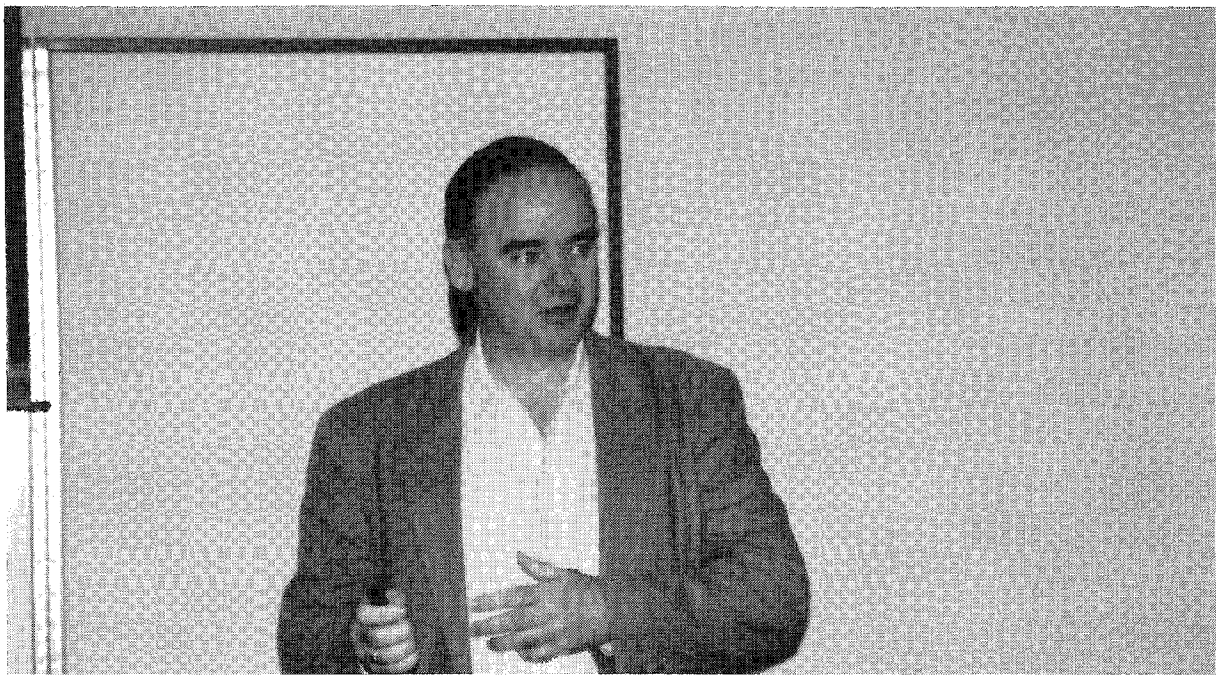

Mike L. Meier

THE ONSET OF TENSILE INSTABILITY

Mike L. Meier, Amiya K. Mukherjee
Department of Chemical Engineering and Materials Science
University of California, Davis
Davis, CA 95616

Key Words:
Tensile test, mechanical properties, Young's modulus, yielding, strain hardening, geometric softening, necking, modulus of toughness, modulus of resilience, fracture.

Prerequisite Knowledge:
Basic knowledge of mechanical properties in tension, digital data acquisition and spreadsheets.

Objective:
Introduction of mechanical properties obtained from tensile testing with an emphasis on being able to fully analyze the data, in particular the phenomenon associated with the onset of necking.

Equipment:
1. Cylindrical tensile specimens
2. Extensometer
3. Tensile test system of suitable load capacity and which acquires data digitally.
4. A computer with Microsoft Excel, Corel Quattro Pro, or another suitable spreadsheet program.

Introduction:
In this experiment the plastic deformation behavior and the onset of plastic instability of some common structural alloys is investigated. The usual mechanical properties are measured from stress-strain curves, but in addition, strain hardening behavior and the onset of plastic instability are studied. Much more is happening during a tensile test than is listed in standard materials properties data tables. The goal of this experiment is to investigate these additional phenomena.

Elastic Deformation: When an isotropic material is loaded to stresses below the yield point and then unloaded again all of the deformation is immediately recovered. This behavior is usually associated with the linear portion of the stress-strain curve, although not all materials exhibit this linear-elastic behavior; for example, rubber is an exception. But for many materials the resistance to deformation in this region is given by Young's modulus Y, which also is often represented by an E, is simply the slope of the stress-strain curve in the linear region

$$Y = \frac{\Delta\sigma}{\Delta\epsilon}. \tag{1}$$

where σ is the true stress and ϵ is the true strain. When measuring Young's modulus one must take into account the stiffness of the testing machine. Ideally, the machine should be perfectly

Young's modulus above is given here in terms of the slope of the true stress-strain curve. In many cases it is measured from the slope of the load-elongation (ΔF - ΔL)

$$Y = \frac{\Delta F}{\Delta L}\frac{L_0}{A_0} = \frac{\Delta S}{\Delta e}$$

or engineering stress-strain (ΔS - Δe) curve. (A_0 is the initial cross-sectional area of the specimen, L_0 is the initial gage length.) ASTM standard E 111-82 recommends using this method unless the strain exceeds 0.25% in which case this standard recommends taking into account the changes in gage length and area, in other words, the true stress-strain curve. The differences in the two values of Young's modulus is only about 0.5% for steel (Y=209 GPa).

stiff but in reality its stiffness may be in the neighborhood of 200,000 pounds per inch. A low machine stiffness will introduce errors in the measured modulus as given by

$$Y_{measured} = Y\left[1 + \frac{A_0 Y}{K L_0}\right]^{-1} \tag{2}$$

where A_0 is the initial cross-sectional area of the specimen, L_0 is the initial gage length, Y is the correct value of Young's modulus and K is the stiffness of the testing machine [1]. The error in the measured modulus results primarily from errors in measurement of elongation. The specimen is a monolithic part while the testing machine has the grips, clevis pins, threaded parts and moving parts that mesh better when loaded means the specimen is generally stiffer than the testing machine. Consider also that the modulus is the ratio of stress, a large number, to strain, a small number. The result is very sensitive to errors in the denominator.

When conducting a constant crosshead speed test one can compute the stiffness of the testing machine K using the equation

$$K = \left(\frac{\dot{x}}{\dot{F}} - \frac{L_0}{A_0 Y}\right)^{-1} \tag{3}$$

where $\dot{x}$ is the crosshead speed and $\dot{F}$ is the loading rate [1]. Or, one can use an extensometer to measure strain directly from the specimen, or one can attach strain gages to the specimen.

Yielding: Yielding occurs when deformation changes from being mostly elastic to mostly plastic. By this definition the method of measuring the yield strength may seems somewhat arbitrary, which it is, however, standard methods have been established so that everyone will get the same result. In fact, there are a number of standard methods available and the method used varies depending on the type of yielding behavior (gradual, sharp, upper/lower), industry, or country. Offset techniques are used when yielding is gradual while sharp and upper/lower type yielding behaviors are easily read from the stress-strain curve. In the case of the upper/lower yielding

behavior which is characteristic of carbon steels and a few other alloys the lower yield stress is taken as the yield strength due to the fact that (1) accurate measurements of the upper yield strength are difficult to make and (2) the lower yield stress is the stress where normal, homogeneous plastic deformation begins.

Strain Hardening: Plastic deformation can occur by three different processes: diffusional processes, twinning and dislocation motion. The contribution of diffusional processes is important at high homologous temperatures, $T > 0.6\ T_{mp}$, and twinning might account for up to a few per cent strain. Dislocation processes are the dominant deformation mechanism of plastic deformation at normal temperatures. Considering only the contribution due to dislocation processes, a shear stress acting parallel to the slip plane causes these dislocations to move through the lattice. As they move they may encounter obstacles such as solute atoms, particles, grain boundaries and other dislocations, effectively impeding their motions until the stress is increased enough to allow the dislocation to overcome the obstacle. As the dislocations glide, climb and cross-slip through the lattice additional dislocations were being generated and start moving through the lattice. With this ever increasing dislocation density the distance between them decreases, they encounter each other more often, and it becomes increasingly difficult to deform the material. This process is called strain hardening.

There are two well known equations that depict the strain hardening phenomenon. The Hollomon equation describes strain hardening as a power law function of stress and strain after yielding. Hollomon's equation is

$$\sigma = K\epsilon^n \tag{4}$$

where σ and ϵ are true stress and strain, n is the strain hardening index and K is the strength coefficient which is equal to the stress at ϵ=1. The second equation is Ludwik's equation which is often preferred because, unlike the Hollomon equation, it does not suggest that strain hardening begins at the very start of the tensile test. It includes a term for the yield stress σ_o

$$\sigma = \sigma_0 + K\epsilon^n \tag{5}$$

where σ_o is given by

$$\sigma_0 = \left(\frac{K}{E^n}\right)^{\frac{1}{1-n}}. \tag{6}$$

In cases where the material has already experienced some plastic deformation (ϵ_0=prior strain) the following equations represent strain hardening:

$$\sigma = K(\epsilon + \epsilon_0)^n \tag{7}$$

$$\sigma = \sigma_0 + K(\epsilon + \epsilon_0)^n. \tag{8}$$

The strain hardening index n is a constant for a given material and can range in value from 0 to 1 but is typically in the range of 0.2 to 0.5. The strain hardening index can be written as

$$n = \frac{d\log(\sigma)}{d\log(\epsilon)} = \frac{\epsilon}{\sigma}\frac{d\sigma}{d\epsilon} \tag{9}$$

and it can evaluated numerically or graphically from the slope of a plot of log(σ) -vs- log(ϵ) where n is equal to the slope of the resulting line. If the Hollomon equation is obeyed the line will be straight, but if the Ludwik equation represents the data or the specimen had been deformed prior to the tensile test the line will be concave up (figure 1). In these cases the values of σ_o and ϵ_o must be known in order to determine the value of n.

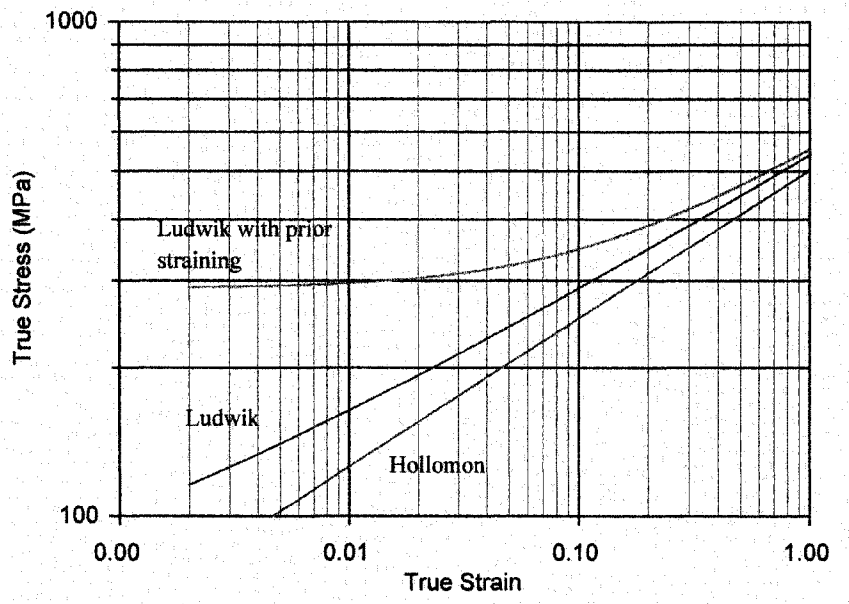

Figure 1. Log-log plots of stress-strain curves calculated using Hollomon's equation, Ludwik's equation and Ludwik's equation with 10% prior straining. (K=500 MPa, n=0.3, E=207 MPa)

The above equation allows one to express strain hardening dσ/dϵ in terms of the rate of increase of stress with respect to strain. Rewriting it as

$$\frac{d\sigma}{d\epsilon} = n\frac{\sigma}{\epsilon} \tag{10}$$

shows that the rate of strain hardening (slope of the stress-strain curve) is proportional to the stress divided by strain.

Strain Rate Hardening: Most materials are sensitive to the rate of deformation, especially at elevated temperatures. This behavior often obeys a power law expression such as

$$\sigma = A\dot{\epsilon}^m \tag{11}$$

where A is a constant at given temperature and metallurgical condition, $\dot{\epsilon}$ is the true strain rate and m is the strain rate sensitivity. This equation can be combined with the Hollomon equation for a general description of the plastic deformation of materials

$$\sigma = B\dot{\epsilon}^m \epsilon^n. \tag{12}$$

At low and ambient temperatures the rate of strain hardening is significant, $0.2<n<0.5$, while the rate sensitivity is small, $0.001<m<0.01$. At higher temperatures just the opposite is true and the strain rate sensitivity can reach values as high as 1.0 (Newtonian viscosity) while the strain hardening index may approach zero. A value of $m=0.5$ is considered characteristic of superplasticity, a condition where elongations of 100's even 1,000's percent strain are possible due to the stability of the neck that may forms at the UTS.

While the strain rate sensitivity can effect the flow stress, it is more important in terms of its effect on ductility. Increased strain rate sensitivity slightly increases the strain at which the material starts to neck, but more significantly it can extend ductility considerably by stabilizing the neck. As the specimen begins to neck the strain rate in the necked region increases and due to the strain rate sensitivity the stress in this region increases and thus the neck stabilizes. So while the strain hardening index is a measure of a material's resistance to the onset of instability, the strain rate sensitivity is a measure of its resistance to necking.

Tensile Strength: The tensile strength S_{TS} [formerly called the ultimate tensile strength (UTS) but now considered an obsolete term] is the maximum nominal stress. This property represents the load bearing capacity of the material. It also occurs at the strain where necking begins. The subsequent drop in stress beyond this point is due to the *geometric softening* associated with the localized thinning and deformation of the specimen.

If a true stress-true strain curve could be obtained directly from a tensile test, rather than an engineering stress-strain curve, one would find that there is no maximum stress prior to failure. There would appear to be no tensile strength. That is not to say that necking has not occurred or that there is no tensile strength, but that other methods must be employed to determine its value and the strain at which it occurred.

There are several methods for determining the tensile strength σ_{TS} from a true stress-strain curve. One method is to plot both the true stress and the rate of strain hardening against true strain as shown in figure 2. The point where these two lines intersect marks the tensile strength and the strain where necking begins. This method is expressed in the following equation

$$\sigma = \sigma_{TS} \text{ when } \frac{d\sigma}{d\epsilon} = \sigma. \tag{12}$$

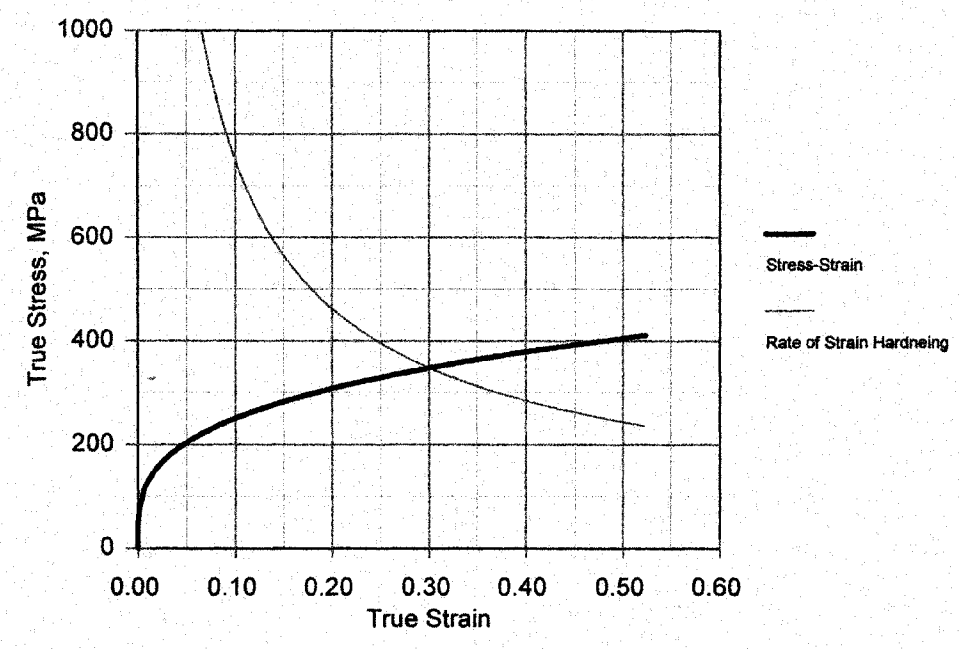

Figure 2. Stress-strain and rate of strain hardening curves calculated using the Hollomon equation. (K=500 MPa, n=0.3)

While this relationship may be derived from the Hollomon equation it also works for stress-strain behaviors which do not obey the Hollomon equation.

The above equation also gives us a second method of determining the tensile strength – the unit subtangent method. Using this method the tensile strength may be found by locating a point on the true stress-true strain curve which has a subtangent of unity (intersects the strain axis at strain ϵ_{TS} -1). Furthermore, it may be shown that

$$\sigma = \sigma_{TS} \text{ when } \frac{d\sigma}{de} = \frac{\sigma}{1+e}. \tag{12}$$

This is Considère's criterion, a third method for determining the tensile strength. It is also a graphical method that requires a plot of true stress versus nominal strain whose origin is set at the yield point. The tensile strength σ_{TS} is obtained by drawing a subtangent from a nominal strain of -1. The nominal tensile strength S_{TS} is the point where this line intersects the stress axis. (See figure 3.) If power law hardening is observed then Considère's criterion may also be used to derive one last expression for the tensile strength

$$S_{TS} = Kn^n(1-n)^{1-n}. \tag{13}$$

Onset of Plastic Instability: Generally, the strain at the maximum load marks the onset of plastic instability. For annealed materials the rate of strain hardening immediately after yielding is

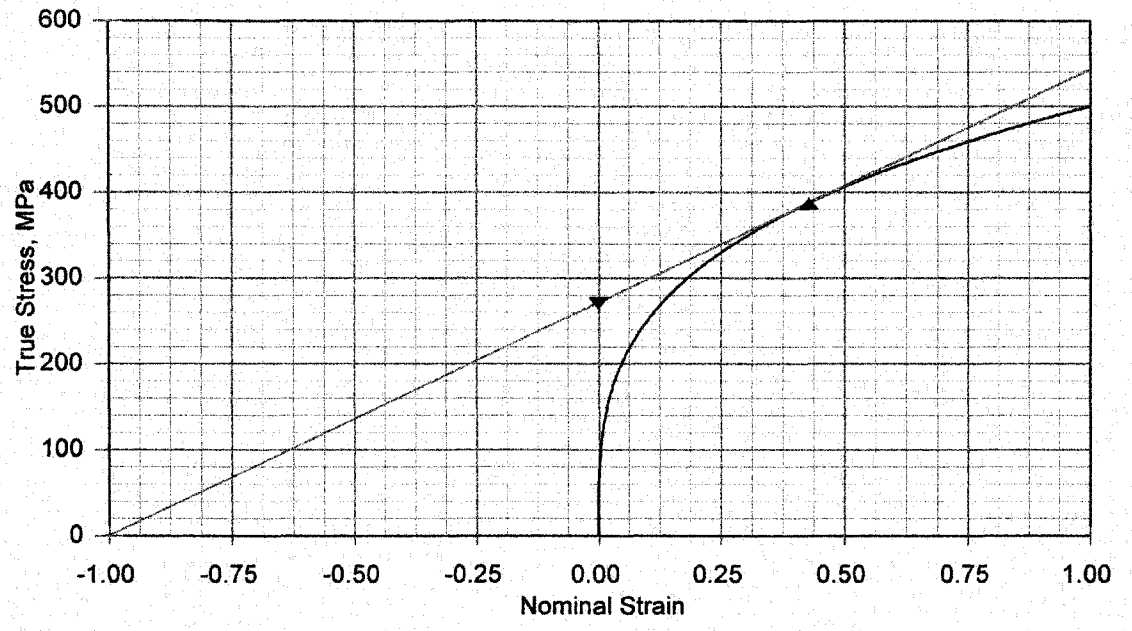

Figure 3. Considère's construction for determining the tensile strengths (S_{TS}=▼=271 MPa, σ_{TS}=▲=388 MPa) of a ductile material. The stress-strain curve was calculated using Hollomon's equation (K=500 MPa, n=0.3).

relatively high, but as deformation continues, the rate of strain hardening steadily decreases. At the same time the specimen is becoming thinner. Eventually the rate of strain hardening and specimen thinning are equal. Beyond this point the rate of specimen thinning is greater than the rate of strain hardening and deformation is unstable, i.e., necking begins. The instability will start in some part of the specimen where an inhomogeneity (soft spot, adjacent to a hard spot) or at a machining defect (stress concentration) exists. Once localized deformation begins the stress in this region will be higher than elsewhere, causing deformation to become even more localized, leading to the formation of a macroscopic neck.

For rate insensitive materials, the onset of unstable deformation occurs at the strain where maximum load is obtained. It was mentioned earlier that the strain hardening index is a measure of the resistance to the onset of instability. It can be shown that the strain hardening index for rate insensitive materials is equal to the true strain where necking begins.

$$\epsilon_{TS} = n \tag{14}$$

For rate sensitive materials the onset of necking will differ but only slightly. The most important aspect of rate sensitivity is that it tends to stabilize the neck, decreasing its degree of localization, and extending ductility well past ϵ_{TS}.

Ductility and Localized Deformation: During nonuniform deformation stresses are concentrated in the necked region of the specimen, leading to a more complex, triaxial, stress state.

Bridgeman [2] has developed a method for computing the stress distribution in the necked region and making corrections to the stress-strain data based on the radius and area at the root of the neck.

The onset of instability often marks the limit of useful deformation. However, neck growth is slow at first and additional straining can occur before the instability is either noticeable or significant. The amount of straining beyond this point is affected primarily by the strain rate sensitivity of the material. For example, maximum load is often reached at about 10-15% strain, which is usually around half the strain to fracture for rate insensitive materials (m ~0.01). Superplastic materials, however, have high rate sensitivities (m~0.5) and may be strained hundreds and even thousands of percent. The maximum load, however, occurred at around 10% strain. The high rate sensitivity stabilized the neck.

Fracture: With continued plastic deformation a material accumulates damage associated with dislocation processes. Dislocations that pile up at grain boundaries and other obstacles can form microcracks. Tensile stresses can open these into voids which grow and eventually coalesce, forming larger cavities. Final fracture occurs when the number and sizes of internal voids is sufficient to exceed the material's ability to withstand the applied load. These voids introduce stress concentrations which can lead to the spontaneous growth of a single crack. (This behavior is the subject of the field of fracture mechanics.) Inspection of the fracture surfaces permits determination of the fracture process involved, i.e., brittle, shear, or ductile. Close inspection of the cup-and-cone fracture surfaces of a ductile material may reveal areas where void formation and coalescence occurred and the area through which the final rupture occurred. A scanning electron microscope is usually required to determine whether the crack propagated intergranularly or transgranularly and how much plastic deformation occurred as the crack propagated.

The strain to fracture is not an intrinsic property of the material. It also depends on the specimen geometry. An expression that relates specimen geometry to ductility is

$$\epsilon_f = C\frac{A_0^{1/2}}{L_0} \tag{15}$$

where C is a proportionality constant [3]. Ideally, comparisons of strain to fracture should be made using specimens of identical design. If this isn't possible, the comparisons should be made on similarly shaped specimens. Corrections based on the $A^{1/2}/L$ ratio may be made. ASTM 370 describes how to make comparisons of round and flat specimens.

Procedure:

Preparation

1. Plot true stress versus true strain for a hypothetical material using either the Hollomon or Ludwik equation. Experiment with the values of K and n to see how their values effect the results. Note the value of the stress as true strain approaches 100%.

2. Determine the tensile strength for the stress-strain curve in the question above.

3. Calculate and plot an engineering stress-strain curve using the data calculated in question 1.

4. Compile mechanical properties data on the specific materials to be tested.

5. Note the specifications of the tensile tester and compare them to the load and elongation requirements for the tensile tests.

6. For the crosshead speed you plan to use, determine the data acquisition rate you will need in order to record enough data in the elastic region to be able to determine Young's modulus.

Materials

Specimens made of plain carbon and low alloy steels, aluminum, and plastics are available. All specimens are round with threaded ends. They all have a 2 inch gage lengths and either an 0.236 or 0.505 inch diameter.

Tensile Testing

Inspect the equipment and become familiar with how it operates. Check the calibration of the load cell and extensometer and make adjustments as required.

Select a specimen to test and measure and record its gage length, diameter, etc. Note the specimen's composition and processing, and then estimate the maximum load that will be generated during the tensile test.

Tensile test the specimen to failure. During the test monitor the load and elongation and watch the specimen carefully to see when necking begins.

After the specimen fractures, remove the broken halves and note the geometry of the fracture and the fracture surfaces. Do not try to fit the halves of the specimen back together again as this will damage the fracture surfaces. You'll probably want to examine the fracture surfaces under a low power microscope or a scanning electron microscope.

Data Analysis

Perform a comprehensive analysis of the data from the tensile tests by importing the data into your spreadsheet program. Construct the stress-strain curves and measure all of the usual mechanical properties including the energy capacities of the material. Analyze the strain hardening behavior and finally, investigate the onset of tensile instability.

Stiffness: Determine the value of Young's modulus using a regression or best fit routine. How does your value compare to the published value?

Optional: Repeat this analysis using data from a tensile test which did not utilize an extensometer. Compare this value to the previous value. This value is typically a factor of 10 to 20 lower than the value obtained using an extensometer. Determine the stiffness of the testing machine.

General Mechanical Properties: Compute the other basic mechanical properties that may be obtained from a tensile test.

- Stress
  - Yield strength, (upper and lower, offset, etc.)
  - Tensile strength (stress at maximum load)
  - Stress at fracture
- Strain
  - Strain at yielding
  - Strain at the onset of necking (observed and from the stress-strain curve)
  - Strain at failure
  - Reduction of area at failure (measured from the specimen)
- Energy capacity
  - Work required to cause failure (area under the whole load-elongation curve)
  - Modulus of resilience (area under the elastic portion of the stress-strain curve)
  - Modulus of toughness (area under the whole stress-strain curve)

Compare these properties to those in reference books.

Strain Hardening: Use a least squares or regression analysis to determine the values of n and K in the Hollomon equation. Comment on the values obtained. Are these typical values? Does the Hollomon equation do a satisfactory job of representing the stress-strain behavior of these materials?

Tensile Strength: Determine the tensile strength using the engineering stress-strain data. Next, determine the tensile strength using the rate of hardening method. Finally, locate the tensile strength on the true stress-strain curve using only the value of the strain hardening exponent. Do all three methods give the same answer?

Optional: Construct a graph similar to figure 3 to determine the tensile strength.

Onset of Instability: At what point in the test did you first observe necking of the specimen? Compare this to the strain where maximum load (tensile strength) occurs on the stress-strain curve. Do the Hollomon strain hardening index and strain at the onset of instability coincide?

Fracture: Examine the fracture surfaces of each specimen. Did fracture occur in a ductile or brittle manner?

Measure the final cross-sectional area of the fractured specimen and compute the true stress at fracture. Compare this to the engineering stress that was obtained at the same strain and the true stress that the Hollomon equation would predict. One would expect it to be lower. Why? Was it?

Comments:
The analysis of the data requires mostly basic spreadsheet skills and the ability to lay out the solution to problem in a sensible and organized manner. A typical spreadsheet will include a header section (owner, file name, creation and revision dates, etc.), a parameters section (gage length, gage area, crosshead speed, etc.), and a results section where the results of the analysis of the data are listed.. The bulk of the data will be in 10 or more columns containing, starting with column 1, the original load-elongation data, elongation data corrected for the toe of the curve, load-elongation data converted to the desired units, nominal stress-strain calculated from the load-elongation data, true stress-strain data calculated from the nominal stress-strain data, and additional columns which are required to measure selected mechanical properties. Building this spreadsheet can be quite a task unless one lays it out in a simple and direct manner.

The difficulty of the analysis of the mechanical properties from the columns of raw data can range from the use of simple @max() and @sum() functions to the more advanced regression analysis procedures. Other clever techniques may have to be devised to be able to determine the offset yield strength (if appropriate). In addition, one must also construct appropriate graphs that both illustrate each property and verify that the analysis has been done correctly. For example, after using a regression routine to determine the value of Young's modulus, one should then calculate the elastic portion of the stress-strain curve using this value and plot it along with the experimental data. One should then calculate the linear elastic portion of the stress-strain curve again but this time applying a strain offset so one can see where this line crosses the experimental stress-strain curve. To accurately locate the offset yield stress one can then subtract the measured stress from the calculated stress and the search the column of data to find the value closest to zero. Similar procedures and graphs should be used to determine the tensile strength using the rate of hardening method, for fitting the Hollomon equation to the strain hardening region of the stress-strain curve, etc.

Employing the rate of strain hardening method to determine the true tensile strength and the onset of instability requires plotting the slope of the true stress-strain curve. Due to the noise in real experimental data the result will be unacceptable unless a smoothing technique such as box car smoothing is employed. We have found that averaging over 21 and sometimes many more data points gives good results.

References:

1. P.P.Gills and T.S.Gross, *Effect of Strain Rate on Flow Properties*, ASM Metals Handbook 9th edition, volume 8, page 44, (1985).

2. Bridgeman, P. W., *Transactions of ASM*, v.32, pp. 553-574, (1944).

3. Wyatt, Oliver H. and Dew-Hughes, David, *Metals, Ceramics and Polymers*, Cambridge University Press, London, p.143, (1974).

4. Polakowski, N.H. and Ripling, E.J., *Strength and Structure of Engineering Materials*, Prentice-Hall, New Jersey, (1966).

Biography:
Michael L. Meier received his B.S. in Materials Engineering from North Carolina State University in 1979 and his M.S. (1986) and Ph.D. (1991) in Materials Science and Engineering from the University of California, Davis. After a two-year post-doctorate position at the Universität Erlangen-Nürnberg in Erlangen, Germany he returned to UC Davis to set up new research laboratories and to manage the laboratory teaching program. He is now the director of Materials Science Central Facilities.

Amiya K. Mukherjee received his M.S. degree in Physical Metallurgy from the University of Sheffield (1959) and D.Phil. degree in Metallurgy and Science of Materials from Oxford University, England (1962). From 1962-65 he was associated with the Lawrence Berkeley National Laboratory and the Department of Materials Science at the University of California, Berkeley, where he worked on application of dislocation theory to the understanding of thermally activated deformation mechanisms in crystalline materials. He was a Senior Scientist at the Battelle Memorial Institute in Columbus, OH (1965-66) primarily working on fracture and failure processes in engineering materials. In 1966 he was the first faculty recruited in the area of materials science at the University of California, Davis and he has been instrumental in developing the materials science program with his colleagues there since. He was promoted to full professorship in 1970.

His current research activities are in the areas of creep properties of metal and intermetallics, superplasticity, high temperature cavitation and failure phenomenon, synthesis, characterizations and processing of nanometals for enhanced plasticity including superplasticity, elevated temperature deformation characteristics of nanocrystalline thin film metallic multlayers, and processing and properties of nanoceramic composites for improved fracture toughness, creep resistance as well as superplasticity. Mukherjee has published over 350 research papers in journals and conference proceedings. He is a past Chairman of Materials Science Division of ASM International and of the Editorial Board of Metallurgical Transactions. He received the Distinguished Teaching Academic Senate Award, University of California, Davis (1978); Special Creativity Award for Research, NSF (1981); Alexander von Humboldt Senior Scientist Award, Germany (1988); AT&T Foundation Award from Amer. Soc. for Engineering Education (1988); University of Tokyo Centennial Gold Medal (1990); Albert Easton White Distinguished Teaching Award, ASM (1992); University of California Prize and Citation for Distinguished Teaching and Scholarly Achievement (1993); Pfeil Medal and Prize for Creativity in Research, Institute of Materials, U.K. (1994); the Bochvar Medal in Metals Physics from the University of Moscow (1996), Humboldt Professor, Max Placnk Institute, Germany (1997); and Senior Fellow, Ecole Polytechnique Federale Lausanne, Switzerland (2000).

Appendix A - Symbols, Conversion Factors and Equations for Stress and Strain

Symbols

Symbol	Description	Preferred Units
F	Force	N
L	Length	mm, cm or m
D	Diameter	mm, cm or m
A	Area	mm^2, cm^2 or m^2
S	Engineering stress	MPa
e	Engineering strain	-
σ	True stress	MPa
ϵ	True strain	-
t	Time	s

Conversion Factors

Description	Conversion Factors
Mass	1 kg = 2.207 lbs
Force	1 N = 10^6 dynes = 0.2248 lbf
Length	1 in = 25.4 mm = 2.54 cm = 2.54×10^{-2} m
Area	1 in^2 = 645.16 mm^2 = 6.4516 cm^2 = 6.4516×10^{-4} m^2
Stress, pressure	1 MPa = 1 MN/m^2 = 145 psi
Energy, work	1 J = 10^7 ergs = 6.242×10^{11} eV = 0.239 cal

Stress and Strain

	Nominal	True
Stress	$s = \frac{F}{A_0}$	$\sigma = \frac{F}{A}$
Strain	$e = \frac{\Delta L}{L_0}$	$\epsilon = \int_{L_0}^{L_f} \frac{dL}{L} = \ln\left(\frac{L_f}{L_0}\right)$
	$e = -\frac{\Delta A}{A_0}$	$\epsilon = \ln\left(\frac{A_o}{A_f}\right) = 2\ln\left(\frac{D_o}{D_f}\right)$ (See note 1)
Strain Rate	$\dot{e} = \frac{\Delta e}{\Delta t} = \frac{1}{L_0}\frac{\Delta L}{\Delta t}$	$\dot{\epsilon} = \frac{d\epsilon}{dt}$

Note 1: Constant volume is assumed ($A_0L_0 = A_fL_f$).

The true stress and strain can be written in terms of the nominal stress and strain, as long as the specimen has not started necking, by the equations

$$\sigma = s(e+1)$$

and

$$\epsilon = \ln(e+1).$$

Elastic Moduli

Modulus	Equation
Young's Modulus	$E, Y = \frac{\Delta\sigma}{\Delta\epsilon}$
Poisson's Ratio	$\nu = -\frac{\epsilon_x}{\epsilon_z}$, For constant volume $\nu = 0.5$
Shear Modulus	$G = \frac{\Delta\tau}{\Delta\gamma} = Y\frac{1}{2(1+\nu)} = K\frac{3(1-2\nu)}{2(1+\nu)}$
Bulk Modulus	$K = \frac{\Delta\sigma_{hyd}}{\frac{\Delta V}{V}} = G\frac{2(1+\nu)}{3(1-2\nu)}$

Appendix B - Sample Data from the Instron 4204 Universal Tester, Header and First 10 Data Points

```
    Sample id : ALUMINUM                    Test date :  30 Dec 1994
      Version : 1.08                      Version date :  30 May 1991
      Machine :  4200                       Robot used :  NO
 Report file# : 45                           Operator : Mike Meier

 X conversion :   .03937008               X A/D offset :          .0000
 Y conversion : ***********               Y A/D offset :          .0000

  Sample rate :        5.00               Extensometer : STD
2nd Sample rate :   1.00
   A/D range :   0                          Autostart : OFF
   Calib type : AUTOMATIC                    Geometry : RECTANGULAR
   Calib load :   11240.4500               Calib extens :        .0000
  Temperature :  25                          Humidity : 50
  Xhead speed :     .1000                   Units type : SI
    Test type : TENSILE                    # specimens :   1
     Bar type : E-45                       Entry dimens : YES
  Break check :    10.00000                Thresh delay :     4.49618
   Load limit : 11240.45000                Extens limit :      .98425

 Sample dimensions :
 A:      .2500   B:      .0559   C:     1.0000   D:  1.0000   E: NO
-------------------------------------------------------------------------------
   Specimen # :     1                     Test end status :   10
 Maximum load :    414.305                Max load point # :        235
   Max extens :       .140                Max extens pnt # :        420
       | 2nd. Speed | Extn. Remv | Relx  Strt | Range  Chg  |
 Point #          ---          ---          ---          ---
 Number of points :   420
 Specimen dimensions :
A:    .2500000 B:    .0559055 C:   1.0000000 D:   1.0000000 E: NO
 Transverse gauge: ---------
 Auxiliary Specimen Inputs:
******* ******* ******* ******* ******* ******* ******* ******* *******
 Auxiliary Sample Inputs:
******* ******* ******* ******* ******* ******* ******* ******* *******

 Calculations from Instron:
   |----------- Maximum ------------|------------ Break -------------|
   |Load        Displ.     Strain   |Load        Displ.     Strain   |
    414.32     .84252E-01********** ********** ********** **********
   |----------- Peak 1 ------------|
   |Load       Displ.     Strain   |
   ********** ********** **********
-------------------------------------------------------------------------------

     1,     .000060,      .000000
     2,     .000390,      .000000
     3,     .000720,      .000000
     4,     .001140,      .000000
     5,     .001470,      .000000
     6,     .001720,      .000000
     7,     .002050,      .000000
     8,     .002470,      .000000
     9,     .002720,      .000000
```

Appendix C - Sample Spreadsheet for 7075 Aluminum

This appendix shows the summary page of the spreadsheet used in the analysis of the tensile test data for 7075-T651 aluminum. Measured values are generally close to the reference values. The accuracy of the analysis of the strain hardening behavior was improved somewhat by assuming a prior strain of 0.02.

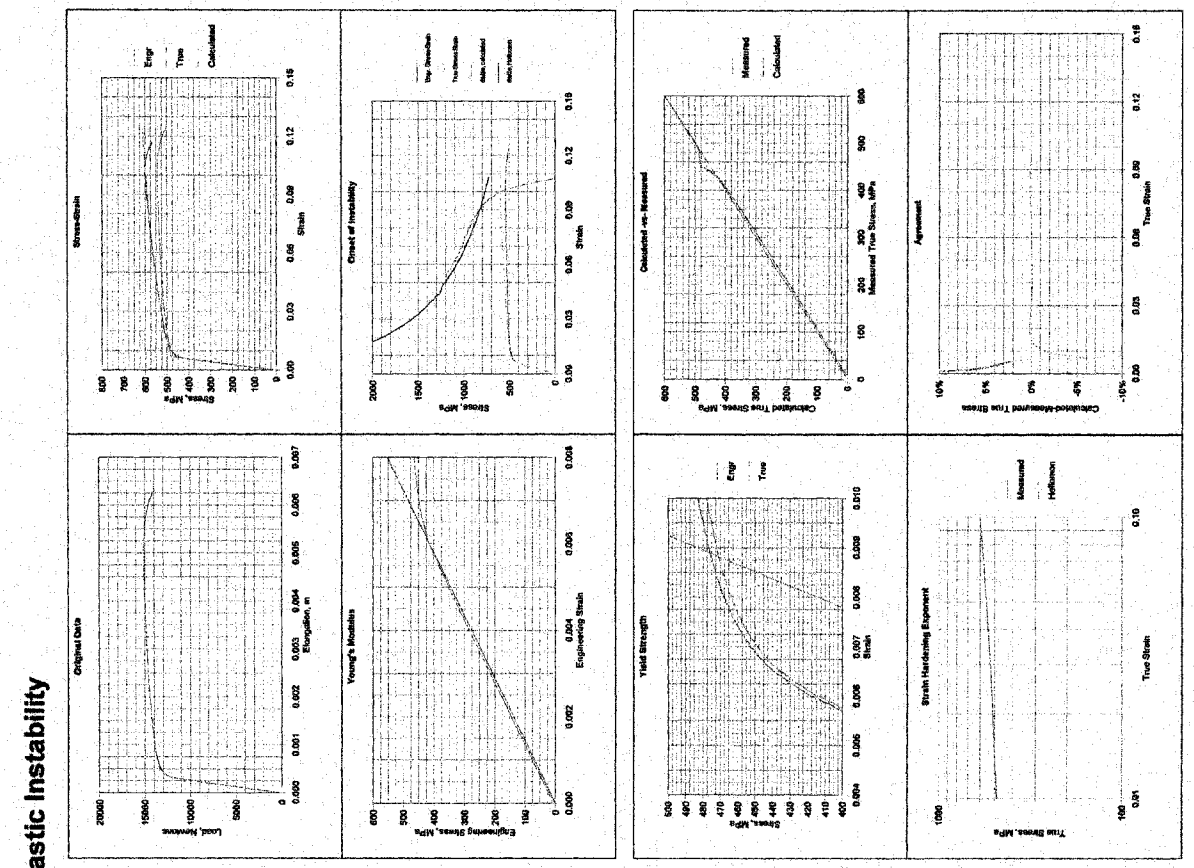

Plastic Deformation and the Onset of Plastic Instability

EMS-138L, Mechanical Properties of Materials Laboratory

File: 7075 Aluminum.wb3
Owner: Mike Meier
Created: January 24, 1995
Revised: July 23, 2001

Misc Constants

Stress:	145	psi/MPa
Offset Strain:	0.002	

Ludwik Parameters

Yield Stress:	0	MPa
Prior Strain:	0	

Specimen dimensions

	Initial	Final	Units
Length	5.08E-02	5.71E-02	m
Diameter	5.95E-03		m
Area	2.78E-05		m^2

Mechanical Properties

Property	Reference Properties	Measured Properties	Units
Young's Modulus	71.7	69.1	GPa
Yield Strength	503.0	480.8	MPa
Yield Strain (start)	0.0070	0.0107	
Yield Strain (end)			
Luder's Strain		0.0000	
Tensile Strength	524.0	543.3	MPa
Strain at TS		0.101	
Ductility	0.110	0.124	
Reduction-Area			
Toughness		89.1	MPa
Strength Factor		821.4	MPa
Hollomon Exponent		0.147	

Regression Analysis of Young's Modulus

Regression Output:

Constant	7.68335513	
Std Err of Y Est	1.6266838	
R Squared	0.99975843	
No. of Observations	295	
Degrees of Freedom	293	
X Coefficient(s)	69119.2568	MPa
Std Err of Coef.	62.7677196	

Regression Analysis of Strain Hardening

Regression Output:

Constant	2.91458067	
Std Err of Y Est	0.00069344	
R Squared	0.99799109	
No. of Observations	761	
Degrees of Freedom	759	
X Coefficient(s)	0.1474888	
Std Err of Coef.	0.00024019	

FIRST ROBOTICS COMPETITION

Lori Aldridge

Northwestern High School
2503 W. Main Street
Rockhill, South Carolina 29732

Telephone: 803-417-0863
e-mail laldridg@rock-hill.K12.sc.us

Lori Aldridge

Welcome to the FIRST Robotics Competition

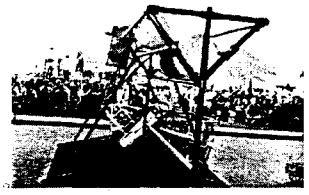

Photograph from the 2000 FIRST Robotics Competition National Championship.

The suggestions provided in this document are designed to help your team develop successfully during the Competition season. The information has been gathered from both rookie and veteran team participants. Remember, not all teams are identical, and what worked for one may not work for all. Read this through and see if any of the ideas work for you. If you need more suggestions, please contact FIRST.

Build Your Team

Start Now

Our teams have provided us with the best advice "Start now." They have told us many times that getting people from diverse areas on board early saves time.

Involve as many people as possible

Involve as many individuals as you think your team can manage. If you must select only a portion of the students who show interest, remember that one of the strengths of the FIRST Robotics Competition experience comes from involving students who are not usually attracted to this type of program. They can add new ideas and perspectives to your team.

Share the Excitement

Work with your team partners to recruit team members from both your company/university partner and team school. Call FIRST for information packets, event programs, or articles from the national press and set up an information table in the corporate cafeteria or at a staff meeting. We also have videos of past Competitions which are sure to get others excited and interested in becoming involved.

Take the time to explain

Some of the students you work with may never have set foot in a machine shop or used a small hand tool. For the first time many will see how their math and science classes are applicable to "Real World" situations. In order to engage the students, be prepared to explain complicated concepts and formulas at a level students will comprehend.

Develop a Team Attitude

Many of our team members have commented that the design and build phase of the Competition is the most intensive work they have experienced . To help things run smoothly, many start at the beginning of the school year with Team Building Workshops that include student, teacher, and corporate team members. Some teams practice brainstorming using the previous year's game. This also serves to recruit new team members and renew the interest of those returning.

Begin Computer Training Now

Learning computer programs ahead of time such as CAD-CAM, drafting, or drawing can also be helpful by speeding up the design process and keeping the cost of "testing" prototypes within budgets.

Develop Sources of Support

Parents

Inform parents about the program by sending home information from FIRST and the school. Include them in your recruiting meetings or have the students make presentations on the team's progress. Open houses or family days at the school or work facility are a great opportunity to introduce parents to the project.

School

Include teachers from outside the science and math departments. Art classes can help design team logos, computer instructors can teach programs, and the shop or tech ed teachers are valuable resources for everyone. Use all the resources of your school to recruit team members. Some schools have their own television studios and in-house broadcast facilities through which videos of the Competition or student-produced documentaries of your progress can be shown. Involve the school administration. Permission slips, insurance issues, and school district clearance are sometimes necessary to allow the students to travel off-site, to work on the machine, or to travel to tournaments. Your school administration can support your team by conducting open houses, school assemblies, pep rallies, or by providing meeting and building space.

Community

The community can support other team needs, such as fundraising and carpools. Students in the same neighborhood can arrange for carpools for travel to and from the work site. Local businesses may donate "fuel" for long work sessions-pizza and doughnuts are always popular. Teams come to the Competition in uniform. Local merchants can supply teams with Team T-shirts, hats, and buttons. Create a team of students to organize fund-raisers and recruit support.

For Inspiration and Recognition of Science and Technology
200 Bedford Street, Manchester, NH 03101 • 800-871-8326 • 603-666-3906 phone • 603-666-3607 fax • http://www.usfirst.org

Proj./Comp/2001/MktToolKit/Team Information Letter 0900

Planning for Success

Use real world Business Models

Some successful teams use a corporate model to organize their efforts. They distribute vision and mission statements, strategic goals, time frames, and they outline, document, and distribute team responsibilties. Teams can create mini corporations complete with design, manufacturing, marketing and budget departments. Even if your team doesn't go to this extent, teams within a team have worked very well.

Divide Responsibilities

Job descriptions, applications, and interviews may allow team members to choose their areas of interest and help team organizers assign responsibilities. You may divide into groups to accomplish specific tasks . Keep each other up-to-date on progress.

Acquire Facilities

If your school administration is unable to provide a facility or work space for your team you will need to find a place where you can set up shop, have meetings and work on the robot. Also, learn the procedures for acquiring materials or having shipments delivered to your work site. If permission, keys, or badges are required for access, get clearance now for all team members to enter facilities. You will not have time during the design and build phase to address these issues.

Choose your traveling team

If you have to choose who will travel and who will stay behind, create a plan for making those decisions. Remember, as a coach you do not have to make these decisions alone. Ask the students to decide on a plan. Their sense of diplomacy and level of maturity will surprise you. Be clear about your expectations of those who make the trip. Talk about acceptable behavior, team spirit, and "gracious professionalism." Be ready to handle emergencies and report good news back home quickly.

Spread the Word

Spreading the word, about your FIRST team among team members and their extended families is a good start. But think BIG! Promote your involvement both in your school and in your community. Use newsletters to recruit team members, a cheering section, or new supporters. Have your school board members, administrators, town or city mayor, and corporate CEOs visit your work site and get your local papers and television stations involved. Again, have students assist your public or community relations staff This will broaden the type of role models you can provide.

Team Promotional Materials

- **Team Media Kit**
- **Competition videos**
- **Competition trifold**
- **Information packets**
- **How to start a FIRST Team**
- **Mentoring Guide**

For FIRST Program Information

Customer Service - 800-871-8326 menu option 2

Engineering Support- 800-871-8326 menu option 2

FIRST
For Inspiration and Recognition of Science and Technology
200 Bedford Street
Manchester, NH 03101
800-871-8326
603-666-3906 phone
603-666-3907 fax
http://www.usfirst.org

Proj./Comp/2001/MktToolKit/Team Information Letter 0900

FIRST ROBOTICS HOW TO WORKSHOP

For Inspiration and Recognition of Science and Technology

www.suggested web site resources.com

- www.usfirst.org
- www.first-sme.org
- www.sharingfirst.mit.edu/
- www.robotics.nasa.gov
- SC Team www.metalinmotion.com
- www.chiefdelphi.com
- SC Team www.teambosch.org
- www.firstlegoleague.org
- www.aiaa.org
- www.pltw.org

*** Team 411 - For Questions email me:
LL1516@Hotmail.Com

South Carolina State Museum
August 30, 2001

Executive Summary

Dean Kamen

President of DEKA Research & Development Corp. & Founder of FIRST (For Inspiration and Recognition of Science and Technology)

Dean Kamen is an inventor, an entrepreneur and a tireless advocate for science and technology. His roles as inventor and advocate are intertwined -- his own passion for technology and its practical uses has driven his personal determination to spread the word about technology's virtues and by so doing to change the culture of the United States.

His vast knowledge of the physical sciences, combined with his ability to integrate the fundamental laws of physics with the most modern technologies, has led to the development of breakthrough processes and products.

As an inventor, Dean holds more than 150 U.S. and foreign patents, many of them for innovative medical devices that have expanded the frontiers of health care worldwide. While still a college undergraduate, he invented the first wearable infusion pump, which rapidly gained acceptance from such diverse medical specialties as chemotherapy, neonatology and endocrinology. In 1976 he founded his first medical device company, AutoSyringe, Inc., to manufacture and market the pumps. At age 30, he sold that company to Baxter International Corporation. By then, he had added a number of other infusion devices, including the first insulin pump for diabetics. Following the sale of AutoSyringe, Inc., he founded DEKA Research & Development Corporation to develop internally generated inventions as well as to provide R&D for major corporate clients. Dean's more recent inventions include: the HomeChoice™ dialysis machine, developed for Baxter (*Design News'* 1993 Medical Product of the Year), the Crown Stent designed for Johnson & Johnson, and the latest invention, the Independence™ 3000 IBOT™ Transporter, also developed for Johnson & Johnson. The IBOT, a personal transporter that was developed for the disabled community was unveiled in 1999. It can climb stairs, traverse sandy and rocky terrain and raise its user to eye-level with a standing person. All three of these products represent extraordinarily innovative responses to extraordinarily daunting challenges.

A decade ago Dean founded FIRST (For Inspiration and Recognition of Science and Technology), and ever since has remained its driving force, its guiding spirit, and, in the eyes of thousands of students across the country, its personal embodiment. FIRST uses wholesale marketing and media techniques to motivate the next generation to want to learn about science and technology. Dean has personally recruited scores of the top leaders of American industry, education and government in this crusade. As a result, the national championship of the FIRST Robotics Competition, which teams professional engineers with high school students from across the country, has set a new record each of the last four years as the largest non-Disney event ever held at Walt Disney World's Epcot Center. The 2000 event attracted almost 400 teams and has impacted tens of thousands of students -- many of them women or minorities from large urban schools.

With the success of the FIRST Robotics Competition, FIRST introduced the FIRST LEGO League (FLL) in 1999 as a means of expanding FIRST's reach to expose younger children to the science and technology fields. As a result of a partnership between FIRST and the LEGO Company, FLL offers hands-on experience for 9-14 year-old kids to explore and invent their own robotic creations. FLL has experienced tremendous growth, reaching more than 25,000 children in the U.S. since its inception.

In addition to his own attempts to master science and technology, Dean has received significant public recognition for his crusade on behalf of science and engineering. He was, for example, labeled by *Smithsonian Magazine* "the Pied Piper of Technology" and profiled by the *New York Times* as "A New Kind of Hero for American Youth".

Dean has received several prestigious awards:

- In 1994 Dean received the Kilby Award which celebrates those who make extraordinary contributions to society through science, technology, innovation, invention and education.
- The Heinz Award was awarded to Dean in 1998 in Technology, the Economy and Employment for a set of inventions that have advanced medical care worldwide.
- Dean was awarded the National Medal of Technology by President Clinton in 2000 for inventions that have advanced medical care worldwide, and for innovative and imaginative leadership in awakening America to the excitement of science and technology.

REGIONAL COMPETITION AWARDS

FIRST will hold an Awards Celebration at each Regional Competition. At these events, a special judging panel will present the following awards:

DaimlerChrysler
Team Spirit
This award celebrates extraordinary enthusiasm and spirit through an exceptional partnership and teamwork.

Delphi
"Driving Tomorrow's Technology™"
This award celebrates an elegant and advantageous machine feature. This award recognizes any aspect of engineering elegance including, but not limited to: design, wiring methods, material selection, programming techniques, and unique machine attributes. The criteria for this award are based on the team's ability to concisely verbally describe, as well as demonstrate, this chosen machine feature.

General Motors
Industrial Design
This award celebrates form and function in an efficiently designed machine which effectively achieves the game challenge.

Johnson & Johnson
Sportsmanship
This award celebrates outstanding sportsmanship and continuous gracious professionalism in the heat of competition, both on and off the playing field .

Motorola
Quality
This award celebrates machine robustness in concept and fabrication.

Xerox
Creativity
This award celebrates creative design, use of a component, or a creative or unique strategy of play.

Imagery
This award celebrates attractiveness in engineering and outstanding visual aesthetic integration from the machine to team appearance.

Leadership in Control
This award celebrates an innovative control system or application of control components to provide unique machine functions.

Incredible Play
This award celebrates the team or alliance displaying the most incredible play of the elimination rounds, including a formidable defensive or offensive move or strategy. The recipient of this award is decided upon by FIRST teams via on-site ballot vote at each regional competition.

#1 Seed
This award celebrates the team which is the top seed at the conclusion of the qualifying rounds.

Featherweight in the Finals
This award celebrates the lightest machine participating in the elimination matches.

Highest Rookie Seed
This award celebrates the highest seeded rookie team at the conclusion of the qualifying rounds.

Rookie All-Star
This award celebrates the rookie team exemplifying a young but strong partnership effort, as well as implementing the mission of FIRST: to inspire students to learn more about science and technology.

Judges' Awards
During the course of the competition, the judging panel may encounter a team whose unique efforts, performance, or dynamics merit recognition.

Regional Finalist
This award celebrates the team or alliance which makes it to the final match of the competition.

Regional Champion
This award celebrates the team or alliance which wins the competition.

January 2001

Sunday	Monday	Tuesday	Wednesday	Thursday	Friday	Saturday
	1	2	3	4	5 2001 Kick-Off Workshops Founders Party	6 2001 FIRST Robotics Competition Kick-Off
7 **Six,Week Build & Design Begins**	8 **Brainstorm & Prototyping begins**	9	10	**11 Prototype Field Complete**	**12 Understand Control System**	13
14	15	16	**17 Test Sub-Mechanism**	18	**19 Movable Drive train ready**	20
21	**22 Prototype Test**	23	**24**	25	26	27
28	**29 Prototype Test**	30	31			

April 2001

Sunday	Monday	Tuesday	Wednesday	Thursday	Friday	Saturday
1	2	3	4	5 National Championship (Orlando, FL)	6	7
8	9	10	11	12	13	14
15	16	17	18	19	20	21
22	23	24	25	26	27	28
29	30					

February 2001

Sunday	Monday	Tuesday	Wednesday	Thursday	Friday	Saturday
				1	2	3
4	5 **Team Uniforms Designed**	6 **Test & Debug**	7	8	9 Chairman Award Submissions Due	10
11	12 Team Party Counts due Regional & Nationals	13 **Driver Practice**	14	15 **Spare Parts Made**	16 **Build Crate To Ship Robot**	17
18	19	20 Ship Robot Regional & Nationals	21	22 Ship Robot Participating in Nationals Only	23	24
25	26	27	28			

March 2001

Sunday	Monday	Tuesday	Wednesday	Thursday	Friday	Saturday
				1 Kennedy Space Center Southeast Regional (KSC, FL) UTC New England Regional (Hartford, CT) * check manual for shipping instructions	2	3
4	5	6	7	8 Long Island Regional (Long Island, NY) NASA Langley/ VCU Regional (Richmond, VI) West Michigan Regional (Grand Rapids, MI)	9	10
11	12	13	14 Autodesk Award Deadline	15 Johnson & Johnson Mid Atlantic Regional (New Brunswick, NJ) Lone Star Regional (Houston, TX) New York City FIRST! (New York City, NY) Southern California Regional (Los Angeles, CA)	16	17
18	19	20	21	22 Great Lakes Regional (Ypsilanti, MI) Motorola Midwest Regional (Evanston, IL) Philadelphia Alliance Regional (Philadelphia, PA) Silicon Valley Regional (San Jose, CA)	23	24
25	26	27				

Sharing Your News
How to Reach The Media

Use the information in this kit to help you share news about your team's involvement in the FIRST Robotics Competition. We recommend that you identify one or two team members who can be in charge of contacting the news media for the duration of the project.

If you have questions about publicizing your team, FIRST national media coordinators are available to help. Call, fax, or e-mail:

Carolyn Eggert or Barbara Trevett
MSA, 20 Park Plaza
Boston, MA 02116
617-695-6364
msacse@aol.com

What is news?

Everyone has their own definition of news . . . in this case, there are several exciting activities and personal stories to share with the news media. For example:

1. You are a group of students building robots from scratch. Invite reporters to visit you while you are building your unique robot. Let reporters see that you started building your robot from a simple crate of nuts, bolts, and wires.

2. You are programming your robot to accomplish a specific task. Once your robot is built, invite reporters to watch you "test" your robot.

3. You are preparing your robot and your team for regional competitions. If there is a competition in your hometown (or somewhere nearby), invite reporters.

4. What happens during the last week of putting together the robots? Packaging it for shipment? Working day and night to make sure things are just right?

5. You are learning real-life science – your participation in the FIRST Robotics Competition could lead to a career in science. Talk to your teammates about why your involvement on the team is so important and what you hope this experience will do for you in the future. Share this information with your local news media.

6. Do any of your team members have personal stories of achievement that lead them to becoming part of your FIRST team?

7. How does this "intellectual" competition compare to athletic competition? Do you use some of the same skills in preparing for competition?

8. Do you have cheerleaders, marching bands rooting for you on the sidelines?

How do I contact newspaper and television reporters?

First, find out the names, addresses, phone and fax numbers of your local newspapers and TV stations. Call to find out which reporter is interested in covering news about:

- EDUCATION
- SCIENCE
- HUMAN INTEREST STORIES
- BUSINESS NEWS

When you have a list of reporters, think about what will interest them. To introduce your team and the FIRST Robotics Competition, use the press releases in this kit. Just fill in the specifics about your team and sponsor. Now, send it off to the reporters.

As your team progresses . . .for example, when you start to build the robot, let reporters know about it.

1. SEND (via mail or fax) a news release that answers the following questions:

- WHO: *Who are you? (FIRST Robotics Competition event, team name, school, sponsor)*
- WHY: *Why are you calling?—Why are you writing this news release?*
- WHAT: *What is interesting about your participation in the FIRST Robotics Competition?*
- WHERE: *Where are you doing it? (Provide exact location, room numbers and phone numbers in case they need directions)*
- WHEN: *When are you doing it? (DATE, TIME)*
- CONTACT: *If they need more information, who has it? Who can they call if they want more information?*

2. CALL THEM

Introduce yourself and tell them why you are calling. Keep in mind that reporters get so many requests, they may not remember receiving your news release. Be prepared to give them a quick description on the phone and after your conversation, FAX the news release to them.

Remember, reporters are busy and are working on deadlines. They may not respond to your news release or call – but feel free to follow up with them.

And, if they are not able to cover your first event, <u>try again</u>.

3. BASIC RULES OF THE ROAD

- Always refer to the our program -- as: FIRST Robotics Competition
- Always refer to your team sponsor whenever writing or talking about your team. Your sponsor makes it possible for you to enter the competition.
- When writing the news release type with double spaces.
- When describing FIRST, use one of these descriptions:

Founded in 1989 by New Hampshire entrepreneur and inventor Dean Kamen, FIRST (For Inspiration and Recognition of Science and Technology) is a non-profit organization that brings together an alliance of business, education, and government organizations through innovative programs to inspire today's youth in the areas of science, engineering and technology. Visit the FIRST web site at <www.usfirst.org> for more information about the FIRST Robotics Competition, and other programs developed by FIRST to inspire youth of all ages.

The rest of this kit offers sample press releases and fact sheets about FIRST Robotics. Feel free to use them to promote regional competitions or as background information for reporters.

Please send copies of any coverage you may receive (articles or news clippings, etc.,) to MSA, 20 Park Plaza, Boston, MA 02116. And remember, call if you have any questions or need help with publicity.

EXAMPLE A: Press Release for Regional Competition

PRESS RELEASE

National Media Contact:
Barbara K. Trevett
(617) 695-6364

Team Contact:
[Contact name, school and team number]
(AREA CODE/NUMBER)

For immediate release
[add today's date]

Region's students prepare to clash on the 'intellectual playing field'

CITY, STATE (DATE) -- Students at more than (number of) schools in the (major city) region this week are pumping up for one of the biggest games of their young lives -- the annual FIRST Robotics Competition. Instead of fine-tuning their shooting style or defensive play, these students test the limits of their own imaginations—using robots they have designed and are sending into technological battle against robots from other FIRST competitors.

In this clash of robots and their student handlers, all the trappings of traditional school sports showdowns--referees, cheerleaders and time clocks--will surround feverish competitors on the "intellectual playing field." Adding to the tension and excitement is the prospect of participating in the national championship for the student teams' marvelous machines at the competition finals at Disney World's EPCOT Center at Orlando, FL in April.

The FIRST Robotics Competition, centered on a new "challenge" each year, is designed to convince young people that science can not only be exciting and rewarding but is as much fun as traditional sports. Details of the annual challenge are kept secret until being unveiled at the "Competition Kickoff" each year, with all teams having an equal start in a fiercely contested day-long event.

Founded in 1989 by New Hampshire entrepreneur and inventor Dean Kamen, FIRST (For Inspiration and Recognition of Science and Technology) is a non-profit organization that brings together an alliance of business, education, and government organizations through innovative programs to inspire today's youth in the areas of science, engineering and technology. FIRST is developing multiple programs to inspire youth of all ages. For more information, visit the FIRST web site at <www.usfirst.org>. Or call (Team Contact name and phone number).

###

EXAMPLE B: Press Release highlighting sponsors

PRESS RELEASE

National Media Contact:
Barbara K. Trevett
(617) 695-6364

Corporate Contact:
[name and title]
(AREA CODE/NUMBER)

For immediate release
[add today's date]

[Headline should include sponsoring corporations and universities. For example:]

___ University and ____ Corporation Partner with Students from _____ School to Prepare for Robotics Competition

CITY, STATE, (DATE) -- (Insert number, spelled out) middle and high schools in the (name of region) will each send their own unique robots into the (location of competition site) contest over the two-day event. The participating schools are (list):

A number of (name of FIRST region)'s top corporations and universities that have partnered with the students on a FIRST team, providing their expertise in technology, science and business organization. They include: (list all corporations and universities, alphabetically):

Founded in 1989 by New Hampshire entrepreneur and inventor Dean Kamen, FIRST (For Inspiration and Recognition of Science and Technology) is a non-profit organization that brings together an alliance of business, education, and government organizations through innovative programs to inspire today's youth in the areas of science, engineering and technology.

Visit the FIRST web site at <www.usfirst.org> or (corporate contact name and number) for more information about the FIRST Robotics Competition.

###

We're Looking for News

Please complete this form and fax to Barbara Trevett of MSA, at 617-695-6366.

Team Name: _____ Team Number: _____

Team Member Name: _____ Age: ____ School: _____

City: _____ State: ___ Zip: _____

Team Member Phone: _____ E-mail Address: _____

Local Newspaper Name: _____

Address: _____ City: _____ State: ____ Zip: _____

Phone: _____ Fax: _____

Important local TV station names, addresses, phone & fax:

_____
_____
_____
_____
_____
_____

About You

Why are you involved? _____
_____
_____
_____

Tell us about you (where are you from? Do you have siblings? Have your siblings been involved with FIRST?) _____
_____
_____
_____

What is your role on the team? _____

How many hours a week do you spend working on the robot/team? _____

Have you ever done anything like this before? If yes, what? _____

If no, would you do it again? _____

Is there anything special you would like us to know? Has anything happened (better grades new career interest) as a result of your joining the FIRST team? _____

Is there anyone else on your team you think has an interesting story to share? Why?

In your opinion, what is the most important part of the robot-building process? _____

Remember, we are doing our best to find stories for newspaper and television stations. We'll be sorting through a lot of information – provided by YOU.

Thanks for all of your help! And GOOD LUCK!

FIRST

Robotics Competition

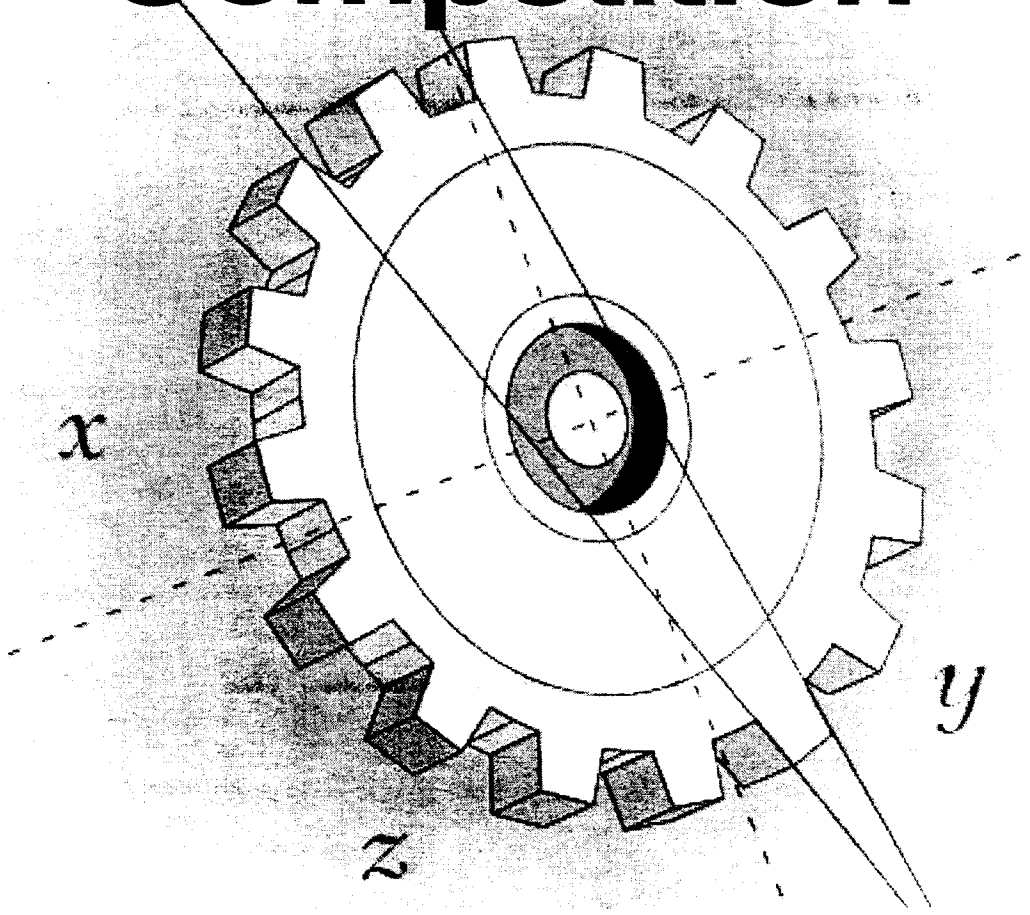

How To Guide

Generic Time Line

September

- Select high school
- Teachers all recruited
- Meet regularly to define roles, set up student selection criteria
- Applications to join team
- First cut on applications
- FIRST applications due
- Student recruiting - presentation to potential new student team members
- Adult professional recruiting
- Determine where the team will meet
- Identify and secure equipment
- Secure funding, do fundraising

October

- Student interviews
- Announce students who made the team
- Parent meeting; expectations
- Distribute SPI catalogs to engineering team
- Discuss overall mission and theme for the year
- Mentoring packet received from FIRST

November

- Review last year's rule book and FIRST website to gain insight into 1st year deadlines, Chairman's Award, team logo, tee-shirts, buttons, etc.
- Students selected
- Assign student job responsibilities
- Meet weekly
- Initiate PR contacts
- Fundraising
- Finalize location for robot work
- Finalize playing field location
- Assign team members to monitor websites (FIRST, Teams)
- Safety training
- Team building
- Site preparation

December

- Team registration deadline
- Meet weekly
- Finalize student roles
- Engineers all recruited
- Team building exercise
- Devise 'Table of Contents' for scrapbook/video
- Determine purchasing method
- Set expectations with adult team members
- Make reservations

January

- Meet as required: brainstorming
- Kickoff ~ Saturday, January 8, 2000 in Manchester, NH

- See 'Robot Timeline'
- Team profiles, logos
- Design
- Animation
- PR ~ follow-up
- Chairman's Award

February

- Meet as required: design, build, test, rebuild
- Animation
- PR ~ follow-up
- Complete Chairman's Award submission by deadline
- Note shipping dates for robot
- Team numbers of Regional parties due

March

- Practice
- PR ~ follow-up
- Team meetings
- Compete in Regional competition
- Team numbers for National party due

April

- Compete in Nationals
- PR ~ follow-up
- Have a few parties, get some sleep

ROBOT TIMELINE

**** Kickoff on Saturday, January 8 ****

week 1:
understand game, brainstorm strategy & design, build playing field, post kit parts and functions

week 2:
brainstorm design, choose concept design, refine concept design, start detail drawings

week3:
mule hardware running, driver/human practice, work on detail drawings, start some fabrication

week 4:
driver/human tryouts, continue fabrication, complete detail drawings, redesigns

week 5:
driver/human practice, initial robot build, testing, rebuild, repair, and retest multiple times

week 6:
driver/human practice, rebuild and retest multiple times, paint

Chairman's Award

The Chairman's Award is the highest award that FIRST bestows upon a team. The award recognizes an extraordinary partnership effort by a team during and beyond the competition season. The Chairman's Award finalists and winner are selected by a panel of competition judges based upon a ten minute review of the teams' Chairman's Award submission, team member interviews, specific judging criteria for the award, as well as format and length restrictions, and submission deadlines which can be found in the competition manual each year.

The Chairman's Award submission is documentation of your team's *'story'*. It is more than a book or a video, it is documentation of the essence of your team. A good way to approach your Chairman's Award submission is to treat it as a permanent record of your team through the eyes of the students. Document team activities that show the partnership you have developed within your team. Consider including human-interest stories and pictures of team members working together. Also include team activities which help spread the FIRST message. These can include things like engagement of a school district, government officials and/or business leaders, presentations and demonstrations at schools and civic functions, recruitment and mentoring of new teams, fundraising, design and build phase experience of your team, and community involvement. Teams will often include things they feel make their team unique. *The possibilities are endless!*

Documentation of your Chairman's Award submission can be submitted in many forms as outlined in the current Competition Manual. Creation of the documentation can be an opportunity to engage students in desktop publishing, digital photography or video production. Unique is great, but keep it simple; it does not need to be fancy or professionally done to be a good submission, but it must be well organized and convey your message succinctly. Many teams in the past have created their submission as a printed document while others have created a video. There is no right or wrong way to create a Chairman's Award submission as long as it follows the FIRST guidelines. Approach the creation of your Chairman's Award submission the same way you approach the building of your robot - develop a plan and follow it. If possible, make a copy of your Chairman's Award submission to keep for your own records. Some teams duplicate some or all of their submission to give to their own team members and for team marketing activities.

When considering whether to create a Chairman's Award submission or not, be practical. Think about all of the activities your team will need to do before the ship deadline and the number of people you have to complete them -- don't commit to something that you cannot follow through on. It is discouraging to team members who put in the effort if there is no end product.

Every FIRST team is unique and many go beyond the basic requirements for a FIRST team. While there is only one team selected as The Chairman's Award winner, every team can get satisfaction from the things they have accomplished which make them a Chairman's Award quality team, so if you have the time and the resources, create a Chairman's Award submission -- for yourself and for FIRST. The experience of creating this documentation is invaluable.

Fundraising

Fundraising is one of the least attractive tasks at first glance and the most difficult for most teams. Fundraising serves two roles in the development of your team. First the chosen fundraising activity raises money for some of the expenses your team will incur during the FIRST experience. Activities such as raffles, candy sales, and car washes are only but a few of the ideas teams have used successfully. Your chosen activities will depend upon your team, community, available time and student resources. Start early, have a plan and do not be shy, always ask for more and give back more to the sponsor than expected.

Second, the fundraising activity serves to bond team members together and give them a sense of purpose early in the FIRST experience. Earning their own way and contributing to the team effort is an important aspect of team development that should not be overlooked. *Consider having students participate in fundraising even if your team is fortunate enough to have their funding fully covered.*

Community support is important. Do not overlook sources of funding locally. This includes additional sponsors and general donations that may include refreshments (for work times), materials to build with and cash donations.

Media/PR

The FIRST experience has proven to have a positive affect on the lives of the young people in America, this is a proven fact. Your team's efforts aimed at Media/PR are efforts to let others know all of the great things that your team has accomplished, while at the same time spreading the news about FIRST. Articles in local publications, radio and TV spots are but a few examples of media that can serve to strengthen your team. Doing great things, changing the way education looks at math and science have more power if others are aware of your activities. Establish strong bonds with the local media, provide them with interesting angles on your team and its activities and the effects of your program on the lives of youth. Spread the word!

Marketing

In this instance, marketing is defined as the things a team does to establish its identity. Marketing efforts result in a team being 'known' for something. This section will attempt to explain some of the marketing efforts that have been successful for other FIRST teams. This section will not cover communications or public relations; those are what a team does to promote its already established identity.

Now the disclaimer: What follows are some ideas that have helped teams establish their identities in the past. The future has yet to be written, and new teams should not depend on just these ideas as they establish their *own* identities!

The way a team acts and looks at events and competitions is a key ingredient of the team's identity. Some teams have a well-defined schedule of tasks and responsibilities for each

competition. Some teams depend on key people to lead important efforts when the time seems right. Some teams have a dress code, with specific details on what is acceptable and what is not. Some teams are instantly recognizable because of the way they dress! A key element in getting the team to act as a team is to communicate the tasks and expectations well in advance of the events. If team members know what the team is going to be doing, they are much more likely to be able to help. Some ideas to help build a consistent identity: pass out a 'roles and responsibilities' checklist; have team meetings before and after events to discuss the good, bad, and ugly; make sure the roles of task leaders are clearly defined; make sure everyone knows and follows the schedule. Some things that past successful teams have done: a well-executed and well timed cheer, a group of seats in the same place every day, a set procedure for the cheering section before/during/after matches, a concerted effort to clean up after each other at the end of the day.

The goodies that teams give out and trade at events are also part of the team's identity. These 'trinkets and trash' leave others with a lasting impression of the team. They don't have to be expensive or complicated! Some common trading items include buttons, dog tags, key chains, and pens or pencils. Some less common items include stopwatches and noisemakers. In addition to trading items, many teams also give items away. Some common giveaway items are candy, business cards, cookies, scorecards, team brochures, and, did we mention food? Originality counts!

The events that a team orchestrates or participates in (at any time of the year) help establish that team's identity. Perhaps they are known for tutoring middle school students or cleaning up a road near school. Perhaps they have had some well known fundraising events. Some teams have floats in parades. Teams should look to their overall mission (yes, teams should define their own mission!) as a guiding force for what types of events they orchestrate or participate in.

Many teams publish information about their team or about FIRST as a way to inform their community or start new teams. Team newsletters, team pictures distributed to school officials, informative guides on how to make college/career choices, and informative guides on how to start/maintain FIRST teams are all examples.

Another means of publishing information is a team website. More and more teams find this a convenient and efficient way to distribute information to anyone who wants it. While it is quite common for teams to include basic information about school, sponsor, and activities on their website, many teams go much further. Discussion forums, chat servers, email list servers, scouting reports from recent regionals, robot pictures, how-to guides on various subjects, informational articles, upcoming events, and private team-only areas are some examples of useful website content. Providing a service that other teams need is a sure-fire way to get a popular website!

Travel Coordinator

If possible, identify one person who will coordinate all aspects of team travel. This cuts down on confusion and duplication of efforts between the school and the corporation.

For air travel, make reservations as early as possible to minimize costs and maximize your chances of traveling at your desired times. If possible deal with the airlines directly and ask for group reduced rates. All travelers are required to have photo identification at the airport and will be required to pass through metal detectors. Each piece of luggage must have a luggage tag with the owner's name, address, and a phone number. Students should be reminded that airport personnel will ask all travelers questions. This must be taken very seriously and is not a time for joking around.

You will need to make ground transportation arrangements to and from the airport. In Florida, if not staying at a Disney hotel, you will also need to arrange ground transportation to and from the Competition.

Hotel packages which provide meal arrangements can save you time and in many cases money. It will make things simpler for you. Many hotels offer buffet or coupon services. Having breakfast together offers the team an opportunity to start the day together. FIRST often arranges for travel companies to provide packages, which include room and meals. Make hotel arrangements with the travel provider or hotel as early as possible.

The hotels and airlines will generally require the finalized list of travelers about 30 days prior to travel.

Animation

Start your animation team as soon as possible learning the animation software. Have computers identified and reserved with the animation software installed as soon as possible. Use the most powerful/fastest computer you can for final rendering. The amount of RAM is critical to the performance of the computer. Slower computers can be used to create objects and save them to disk for later import. Practice rendering and transferring to video tape early so that you have time to work out the process. There are many low cost video cards that have video out and will handle the process of putting your animation to VHS tape.

Develop a storyboard before starting the animation, and stick to it. Careful planning and development of the story will save you many hours of work. It is important that you divide the animation among the animation team maximizing computer time. A calendar of deadlines and the ship date should be posted as a reminder.

Participation in this competition will allow students to develop skills in design and animation. This animation is a good opening act for many team activities and demonstrations after the competition has concluded.

Mentor Sign Up Form (send in registration package or email)

FIRST is starting a Team Mentor program this year administered from the FIRST Web site. The Mentor program is aimed at making the *'FIRST Experience'* a little less stressful for the rookie teams and others needing assistance. Your team can help in this process by agreeing to be a mentor. As a mentor, your team would be listed on the FIRST web site and in printed material as a resource.

Please consider being a mentor resource. The amount of time and effort you will provide will depend on the needs of the team seeking help. Most of all, you will answer questions, give guidance and direct them to resources available in the FIRST community.

Please send this completed form to Theresa Clement at FIRST. tclement@usfirst.org or call (800) 871-8326. ext. 432.

****

Select a main contact for this mentor program.
Main contact information .....print please
First _____ Last _____
Team # _____ Team Name _____
Phone # ( ) _____ E-Mail _____
City _____ State _____
Business _____
School _____
Best time for a phone contact: _____

****

Burnout and Retention

All teams need to be aware that in the course of events, that a change in a team's structure will allow your team to evolve. Students, engineers, teachers and the roles that they play on a team often fluctuate with the needs of their personal and professional lives. Adjusting to these changes often puts stress on the structure of the team. The community of FIRST will support each other with all the resources that are available. The true power of FIRST is the willingness of teams to assist each other in difficult times and rejoice with each other in their successes. With this in mind, we all need to share our expertise and lend a hand to a team that may be having a change in team structure.

View change as a healthy condition that serves to strengthen and bind your team.
Ask for assistance if there is a need.
Lend a hand and do whatever your team can to assist others.
Understand you are not alone.
Educate others as to the resources that are available.

We all see the **VALUE** in a strong **FIRST** organization.

****

THE CENTER FOR THEORETICAL AND COMPUTATIONAL MATERIALS SCIENCE

James Warren

Director, Center for Theoretical and
Computational Materials Science
Theoretical Physicist
Metallurgy Division
Materials Science and Engineering Laboratory
National Institute of Standards and Technology
100 Bureau Drive, Stop 8554
Gaithersburg, Maryland 20899-8554

Telephone: 301-975-5708
e-mail jwarren@nist.gov

The Center for Theoretical and Computational Materials Science

Materials Science and Engineering Laboratory

MISSION: to investigate important problems in materials theory and modeling with novel computational approaches; to create opportunities for collaboration; to develop powerful new tools for materials theory and modeling and accelerate their integration into industrial research.

Focus Areas Include:

OOF: Object Oriented Finite Element Software
First Principles Prediction of Phase Diagrams
Multiscale Simulations of Filled Polymers
Phase Field Modeling of Microstructure
Green's Functions for Elastic Properties
Solder Interconnect Design Tools
Micromagnetic Modeling Tools
Deformation of Aluminum

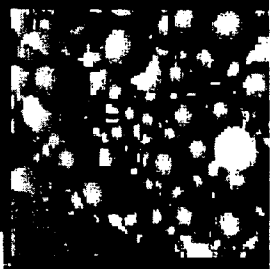
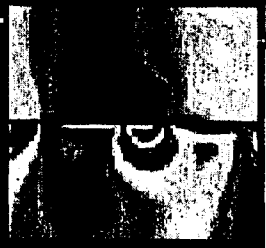
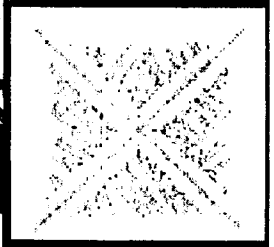
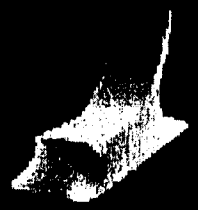

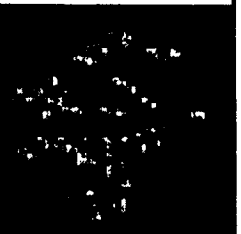
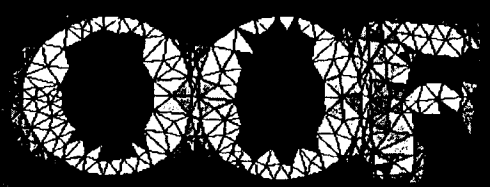


NIST

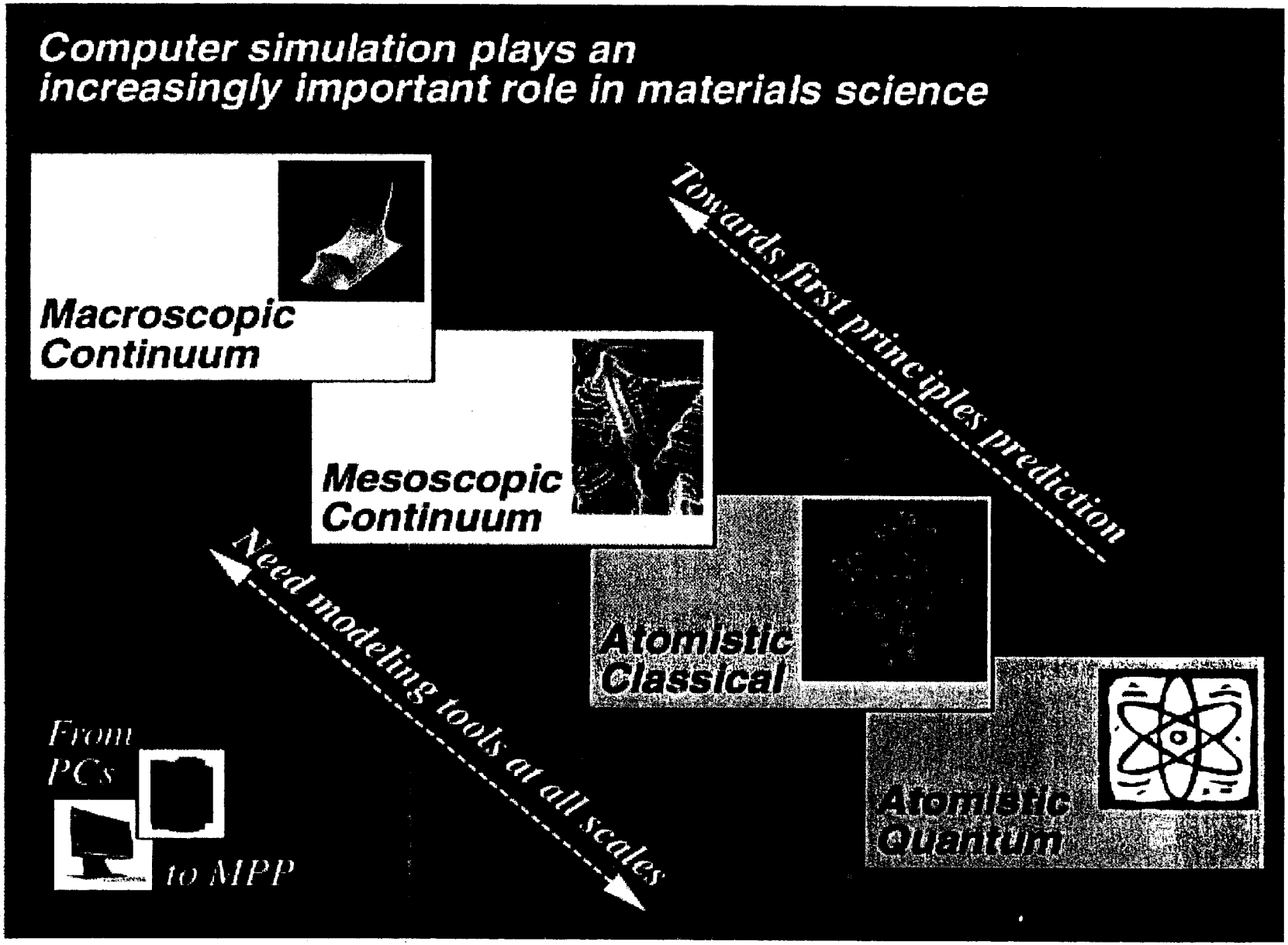
Computer simulation plays an increasingly important role in materials science
Macroscopic Continuum
Mesoscopic Continuum
Atomistic Classical
Atomistic Quantum
Towards first principles prediction
Need modeling tools at all scales
From PCs
to MPP

OOF: Object oriented Finite Element Software: edwin.fuller@nist.gov

First Principle Prediction of Phase Diagrams: ben.burton@nist.gov

Green's Functions Library for Elastic Properties: vinod.tewary@nist.gov

Deformation of Aluminum: lyle.levine@nist.gov

CTCMS
Working Groups

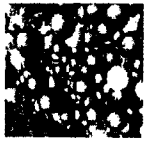

Multiscale Simulations of Filled Polymers: francis.starr@nist.gov

Micromagnetic Modeling Tools: robert.mcmichael@nist.gov

Solder Interconnect Design Tools: james.warren@nist.gov

Phase Ordering Modeling Tools: james.warren@nist.gov

Simulation Tools for Microstructure Evolution in Multiphase Blends:
charles.han@nist.gov

The NIST Center for Theoretical and Computational Materials Science

a resource of expertise and collaboration in materials theory and simulation

www.ctcms.nist.gov

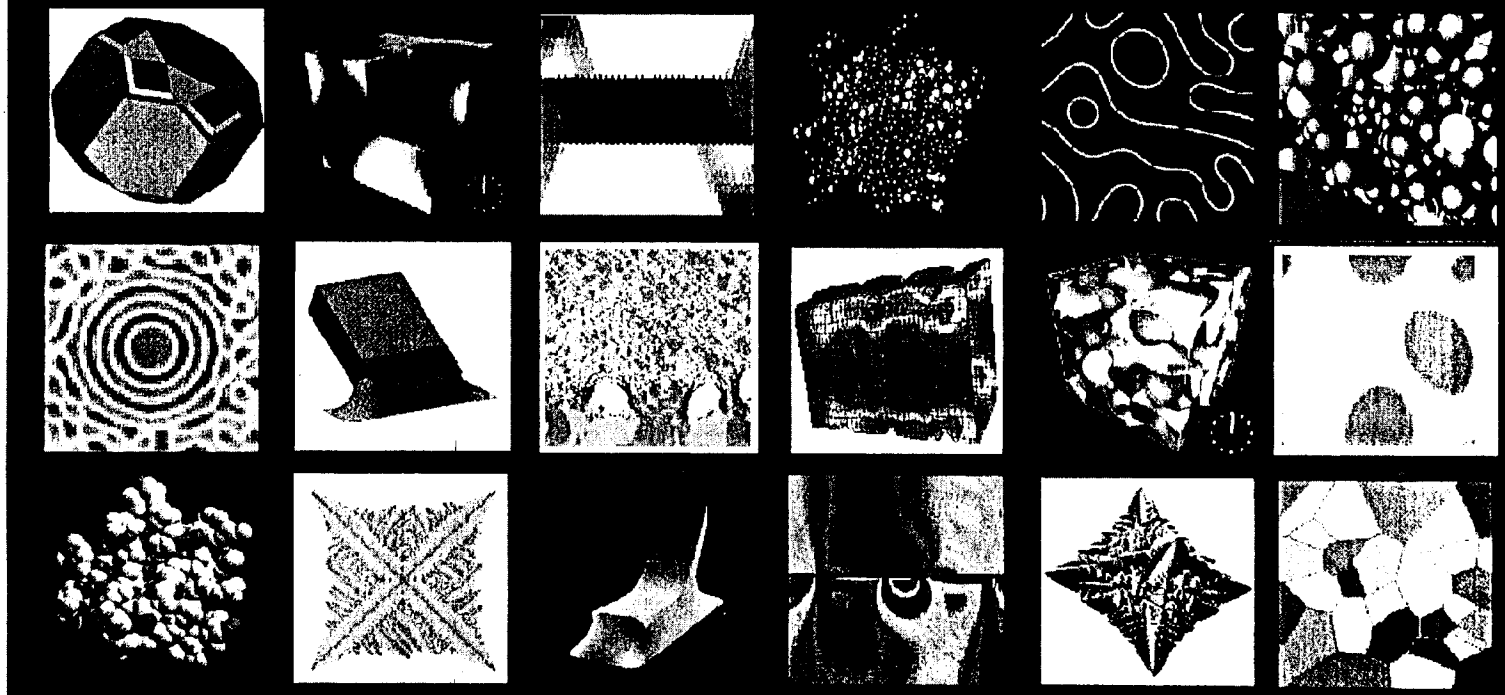

LOAD TESTING OF TEMPORARY STRUCTURAL PLATFORMS

Harvey Abramowitz

Ralph E. Bennett III, PE

John Bennett (student)

Rick J. Hendrickson (student)

Caris Koultourides (student)

and

Brandon W. Tredway (student)

Department of Engineering
Purdue University - Calumet
2200 169th Street
Hammond, Indiana 46323

Telephone: 219-989-2473
e-mail harveya@calumet.purdue.edu

Walter Kuchariski (student)
Construction Technology

Harvey Abramowitz

Load Testing of Temporary Structural Platforms

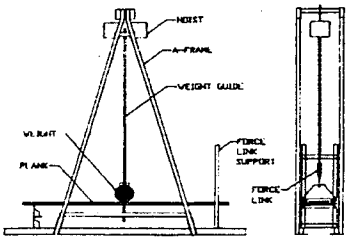

Load Testing of Temporary Structural Platforms

Harvey Abramowitz
Department of Engineering
Ralph E. Bennett III, PE
Department of Construction Technology

Engineering Students
John H. Bennett, Rick J. Hendrickson,
Caris Koultourides and Brandon Tredway

Construction Technology Student
Walter Kucharski

Background

1. Scaffold Platform is Weakest Link of Temporary Structure

2. Current Platform Design is Based on Static Loading

Background (cont)

3. Normal Platform Usage Includes Application of Dynamic Loads

   e.g., Workers Jumping and
   Material Dropped onto Structure

Needs

1. Develop Standardized Dynamic Loading Test Procedure

2. Develop Dynamic Loading Design Criteria

Objectives

For Temporary Structural Platforms, such as Scaffolding Planks

1. Introduce Student to Concept of Dynamic Loading, as Compared to Static Loading

2. Demonstrate a Method for Determining Dynamic Loading

Objectives (cont)

For Temporary Structural Platforms, such as Scaffolding Planks

3. **Compare Theoretical and Actual Static and Dynamic Loading Results**

4. **Develop and Recommend Dynamic Loading Criteria**

Prerequisite Knowledge

The Student

1. **Should be Familiar with PC's**

2. **Should be Familiar with Determining a Stress Strain Curve, and the MOE (Including Flexural)**

Testing Apparatus

- **Static**
- **Dynamic**

Static Testing Apparatus

Vibration Analysis Machine

DynaMOE^{tm}

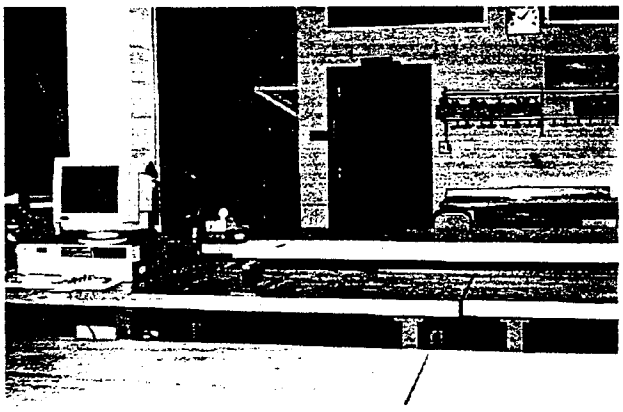

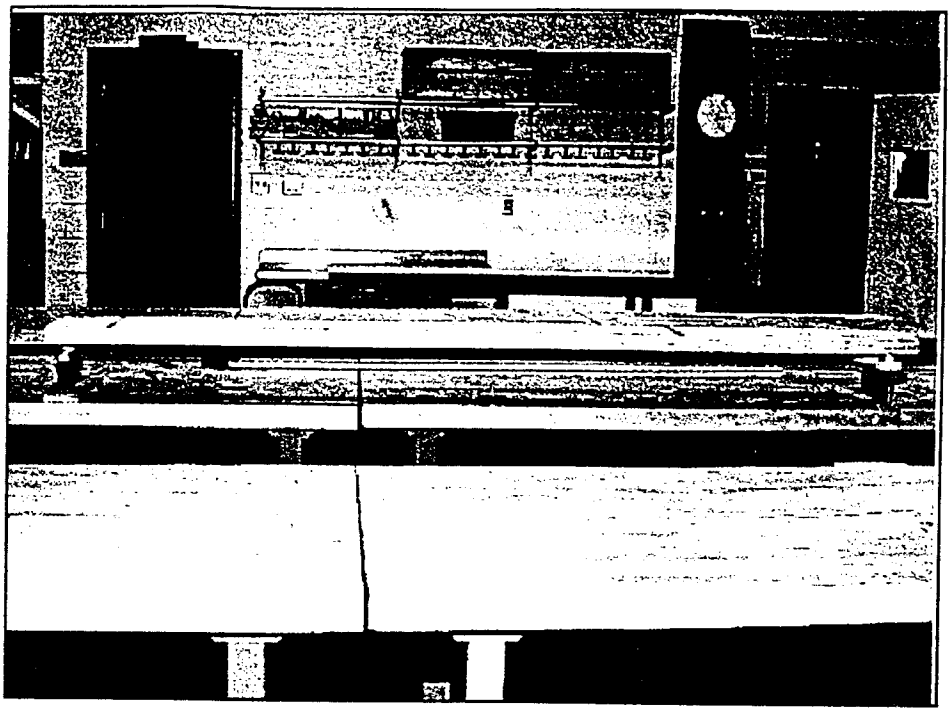

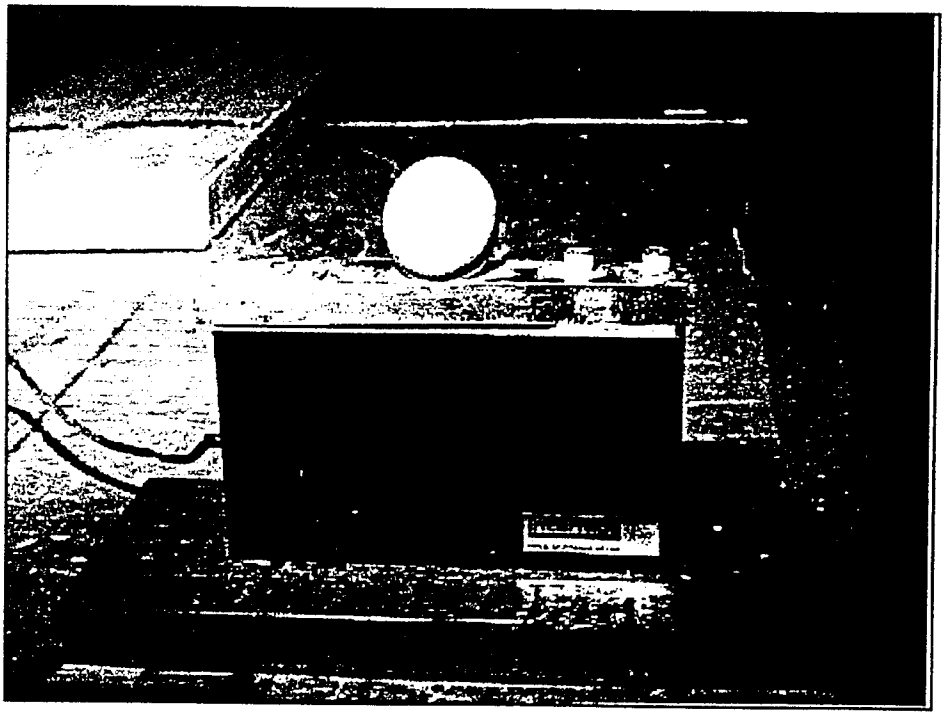

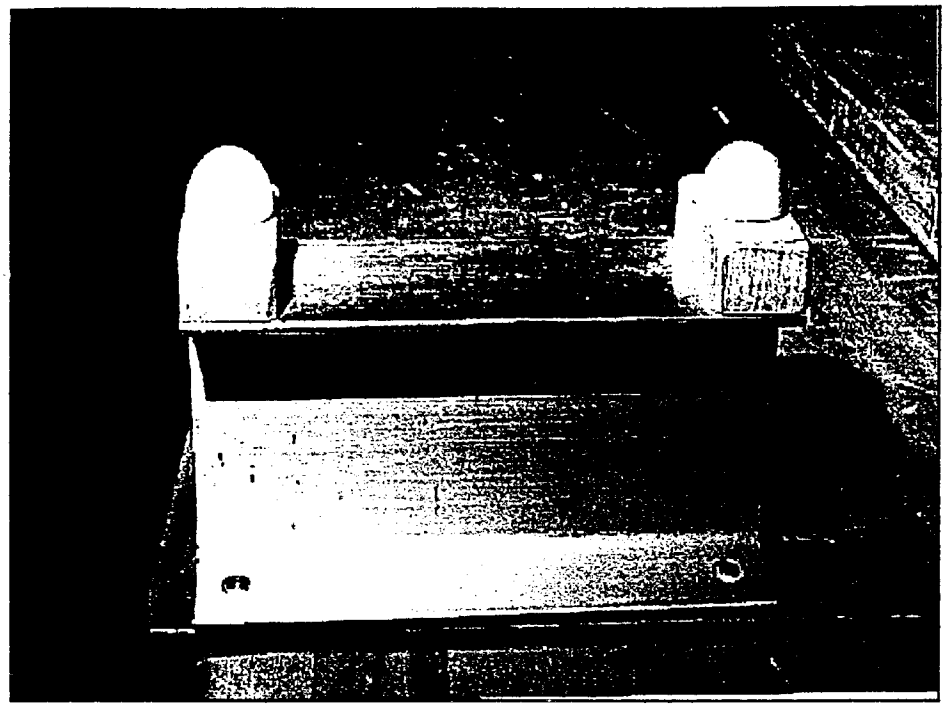

$$E_d$$

$$E_d = \boxed{\frac{f^2 WL^3}{2.46gI}}$$

or

$$= \frac{f^2 WS^4}{2.46gIL}$$

INPUTS

- WEIGHT
- LENGTH / SPAN
- HEIGHT / DIAMETER
- WIDTH

OUTPUTS

- DENSITIES
- f
- I
- E_d
- EI

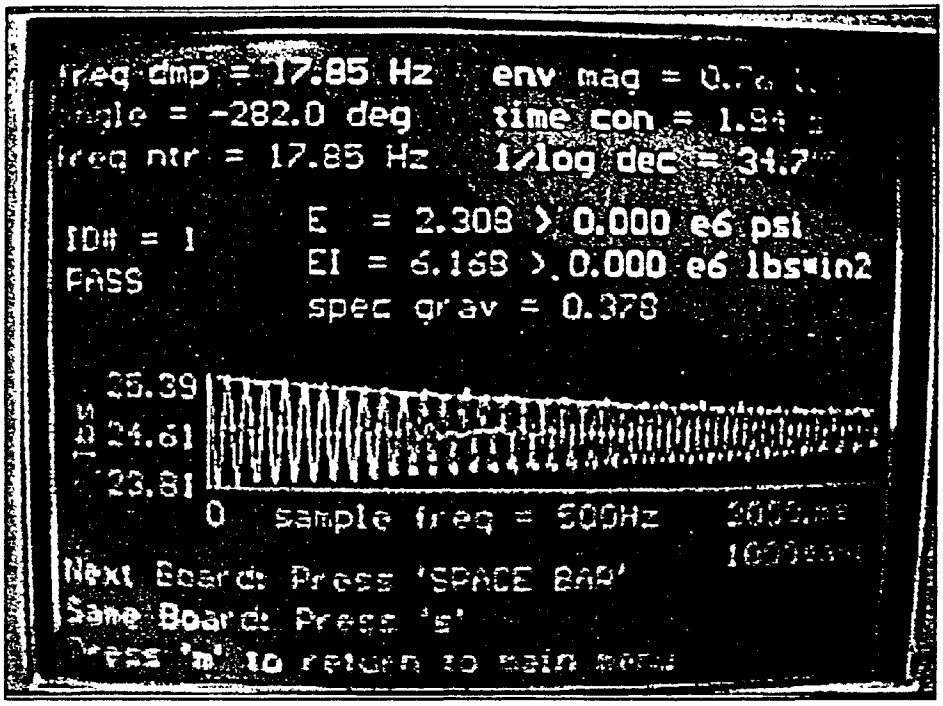
freq dmp = 17.85 Hz
env mag =
angle = -282.0 deg
time con =
freq ntr = 17.85 Hz
1/log dec =
ID# = 1
PASS
E = 2.308 > 0.000 e6 psi
EI = 6.168 > 0.000 e6 lbs*in2
spec grav = 0.378
25.39
24.61
23.81
0 sample freq = 500Hz
Next Board: Press 'SPACE BAR'
Same Board: Press 's'
Press 'm' to return to main

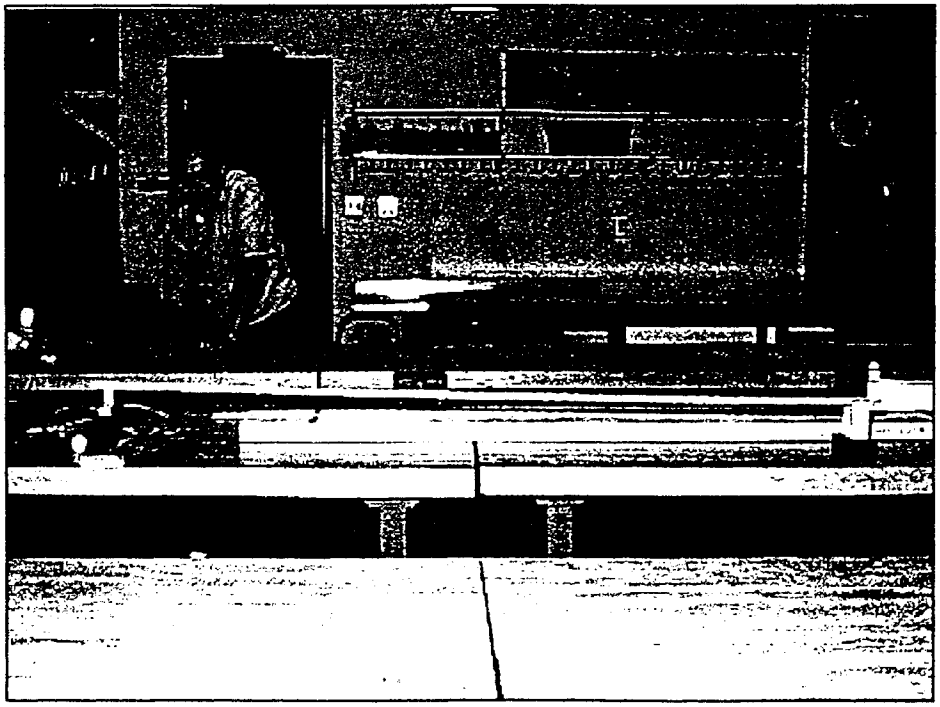

Conventional
Three Point Test Assembly

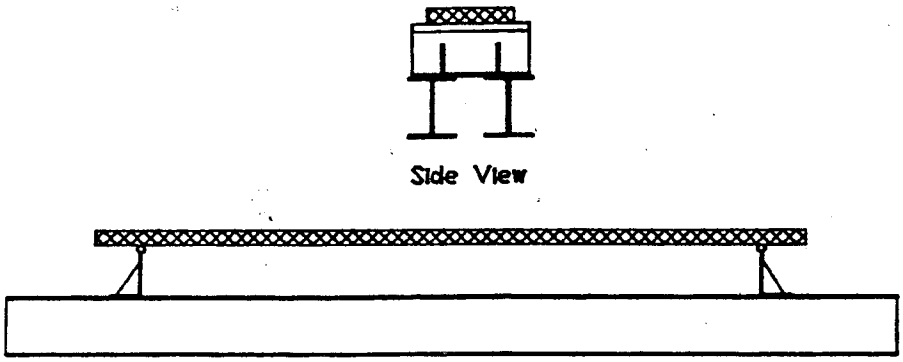

Static Testing Apparatus

Actual Static Load Apparatus

Tinius Olsen Testing Machine

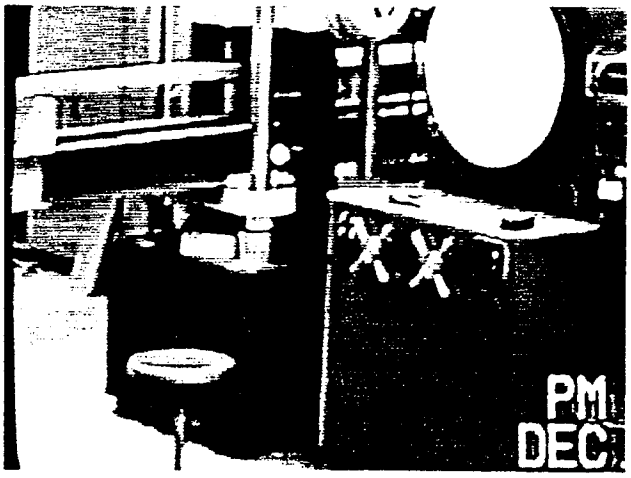

Dynamic Testing Apparatus

Designed and Built
(Senior Projects)

Dynamic Testing Apparatus

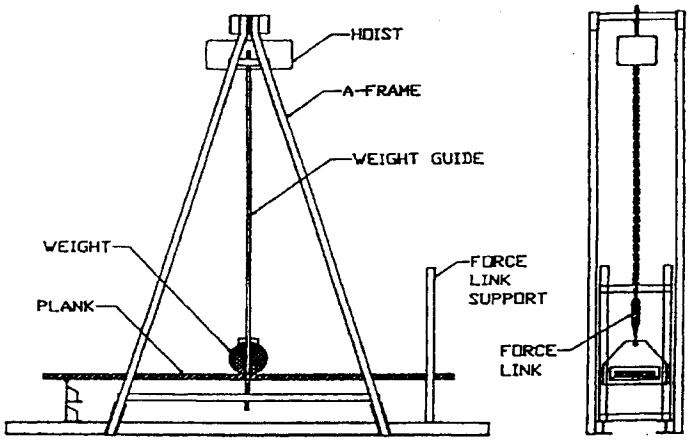

Samples Tested

1. Solid Sawn Wood Plank
   a. Finish
      i. Rough
      ii. Dressed
   b. Types
      i. Southern Yellow Pine
      ii. Douglas Fir

Samples Tested

2. Manufactured Wood Plank
   a. Veneer Type
      i. Horizontal
      ii. Vertical
   b. Suppliers
      i. 3 Manufacturers

Manufactured Wood Plank

VariablesTested

Solid Sawn & Manufactured Plank

1. Span
2. Height
3. Width
4. Moisture Content
5. Stiffness
6. Specific Gravity

VariablesTested

Load Tests

1. **Static Load**

2. **Dynamic Load**

Solid Sawn & Manufactured Plank

Test Procedures

Static-Nondestructive

- Measure Plank Width, Weight & Length
- Calibrate DynoMoe Test Apparatus
- Vibrate Plank
- Read & Tabulate MOE, Weight & Frequency

Static – Destructive

- Insert Test Platform into Tinius Olsen Testing Machine
- Set Platform Span
- Set Deformation Dial
- Calibrate Tinius Olsen Testing Machine
- Read Applied Load at Prescribed Deflections

Solid Sawn & Manufactured Plank

Test Procedures

Dynamic

- Inspect Apparatus
- Install Force Link, Force Link Cable & Moveable Support
- Set Span Length
- Install & Power Quick Release
- Power Peak Meter & Hoist
- Calibrate Force Link & Peak Meter
- Raise Weight
- Center Plank on Span
- Set Test Weight at Proper Height
- Release Weight
- Read & Record Load from Peak Meter
- Re-raise weight to Prescribed Drop Heights Until Failure Occurs
- Read & Record Load from Peak Meter Until Failure Occurs

Results and Discussion

Typical Dynamic Loading Results

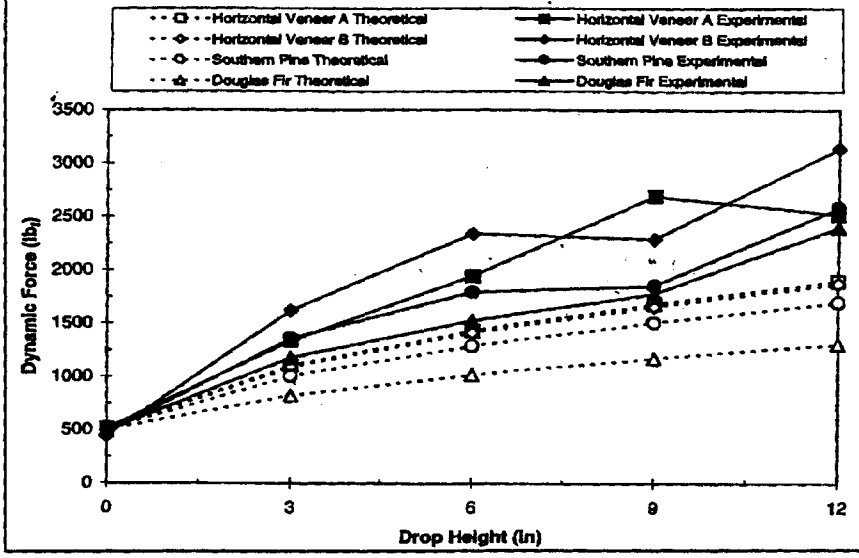

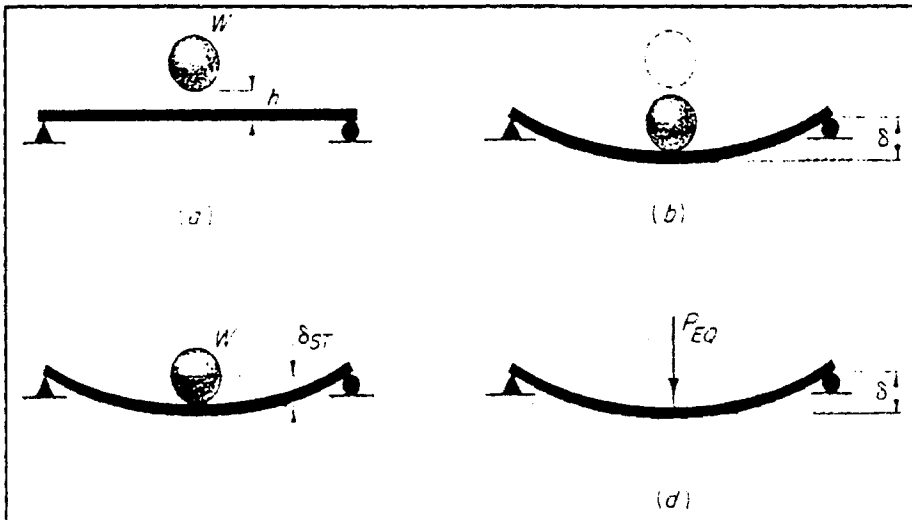

FIG. 13.5 Derivation of impact factor. (*a*) Impact load. (*b*) Deflection under impact load. (*c*) Deflection under gradually applied load W. (*d*) Equivalent gradually applied load to give same deflection as impact load W

Equation for Theoretical Equivalent Static Loads

$$s = \left(1 + \sqrt{1 + \frac{2h}{\delta_{ST}}}\right) s_{ST}$$

Dynamic Loading Results

TABLE I: DYNAMIC LOADING RESULTS

Plank	MOE Dynamic ($x10^6$psi)	MOE Static ($x10^6$psi)	Density (lb_m/in^3)	Moisture Content (%)	Ratio Experimental/ Theoretical
Southern Pine	1.50-3.00	2.02-2.80	.020-.029	10.00-13.00	1.41-2.21
Douglas Fir	1.75-2.60	ND	ND	11.00-12.50	1.51-2.67
Horizontal Veneer A	1.97-2.35	ND	.024-.026	12.50-16.50	1.52-1.88
Horizontal Veneer B	1.90-1.99	1.872-2.050	0.019	14.50-16.00	1.22-1.60
Vertical Veneer	1.75-2.42	1.975-2.403	.021-.026	9.25-12.75	1.40-1.65
	ND: Not Determined		Thickness	1.50-1.63 in	
			Width	9.06-11.75 in	
			Length	96.00-145.13 in	

Ratios
Experimental/Theoretical

Range

1.1 – 2.4

Results and Discussion (cont)

- **Manufactured wood planks have less variable stiffness characteristics than solid-sawn scaffold planks.**

Results and Discussion (cont)

- Manufactured wood planks have a more predictable ultimate failure load range than do solid sawn planks.

Results and Discussion (cont)

- Laminated joints or laminated veneer placement in manufactured planks, like annular rings spacing, knot size and placement of solid sawn scaffold planks, proved to affect specimen dynamic resistance.

Dynamic Loading Criteria

Recommendation:

Safety Factor $\geq$ 3
to Prevent Failure

Summary

- **Concept of Dynamic Loading Introduced**
- **Method for Determining Dynamic Loading Demonstrated**
- **Comparison of Equivalent Static and Actual Dynamic Loads Made**
- **A Safety Factor of at Least 3 is Recommended as the Dynamic Loading Criteria**

NON-LINEAR ACOUSTIC SYSTEM FOR DAMAGE ASSESSMENT

Yulian Kin

Purdue University Calumet
Hammond, Indiana 46323

Telephone: 219-989-2684
e-mail kin@hwi.calumet.purdue.edu

and

Alexander Sutin

Eric Roades

Karen Dalton

Kimberly Bateman

Yulian Kin

Non-Linear Acoustic System for Damage Assessment

Yulian Kin
Alexander Sutin
Eric Roades
Karen Dalton
Kimberly Bateman

Key Words:
Fatigue, fatigue damage, crack, non-destructive fatigue testing, non-linear acoustic instrumentation

Prerequisite Knowledge:
Fatigue crack propagation
Basic understanding of oscilloscopes and function generators
Failure prediction techniques

Objective:
Damage assessment on the basis of wave modulation change.

Equipment:

1. Digital Oscilloscope with FFT capabilities
2. Digital Function Generator
3. Piezoelectric Ceramic Sensors (Disc, 10mm by 2mm)
4. High Pass Filter (20-40 kHz cutoff)
5. Striker
6. BNC to Alligator leads
7. Test Specimens, damaged and undamaged (for reference)

Introduction:

This project is based on a nonlinear acoustic approach to damage detection. This approach is based on the fact that cracks, surface flaws, disbonding or other damage have high nonlinear elasticity. This causes nonlinear acoustic responses, especially the modulation of an ultrasound wave passing through a crack [1]. These responses were of particular interest in the conducted experiments.

In these experiments, the specimens were induced with a high frequency ultrasonic wave and a low frequency vibration, and the interaction modulation provided a reliable measure of the quantity of the accumulated damage. This method is known as nonlinear wave modulation spectroscopy (NWMS) [2]. The physical nature of this modulation can be explained with the help of a simple model. Consider the sample in Fig 1, with a single crack as the only flaw. The method uses the interaction of a high-frequency ultrasonic signal, transmitted through the part, with the low-frequency vibration of the part. The low-frequency vibration alternates between compression and dilation of the flaw. Suppose the ultrasonic signal has a frequency at least an order of magnitude larger than

the low-frequency signal, and that the amplitude of the low-frequency vibration is sufficiently large to close the crack during the compression phase (Fig. 1a), and to open it during the subsequent tension (Fig. 1b). During the dilation phase of the low-frequency cycle, the high frequency signal is partially decoupled by the opened crack. This reduces the amplitude of the high-frequency signal that passes through the crack. During the other half of the low-frequency cycle, the signal produces compression and the crack is closed. The closed crack does not decouple the ultrasonic signal and the amplitude of the transmitted signal increases. This results in amplitude modulation of the ultrasonic signal as shown in Fig. 2; *i.e.* observation of low amplitude during the dilation part of the low-frequency vibration signal and high amplitude during its compressive phase. Fourier transformation of this signal reveals sideband frequencies that are the sum and difference of the frequencies of the ultrasonic and vibration signals. The presence of these new frequency components is a clear sign that a flaw or crack is present.

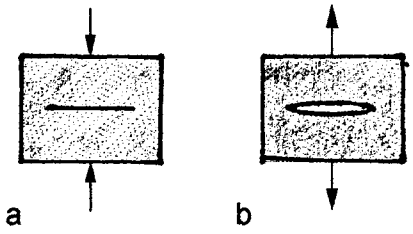

Figure 1. *Crack Behavior Under Low Frequency Vibration (a) in compression (b) in tension.*

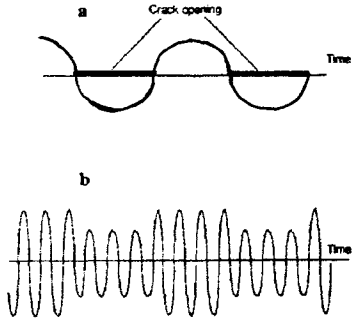

Figure 2. *Amplitude modulation of probe signal; (a) vibration, (b) ultrasonic signal.*

Specimen:

Tests were conducted on three Ford Alternator Housings. (Figure 3) Two of the housings exhibit damage, one visible and one not apparent to visual inspection. The third housing is undamaged and is used for reference purposes.

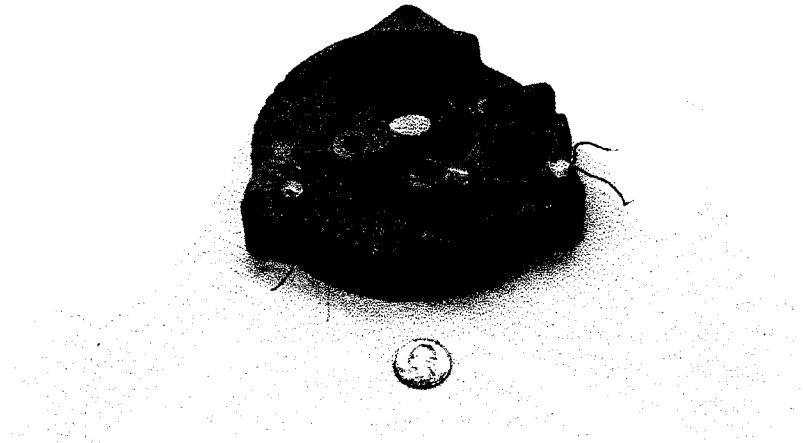

Figure 3. *Ford Alternator Housing (test specimen).*

Experimental Setup:
The basic electrical setup of the system is shown in Figure 4. A signal generator, generating a sine wave signal is connected to an input sensor attached to the specimen. A constant high frequency sinusoidal wave is inputted. A second, output, sensor on the specimen is connected to the oscilloscope through a high pass filter. The impact from the striker or firing mechanism induces low frequency vibration into the specimen. The striker is equipped with a sensor used for synchronization with the digital oscilloscope, which conducts spectral analysis of the received signal.

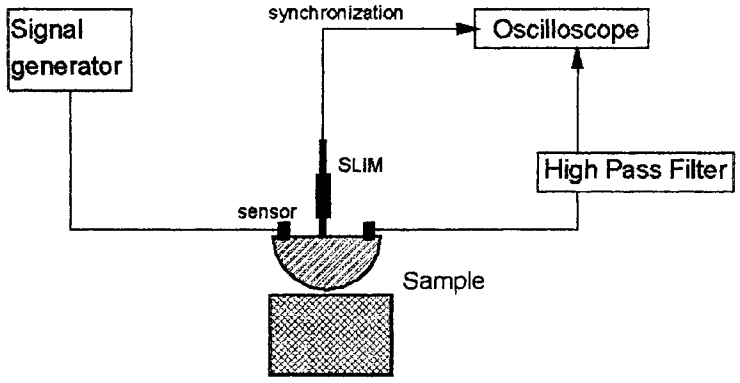

Figure 4. *Electrical Schematic*

Figure 5. *Current Lab Setup.*

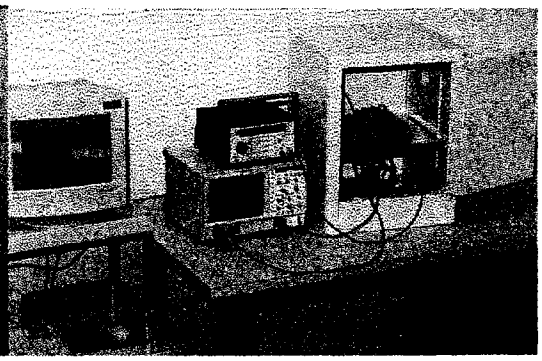

Figure 6. *Mock-up of future instrumentation.*

Observations:
It can be seen that the modulation (high level side components) takes place just after the impact in the damaged specimen. (Figure 7) The undamaged specimen has no such side components. (Figure 8)

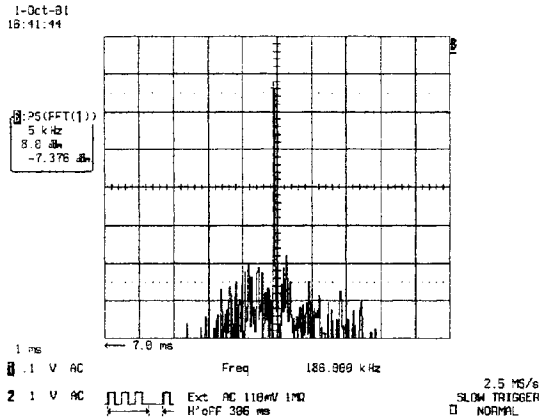

Figure 7. *Spectral analysis of the sample with a tiny crack*

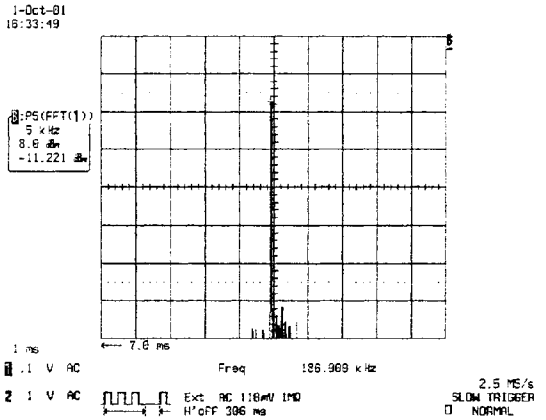

Figure 8. *Spectral analysis of intact sample.*

Applications:

The NWMS experiments, described and demonstrated here, possess two significant benefits for detection of nascent damage. First, its sensitivity to damage is orders of magnitude greater than competing techniques. Second, its ability to examine the entire part at one time allows rapid and efficient testing of complex specimens. The possible applications of this method are the observation of fatigue damage in buildings, bridges, aircraft, automobiles, etc. This technology would allow for more accurate maintenance schedules, safer supports, and preventative repair measures of the damaged structures.

References:

1. Didenkulov I.N., Sutin A. M., "Nonlinear Acoustic Technique of Crack Location," American Institute of Physics Conference Proceedings, no. 524, pp.329-332, 2000.

2. Chudnovsky A., Kin Y., Sutin A. "Non-Linear Acoustic Technology for the Investigation of Structure Damage". *SEM Annual Conference on Experimental and Applied Mechanics, Portland Oregon,* #184, 2001.

3. Sutin A. "Quantitative Nondestructive Evaluation in Reliability Assessment of the Aging Aircraft Structure Components". Smart Material Design Inc., Highland Park, IL. Report, F49620-99-C-0038. 2000.

4. Kin Y., Sutin A., Chudnovsky A. "Non-Linear Acoustic Instrumentation for Detection of Damage in Aging Metal, Plastic, and Composite Structures". *Eighth Annual International Conference on Composites Engineering, Tenerife Canary Islands, Spain*, 2001.

MOTORLESS MOTION WITH NiTi: A SENIOR DESIGN PROJECT

Suzanne Keilson

and

Robert Redfield

Department of Electrical Engineering and Engineering Science
Loyola College
4501 North Charles Street
Baltimore, Maryland 21210

Telephone: 410-617-2722
e-mail skeilson@loyola.edu

and

Michael Guarraia
currently at Lockheed Martin Corp.

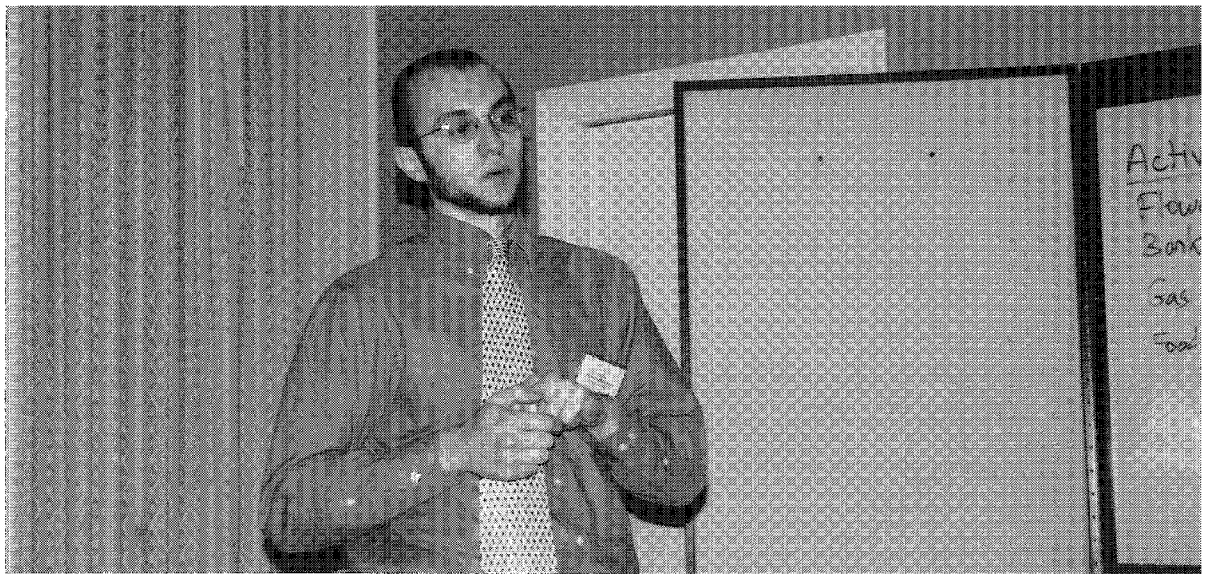

Biographies:

Michael Guarraia graduated from Loyola College in May, 2000 with a degree in Engineering Science specializing in Materials Science, and is currently employed at Lockheed Martin Corporation and is pursuing his MBA at Loyola College.

Robert Redfield graduated from Loyola College in May, 2000 with a degree in Engineering Science specializing in Materials Science, and is pursuing a medical career.

Suzanne Keilson, assistant professor, at Loyola College since 1994, has worked in various areas of materials science, including point defects in crystals and biomaterials. She also does research in biosensory systems (the auditory system) and signal processing.

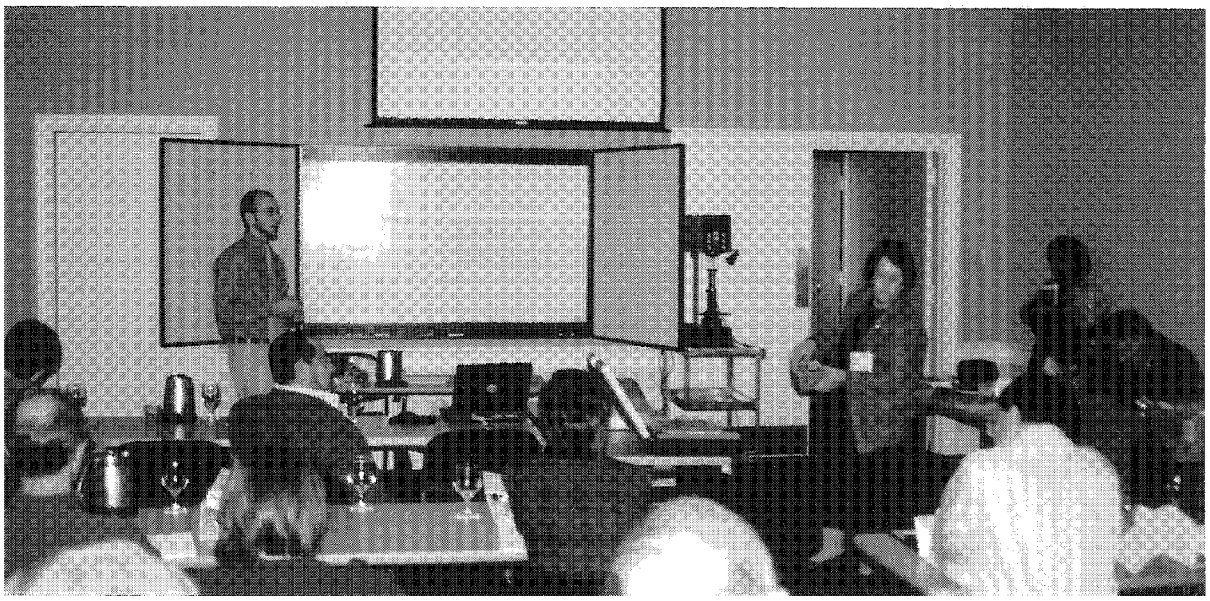

Motorless Motion with Ni-Ti: A Senior Design Project

Michael Guarraia*, Robert Redfield, Suzanne Keilson
Electrical Engineering and Engineering Science
Loyola College, Baltimore, MD
*currently at Lockheed Martin Corp.

Key Words: Nickel-Titanium alloy, shape memory alloys, senior design, motorless motion, robotics, biomechanics

Prerequisite Knowledge: Knowledge of basic materials science, electronics and mechanics. An introductory materials science course covering phase transitions and alloys. In addition, undergraduate courses in mechanics and electronics and some review in biomechanics and robotics would prove helpful.

Objective: To understand the interaction between design, design criteria and materials properties. Design of an application based on a materials property study/exploration. Can be used as both a "cookbook" lab to build and understand some basics of mechanics, materials, and electronics in the context of a robotics application, or in a more open-ended form to explore the interrelationship between design, design constraints, and materials properties.

Equipment and Materials:
Erector Millenium® set:
screws, nuts, frame members, plastic spacers

Ni-Ti wire:
Dynalloy® NITINOL (8 meters)

Electronic components:
Resistors (15 ohms), batteries (9 volt), switches (single pole double throw, one for each robot digit), circuit board for mounting, sheet metal box to contain circuitry, Dremel® tool cutter, rubber bands and/or biasing springs, two-part epoxy

Introduction:

Design course:
The senior design capstone course at Loyola College is intended to be a culmination of undergraduate coursework. All students in both the electrical engineering and engineering science programs take the same course and learn project management and professional skills together. The design project should consider realistic engineering constraints such as cost, time, manufacturability (such as the ability to solder parts together), and power consumption. From the students' perspective, some of the project goals include gaining a more thorough understanding of a material and its properties (based on theoretical knowledge and current manufacturing practice), to design a socially beneficial project, and to construct a working model

under the aforementioned constraints. The budget constraints are $400 for the design team and the time constraint is that all work, beginning in September, is completed by the end of April.

The goal of this project was to develop a senior design project around the principle of motorless motion utilizing the shape memory properties of a Nickel-Titanium (NiTi) alloy. Ultimately, this was incorporated into a working prototype of a three-fingered robotic hand.

The material (NiTi):

NiTi or NITINOL (named for the alloy development at the Naval Ordinance Laboratory) has been getting increasing attention in a number of applications including eyeglass frames, fishing lures, cellular phone antennas, medical guide wires, and surgical tools. The particular alloy composition that is generally used is 55 weight % Ni and 45 weight % Ti. The crystal structure of NiTi is the B-2 structure, and is similar to the BCC structure, but with two differing atoms in the unit. The nickel atoms are on the cube corners and the titanium is in the center of the unit cube (Figure 1).

The NiTi alloy exhibits two very unique properties that have great potential for application. The first is superelasticity. This is the ability to undergo excessive stress (to the point of substantial elastic deformation) without plastic deformation. It is also called mechanical memory, whereby the deformed part returns to its pre-deformed or constrained shape upon release of the stress. The other unique property of NiTi is the shape memory effect. This is the ability to return to a predetermined shape by heating the material. This is also sometimes called thermal memory. These effects are achieved via a phase transformation (Figure 2). At the relaxed or low temperature state, the material is in a martensitic phase; upon heating above a critical temperature the NiTi goes into an austensitic phase (high temperature form). The recursive phase transformation returns the structure to its original mechanical configuration.

Design Project:

During the brainstorming sessions, some project ideas that were generated included using the superelastic properties of NiTi for its dynamic qualities in rock climbing gear, using the shape memory effect for safety devices such as sprinkler systems or in valves, or snake-like flexible objects. The actuation of the NiTi was seen to be similar to the action of human muscles. It is well known in biomechanics that muscles act in pairs, as one element of the pair contracts the other extends to create the appropriate smooth control of motion around a joint. The tendons are the whitish tissue that attaches the muscle to the bone and the muscle will usually wrap itself over the joint. As the muscle contracts, force is exerted on the joint forcing it to move or rotate. These same principles of biomechanics were applied in this design project. An anchoring point, joint design, and biasing spring were some of the necessary elements to create a potentially useful robotic part (Figure 3).

The final project idea was a three-fingered robotic hand. Many researchers are intrigued by the far-ranging potential of robotic applications. What makes this example so interesting is that no gears, hydraulics or motors are used for actuation of the moving parts. Some of the advantages to this design, which relies on a materials property of the NiTi alloy as compared with more conventional mechanical designs, are its high strength-to-weight ratio, small size, silent operation, low power requirements, easy maintenance, and potential biocompatibility. Additionally, NiTi possesses very good corrosion resistance. The alloy forms a thin oxide layer (TiO_2) on the exterior, which is more corrosion resistant than stainless steel. It is already in use as surgical equipment, so its use in prosthetic devices is certainly a possibility as well. As with

other robotic designs, this would also have the advantage of being able to work in extreme environments for extended periods of time[1].

Most of the design specifications were determined through a combination of extensive experimentation, trial and error, and literature and web research. From the basic information about the material, it was known that upon receiving a specified amount of current, which causes heating, the NiTi contracts as its phase changes. Key design issues were the diameter and length of wire, and the amount of current required for resistive heating (which would cause the necessary phase transformation, thus inducing contraction and movement of the robotic part). The percent composition of the alloy determines the percent shape change, which in turn determines the total movement of the robotic finger. For the material purchased for this project, a maximum length change of 6.6 % was observed. Geometric parameters of the design such as minimum bend radius and the corresponding minimum radius of the pulleys were set to avoid fatigue and destruction of the alloy matrix.

The final design used 150 μm diameter Dynalloy® NiTi, requiring a current of approximately 0.4 amps to fully contract the wire. The finger members were constructed from an Erector® set. The mechanical properties of the metal and plastic spacers from the set played an important role in the final design, as discussed in more detail in the procedures section. The design evolved through a number of iterations in order to achieve some desired level of performance.

Testing was necessary in order to finalize design parameters[2]. One of the tests performed was for the thermal characteristics of the plastic spacers. They were used for the pivot point of the joint. The NiTi, upon applying a current, heats up to 70° C, a sizeable thermal challenge for plastic, which also must withstand repeated heating cycles for the lifetime of the robotic part. A conservative test was performed in which the spacers were placed in an oven and placed under load, edge on (diametrically). All spacers withstood an environment of 90-95° C for 10 minutes with no observable deformation, even under a load of 52.1 grams. Another test that was performed was a radial strength test of the finger and pivot joint configuration. This was done to get an idea of how strong the individual robotic fingers would be. The design was able to achieve a maximum 50 degree rotation of the joint upon joule heating with a load of 70 grams and a maximum 90 degree rotation with a 10 gram load.

A working prototype was meticulously constructed giving the students great satisfaction and meeting all of the design criteria and learning objectives[3] (Figure 4).

Procedure:

To duplicate the process of building a robotic hand, one starts with a single "finger" or digit. Some examples of the early design evolution of the project are shown in Figure 5. A single finger with a single hinged joint consists of four frame members used in pairs to create two segments attached at the hinge joint. A segment is made by two frames held together by screws and nuts and separated by plastic spacers. For each such finger, a complete electrical circuit must be created. The NiTi wire is fixed at the proximal spacer (attachment point to the base of the "hand") and runs to the hinge joint. A groove should be cut in a plastic spacer to accommodate one end of the loop of NiTi wire, which is then secured with epoxy into the groove[4]. This plastic spacer, residing in the hinge joint must be rigidly fixed to the distal segment, but free to spin about the screw axis, in order to insure rotation of that distal segment

(Figure 6). In the final design a rubber band provides the restoring force (acts as the complementary muscle in the muscle pair), and wraps around the entire digit.

When the NiTi contracts under heating, the wire, which is fixed to the outer diameter of the plastic spacer, creates a torque around the axis of the spacer. If the distal segment is rigidly attached to the spacer, it too will rotate in response to that torque[5]. This is what gives rise to the gripping or grasping motion of the fingers. When the current is turned off and the NiTi wire relaxes to its original length, the rubber bands (or biasing springs) supply the force to rotate the distal segments back to their original positions, releasing the "grasp" of the robotic hand. The basic circuitry is very simple, with each finger employing its own mechanical switch placed on the sheet metal box and a simple resistor (15 ohms) and battery (9 volts) connected in series in the NiTi wire loop (Figure 7). When the switch is thrown and the circuit is closed, current flows, thereby heating the NiTi. No safety or automated options were placed in this initial prototype. The operator must open the switch to prevent the wire from overheating or damaging the spacers. No attempt was made to coordinate the operation of the digits. These are all possible extensions to the basic design[6].

Comments and Instructor Notes:

1. Another possible environment to employ the NiTi robotic hand is in a clean room, especially for silicon wafer and IC manufacturing.

2. This also helps to emphasize the point that the design process is an iterative one, and that testing plays a crucial role in product development.

3. Total expense report for the project was $273.

4. Great care must be used with the plastic spacers and the wrapping of the NiTi wire. When the finger is loaded and the current is increased, the plastic spacer can be cut or damaged.

5. Due to the constraint of the percent contraction of the NiTi, a direct attachment of the wire to the distal segment would only have resulted in a small radial motion about the joint. With this design about 70 degrees of rotation is achievable. This is applying a mechanical principle akin to that of gearing ratios. By attaching the NiTi to a small diameter spacer, you can achieve maximal rotational output for that percent length change.

6. Several possibilities for design expansion and projects exist, such as more complicated joints and robotic action, and utilizing a computer or digital interface to control the circuitry. The robotic hand could also be put under remote or radio control. Variable contraction and feedback systems could be explored to control the grip of the robotic hand to enable it to pick up objects of varying weight, size, and fragility.

References:

Duerig, Melton, Stockel, and Wayman. Engineering Aspects of Shape Memory Alloys. Boston: Butterworth-Heinmann. 1990.

Porter, Easterling. Phase Transformations in Metals and Alloys. New York: Chapman & Hall. 1992.

Web sites:

www.dynalloy.com

www.sma-inc.com

www.nitinol.com

Acknowledgements:
Thanks to Dr. Robert Pond Jr. for his invaluable editorial and technical input.

Figure 1 B2 structure of NiTi alloy

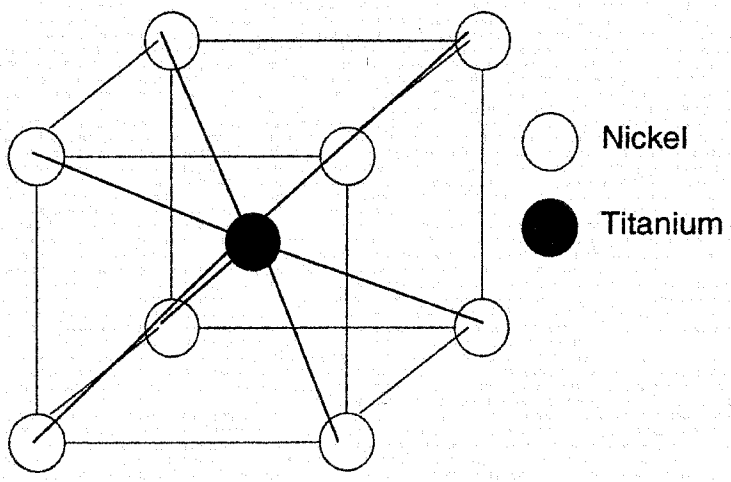

Fig. 2

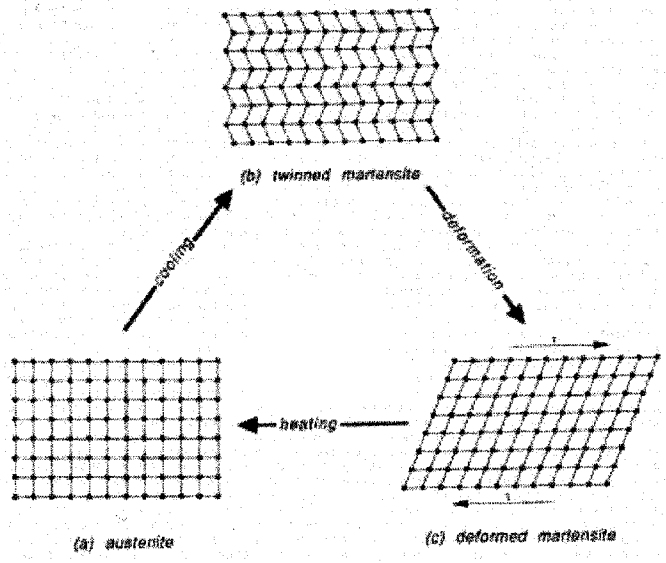

†Duerig, Melton, Stockel, Wayman. *Engineering Aspects of Shape Memory Alloys.* Boston: Butterworth-Heinemann. 1990. (p. 11)

Figure 3. Analogy between biomechanical operation of a muscle and NiTi robotic action.

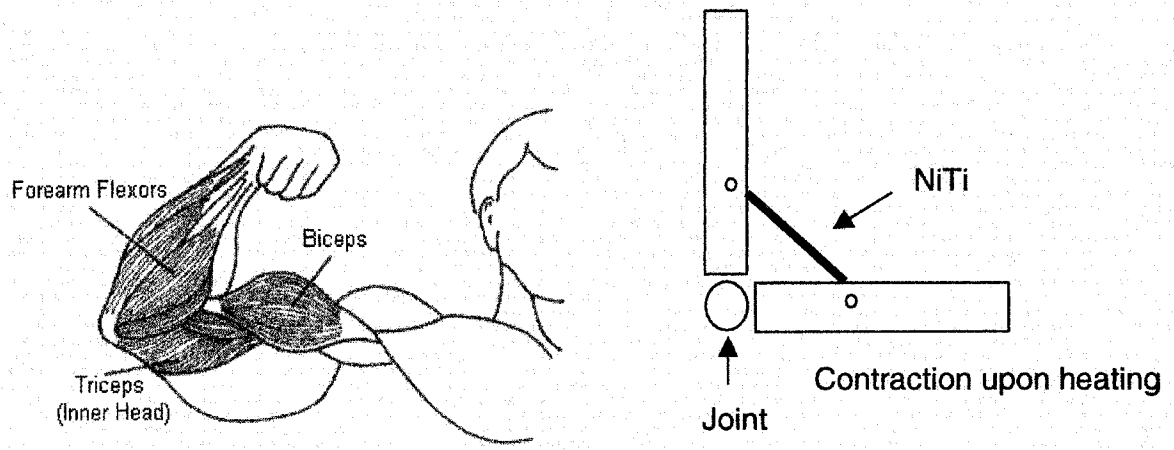

Figure 4. Photos of prototype robotic hand. Different views.

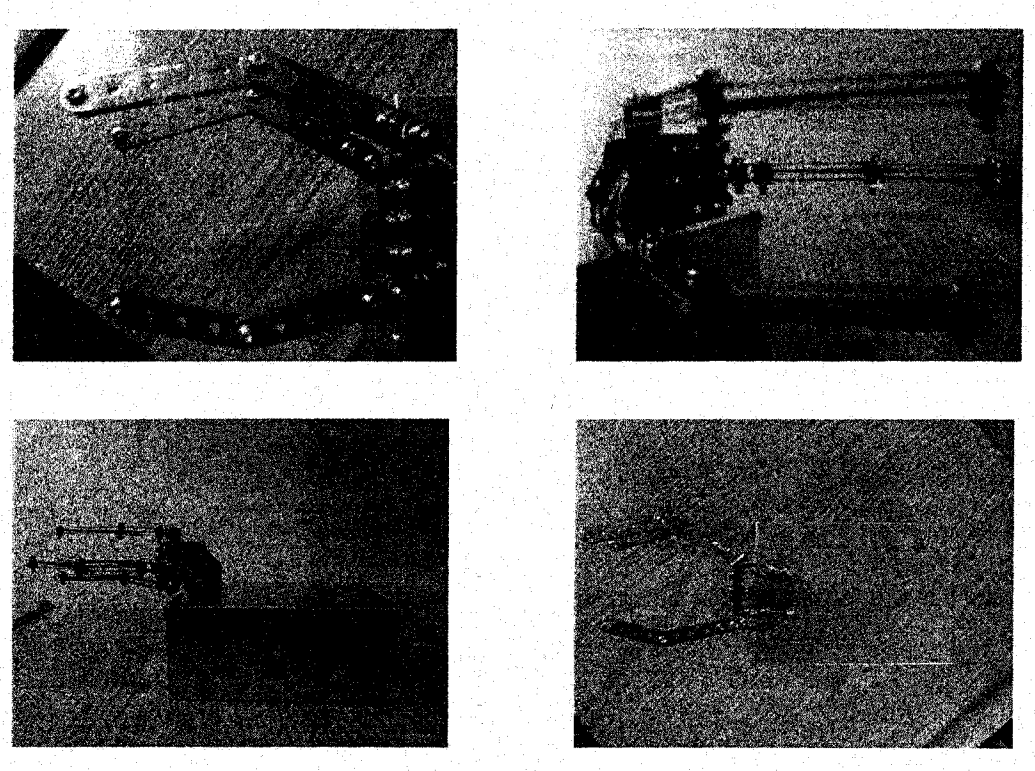

Figure 5. Some examples of the design evolution of the robotic digit.

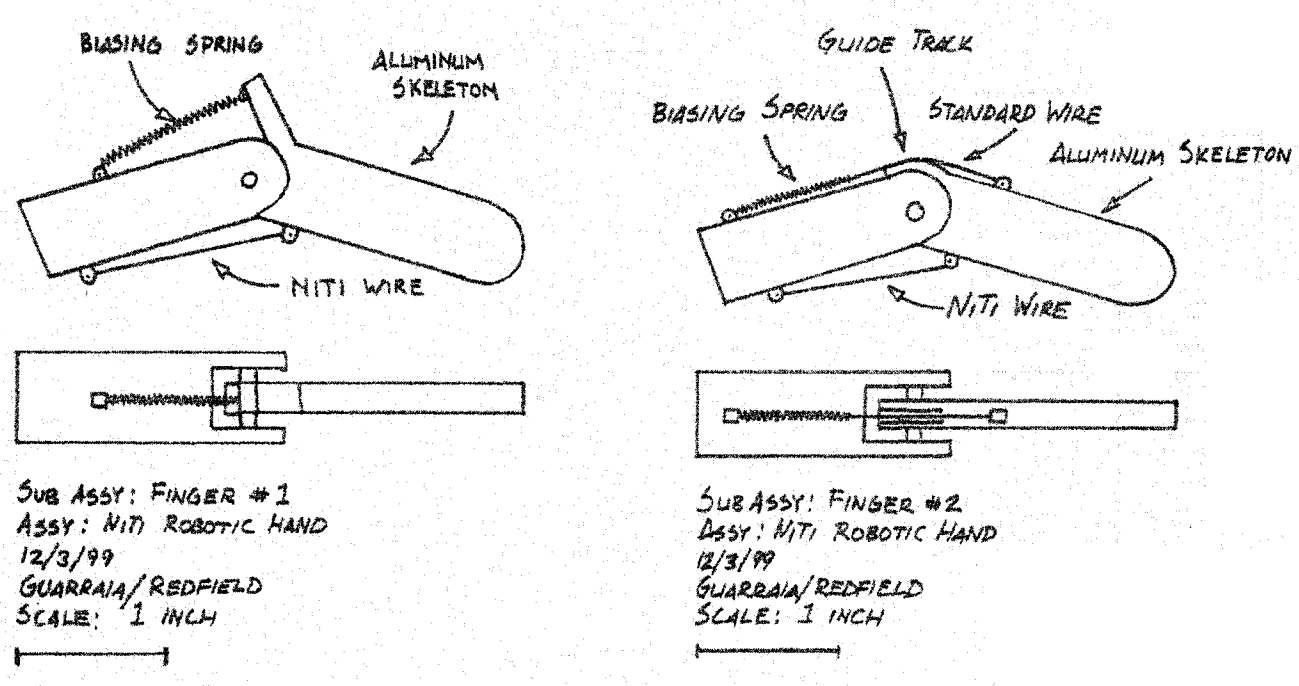

Figure 6. Schematic of final design of a single "digit". Securing wire around the plastic spacer allows for more angular motion of segment (yellow arrows) for a given length change of NiTi wire.

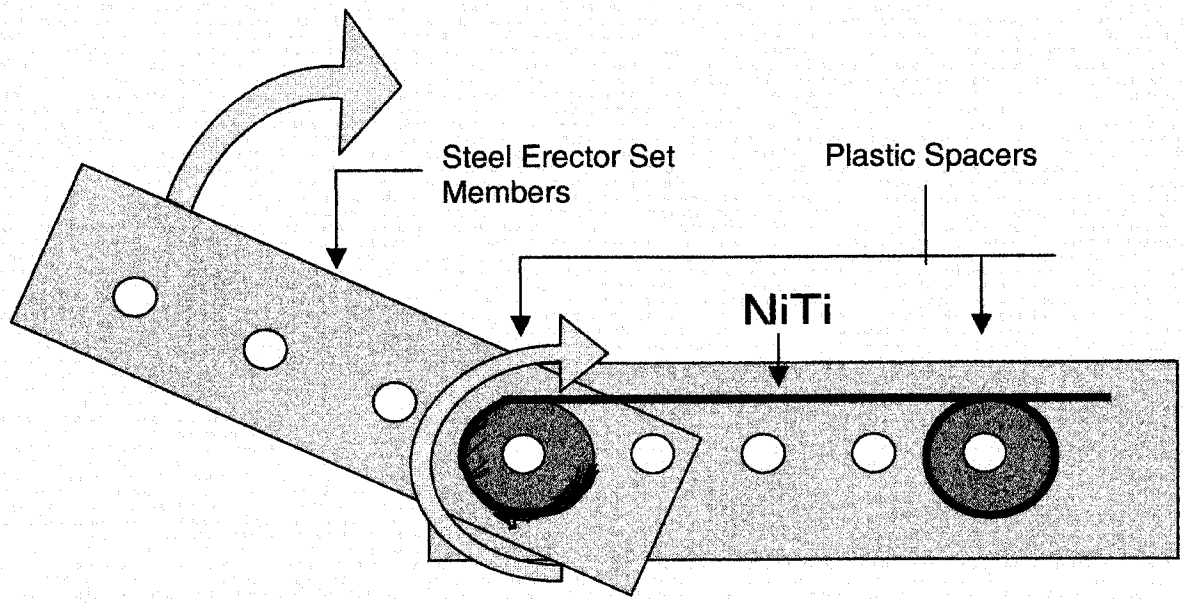

Figure 7. Electrical circuit for control of NiTi phase transition. Note that current is only at 75% of the current for maximum contraction (0.4 amps).

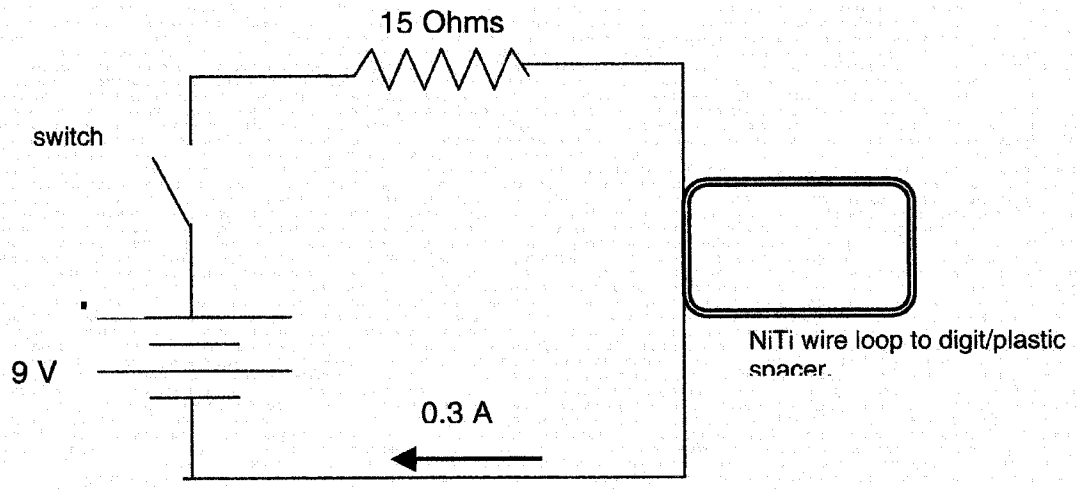

AN INSTRUCTIONAL SOFTWARE PACKAGE ON FTIR SPECTROMETRY

Leonard W. Fine

L. Avila

and

B. Venkataraman

Department of Chemistry
Columbia University in the City of New York
Havemeyer Hall
New York, New York 10027

Telephone: 212-854-2017
e-mail fine@chem.columbia.edu

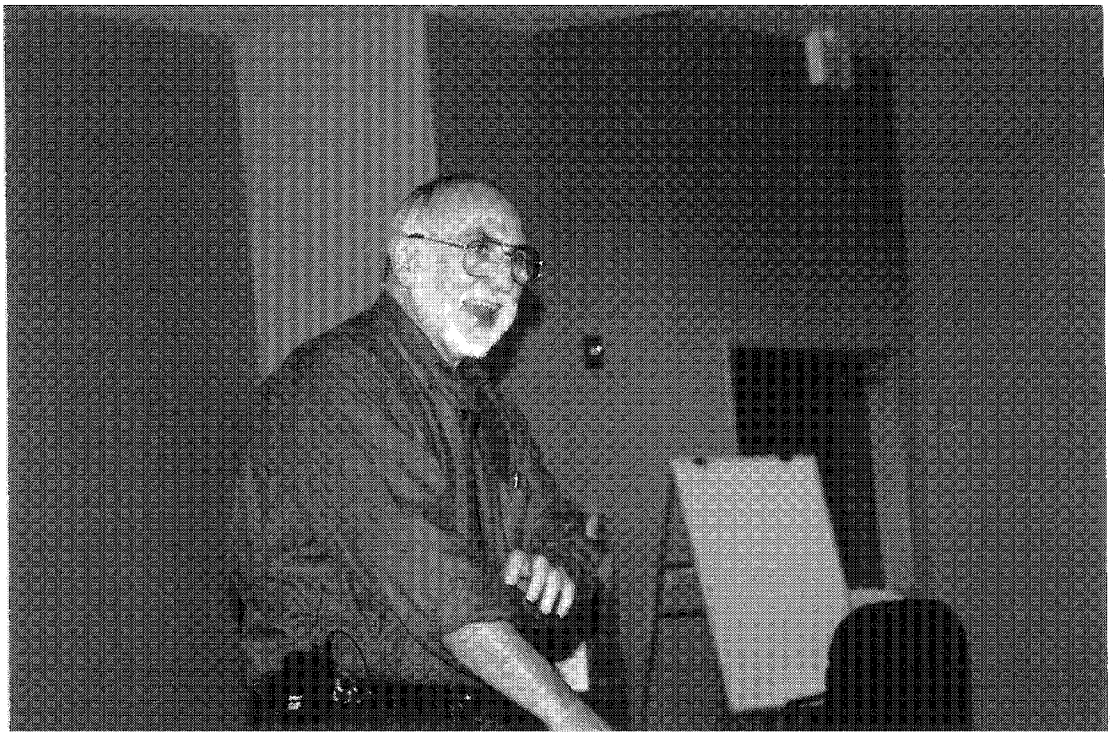

Leonard W. Fine

B. Venkataraman

AN INSTRUCTIONAL SOFTWARE PACKAGE ON FTIR SPECTROMETRY

L. AVILA, L. FINE AND B. VENKATARAMAN
Department of Chemistry, Columbia University, NY, NY 10027

We have developed an interactive software package on the theory and practice of spectrometry. While the focus of the package is on an experimental technique use chemical analysis, the mathematics, physics, and engineering of the technique are emphasized. In particular, the package illustrates how the Fourier transform and interferometery are combined to extract spectral information from interferograms.

After introducing the Fourier Transform with illustrations and applications drawn fro different fields (e.g. music and medicine), the software turns the user's attention to question of how the Fourier Transform and interferometry work together in recordir infrared spectrum. It starts by showing how the Michelson Interferometer is used t determine an absorption spectrum with a monochromatic light source. From there expands to a two-frequency light source and then to a polychromatic light source s how the principles are the same, just that the interferogram gets more complex. Is related to resolution and optimum usage of apodization functions are also discusse

Where possible, interactive animations have been included to help explain concep example, in a section contrasting a dispersive spectrometer with an FTIR spectrom user "walks" through the instrument with the components "clickable" to view additio information or simple animations on the working principle of the component.

SUBSTRATE ANALYSIS GRIT BLASTING

Rodney D. Jiggetts

Metallurgy Division (855)
National Institute of Standards and Technology
100 Bureau Drive, Stop 8555
Gaithersburg, Maryland 20899-8555

Telephone: 301-975-5122
e-mail rodney.jiggetts@nist.gov

F. Biancaniello

S. Ridder

S. Mates

M. Stoudt

R. Schaefer

P. Boyer

Rodney D. Jiggetts

Substrate Analysis
Grit Blasting

The National Institute of Standards & Technology
MSEL
Metallurgy Division
Materials Processing Group

Rodney D. Jiggetts

F. Biancaniello

S. Ridder

S. Mates

M. Stoudt

R. Schaefer

P. Boyer

Substrate Based Analysis

Needs:

- Thickness and deposition efficiency sensors; substrate preparation vs. adhesion

NIST Role:

- State of the Art Microanalysis Lab
- Expertise in developing new technologies in sensor application and calibration

Substrate Based Analysis

Goals:

Short Term:

- Profilometry Measurements
- Reflectometry Measurements
- Confocal Microscopy Measurements
- Image Analysis & SEM
- Evaluate new Peel/Adhesion Test

Long Term:

- Compile and Correlate Surface Roughness Data using the Various Techniques
- Correlate Surface Roughness Data of the Various Techniques with Adhesion Tests
- Publish paper(s) of the correlation between the various measuring techniques, and adhesion

GRIT BLASTING

One of the commonly used processes in Substrate Preparation

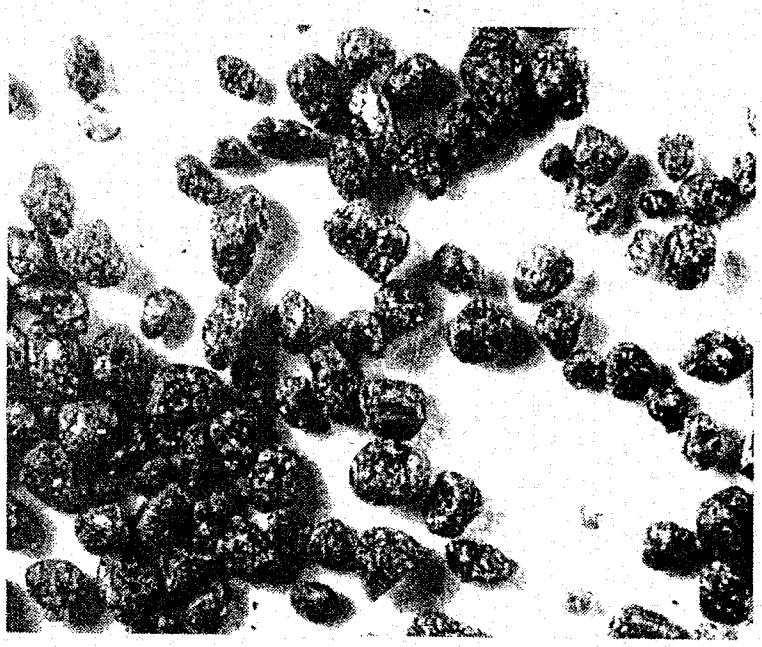

How do you determine what is a "PROPERLY" Grit Blasted Surface?

1) By the "Maximum" roughness measurement?
2) By the "Maximum" number of peaks per length measured?
3) By an Adhesion Test?

Outline

- NIST's Grit Blasting Facility
- Grit Impact on Surface
- Substrate Surface Analysis Results:
    1) Profilometry
    2) Metallography
    3) Image Analysis
    4) Reflectometry
    5) Confocal Microscopy
- Summary
- Future Work/Goals

Grit Blasting Facility

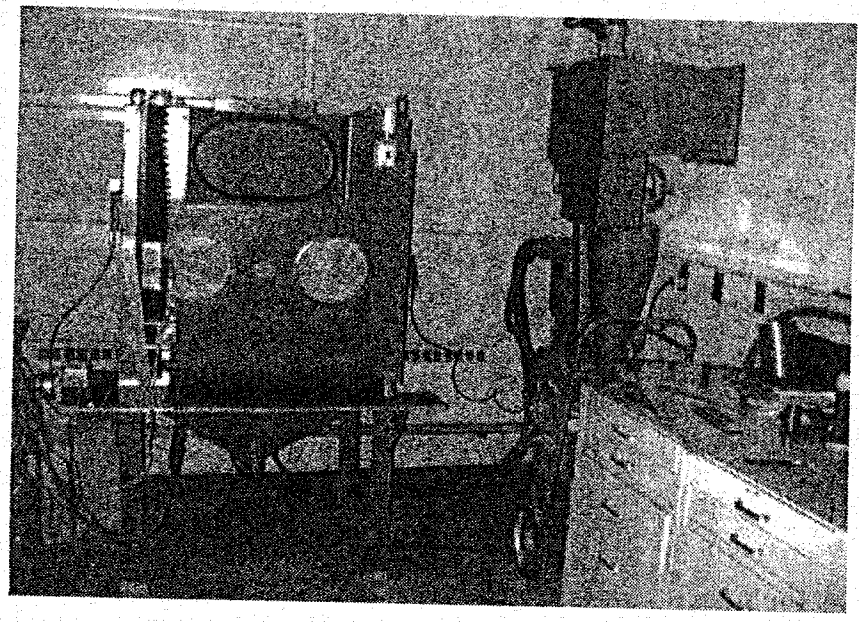

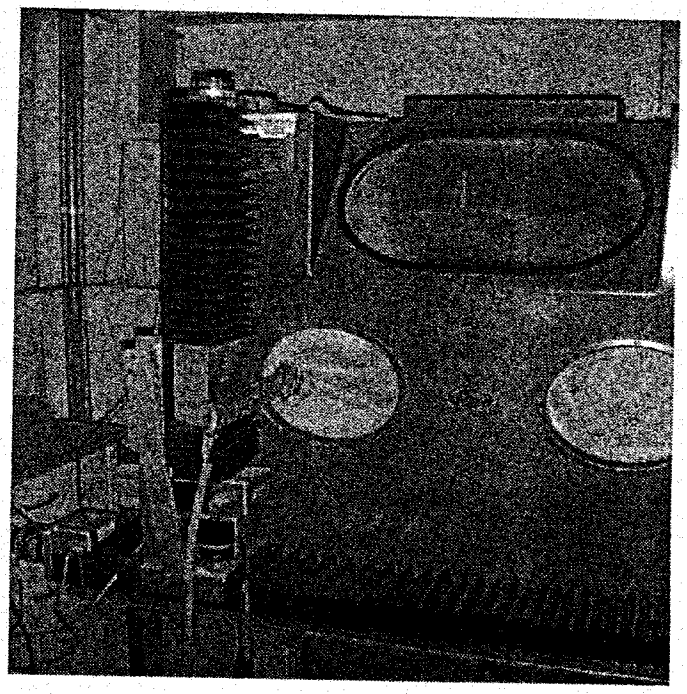

- Suction/Vacuum
- Recirculating
- 800 kPa (100 psig) adjustable Line

<u>Robotics</u>

Consistency/Repeatability

Software - Labview
- Speeds
- Positionings

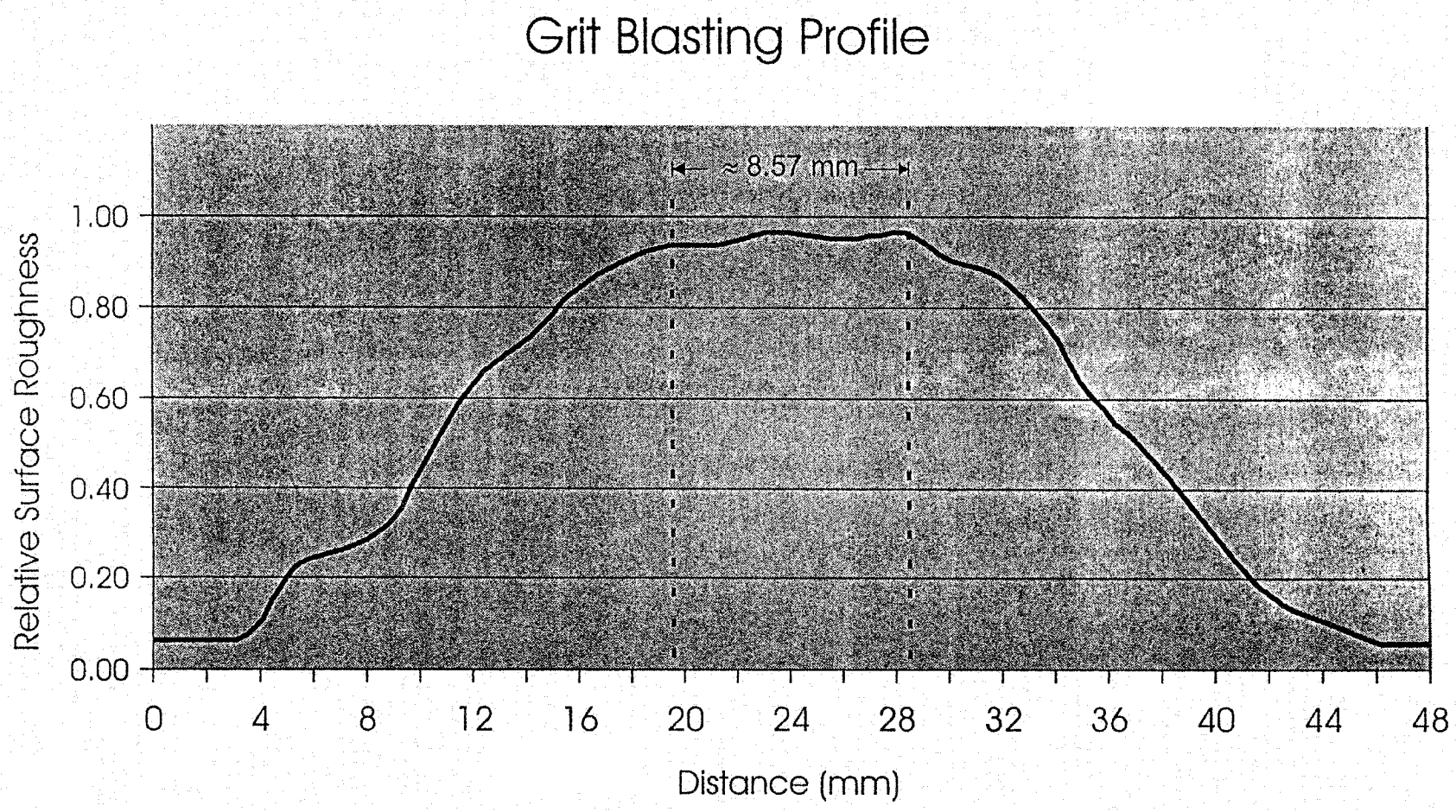
Grit Blasting Profile
≈ 8.57 mm
Relative Surface Roughness
1.00
0.80
0.60
0.40
0.20
0.00
0
4
8
12
16
20
24
28
32
36
40
44
48
Distance (mm)

Grit Impact on Surface

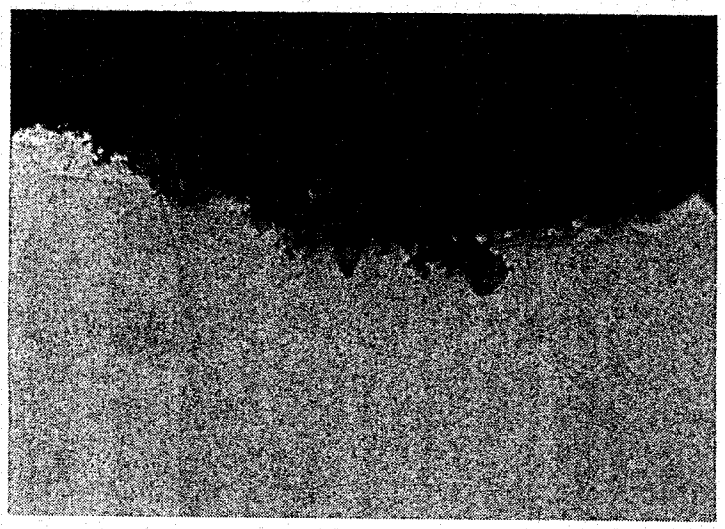

Ni Coating
(electro deposited)

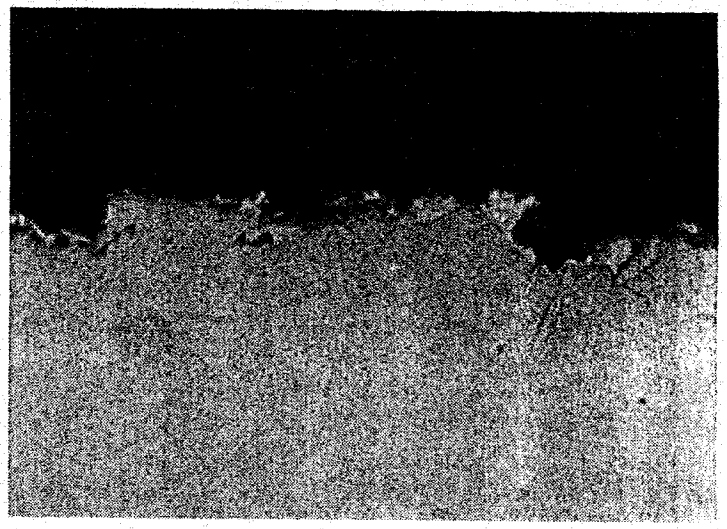

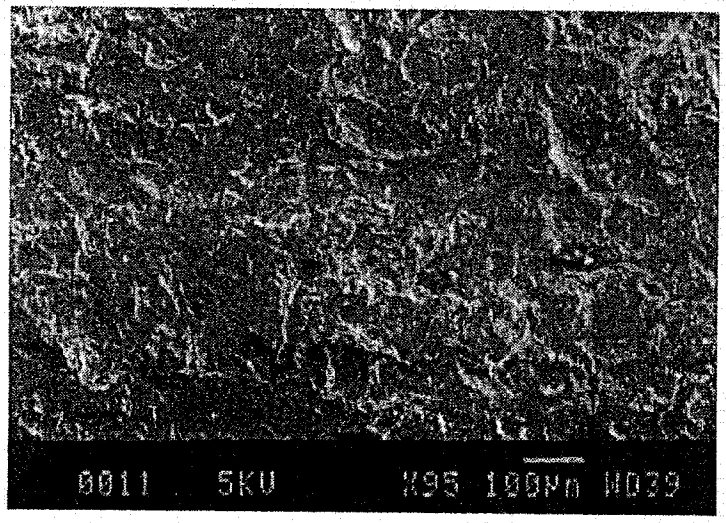

SEM
(Grit Blasted Surface)

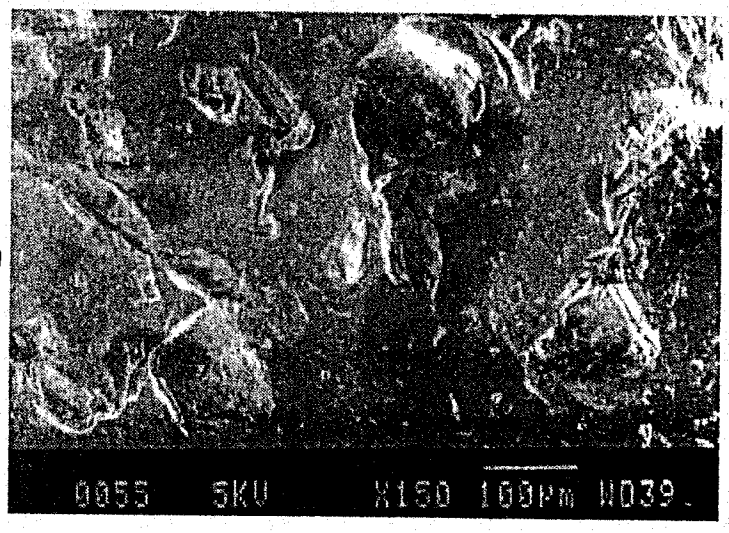

Profilometry

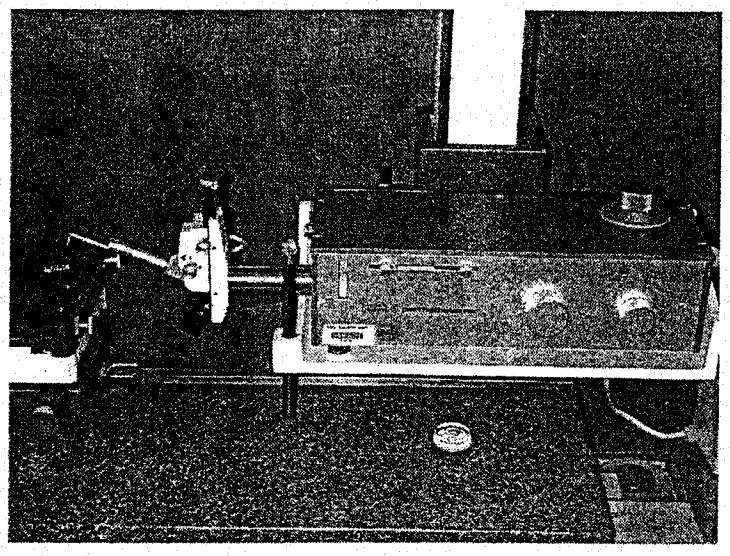

Praxair Substrates

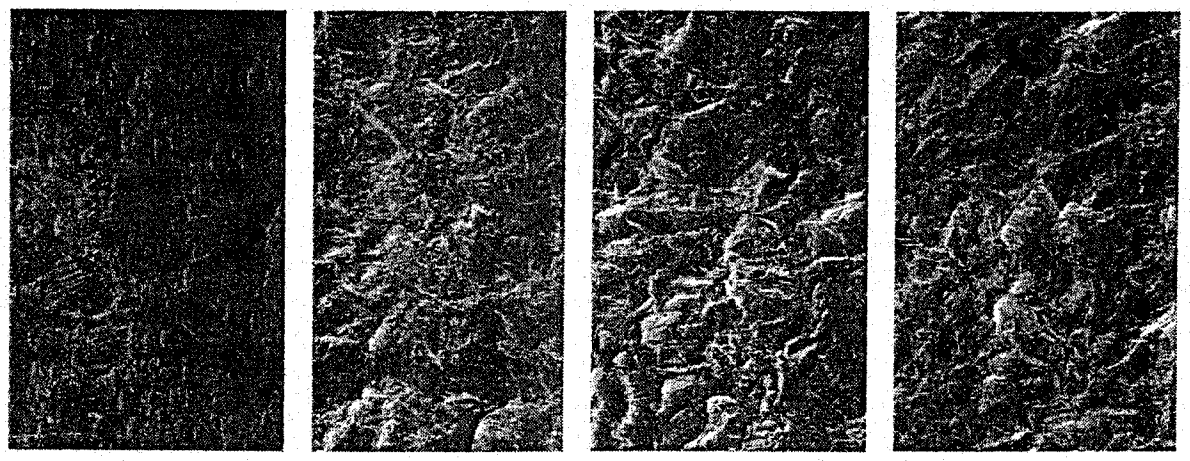

Grit Blasted Samples

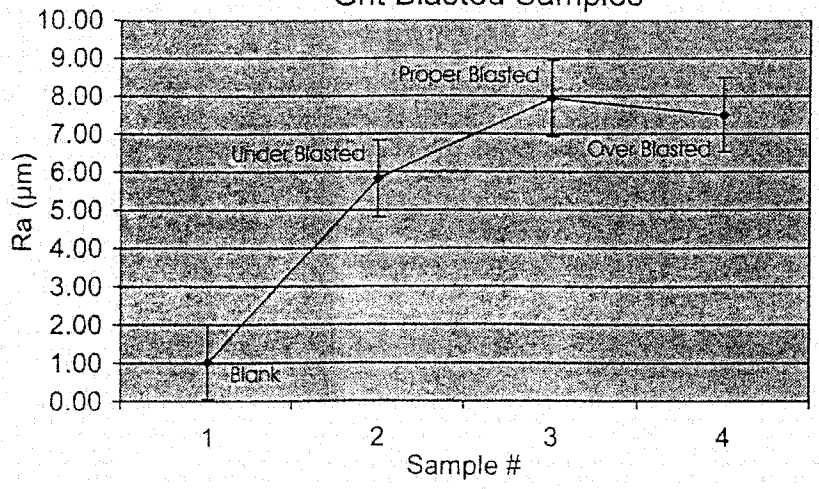

Profilometry Results

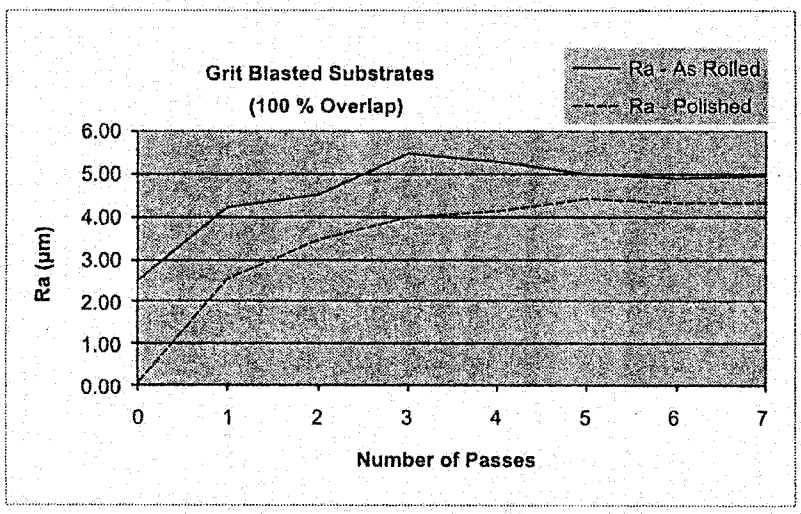

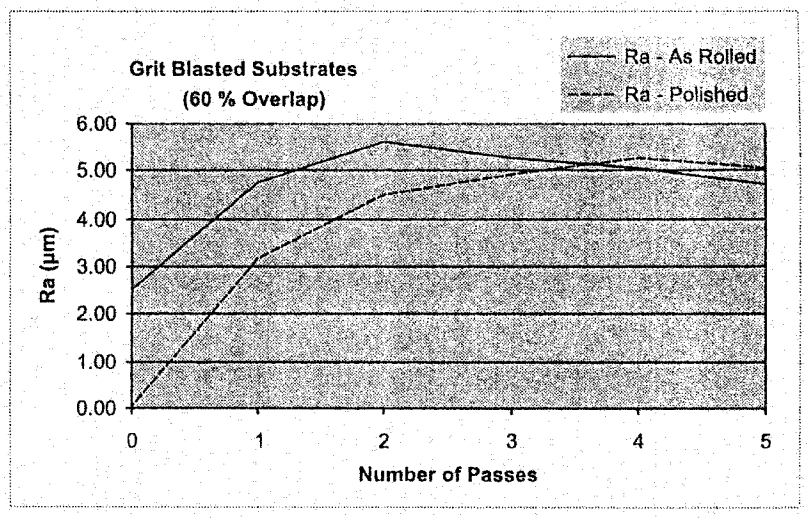

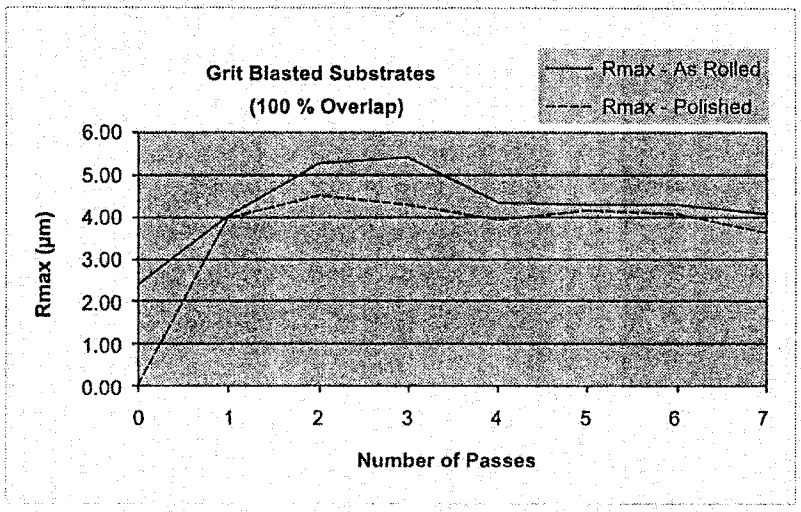

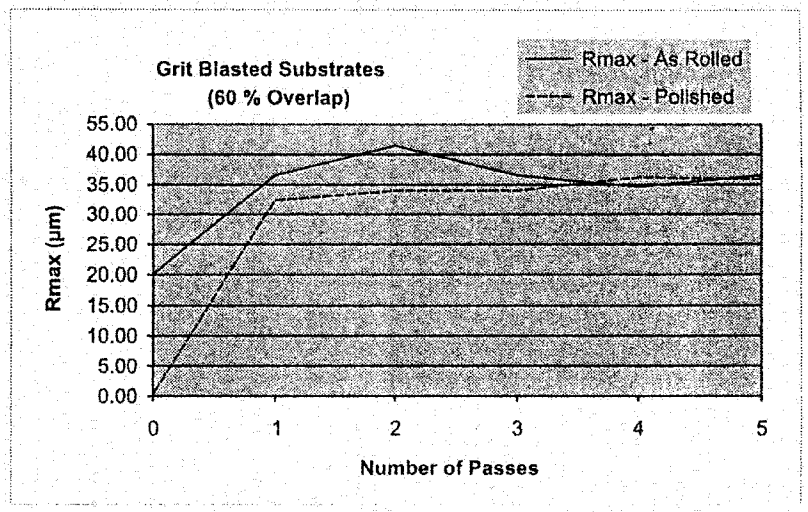

Bi -Directional Reflectometer

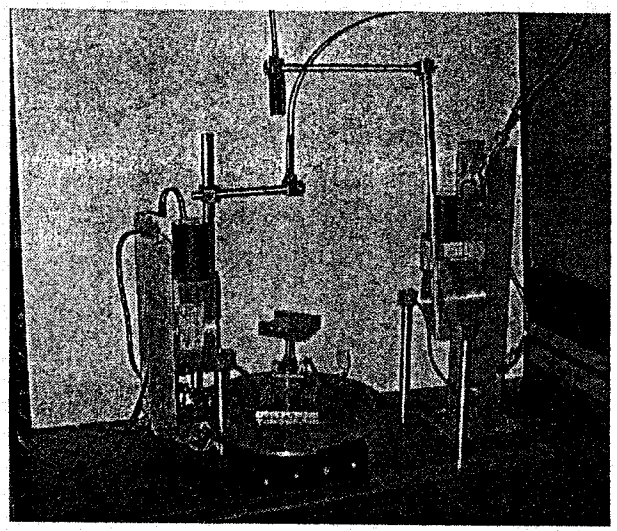

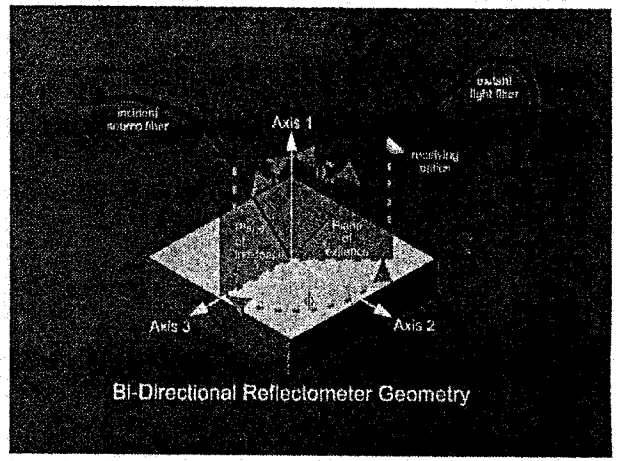

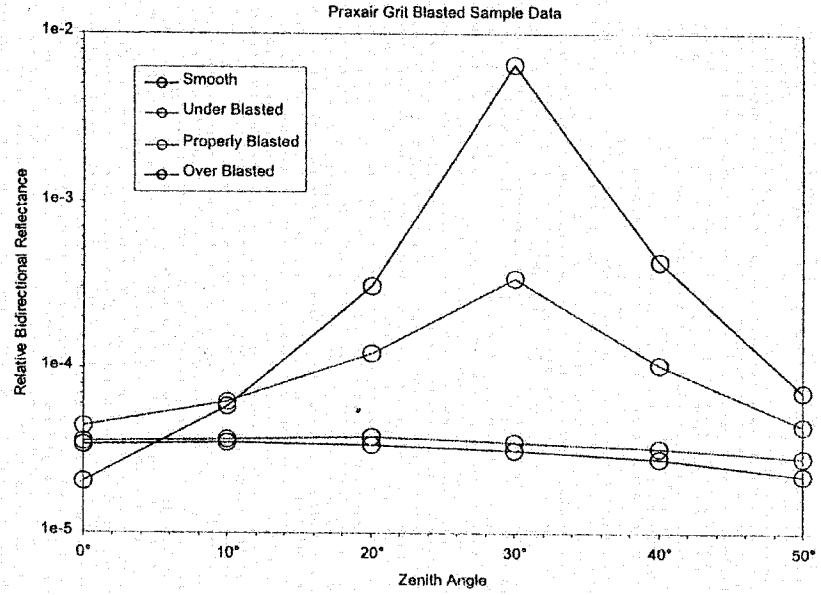

Confocal Microscope

System

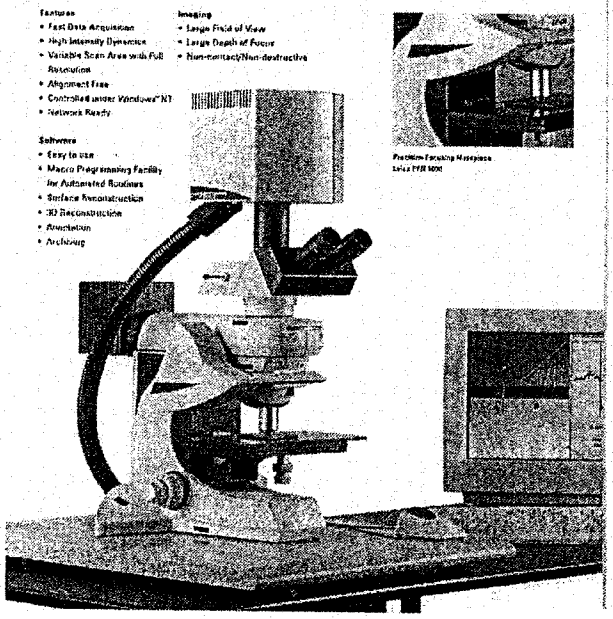

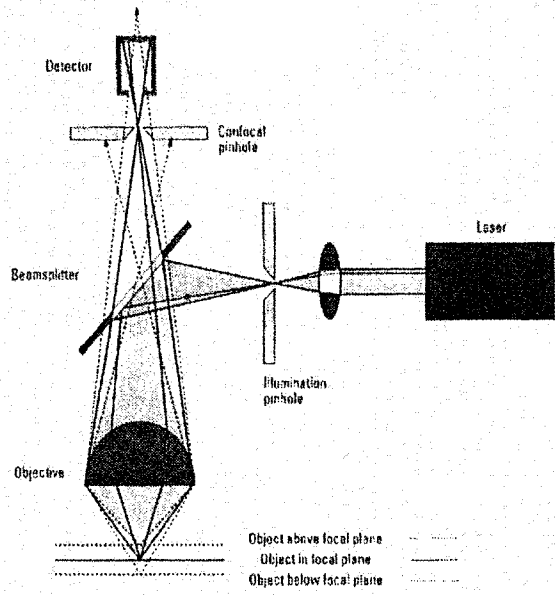

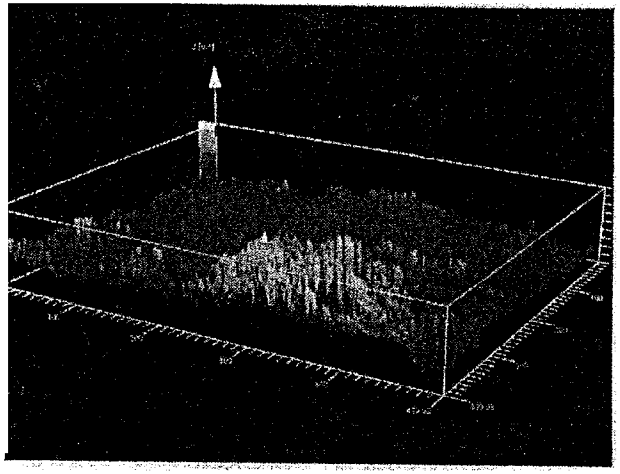

Summary

Under Blasted

Properly Blasted

Over Blasted

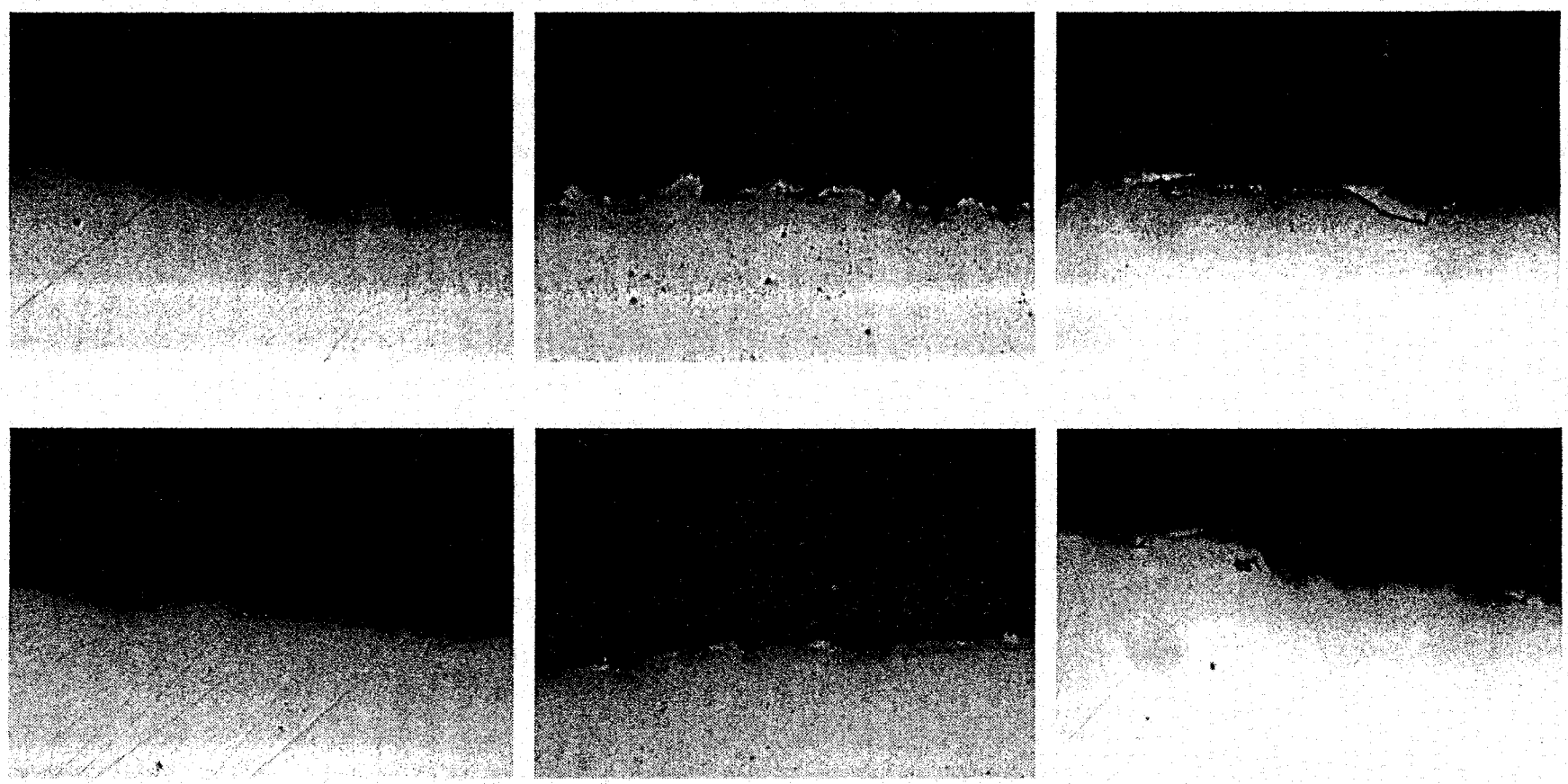

Future Work/Goals

- Correlate Data with the Reflectometry Work in progress
- Correlate Data with Adhesion Test
- Correlate Substrate Roughness with Coating Roughness

THE DYNAMIC YOUNG'S MODULUS

R. E. Smelser

E. M. Odom

and

K. V. Organ

Mechanical Engineering Department
University of Idaho
Moscow, Idaho 83844-0902

Telephone: 208-885-4049
e-mail rsmelser@uidaho.edu

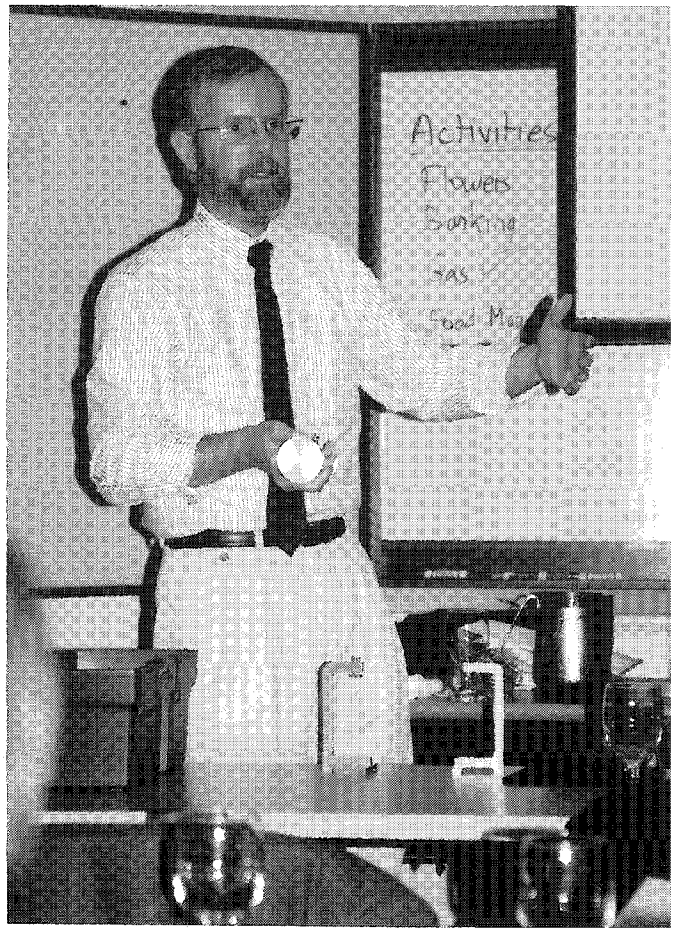

Ron Smelser

RONALD E. SMELSER
Ronald E. Smelser is a Professor of Mechanical Engineering at the University of Idaho. He holds a Bachelor's degree from the University of Cincinnati, a Master's degree from MIT, and a Ph. D. from Carnegie Mellon University. Prior to joining the faculty at the University of Idaho, he worked for fourteen years at U. S. Steel, Alcoa, and Concurrent Technology Corporation. He currently teaches the mechanics, materials, and Sophomore Laboratory courses and is involved with the Idaho Engineering Works (IEW). The IEW is a group of graduate students who develop leadership skills through mentoring the Senior Design program under the tutelage of faculty. His interests include materials process modeling, structure-property relations of materials, and material failure and fracture. He is a member of ASME, ASEE, and AAM. He has published numerous papers on materials processing and fracture and has contributed to the ASEE Annual Conference.

EDWIN M. ODOM
Edwin M. Odom, an Associate Professor of Mechanical Engineering at the University of Idaho, obtained his undergraduate and graduate degrees from the University of Wyoming. His interests include experimental mechanics and the design process. Dr. Odom joined the University of Idaho in 1992 and takes an active interest in the ME Machine Shop as a key element in design education. The ME department benefits enormously from his experience in the US Army at the Material Test Directorate as well as his experience as a gas turbine design engineer for the General Electric Company. Dr. Odom developed the Sophomore Laboratory. He also maintains an avid interest in the subject of creativity and management and is a recognized leader in the areas of team dynamics and leadership styles. He was recognized for his role in the development of the Senior Design program and the IEW by a university teaching award in 1998.

K. V. Organ
Kevin V. Organ is a candidate for the Master of Science Degree in the Mechanical Engineering Department at the University of Idaho.

THE DYNAMIC YOUNG'S MODULUS

R. E. Smelser, E. M. Odom, and K. V. Organ

Mechanical Engineering Department
University of Idaho
Moscow, ID 83844-0902

Key Words: Young's Modulus, Pendulum, Bending, Moments of Inertia

Prerequisite Knowledge: A knowledge of statics and a curiosity to learn.

Objective: The elastic modulus of a material is of primary importance in mechanical design. The determination of this modulus for thin rods is quite difficult. Traditional methods using strain gages or extensometers are problematic. Applying strain gages around small diameter rods is difficult. Extensometers can be damaged and can bend the thin rods when mounted on them. The experiment measures the elastic modulus of thin rods using the principles of dynamics.

This experiment employs a simple apparatus to determine a fundamental property of engineering materials. The experiment provides a rich ground for introducing and discussing the difference between mass moments of inertia and area sectional properties. The analysis of the experiment also offers an opportunity to explain engineering approximations and how to validate the approximations.

Equipment and Methodology: We employ two torsional pendulums connected by a thin rod to determine the elastic modulus of the rod, Fig. 1. The pendulums are set into a small amplitude vibration in a horizontal plane. The pendulums place the rod in pure bending. The moments that bend the rod are related to the geometry of the deformation and the elastic modulus through the moment - curvature relationship. The moments created by the rod on the pendulums determine the period of the vibration of the pendulums. The period of vibration is easily measured with a stopwatch. The oscillations are a function of the applied moment and the mass moment of inertia of the pendulum. The coupling of the two systems allows the determination of the elastic modulus of the rod. The details are explained in the following experiment.

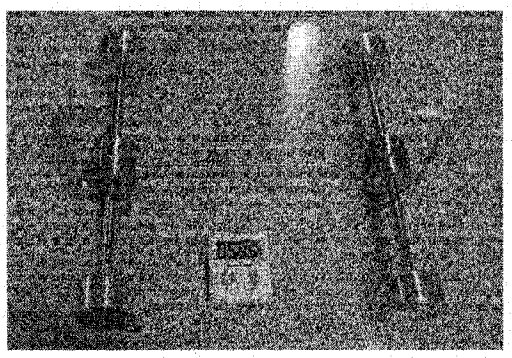

Figure 1. The torsional pendulum apparatus.

THE DYNAMIC YOUNG'S MODULUS

Introduction:

One of the most common design requirements for engineered structures is an elastic response. An elastic structure returns to its initial geometry when the force is removed. To achieve this response, a designer often uses the Young's modulus or the elastic modulus to design the structure. Young's modulus is a material property that linearly relates the material stretching to the force that causes the stretching or deformation. If the material obeys this linear relationship, we call the response linearly elastic or simply elastic. Why is this desirable in design?

The material deformation is described using a computed quantity called strain, ε. The material deformation, δ, is the difference between the specimen length before the load is applied, L_i, and after the load is applied, L_f. The ratio of the deformation to the initial length of the specimen, L_i, defines the engineering strain. The force, F, causing the deformation is usually divided by the initial cross-sectional area of the member, A_i, to give the engineering stress, σ. Can you think of reasons why engineers use these definitions for stress and strain?

$$\varepsilon = \frac{L_f - L_i}{L_i} = \frac{\delta}{L_i} \qquad \sigma = \frac{F}{A_i} \tag{1}$$

The Young's modulus, E, relates the stress to the strain linearly.

$$\sigma = E\varepsilon \tag{2}$$

This linear relationship together with Eqs (1) allows designers to predict the amount of elongation of a part subjected to a certain amount of load. It also allows the determination of the load if the part is to only deform by a known amount. Be sure that you can use Eqs (1) and (2) to show this.

Objective:

The objective of this experiment is to determine the Young's modulus of wire-like specimens of engineering materials using a torsional pendulum device.

Laboratory Equipment:

1. Torsional pendulum apparatus.
2. Stopwatch.

Procedure:

The following figure shows a plan view of a torsional pendulum device. The specimen that is being studied is attached between the two arms of the pendulum device. The specimen is long compared to its cross section. The specimen is bent into a circular arc. These are

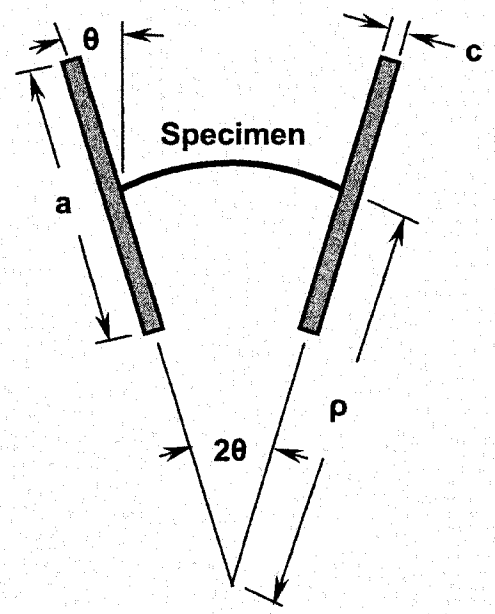

Plan View of the Torsional Pendulum

characteristics of a beam. In Mechanics of Materials, you will study the deformation of beams and the way that they are bent. Many relationships will be developed. One important relationship that relates the bending moment, M_b, the elastic modulus, and the geometry is

$$M_b = \frac{EI_A}{\rho} \tag{3}$$

This is the moment-curvature relationship. ρ is the radius of curvature of the deflected beam, and I_A is the area moment of inertia of the cross section about the neutral axis of bending. For a beam with a circular cross section, the area moment of inertia is

$$I_A = \int_A y^2 dA = \frac{1}{4}\pi r^4 \tag{4}$$

Statics tells us that there is an equal and opposite moment, M_r, to the bending moment M_b acting on the pendulum arm, $M_r = -M_b$. This moment acts to restore the pendulum arm to its original position. From elementary physics, we know that Newton's Law of Motion tells us that forces on bodies produce accelerations, $F = ma$. There is an analogous relationship for moments.

$$M = I_m \alpha \tag{5}$$

In Eq. (5), I_m is the mass moment of inertia, and α is the angular acceleration. The mass moment of inertia for rectangular bars oriented as shown in the figure is

$$I_m = \int_m r^2 dm = \frac{1}{12} m(a^2 + c^2) \tag{6}$$

Here, m is the mass of the pendulum arm, and the dimensions of the arm are shown in the figure. You will study Eq. (5) in more detail in dynamics.

The angular acceleration is related to the angle of rotation by

$$\alpha = \frac{d^2\theta}{dt^2} \tag{7}$$

Combining Eqs (3), (5), and (7) and recognizing that $M = M_r = -M_b$, we have

$$I_m \frac{d^2\theta}{dt^2} = M_r = -M_b = -\frac{EI_A}{\rho} \tag{8}$$

The minus sign shows that the moment produced by the beam on the pendulum arm acts to restore the arm to its initial position. The radius of curvature can be eliminated from Eq. (8) by using geometry. The neutral axis of bending does not deform, and the length equals the specimen length. The specimen length, l, is related to the radius of curvature by the arc length.

$$l = 2\rho\theta \tag{9}$$

We can rewrite Eq. (8) as

$$\frac{d^2\theta}{dt^2} = -\frac{2EI_A}{I_m l}\theta \tag{10}$$

This is the differential equation for a simple harmonic oscillator. You will study this in more detail in your differential equations course. The period of oscillation, T, is

$$T = 2\pi\sqrt{\frac{I_m l}{2EI_A}} \tag{11}$$

Rewriting Eq. (11) gives the elastic modulus as

$$E = \frac{2I_m l}{I_A}\left(\frac{\pi}{T}\right)^2 \tag{12}$$

To find the Young's modulus, you will measure the time required to complete approximately 50 oscillations of the pendulum. This will need to be done several times to give reliable statistics for the period of oscillation. The period of oscillation is

$$T = \frac{\text{total time}}{\text{total cycles}}$$

Why do we need to make multiple measurements for the period? How can you characterize the quality of your data?

Laboratory Write-up:

Follow the instructions for writing a quality laboratory report. How do your values for Young's modulus compare with the values provided in a standard reference for elastic properties? Also find two other sources for Young's modulus. Are the various sources consistent? How well should they compare? You measured r, a, c, m, and T during this experiment. An error in which of these would cause the most error in the resulting calculation of Young's modulus? Include the answers to all the questions posed throughout the laboratory description in your report.

Data Sheet

Data that you will need before you begin the experiment:

Specimen Steel Wire

Radius of the wire specimen, r, 0.092/2 in

Length of the wire between pendulum arms, l, 12 in

Mass of the pendulum arm, m, _____

Length of the pendulum arm, a, _____

Width of the pendulum arm, c, _____

Period of Oscillation, T				
Trial	Time (sec)	Oscillations (cycles)	Period (sec/cycle)	Elastic Modulus (GPa)
1	95	100	0.95	208
2	49	50	0.98	215
3	25	25	1.00	219
4	58	60	0.97	212
Average			0.98	214
Std. Dev.			0.02	4.3

Comments:

1. A second experiment was conducted on a 0.062 diameter steel rod. The period of oscillation was 2.2 seconds. This gave a modulus of 208 GPa.

2. Figure 1 shows the torsional pendulum apparatus. The design using the dumbbell-shaped arms allows the device to be compact and keeps it on a scale suitable for a tabletop device.

3. The experiment shows the difference between area moments of inertia and mass moments of inertia. This encourages the discussion and understanding of these two important measures in mechanics and provides concrete examples of these difficult concepts.

4. The dumbbell-shaped arms also allow a further discussion of the parallel axis theorem. This is often only briefly discussed in introductory mechanics courses. The dumbbell arms also allow for easy adjustment of the period of oscillation for specimens of different dimensions. Different end weights allow easy adjustment of the mass moment of inertia.

5. It is recommended that the students measure the weight or mass of the components that comprises the pendulum arms. This, together with the part dimensions, allows the computation of the mass moment of inertia. It is important for students to understand that one should not simply take density values from textbooks and use that together with dimensions to calculate mass. Errors can result in the modulus calculations since the textbook values are averages.

6. The apparatus demonstrates the fact that the wire specimen is inextensible. An initial prototype was constructed using instrument bearings to support the pendulum arms. The bearing supports introduced a severe damping into the system. The damping was the result of the wire trying to move the bases that held the bearing needles. The bearings would have been successful if the nodes of the vibrating wire were located on the pivots. This is not practical given the requirement to accommodate various wire sizes. We use nylon fishing line connected to lure swivels to accommodate the small inward motions of the oscillating pendulums. This also gives an extremely low friction suspension of the arms.

7. The connection of the wire to the apparatus has also proved to be a challenge. The connection must ensure the theoretical boundary condition of a fixed end on the specimen. The fixed end condition is only approximated by a setscrew or a similar attachment. The lack of complete constraint can be handled by using an effective length of the wire in the theoretical development. The determination of an effective length is difficult. We have found that one solution is to embed the wire and attach it with solder in a bolt with a drilled hole. This is shown in the following figure.

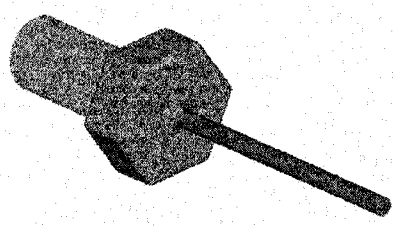

8. Pro/ENGINEER® drawings will be supplied on request for a small fee to cover the cost of reproduction.

Bibliography:

1. F. P. Beer and E. R. Johnston, Jr. (1997) *Vector Mechanics for Engineers, Statics and Dynamics, Sixth Edition*, WCB McGraw-Hill.

2. R. A. Serway and R. J. Beichner (1999) *Physics for Scientists and Engineers, Fifth Edition*, Saunders College Publishing.

3. G. F. C. Searle (1933) *Experimental Elasticity, Second Edition*, Cambridge University Press.

CASE STUDY: USING A NEURAL NETWORK TO IDENTIFY FLAWS DURING ULTRASONIC TESTING

A. Kayabasi

Glenn S. Kohne

and

P. J. Coyne, Jr.

Loyola College in Maryland
Department of Electrical Engineering and Engineering Science
4501 N. Charles Street
Baltimore, Maryland 21210

Telephone: 410-617-2249
e-mail kohne@loyola.edu
e-mail pcoyne@loyola.edu

Alp Kayabasi is a Lead Technical Specialist at United Parcel Service Information Services in Timonium, Maryland. He has a bachelor's degree in Electrical Engineering from University of Maryland at College Park, a master's degree in Engineering Science from Loyola College in Maryland and a master's degree in Electrical Engineering from University of Maryland Baltimore County. He is an adjunct faculty member at Loyola College and Towson University.

Mr. Glenn S. Kohne earned his BSEE (High Honors) at the University of Maryland in 1970. He completed his MES in Digital Systems at Loyola College in 1981. He worked as a Lead Electrical Engineer with Raytheon Co. in Massachusetts, served as a Lieutenant Commander in the USPHS for 10 years, and is currently an Associate Professor of Electrical Engineering at Loyola College. His interests include teaching, developing educational software, and flying.

Paul J. Coyne, Jr. is a Professor of Electrical Engineering and Engineering Science at Loyola College in Maryland. He has bachelors and master's degrees in Electrical Engineering from the University of Delaware. He received his Ph.D. in Applied Sciences-Metallurgy/Materials Science also at the University of Delaware. Further information on teaching and research activities is available at his homepage, http://eees.loyola.edu/~coyne/.

Case Study: Using a Neural Network to Identify Flaws during Ultrasonic Testing

A. Kayabasi, G. S. Kohne and P. J. Coyne, Jr.
Loyola College in Maryland
Department of Electrical Engineering and Engineering Science
Baltimore MD 21210-2699

Key Words: neural networks, ultrasonic nondestructive evaluation.

Prerequisite Knowledge: A basic exposure to windows based applications to operate the program, Neural~1, and a mathematical background which includes elementary calculus and linear algebra.

Objective: The construction of a neural network implemented in software which can be trained to classify objects based on certain features and then when presented with new objects to classify them based on previous experience.

Equipment and Materials:
1. A personal computer using the Windows 95/8 to execute the downloadable software.
2. A set of numeric data with which to train the neural network to classify objects.
3. A subsequent set of similar data, which must be classified.

Introduction:

A neural network or more formally an artificial neuronal network involves the implementation, either in hardware or software, of a parallel distributed processing computation structure or neurocomputers that is capable of tasks such as pattern recognition in nondestructive testing, which is the example chosen for this case study. These neurocomputers can function similarly to the human brain, although they are not limited to this function. It is estimated that the human brain is composed of 10^{11} neurons; each connected to 10^4 other neurons [1], which implement a massively parallel computation structure capable of very complex tasks, some still far beyond the capabilities of the today's computers.

The neuron is the fundamental processing unit in the brain and in the artificial neuronal network. Each neuron, Figure 1, receives inputs from many other neurons or from sensory processing elements. Each input is weighted, positively or negatively, by a connection strength and then combined or summed. When the weighted-combined inputs exceed a threshold, the neuron fires or activates its output line, which is then used as the input to another neuron. The key to this parallel processing unit is the connecting weights, which have been arrived at as a result of evolution in humans but must be learned or trained, in an artificial neuronal network. Additionally, many artificial neurons use a constant input or bias, Figure 1, to increase the ability of the neuron to learn complicated relationships.

The human operator in a particular nondestructive test learns, by experience, to recognize that certain features, such as a particular shape on an oscilloscope trace, correlates with a certain condition of the piece under test. If we wish to assist the human operator with a neural network, the same procedure must be followed. The network must be presented with a sequence of input features and the corresponding characteristics of the piece under test. During this training phase the connecting weights are adjusted such that the difference between the network output, which is an indicator of the state of the test piece, and the desired output are reduced. This weight adjustment gives the network a memory of the correlation between the trace characteristics and the corresponding state of the test piece. After a suitable training period, the neural network should be tested with features from a different test piece, much as one would test an inexperienced operator after training.

This case study will focus on the utility of neural networks for the development of a flaw size identifier, which could be used as part of a computer-based classifier of flaws during ultrasonic pulse-echo nondestructive testing. Additionally, the various options available and decisions required in the selection of particular neural network topologies as well as the corresponding training and testing signals will be presented.

A number of decisions are required for the construction of a neural network to be used as a pattern recognizer. The first decision concerns whether the physical implementation of the network will be in hardware or software. A software implementation, on a general-purpose computer, was selected to maximize flexibility. The next decision concerns the numeric characteristics of the data at the input, at internal nodes, and at the output. The data values can be either continuous or discrete and either bipolar or unipolar. Given that the source of the data is an electrical signal, which is bipolar and continuous; the use of bipolar and continuous data should maximize the information provided to the network. The selected data values will be taken from a digitized version of the electrical signals.

The next decision concerns the network architecture, the interconnection of the network nodes and the number of layers of nodes. A feed-forward network topology allows a flow of information only from the input layer of nodes to the output layer of nodes, which may proceed through one or more hidden layers of nodes. A feedback configuration would allow signal information to flow from the output node layer or any hidden node layer to previous layers. A feed-forward network will be implemented in this case study since a feed-forward network avoids stability problems inherent in feedback topology. A single hidden layer of nodes was selected and since this proved successful the complexity of additional layers was avoided.

The next decision concerns the neuron activation function and the inclusion of a bias term at each neuron. There are two general categories of activation functions: a hard limiting threshold for activation or a continuous activation function, which may take on a variety of mathematical forms. While the hard limiter more closely mimic the human neuron, the continuous activation function was selected based on constraints imposed by the training or learning algorithm. A sigmoidal activation function for bipolar data was selected as shown below where Σ represents the summation of the neuron inputs as shown in Figure 1.

$$\text{ACTIVATION } (\Sigma) = A(\Sigma) = \frac{2}{1+\exp(-\Sigma)} - 1 \qquad (1)$$

A bias term allows a constant input value, in this case unity, to be connected to each neuron through an adjustable weight. This allows a greater degree of flexibility [2] as the neural network learns the relationship between the input and the output during training.

Given a signal characteristic and neural network architecture; a mode for learning and a learning rule must be selected. There are two general categories of learning modes – supervised and unsupervised. Since the desired network output, i. e. the identification of the simulated flaw was known during training, the supervised learning mode was selected. The training rule selected was the backpropagation rule or the generalized delta rule [3], which minimizes the mean square error of the difference between the desired or target output and the current output by making incremental adjustments in the connecting weights between layers in the neural network proportional to the difference between the desired output and the current output. A portion of a two-layer feedback neural network is illustrated in Figure 2. The updated weight linking the j^{th} hidden node to the k^{th} output node, W_{jk}^{n+1}, at the n+1 instant in the training sequence is given by

$$W_{jk}^{n+1} = W_{jk}^{n} + \Delta W_{jk}. \qquad (2)$$

W_{jk}^{n} is the prior weight and ΔW_{jk} is the weight adjustment given by

$$\Delta W_{jk} = \text{lrc}\left(D_k - O_k^n\right) A'\left(\Sigma_k^n\right) Z_j^n, \qquad (3)$$

where lrc is the data dependent learning rate constant, D_k is the desired k^{th} output node value, O_k^n is the k^{th} output node value at the n^{th} instant, $A'\left(\Sigma_k^n\right)$ is the first derivative of the activation function at the k^{th} output node at the n^{th} instant, and Z_j^n is the output value at the j^{th} hidden node at the n^{th} instant. The first derivative of the activation function in the weight adjustment equation is what necessitates using a continuous activation function. The weight adjustment equation for the weights connecting the bias to each neuron is the same except that Z_j^n is set equal to unity in Equation (3).

The updated weight linking the i^{th} input node to the j^{th} hidden node (Figure 2), V_{ij}^{n+1}, at the n+1 instant in the training sequence is given by

$$V_{ij}^{n+1} = V_{ij}^{n} + \Delta V_{ij}. \qquad (4)$$

V_{ij}^{n} is the prior weight and ΔV_{ij} is the weight adjustment given by

$$\Delta V_{ij} = lrc \sum_{k} \left(W_{jk}^{n} \left(D_k - O_k^n \right) A' \left(\Sigma_k^n \right) \right) A' \left(\Sigma_j^n \right) X_i , \quad (5)$$

where $\sum_{k} \left(W_{jk}^{n} \left(D_k - O_k^n \right) A' \left(\Sigma_k^n \right) \right)$ acts as an effective error at the j^{th} hidden node by propagating back the error from all the output nodes weighted by the appropriate connecting weight, $A' \left(\Sigma_j^n \right)$ is the first derivative of the activation function at the j^{th} hidden node at the n^{th} instant, and X_i is the value at the i^{th} input node. The weight adjustment equation for the weights connecting the bias to each neuron is the same except that X_i is set equal to unity in Equation (5). Given a physical implementation, the characteristics of the internal data, network architecture, an activation function, a learning mode, and a learning rule; the remaining decisions will be based on the experimental data used for training and testing.

The preceding neural network has been implemented as a windows application called Neural~1. This application, example input files and users guide is downloadable as a self-extracting compressed file from the software area on one of the author's homepage, http://www.kohne.net/. All parameters discussed in the paper are adjustable from the windows interface including the size of each layer in the neural network.

Procedure:

Flaws were simulated using the polished cross-section of acrylic rods immersed in water at 22°C. Table I lists the simulated flaws, their respective cross-sections, the range of distance that the samples were placed relative to the transducer wearplate, the number of experiments available, and the neural network output binary code for each sample.

The simulated flaws were positioned at varying distances from a Panametric™ V114 transducer, 1.91 cm. in diameter, with the flaw cross-section parallel to the wear plate. The transducer-amplifier system, a Panametric™ 5050 P/R operated in the pulse-echo mode, generated short pulses of longitudinal ultrasonic waves with a nominal center frequency of 1 MHz. The first echo from each simulated flaw was amplified and stored in a LeCroy™ 9400 digital oscilloscope configured to sample the return echo at a sampling frequency of 100 MHz. The data was then electronically transferred to a computer for analysis.

The next decision required was the selection of relevant echo features, which would be presented to the neural network during training and the subsequent testing phase. The features selected were dictated by two factors. The input features should require a minimum of preprocessing, with no human interaction, and the number of features should be small so as to limit the number of data sets required for training the network. A lower bound [4] on the number of training sets required is given by a product of the number of different samples to be classified, five in these experiments, and the minimum of the number of input features/nodes or the number of hidden nodes, which are both to be determined. Given these constraints, time domain samples of each echo were used as input to the neural network. The samples were taken directly from the LeCroy™ data file representing each echo. The samples were taken after the echo voltage exceeded a negative going threshold. A total of eight samples were taken, skipping twenty samples

between each selected sample. These allowed the major portions of each echo to be represented by voltage deflections at pre-set points on the time axis. Figure 3 illustrates an example echoes from sample b with the corresponding data samples used in the analysis indicated by asterisks. While eight samples would not correspond to a correct data reduction of the sampled echo; it does allow a mixture of both amplitude information and time location information about each echo. In addition to greatly reducing the number of potential input features, this scheme simplifies the preprocessing phase, which would otherwise require a feature extraction exercise to identify amplitude features, time features or any transform domain features.

The eight sample input values define the number of nodes at the input of the neural net, while the number of nodes in the hidden layer was set to five for most of the experiments. The output layer of the neural network was set to three nodes, as determined by the binary encoded identifications listed in Table I. The desired output values are set to a three-bit binary code, with three binary digits allowing the classification of eight different items although only five were used in these experiments. Variations on the actual binary code assignments showed no effect on the networks ability to recognize samples. The output coding was motivated by the desire to reduce the number of connecting weights in the overall neural network. A logical alternative to this output identification scheme would have been to have the number of output binary digits equal to the number of different samples. In this scheme, in order to identify a given sample, only one output binary digit equals one while the remainders are at minus one. This would have been the next course of action if the training and subsequent testing were unsuccessful in correctly identifying the samples using a binary encoded version. Additionally, the number of nodes in the hidden or intermediate layer was varied to illustrate the effect of this variable. The final decision prior to training the neural network was the selection of initial connecting weight values. All connecting weights were set to random numbers between -0.5 and 0.5, using a Nguyen-Widrow normalization [3].

Note that the target values are in binary but the network output is continuous to assure the existence of the derivative of the activation function as stated earlier. An adjustable error was allowed when comparing the network output with the target values. A correct match of network output and target values occurs if all network output values are within 0.2 of the target values. The adjustable parameter is a required input parameter at the windows application interface.

A data set consists of eight samples from an echo with the corresponding output or sample identification binary code listed in Table I. The fifty-seven data sets were ordered from sample a through e, with each sample ordered in increasing distance from the transducer face. This allowed for three different types of training and testing on the neural network. Experiment H1 used half of the data sets to train, selecting every other data set, and the remaining half to test the network, with Experiment H2 reversing the training and testing data groups. Experiment T1 used one-third of the data sets to train, selecting one data set and skipping two data sets, and testing with the remaining two-thirds of the data sets, with Experiments T2 and T3 each using a different one-third of the data sets for training and the remaining two-thirds for testing. Experiment Q1 used one-forth of the data sets to train, selecting one data set and skipping three data sets, and testing with the remaining three-fourths of the data sets, with Experiments Q2, Q3 and Q4 each using a

different one-forth of the data sets for training and the remaining three-fourths for testing. Each training run was continued until the training error was reduced to a preset root-mean-square (RMS) value. Multiple training runs, each with a different set of initial random network weights, were done to maximize the percent correct before a single testing run was executed. The RMS error was reduced during training only when a series of training runs failed to achieve a ninety percent correct testing run.

Table II list the results of all experiments performed on the neural network with eight input nodes, five nodes in the hidden layer, and three nodes in the output layer. In all cases the network weights were started at random values, even when a training sequence was repeated with a smaller RMS goal. Given the network size, a desired minimum number of training sets should be greater than 25. The H-series experiment exceeds this goal, while both the T-series and Q-series use less than the desired minimum. This will allow some exploration of the exactness of this minimum number of training sets.

The H-series of experiments have the highest percent correct in testing on average for 0.1 RMS training error as expected, since these two experiments used the largest data sets for training. Subsequent random starts for the H2 series with a smaller RMS goal leads to an increase in the percent correct in testing to the lower 90% range with the network able to memorize, 100% recognition, the input training set at 0.05 RMS training error. The T-series of experiments had a somewhat lower percent correct in testing on average for 0.1 RMS training error than the H-series as would be expected since less information was provided in the training phase. As the training was extended to 0.01 RMS training error the percent correct in testing for the T-series also increased to the low-to-mid 90% range. This illustrates two expected results. Increasing the number of training samples or the length of training increases the percent correct recognition in testing. The T-series results seem to indicate that a maximum number of training set at 25 is a conservative estimate.

The Q-series of experiments proved to have the most variability. The percent correct for 0.1 RMS training error ranged from the low 60%'s to upper 70%. Two causes for this are possible. First, the effect of the random start can put the initial weights near a global minimum that produces a high percent correct or the initial weights may position the start point near a local minimum which has a much lower percent correct. The algorithm, which reduces the RMS training error, adjusts the weight values to move down an error surface, which may have many local minima. This is illustrated by the poor results for the Q4 experiments. Secondly, a small training set may provide insufficient information to form a general solution to the problem at hand. This is also illustrated by the Q4 experiments which never produced a percent correct above the low 80%'s range, but the other Q-series experiments were able to generalize to a percent correct which went into the 90% range. In the case of increasing the training time by reducing the RMS error, it is possible for the network to memorize the training data as opposed to obtaining a general solution to the problem at hand. If this occurs, subsequent testing with data not used in training should reveal a low percent correct and thus identify this shortcomings of the neural network. The Q4 experiment with a 0.0001 RMS error showed that the network did not form a general solution to the problem it just memorized the training data.

Figure 4 illustrates the percent correct for the Q3 experiment as a function of the number of training iterations for three different numbers of nodes (three, five, eight), in the hidden layer of the neural network. The results indicate that a network with more internal neurons will learn more quickly and will be able to generalize a better solution to the problem at hand. The figure also indicates only a modest improvement when eight internal neurons are used as opposed to five. No general solution exists for the correct number of neurons in a hidden layer, but a general rule would start with a low number of neurons in the hidden layer and then increase the number the until an acceptable solution is reached.

Comments:

A neural network can be trained to recognize samples using features in time traces of ultrasonic echoes. The complexity of the network is limited by the quantity of training/testing data available. In general, the more complex a network is the better the generalization of a solution for the problem under study. The quality of the training set and the length of training limit the success of the neural network. The potential for a network to arrive at a local minimum with a high RMS error is possible, but this can usually be avoided by using a quality training set.

The windows based application Neural~1 can be used to solve a very general class of problems. Any length input vector, with continuous or discrete values, can be used; the length equals the number of neurons in the input layer. The number of hidden neurons can be varied, starting with a small number relative to the size of the input layer. The form and size of the output layer would be problem dependent. The algorithm is based on the contents of Chapter 6 of Fausett's textbook [3].

References:

1. J. M. Zurda, Introduction to Artificial Neural Systems, West Publishing, St. Paul (1992).
2. B. Widrow and S. D. Stearns, Adaptive Signal Processing, Prentice-Hall, Englewood Cliffs (1985).
3. L. Fausett, Fundamental of Neural Networks: Architectures, Algorithms, and Applications, Prentice-Hall, Englewood Cliffs (1994).
4. K. G. Mehrotra, C. K. Mohan, and S. Ranka, IEEE Trans. on Neural Net., **2**, 6 (1991).

Table I: Sample designation, sample cross-section area, variation in sample-to-transducer distances, the number of experiments available, and neural network output code for each sample.

SAMPLE	AREA (cm^2)	DISTANCES (cm)	NUMBER	OUTPUT CODE
a	45.8	1.809-10.922	14	1 -1 -1
b	1.31	1.267-10.054	13	-1 -1 -1
c	0.709	0.024-5.556	9	-1 -1 1
d	0.312	1.730-7.588	10	-1 1 1
e	0.0855	0.072-10.486	11	-1 1 -1

Table II: Results for all experiments performed on a neural network with an eight-five-three structure.

Experiment	Percent used in training	Percent used in testing	RMS Error	Percent Correct Train / Test
H1	50.9	49.1	0.1	100 / 96.4
H2	49.1	50.9	0.1	89.3 / 82.8
			0.05	100 / 89.7
			0.01	100 / 93.1
T1	33.3	66.7	0.1	84.2 / 81.6
			0.05	100 / 89.5
			0.01	100 / 92.1
T2	33.3	66.7	0.1	84.2 / 78.9
			0.05	100 / 78.9
			0.01	100 / 92.1
T3	33.3	66.7	0.1	94.7 / 89.5
			0.05	100 / 89.5
			0.01	100 / 94.7
Q1	26.3	73.7	0.1	93.3 / 78.6
			0.05	100 / 88.1
			0.01	100 / 92.9
Q2	24.6	75.4	0.1	85.7 / 74.4
			0.05	100 / 93.0
Q3	24.6	75.4	0.1	85.7 / 65.1
			0.05	100 / 86.0
			0.01	100 / 93.0
Q4	24.6	75.4	0.1	85.7 / 62.8
			0.05	100 / 65.1
			0.01	100 / 76.7
			0.001	100 / 83.7
			0.0001	100 / 81.4

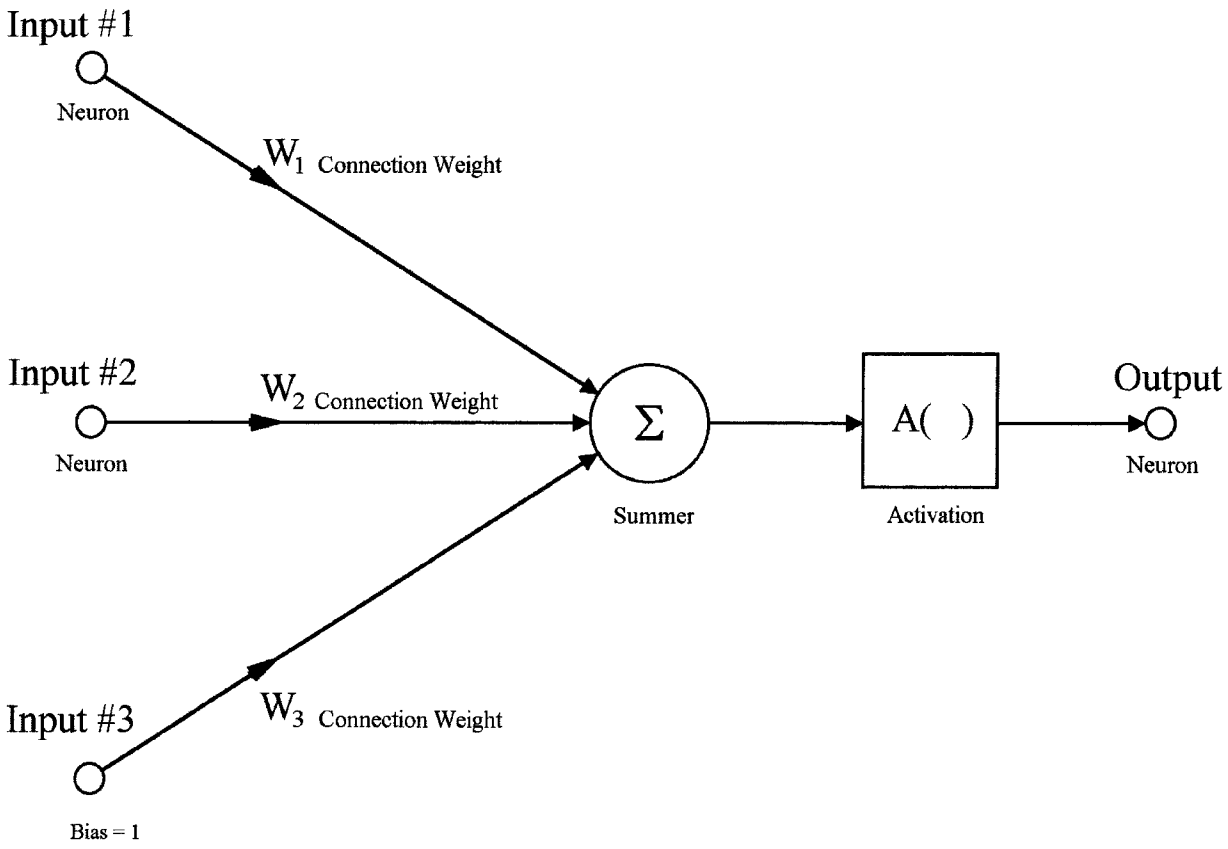

Figure 1. A single neuron receiving input from two other neurons and a bias

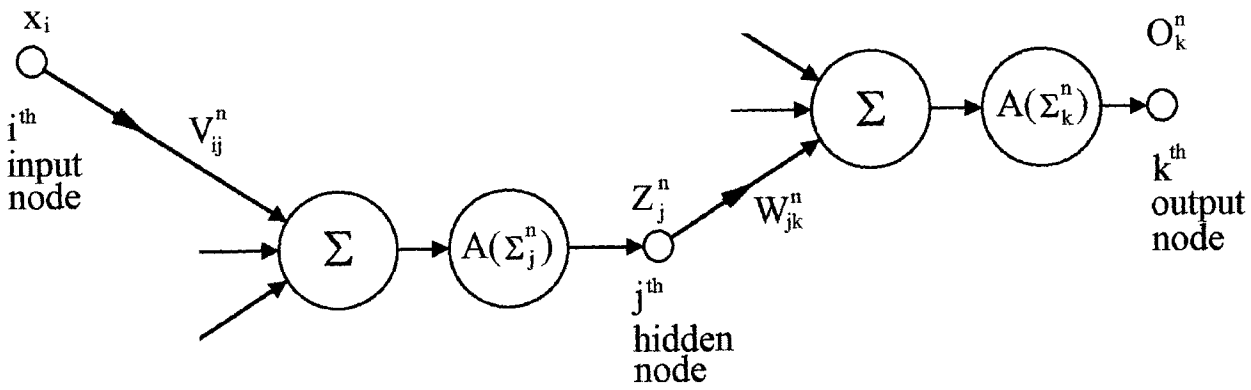

Figure 2. A portion of a two-layer feedforward neural network.

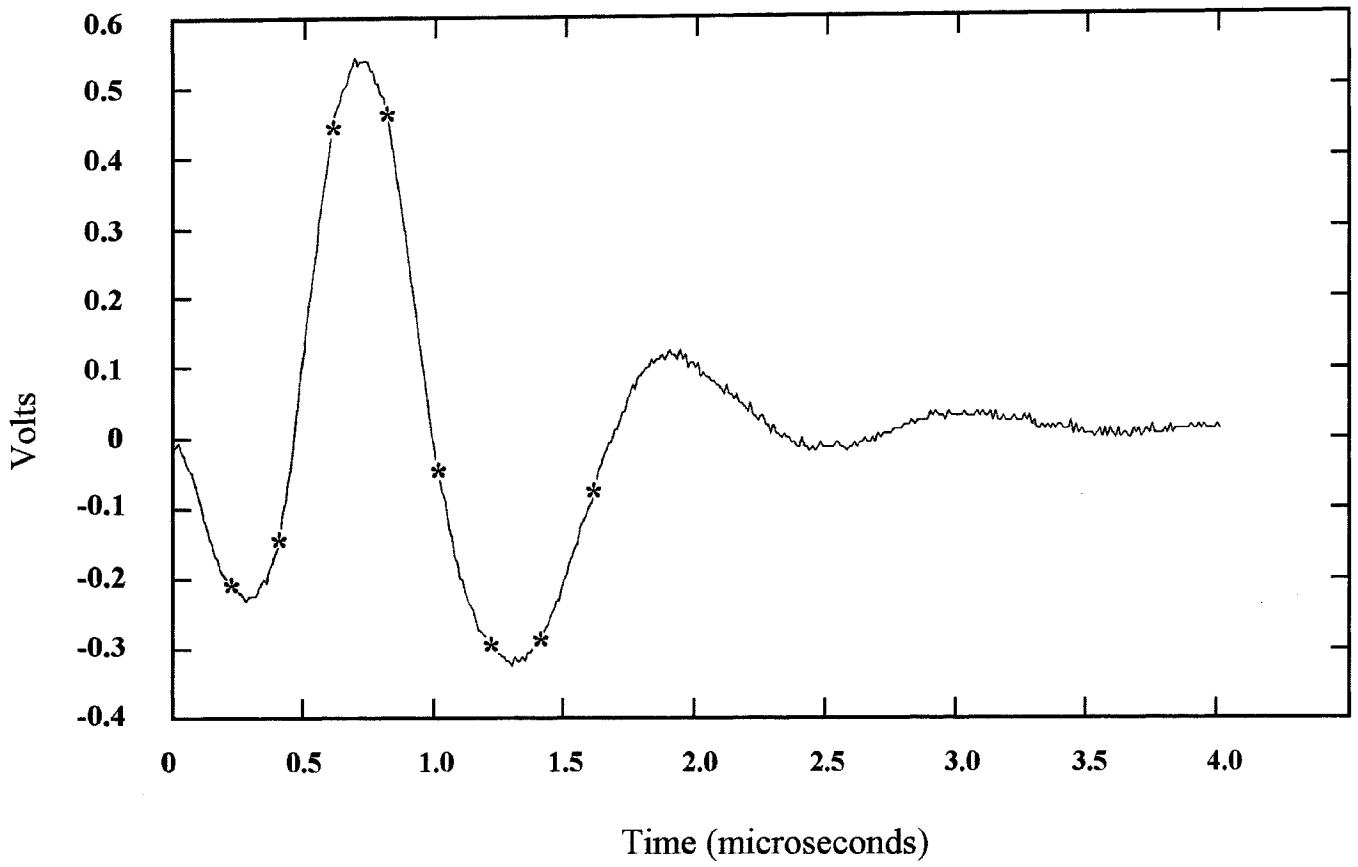

Figure 3. Example time trace with data values used in the analysis indicated by an asterisk.

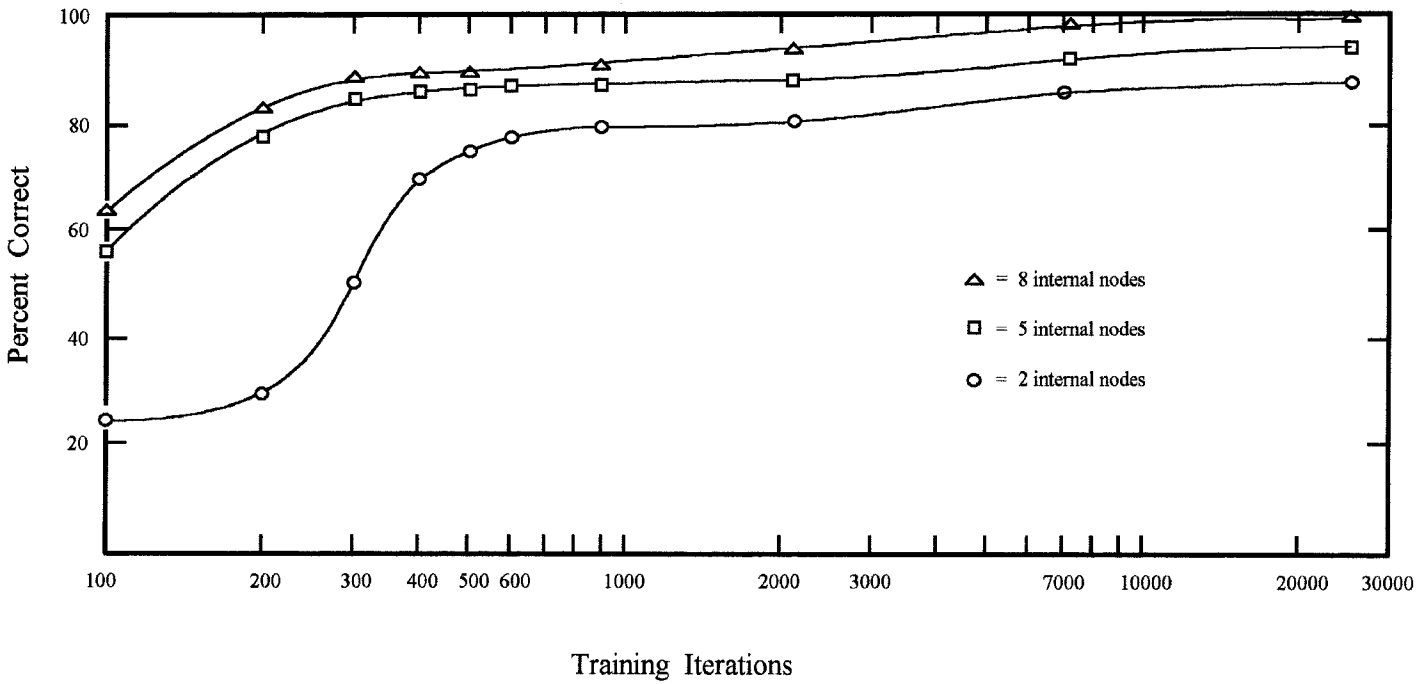

Figure 4. Training results as percent corrrect versus training iterations for three different numbers of internal or hidden nodes.

DEMONSTRATIONS OF SOME FUNDAMENTAL CONCEPTS CONCERNING FUELS AND ENGINES

John J. Fortman

Professor Emeritus of Chemistry
Wright State University
Dayton, Ohio 45435

Sponsored by Wright-Patterson Air Force Base ARL/ML

Telephone: 937-775-2188
e-mail john.fortman@wright.edu

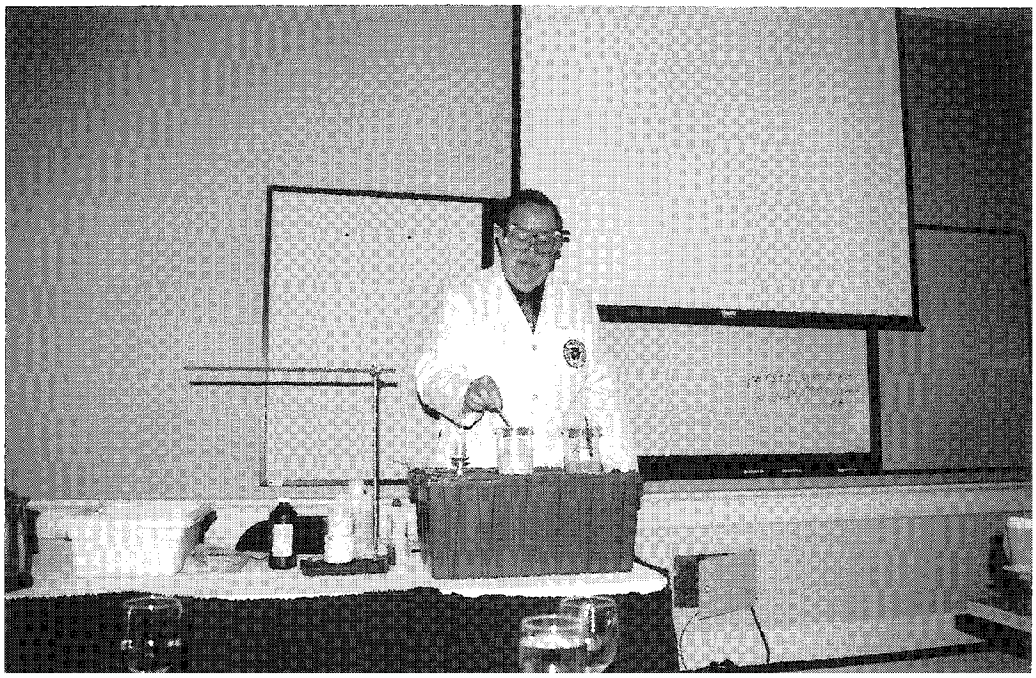

Biography:

John J. Fortman is Professor Emeritus of Chemistry at Wright State University, Dayton, OH, where he has taught for 36 years. He received his B.S. from the University of Dayton in 1961 and his Ph.D. in physical inorganic chemistry from the University of Notre Dame in 1965. At WSU he has received six outstanding teaching awards and was appointed the Robert J. Kegerreis Distinguished Professor of Teaching. In 1998 he was recognized with the Chemical Manufacturers Association National Catalyst Award for Outstanding College Chemistry Teaching. He has published 71 papers with almost half of them dealing with chemical demonstrations. He has given many presentations at national meetings and for eight different states or regional meetings of high school chemistry teachers. As a tour speaker for the American Chemical Society he has given over 200 local section talks in 49 of the 50 states.

Demonstrations of Some Fundamental Concepts Concerning Fuels and Engines

John J. Fortman
Professor Emeritus of Chemistry
Wright State University
Dayton, OH 45435

Sponsored by Wright Patterson AFB ARL/ML

Key Words: Combustion, fuels, engines, fires, explosions, demonstrations, analogies.

Prerequisite Knowledge: Basic ideas of chemical reactions, the piston function in the internal combustion engine.

Objective: Demonstrations presented are suitable for both younger students and high school and college classes. An appreciation of how fundamental scientific knowledge can explain the technology of useful applications can be gained.

Equipment and Materials: See the instructions for the individual experiments under the Procedure section.

Introduction: In order to produce combustion one needs a fuel, a source of oxygen, and an initiator. This is presented in a surprising manner using a burning book while relating this information. Carbon dioxide and oxygen gases are produced to illustrate the difference between gases which do or do not support combustion. The vapor nature of burning is illustrated with a demonstration which dates back to Michael Faraday and his lectures on the candle. This open burning of fuel vapor which occurs when the fuel and oxygen come from different sources and burn at the interface of mixing is contrasted to explosions which occur when the fuel and oxygen gases are pre-mixed. Since oxygen is the limiting reagent there is a need for an exhaust stroke in order to have repeated explosions which produce thrust. The timing cycle in a four-cylinder four-stroke internal combustion engine is shown by a participatory analogy. A visual illustration is presented comparing a rapid rough explosion and a slower smooth explosion and the difference is related to the octane rating of fuels for anti-knock.

Procedure:

1. The Three Things Required for Combustion (1)
   A book bursts into flames while one reads from it that you need a fuel, a source of oxygen, and an initiating spark or flame in order to have combustion. The workings of the trick book is shown to expose fire proof ceramic ribbon saturated with cigarette lighter fluid which supplies the fuel vapor and a battery operated glow bar which initiates its combustion which the oxygen in the air. The need for the oxygen is illustrated when the book is closed,

suffocating the flame. "Burning" books may be purchased from suppliers of magic products or made with instructions given in reference 1.

2. Gases Which Support or Do Not Support Combustion. (2,3)

(a) Carbon Dioxide Does Not Support Combustion.
One or two alka-seltzer tablets are dropped into a 600 mL beaker which is about one-fourth full of water. Insert a burning splint into the top of the beaker and it will go out since CO_2 does not support combustion. Since CO_2 is heavier than air the gas will remain in the beaker for a long enough time to do the second part. If air is circulating over the beaker too rapidly the CO_2 gas may escape from the beaker too quickly and the flame is not extinguished.

(b) Oxygen Gas Does Support Combustion. (3)
In a second 600 mL beaker place about one-third of the contents of an envelope of dry yeast. Pour in some 3% hydrogen peroxide until the beaker is one-fourth to one-third full. Suds will start rising up in the beaker. (Just as yeast will release carbon dioxide from sugars, ingredients in the dry yeast will catalyze the release of oxygen gas from hydrogen peroxide; there is no carbon present). Touch the top of the foam with a glowing splint and it will burst into flames as oxygen does support combustion.

Now you may place the burning splint into the CO_2 beaker and the flame will go out but remove it while it is still glowing. Return the glowing splint to the O_2 foam and it will again burst into flames. With a little practice you can cycle the splint back and forth six or more times, igniting and extinguishing the flame. For a more humorous effect get a big smile on your face and shift back and forth on your feet like a young boy playing with matches.

3. The Vaporous Nature of the Fuel in Combustion (3)

Make about 100 mL of a 50:50 mixture of water and ethyl (or methyl or isopropyl) alcohol and add a little sodium chloride to make the flame more visable . Place it in a large container and thoroughly wet a cloth towel in it. Squeeze out the excess liquid and drape the towel over a rod. Light the cloth from the bottom after dying your hands. (The burning hands trick is too dramatic!) After it has flamed for a while extinguish the fire by giving it a quick jerk using a pair of tongs. The towel will not be burnt.

4. Alcohol Explosions Demonstrating Combustion in an Internal Combustion Engine. (4)

A copy of reference 4 is attached. Reprinted with permission of Chem 13 News. Part A describes the demonstration.

5. The Need for the Exhaust Stroke (4)

The procedure is given in the last paragraph of Part A of reference 4, which is attached.

6. An Analogical Demonstration of the Four Stroke, Four Cylinder Engine. (4)

   See Part B of the attached copy of reference 4. Full sized masters of the figures are supplied for making overhead transparencies.

7. Demonstrations Contrasting Rough and Smooth Alcohol Explosions for Analogy to Octane Rating (5,6)

   About 25 to 40 mL of methanol is shaken and swirled in a 5-gallon plastic water jug for 10 to 15 seconds to hasten the volatilization of the liquid and to make the gas concentration uniform throughout the bottle. The stopper or lid is removed and the excess liquid alcohol is poured out. The jug is placed behind a shield, the lights are dimmed, and a long fireplace match or kitchen match taped to a meter stick is brought over or slightly into the mouth of the bottle. Blue flames are thrust out of the mouth of the bottle followed by some dancing flames of burning vapor in the center of the jug. This rapid, rough explosion of methanol can be compared to the combustion of low octane rated fuels with straight chain hydrocarbons.

   In a second jug the demonstration is repeated using cool 70% isopropanol which produces a slower, less violent explosion followed by ring of flames moving down the inside of he jug. This smoother, slower explosion can be compared to combustion of high-octane fuels with branched hydrocarbons, which is more suitable for driving the piston.

   Before reuse each jug should be totally filled with water to exhaust the oxygen-depleted air and allowed to fully dry.

   The most important precautions to be taken in these demonstrations are:
   - never use a glass bottle;
   - pure oxygen or any gas mixture with a concentration of oxygen higher than air should not be used;
   - when using methanol or ethanol, neither the alcohol nor the bottle should be heated above room temperature;
   - plastic jugs should be replaced when they begin to show grazing, frosting, or cracking;
   - Safety shields must always be in place, because even the mildest of these explosions have some chance of the bottle shattering; and, of course safety goggles must be worn.

Comments:

This program in its entirety gives a short course in combustion reactions of fuels relevant to use in engines. Individual experiments can be used to focus on specific aspects if desired. The experiments all have an element of danger as they involve fires and explosions so proper safety precautions must be followed. In particular explosions of alcohols in jugs given in section 7 of the procedure have led to several serious accidents due variations of "short cuts" in the instructions. A more complete list of safety concerns are given in reference number 6.

References:

1. R. Battino and J. Fortman, "The 'Burning' Book - a Guide to Its Construction", Chem 13 News, Number 249, p. 18, May 1996.

2. J. Fortman, "Complementary Demonstrations #6: Gases Which Support or Do Not Support Combustion," Chem 13 News, Number 236, p. 13, January 1995.

3. J. Fortman, "Updated Versions of Some Demonstrations Faraday Used with His Christmas Lectures on 'The Chemical History of a Candle'," Chem 13 News, Number 205, pp. 9-12, September 1991.

4. J. Fortman, "Demonstrating the Chemistry of the Internal Combustion and Jet Engines: Alcohol Explosions," Chem 13 News, Number 285, pp. 10-11, May 2000.

5. J. Fortman, "Safety Precautions for the 'Ring of Fire' and 'Whoosh Bottle' Demonstrations" Chem 13 News, Number 277, p. 1, September 1999.

6. J. J. Fortman, A. C. Rush, and J. E. Stamper, "Variations on the 'Whoosh' Bottle Alcohol Explosion Demonstration Including Safety Notes," J. Chem. Educ. 76, 1092-3 (1999).

Demonstrating the chemistry of internal combustion and jet engines: alcohol explosions

John J. Fortman
Department of Chemistry
Wright State University
Dayton OH 45435

Students often know more about the mechanics of a car engine than they know about the chemical reaction that propels them. The following demonstrations will help them to understand the chemistry that occurs in both car and jet plane engines.

A. An enclosed explosion—the internal combustion engine in a car

Two 3d nails are pushed through opposite sides of a polyethylene bottle (125 mL to 500 mL in size) which is also fitted with a cork. (Clear plastic bottles must not be used as they may shatter.) The nails must be in tight and almost touching. By pushing the nails through the walls without drilling holes, the plastic will seal around the nails and if some water is placed in the bottle the internal rusting of the nails will secure the nails better than glues, which might soften at firing temperatures. When firing occurs the nails should be pointed towards the side walls of the room and not towards the audience.

Two to five mL of alcohol (ethanol, methanol or 2-propanol) are placed in the bottle. It is stoppered and shaken. The excess liquid can be poured out before firing to show that this is a vapor phase reaction. A Tesla coil is brought in contact with one of the nails causing a spark to jump between the nails and firing the cork to the ceiling.[1,2,3] Alternatively, the spark may be supplied by a push button ignition device (used on many gas barbecue grills) that has been modified with two lengths of wire and alligator clips.[4,5] Water-proof wick or electrical rocket ignitors[6] could also be used but they are harder to relate to the spark plug in the internal combustion engine.

You may want to ask a member of the audience to repeat this demonstration. If you immediately restopper the bottle and add more alcohol the bottle will not fire again. Ask the volunteer or the class why not. The reason is that the bottle lacks sufficient oxygen.[2] Fill the bottle with water, empty it, add alcohol, shake and then repeat. It explodes again. After the students have seen that the second explosion cannot occur without first exhausting the cylinder and taking in a fresh air fuel mixture, the lesson can be connected to the four strokes in a cylinder of the internal combustion engine: intake, compression, power and exhaust.

B. An analogical demonstration of the four stroke, four cylinder engine

Ask for four volunteers from your audience, perhaps those who like to do line dances. Line them up shoulder to shoulder facing the audience. First have them practice the up and down stroke of the piston by having them bend their knees and go up and down like an "ump-pah" band. Then tell them that their two fists will represent the valves, their left fists being the intake valves and their right fists being the exhaust valves. When their fists are against their shoulders the valves are closed and when extended they are open. Refer them to an overhead transparency of Fig. 1 and slowly lead them through the four steps beginning with them upright with the left fist extended and squatting down (the intake stroke). They now bring their left

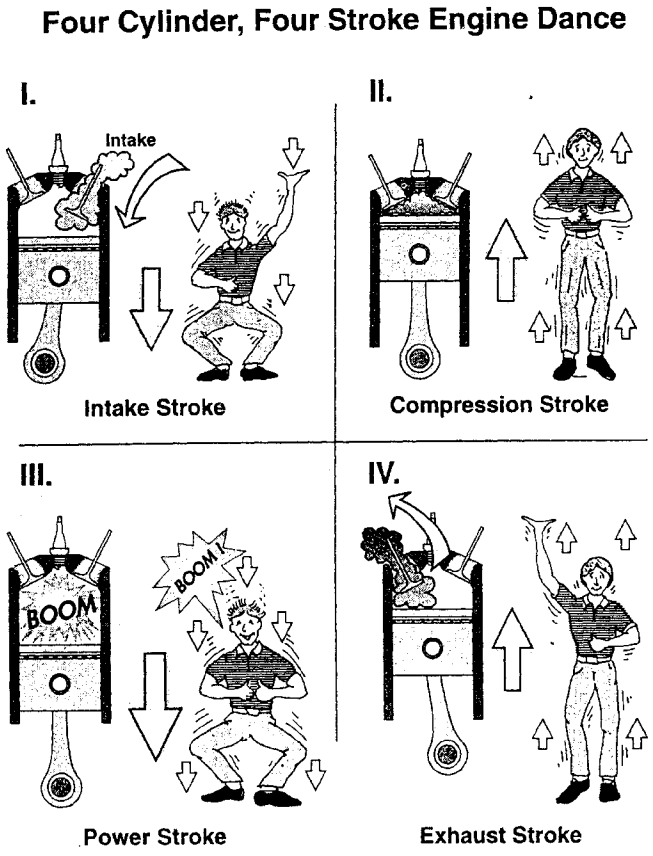

Fig. 1.

Four Cylinder, Four Stroke Engine Dance Timing

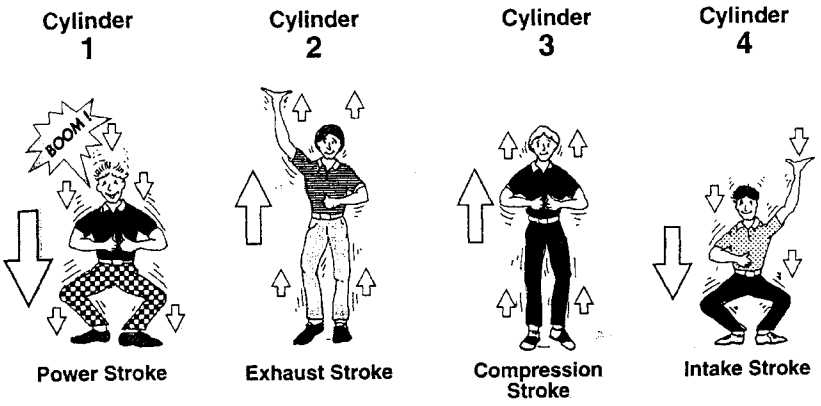

Fig. 2.

fists to their shoulder and straighten back up (the compression stroke). Together they all say "boom" and stoop down again with both fists at their shoulders (the power stroke). Finally they extend their right arms upwards with fist open (the exhaust stroke). You may have them practice the four steps together several times before you break the news to them that to represent a real engine they must each be doing a different step at any given time. Show them an overhead of Fig. 2 and point out that the correct firing sequence has the outer pair in phase with each other but out of phase with the middle two. For mass and power balance the firing sequence is 1-3-4-2, so point at the correct student and sing "BOOM – boom – BOOM – boom." While everyone is still laughing thank them for participating and send them off with a suggestion that they practice before the next school dance or variety show and they may start a new dance craze.

C. An open explosion—a jet engine

About 25 mL of methanol or ethanol is shaken in a 5 gallon plastic water jug. Remove the cap and pour out the excess alcohol. Place the bottle behind a safety shield. Dim the lights and bring a match taped to a meter stick over the mouth of the jug. A blue flame will shoot out and flames will dance and pulsate in the jug as more air is sucked in. Compare this to the thrust of an external-combustion jet engine. This is an old demonstration, which has apparently been passed on without being formally published. The first citable reference of which I am aware was at the BCCE at Purdue in 1988[7] and there have been several newer modifications.[8,9,10]

CAUTION

There have been recent warnings of bottles shattering during this experiment.[11,12] Do not use a glass bottle; do not use alcohol above room temperature, and do not use oxygen in any higher concentration than found in air. Always use a safety shield. A more complete analysis of this experiment and its safety requirements has been published[13] along with a shorter warning.[14]

Literature cited

1. J.W. Bozzelli, *Journal of Chemical Education*, December 1983, pages 1069-1070.
2. B.Z. Shakhashiri, "Vapor-Phase Oxidations," *Chemical Demonstrations*, University of Wisconsin Press, Madison WI, volume 2, 1985, pages 216-219.
3. L. Summerlin, J.L. Ealy, Jr., "The Methanol Cannon," *Chemical Demonstrations: A Sourcebook for Teachers*, American Chemical Society Publications, Washington DC 1985, page 170.
4. R. Battino and J.J. Fortman, *Journal of Chemical Education*, February 1992, page 172.
5. H. Brouwer, *Journal of Chemical Education*, April 1993, page 329.
6. J.J. Fortman and J. Schreier, *Journal of Chemical Education*, April 1993, pages 328-329.
7. M.H. Bailey, *Abstracts of the Tenth Biennial Conference on Chemical Education*, Purdue, IN, 1988, Abstract No. 295 and handout.
8. D.A. Robinson, 209th ACS National Meeting, Anaheim, CA, April 1995, Abstract No. CHED-038.
9. D.A. Robinson, 211th ACS National Meeting, New Orleans, LA, March 1996, Abstact No. CHED-061.
10. W.C. Deese, *CHEM 13 NEWS*, November 1996, pages 8-9.
11. C. Lee, *Journal of Chemical Education*, May 1998, page 543.
12. W.C. Deese, *CHEM 13 NEWS*, May 1998, page 3.
13. J.J. Fortman, A.C. Rush, J.E. Stamper, *Journal of Chemical Education*, August 1999, pages 1092-1094.
14. J.J. Fortman, *CHEM 13 NEWS*, September 1999, page 1. ■

Four Cylinder, Four Stroke Engine Dance

I.

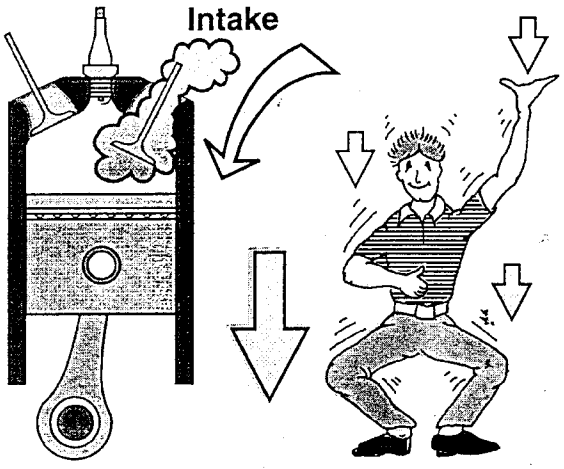

Intake Stroke

II.

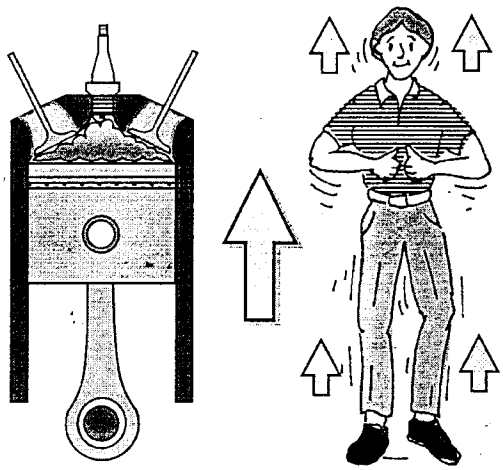

Compression Stroke

III.

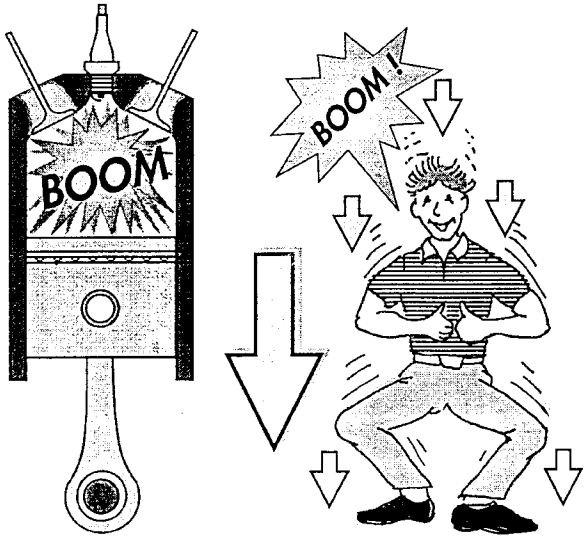

Power Stroke

IV.

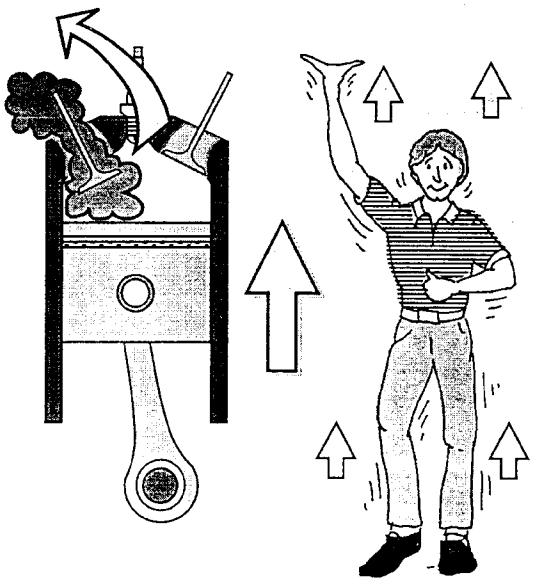

Exhaust Stroke

Four Cylinder, Four Stroke Engine Dance
Timing

Cylinder 1

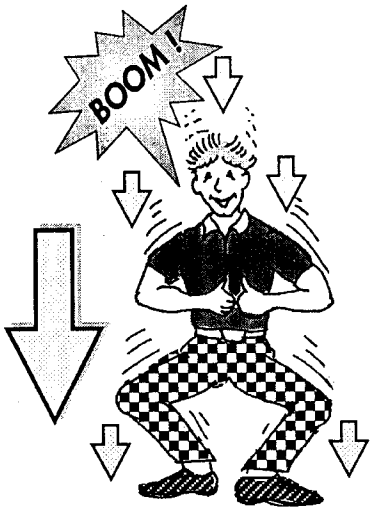

Power Stroke

Cylinder 2

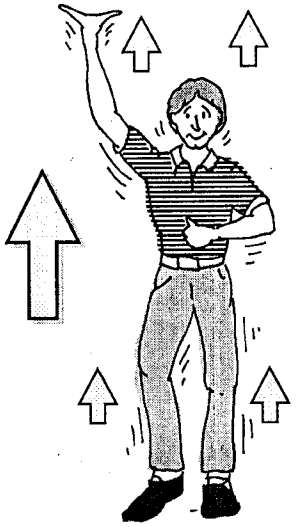

Exhaust Stroke

Cylinder 3

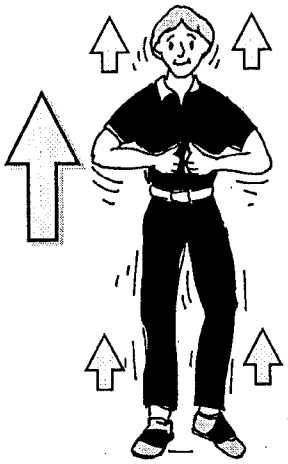

Compression Stroke

Cylinder 4

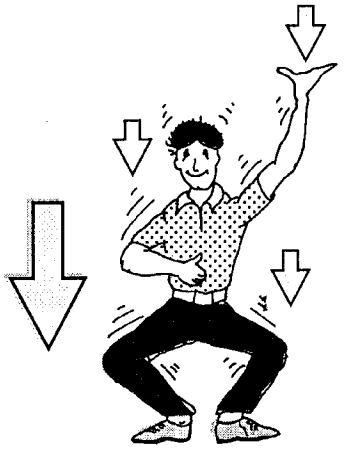

Intake Stroke

HARDNESS INDENTATION ANALYSIS

Richard J. Fields

MATLS B252
National Institute of Standards and Technology
100 Bureau Drive, Stop 8553
Gaithersburg, Maryland 20899-8533

Telephone: 301-975-5712
e-mail rjf@nist.gov

and

Thomas A. Pierce

Student
Norfolk State University
700 Park Avenue
Norfolk, Virginia 23504

e-mail tapnsu@yahoo.com

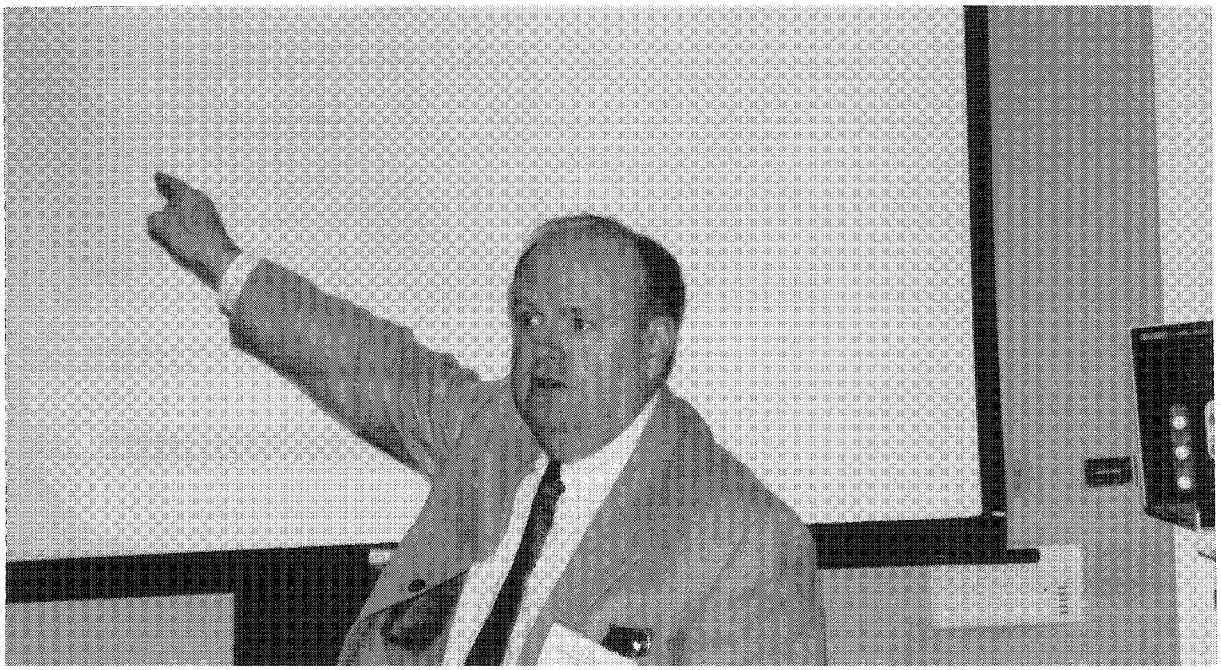

Richard Fields

Thomas Pierce

Hardness Indentation Analysis

R. J. Fields and T. A. Pierce
National Institute of Standards and Technology
Gaithersburg, Maryland

Key Words:

Hardness testing, indentation, metals, mechanical properties, and residual stress.

Prerequisite Knowledge:

Physics (mechanics and optics) and algebra.

Objective:

Demonstrate the usefulness of hardness testing for characterizing the mechanical properties of metals and show the effect of residual stress on hardness measurements.

Equipment and Materials:

Hardness tester, pieces of metal, optical flat, and monochromatic light source.

Introduction:

Hardness is measured by forcing a hard sphere or diamond brale into a surface using a known load; the size (area or depth) of the resulting indentation is a measure of the hardness. {1} The hardness is related to other mechanical properties. The ease and speed of hardness testing makes it the measurement of choice by industry, especially for quality control. Besides simply characterizing the hardness of a product, hardness testing can be used to analyze structures. For example, it can be used to find welds in structures and to determine if some regions are brittle. {2} Its value is affected by residual stresses in metals and it is the purpose of this experiment to show this effect.

Procedure:

Hardness testing of several metals will be carried out using a typical hardness tester. The hardness test will be explained and the measured value correlated with known mechanical properties of these metals. The test will then be used to scan across a weld in a steel plate to show how mechanical properties vary in a weldment. To demonstrate how residual stresses effect the measurement, a metal bar will be bent. The hardness will be measured on the top and bottom surface. An analysis will be worked through showing how to separate the actual hardness from the residual stress effects. The magnitude of the residual stress will be determined. Finally, a block of metal will be repeatedly indented and its curvature monitored, using an optical flat and monochromatic light, to demonstrate the build up of residual stress by

indentation. Analysis and plotting will be used to elucidate the phenomenon.

Comments:

A complimentary copy of NIST's Recommended Practice Guide for Rockwell Hardness Measurement of Metallic Materials will be provide to each attendee.

References:

1. Annual Book of ASTM Standards, Metal Test Methods and Analytical Procedures, Vol 03.01, Publ. by ASTM, West Conshohocken, PA, 2000.

2. ISO Standard 14271, "Vickers hardness testing of resistance spot, projection and seam welds", ISO Geneva Switzerland.

Bibliography:

Rockwell Hardness Measurement of Metallic Materials, Samuel R. Low, NIST Spec. Publ. 960-5, U. S. Government Printing Office, Washington, D. C., 2000.

The Hardness of Metals, David Tabor, Publ by Clarendon Press, Oxford, England, 1951

OVERVIEW OF NEW:UPDATE 2002

W. Richard Chung

Department of Chemical and Materials Engineering
San Jose State University
San Jose, California 95192-0082

Telephone: 408-924-3927
e-mail wrchung@email.sjsu.edu

Richard Chung

17th Annual National Educators' Workshop
NEW: Update 2002

October 13 – 16, 2002

To be held at

Semiconductor Equipment and Materials International (SEMI)

Ultratech Stepper, Inc.

IBM Seagate

San Jose State University

Workshop Sites

- SEMI: (Selected form http://www.semi.org)

SEMI represents its members in every significant semiconductor manufacturing region in the world, with offices in Belgium, Japan, Korea, North America, Russia, Singapore, and Taiwan. Member companies in each region profit from our global viewpoint. Check below for SEMI information in your region.

Worldwide Offices - Regions

SEMI North America

SEMI San Jose - Headquarters

3081 Zanker Road
San Jose, CA 95134-2127
Phone: 408.943.6900
Fax: 408.428.9600
Email: semihq@semi.org

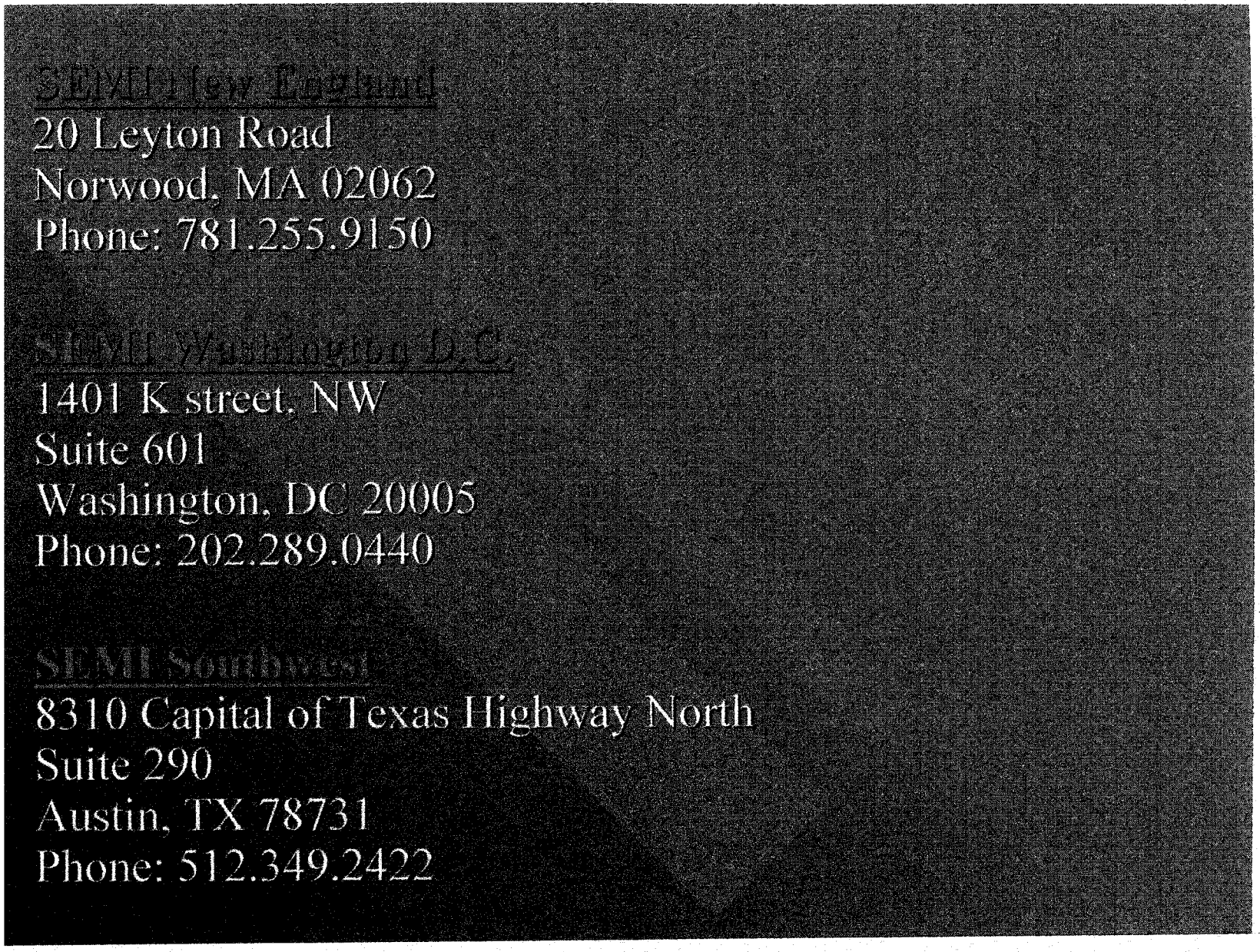
SEMI New England
20 Leyton Road
Norwood, MA 02062
Phone: 781.255.9150
SEMI Washington D.C.
1401 K street, NW
Suite 601
Washington, DC 20005
Phone: 202.289.0440
SEMI Southwest
8310 Capital of Texas Highway North
Suite 290
Austin, TX 78731
Phone: 512.349.2422

SEMI China

SEMI China Contact
Wei-Fang Zhou
E-mail: wzhou@semi.org
Phone: 1-408-943-6947

SEMI Korea

SEMI Korea
4005 World Trade Tower
159-1 Samsung-Dong, Kangnam-Ku
Seoul, Korea 135-729
Tel: 82.2.551.3401

SEMI Europe & CIS

SEMI Europe

40 Avenue des Arts
B-1040 BRUSSELS
BELGIUM
Phone : 32.2.289.64.90

SEMI Moscow

24/2, Usievicha Str.,
Moscow, 125315
Russia
Phone: 7 (095) 931 9647

SEMI Asia

SEMI Taiwan

14 F-1, Empire Commercial Building
No. 295, Section2, Kuang Fu Road
Hsinchu, Taiwan, 300
Phone: 886.3.573.3399

SEMI Japan

7F Kenwa Bldg., 4-7-15 Kudan-minami
Chiyoda-ku, Tokyo 102-0074
Japan
Phone: 011.81.3.3222.5755
Fax: 011.81.3.3222.5757

SEMI Singapore

9 Temasek Boulevard
#42-03 Suntec City Tower Two
Singapore 038989
Republic of Singapore
Phone: 65.339.6361

- Ultratech Stepper Inc. (cited from http://www/ultratech.com)

  Founded in 1979, Ultratech Stepper, Inc. designs, manufactures and markets photolithography equipment used worldwide in the fabrication of integrated circuits, microsystems devices and thin film heads for disk drives. The company produces products that substantially reduce the cost of ownership for manufacturers in the electronics industry. Ultratech's common stock is traded on the NASDAQ Stock Market under the symbol UTEK. The statements contained herein that are considered forward looking statements involve numerous risks and uncertainties. Such risks and uncertainties are set forth in the company's SEC reports.

Preliminary Program

- Sunday afternoon reception and Lab Tours– College of Engineering, San Jose State University
- Monday Workshop Presentations –
  - Ultratech Stepper – Assembly room
  - SEMI – Break-out rooms
  - Monday Mini Workshops --Seagate Material Analysis and Tribology Testing
- Tuesday IBM Almaden Research Center—
  - Plenary Presentations -- Auditorium
  - Facility Tours – Material Syntheses & Characterizations
- Wednesday Workshop Presentations – Ultratech Stepper and SEMI

Workshop Schedule

NEW2002 workshop schedule-rev 3.doc

17th National Educators' Workshop Schedule
October 13-16, 2002, San Jose, California

Date/Time	SUNDAY	MONDAY		TUESDAY			WEDNESDAY
7:00-8:00	N/A	**Breakfast Reception**		**Breakfast Reception**			**Breakfast Reception**
8:00-10:00	N/A	Plenary Session & Presentations ***SEMI/Ultrateh Stepper***		8:00-9:00 a.m. Bus travel to IBM **9:00 a.m. Plenary Session** Host: Dr. John Baglin IBM Almaden Research Center Auditorium A&B - *Overview: Future Computing* - *Single-atom Cryogenic STM.*			Plenary Session & Presentations ***SEMI/Ultrateh Stepper***
10:00-10:30	N/A	**Coffee Break/Exhibits**		**Coffee Break** *(2 Demos available in Foyer now thru to Lunch time);* *(Poster set-up time)*			**Coffee Break/Exhibits**
10:30-12:00	N/A	Presentations ***SEMI/Ultrateh Stepper***		**Hot Topics/Tutorials and Demos** *IBM*			Presentations ***SEMI/Ultrateh Stepper***
				Aud. A *Hot Topics A (Four 20-min talks)*	**Aud. B** *Hot Topics B (Four 20-min. talks)*	**Foyer** *2 Hands-on Demos*	
12:00-13:00	N/A	**Luncheon**		**Luncheon**			**Box Lunch**
13:00-15:00	**Lab Tours and Networking**	Plenary Sessions Mini-workshop Dr. Susan Chang *Materials Analysis, Seagate*	Plenary Sessions **Mini-Workshop** **open**	**1:30 p.m. Plenary Session** ***Auditorium A&B*** *Invited presentations*			Collaborative Effort (advisory board meetings)
15:00-15:30	**Coffee Break**	**Coffee Break**		**2:30 p.m. Posters, Lab Tours, Coffee**			Collaborative Effort (advisory board meetings)
15:30-17:00	**Welcome Reception, Dean Kirk** ***Engineering Bldg, SJSU*** Plenary Sessions	Mini-workshop Dr. Susan Chang *Materials Analysis, Seagate*	**Mini-Workshop** **open**	**Aud. A** **Presentations**	**Aud. B** **HighSchool/Community College Track**		
18:00-21:00	N/A	**Reception in Hotels**		**Banquet at Tech Museum?**			

A Proposal for Mini Workshops for NEW:2002

Mini Workshops to be conducted at Seagate on Monday, October 14, 2002

Location:

Seagate Recording Media
311 Turquoise Street
Milpitas, CA 95035

Contact Person:

Dr. Susan Chang
Executive Director
Material Analysis and Tribology Testing
(408) 941-5403
Susan.S.Chang@seagate.com

Format and Topics: (12- 5PM)

Lunch and refreshments may be provided by Seagate (will work with company authorities!)
An overview of disk manufacturing process (1 hour)
Tour of the manufacturing facilities (30 minutes)
The attendees will then participate in a chosen area to get their hands-on experience:
The workshop size is limited to 10 people per area.

1) Failure Analysis
2) AFM/MFM (Atomic Force Microscopy/ Magnetic Force Microscopy)
3) Corrosion engineering
4) Tribology
5) Measurement of Surface Texture
6) Disk Characterization
7) Function Tests
8) Measurement of Magnetic Properties

NEW-2002
Tuesday, October 15, 2002
IBM Almaden Research Center

Tentative Program
(version 9/27/01)

8:45 a.m. Buses arrive at IBM. Visitor badging.

9:00 a.m. ***Plenary Session*** Auditorium A and B

- Overview: "Computing: The Future is not What it Used to Be"
- "Manipulating Single Atoms on Surfaces – the Cryogenic STM"

10:00 a.m. ***Coffee Break*** Aud. Foyer

[Posters to be pinned up now; formal session later]

- Hands-on STM demos – (remote)
- Hands-on Simulation of Ion-Solid Interaction (SRIM at 5 computers in Foyer)
  [These demos, and coffee, to remain available thru the a.m.]

10:30 a.m. ***Hot Topics / Tutorials*** *and* ***Demos***

[Parallel activities; attend the 20-min. talks of your choice]

Aud. A:
- Holographic Storage
- Magnetic Tunnelling – Spintronics
- Polymer Synthesis / Flat Panel Displays
- MEMS

Aud. B:
- Ion Beam Modification of Materials
- Multi-scale Modelling – Fracture
- Focused Ion Beam Technology
- Materials Characterization

Foyer: *[continuing]*
- Hands-on STM Demos
- Hands-on Simulation of Ion-Solid Interactions

12:10 p.m.	***Lunch***	IBM Cafeteria
1:30 p.m.	***Plenary Session***	Auditorium A and B
2:30 p.m.	***Poster Session*** *and* ***Lab. Tours***	

[Refreshments during poster session]
[Tours will make brief stops at 3 or 4 labs of interest]

3:40 p.m.	***Presentations***	Aud. A / Aud. B

[Parallel sessions in Aud. A and Aud. B]

5:00 p.m. Return to buses

Organizing Committee

- San Jose State University – Richard Chung, Emily Allen, Seth Bates
- IBM – John E. E. Baglin
- SEMI – Lisa Anderson, Bruce Gheman
- Ultratech Stepper – Barbara Womack, Michelle Rhodes
- Seagate – Susan Chang, Jeff Mack
- Intel – Jerry Kinsinger
- Workforce Silicon Valley – Ruth Medalina, Rendee Dore
- Silicon Valley Engineering Council – Cliff Monroe
- UC-Davis – Mike Meier

CARBON FIBER: THE MATERIAL OF THE FUTURE

C. David Warren

Oak Ridge National Laboratory
Building 9204
P. O. Box 2009, MS 8050
Oak Ridge, Tennessee 37831-8050

Telephone: 865-574-9693
e-mail WarrenCD@ORNL.GOV

C. David Warren

National Educators Workshop
Carbon Fiber: The Material of the Future

Vehicle Systems

C. David (Dave) Warren

Technical Manager
Transportation Composite Materials Research

Oak Ridge National Laboratory
P.O. Box 2009, M/S 8050
Oak Ridge, Tennessee 37831-8050
Phone: 865-574-9693. Fax: 865-574-0740
Email: WarrenCD@ORNL.GOV

The Challenges Facing Us

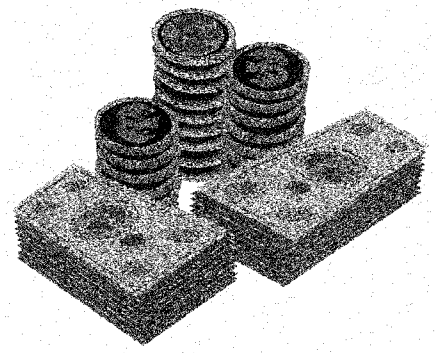

American Jobs

Growing Petroleum Consumption

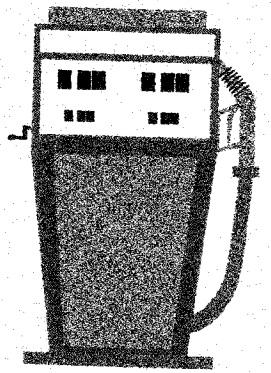

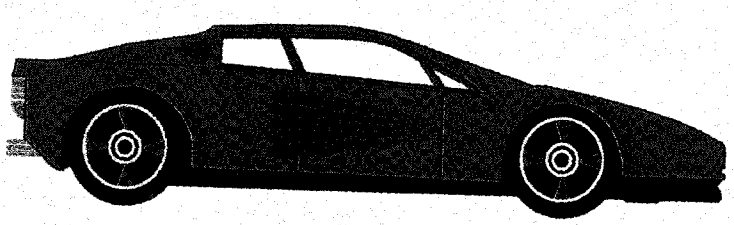

Urban Pollution

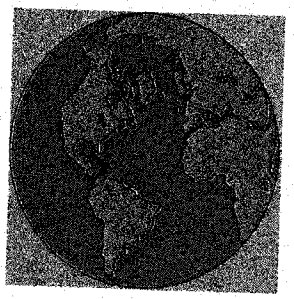

Global Climate Change

U.S.PETROLEUM DEPENDENCE, 1994
TRANSPORTATION SECTOR IS KEY CONTRIBUTOR

TOTAL U.S. PETROLEUM USE:
16.5 MBPD

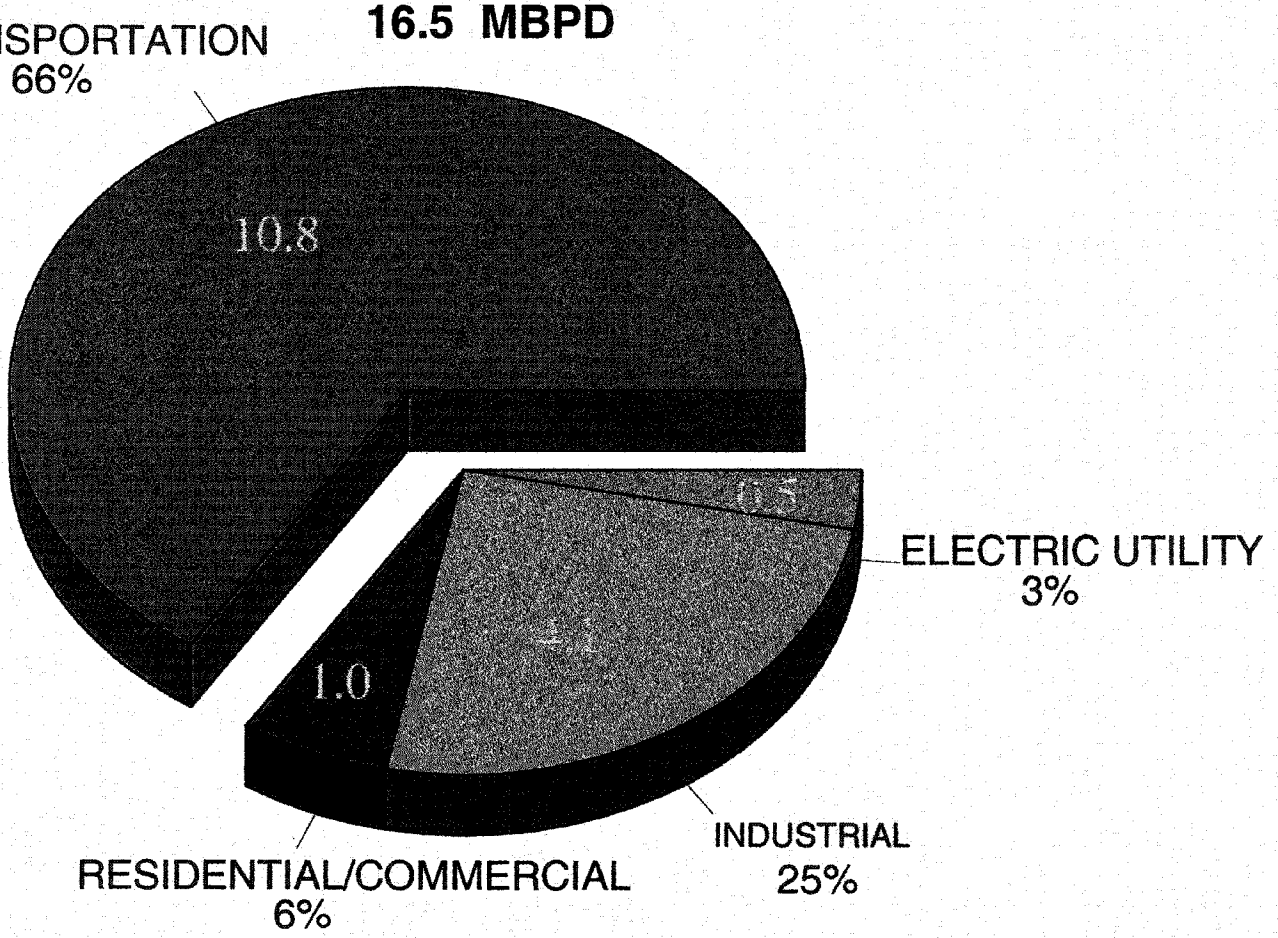

SOURCE: MONTHLY ENERGY REVIEW, AUGUST 1995
DOE ENERGY INFORMATION ADMINISTRATION

U.S. MERCHANDISE TRADE DEFICIT: DOMINATED BY OIL AND VEHICLE IMPORTS

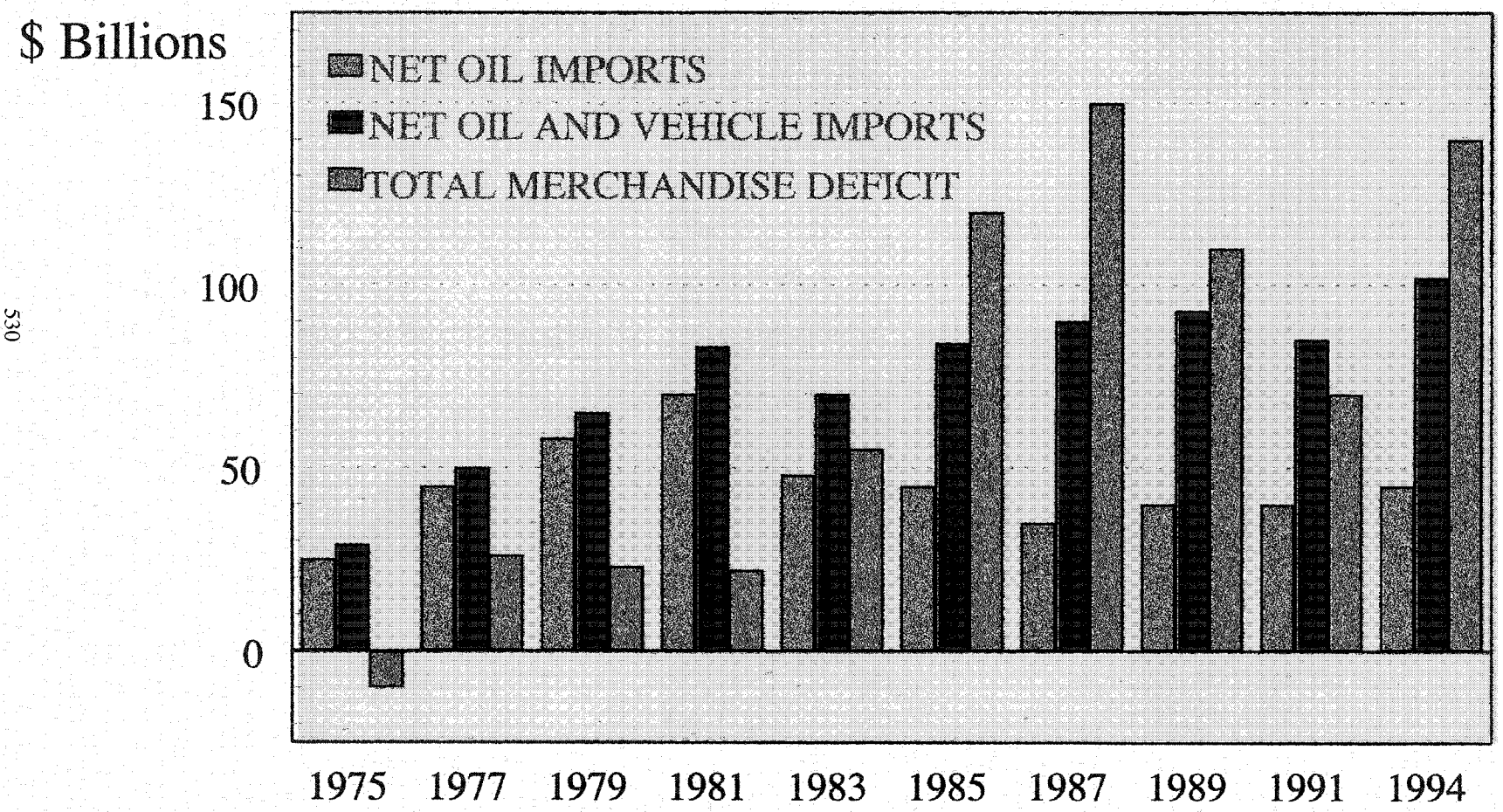

SOURCE: MONTHLY ENERGY REVIEW, AUGUST 1995, DOE ENERGY INFORMATION ADMINISTRATION.
AMERICAN AUTOMOBILE MANUFACTURERS ASSOCIATION, ECONOMIC INDICATORS, SECOND QUARTER: 1995.

OAAT MATERIALS PROGRAM GOALS

1. Significantly improve national competitiveness in manufacturing.
   - Agile/Flexible manufacturing
   - Reduction of costs
   - Reduced environmental impact
   - Improved quality

2. Implement commercially viable innovation from research on conventional vehicles.
   - Reduced emissions
   - Improved safety
   - Increased thermal efficiency
   - Reduce drivetrain losses

3. Develop a vehicle to achieve up to 3X fuel efficiency of today's comparable vehicle. (Chrysler Concorde, Ford Taurus, Chevrolet Lumina)
   - 80 mpg BTU equivalent
   - Equivalent consumer cost to own and drive
   - Comparable size, performance & utility

4. Develop advanced technologies beyond the PNGV time frame.
   - 100 mpg equivalent by 2011 - 2015.
   - Advanced materials and processing technologies

ENERGY DISTRIBUTION
TYPICAL MID-SIZE VEHICLE

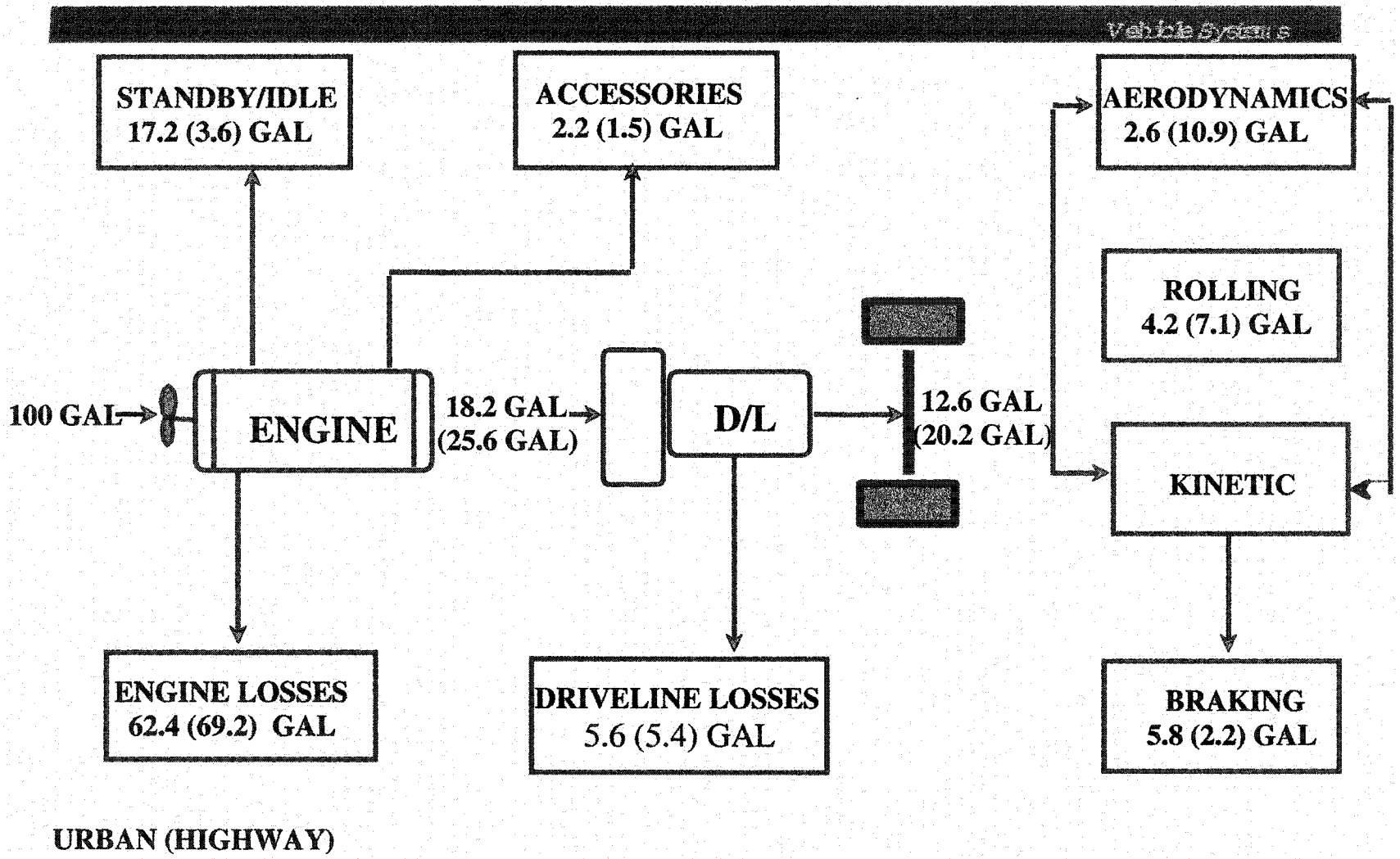

URBAN (HIGHWAY)

ENERGY DISTRIBUTION

TYPICAL MID-SIZE VEHICLE LESS 30% WEIGHT

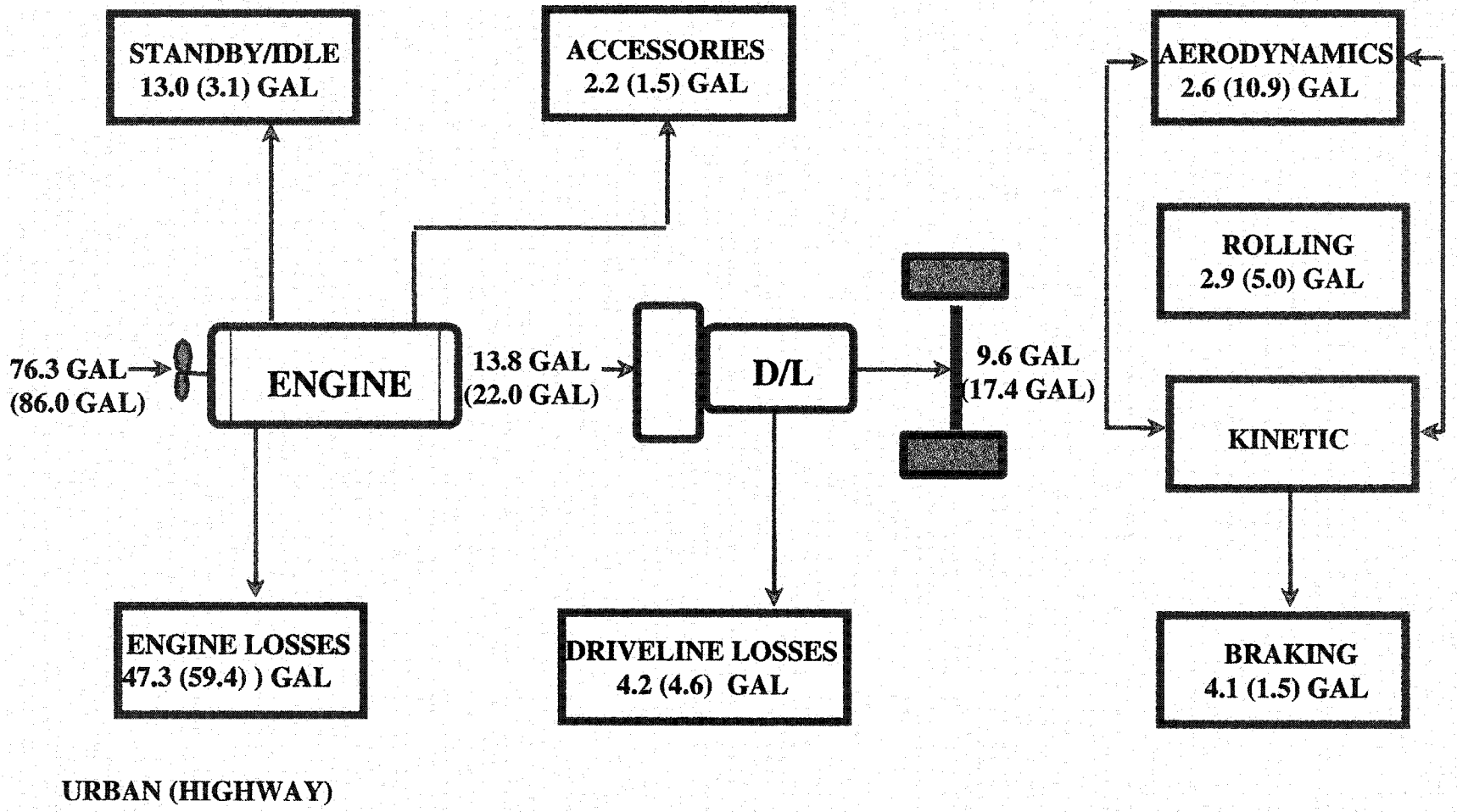

URBAN (HIGHWAY)

Composite Material Advantages

	Density (lb/cu. ft.)	Strength (Kpsi)	Modulus (Mpsi)
Automotive Steel	480	60-200	30
6061 Aluminum	167	30-40	10
Glass Fiber Composite	93	30-100	5-8
Carbon Fiber Composite	79	60-150	10-35

Advantages

Less Expensive Tooling

Parts Integration

Net Shape Forming

No Corrosion

Energy Absorption

Disadvantages

Raw Material Cost

Repair Processes

Processing Methodologies

Recyclability

Design Databases

Why Composites for Cars and Trucks

Vehicle Systems

Body Weight Savings Potential

Glass Fiber Composites	20-30%
Carbon Fiber Composites	40-60%

Weight Reduction = Fuel Economy = Emission Reductions

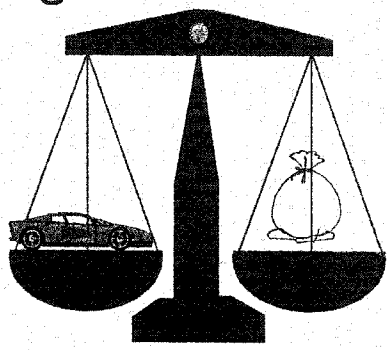

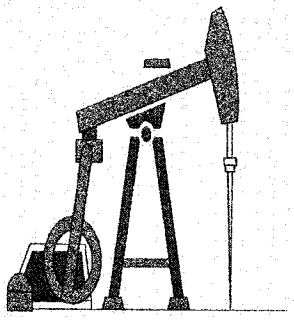

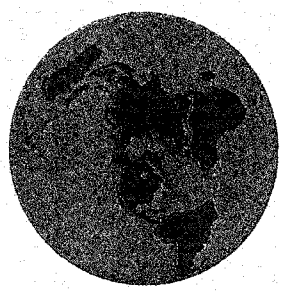

COMPOSITE MATERIALS RESEARCH
What Was Done --- Glass Fiber Composites

Vehicle Systems

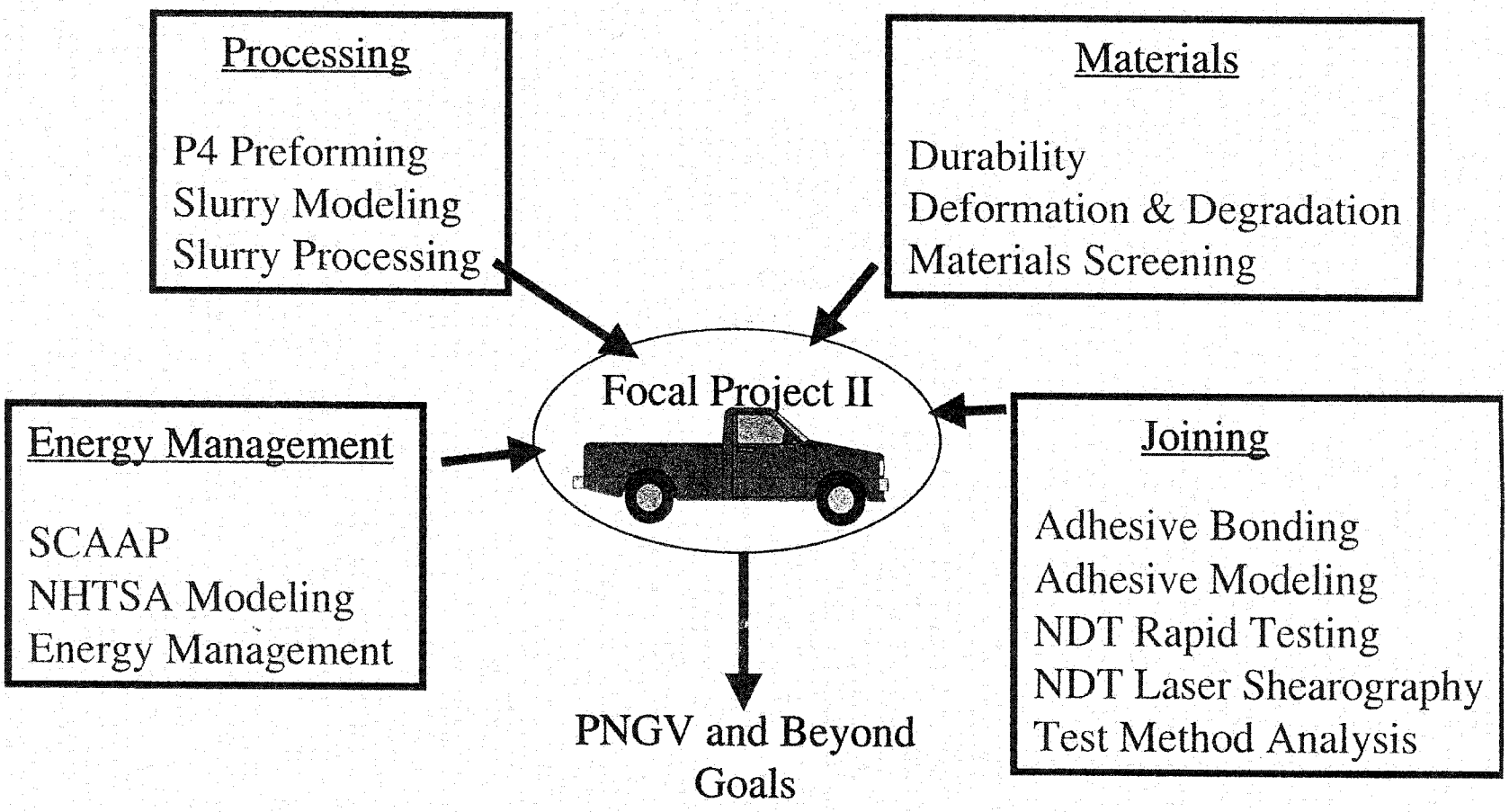

AUTOMOTIVE COMPOSITES CONSORTIUM

Focal Project 2

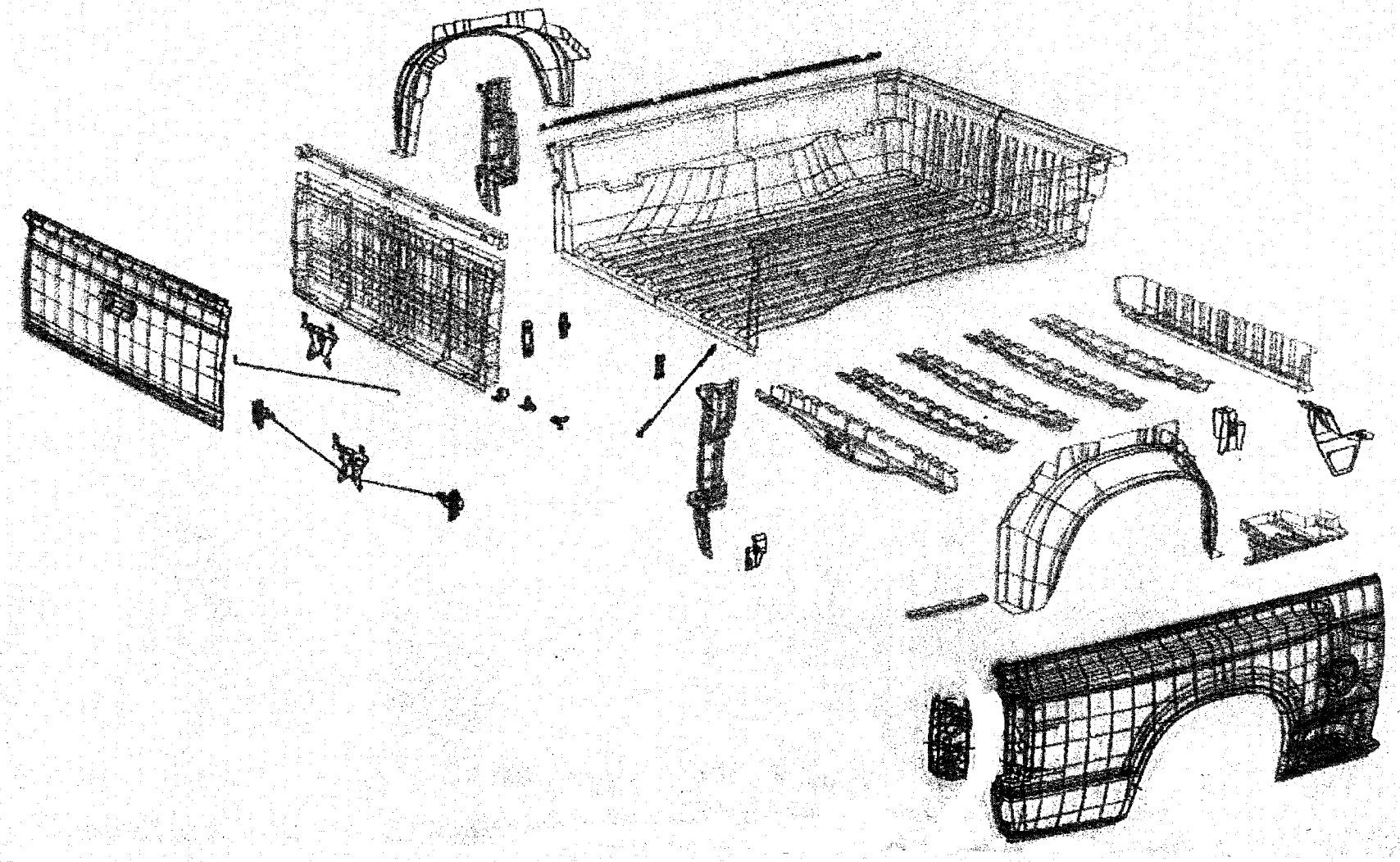

Focal Project II - Glass Fiber

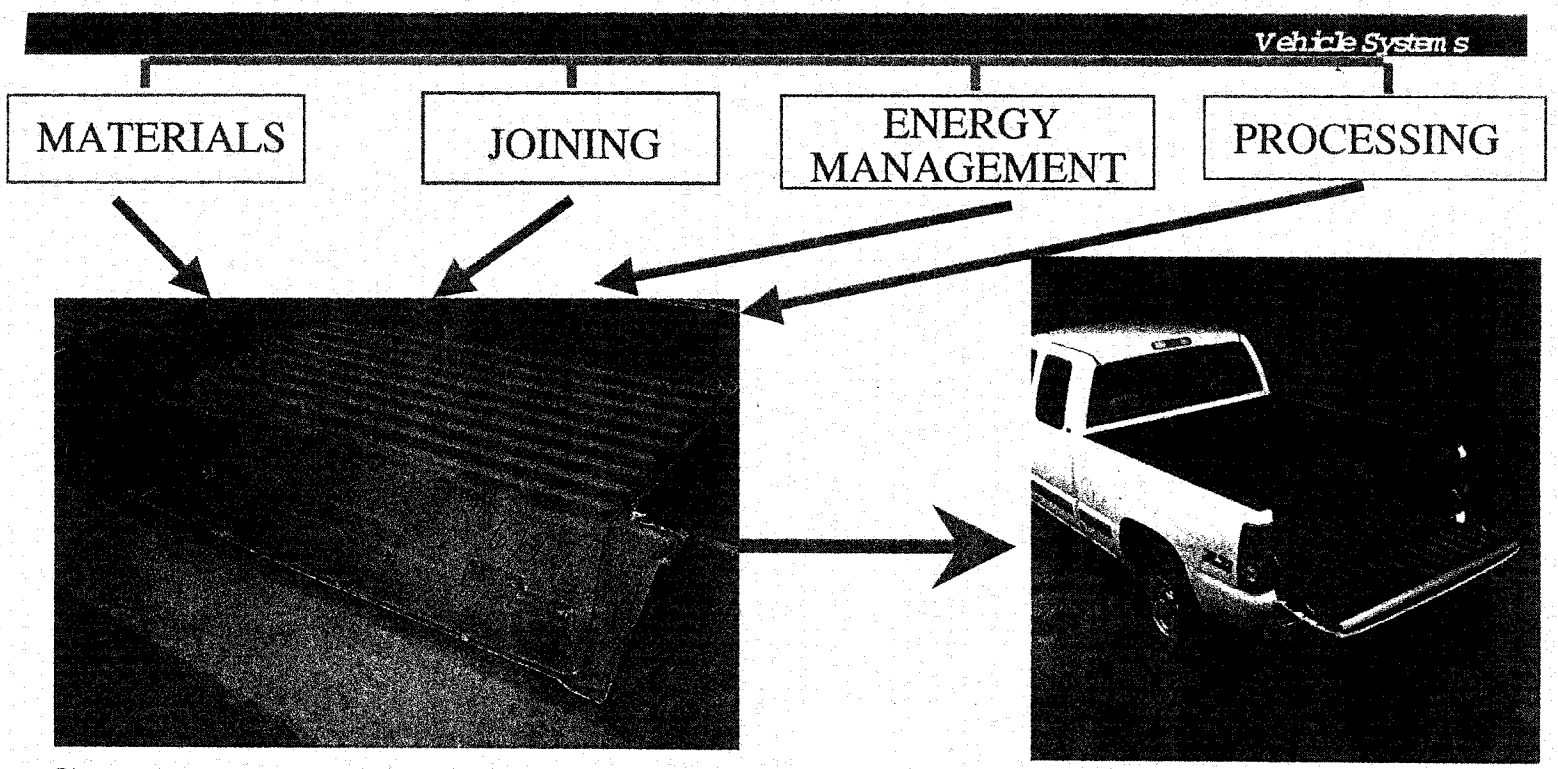

Compared to Steel Baseline

25% lighter — Greater Durability

Equal cost — Equal Safety

1 part every 4 min achieved

50 lb lighter - 15 lb lighter tailgate

No painting necessary

Impact and Corrosion Resistant

Tailgate Load Capacity 1000lb vs 600lb steel

Carbon Fiber

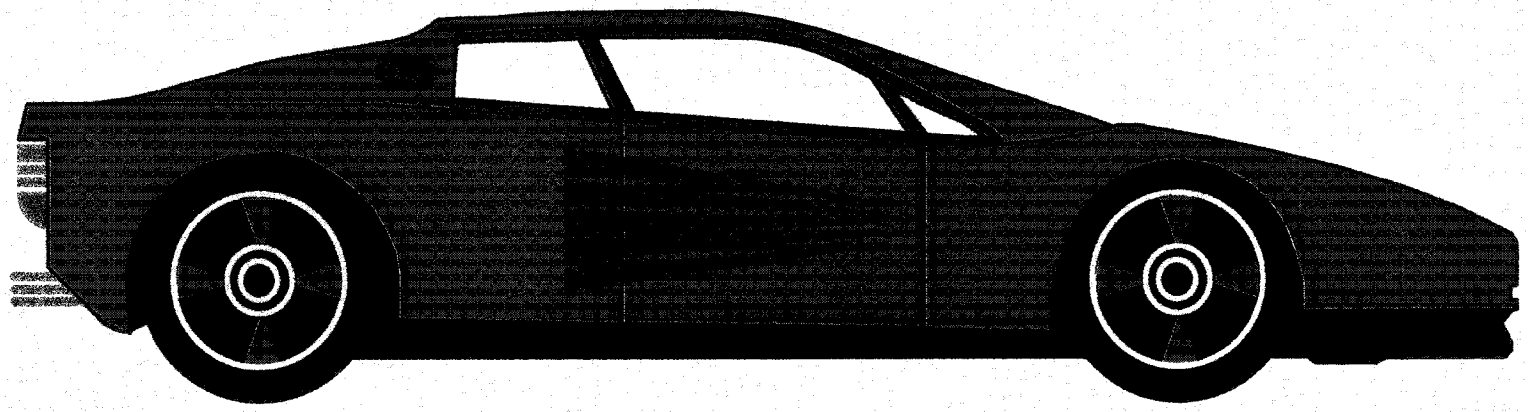

PRODUCT FORMS

- **Tows**
  - 2,3,6,12 K
  - 'Fat' or Large Tow
  - Commingled
- **Unidirectional, Continuous Prepreg Tapes**
- **Powder Prepreg**
- **Fabrics**
  - Weaves (2-D)
  - Commingled
- **Preforms**
  - 2-D Weaves, Braids, Knits
  - 3-D Weaves, Braids
- **Discontinuous Fibers**
  - Chopped
  - Vapor Grown, Whiskers

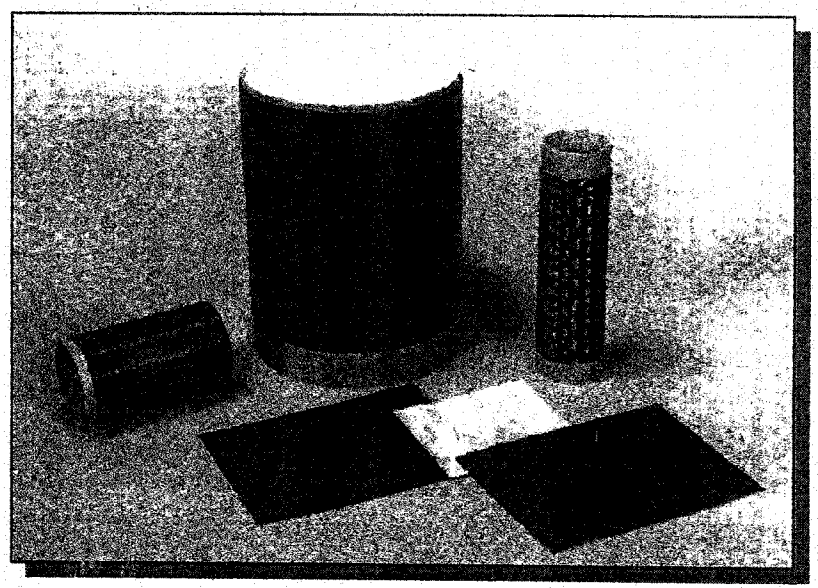

COMMON WEAVE STYLES

Plain

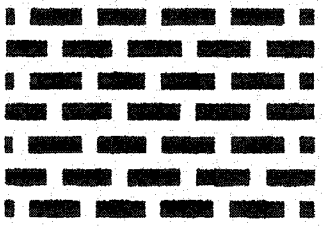

Crowfoot Satin

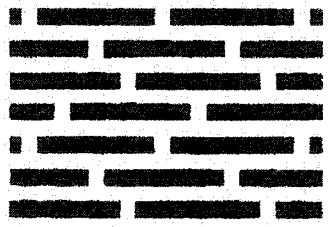

2x2 Basket

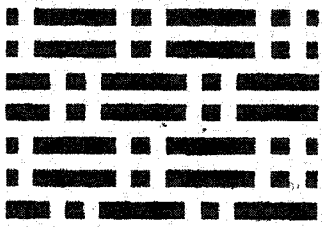

±45° Plain

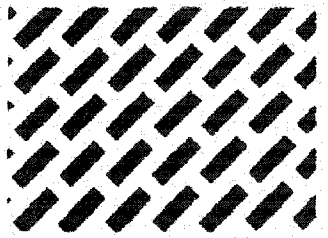

5HS

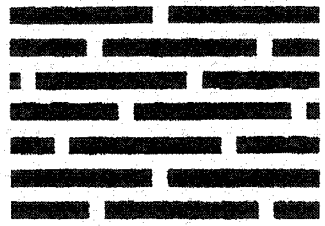

8HS

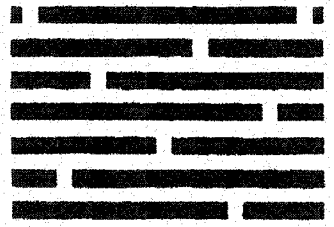

Leno

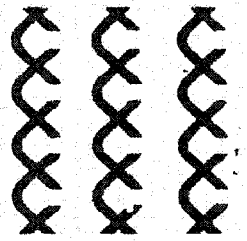

±45° 8HS

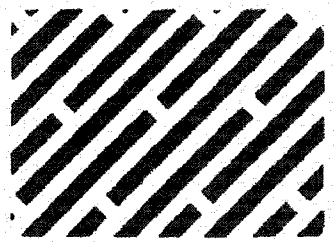

2/2 Twill

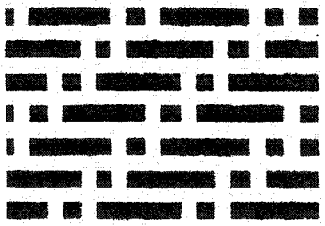

2/1 Twill

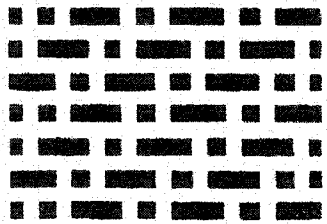

Non-Crimp

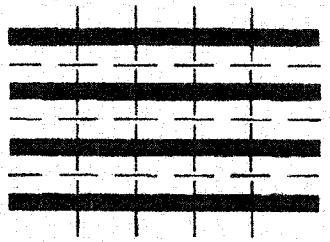

±45° Crowfoot Satin

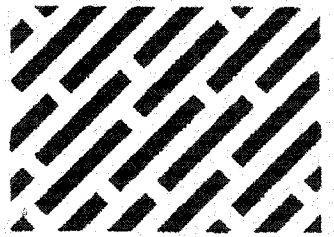

TYPICAL PAN-BASED CARBON FIBERS FOR AEROSPACE

- **Standard Modulus: E 32-35 Msi**
  - Cost Relatively Low
  - Large Database
  - AS4, Panex
- **Intermediate Modulus: E 42-47 Msi**
  - Highest Strength, Good Stiffness
  - IM7, IM8, T650-42,...
- **High Modulus: E 50-70 Msi**
  - High Stiffness
  - Cost
  - M40J, M50J, etc.
- **Ultra-High Modulus: E 71-85 Msi**
  - Highest Stiffness
  - M55J, GY-70,...

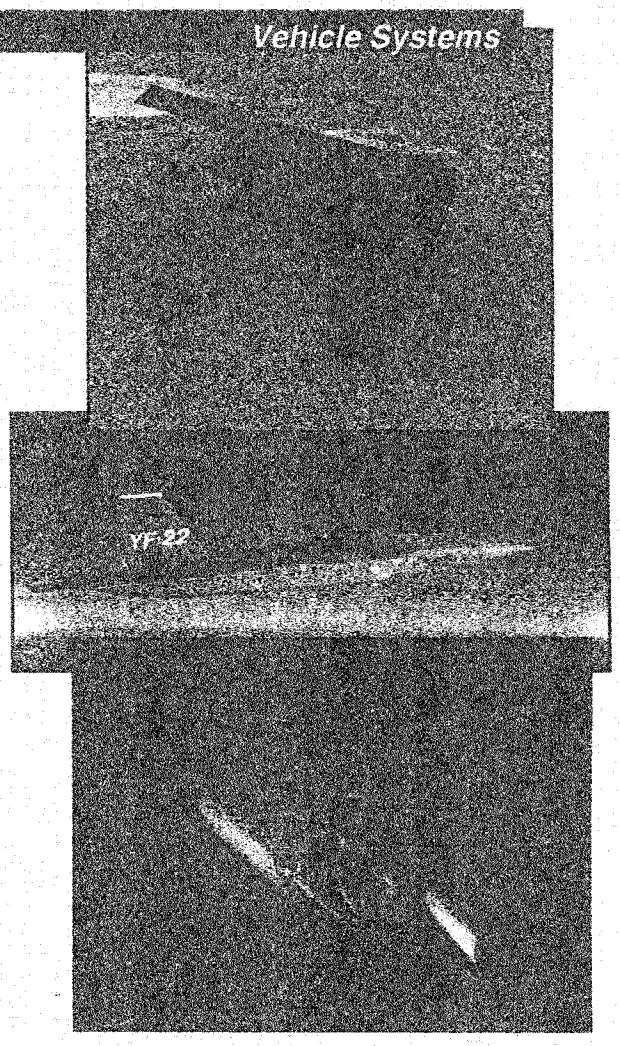

AEROSPACE APPLICATIONS

Military

- F-15 - Empennage/Speed Brake
- F-16 - Empennage
- F-18 - Wing Skins/Empennage
- AV8B - Wings/Empennage/Fuselage
- B-1B - Secondary Structure
- Space - Tubular Structures
- Helicopters - Blade/Rotor Hub/Fuselage
- Missiles - Control Surfaces
- Rocket Motor Cases
- Engine Components
- A-6 - Wings
- B-2
- C-17 - Nacelles/Fairings/Control Surfaces
- F-22 - Wings/Empennage/Fuselage

COMMERCIAL AEROSPACE

COMMERCIAL AEROSPACE

Boeing 777

- Weight Reduction
- Fatigue Resistance
- Corrosion resistance
- Impact Damage Resistance
- Reduction in Need for Structural Repairs

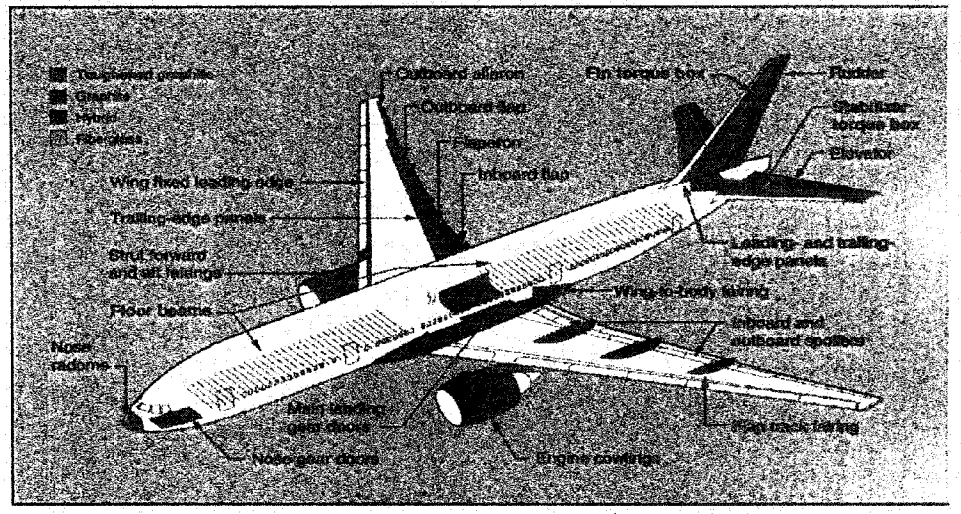

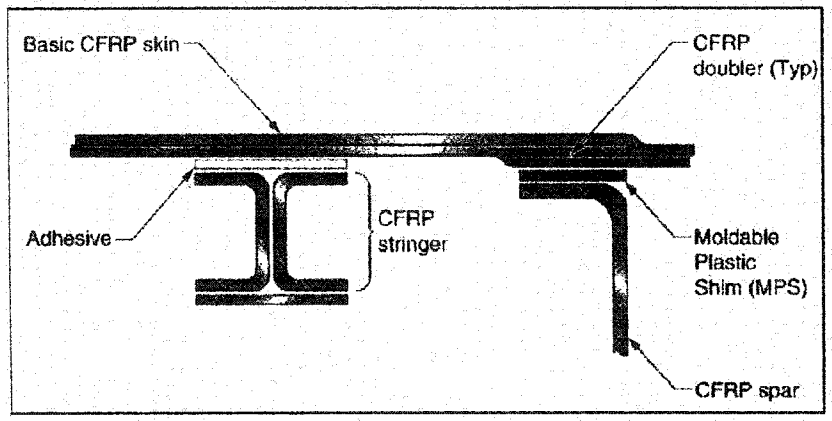

Cost-Effective Composite Structures

- Automated Fabrication Methods where Practical
- Automated Assembly Methods where Practical
- Process Controls to Minimize Manufacturing Discrepancies
- Integrated Product Design Teams
- Design for Damage Resistance, Maintainability, Repairability - Customer/Operator Needs

BUSINESS JETS

Vantage Single-Engine Jet VisionAire

- Lower Cost ($1.65M vs $2-3M)
- Lower Operating Costs (60% of Similar Type Jets)
- Composite Airframe + Single Engine

NON - AEROSPACE APPLICATIONS

- **Corvette - Door, hood, and roof panels, floor pan**
- **Many GM Vehicles - Bumper beams**
- **Paradigm - All composite (thermoplastic) for introduction in China.**
- **CCV - All composite - 4 piece auto body (for introduction to third world countries)**
- **Bridges - Seismic retrofit, replacement of bridges**
- **GM Trucks - Drive shafts**
- **Natural Gas Vehicles - Fuel storage tanks**
- **Sporting Goods - Golf shafts, skis, snowboards**
- **Boats - Hulls and support structures**

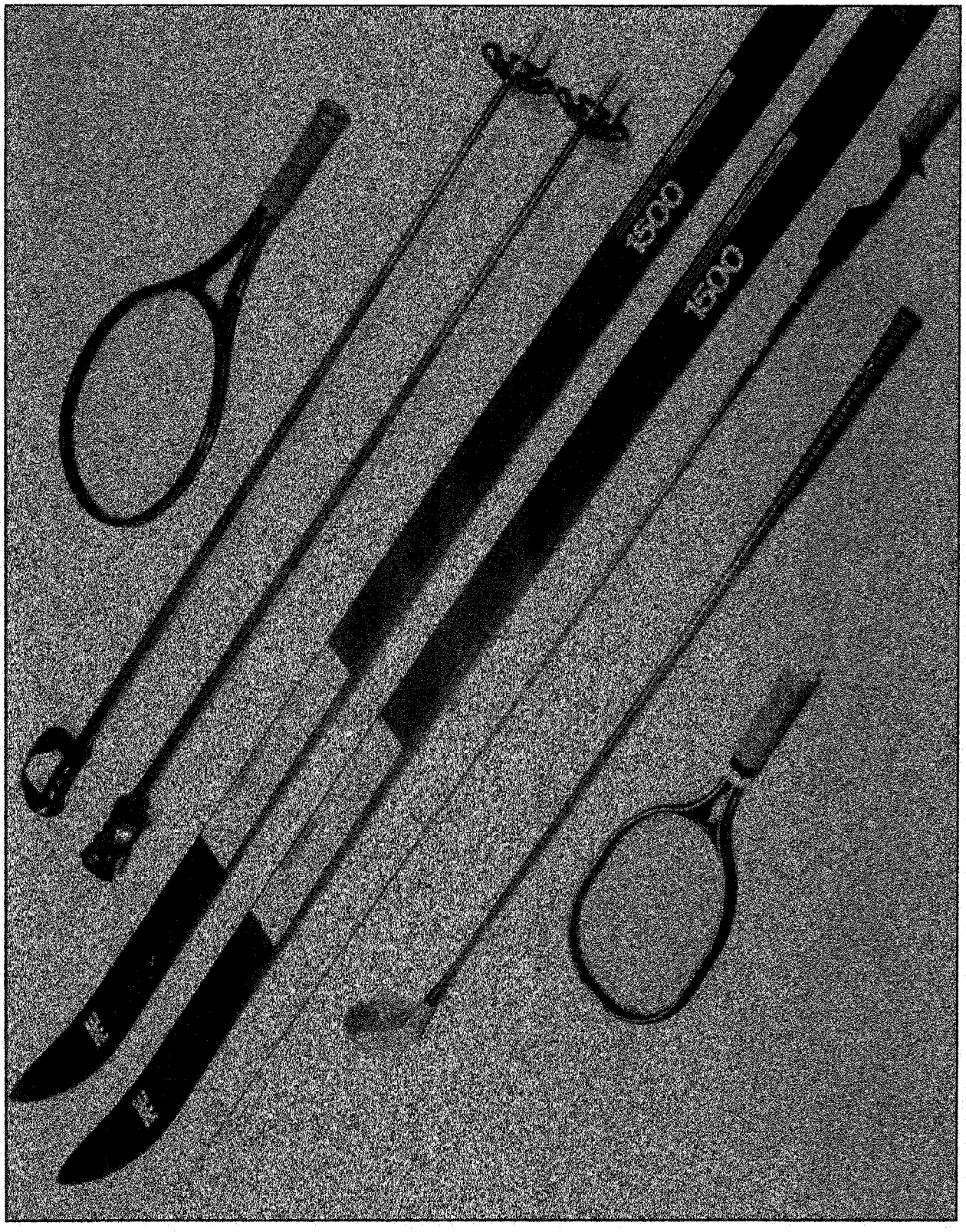

INFRASTRUCTURE

- **Value of U.S. Infrastructure (Roads, Bridges, Highways, Pipelines, Rail Lines, etc.) est. $2.4 Trillion (USDOT)**
- **~39% (225,826) of US Bridges Structural Deficient or Obsolete (1992 FHWA Data)**
  - $91B Backlog in Bridge Construction
  - est $78B Over Next 20 Years Budgeted for Major Infrastructure Rehabilitation (Government)
- **Average Lifespan of U. S. Steel Rail Cars is 25 Years; Average Age is 23 Years**

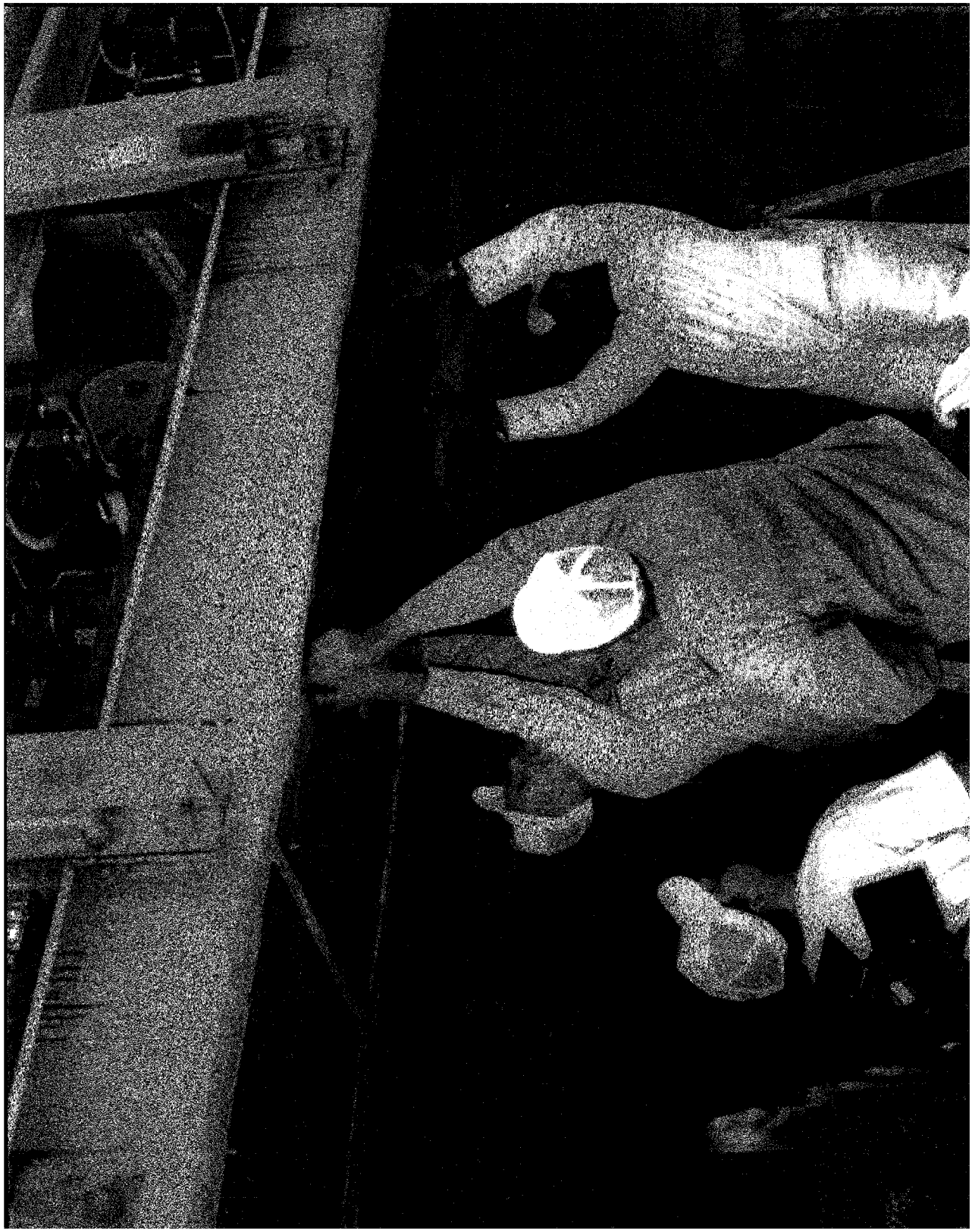

THE CHALLENGE

MILITARY VS COMMERCIAL

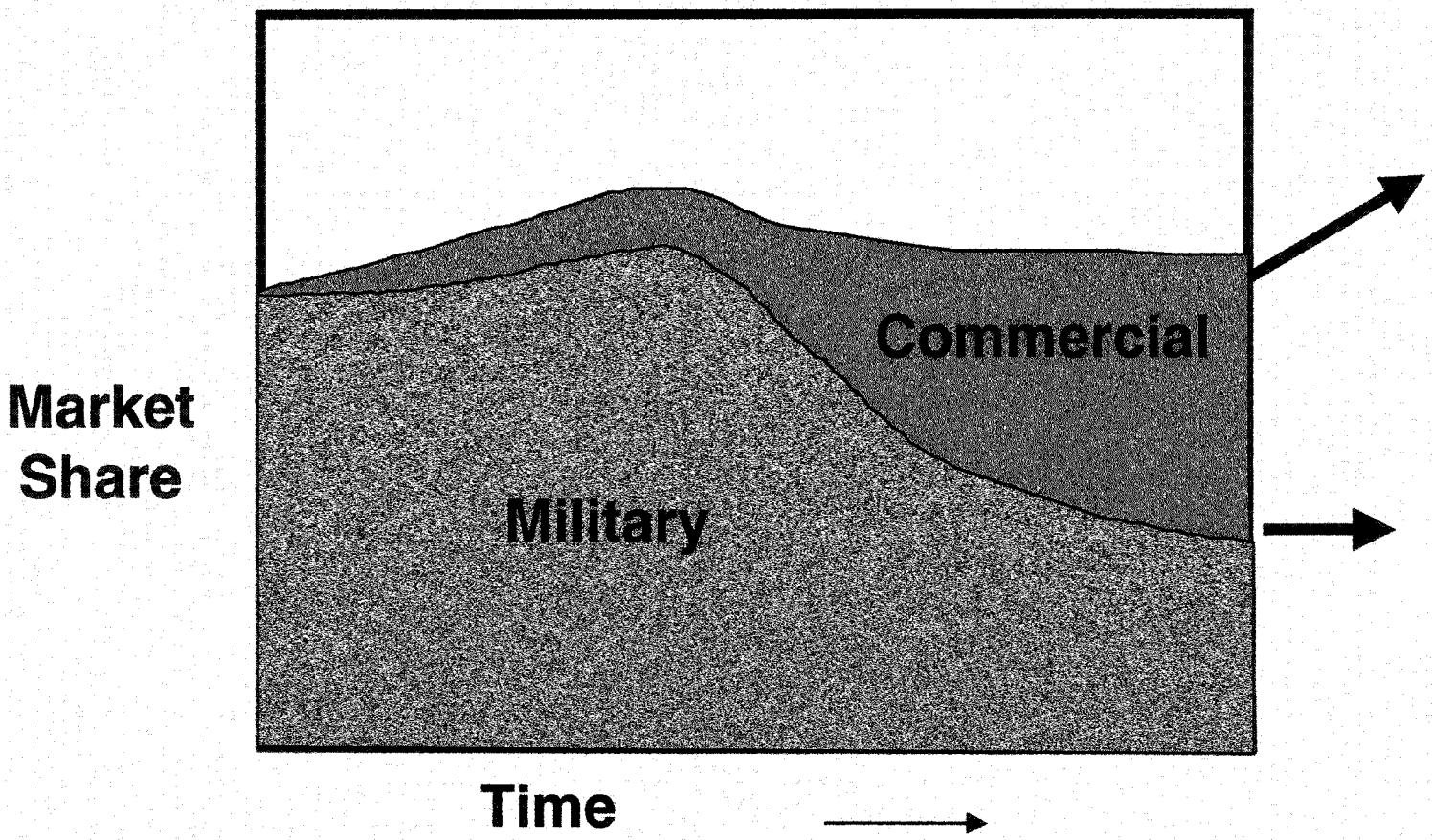

CARBON FIBER MARKET HISTORY

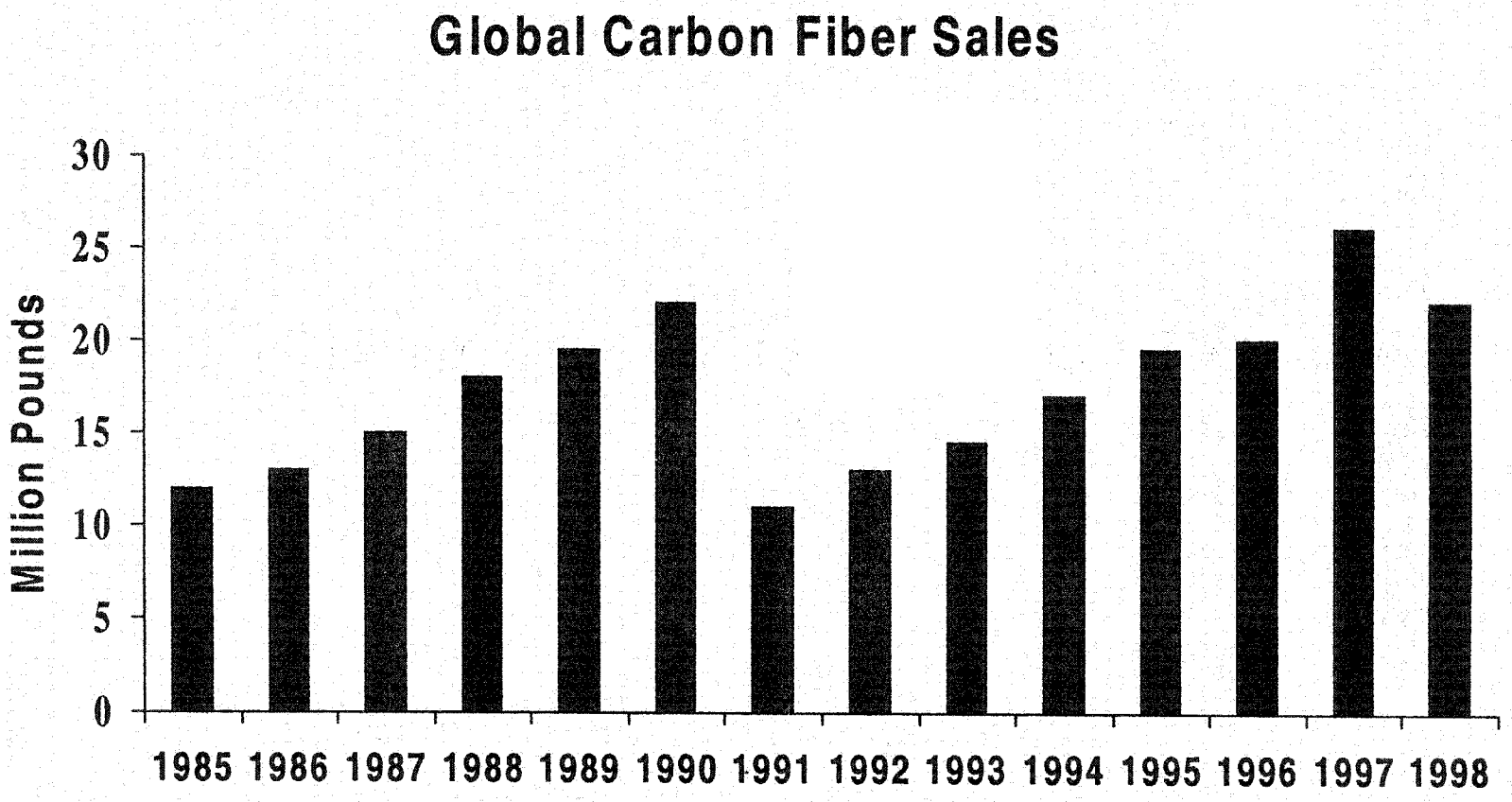

W.H. Werst, Jr., "Advanced Composites in the 90's (and 80's)
Carbon Fibers '99, November 1999, Intertech

Why Composites for Cars?

Glass Fiber Composites can reduce weight by 20 -30%

- Data Bases
- Design Methodologies
- Processing Technologies
- Material Crash Models
- Rapid Cure Technologies
- Joining Methods
- NDT
- Recycling

Carbon Fiber Composites can reduce weight by 40-60%

- All of the above
- Fiber Cost

Weight Reduction = Fuel Economy & Emission Reductions

COMPOSITE MATERIALS RESEARCH
What we are Doing --- Carbon Fiber Composites

Vehicle Systems

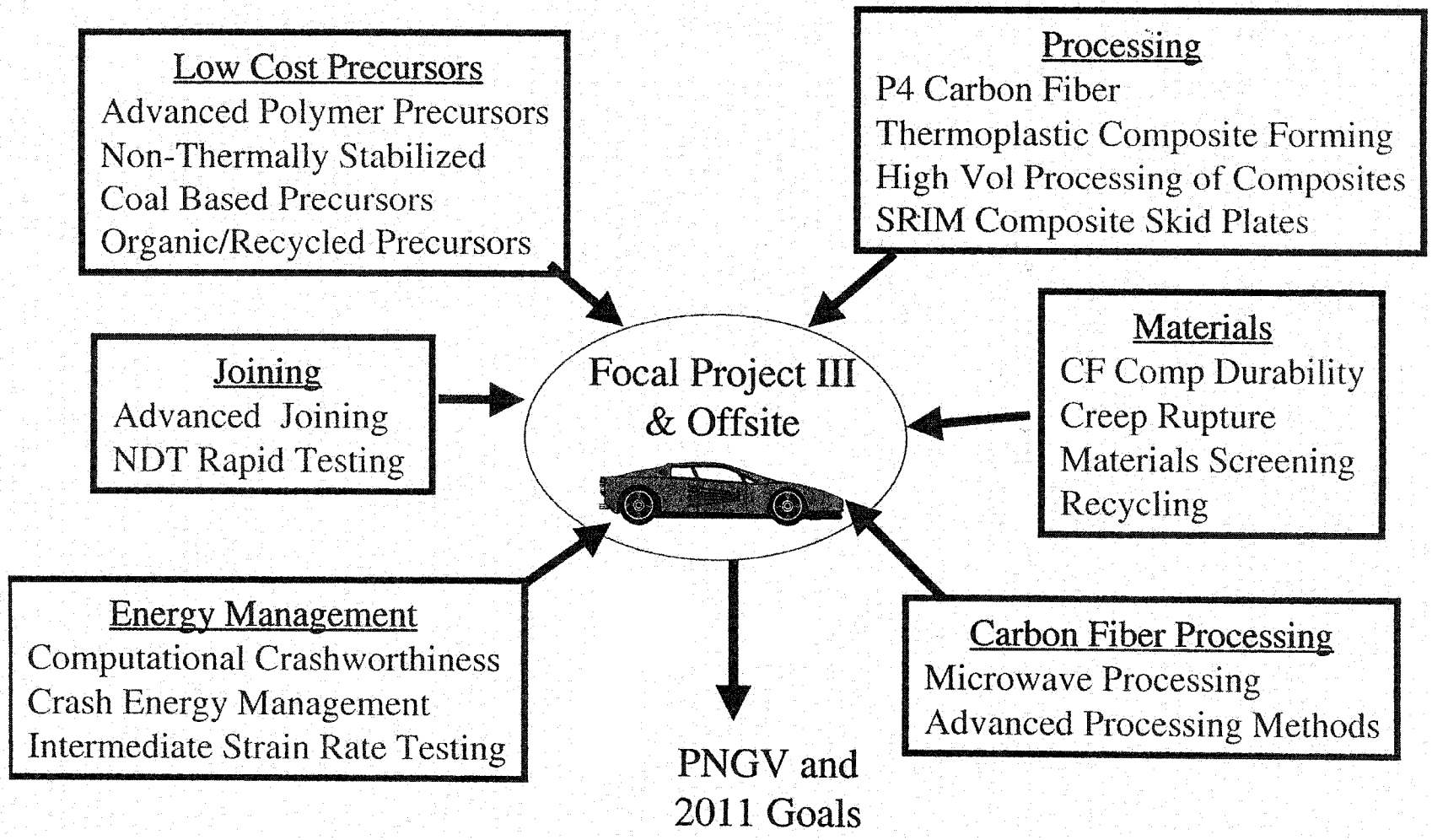

Focal Project 3
Composite Intensive Body-In-White

- Initiate body-in-white concept developed
- Potential processes identified
- CAD/Analysis firm identified to begin math model development

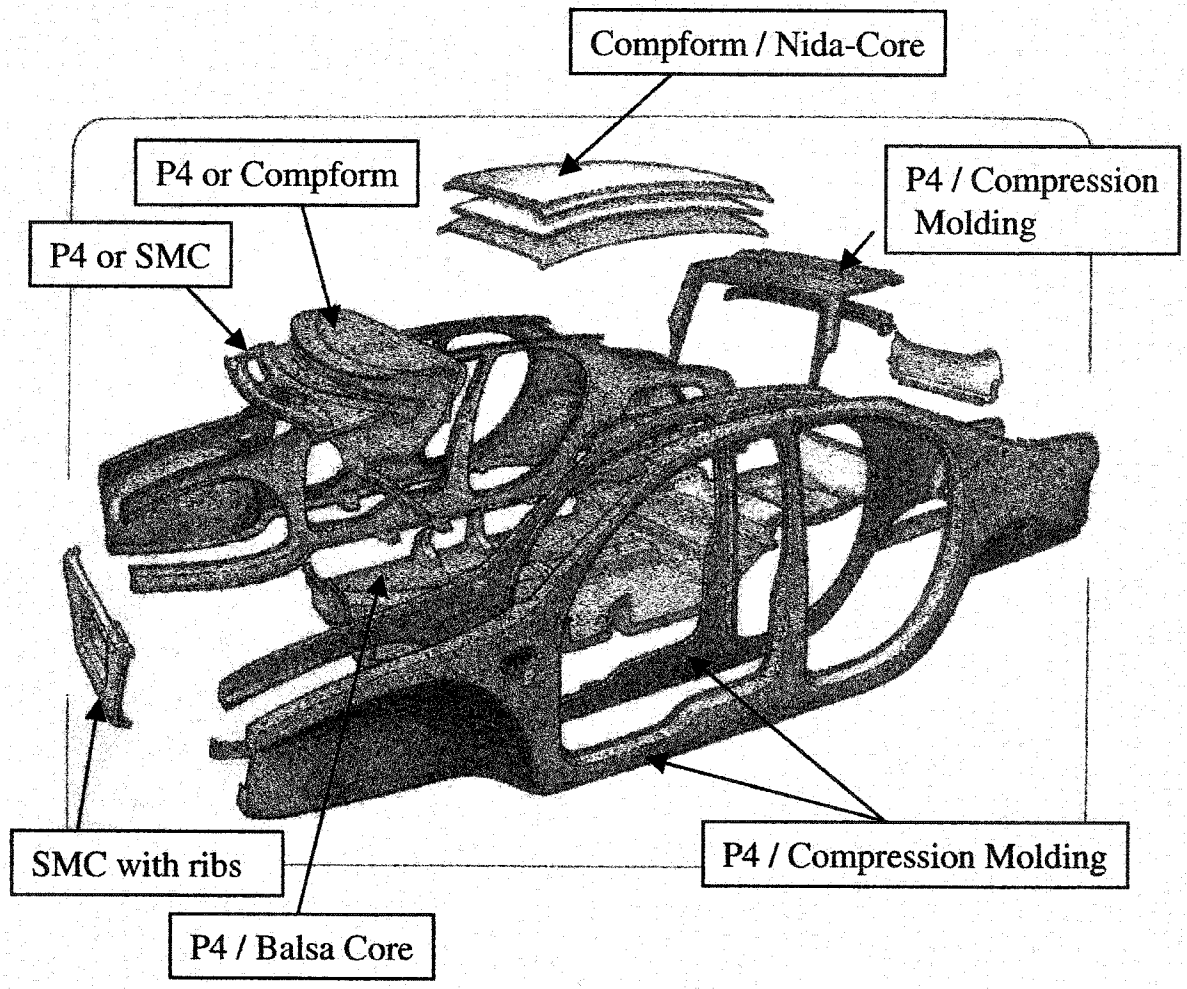

ACC Focal Project III

Phase 1 Results:

- 67% mass savings over baseline
- Bending stiffness exceeded 20%
- Torsional stiffness exceeded 140%
- Durability and abuse load cases satisfied
- Manufacturing strategy developed

Materials / Mass Distribution:

- Chopped carbon - 5.8 kg
- Carbon fabric - 17.7 kg
- Core - 3.2 kg
- Adhesive - 1.6 kg
- Inserts - 8.8 kg

CARBON FIBER

#1 Priority

$3 - $5 Per Pound

THE MARKET

North American Vehicle Production

> 18M / year

10 pounds of Carbon Fiber per Vehicle:

180M lb/year

Nearly 4X Current Worldwide Capacity

THE MARKET

Potential Use of Carbon Fiber in a Typical Vehicle

Structural Steel Material	1997 Weight (Kg)	Potential Weight Savings (Kg)	Final Total Weight (Kg)	Carbon Fiber 40 wt% (Kg)	Carbon Fiber 40 wt% (lbs)
Regular steel sheet, tube, bar, and rod	641.4	404.5	236.9	94.8	208.5
High & medium strength steel	134.3	68.2	66.1	26.4	58.2
TOTAL	775.7	472.7	303.0	121.2	266.7

266.7 pounds per vehicle

4,800,000,000 pounds per year

Nearly 100X Current World Capacity

This is Just North American Vehicles

Carbon Fiber Production

Thermal reduction of a limited number precursors by pyrolysis of all but the carbon followed by heat treatment of the carbon to obtain desired structure.

Are these the only materials and the only way?

Historically: No cost driver for lower cost.
Only better Performance.

Historical Background

Rayon

1950's - Rayon to C process developed
Ablative composites - 40 KSI
1959 - Union Carbide - 50 -130 KSI carbon cloths

Space Race

1967 - Stiffness improvement E = 6 Msi
1968 - Process Stressing included - Thornel 25
E = 25 Msi
1970 - Process optimized - Thornel 75
E = 75 Msi

Historical Background

Polyacrylonitrile (PAN) - Consumer and Aerospace

1960 - PAN use patented
1961 - Modulus increase developed E = 25 Msi
1966 - Inclusion of tensioning E = 70 Msi

Current - Improvements in technology
but no major changes
E = 32 - 75 Msi
Max Stress = 550 to 750 KSI

Historical Background

Pitch - Aerospace

1965 - Melt spinning of Petroleum By Product
E = 10 Msi

1973 - First patents using mesophase pitch

Current - Little change in process.

E = 55 - 120 Msi
Max Stress = 200 - 550 Ksi

Carbon Fiber from PAN
Step 1: Pan Preparation

PAN:

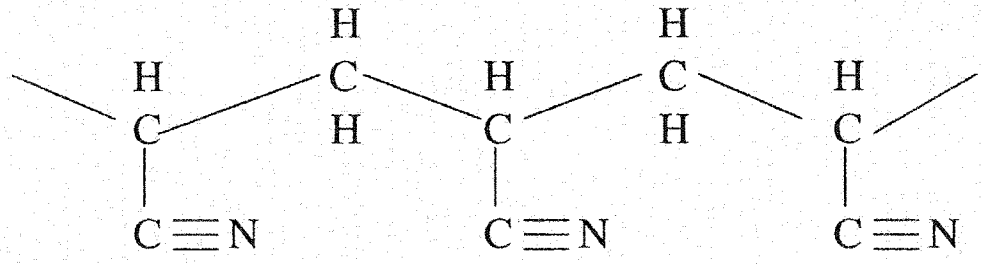

Process:

Polymer Solution
Spun into coagulating bath
Washed
Stretched
Dried

Stretching:

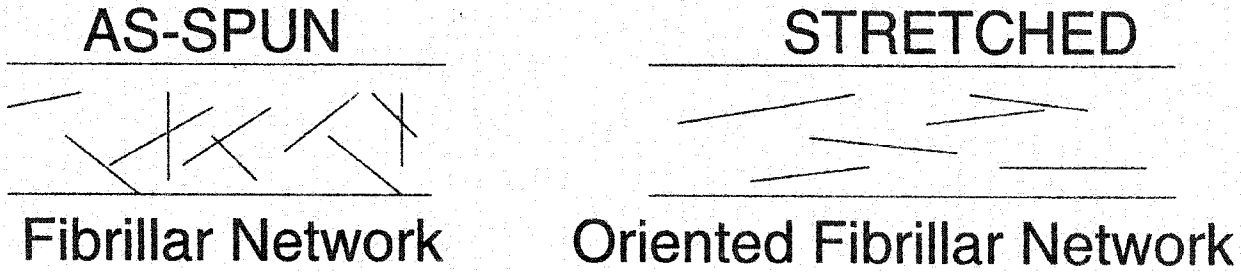

Carbon Fiber from PAN
Step 2: Pan Stabilization

PAN fiber is stabilized to prevent polymer relaxation or softening (loss of preferred orientation) and chain reactions during subsequent elevated temperature processing steps

PAN Tg = 120 C	vs	Carbonization = >1000C

Heat to 200 - 220C

Oxidizing Atmosphere

Carbon Fiber from PAN
Step 3: Pan Carbonization

Pan Fiber is pyrolyzed to C fiber

Process:

Inert Atmosphere
1000 - 1500 C
Stress

Key Features:

Most non-carbon elements are driven from fiber
55-60% of original weight lost
Carbon yield from PAN 40-45% (Rayon 10-30%)
Pan Density - 1.2 g/cc CF density = 1.8 g/cc
C fiber diameter = 60% of PAN diameter
C content = 80-95%
C/Gr fibrils with "turbostratic graphite" structure.

Carbon Fiber from PAN
Step 4: Pan Graphitization

Produces graphite fiber with higher C yield and more graphitic microstructure than carbonization step (similar to heat treatment)

Inert Atmosphere
Stress
2000 - 3000 C

Key Features

C content > 99%
Density - 2.1 g/cc
More graphitic structure
Diameter = 7 to 10 microns

Carbon Fiber - Production

Carbon Fiber Production

Historically: Thermal reduction of a precursor by pyrolysis of all but the carbon followed by heat treatment of the carbon to obtain desired structure.

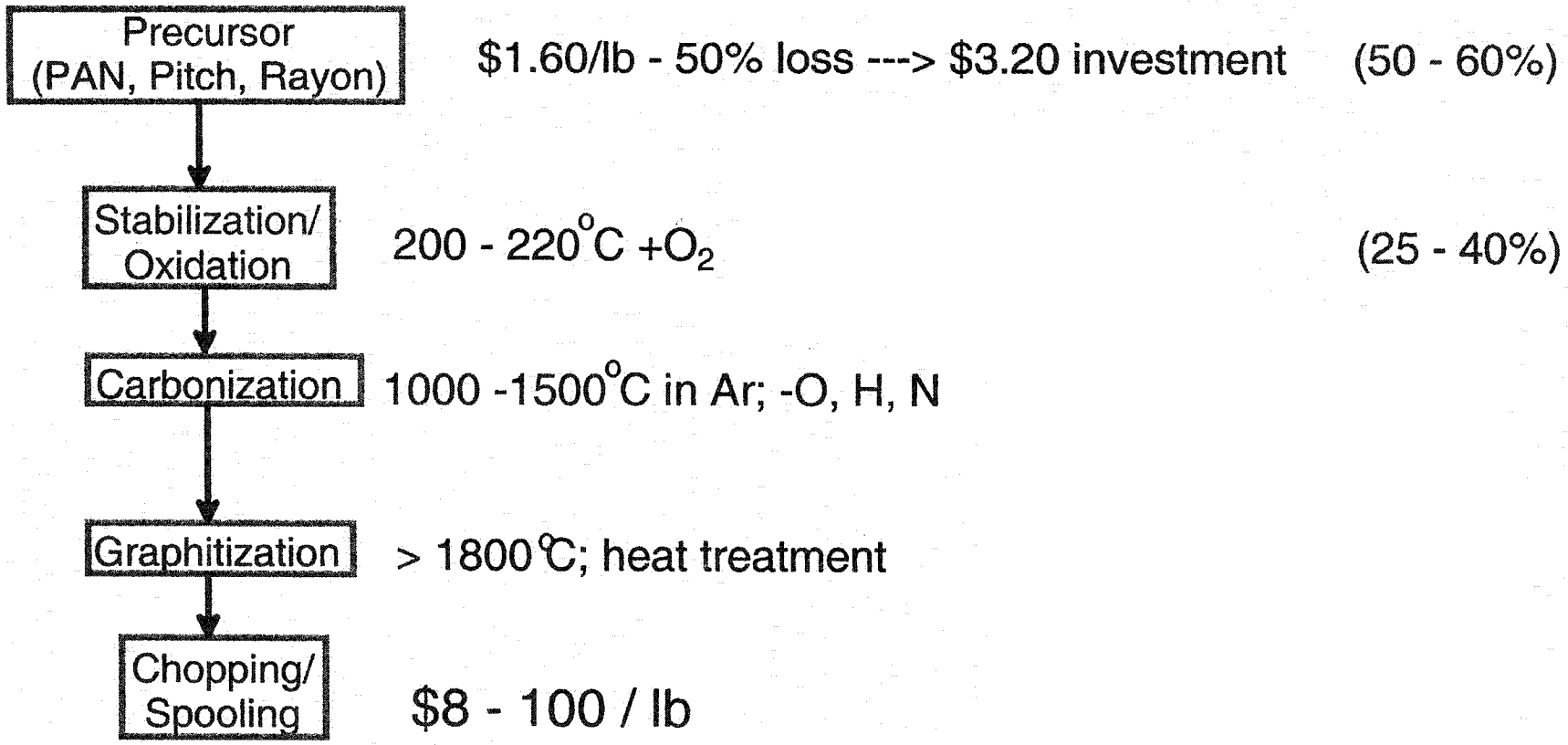

Carbon Fiber Price

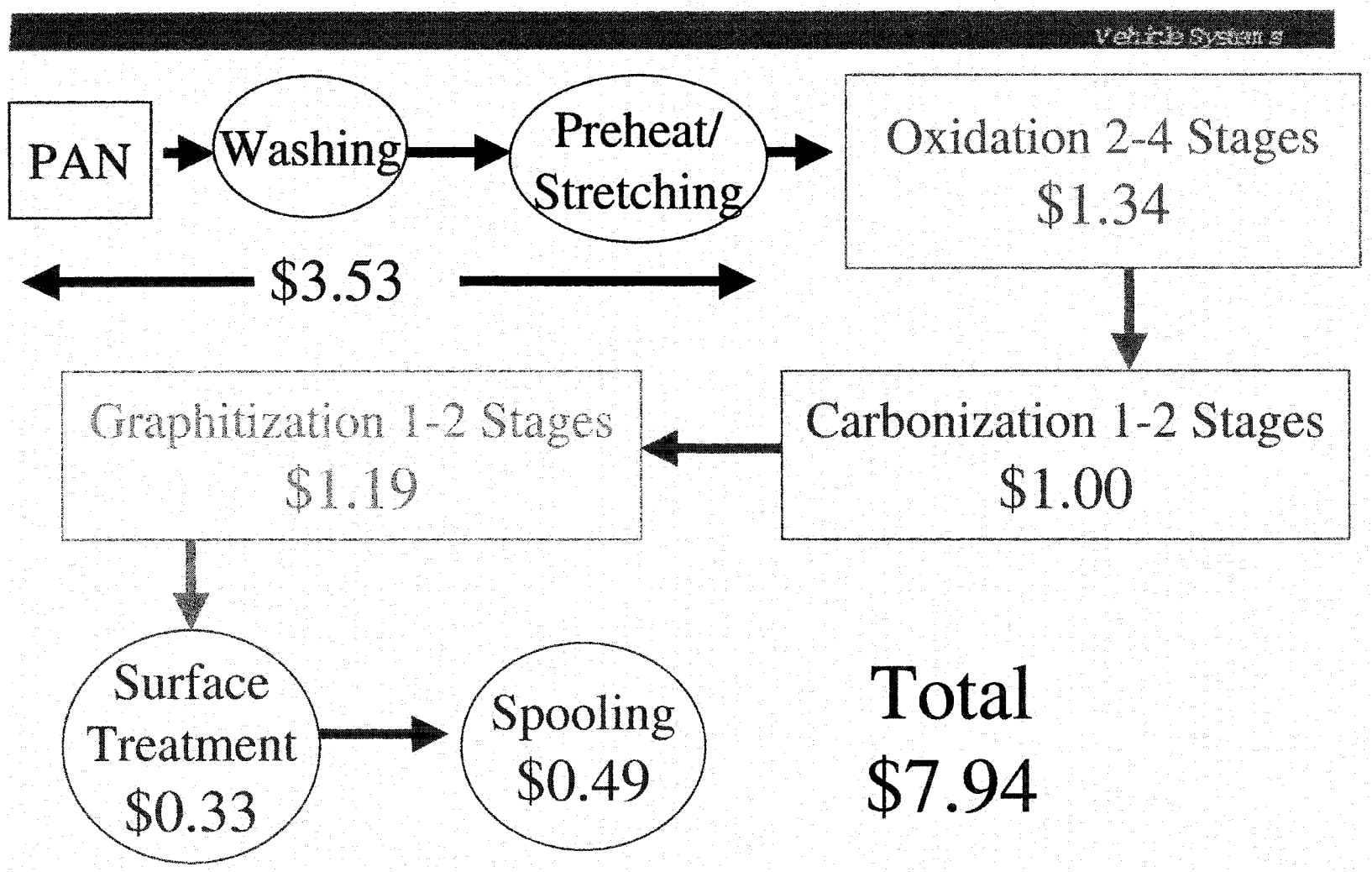

Microwave & RF Processing of Carbon Fibers

Single Tow Continuous

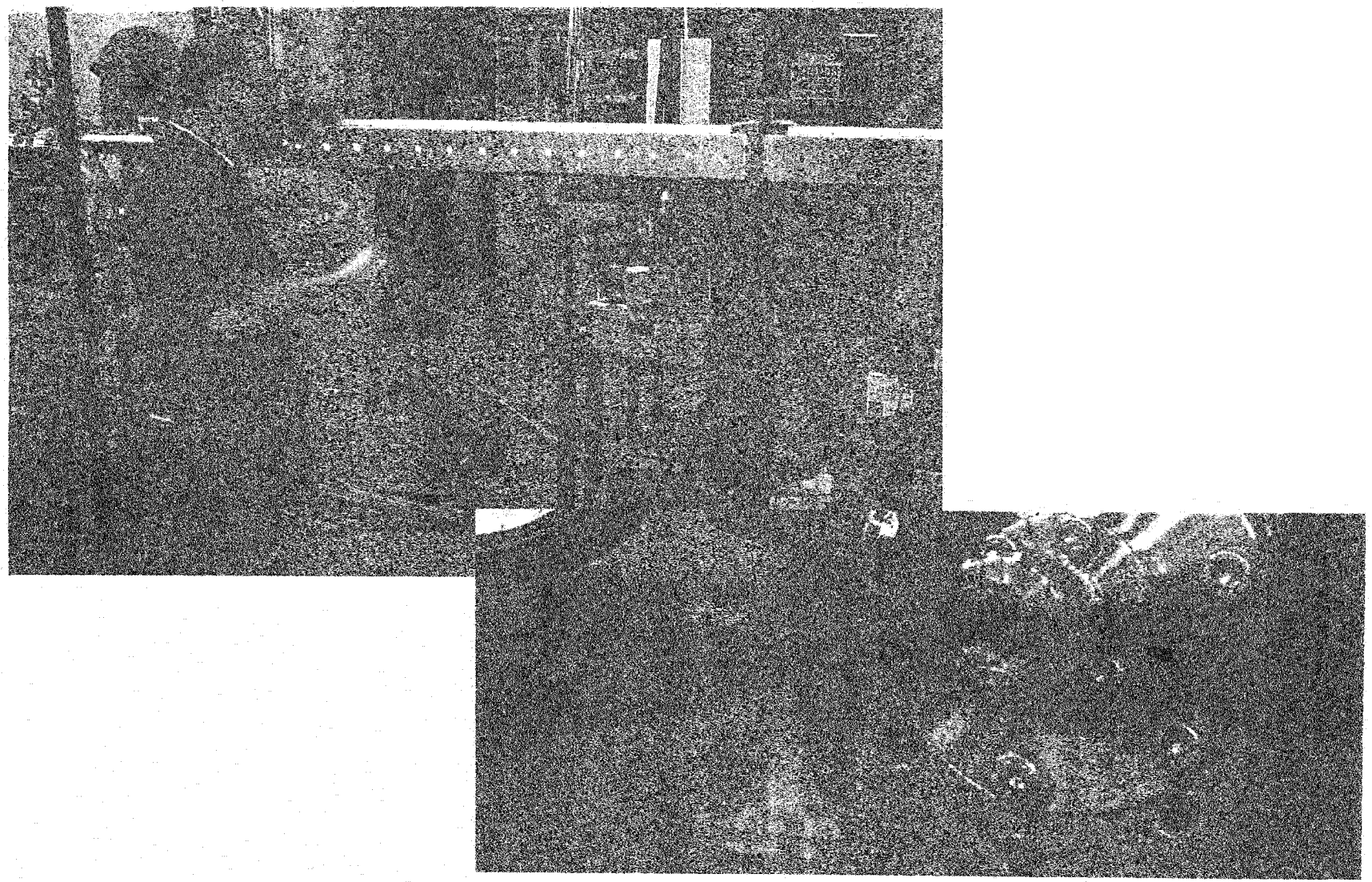

Microwave Assisted Manufacturing of Carbon Fibers

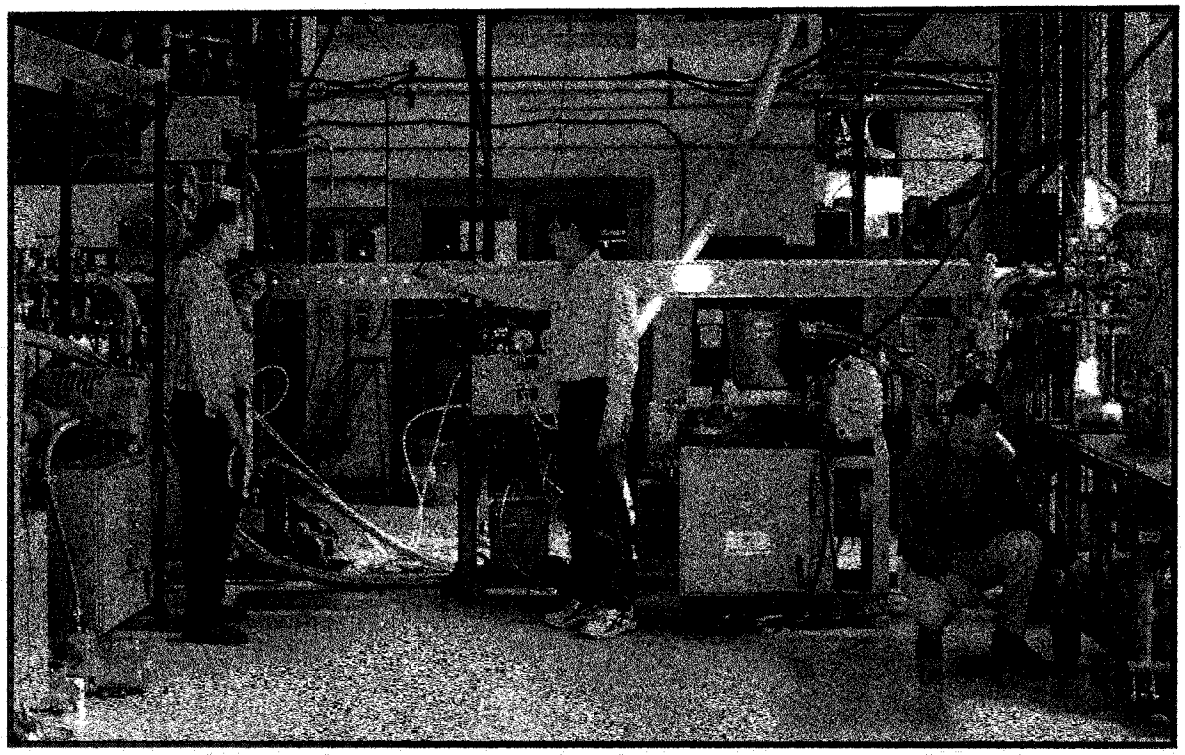

ORNL researchers monitor the output temperature of carbon fiber produced by the ORNL Microwave-Assisted Plasma (MAP) Carbon Fiber Manufacturing Process.

Washed Hardwood Kraft Lignin
Lignin content (%)
100%
95%
87.5%
75%

Lignin Single Fiber Results

Process for Desalting Developed

Co-monomer mixtures determined, spun and carbonized.

Oxidation and Carbonization scheme developed. (stretching, heating, atmospheric control - sensitivity determined)

Currently long single filament "fat" fibers have been produced.

Goals:	25Msi	>400Ksi	>1% elongation
"Fat Fibers"	26Msi	150Ksi	1.3% elongation

Next: Equipment modification for twin screw extruder - Nov
Spinning of 28K Tows - December

Exfoliated Graphitic Nanostructures ("EGN") as Economic Polymeric Fillers

Exfoliated Graphitic Nanostructures Magnification 3,000x. Note aspect ratio exceeds 100:1

Crystalline Graphite Precursor (non-expanded). Magnification 90x

EGN is (1) an exfoliated (separated) graphitic platelet consisting of multi-aromatic carbon ring nanostructures (50-100 nm thickness), (2) characterized by a 3D structure of highly conductive platelets, and (3) a microparticle that should act as an interrupter for microcrack growth.

Summary Coal-Based Precursor

1. Developed EGN (Exfoliated Graphite Nanostructure) particles to use as reinforcement. Micro-particles-Not Carbon Fiber.

2. Could be used as a reinforcing additive while preserving the benefits of injection molding.

3. Particles function different from toughners. Act more like carbides in metals. Can modify conductivity and thermal properties.

4. A good start on micro-particle technology. Surfaces will need modifying.

5. Project terminated since it is not carbon fiber.

Summary Chemistry Project

1. Used MA as a comonomer - Achieved melt spinnable fiber
2. Used itaconic acid to aid stabilization
3. Used a CO_2 plasticizer to aid stabilization
4. Good initial work in UV stabilization - Widely applicable
5. Cost of melt spun not advantageous over commodity grade.

Redirection

Itaconic acid, CO_2 plasticization and UV pretreatment will make commodity PAN processable.

Summary Commodity PAN

1. Limited success with non-PAN based materials.

2. Have developed small scale capability for commodity PAN.

3. Chemical solution for stabilizing PAN similar to Chemistry.

4. Radiation stabilization proven but relied on e-beam and gamma.

5. Refinement of stabilization scheme and pretreatment necessary for completion.

<u>Redirection</u>

All non-commodity PAN work stopped. Chemistry will work with them to develop pretreatment and stabilization scheme.

Future Directions

Current research focusses on precursor and carbonization.

Oxidation/Stabilization is the most capital equipment intensive and rate limiting step of the process.

Concentrated effort needs to begin in oxidation/stabilization
- Cold Plasma oxidation
- Radiation Stabilization (UV, E-beam)
- Post spinning chemical modification for the above.

Additional work may be needed to integrate all technologies into one to achieve optimization

SMART MATERIAL ACTUATORS

Charlie E. Woodall
Student

Won J. Yi*

Walter Golembiewski

and

Kyo D. Song

Department of Technology
Center for Material Research
Norfolk State University
700 Park Avenue
Norfolk, Virginia 23504

Telephone: 757-823-8105
e-mail ksong@nsu.edu
brickcha@hotmail.com

*ICASE
NASA Langley Research Center

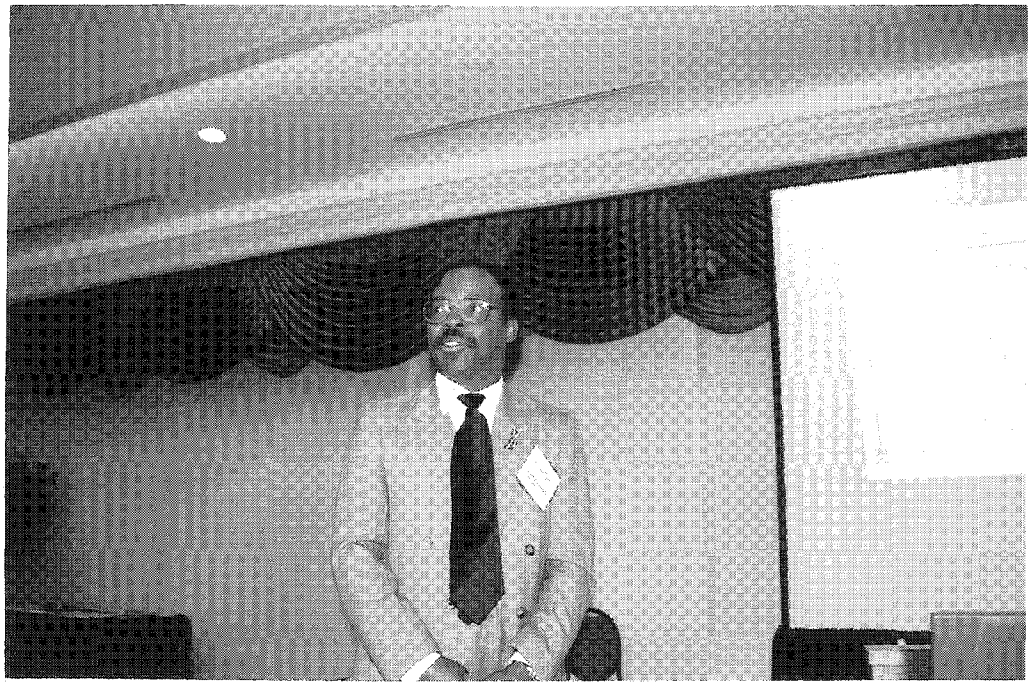

Charlie Woodall

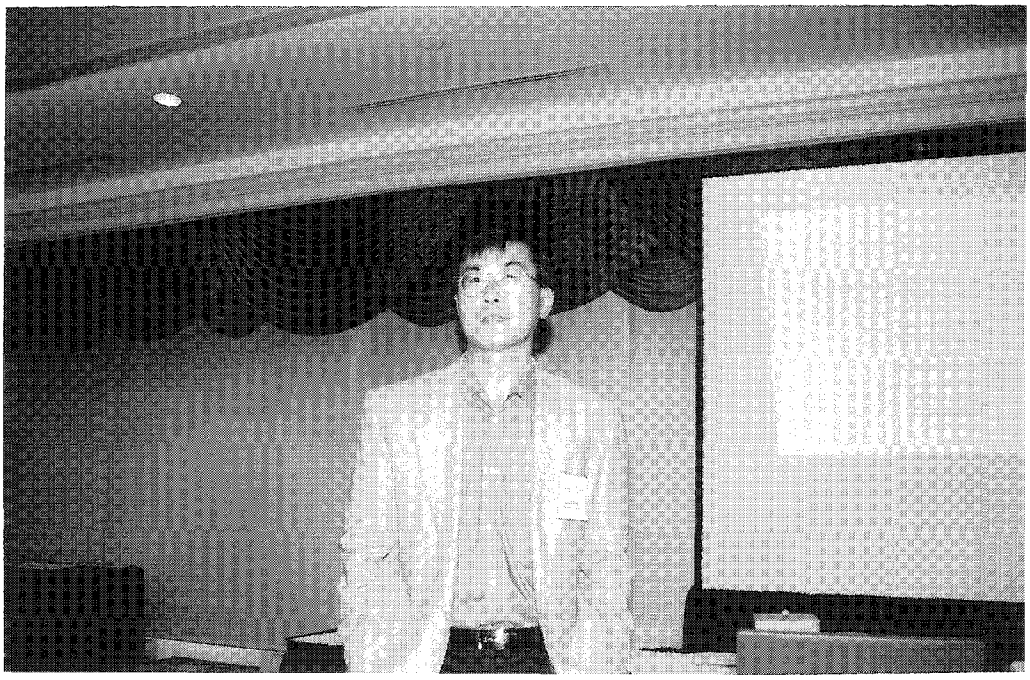

Kyo D. Song

Smart Material Actuators

National Educators' Workshop
October 14 - 17, 2001
at National Institute of Standards and Technology

Charlie E. Woodall, Won J. Yi*, Walter Golembiewski and Kyo D. Song

Department of Technology, Center for Material Research, Norfolk State University
*ICASE, NASA Langley Research Center

Key Words: Piezoelectric, Unimorph, Smart Materials, THUNDER and Actuators

Prerequisite Knowledge: Basic knowledge of electronics, electromagnetic wave propagation, smart materials, rectenna operations

Objective: To provide the proof of concept that smart materials can be actuated by microwave power.

Equipment and Materials:
1. Anechoic chamber
2. Narda X band horn antenna model 601A (8.2 - 12.4GHz)
3. JPL 6 x 6 rectenna array
4. Hewlett Packard 8684B signal generator (5.4 - 12.5GHz)
5. Logi Metric Amplifier
6. Adjustable recycle time delay relay (HDFA Series by Amperite)
7. Hameg Instruments Oscilloscope (HM1507 150MHz 200Ms/s Analog/Digital)
8. Tekronix DMM916 (Analog/Digital Multimeter)
9. Resistors (1.5 ohm, 2.7 ohm, 3.9 ohm, 5.6 ohm, 1.2k ohm, 3.5k ohm, and 270k ohm)
10. THUNDER (Thin Layer Composite Unimorph Ferroelectric Driver and Sensor)
11. Coaxial cables and wiring fixtures

Introduction:

An experimental study of a smart materials actuator driven by microwaves is presented in this paper. A proof of concept experiment using THUNDER (Thin Layer Composite Unimorph Ferroelectric Driver and Sensor) Materials has been set up and demonstrated using microwaves. The smart material actuator system driven by microwaves may have applications, such as the Next Generation Space Telescope (NGST) with fragmented optics control.

Procedure:

A feasibility experiment was set up and demonstrated using a microwave source to provide the power needed to actuate the smart materials, as shown in Fig. 1.

A combination of signal generator and amplifier provided 20 W of microwave power to a Narda horn antenna at a frequency setting of 8.5GHz. The 20 W microwave power irradiated a JPL (Jet Propulsion Laboratory) 6 x 6 rectenna array. The rectenna, which is a rectifier and an antenna, converts the microwave power into DC power. The horn antenna, the 6 x 6 rectenna array, and the required wiring fixtures were inside an anechoic chamber as shown in Fig. 2(a) and 2(b). All other items listed in the equipment and material section were externally connected to the horn antenna and the rectenna via a backplate at the rear of the chamber. The Narda horn antenna is connected to the amplifier by a coaxial cable, and the signal generator is connected to the amplifier by a separate coaxial cable. The 6 x 6 rectenna array is connected to the exterior of the anechoic chamber by means of a dual output BNC connector. The distance between the horn antenna and the 6 x 6 rectenna array was 65 cm.

Comments:

In this experiment, the Narda horn antenna's 20 W microwave power was converted into a measured 192 V DC by a digital multimeter. The estimated current being produced from the 6 x 6 rectenna array was 0.38mA. This was computed using various measured resistor values and the measured voltage across each resistor. The DC voltage output of the 6 x 6 rectenna array was connected to the resistors in separate operations, and the current through each of the resistors was calculated.

A schematic diagram of the experimental setup is shown in Fig. 3. The positive terminal of the rectenna was connected to the normally open connection of the recycle timer, and the negative terminal was connected to the common/ground connection as shown in Fig.4. A R-C circuit was constructed using a THUNDER and a 27K ohm resistor. One of the two terminal connections of the R-C circuit was connected to the recycle timer's normally open connection, and the other was connected to the common/ground. The recycle timer setting was set at .5 seconds, which was the recycle timer's fastest setting possible. The Amperite recycle timer had a range of settings from 0.5 seconds to 24 hours. This time setting was verified with a Hameg Instruments Oscilloscope. The measured capacitance of THUNDER was 260nF.

When the recycle timer switch was closed, the path of least resistance for the R-C circuit was via the THUNDER, thus charging the circuit. When the recycle timer switch changed to the open position, the connection between the rectenna and the THUNDER was broken. The voltage polarity at this point was reversed. The THUNDER and the resistor circuit performed in the same manner as a capacitor and a resistor in a R-C circuit when a voltage was applied or removed.

This on/off switching of the recycle timer created a pulse to demonstrate that the THUNDER device could be actuated by a microwave power. This pulse was captured in a pictorial. The pulse rise and decay times were measured as 0.5 and 0.3 sec, respectively.

THUNDER is a ferroelectric device made of multiple layers of materials, typically stainless steel, aluminum and PZT (Lead Zirconate Titanate) piezoceramic. These layers of materials are sandwiched together with an adhesive bond. A piezoceramic material is composed of randomly oriented crystals or grains. By applying electrodes to the ceramic and a strong DC electric field, the dipoles are aligned in the direction of the electric field. By aligning in this manner, the smart material will have a permanent residual polarization. The result of this polarization is a change in the geometric dimension. Through the piezoelectric effect, THUNDER has the capability to expand or contract, based on the polarity of the voltage applied. When the applied voltage is positive, THUNDER will flatten, and if the applied voltage were negative, the THUNDER arches.

References:

1. T.K.Wu, "Multiband FSS," in T. K. Wu (Ed.), *Frequency Selective and Grid Array,* John and Wiley & sons, New York, 1995.
2. W. Schneider, J. Moore, T. Blankney, D. Smith, and J. Vacchione, "An Ultra-Lightweight High Gain Spacecraft Antenna," *IEEE Antennas Progagat. Int. Symp.*, Seattle, WA, June, pp. 886-889, 1994.
3. T. H. Lee, R. C. Rudduck, T. K. Wu, and C. Chandler, "Structure Scattering Analysis for Sea Winds Scatterometer Reflector Antenna Using Extended Aperture Integration and GTD," *IEEE Anetnnas Propagat. Int. Symp.*, pp. 890-893, Seattle WA, June 1994.
4. W. C. Brown, et al., *US Patent 3 434678*, Mar. 25, 1969.
5. W. C. Brown, "Experiments involving a microwave beam to power and position a helicopter," *IEEE Trans. Aerosp. Electron. Syst.*, Vol AES-5, No. 5, pp. 693-702, 1969.
6. W. C. Brown, "Solar Power Satellite Program Rev. DOE/NASA Satellite Power System Concept Develop. Evaluation Program," *Final Proc. Conf.*800491, 1980.
7. J. Schlesak, A. Alden and T. Ohno, "A microwave powered high altitude platform," IEEE MTT-S Int. Microwave Symp. Dig., pp. 283-286 1988.
8. W. C. Brown, "Design study for a ground microwave power transmission system for used with a high-altitude powered platform," *NASA Final Contractor report 168*344, Raytheon Rpt. PT-6052, 1983.
9. NASA JPL, "Patch Rectenna for Converting Microwave to DC Power," *NASA Tech Briefs,* Vol. 21, January, p. 40, 1997.
10. Brown, W. C., Draft of Paper Prepared for Presentation at the 8th Biennial SSI/Princeton Conference on Space Manufacturing, May 6-9, 1987.

Biography:

Dr. Kyo D. Song is a P.I. of Faculty Awards Research (FAR) funded by NASA starting March 5, 1998 to March 4, 2002. He has been involved in many research projects, such as: Hypersonic Flow Research, Testing high temperature materials for Scram-jet Engine Components, Study on effects of atomic oxygen on space materials,

and Smart materials research for Next Generation Space Telescope (NGST) under NASA supported grants. Mr. Charlie Woodall is a senior student in Computer Technology at Norfolk State University. He is a retired Navy engineer who had been working 23 years on communication system. Dr. Won Yi is working as a research scientist at NASA Langley Research Center. His specialized area is high voltage, pulse power, and lasers. Dr. Golembiewski is an Associate Professor working at Computer Technology. He has considerable experience in the design and testing of circuitry and communications.

Note: * The subject mater is under the invention disclosure (LAR 15754-1) at NASA Langley Research Center.

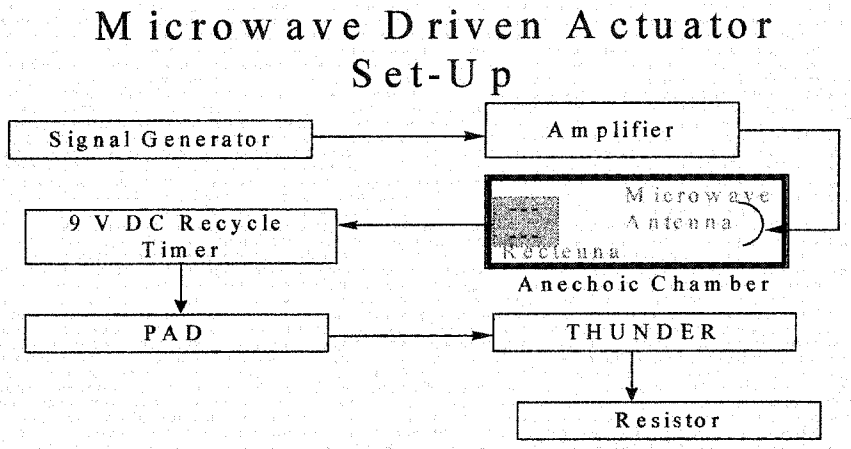

Figure 1: Block diagram

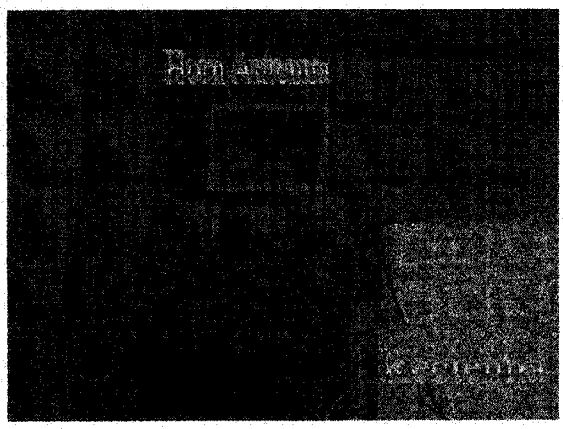

Figure 2(a): Inside the anechoic chamber

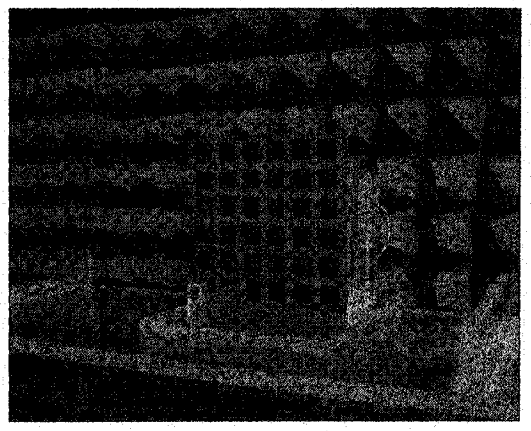

Figure 2(b): The rectenna inside the anechoic chamber

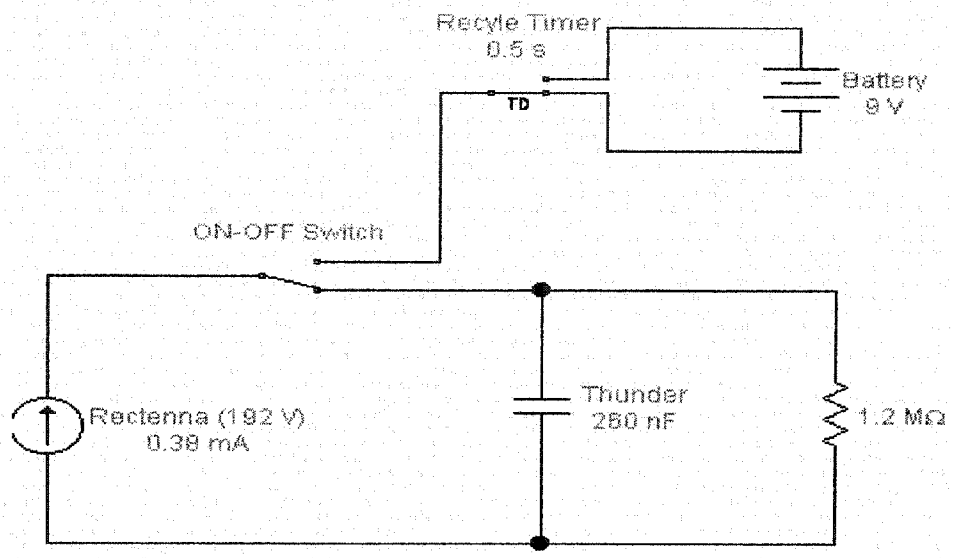

Figure 3: Schematic diagram

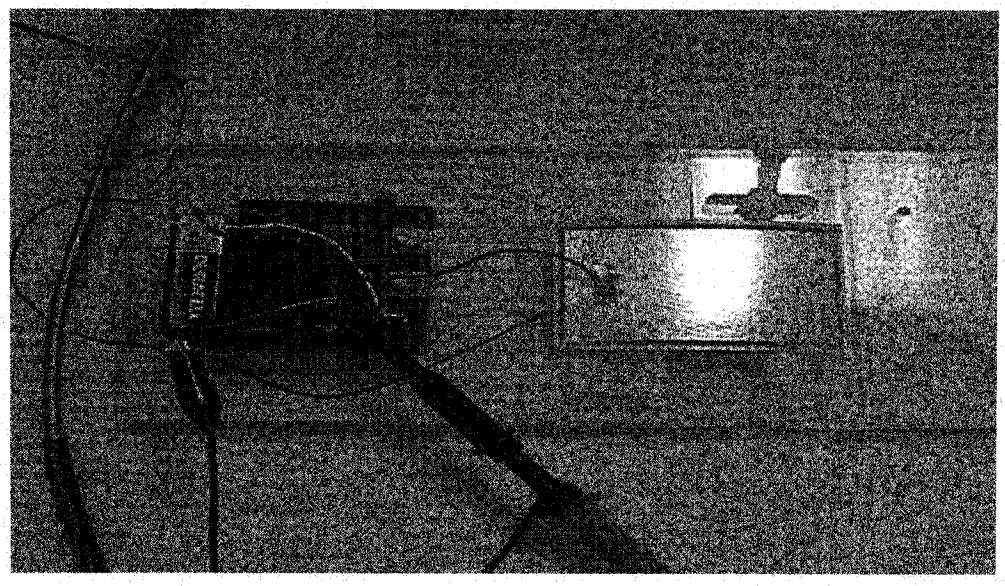

Figure 4: Recycle timer and THUNDER

COLLOIDAL SELF-ASSEMBLY PHENOMENA

O. C. Wilson, Jr.

and

L. J. Martinez-Miranda

Department of Materials and Nuclear Engineering
University of Maryland
College Park, Maryland 20742-2115

Telephone 301-405-0253
e-mail martinez@eng.umd.edu

Biography

Otto C. Wilson, Jr. is an Assistant Professor in the Department of Materials and Nuclear Engineering at the University of Maryland. His undergraduate and graduate education (M.Sc. and Ph.D.) was completed at Rutgers University in Ceramic Science and Engineering. Otto has developed the BONE lab (Biomimetics, Orthopedics, and Nanomaterials Exploration) at UMCP where he and his students are studying ways to improve the synthesis and remodeling response of hard tissue implants. Additional reserach areas include composite research and microwave processing of materials. He enjoys teaching classes in biological materials and biomaterials and is actively involved in K-12 educational outreach.

L. J. Martínez-Miranda is Associate Prof. of Materials in the Dept. of Materials and Nuclear Eng at the University of Maryland – College Park. She received her bachelor's and master's degree in Physics from the Universidad de Puerto Rico in Río Piedras, a bachelor's in Music degree from the Conservatory of Music of Puerto Rico and her doctoral degree in Physics from Massachusetts Institute of Technology. At Maryland she has been responsible for designing the junior level laboratory undergraduate course with the help of her colleagues, and has taught the introductory design course and the physics of materials course. Her interest is in X-ray scattering from liquid crystals and solid films.

Colloidal Self-Assembly Phenomena

O. C. Wilson, Jr. and L. J. Martínez-Miranda
Department of Materials and Nuclear Engineering
University of Maryland
College Park, MD 20742

Key Words: Colloid, self-assembly, silica, hydrous iron oxide, akageneite, chemical precipitation

Prerequisite Knowledge: Basic chemistry and physics of light diffraction

Objective: To observe the influence of self assembly and order on the propagation of light in colloidal cystals

Equipment and Materials: Oven capable of heating up to 100-120 C, chemical glassware (beakers, pipettes), magnetic stirrer and stir bar, high speed centrifuge (minimum speed is 3000 rpm), deionized water, tetraethyl ortho silicate (TEOS), ammonium hydroxide (reagent), ethyl alcohol, FeCl3.9H2O, urea, glass microscope slides.

Introduction:

The discovery of x-rays in the early 1900's by Bragg opened up a whole new world by providing a tool that allowed materials scientists to probe the atomic structure of crystalline materials. By definition, a crystal is a material that exhibits long range atomic order where atoms occupy specific locations on a crystal lattice. The basic building unit of a crystal is the unit cell. The unit cell is the smallest arrangement of atoms that can be translated in three dimensional space to build the crystal lattice. The basic equation that relates the atomic plane spacing (d), the wavelength of the incident radiation (λ), and the angle of diffraction (θ) is known as Bragg's Law and can be expressed as follows:

$$n\lambda = 2d \sin\theta \qquad (1)$$

The geometry of diffraction event for a crystalline material is shown in Figure 1. With state of the art transmission electron microscopes, scientists can now actually see regularly spaced atomic planes in biological and synthetic materials by visualizing features that are on the order of a 0.1-1 nm.

Although we can not directly see a crystal lattice with the unaided eye because the wavelength of x-rays is too short for our eyes to detect, there are optical analoques to diffraction that can be readily observed. The brilliant, iridescent colors of some species of beetles and butterflies result from the diffraction of visible light from regularly spaced structural units that have dimensions on the order of the wavelength of visible light (300-700 nm). Another example of optical diffraction in nature involves the semi-precious gemstone opal. In natural opal, uniformly sized amorphous silica (SiO_2) spheres form

under geological conditions and slowly settle into close packed, ordered arrays. High temperatures in excess of 1000 °C cause the particles to partially sinter and form bonds between particles that give the opal structural integrity. The colors that are observed in opal result from the interplay of light with the regularly spaced planes of monodisperse silica spheres based on equation (1). If the planes are not ordered properly, the light that is diffracted from the opal interacts in a destructive manner and the resulting opal has a white appearance and is sometimes called milk opal. It is possible to make synthetic opals based on the availability of chemical techniques to synthesize submicron silica spheres with uniform (monodisperse) size (Stober et al., 1968). Typical chemicals for this process include tetraethylorthosilicate (TEOS), ethyl alcohol, water and ammonia. The water promotes a hydrolysis based chemical reaction that breaks the bond between the Si atom and the ethyl functional group and allows the Si-O to form various species that can polymerize and form a long chain network that results in the formation of uniform spheres of various sizes from a few nanometers (nm) up to microns in size. Synthetic opals are produced commercially by synthesizing uniform silica spheres in large quantities and allowing the particles to settle into ordered, crystalline arays by slow sedimentation or solvent removal.

The diffraction of light from ordered arrays of non isotropic (rod shaped) particles can also give rise to interesting diffraction phenomena. Akageneite (β-FeOOH) is the the most famous inorganic system in this class of materials. It can be formed by the slow hydrolysis of aqueous solutions of iron (III) chloride ($FeCl_3$, typically 0.03-0.06 M). In order to form particles with a suitable degree of monodispersity, aging times can be as long as a few months to a year. For this system, patience is a virtue and yields a nice reward because the bright, iridescent colors that can be observed for this system are very remarkable. Under the right conditions, the akageneite particles self assemble into ordered two dimensional rafts where all the particles are oriented perpendicular to the plane of the raft as shown in Figure 2. Numerous layers of these rafts can form and the spacing between successive raft layers determines the conditions for color formation. These layers are called Schiller layers.

In recent years, a number of unique applications for colloidal crystals are being investigated as more elegant methods are devised to control the spatial extent and degree of ordering. One of the more far reaching applications for colloidal crystals with a big technological payoff involves the use of self assembled colloidal crystals that can control the propagation of light and other types of electromagnetic radiation. These "photonic crystals" are projected to revolutionize the information age by making it possible to make optical based computer systems.

Procedures:

Synthesis of monodisperse silica spheres

A.) Pour 85 ml of 200 proof ethyl alcohol into a 200 ml beaker. Place the magnetic stir bar in the solution and stir on the magnetic stirrer at a moderate rate.

B.) Add approximately 2 ml of tetraethyorthosilicate (TEOS) to the ethyl alcohol solution. Allow a few minutes for the liquids to completely mix

C.) Carefully measure out 10-15 ml of reagent ammonium hydroxide (12 M) and add to the TEOS/ethyl alcohol solution. ***Caution: Make sure that this is done under a fume head due to the very strong ammonia vapors that will be present.***

D.) Allow the solution to stir for 3-10 hrs. You can have students observe the reaction for the first 10-15 minutes and record the time that it takes for the initially clear solution to turn light blue in color. This time corresponds roughly to the induction time (the time it takes for the nuclei to reach a sufficient size to scatter visible light). The explanation for the bluish color of the solution is related to the phenomena that accounts for the blue color of the sky i.e. scattering of light by very small particles (molecules, colloids). After more time has elapsed, students can observe the solution gradually turn milky white and opaque.

E.) After aging for 3-10 hrs, the silica particles should be washed to remove excess ammonia. This can be accomplished by placing the silica suspension in centrifuge tubes or bottles. Centrifuging the suspensions at 3000-5000 rpm will cause them to settle to the bottom of the tube (or bottle). Carefully pour of the clear supernatant liquid, replace with fresh water, and re-disperse particles by shaking or using an ultrasonic bath or probe. The first wash should be performed using ethyl alcohol, and subsequent washes should be done in water. During centrifugation, you may observe the formation of colored regions in the sediment cake that forms on the bottom of the centrifuge tube. Five to ten centrifuge cycles should be sufficient. After the last wash in water, re-disperse the silica spheres in ethyl alcohol and centrifuge one more time. Pour off the alcohol and re-disperse the silica particles in a minimum amount of ethyl alcohol (approximately 25-50 ml).

F.) Opals can be formed by three methods. In method 1, concentrated suspensions of silica spheres can be allowed to settle into ordered arrays on the bottom of glass sample vials (20 ml). Vivid colors will be seen in the ordered sediment that forms on the bottom of the beaker. Method 2 involves carefully removing the ethyl alcohol by evaporation at room temperature or under moderate heat (60 °C) in an oven. The resulting silica compact may appear white and chalky, but if it is placed in ethyl alcohol or water, it will bubble and display opalescent colors. The bubbles occur because the liquid displaces the air that occupies the pores that exist between adjacent particles. Method 3 is the quickest method. Drops of the concentrated silica suspension in ethyl alcohol can be placed on microscope slides and allowed to dry (within a few minutes). Instruct the students to view the flat "opals" in transmitted light and reflected light in which the slide is perpendicular to the light source and then have the students view the flat opal at an angle to the incident light. Students should be able to see that there are specific angles which cause opalescent colors to appear.

Synthesis of monodisperse akageneite rods

A.) Add 4000 ml of de-ionized water to a gallon sized container. Weigh 54 grams (0.2 mol) of $FeCl_3 \cdot 6H_2O$ and add this to the water. Allow to dissolve and place in a quiet location for a few months. The solution will turn from the initial brown color to a

more darker brown, turbid suspensions as the akageneite particles nucleate and grow. Alternate method: Urea and heat can be used to make akageneite rods that are not as uniform in size but still display irridescent phenomena if a shorter experiment is required. Add 30 g of urea to 100 ml of deionized water and then add 5.4 grams of $FeCl_3 \cdot 6H_2O$. Use a magnetic stirrer to stir the solution on a hotplate at 90-95 oC for 3-5 hrs. The initial pH of the solution will be 2-3, but the urea hydrolyzes and produces carbonate and hydroxide ions that raise the pH of the solution to a final value of 6-7.

B.) The particles should be washed by centrifugation using water. Higher speed may be required (10,000-15,000 rpm). After cleaning the particles, they should be re-dispersed in a minimum volume of water (50-100 ml) and allowed to settle. It may be easier to observe the formation of Schiller layers by putting some of the suspension into a 20-40 ml sample bottle and tilting it on an angle and allowing the suspension to sediment undisturbed for a few day. Iridescent colors will be visible in the sediment layer.

Student excercises:

Calculation for estimating particle spacing using Braggs law

A.) Using the flat opal, have students measure the angle that corresponds to opalescent color formation. This could be done using a protractor. Note the color or colors that can be seen for a particular angle. Find the wavelength of light that corresponds to the particular colors that are observed. This value (in nm) will be used for l in equation 1. The angle q represents the angle at which the colors were observed. Setting n=1 for this example, students can calculate the spacing for the array that roughly corresponds to the silica particle diameter.

Building a structural model for the opal and Schiller layers

A.) Opal: Uniform size marbles or ping pong balls can be distributed to students for stacking layers of the balls in a close packed structure to form a large scale model of opal.

B.) Schiller layers: Straws can be bundled together in large mats. Placing 2-3 mats on top of each other at various spacings will give students a visual picture of what happens in the case of the self assembly of rod shaped particles into colloidal crystals.

Comments:

The chemical synthesis procedures may be too extensive in terms of time and resource availability. Alternate arrangements can be made to accommodate these cases such as preparing the colloids beforehand, getting the colloids from commercial sources, or contacting the authors to request samples. The silica should be easy to obtain from commercial suppliers, but the akageneite is probably not available.

References:

1.) W. Stober, A. Fink, and Bohn, "Controlled Growth of Monodisperse Silica Spheres in the Micron Size Range," J. Colloid Interface Sci., 26, 62 (1968).

THE MAGIC OF CRYOGENICS

Daniel P. Vigliotti

James B. Alcorn

Brian P. Marsh

and

Nicole A. Neumeyer

National Institute of Standards and Testing
Division 853
325 Broadway-360
Boulder, Colorado 80303-3328

Telephone: 303-497-3351
e-mail vigliotti@boulder.nist.gov

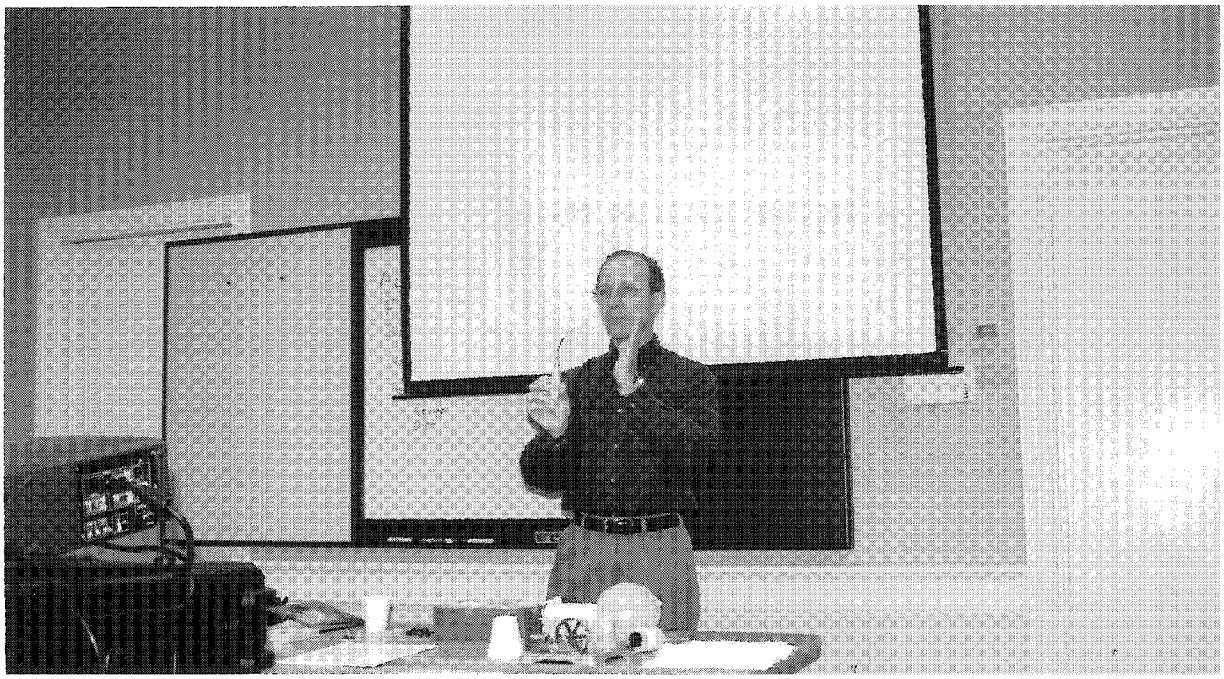

Daniel P. Vigliotti

The Magic of Cryogenics*

Daniel P. Vigliotti, James B. Alcorn, Brian P. Marsh, Nicole A. Neumeyer
Materials Reliability Division
National Institute of Standards and Technology
Boulder, Colorado 80305

Key Words: bimetallic; brittle; coefficient of thermal expansion; contraction; cryogenics; ductile; levitation; liquid nitrogen; magnetism; pressure; superconductor.

Prerequisite Knowledge: The presenter should be familiar with safety precautions involving cryogenic liquids.

Objective: The purpose of this presentation is to introduce teachers to a demonstration that exposes K-12 students to a variety of scientific areas through experiments using liquid nitrogen. This presentation demonstrates how changing the temperature of materials changes their size and shape. During the presentation, there are many opportunities to explore subjects for which changes in temperature are important such as magnetism, biology, the relationship between pressure and volume, and the composition of air. Students may perform some of the experiments in this presentation.

Equipment[1]:

1. Liquid Nitrogen In Dewar
2. Insulated Container
3. Styrofoam Cups
4. Funnel
5. Tongs
6. Leather Gloves
7. Safety Glasses
8. Popgun
9. Balloons
10. Steam Engine
11. Brass Ball And Ring
12. Bimetallic Knife
13. Strips Of Soft Steel
14. Strips Of Rubber
15. Wood Block
16. Superconductor Kit
17. Carnation
18. Banana
19. Mighty Miniature Mass Mover

List of Demonstrations:

1. Popgun
2. Exploding Balloon
3. Steam Engine
4. Contracting - Expanding Balloon
5. Bimetallic Knife
6. Brass Ball and Ring
7. Rubber and Metal Strips
8. Carnation
9. Banana
10. Mighty Miniature Mass Mover
11. Superconducting Magnet

---

[1] If you have questions about acquiring any of these materials, contact Daniel P. Vigliotti at 303-497-3351 or vigliotti@boulder.nist.gov.

Presentation:

This presentation deals with cryogenics. The word cryogenics comes from the Greek language, *kryos,* meaning "cold", and *genic,* meaning "the production of". The teacher should ask the question, "What is the coldest temperature that anyone has experienced outside?" You will get a range of answers from about 0 °C (32 °F) to -40 °C (-40 °F). Next ask, "What do you think is the coldest temperature ever recorded on Earth and where was it?" The correct answer is -106.7 °C (-160 °F) at the South Pole. Now inform the students that this presentation involves liquid nitrogen and that the temperature of liquid nitrogen is -196 °C (-320.5 °F). Liquid nitrogen is so cold that if it touches the skin, it will damage the skin causing a burning sensation just as if one puts their hand on a red-hot stove. It may cause a blister to form, which is really due to a severe case of frostbite. Basic safety precautions should be stated to the classroom prior to beginning the demonstrations: 1. Do not pick up anything that falls on the floor. 2. Do not touch anything unless told to. Remind students that it is important to follow these rules because liquid nitrogen kills cells. This is the very same liquid that a doctor may use to kill warts.

Liquid nitrogen has many uses in industry. Since liquid nitrogen is inert, meaning it does not readily react with other compounds, it is used to freeze frozen foods available in the grocery store. Conveyer belts move foods through a "cold tunnel" that is cooled by liquid nitrogen to about –184 °C (-300 °F). Freeze-dried foods are sprayed with or immersed in liquid nitrogen to freeze them very quickly. Similar techniques are used to freeze blood and other human cells. Liquid nitrogen is also used in the medical field to perform cryosurgery.

Liquid nitrogen is a colorless, odorless liquid, such that when poured into the insulated container, it will look like steaming water (See Figure 1). When the insulated container is full, the liquid nitrogen will then look like boiling water (See Figure 2). The liquid nitrogen will continue to boil violently until the inside of the insulated container reaches -195.6 °C (-320 °F). At this point, the liquid nitrogen will appear relatively stable. However, the liquid will continue to slowly turn into a gas (See Figure 3).

Figure 1 - Pouring Liquid Nitrogen

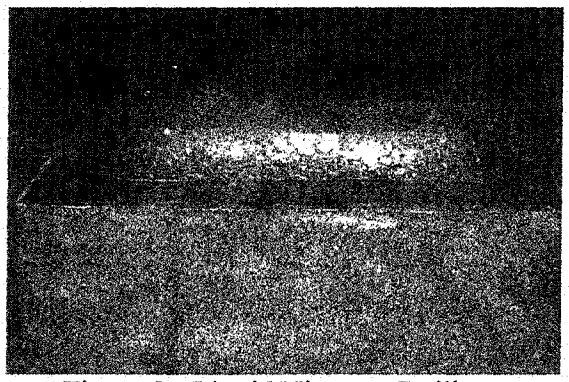

Figure 2 - Liquid Nitrogen Boiling Violently

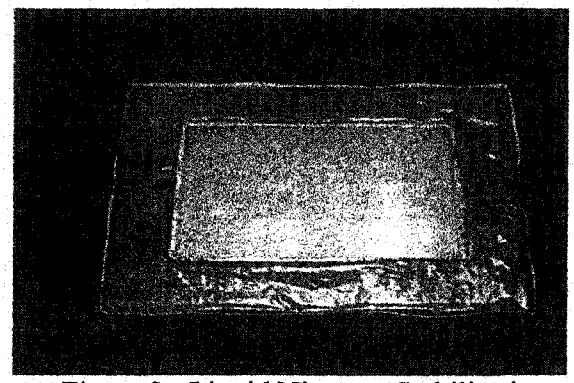

Figure 3 - Liquid Nitrogen Stabilized

At this point, ask the students, "Is it a good or a bad thing that this liquid is turning into a gas and we are breathing it?" Most students will say it is a bad thing. We will later determine this is not true, because nitrogen is a gas that comprises much of our atmosphere. As a follow-up question, ask the students, "What is in the air that we breathe?" Most classes will say oxygen, smog, hydrogen, and carbon dioxide. This immediately leads into a new subject: "Where does the carbon dioxide in this room come from?" In every classroom, usually one student knows that it comes from people exhaling. Now discuss the process of photosynthesis. After students name as many gases as possible that make up air, ask: "Does anyone know which gas makes up most of the air that we breathe?" The majority of students will agree that most of what we breathe is oxygen. Most students are surprised to find out that only 21 % of the air is oxygen but 78 % is nitrogen, which leaves only 1 % for all other gases including carbon dioxide. (If the students understand percentages, use them; however, younger students may need further explanation.)

DEMONSTRATIONS:

Pressure-Volume-Temperature Relationships (Experiments 1-4):

The first set of experiments will examine one interesting characteristic of liquid nitrogen as it changes into gas. During this process, it increases in volume about 700 times. In the dewar there is about a gallon of liquid nitrogen. If we could remove the cap and all of the liquid nitrogen were changed into a gas, then it would take 700 dewars of that same volume to catch all of the gas. That is a dramatic increase in volume.

1. Popgun

This experiment uses a popgun (See Figure 4) to show the result of liquid nitrogen heating up and turning into a gas. Use a styrofoam cup to remove a small amount of liquid nitrogen from the insulated container and pour it into the popgun. (Make sure that a string is attached to the cork prior to demonstration to ensure that it does not fly away and cause damage.) Quickly force the cork into the popgun. It will immediately pop off (See Figure 5). You may continue to force the cork into the popgun and it will continue to pop off until all of the liquid nitrogen has turned into a gas. By the time all of the liquid turns into gas, the sealed end of the popgun will be white and smoking. This is oxygen and water condensing on the outside of the popgun.

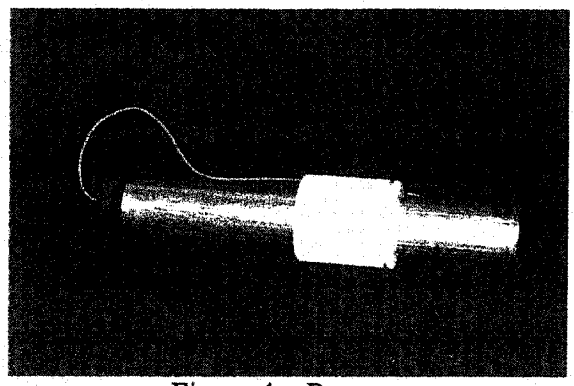

Figure 4 – Popgun

Figure 5 - Cork Popping Off Popgun

2. Exploding Balloon

Next, we will inflate a balloon using the expansion property of liquid nitrogen. Take the funnel and put it in the balloon. Seal the balloon around the funnel with your fingers and pour in a small amount of liquid nitrogen using the styrofoam cup (See Figure 6). As soon as a small amount is in the balloon, remove the funnel, pinch the balloon closed, and shake the balloon to keep the liquid nitrogen from freezing the bottom of the balloon (See Figure 7). The balloon will inflate, and if there is enough liquid nitrogen inside, the balloon will expand to its limit and explode (See Figure 8).

Figure 6 - Pour Liquid Nitrogen in Balloon

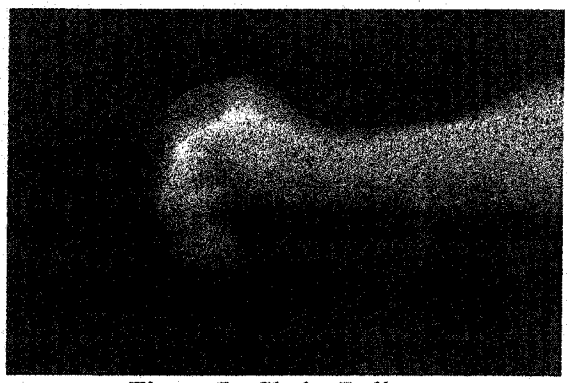

Figure 7 - Shake Balloon

Figure 8 - Balloon Exploding

3. Steam Engine

The next experiment uses a steam engine (Figure 9) to demonstrate the expansion property of liquid nitrogen. (Before beginning the presentation, ensure that steam engine is in proper working condition.) Since, most students can identify with a steam locomotive, ask students to explain the principle of a steam engine. (Older students may be able to explain it.) Explain that on a steam locomotive the boiler is filled with water. Fire is used to boil the water to create steam. This steam trapped in the boiler creates pressure that is guided through a series of pipes and valves to cylinders containing pistons. The pistons are connected to the wheels, which make the locomotive go down the tracks. Explain that we will create pressure to run the flywheel on our steam engine; however, we need neither water nor fire, just the heat in the room. Remove the whistle and the relief valve from the top of the steam engine. Put the funnel in one of the holes and pour about half a styrofoam cup of liquid nitrogen into it (Figure 10). Quickly install the whistle first, and then the relief valve. Give the flywheel a light spin to get it started. The flywheel will turn at a high rate of speed and slow down when all of the liquid nitrogen turns into gas. As the liquid nitrogen cools the steam engine, oxygen and water will condense on the boiler (See Figure 11).

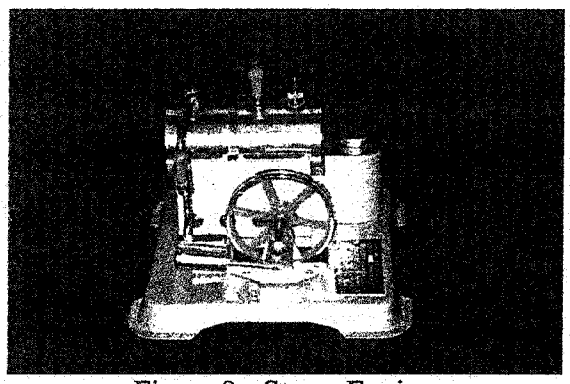

Figure 9 - Steam Engine

Figure 10 - Pour Liquid Nitrogen into Steam Engine

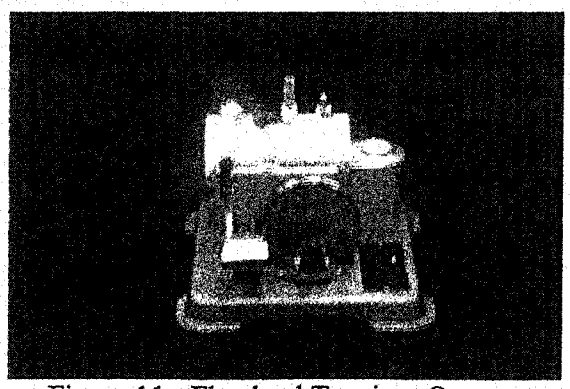

Figure 11 - Flywheel Turning, Oxygen and Water Condensing on Boiler

4. Contracting – Expanding Balloon

We will now use a balloon to demonstrate how gases contract when exposed to cryogenic temperatures while simultaneously making dry ice. Blow up a balloon until it is slightly larger than the insulated container (See Figure 12). Push the balloon directly into the liquid nitrogen (See Figure 13). The balloon will begin to shrink where it touches the liquid nitrogen. You must periodically rotate the balloon in the surface of the liquid until the balloon is collapsed (See Figure 14). At this point, you may ask the students what gases are in the balloon. Because you exhaled into the balloon to inflate it, some carbon dioxide is present inside in addition to the exhaled nitrogen from the air you breathed into it. The carbon dioxide has contracted and frozen into a small block of dry ice. (Also, the water vapor in your breath has been frozen into small particles of ice.) You can demonstrate that dry ice has formed in the balloon by shaking the balloon, and listening for the dry ice bouncing around inside of the balloon. Before the balloon heats up and inflates, return it to the container to shrink it again. After the balloon collapses again, quickly remove it and set it on the table for the students to see. (See Figure 15) The balloon will warm up quickly and start to inflate again. (See Figure 16) Because the rubber in the balloon is not of a consistent thickness, the balloon will appear distorted as it inflates and will probably explode before completely inflating.

Figure 12 – Inflate the Balloon

Figure 13 – Push the Balloon into Liquid Nitrogen

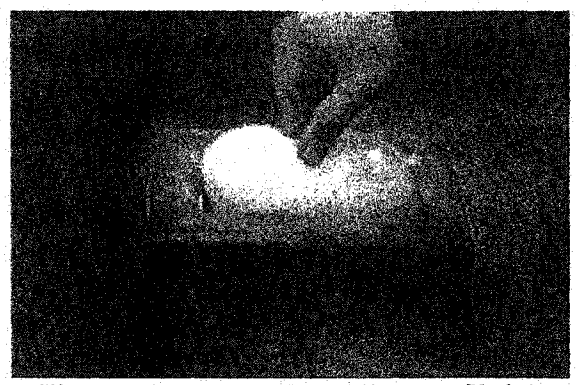

Figure 14 – Rotate the Balloon to Shrink Balloon

Figure 15 - Balloon Deflated

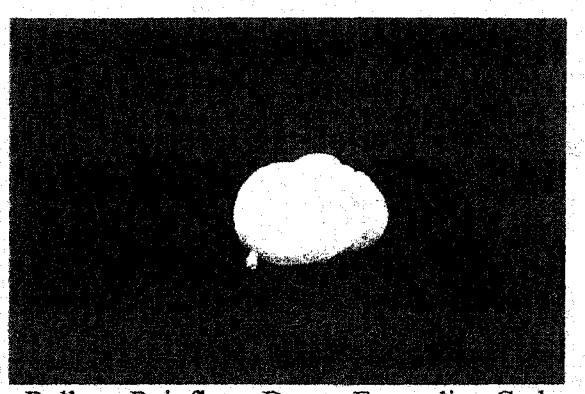

Figure 16 - Balloon Reinflates Due to Expanding Carbon Dioxide

Coefficients of Thermal Expansion (Experiments 5-6):

Describe the coefficient of thermal expansion as, loosely speaking, the rate at which something expands or contacts as a function of temperature. Materials are tested and assigned coefficients of thermal expansion at various temperatures. These coefficients are valuable to engineers when they are designing and choosing materials with which to build things such as buildings, bridges, ships, submarines, spaceships, and satellites. It is important to choose materials that when bonded together are compatible by expanding and contracting at approximately the same rates when they are exposed to changes in temperature, rather than at different rates, which could damage them.

5. Bimetallic Knife

There are two materials with very different coefficients of thermal expansion. The bimetallic knife is made of brass bonded to steel. At room temperature, the knife is straight (See Figure 17).

Figure 17 - Bimetallic Knife at Room Temperature

After the knife is submerged in liquid nitrogen and removed, the knife is significantly bent (See Figure 18). Brass has a high coefficient of thermal expansion and will become shorter when it is cooled. Steel has a lower coefficient of thermal expansion and does not shrink nearly as much as

the brass The steel is forced to bend, as the brass gets shorter. Therefore brass and steel are thermally incompatible if the shape of a structure is to be preserved and not warped

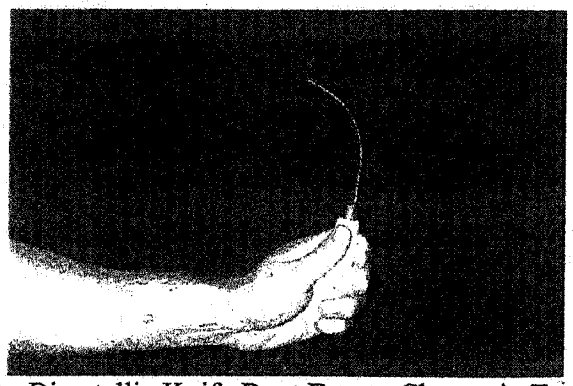

Figure 18 - Bimetallic Knife Bent Due to Change in Temperature

6. Brass Ball and Ring

In contrast to the bimetallic knife, here are two objects of the same material and therefore having the same coefficients of expansion and contraction. We have a brass ball and a brass ring (See Figure 19). The brass ball is sized so that it just fits through the ring (See Figure 20) The brass ring is submerged in the liquid nitrogen for about two minutes When the ring is removed, it has shrunk enough that the ball can no longer fit through the ring (See Figure 21)

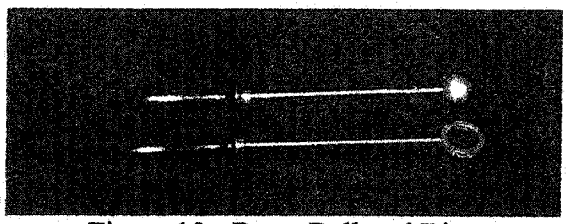

Figure 19 - Brass Ball and Ring

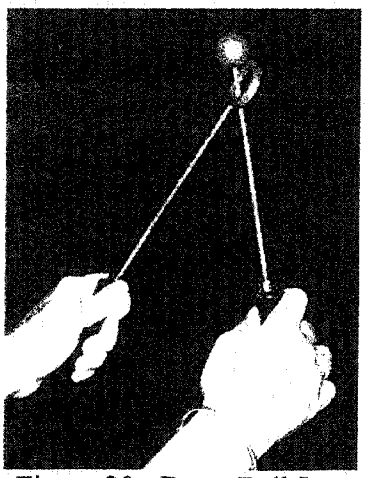

Figure 20 - Brass Ball Just Fits Through Ring

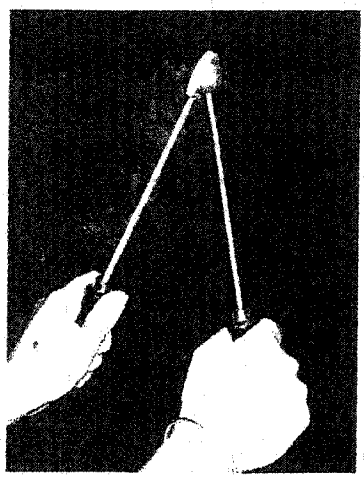

Figure 21 - Brass Ring Shrunk; Ball Will Not Go Through Ring

Transition from Ductile to Brittle (Experiments 7-8):

To the students, define brittle as hard, rigid, fragile, and not flexible A brittle object breaks easily and shatters when it breaks. Define ductile as being elastic, able to bend and then recover its original shape undamaged. A ductile object is hard to break, but easy to bend

7. Rubber and Metal Strips

This experiment shows that rubber is very ductile at room temperature but becomes extremely brittle at cryogenic temperatures. Show the flexibility of a strip of common rubber by bending it between your finger and thumb (See Figure 22). Drop the rubber strip into the liquid nitrogen and have a student volunteer to put on some leather gloves. Using tweezers, quickly remove the rubber strip from the liquid nitrogen, put it in the students gloved hand, and ask the student to try to bend it. Instead of flexibly bending, the rubber is now rigid and inflexible and will snap into several pieces (See Figure 23).

Figure 22 Flexible Rubber Strip

Figure 23 - Brittle Rubber Strip

It is easy to see that rubber is ductile at room temperature; it is not as easy for students to think that steel, aluminum, or other metals can be ductile For applications of ductile metals, you may talk about the following examples· Think about the steel that will be used to build a skyscraper in California where there is a very good chance that the building will experience an earthquake. Ask the students, "Would you want to use ductile or brittle steel?" Think about an airplane wing. Again, ask them, "Have you ever been on an airplane that is flying in rough weather?" Most students will say yes. Then ask if anyone was able to look out the window and see the wing tip. Question, "What was the wing tip doing?" The careful observer will have noticed the wing tip was bouncing up and down. That means that the aluminum in the wings must be ductile If the aluminum were brittle, the wings would break and fall off. To display this, take a metal strip and bend it between your finger and thumb (See Figure 24). The metal strip will bend easily. Submerge the bent metal in the liquid nitrogen and have a student volunteer put on some leather gloves. Using tweezers, remove the bent metal from the liquid nitrogen and hand it to the student to try to bend it (See Figure 25). It will snap very easily. In fact, it will take less force to break it than it did to bend it to the same deflection at room temperature

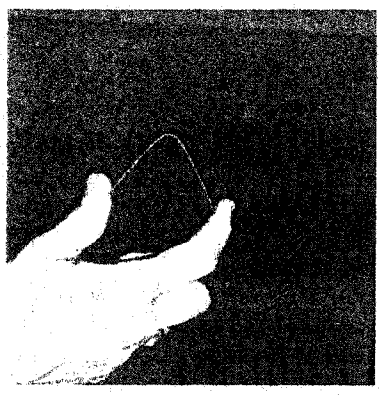

Figure 24 - Flexible Metal Strip

Figure 25 - Brittle Metal Strip

8. Carnation

Next, hold a carnation, (See Figure 26) and ask whether a flower is ductile or brittle. It is usually difficult for a class to reach a consensus because of our previous definitions of ductile and brittle. A carnation is soft and flexible but it is also fragile. Therefore it is obviously ductile. Before submerging the carnation in the liquid nitrogen, tell the students that you are going to put the flower into the liquid nitrogen and then take it out. Ask if they think it will look the same or will it look "yucky". Remember, we said earlier that when liquid nitrogen touches skin and warts, it kills cells. Most will say that it will look "yucky" Remove the carnation and they will see that it looks normal, except that it appears to be smoking. Now is the time to ask for an adult volunteer (as this should not be done by students). Submerge the flower in the liquid nitrogen again (See Figure 27). Explain to the volunteer that you will remove the flower and shake most of the liquid nitrogen off so that his/her hand will not be frostbitten, when he/she slowly crushes the flower. Remove the flower, shake off all liquid nitrogen and then quickly hold it over a paper towel for the volunteer to slowly crush the flower (See Figure 28). The petals will break off easily and will sound somewhat like glass shattering (See Figure 29). The petals are so delicate that they will warm up and become ductile almost immediately upon hitting the paper towel

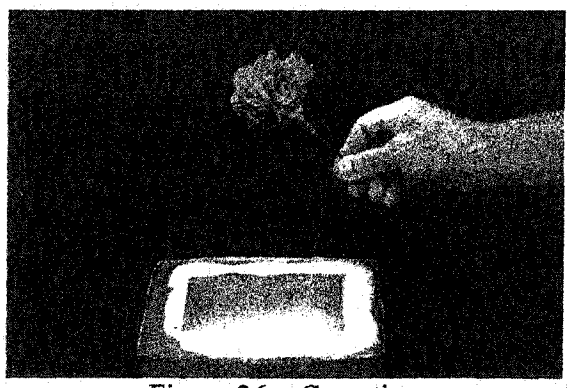

Figure 26 – Carnation

Figure 27 - Carnation Submerged in Liquid Nitrogen

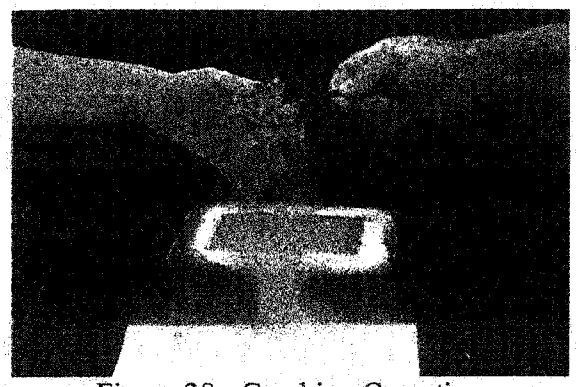

Figure 28 - Crushing Carnation

Figure 29 - Petals Falling

Creating Toughness at Cryogenic Temperatures (Experiment 9):

9. Banana

For this experiment, hold up a banana and ask the students for the best use of a banana. They will say bananas should be eaten. Ask if any of them have ever used a banana as a hammer. Of course nobody has, because when you try to pound in a nail, it will stick in the banana (See Figure 30). Demonstrate this, then remove the nail and submerge the banana in the liquid nitrogen (See Figure 31). Explain that you can create toughness in materials by making them cold, although, it is difficult to determine whether something has gone beyond tough and has become brittle. The banana will need to stay submerged for approximately five minutes. This is a good time to review some of the concepts that have been discussed to this point. You may also ask for questions. Put on the leather gloves, and take the banana by the warm end sticking out of the container and try to pound the nail into a piece of wood (See Figure 32). You want to break the banana to display that it is frozen all the way through. You may have to hit the banana hard in order to break it (See Figure 33).

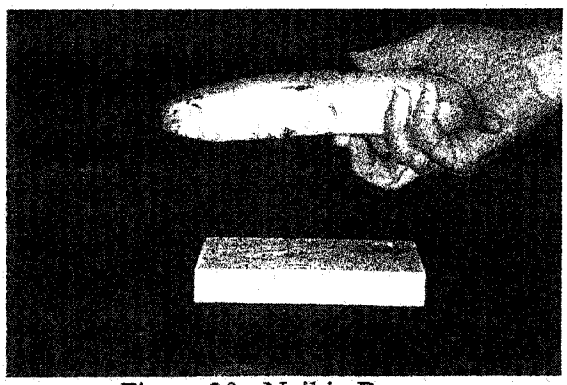

Figure 30 - Nail in Banana

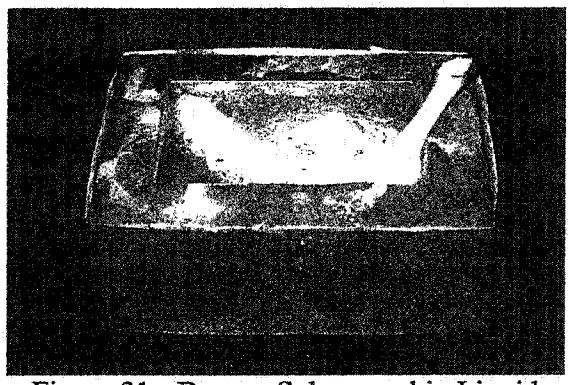

Figure 31 - Banana Submerged in Liquid Nitrogen

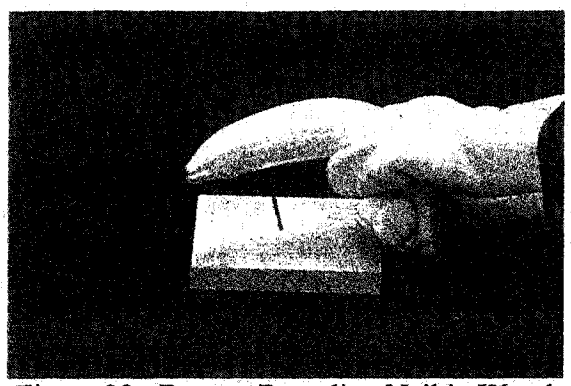

Figure 32 - Banana Pounding Nail in Wood

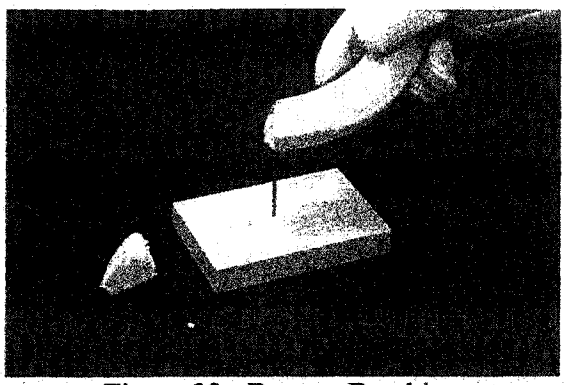

Figure 33 - Banana Breaking

Electrical Resistivity (Experiments 10-12):

10. Mighty Miniature Mass Mover

The "Mighty Miniature Mass Mover", contains electronic circuitry, a capacitor, a switch and a copper coil positioned in a Petri dish (See Figure 34). The electric charge stored in a capacitor is dumped into a coil to create a magnetic pulse that is opposed by an electrical eddy current in the dime. A dime will be placed on the coil and repelled by the magnetic forces created by the currents. The capacitor is a storage device for electrical charge. When the capacitor is discharged, it sends current through the coil that creates an electromagnetic reaction for an instant The magnetic field produced by the electromagnet induces eddy currents within the conducting dime and causes it to jump away from the electromagnet

First, demonstrate what happens at room temperature Plug in the unit to charge the capacitor. Place a dime on top of the coil and push the button to discharge the capacitor. Note that the dime is repelled only slightly.

Then, with the styrofoam cup, pour liquid nitrogen into the Petri dish, covering the coil. Once the coil has reached liquid-nitrogen temperature, place the dime on the coil and again push the button to discharge the capacitor (See Figure 35). The lower resistance in the coil will allow a greater electrical current to flow and cause the dime to be repelled higher than during the initial test.

Repeat the above procedure, but this time with the dime also cooled to liquid-nitrogen temperature The opposing field created in the dime is now even greater, and the dime will be repelled even higher (See Figure 36)

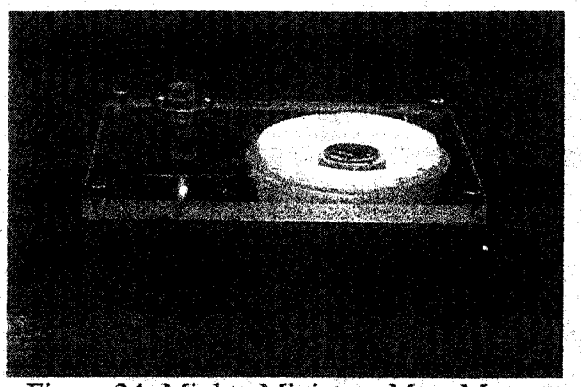

Figure 34- Mighty Miniature Mass Mover

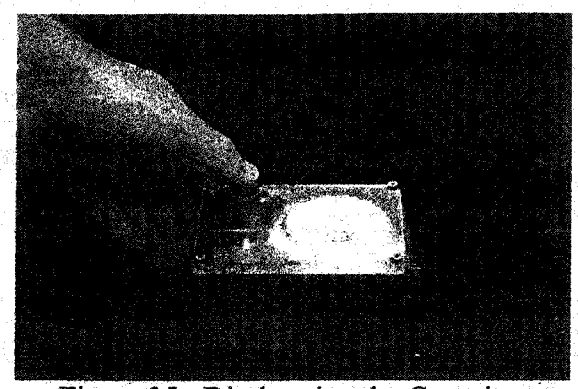

Figure 35 - Discharging the Capacitor

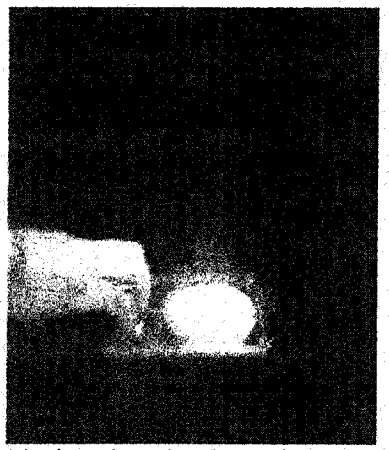

Figure 36 - Discharging the Capacitor with Cold Dime

11. Superconducting Magnet

This kit contains a ceramic superconducting magnet made from yttrium, barium, and copper oxides. It is important to point out that superconducting behavior only occurs in superconductors at cryogenic temperatures. Superconductors are strongly diamagnetic. That is to say that they will repel a magnet. The kit also contains a rare-earth magnet and a Petri dish (See Figure 37).

This experiment will demonstrate levitation. Position the superconducting magnet in the Petri dish. Use a styrofoam cup to fill the Petri dish with liquid nitrogen. Continue to fill the Petri dish until the superconducting magnet reaches liquid-nitrogen temperature and no longer causes the liquid nitrogen to boil vigorously. Place a styrofoam cup upside down on the table. Remove the superconducting magnet from the Petri dish and set it on top of the cup. Place the rare-earth magnet above the superconducting magnet (See Figure 38). Start the levitated rare-earth magnet spinning by pushing down on one edge. It will spin with little resistance (See Figure 39). The levitated rare-earth magnet will spin above the superconducting magnet until it warms up. When it is no longer superconducting, the magnet will no longer levitate and will drop into the cup.

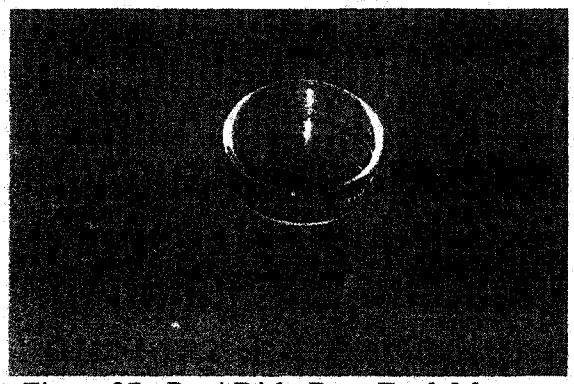

Figure 37 - Petri Dish, Rare-Earth Magnet, Superconducting Magnet

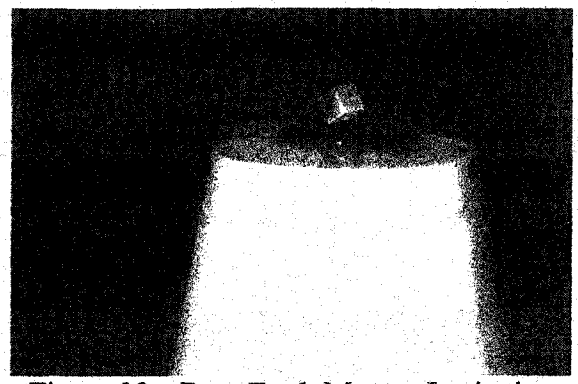

Figure 38 – Rare-Earth Magnet Levitating

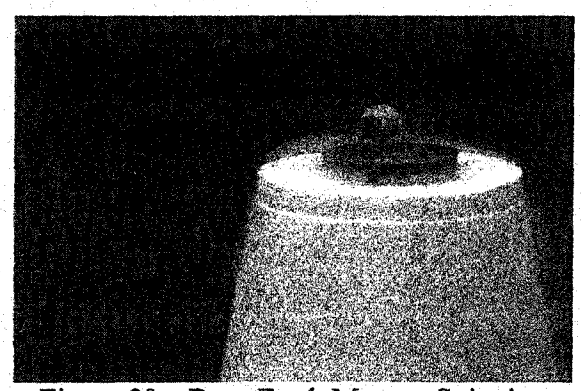

Figure 39 – Rare-Earth Magnet Spinning

Acknowledgement:

Special thanks to Phyllis Wright, Career Awareness and Resource Education (CARE) Coordinator, for her remarkable dedication to the program and for furnishing this kit.

This cryogenics kit is available from the CARE program at the National Institute of Standards and Technology, Boulder, CO[2]. The CARE program was established in 1979 to promote interest and awareness in math and science. Awareness and exploration of the sciences are encouraged through science kits, videos, field trips, and presentations by the scientific staff.

Some parts of this kit are available commercially and some parts are produced by NIST Divisions in Boulder, Colorado.

[2] Phone: 303-497-3244 E-mail: phyllis.wright@nist.gov

MOLECULAR DYNAMICS SIMULATIONS OF CRACKING PHENOMENA IN POLYMER LIQUID CRYSTALS (PLCs)

Witold Brostow

Laboratory of Advanced Polymeers
and Optimized Materials
Department of Materials Science
University of North Texas
Denton, Texas 76203-5310

e-mail brostow@unt.edu

António M. Cunha

Department of Polymer Engineering
University of Minho
4800 Guimaraes
Portugal

and

Ricardo Simões

Laboratory of Polymers
Department of Materials Science
University of North Texas
Denton, Texas 76203-5310

e-mail rsimoes@unt.edu

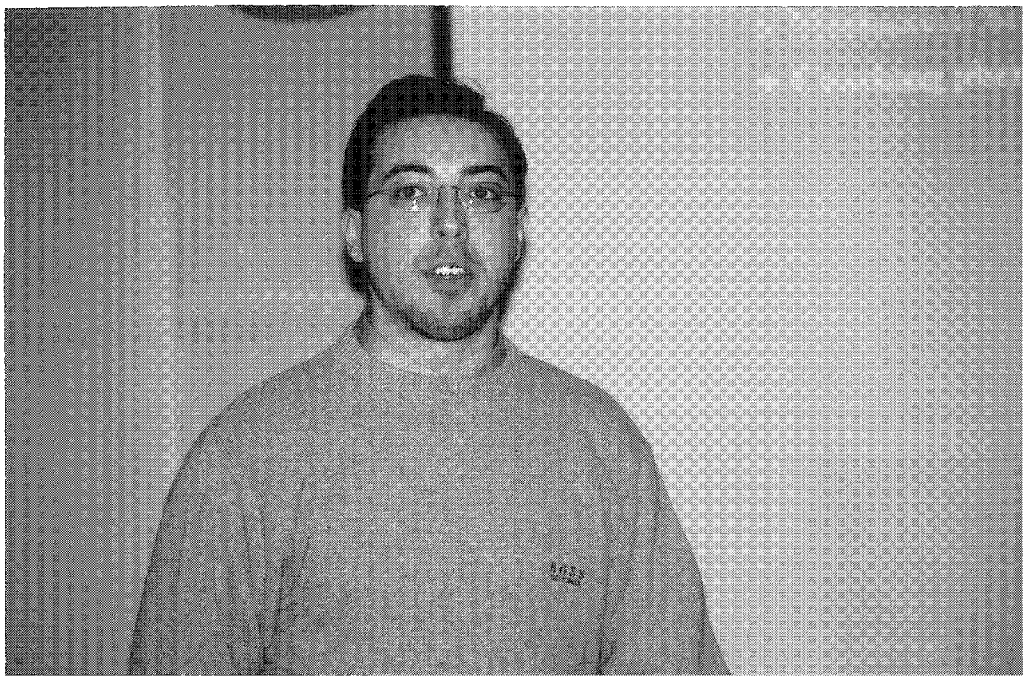

Ricardo Simões

Biography:

Ricardo Simoes is a PhD student of Materials Science and a Teaching Assistant of Physics at the University of North Texas, Denton, Texas. He has a 5-year bachelor's degree from the University of Minho, Guimaraes, Portugal. He is a member of the *Ordem dos Engenheiros* and the *Society of Plastics Engineers (SPE)*. He is the President of the North Texas Chapter of SPE and the vice-chair of the organizing committee of Polychar - World Forum on Polymer Applications and Theory.

MOLECULAR DYNAMICS SIMULATIONS OF CRACKING PHENOMENA IN POLYMER LIQUID CRYSTALS (PLCs)

Witold Brostow (a), António M. Cunha (b), and Ricardo Simões (a, b)
(a) Laboratory of Advanced Polymers and Optimized Materials (LAPOM), Department of Materials Science, University of North Texas, Denton, TX 76203-5310, USA; brostow@unt.edu; http://www.unt.edu/LAPOM/
(b) Department of Polymer Engineering, University of Minho, 4800 Guimaraes, Portugal

Key Words: crack propagation, computer animation, molecular dynamics, polymer simulation.

Prerequisite Knowledge: Basic knowledge of polymer systems, interaction potentials, mechanical properties, failure analysis and reliability of polymeric materials. Some knowledge of computer graphics and animation is advised.

Objective: To study the cracking phenomena in PLCs and to develop tools to graphically represent crack formation and propagation, while at the same time creating the basis for the three-dimensional representation of polymeric, metallic or ceramic systems.

Equipment and Materials: PC with Windows environment and Microsoft Visual C++.

Introduction:

Reliability of polymeric materials is important not only for scientists and engineers, but also for all the users of these materials, that is, for all of us [1, 2]. The users do not know about the chemistry of synthesis, processing, thermodynamics, or rheology. However, when buying a product that contains polymeric components, they want appropriate quality assured. Although mechanics of polymers exists for quite some time, there are still no answers to fundamental questions such as: "where does a crack begin" or "how does it grow". Scanning electron microscopy (SEM) allows us to study the surface of cracks after fracture has occurred; however, it provides no information to answer the questions above. For obvious reasons these issues are important also for students of Materials Science and Engineering (MSE) and related disciplines. There is by far not enough about computer modeling and simulations in MSE textbooks.

An approach exists to answer these questions: computer simulations. One can create a polymeric material on a computer, apply an external force to it, and observe how cracks form, how they propagate through the material, and how fracture eventually occurs. A particular problem with computer simulations is the large amount of information they produce. Effective methods to analyze this information are therefore needed. The solution found was three-dimensional (3D) graphical representation of the results through OpenGL rendering.

Procedure:

One can use two methods [3]: Monte Carlo or Molecular Dynamics. Cartesian coordinates are assigned to each segment of each polymeric chain. The chains are contained inside a rectangular box. The segments interact according to interaction potentials. Different potentials

dictate the behavior of different types of segments. In the Monte Carlo method, developed by Norbert Metropolis and Stanislaw Ulam [4], the particles are moved one at a time; for this reason this method is more adequate for equilibrium properties.

In the molecular dynamics method, originally developed for gaseous molecules by Berni J. Alder and his collaborators [5], all particles are moved simultaneously. Besides the cartesian coordinates, each particle is also assigned three momentum components along the cartesian axis. In this way it is possible to observe and follow the movement of the particles – chain segments in our case – and also to observe the effect of applied external forces.

An obvious question is: what happens when a particle wants to escape the system? The problem was solved by applying boundary conditions; it is considered that the system space is full of periodic copies of the basic rectangular box, which are usually called "ghosts". Whenever a particle is displaced outside the basic box, its "ghost" automatically enters the box from the opposite side.

In order to graphically represent the results of the simulations, a 3D graphics program was written. This program represents the segments as solid spheres in the coordinates calculated by the simulation, as shown in Figure 1. An animation of the cracking phenomena as a function of time can be obtained by changing the position of the particles at each simulation step, as shown in Figure 2. The reason for the use of the OpenGL environment in Microsoft Windows operating system is the accessibility, since the program will run in any common secretary computer, without need to resort to supercomputers.

Comments:

In spite of the advantages, the simulations require advanced knowledge of molecular physics, polymer science and engineering, and computer programming. For this reason, the number of simulations of polymers under stress producing deformation is limited. Stress relaxation simulations for single-phase polymers [6] also exist.

In our current simulations we consider two-phase polymeric systems – as is the case of polymer liquid crystals [3]. The rigid phase with high concentration of liquid crystal segments forms islands in the matrix consisting of flexible segments. Each polymer liquid crystal chain contains both types of segments.

Generally, cracks could be expected to appear inside the islands (since they are rigid), or inside the matrix (which is flexible and therefore has little resistance to stress) on the boundary of the two phases. In the conference, we will present results that will allow us to answer this question.

Some of our results were already published in 2001 [7]. In the conference we shall present those results along with other unpublished ones.

Although our simulations are dedicated to polymer liquid crystals, the developed method can be adapted to other single-phase or two-phase polymer systems. The simulations allowed us to observe interesting features about the cracking phenomena.

The graphic programming implemented allows for representation of any three-dimensional structures. This type of graphical representation of polymeric systems is still practically inexistent, however, its uses and advantages are obvious. A particularly interesting possibility of OpenGL graphic programming is its use as an instructional tool. It simplifies teaching the structure of two-phase polymers, the step-wise polymerization process and the 3D arrangement of the resulting non-longitudinal polymeric chains, as shown in Figure 3. The same method can be used to represent structures of metals and ceramics.

Acknowledgements:

We acknowledge financial support of the Robert A. Welch Foundation, Houston (Grant #B-1203) and the Fundação para a Ciencia e a Tecnologia, 3° Quadro Comunitário de Apoio, Lisbon.

References:

1. W. Brostow and R.D. Corneliussen, editors, Failure of Plastics, Hanser, München – Wien – New York 1986, 1989, 1992.
2. W. Brostow, editor, Performance of Plastics, Hanser, Munich – Cincinnati, 2000.
3. W. Brostow, chapter 15 in Mechanical and Thermophysical Properties of Polymer Liquid Crystals, W. Brostow, editor, Chapman & Hall, London, 1998.
4. N. Metropolis and S. Ulam, J. Amer. Statist. Assoc. 44, 335 (1949).
5. B.J. Alder and T.E. Wainwright, J. Chem. Phys. 27, 1208 (1957).
6. S. Blonski, W. Brostow and J. Kubát, Phys. Rev. B 49, 6494 (1994).
7. W. Brostow, M. Donahue III, C.E. Karashin and R. Simoes, Mater. Res. Innovat. 4, 75 (2001).

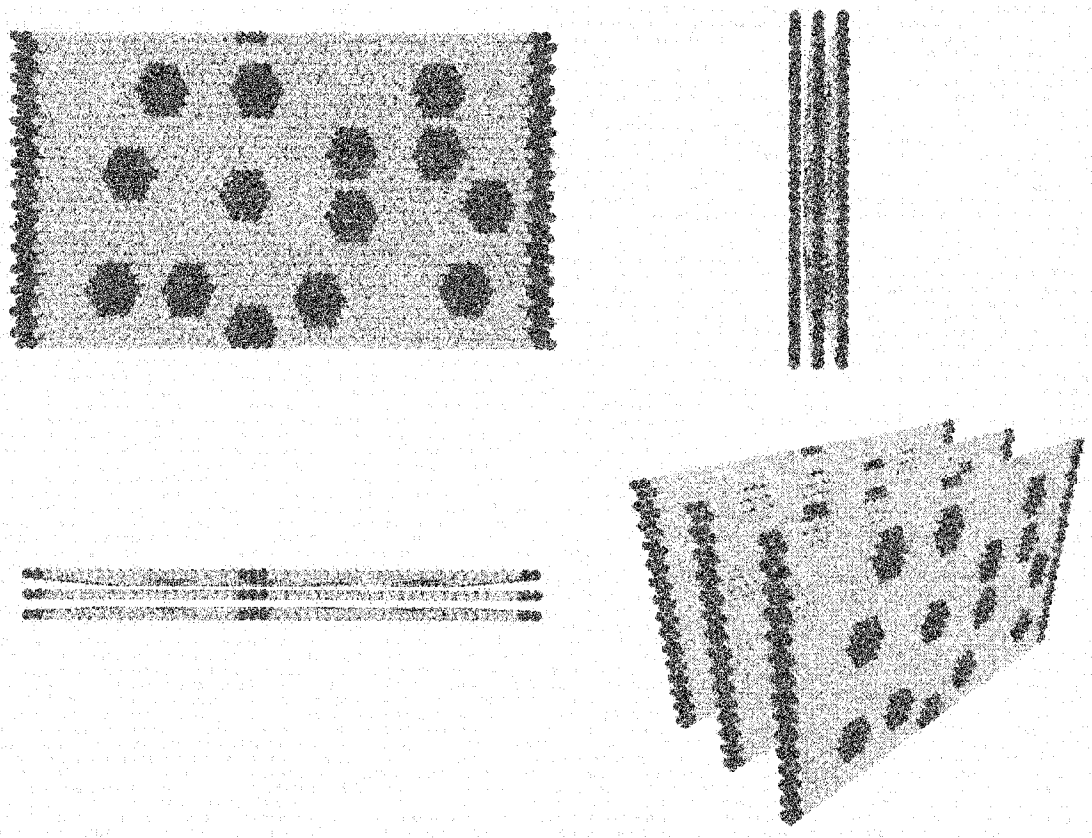

Figure 1 – Visualizing the simulated PLC in three-dimensions.
Rigid segments are represented as dark spheres and flexible segments are represented as light spheres. The material represented has 3 layers, each with 30 chains of 50 segments.

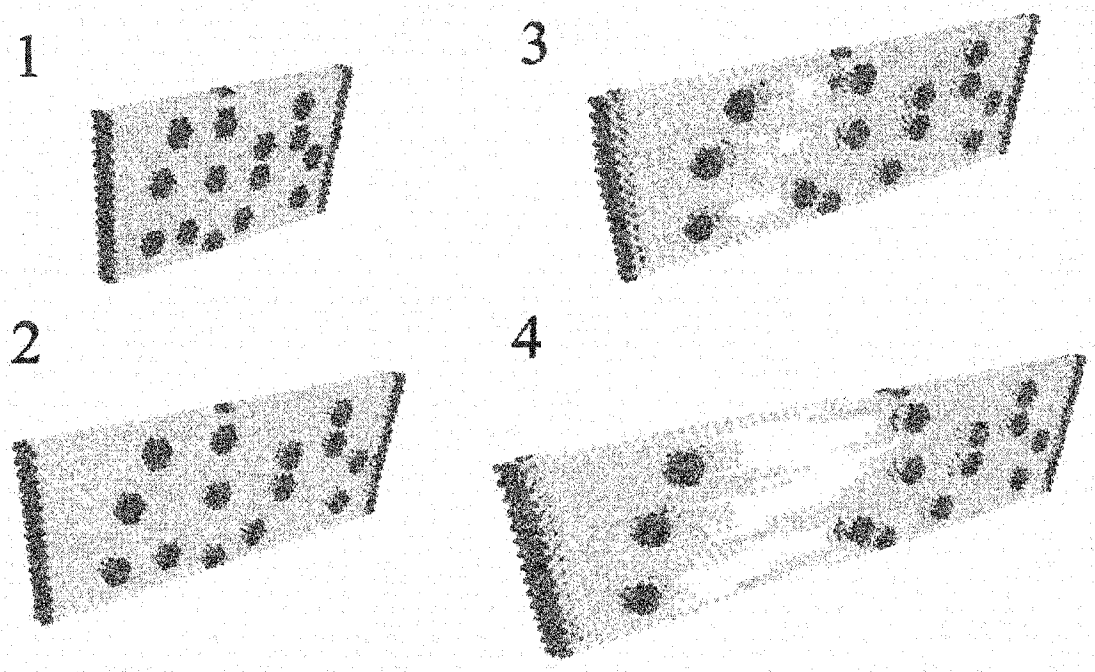

Figure 2 – Some frames from the animation of the cracking phenomena. Crack formation and propagation up to failure can be visually observed as an animation. Rigid segments are represented as dark spheres and flexible segments are represented as light spheres.

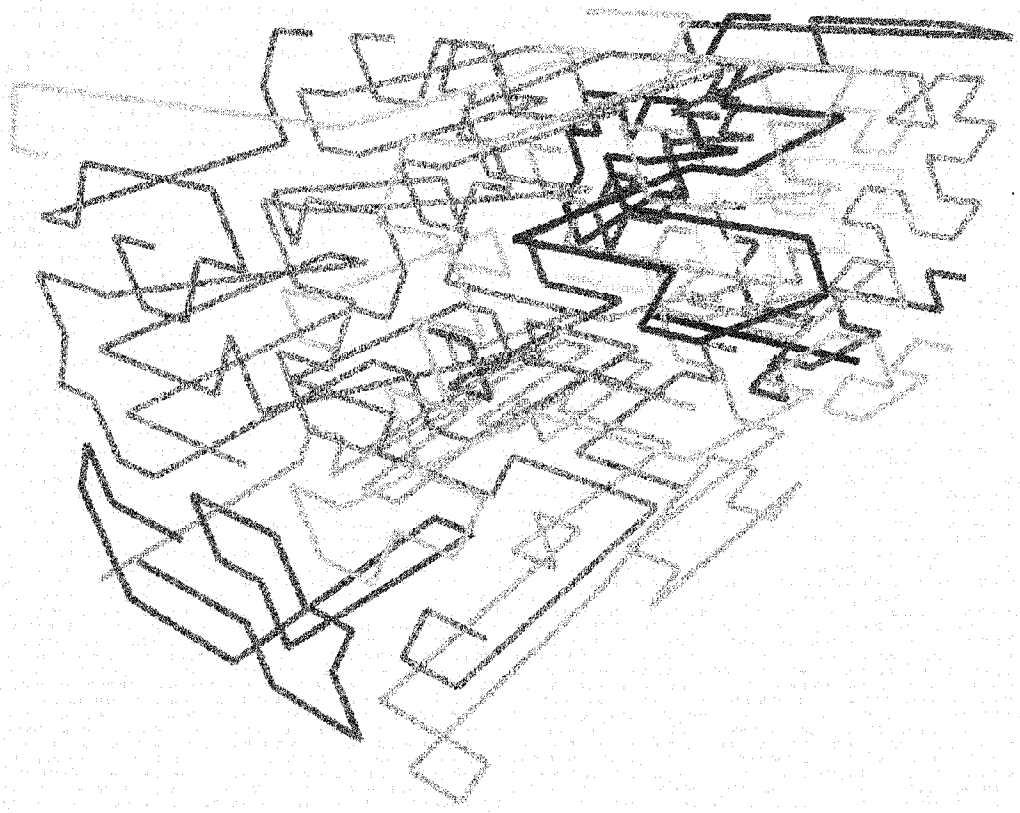

Figure 3 – Three-dimensional representation of non-longitudinal polymeric chains. For ease of visualization, each chain has been represented in a different shade of gray.

DEVELOPMENT OF A DEFORMATION PROCESSING LABORATORY

Richard B. Griffin

Mahan Hall, C&ME (2001 - 2002)
United States Military Academy
West Point, NY 10996-1792

845-938-4093
Richard.Griffin@USMA.edu

K. Ted Hartwig

Robert Barber

Tiffany New

and

Ibrahim Karaman

Mechanical Engineering Department 3123
Texas A&M University
College Station, Texas 77843-3123

Telephone 979-845-9779
e-mail rgriffin@mengr.tamu.edu

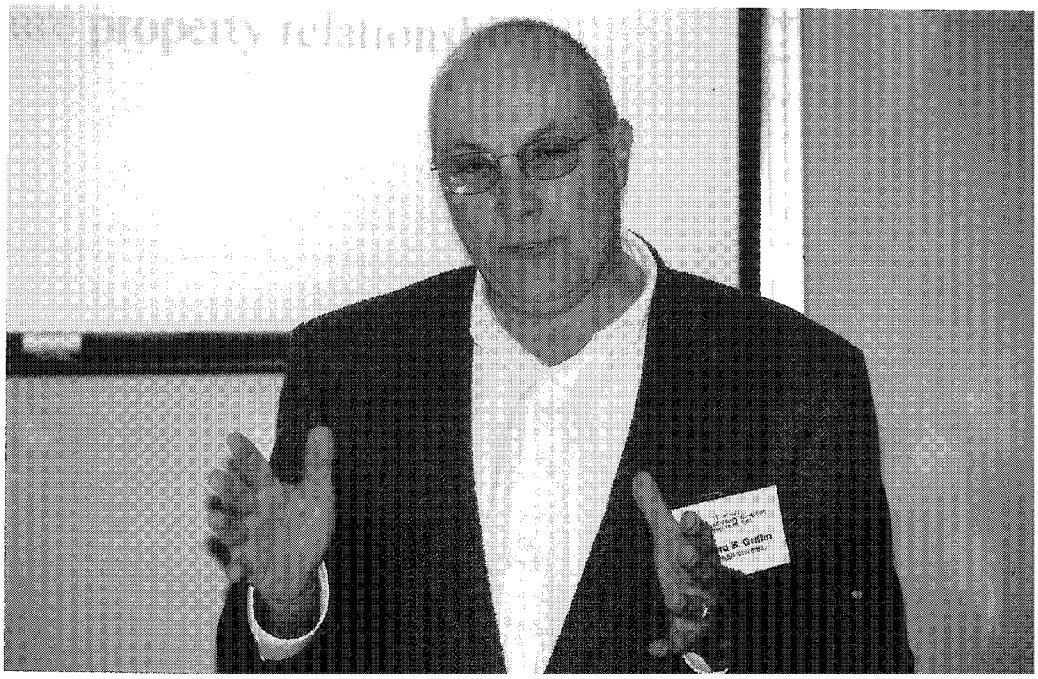

Richard B. Griffin

National Educators Workshop
New: Update 2001

Development of a Deformation Processing Laboratory

Authors

Richard B. Griffin, K. Ted Hartwig, Robert Barber, Tiffany New, and Ibrahim Karaman
MEEN Dept. 3123
Texas A&M University
College Station, TX 77843-3123

Abstract:
Deformation processes have substantial effects on the mechanical properties of materials. A recent innovation called equal channel angular extrusion (ECAE) has been developed. The ECAE process forces a billet around a sharp corner and as a result large uniform simple shear strain is induced into the billet. This is opposed to the nonuniform strains associated with conventional area reduction extrusion, where a billet is forced through a die orifice. Since the die inlet and outlet chambers maintain the same cross-section in ECAE, the geometry of the billet remains the same before and after the extrusion, which allows the billet to be processed multiple times resulting in high strains. A comprehensive comparison of the effects of rolling, conventional extrusion, and ECAE has been developed into a laboratory activity for a junior level materials/manufacturing course. A comparison between deformed grid patterns of extruded copper and Play-Doh specimens from a small extrusion press are compared. Hardness measurements on deformed copper specimens are used to validate these results. Deformation is carried out at room temperature on one-inch square ECAE and one inch diameter copper bars. Explanations of the deformation processes and results from the laboratory activity are discussed.

Introduction:

Deformation of material components can significantly alter the properties and microstructures of the material. Of the many available methods of material deformation, extrusion is one of the most common. The extrusion process first appeared in a 1797 patent to Joseph Bramah for a lead press (Sheppard)[1]. The application of this method to a common engineering procedure occurred in the late 1800's. Since then, extrusion has grown and changed to incorporate a broader range of methods. With current advances, extrusion maintains its potential in diverse engineering applications.

There are multiple extrusion techniques. One method, conventional extrusion, reduces the cross-sectional area of a billet of material by forcing the specimen through a die orifice under high pressure (Dieter)[2]. The setup for this method can be seen in Figure 1. Usually, solid and tubular shapes are created; however, irregular cross-sectional shapes can also be fabricated using this method. The large forces that are required often result in extrusions being performed near the recrystallization temperature. In metals, these temperatures correspond to increased ductility and decreased flow stress

(ASM Committee on Cold Extrusion)[3]. Extrusion at lower temperatures is possible and useful mechanical properties often result.

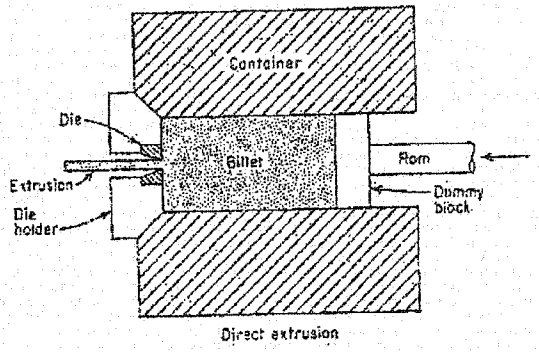

Figure 1: Equipment Setup for Conventional Extrusion Deformation

The deformation process causes changes in material characteristics. As the billet is pushed through the die, high hydrostatic pressure occurs within the block of material. The pressure results from the compressed material being constrained as it is pushed through the die. The imposed conditions of the deformation method can have effects on the success of the extrusion. Under the correct conditions, many materials that are difficult to deform are easily extruded at high temperatures. Temperature, speed, friction, and the extrusion ratio are the main parameters that affect the extrusion process. Internal voids and pores are healed, and crack propagation is inhibited. Also, the course microstructures within the starting material are effectively broken down [2]. The material exhibits significant changes as a result of this deformation process.

The extrusion ratio (R) is defined as the ratio of the original cross-sectional area (A_o) of the sample, which is also the cross-sectional area of the extrusion chamber, to the extrudate cross-sectional area (A_f) ($R = A_o / A_f$). The true strain for conventional extrusion (ε_t) is found as the natural log of the extrusion ratio:

$$\varepsilon_t = \ln (A_o / A_f) = \ln (R). \qquad \text{Eq. 1}$$

The pressure required for conventional extrusion (P) is related to the extrusion ratio and the true strain:

$$P = k \bullet A_o \bullet \ln (A_o / A_f) = k \bullet A_o \bullet \varepsilon_t. \qquad \text{Eq. 2}$$

The extrusion constant, k, is dependent upon the friction, flow stress, and any inhomogeneous deformation [2]. The interdependence between the extrusion variables enables the process to be easily altered to fit many material requirements.

There are certain disadvantages to the conventional method of extrusion. This process usually induces a nonuniform deformation field in the billet.* Strain

---

Special "stream line" dies can be made which produces uniform strain but such dies are costly to design and manufacture.

---

variations are seen from the front to the back of the extrusion in longitudinal and transverse directions. This nonuniformity of deformation results in variations within the microstructure and the properties of the extruded material. Areas with exaggerated grain growth are often found after hot extrusion [2].

A relatively new innovation in extrusion processes is equal channel angular extrusion (ECAE) (Segal)[4]. The hallmark of this method is that the die inlet and exit channel cross-sectional areas are nearly identical. Instead of forcing the specimen through a die, the billet is forced around a sharp corner between the exit and inlet chambers; this can be seen in Figure 2. The billet experiences uniform, simple shear stress instead of the nonuniform stress experienced in conventional extrusion [3]. Since the shape of the billet does not change during extrusion, the sample can be extruded multiple times resulting in high strains. These uniform, unidirectional, and extremely high deformations that result from relatively low pressure and load are not easily achieved with conventional extrusion [4]. The virtually unlimited plastic strain that the specimen can experience causes changes in material characteristics.

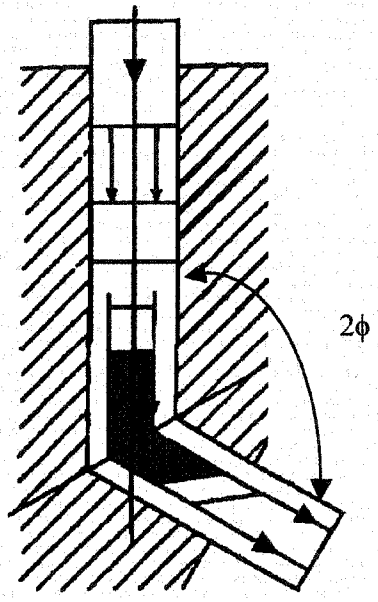

Figure 2: Equipment Setup for ECAE Deformation

The total strain for N extrusion passes is a function of the angle (2ϕ) between the extrusion channels and is:

$$\varepsilon_t = 2 \bullet N \bullet \cot(\phi) / \sqrt{(3)}. \qquad \text{Eq. 3}$$

The equivalent reduction ratio (RR) is also related to the 2ϕ angle:

$$RR = \exp(2 \bullet N \bullet \cot(\phi) / \sqrt{(3)}). \qquad \text{Eq. 4}$$

The percent reduction in area (AR) is a function of the reduction ratio:

$$AR = (1-(1/RR)) \bullet 100. \qquad \text{Eq. 5}$$

The pressure for extrusion (P) can be derived as a function of flow stress (σ_o) as:

$$P = 2 \bullet \sigma_o \bullet \cot(\phi) / \sqrt{(3)}. \qquad \text{Eq. 6}$$

The conventional extrusion process has drawbacks that can be avoided with the new ECAE innovation. Uniformity of strain and distortion reduce variations of properties within the material. Also, the ability to process bulk materials in ECAE adds to its positive aspects.

The effects of different processing techniques on materials can result in variations in mechanical properties and in microstructure. A comparison of the deformation patterns

and hardness values of extruded specimens are utilized to determine strain uniformity. In this laboratory activity students are provided the opportunity to examine the effects of annealing on specimens deformed by ECAE, conventional extrusion, and rolling..

Procedure:

Modeling the Process

In order to model conventional extrusion deformation, an experiment is performed using a two-colored checkerboard array of Play-Doh (Kridli)[5]. The Play-Doh billets are extruded with data collected at various points in the operation. Photographs of the sample are taken before extrusion, during extrusion at small strains, during extrusion at larger strains, and after extrusion. The extruded sample is cut apart to photograph the deformed cross-section after extrusion is complete. The geometrical alterations of the arrayed blocks are analyzed to determine the shear strains in the sample. Each block of the arrayed Play-Doh sample is considered as a single strain element for strain field calculations. The strain variations are examined as a function of the block locations.

Deformation Processes

Students' process annealed oxygen free copper samples (400°C for 30 min.), with a 6.5 cm^2 (1 in^2) cross-sectional area by rolling, conventional extrusion, and equal channel angular extrusion at room temperature. The students do the rolling, while the ECAE and conventional extrusion are done by a research associate and observed by the students. For the laboratory, the students use solid specimens. However, prior to the laboratory split and gridded specimens were prepared for helping the students compare the two extrusion processes. The temperature, punch speed, and extrusion pressure-ram displacement curve for each process are recorded. An examination of material characteristics (hardness and metallography) before and after the extrusion processes illustrates differences in the processing methods. The extrusion press is a 250 ton MTS test machine with a 20 in stroke and a maximum ram speed of 2.5 in/s.

The extruded copper sample is cut into appropriate specimen sizes for Rockwell hardness measurements, which are completed according to ASTM standard E10.

Some specimens may be mounted, ground, and polished for Vickers microhardness measurements (utilizing ASTM standard E384), in comparing between the original billet and the processed specimens. The Vickers microhardness tests are not typically done during laboratory classes.

The distorted grid patterns and quantified grid distortions for the extruded, gridded samples are utilized to determine the strain of the sample and the regions of nonuniform deformation. The hardness values and strain fields that are found are utilized in the comparison of the two extrusion methods. The uniformity of strain can be determined with these measurements.

An analysis of the effects of different annealing temperatures on the processed copper specimens is also undertaken. Students select the number of specimens and the temperatures and times for annealing. The processed samples are cut into appropriate pieces for the different heat treatments. Samples of each processed specimen are annealed for thirty minutes at room (typical) temperature ($\approx$ 25°C), 100°C, 150°C, 175°C, 200°C, 300°C, and 400°C in an air furnace. Hardness measurements are completed on each annealed specimen to determine the amount of recovery. These measurements are also

used for determination of the recrystallization temperature of the copper, which is about 225°C, as shown in Figure 3. Annealing has significant recovery effects on the properties of deformed specimens. Figures 3 and 4 illustrate the effect of annealing temperature, for a constant time, on the recrystallization temperature of material tested.

Optical metallography is undertaken on the initial annealed samples, the deformed specimens, the deformed specimens annealed at 200°C for thirty minutes in air, and the deformed specimens annealed at 400°C for thirty minutes in air. The samples are prepared by first cutting, mounting (use cold mount), and polishing sections from samples representing each deformation method. The variations in grain size and shape are compared for a better understanding of the microscopic effects of cold working and annealing.

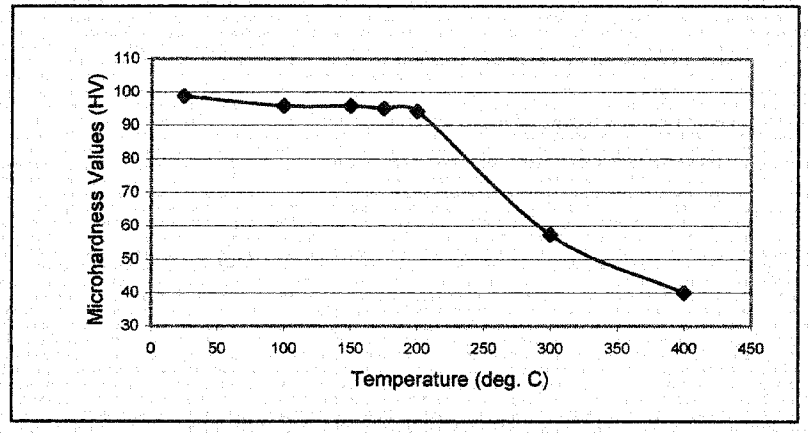

Figure. 3. Hardness variation of the rolled specimen as a function of annealing temperature.

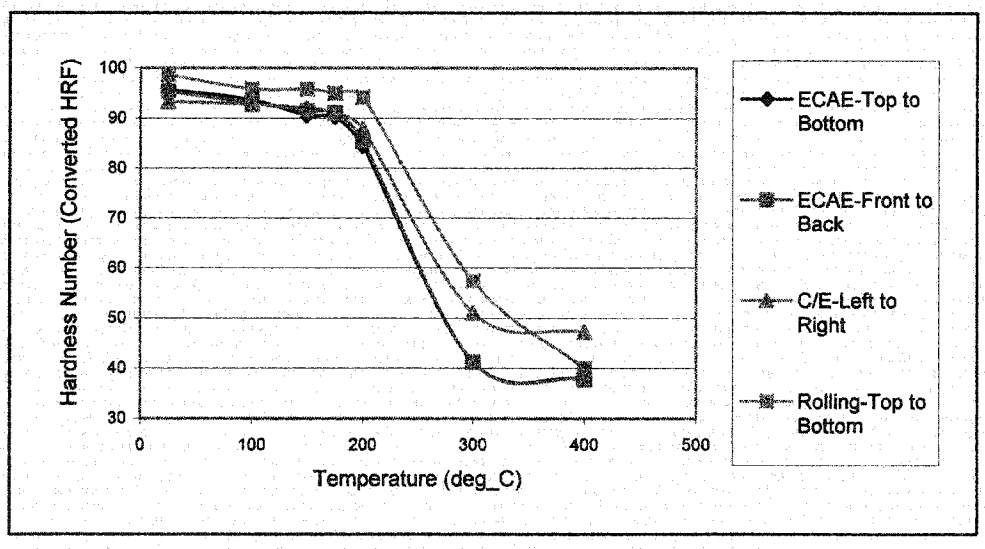

Figure 4. The variation of the hardness as a function of the annealing temperature.

Discussion:

The deformation patterns of the extruded specimens are compared for uniformity. The pattern on the ECAE extruded sample was uniform; the deformed squares all displayed a uniform geometrical change that is shown in Figure 5. This uniform shape change is correlated to a uniform strain field. However, nonuniform deformation can be viewed for the bottom 10% of the sample; this was attributed to friction experienced by the bottom of the billet during the extrusion process. The uniform strains associated with ECAE should be supported by uniform hardness values on the cross-section of the processed samples. The deformed microstructure should also display uniform microscopic alterations The uniformity of properties in ECAE increases its applicability to numerous engineering applications.

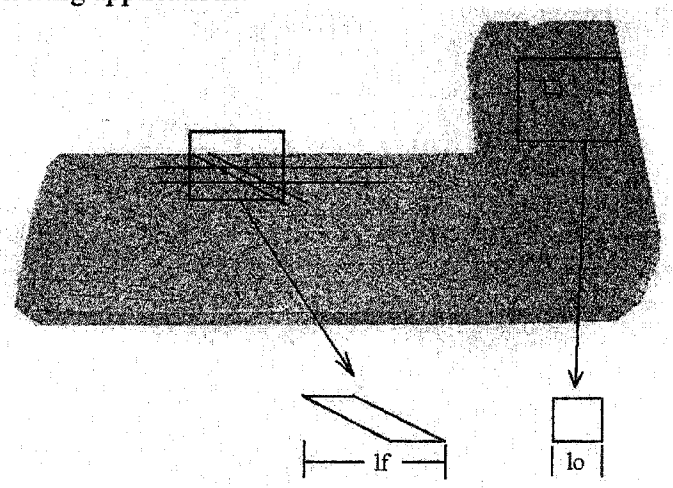

Figure 5. Deformation grid for ECAE deformation.

A significantly different situation is encountered in the analysis of the conventionally extruded specimens The deformed grid pattern shown in Figure 6 is nonuniform; center grid squares experienced greater size and shape changes than on the specimen edges. Variations in hardness values on the cross-section of the extruded specimen show that there are varying amounts of cold work across the billet. The nonuniform hardness profile is also seen in the rolled specimen, which should experience greater hardness values at the edges of the sample The deformed microstructures should further support these findings. Nonuniform distortion causes nonuniform properties, and this may cause difficulty in structural applications

The effects of annealing on the properties of the samples are most notable near the recrystallization temperature, where the heavily worked structure recrystallizes to strain free well defined grains. The specimens annealed near the crystallization temperature (approximately 160°C) experience a significant decrease in hardness values. Variations in hardness between specimens annealed at temperatures lower than the recrystallization temperature are much less dramatic. Microstructural analysis should delineate the stages of recrystallization and grain growth as the grain structure changes. The experimental results elucidate the results of deformation and annealing giving a greater understanding of cold working and material response to heat treatment. The variation in hardness values

shown in Figure 7 is used to demonstrate the variation in processing for the three processes used during the laboratory.

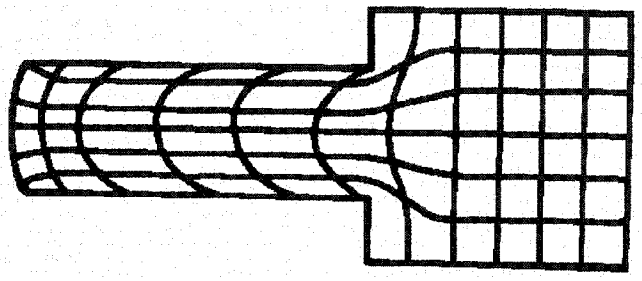

Figure 6. Deformation grid for conventional extrusion deformation.

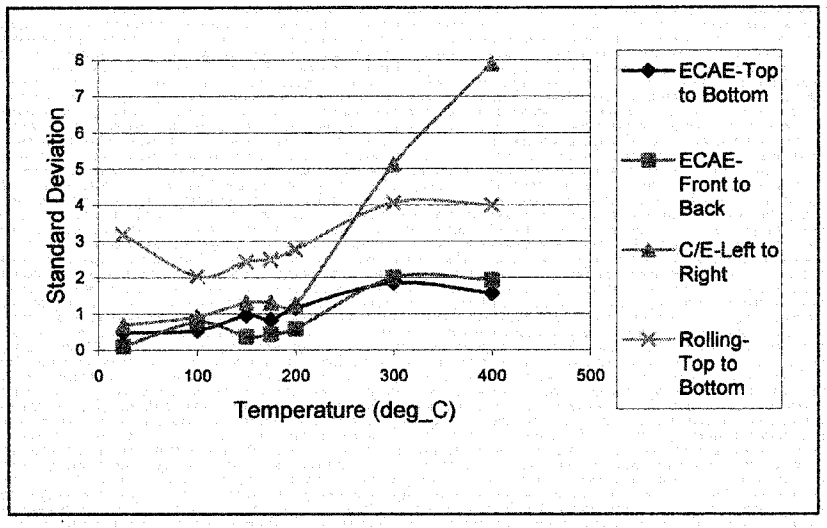

Figure 7. The effect of different annealing temperatures on the standard deviation of hardness values of copper.

The ECAE deformed material exhibits less variation in the standard deviation of the hardness values than either of the other two deformation processes as the specimens were traversed.

Conclusion:

The laboratory groups evaluated three methods of deformation and, were able to compare the relative characteristics of ECAE, conventional extrusion, and rolling. The students were able to choose different annealing times and temperatures and observe the results of their choices. For evaluating the effects of annealing temperature, they used hardness testing. In addition, they used Play Doh to model the deformation process.

References:

1. Sheppard, T., Extrusion of Aluminum Alloys, Kluwer Academic Publishers, 1999.
2. Dieter, G.E., Mechanical Metallurgy, Third Ed., McGraw-Hill, 1986.
3. ASM Committee on Cold Extrusion, "Cold Extrusion," Metals Handbook, Volume 4, pp.475-489.
4. Segal, V.M., "Materials Processing by Simple Shear," Materials Science and Engineering A197, 1995, pp.157-164.
5. Kridli, Ghassan K., "Visio-Plastic Modeling of Metal Forging and Extrusion," National Educators' Workshop: Update 99, 2000, pp. 477-480.

BIPMAP (Binary Isomorphous Phase Map) AN INTERACTIVE COMPUTER TOOL FOR PHASE DIAGRAM INSTRUCTION

J. Csernica

J. Stolk[1]

M. E. Hanyak

and

V. Subramanian

Department of Chemical Engineering
Bucknell University
Lewisburg, Pennsylvania 17837

Telephone: 570-577-1257
e-mail csernica@bucknell.edu

[1]current address:
Franklin W. Olin College of Engineering
1735 Great Plain Avenue
Nedham, Massachusetts 02492

Jeffrey Csernica

BIPMAP (Binary Isomorphous Phase Map) – An Interactive Computer Tool for Phase Diagram Instruction

J. Csernica, J. Stolk[1], M.E. Hanyak, V. Subramanian
Department of Chemical Engineering
Bucknell University
Lewisburg, PA, 17837

Abstract

BIPMAP, a program that can be accessed over the internet, is designed to assist with phase diagram instruction for beginning materials science students. Using a mouse and/or navigation buttons, the user can select a point anywhere in a binary isomorphous phase diagram to view information including phase amounts and compositions. Schematic alloy microstructures are also shown, which, together with corresponding color-coded phase fields, tie lines (in two-phase regions), and numerical results, help students visualize concepts such as the lever rule and microstructural development.

Key words: Equilibrium, phase diagram, solubility, microstructure, lever rule.

Introduction

The understanding and proper use of metallurgical phase diagrams is typically considered a vital component of introductory materials science instruction, with textbooks (1,2) devoting entire chapters and/or self-paced tutorials (3) to this topic.

A number of web-based computer tools dealing with phase diagrams are also available, which are generally intended to supplement traditional textbook information. These include sites at the University of Southampton (4) and Virginia Tech (5), which include self-paced lessons that lead students through phase diagram definitions and concepts. These useful sites contain text, pictures, graphics, quizzes and hyperlinks to phase diagram related topics, much as static renditions of textbook content. Both offer a phase diagram page which allows the user to click on a few pre-designated points to see schematic images of alloy microstructures.

Electronic renditions of phase diagrams designed for experienced users, with varying levels of interactivity, are also available. These include CD-ROM collections from ASM (6) and the BiPhaser Trial (7).

---

[1]current address: Franklin W. Olin College of Engineering, 1735 Great Plain Ave., Needham, MA 02492

From our experience with introductory materials science instruction at Bucknell, we felt that a need existed for a different type of electronic phase diagram instructional tool. Major goals were that it be truly interactive (able to respond to students' free and unstructured exploration), and appropriate for beginners, with an interface designed to organize and display information to help students conceptualize and integrate phase diagram basics. The result, applied to a binary isomorphous system, is called BIPMAP. This is a internet Java-based applet which can be accessed at:

www.departments.bucknell.edu/chem_eng/bipmap

Key Features

Diagram. As seen in Figure 1, which is a grayscale snapshot of the BIPMAP screen, the majority of the screen area is taken up by the phase diagram itself, with appropriate temperature and composition axes. Represented is the actual Bismuth-Antimony (Bi-Sb) phase diagram (8). Not visible in Figure 1's black-and-white rendition is the color-coding visible on the computer monitor, which provides connection with some other features described below. In particular, the liquid solution region is blue, the solid solution region is red, and the two phase region is white.

Selection and Movement of Composition-Temperature Point. Any point within the phase diagram can be selected with a mouse click, to a resolution of 0.25 wt% Sb and 1.25 °C. Once a point has been established, it can be moved horizontally or vertically using the sets of fast ("ff") and normal motion buttons to the upper right of the diagram. This makes it possible for constant temperature or constant composition (heating and cooling) analyses.

Quantitative Results Display. The boxes below the cursor motion buttons on the right of the screen indicate the coordinates of the currently selected composition-temperature point, and the equilibrium state or constitution of the alloy at that point. The state information given includes the phases present, phase compositions, and relative phase amounts (in this order, as that mimics the order information is normally attained manually from the diagram). Some of this information is color-coded to match the diagram. For example, the individual liquid and solid phase fractions are displayed in blue and red, respectively.

Tie Line. When a point is selected in the two phase region, a tie line is drawn. This line is "inverse" color-coded. That is (see Figure 1), the right arm of the tie line is colored blue (liquid region color), and the left arm is red (solid region color). The color-coding helps students make the connection between the desired phase amount in the lever rule and the appropriate segments of the lever. Also, vertical dashed lines are dropped at the ends of the tie line to indicate individual phase compositions on the abscissa (also displayed in the results box).

Microstructure. While only simplified schematics, we feel that the representative microstructures shown in the lower right box are instrumental in helping students conceptualize the meaning of phase diagram navigation and the quantitative results that are displayed. Again,

color-coding to match the phase diagram regions is employed. For various solid/liquid fractions, the microstructure will show red solid grains, contained in a blue liquid matrix (see Figure 2 a-d). At low solid fractions, small spherical nuclei are present. As higher solid fractions are encountered (say, upon cooling in the two-phase regions), these same nuclei grow (for simplicity, no new nuclei are added). When the spherical grains impinge, a straight grain boundary is formed.

In-Class Use and Assessment

In Spring 2001, BIPMAP was introduced to a group of 32 first-year chemical engineering students in their required introductory materials course. With no in-class introduction to the program, they were referred to the site as part of a homework assignment, the text of which appears in Appendix A. Many of the standard textbook question types concerning concepts such as melting point, solubility, liquidus temperature, phase composition, and the lever rule are appropriate for such exercises. Later in the semester and prior to an examination covering phase diagram topics, another assignment asked students to first answer on paper questions dealing with the Bi-Sb diagram, then check their answers using BIPMAP. At that time, they were asked to complete an electronic survey which asked for their feedback on the program.

The student survey response to the use of BIPMAP and its features was overwhelmingly positive. Table 1 summarizes averages responses on a 5-point scale (1 = strongly disagree, 5 = strongly agree).

Question	Avg. Response
1. BIPMAP was easy to use.	4.69
2. The labels on the results display are self-explanatory.	4.08
3. BIPMAP helped me understand phase diagrams.	4.44
4. The color coding of the tie lines aided my understanding of the lever rule.	4.38
5. Pictures of the microstructures helped me understand what happens physically when an alloy is cooled/heated.	4.63
6. BIPMAP is a good learning tool.	4.75
7. I would consider using BIPMAP as a review tool for subsequent exams.	4.55
8. I would recommend using BIPMAP in future Science of Materials classes.	4.91

Table 1. Average student responses to 5-point scale questions on BIPMAP survey (1 = strongly disagree, 5 = strongly agree)

In particular, we see that students strongly felt the software was an effective learning tool that should be used again in the course, and they benefited from some of its key features like the microstructures and colored tie lines.

We also asked for written responses describing what students liked about BIPMAP, and what they saw as areas for improvement. Again, we were pleased that students favorably commented on many of the design features of the program, and overwhelmingly felt that it helped them understand phase diagrams. Comments also suggested that students spent a good deal of time with the program beyond the straight solution of the homework problems. Suggestions for improvement were few, although some suggested added features, and several thought there would be a benefit to including more (and more complex) phase diagrams. Table 2 contains several representative comments.

1. BIPMAP has helped me greatly in understanding phase diagrams. I am a visual learner, so to have a program like this was quite beneficial.
2. The interface was very easy to use.
3. I like that I can make can make up my own problems and then check to see that I am doing the right thing, and am not confused about compositions vs. amounts.
4. I liked the way I could check instantly my hand calculations, and observe trends as I move the cursor in different directions.
5. I like the color coded tie lines.
6. The pictures of the microstructures were especially helpful.
7. It gives me a good idea of how the phase diagram really works.
8. If you didn't know how to use phase diagrams, you could learn just by doing this.
9. Perhaps have an area where you can type in coordinates.
10. You could add a more complicated phase diagram, with a eutectic point.

Table 2. Representative student comments from BIPMAP survey.

Summary

The BIPMAP phase diagram program is an effective learning tool for the beginning study of phase diagrams. Introductory materials science students can comfortably learn and use BIPMAP at their own pace. We plan to expand the program beyond the binary isomorphous case to include a simple eutectic diagram. [Instructors with experienced students may find eutectic

diagrams at the BiPhaser Trial site (7) useful.] Materials science faculty and students are encouraged to try BIPMAP, and the authors welcome comments which can be sent to csernica@bucknell.edu.

References

1. Callister, W.D., *Materials Science and Engineering – An Introduction*, 5th ed., Wiley, New York, 2000.
2. Shackelford, J.F., *Introduction to Materials Science and Engineering*, 5th ed., Prentice-Hall, Upper Saddle River, New Jersey, 2000.
3. Ashby, M.F., Jones, D.R.H., *Engineering Materials 2 – An Introduction to Microstructures, Processing and Design*, Pergamon Press, New York, 1986.
4. Phase Diagrams, *www.soton.ac.uk/~pasr1/.*
5. 96 Class Project; Phase Diagram Basics, *www.sv.vt.edu/classes/MSE2094_NoteBook/96ClassProj/proj.html.*
6. Binary Alloy Phase Diagrams CD-ROM Demo Disk, ASM International, Metals Park, OH.
7. BiPhaser Trial, *www.home.ivm.de/~gollog/biuk.htm.*
8. *Metals Handbook - Metallography, Structures and Phase Diagrams*, vol. 8, 9th ed., ASM International, Metals Park, OH, 1989.

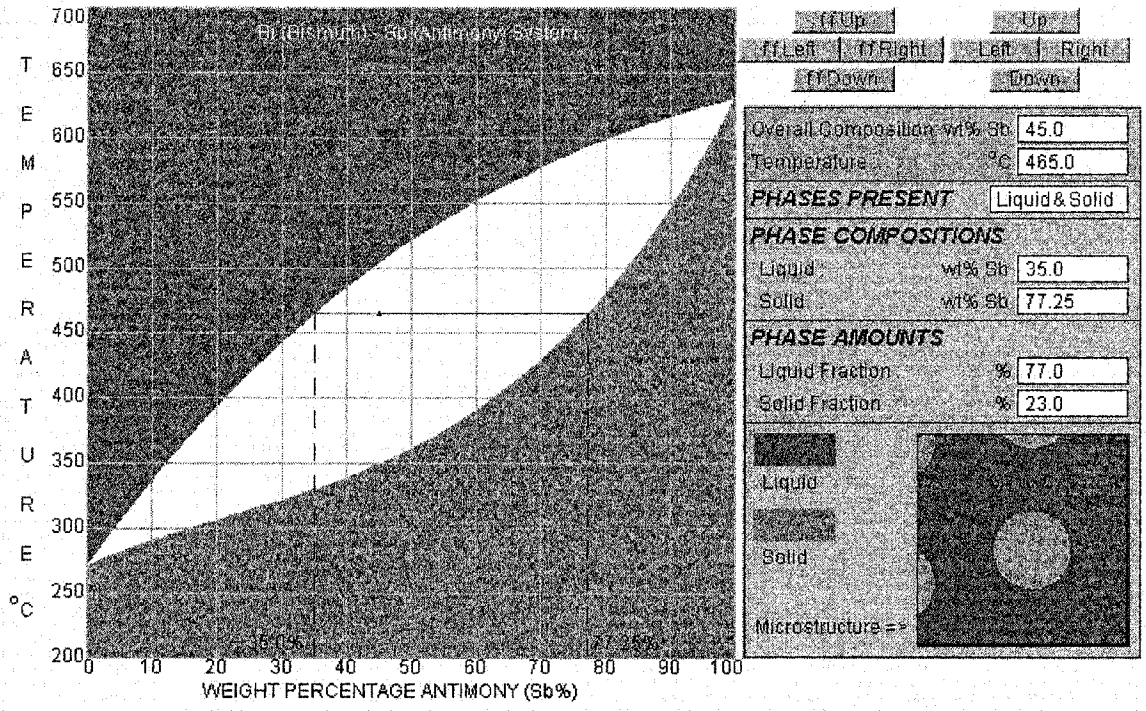

Figure 1. Grayscale snapshot of BIPMAP screen with coordinate of 45 wt% Sb and 465 °C selected.

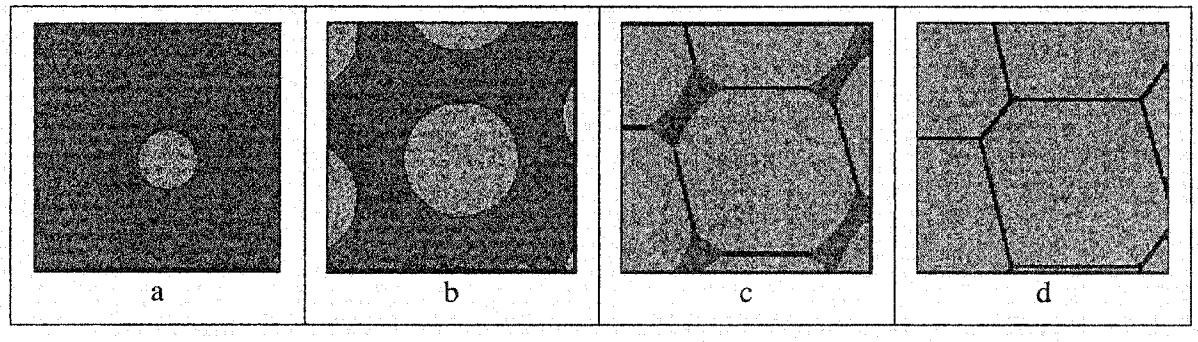

Figure 2. Schematic solid/liquid (light/dark) microstructures at solid percentages of: (a) 10; (b) 20; (c) 85; (d) 100.

Appendix A – sample first homework assignment

1. Open the BIPMAP program, using the link at the course "lecture" homepage.

   Place the cursor at the left edge of the diagram (0% Sb), and use the click-buttons to move it up and down. Find as precisely as possible the melting temperature of Bi. Note the changes in the "results" windows to the right of the diagram as you move through the melting region. What is the melting temperature?

Similarly, move the cursor and use the program to find answers to the following:

2. At 500 °C, a mixture containing 20 wt% Sb exists as a single phase liquid. If more antimony is added to this system, at what concentration would the solubility be exceeded (indicated by the presence of a second phase)?

3. A mixture of antimony and bismuth (70 wt% Sb) is heated to 650 °C to form a well mixed liquid. This liquid is slowly cooled to room temperature.

   a) At what temperature does the first solid form, and what is the composition of this solid?

   b) At what temperature will the mixture contain equal amounts of liquid and solid and what are the compositions of each phase at this temperature?

   c) At what temperature will the mixture contain 10 wt% liquid, and what are the compositions of each phase at this temperature?

   d) At what temperature will the last amount of liquid disappear?

   e) Collect information from the program, and then make a plot of the liquid composition (wt% Sb) as a function of temperature in the range of 300 – 650 °C.

TEAPOT DRIBBLES & LADLE POURS

Edward L. Widener

School of Technology
Mechanical Engineering Technology
Purdue University
Knoy Hall, Room 119
West Lafayette, Indiana 47907-1317

Telephone: 765-494-7521
e-mail elwidener@tech.purdue.edu

Ed Widener

TEAPOT DRIBBLES & LADLE POURS

by Edward L. Widener, PE
Purdue University, MET Department
West.Lafayette, IN

Key Words: Open-channel flow; potential-flow nets; capillarity; surface tension.

Prerequisite Knowledge: Consistent Units = F, L, T, t
Force (F) = Mass (m) x Acceleration (a)
Velocity (V) = Length (L) / Time (T)
Acceleration = Velocity / Time
Stress (s) or Pressure (p) = Force / Area (A)
Capillarity (c) = Force / Length
Weight (w) = Force
Absolute or Dynamic Viscosity (v) = Stress x Time

Objectives: To specify dimensions; to contrast surface tension and tensile stress; to test theory with observations; to investigate flow-nets; and to explore molten-metal pouring.

Equipment & Supplies: Several teapots, pitchers, and drinking glasses
Several beakers or graduated cylinders
Assorted paper cups or plastic tumblers
Tap water (between 0 – 100 degrees Celsius)
Catch basin (sink or tub)

Abstract: Why do bad teapots dribble on your fine linen tablecloth? Some physics books blame surface tension (capillarity) between the hot-tea and china-pot; but simple experiments disprove simplistic explanation. The "wetting" ability of liquid water is enhanced by temperature rise, as surface tension decreases. Also, changing the materials of a liquid-solid interface may greatly change capillarity. But bad teapots still dribble. Misshapen spouts cause spillage, regardless of metal-ceramic-plastic material selection. Applications are obvious: 1)Broad-crested weirs; 2)Dam spillways; 3)Molten-metal ladles; 4)Flow-nets; 5) Fourdrinier wires on Table-rolls.

Introduction: Early courses in Materials tend to stress solids, but fluids are fascinating. Pouring liquid from one container into another is an example of "open-channel flow". Spills of hazardous material are unacceptable, so design of vessels is important. Must we suffer the "bottom-teeming" of molten steel, from ladles with costly maintenance? Let us explore some "dribble phenomena", using a collection of various cups, cans, jars, and tumblers. Classify by differences in diameter, height, taper, flare, wall thickness and lip.

Procedure:

1) Start with a simple plastic cup of clear styrene (SPI #6, ASTM-PS). Note its tapered shell, thin-wall, circular cross-section, and sharp lip. Fill with water and pour swiftly, discharging a convex arc into your tub. This free-falling stream

looks braided and turbulent, because surface tension pulls the flattened overflow into a round jet, then rotates into an oval, then round again. As the cup empties, your stream will separate more abruptly, with less tendency to dribble. Thus, when comparing vessels, refill at each startup.

2) Refill the same cup, pour more slowly, and form a different stream. After curving around the lip, this stream will separate from the lip to make an "S-curve". This is a convex/concave inflection , which falls into your tub. Aiming cream at your coffee mug would require some "offset".

3) Refill the same cup, pour even slower, and form a third type of stream. Curving around the lip, this stream flows on the outside wall of the cup, separating at the bottom to form a backward arc (concave) into your tub. Aiming cream at your coffee mug requires even greater "offset".

4) Refill the same cup, but squeeze the rim into an oval, before pouring fast and slow. This tends to exacerbate dribbling, to produce simultaneous forward and backward streams, or to exhibit unstable movement (front to back).

5) Shift to a paper cup, which allows a sharply-folded "V-lip", makes our stream more 3-dimensional, and reduces dribbling. This accounts for the pointed lip on lab beakers and cream pitchers.

6) Finally test your teapots, which have various side-outlets, curvatures, extensions, and end configurations. The best design has a hooked spout and downward free-fall. However, this is vulnerable to chipping and breaking. We need a slip-on attachment, suitable for any spout.

Conclusion: Dam spillways and broad-crested weirs are described by 2-dimensional flow-nets, with streamlines (flux) intersected by isobars (pressure) at right angles. These so-called "potential-flow fields" apply as well to electric current, heat transfer, gravity pull, magnetism, and solid mechanics. For an "ideal fluid" (having no energy losses from friction, viscosity, hysteresis, or capillarity) there is a unique flow-net for any given boundary-condition. The solution can be found by sketching (graphics), arithmetic (relaxation) , conformal mapping (algebra), or finite elements (software). Thus, water and air are virtually ideal fluids, as are many industrial fluids. Thomas Jefferson designed "self-scouring plows" with conic sections (hyperbolic). Therefore, teapot dribble can be predicted for "potential-flow" boundaries. Similarly, water is hydraulically pumped through paperformer wires, running over "table rolls".

Acknowledgements:

1) "Teapot Experiments", Scientific American Magazine, Puzzles & Games, Simon Gardner (ed), circa 1970.
2) "The Amateur Scientist", C.L.Strong (ed), Simon & Schuster, NY,1960.
3) "Fluid Mechanics for Hydraulics Engineers", Hunter Rouse, Dover, 1960
4) "McGraw-Hill Dictionary of Scientific & Technical Terms", 5th ed., 1994.

NATIONAL COMPOSITE CENTER AND DIRECTED FIBER PREFORMING

Tobey Cordell

National Composite Center
2000 Composite Drive
Kettering, Ohio 45420

Telephone: 937-369-1174
e-mail tcordell@compositecentr.org

National Composite Center and Directed Fiber Preforming

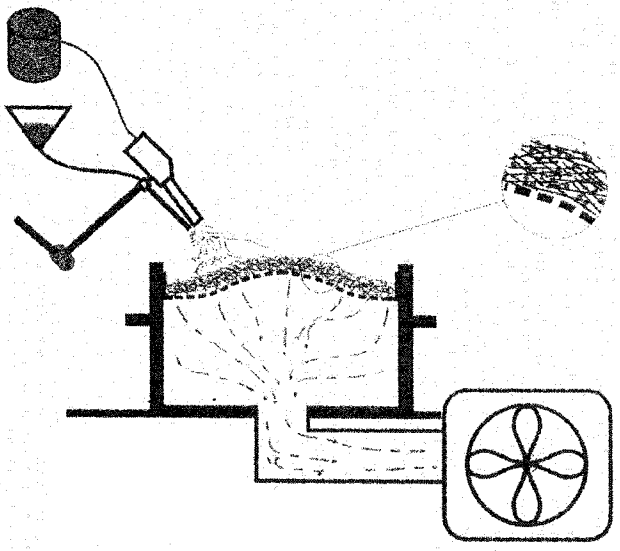

N·C·C
NATIONAL COMPOSITE CENTER

Tobey Cordell

National Educators'Workshop
October 2001

Programmable Powdered Preform Process (P4)

Fiber Deposition

Chopped fiber and binder applied to lower screen.
Held by vacuum.

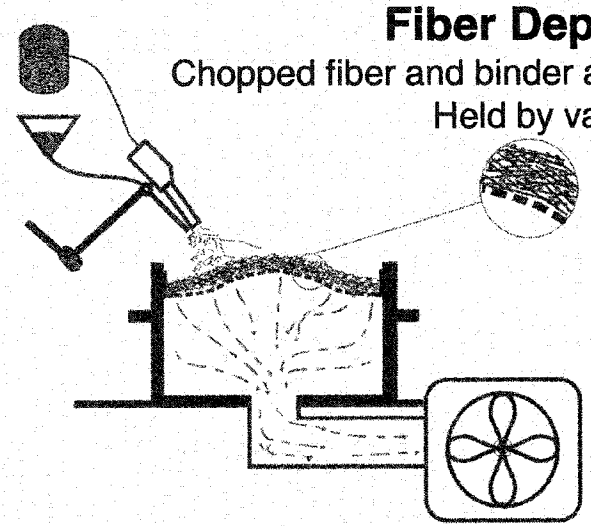

Consolidation

Upper screen compacts preform.
Hot air cures binder.

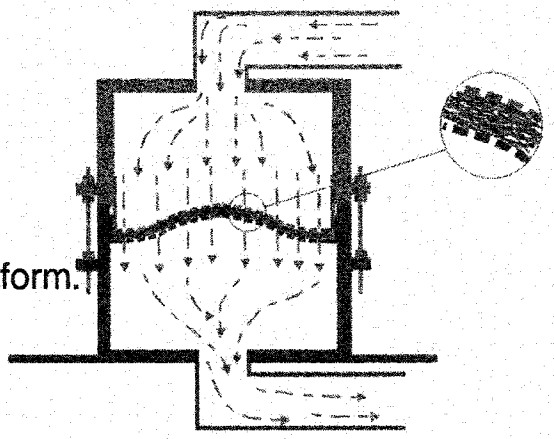

Cooling

Ambient air cools preform.

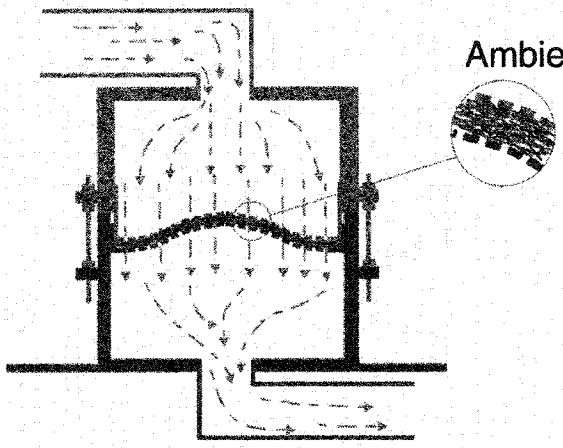

De - Molding

Preform removed from the lower screen.

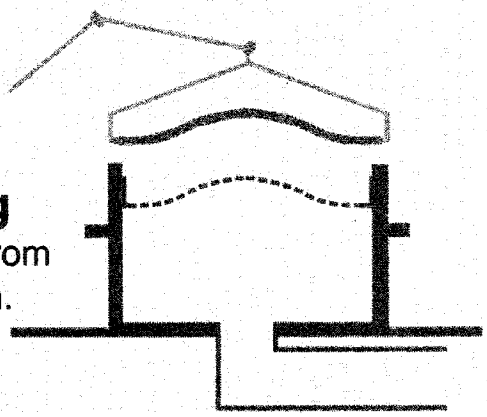

Lower Cost Preforms for Lower Cost Molding Processes

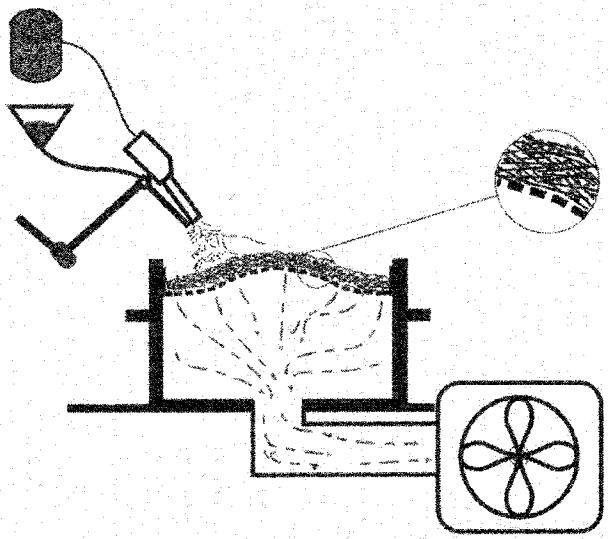

Directed Fiber Preforms

- **Chopped Fiber**
- **Binder to hold fibers in part shape**

Structural Reaction Injection Molding (**SRIM**)

Resin Transfer Molding (**RTM**)

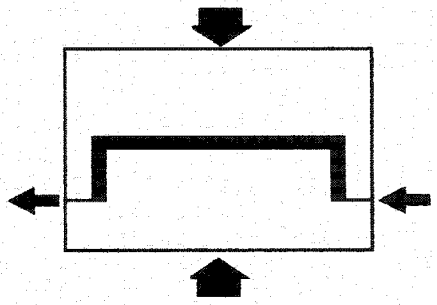

Vacuum Assisted RTM (**VARTM**)

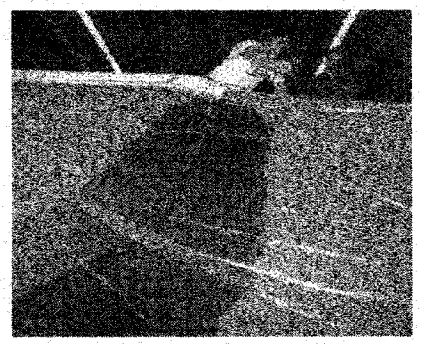

DFP Composite Firefighter Helmets

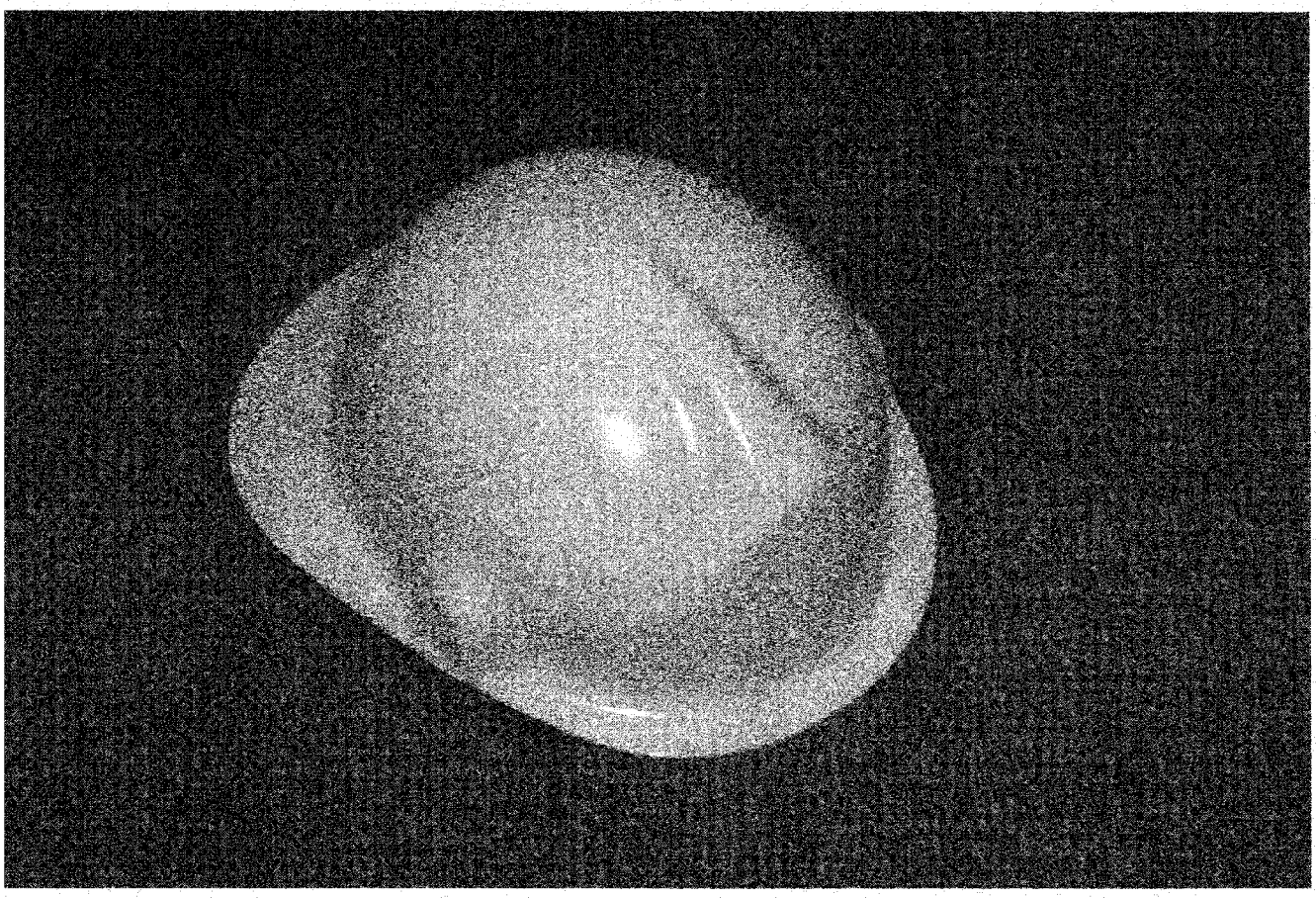

Directed Fiber Preform Niche

- **Performance (Properties)**
  - SMC < DFP < Continuous Fiber
- **Part Design**
  - Complex shapes
  - Large parts take advantage of robotic automation
- **Quantity**
  - Medium to high volume: automation; amortize tooling & equipment costs
- **Cost**
  - Raw material lowest cost form; negligible scrap rate

P4 Composite Pickup Truck Box

- Automotive Composites Consortium (ACC) Focal Project
- Fiberglass / Polyurethane
- Structure, not just Liner

- Performance Goal: 30% lighter than Conventional Steel + Liner

- Cost Goal: "Competitive" Rate
  - 4 Minutes to Produce Preform (P4)
  - 4 Minutes to Infuse (1000 ton SRIM Press)

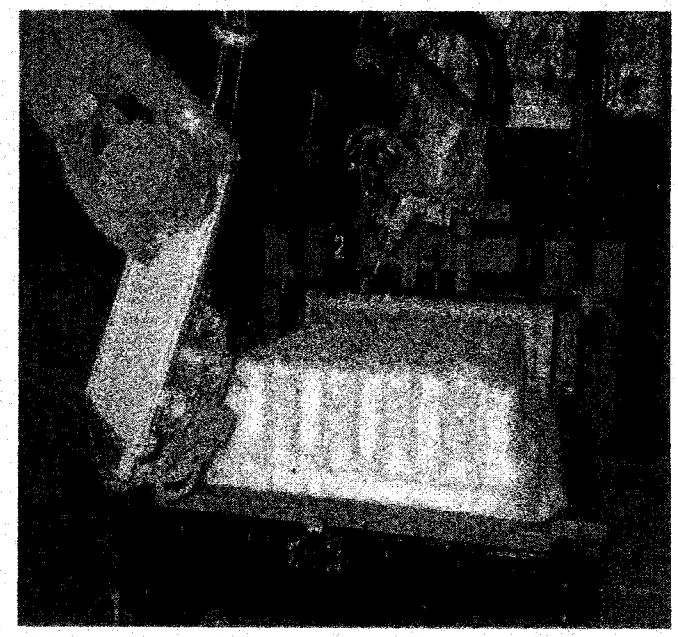

Chevrolet Silverado Pickup Truck
Composite Box and Tailgate
Int'l Body Engineering Conf., Detroit Sept 99

Programmable Powdered Preform Process for Aerospace: Technology Spin-on!

$ / lb.

Cost

lb. / $

Aerospace

Automotive

Performance

Fiber orientation, continuity, properties

P4A Program Results

- **Useful engineering properties**
  - 90% stiffness retention
  - 80% strength retention
  - Better Compression After Impact
- **Process enables complex shapes to be fabricated**

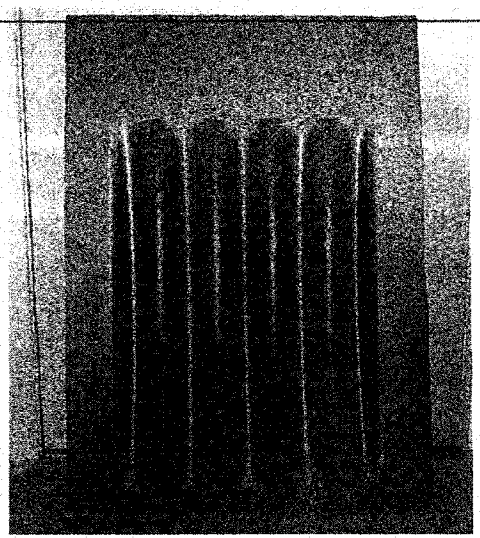

- **Cost Savings**

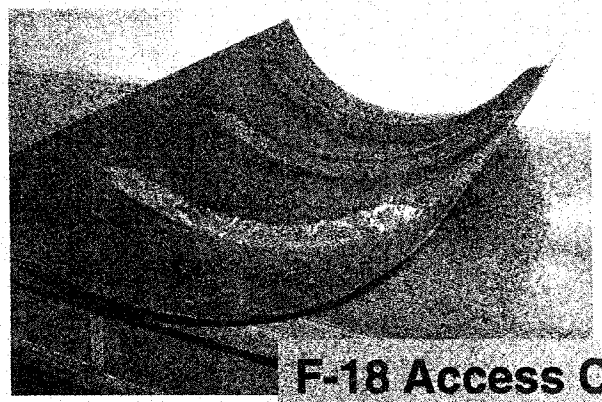

F-18 Access Cover
46% Cost Saving

YC-15 Tailcone
80% Cost Saving

P4A Phase 2

C-17 applications

General Cost Trend for Carbon Fiber Tow Sizes

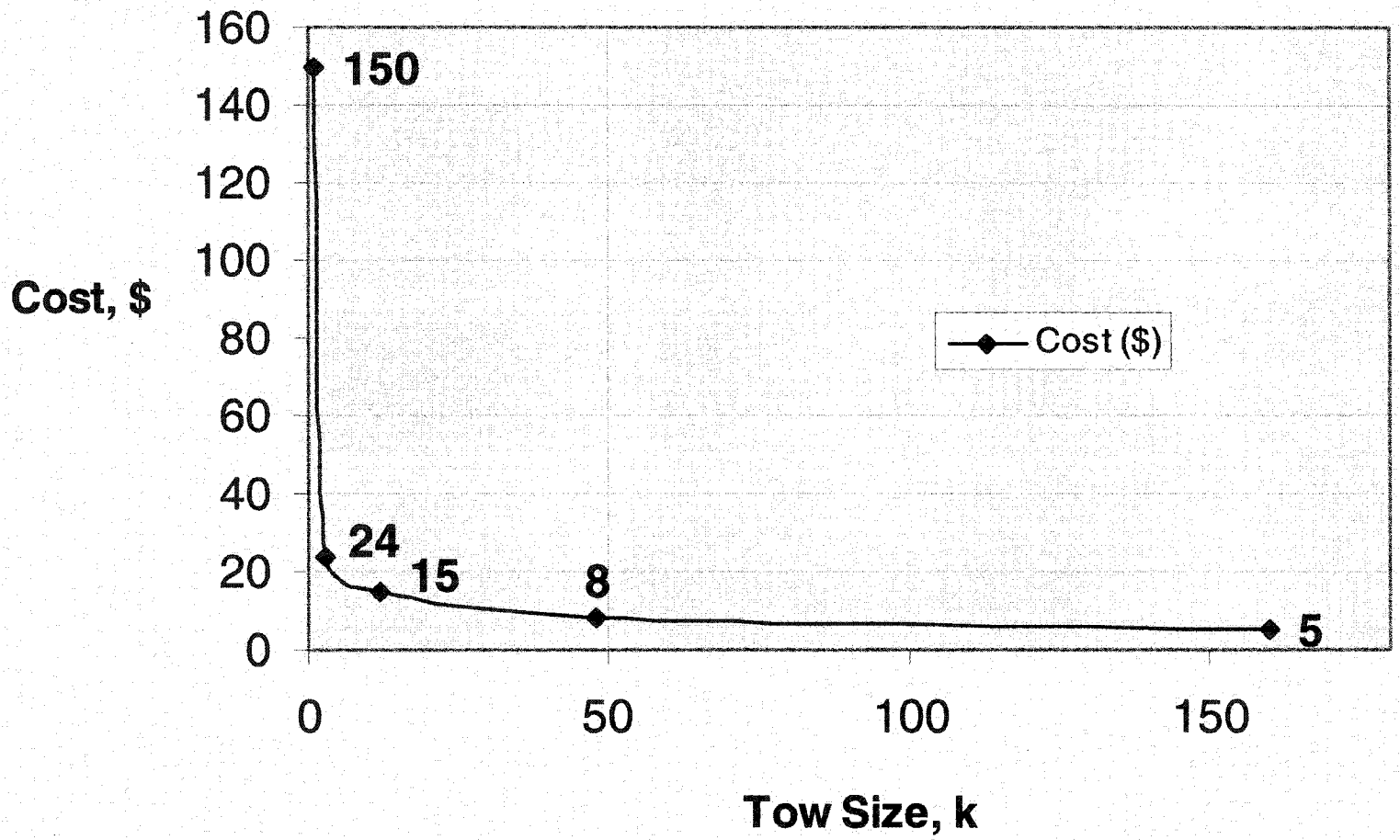

Conclusions

- **Directed fiber preform applications are growing**
  - **Automotive**
  - **Commercial**
  - **Aerospace**
- **Multiple resin infusion processes are successful**
- **Strong customer interest**

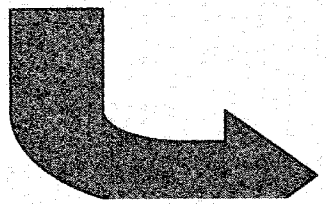

Towards ultimate goal of more affordable fiber-reinforced

REPORT DOCUMENTATION PAGE

Form Approved
OMB No. 0704-0188

1. AGENCY USE ONLY *(Leave blank)*	2. REPORT DATE	3. REPORT TYPE AND DATES COVERED
	June 2002	Conference Publication

4. TITLE AND SUBTITLE
National Educators' Workshop: Update 2001
Standard Experiments in Engineering, Materials Science, and Technology

5. FUNDING NUMBERS
WU 772-30-10-32

6. AUTHOR(S)
Compiled by Edwin J. Prior, James A. Jacobs, and Said Jahanmir

7. PERFORMING ORGANIZATION NAME(S) AND ADDRESS(ES)
NASA Langley Research Center
Hampton, VA 23681-2199

8. PERFORMING ORGANIZATION REPORT NUMBER
L-18193

9. SPONSORING/MONITORING AGENCY NAME(S) AND ADDRESS(ES)
National Aeronautics and Space Administration
Washington, DC 20546-0001

10. SPONSORING/MONITORING AGENCY REPORT NUMBER
NASA/CP-2002-211735

11. SUPPLEMENTARY NOTES
Prior: Langley Research Center, Hampton, VA; Jacobs: Norfolk State University, Norfolk, VA; Jahanmir: National Institute of Standards and Technology (NIST), Gaithersburg, MD

12a. DISTRIBUTION/AVAILABILITY STATEMENT
Unclassified—Unlimited
Subject Category 23 Distribution: Standard
Availability: NASA CASI (301) 621-0390

12b. DISTRIBUTION CODE

13. ABSTRACT ***(Maximum 200 words)***
This document contains a collection of experiments presented and demonstrated at the National Educators' Workshop: Update 2001 held in College Park, Maryland, October 14–17, 2001.

14. SUBJECT TERMS
Materials; Experiments; Education; Structures; K–12; Materials Science; Composites; Plastics; Nanomaterials; Metals; Testing; Ceramics; Polymers; Optical materials; Materials curriculum

15. NUMBER OF PAGES
724

16. PRICE CODE

17. SECURITY CLASSIFICATION OF REPORT	18. SECURITY CLASSIFICATION OF THIS PAGE	19. SECURITY CLASSIFICATION OF ABSTRACT	20. LIMITATION OF ABSTRACT
Unclassified	Unclassified	Unclassified	UL